

VENTILATION FOR CONTROL OF THE WORK ENVIRONMENT

VENTILATION FOR CONTROL OF THE WORK ENVIRONMENT

SECOND EDITION

William A. Burgess

Harvard University

Michael J. Ellenbecker

University of Massachusetts Lowell

Robert D. Treitman

Concord, Massachusetts

 **WILEY-INTERSCIENCE**

A John Wiley & Sons, Inc., Publication

Copyright © 2004 by John Wiley & Sons, Inc. All rights reserved.

Published by John Wiley & Sons, Inc., Hoboken, New Jersey.
Published simultaneously in Canada.

No part of this publication may be reproduced, stored in a retrieval system, or transmitted in any form or by any means, electronic, mechanical, photocopying, recording, scanning, or otherwise, except as permitted under Section 107 or 108 of the 1976 United States Copyright Act, without either the prior written permission of the Publisher, or authorization through payment of the appropriate per-copy fee to the Copyright Clearance Center, Inc., 222 Rosewood Drive, Danvers, MA 01923, 978-750-8400, fax 978-646-8600, or on the web at www.copyright.com. Requests to the Publisher for permission should be addressed to the Permissions Department, John Wiley & Sons, Inc., 111 River Street, Hoboken, NJ 07030, (201) 748-6011, fax (201) 748-6008.

Limit of Liability/Disclaimer of Warranty: While the publisher and author have used their best efforts in preparing this book, they make no representations or warranties with respect to the accuracy or completeness of the contents of this book and specifically disclaim any implied warranties of merchantability or fitness for a particular purpose. No warranty may be created or extended by sales representatives or written sales materials. The advice and strategies contained herein may not be suitable for your situation. You should consult with a professional where appropriate. Neither the publisher nor author shall be liable for any loss of profit or any other commercial damages, including but not limited to special, incidental, consequential, or other damages.

For general information on our other products and services please contact our Customer Care Department within the United States at 877-762-2974, outside the United States at 317-572-3993 or fax 317-572-4002.

Wiley also publishes its books in a variety of electronic formats. Some content that appears in print, however, may not be available in electronic format.

Library of Congress Cataloging-in-Publication Data:

Burgess, William A., 1924-

Ventilation for control of the work environment/William A. Burgess,
Michael J. Ellenbecker, Robert D. Treitman.— 2nd ed.
p. cm.

Includes bibliographical references and index.

ISBN 0-471-09532-X (cloth)

1. Factories—Heating and ventilation. 2. Industrial hygiene.
- I. Ellenbecker, Michael J. II. Treitman, Robert D. III. Title.
TH7684.F2.B86 2004
697.9'2—dc22

2004006447

Printed in the United States of America

10 9 8 7 6 5 4 3 2 1

CONTENTS

List of Units	xiii
Preface	xv
1 Ventilation for Control	1
1.1 Control Options / 2	
1.2 Ventilation for Control of Air Contaminants / 3	
1.3 Ventilation Applications / 5	
1.4 Case Studies / 7	
1.5 Summary / 9	
References / 11	
2 Principles of Airflow	12
2.1 Airflow / 13	
2.2 Density / 13	
2.3 Continuity Relation / 14	
2.4 Pressure / 16	
2.4.1 Pressure Units / 16	
2.4.2 Types of Pressure / 17	
2.5 Head / 18	
2.6 Elevation / 20	
2.7 Pressure Relationships / 22	
2.7.1 Reynolds Number / 24	
2.8 Losses / 26	
2.8.1 Frictional Losses / 26	
2.8.2 Shock Losses / 28	
2.9 Losses in Fittings / 30	
2.9.1 Expansions / 30	
2.9.2 Contractions / 32	
2.9.3 Elbows / 35	
2.9.4 Branch Entries (Junctions) / 36	

- 2.10 Summary / 38
- List of Symbols / 38
- Problems / 39

3 Airflow Measurement Techniques

43

- 3.1 Measurement of Velocity by Pitot–Static Tube / 45
 - 3.1.1 Pressure Measurements / 47
 - 3.1.2 Velocity Profile in a Duct / 50
 - 3.1.3 Pitot–Static Traverse / 57
 - 3.1.4 Application of the Pitot–Static Tube and Potential Errors / 60
- 3.2 Mechanical Devices / 61
 - 3.2.1 Rotating Vane Anemometers / 61
 - 3.2.2 Deflecting Vane Anemometers (Velometer) / 68
 - 3.2.3 Bridled Vane Anemometers / 71
- 3.3 Heated-Element Anemometers / 72
- 3.4 Other Devices / 75
 - 3.4.1 Vortex Shedding Anemometers / 75
 - 3.4.2 Orifice Meters / 76
 - 3.4.3 Venturi Meters / 76
- 3.5 Hood Static Pressure Method / 77
- 3.6 Calibration of Instruments / 79
- 3.7 Observation of Airflow Patterns with Visible Tracers / 80
 - 3.7.1 Tracer Design / 81
 - 3.7.2 Application of Visible Tracers / 84
 - List of Symbols / 85
 - References / 86
 - Manufacturers of Airflow Measuring Instruments / 87
 - Manufacturers of Smoke Tubes / 87
 - Problems / 87

4 General Exhaust Ventilation

90

- 4.1 Limitations of Application / 91
- 4.2 Equations for General Exhaust Ventilation / 93
- 4.3 Variations in Generation Rate / 99
- 4.4 Mixing / 100
- 4.5 Inlet/Outlet Locations / 101
- 4.6 Other Factors / 102
- 4.7 Comparison of General and Local Exhaust / 105
 - List of Symbols / 106
 - References / 106
 - Problems / 107

5 Hood Design **108**

- 5.1 Classification of Hood Types / 109
 - 5.1.1 Enclosures / 109
 - 5.1.2 Exterior Hoods / 110
 - 5.1.3 Receiving Hoods / 115
 - 5.1.4 Summary / 116
- 5.2 Design of Enclosing Hoods / 116
- 5.3 Design of Exterior Hoods / 120
 - 5.3.1 Determination of Capture Velocity / 120
 - 5.3.2 Determination of Hood Airflow / 125
 - 5.3.3 Exterior Hood Shape and Location / 135
- 5.4 Design of Receiving Hoods / 135
 - 5.4.1 Canopy Hoods for Heated Processes / 135
 - 5.4.2 Hoods for Grinding Operations / 138
- 5.5 Evaluation of Hood Performance / 141
 - List of Symbols / 142
 - References / 142
 - Appendix: Exterior Hood Centerline Velocity Models / 144
 - Problems / 148

6 Hood Designs for Specific Applications **151**

- 6.1 Electroplating / 152
 - 6.1.1 Hood Design / 152
 - 6.1.2 Airflow / 155
- 6.2 Spray Painting / 159
 - 6.2.1 Hood Design / 159
 - 6.2.2 Airflow / 163
- 6.3 Processing and Transfer of Granular Material / 165
- 6.4 Welding, Soldering, and Brazing / 169
- 6.5 Chemical Processing / 177
 - 6.5.1 Chemical Processing Operations / 178
- 6.6 Semiconductor Gas Cabinets / 187
 - 6.6.1 Entry Loss / 190
 - 6.6.2 Optimum Exhaust Rate / 191
- 6.7 Low-Volume/High-Velocity Systems for Portable Tools / 192
 - Example 6.1 Calculation of Exhaust Rate for Open-Surface Tanks / 199
 - Example 6.2 Design of a Low-Volume/High-Velocity Exhaust System / 200
 - List of Symbols / 201
 - References / 202

7 Chemical Laboratory Ventilation 204

- 7.1 Design of Chemical Laboratory Hoods / 205
 - 7.1.1 Vertical Sliding Sash Hoods / 205
 - 7.1.2 Horizontal Sliding Sash Hoods / 209
 - 7.1.3 Auxiliary Air Supply Hoods / 212
- 7.2 Face Velocity for Laboratory Hoods / 214
- 7.3 Special Laboratory Hoods / 216
- 7.4 Laboratory Exhaust System Features / 217
 - 7.4.1 System Configuration / 217
 - 7.4.2 Construction / 218
- 7.5 Factors Influencing Hood Performance / 220
 - 7.5.1 Layout of Laboratory / 220
 - 7.5.2 Work Practices / 222
- 7.6 Energy Conservation / 224
 - 7.6.1 Reduce Operating Time / 224
 - 7.6.2 Limit Airflow / 225
 - 7.6.3 Design for Diversity / 227
 - 7.6.4 Heat Recovery / 227
 - 7.6.5 Ductless Laboratory Hoods / 227
- 7.7 Performance of Laboratory Hoods / 228
- 7.8 General Laboratory Ventilation / 229
 - References / 229
 - Problems / 230

8 Design of Single-Hood Systems 232

- 8.1 Design Approach / 233
- 8.2 Design of a Simple One-Hood System (Banbury Mixer Hood) / 234
- 8.3 Design of a Slot Hood System for a Degreasing Tank / 241
 - 8.3.1 Loss Elements in a Complex Hood / 241
 - 8.3.2 Degreaser Hood Design Using Velocity Pressure
Calculation Sheet (Example 8.2) / 245
- 8.4 Pressure Plot for Single-Hood System / 247
 - List of Symbols / 247
 - Example 8.1 Banbury Mixer System Designed by the Velocity
Pressure Method / 248
 - Example 8.2 Degreaser System Designed by the Velocity
Pressure Method / 250
 - References / 251
 - Appendix: Metric Version of Example 8.1 / 252
 - Problems / 252

9 Design of Multiple-Hood Systems 254

- 9.1 Applications of Multiple-Hood Systems / 254
- 9.2 Balanced Design Approach / 256
- 9.3 Static Pressure Balance Method / 260
 - 9.3.1 Foundry Cleaning Room System (Example 9.1) / 260
 - 9.3.2 Electroplating Shop (Example 9.2) / 262
- 9.4 Blast Gate Balance Method / 265
- 9.5 Other Computational Methods / 265
 - List of Symbols / 266
 - Example 9.1 Foundry Cleaning Room Designed by Static Pressure Balance Method / 267
 - Example 9.2 Electroplating Shop System Designed by Static Pressure Balance Method / 272
 - References / 278
 - Additional Reading / 279
 - Appendix: Metric Version of Example 9.1 / 280

10 Fans and Blowers 282

- 10.1 Types of Air Movers / 283
 - 10.1.1 Axial Flow Fans / 283
 - 10.1.2 Centrifugal Fans / 285
 - 10.1.3 Air Ejectors / 287
- 10.2 Fan Curves / 288
 - 10.2.1 Static Pressure Curve / 289
 - 10.2.2 Power Curve / 291
 - 10.2.3 Mechanical Efficiency Curve / 293
 - 10.2.4 Fan Laws / 295
 - 10.2.5 Relationship between Fan Curves and Fan Tables / 297
- 10.3 Using Fans in Ventilation Systems / 298
 - 10.3.1 General Exhaust Ventilation Systems / 298
 - 10.3.2 Local Exhaust Ventilation Systems / 300
- 10.4 Fan Selection Procedure / 305
 - List of Symbols / 308
 - References / 309
 - Problems / 309

11 Air-Cleaning Devices 311

- 11.1 Categories of Air-Cleaning Devices / 312
 - 11.1.1 Particle Removers / 312
 - 11.1.2 Gas and Vapor Removers / 322
- 11.2 Matching the Air-Cleaning Device to the Contaminant / 325
 - 11.2.1 Introduction / 325
 - 11.2.2 Device Selection / 326

- 11.3 Integrating the Air Cleaner and the Ventilation System / 326
 - 11.3.1 Gravity Settling Devices / 330
 - 11.3.2 Centrifugal Collectors / 330
 - 11.3.3 Filters / 331
 - 11.3.4 Electrostatic Precipitators / 334
 - 11.3.5 Scrubbers / 334
 - 11.3.6 Gas and Vapor Removers / 335
 - List of Symbols / 336
 - References / 337
 - Problems / 337

12 Replacement-Air Systems 338

- 12.1 Types of Replacement-Air Units / 340
- 12.2 Need for Replacement Air / 341
- 12.3 Quantity of Replacement Air / 342
- 12.4 Delivery of Replacement Air / 344
 - 12.4.1 Replacement-Air System 1 (RAS-1), Melting Furnaces / 349
 - 12.4.2 Replacement-Air System 2 (RAS-2), Floor Casting / 349
 - 12.4.3 Replacement-Air System 3 (RAS-3), Sand Handling / 350
 - 12.4.4 Replacement-Air System 4 (RAS-4), Shakeout / 351
- 12.5 Replacement Air for Heating / 352
- 12.6 Energy Conservation and Replacement Air / 353
- 12.7 Summary / 356
 - References / 356

13 Quantification of Hood Performance 358

- 13.1 Hood Airflow Measurements / 359
- 13.2 Hood Capture Efficiency / 360
 - 13.2.1 Influence of Cross-Drafts on Hood Performance / 361
 - 13.2.2 Relationship between Airflow Patterns and Capture Efficiency / 363
 - 13.2.3 Shortcomings of the Centerline Velocity Approach / 370
- 13.3 Use of Capture Efficiency in Hood Design / 372
 - List of Symbols / 372
 - References / 373

14 Application of Computational Fluid Dynamics to Ventilation System Design 374

- 14.1 Introduction / 374
- 14.2 Methods / 376
 - 14.2.1 Grid-Based Methods / 377
 - 14.2.2 Grid-Free Methods / 378

14.3	Applications / 379
14.3.1	Historical Perspectives / 379
14.3.2	Current Progress / 380
14.4	Issues on the Use of Computational Fluid Dynamics / 386
14.5	Commercial Codes: Public-Domain Information / 387
	References / 387
	Appendix / 389

15 Reentry 391

15.1	Airflow around Buildings / 393
15.2	Measurement of Reentry / 396
15.3	Calculation of Exhaust Dilution / 401
15.4	Scale Model Measurement / 404
15.5	Design to Prevent Reentry / 406
15.5.1	Stack Height Determination / 407
15.5.2	Good Engineering Practices for Stack Design / 408
	List of Symbols / 412
	References / 413
	Problems / 415

Index 417

LIST OF UNITS

atm	atmosphere
Btu/h	British thermal units per hour
°C	degree Celsius
cfm, ft ³ /min	cubic feet per minute
clo	thermal insulation of clothing, 1 clo = 0.88 ft ² -h-°F/BTU
cm	centimeter
d	day
°F	degree Fahrenheit
fpm, ft/min	feet per minute
ft	foot
ft ²	square foot
ft/sec	feet per second
ft-lb/min	foot-pounds per minute
g	gram
g/min	grams per minute
gal	gallon
h	hour
hp	horsepower
in.	inch
in. Hg	inch of mercury
in. H ₂ O	inch of water
in. H ₂ O/fpm	inches of water per foot per minute
in. H ₂ O/fpm-lb/ft ²	inches of water per foot per minute per pound per square foot
°K	Kelvin
kcal/h	kilocalories per hour
L	liter
lb/ft ²	pound per square foot
lbf	pound-force
lbm	pound-mass
lpm	liters per minute
m	meter
m ²	square meter

xiv LIST OF UNITS

m/s	meters per second
m ³ /s	cubic meters per second
met	unit of metabolism: 1 met = 50 kcal/m ² /h
mg	milligram
mg/m ³	milligrams per cubic meter
min	minute
ml	milliliter
mm Hg	millimeters of mercury
mph	miles per hour
mppcf	million particles per cubic foot
Pa	pascal
ppm	parts per million
psf	pounds per square foot
psi	pounds per square inch
psia	psi-absolute
psig	psi-gage
°R	degree Rankine
rpm	revolutions per minute
s	second
W	watt
y	year
μm	micrometer
μg/m ³	micrograms per cubic meter

PREFACE

We estimate that tens of thousands of new industrial exhaust ventilation systems are installed annually in the United States alone. If we assume that the average capacity is 1000 cubic feet per minute (cfm) with installation costs of \$5 per cfm and yearly operating expenses of \$2 per cfm, it is apparent that this represents a considerable investment. However, many of these systems are improperly designed, not installed according to the plans, or poorly maintained, leading to tremendous loss as a result of inefficiency.

In an attempt to improve this situation, we wrote this book to provide information to those responsible for the specification, design, installation, and maintenance of industrial ventilation systems. This audience includes plant engineers, industrial hygienists, and students of industrial ventilation. We hope to provide a theoretical background to the plant engineer who, while intimately familiar with the equipment and hardware, may not have an appreciation of the principles of ventilation. For the industrial hygienist, we have attempted to bring the concepts and principles of ventilation into an industrial setting. Finally, for the student, we have written a textbook that demonstrates both the theoretical and practical aspects of the subject.

This book is not a reference manual. We wrote it to be used with the American Conference of Governmental Industrial Hygienists (ACGIH) *Industrial Ventilation Manual* and its companion study guide by D. Jeff Burton. Throughout the text, we refer the reader to specific designs, charts, and tables in the *Ventilation Manual*. We did not want to repeat the information provided there, but rather concentrated on explaining the rationale *behind* the material and providing a framework within which to use the *Ventilation Manual*. We have successfully used this approach in the instruction of hundreds of students. Although we refer to the specific figure and table numbers in the 24th edition of the *Ventilation Manual* we appreciate there may be occasional changes in these numbers in future editions. However, it is our experience there is little difficulty in picking up these changes and locating the correct materials since the titles of the figures and tables are rarely changed. If the ACGIH manual is not currently on the reader's bookshelf, we strongly recommend its purchase. Successful use of this book requires it. Although this volume continues to rely on the English system of units, the equivalent Systeme International d'Unites (SI) units are shown in parentheses. To eliminate confusion in the local exhaust ventilation system design calculations only English units are used in Chapters 8 and 9. However, in each of these chapters one of the design problems is presented in its entirety in SI units in an Appendix. End-of-chapter problem

sets including sample problems in both English and SI units are now presented to reinforce the content of selected chapters. The problems are representative of those encountered in certification examinations in occupational health and safety specialties.

We have not attempted to write a fluid mechanics textbook, nor did we try to prepare a “troubleshooting” guide to solving ventilation problems. This is also not a compendium of design solutions for a myriad of specific situations, nor is it a catalog of charts, nomograms, and tables. The first two chapters of the book provide background material, with the introductory chapter presenting an overview of industrial ventilation and its historical and technical relationship with other methods of environmental control. The principles of fluid mechanics, required information for proper application of design techniques, are presented in Chapter 2.

We present methods and instrumentation for measuring airflow in Chapter 3. Although this may seem out of place, we have found not only that it dovetails well with the principles of airflow presented in Chapter 2 but that it improves the reader’s ability to grasp concepts presented in subsequent chapters. The topic of general ventilation (also called dilution ventilation) is covered in Chapter 4.

Hood design selection, and performance are addressed in Chapters 5, 6, 13, and 14, respectively. The introduction to computational fluid dynamics in Chapter 14 is new to this volume, and we are indebted to Michael Flynn for this contribution. We have given a great deal of attention to the subject of hoods because they are a critical part of any local exhaust system. Special attention is given to chemical laboratory hoods and associated ventilation systems (Chapter 7) because of the great number of these in use. Chapters 8 and 9 cover the design of local exhaust ventilation systems, building on the principles provided in Chapter 2. Examples of single- and multiple-hood systems designs are presented.

Two other components of the local exhaust system are the fan or blower and the air cleaning device. Information on fan design and performance is found in Chapter 10, and a summary presentation on air-cleaning devices is covered in Chapter 11, although the reader should be fully aware that this is only an overview of this subject.

One aspect of an industrial ventilation system often overlooked is the provision of air to replace the air that is mechanically exhausted, either locally or generally. The rationale for designing and installing replacement-air systems is provided in Chapter 12, with specific guidelines and examples.

Finally, Chapter 15 presents the topic of reentry of exhausted air back into the building. The problem of air from exhaust stacks reentering the building either through windows or via mechanical air intakes presents unique challenges to ventilation engineers as well as building architects. We thank Martin Horowitz for preparation of this chapter.

We acknowledge colleagues who provided many helpful criticisms of early drafts of this book. We are grateful to Robert Gempel for the series of design problems in Chapters 8 and 9. Special thanks to the numerous students who have helped to hone this material into what we hope is an instructive text.

WILLIAM A. BURGESS
MICHAEL J. ELLENBECKER
ROBERT D. TREITMAN

PRINCIPLES OF AIRFLOW

Under normal conditions of temperature and pressure, matter can exist in three states: solid, liquid, and gas. Liquids and gases are both fluids and are thus governed by many of the same laws of physics. The fundamental differences between solids and fluids are that the former have definite shapes and are able to sustain shear forces while at rest, whereas the latter assume the shape of the container in which they reside and can sustain shear forces only while in motion. Within the class of fluids, liquids and gases differ in their ability to form interfaces with other liquids or gases (gases do not form interfaces with other gases), in the way they fill a volume (gases disperse evenly throughout), and in their compressibility (liquids cannot be compressed significantly). Other properties, such as flow patterns, boundary layers, and shear forces in motion, are common to all fluids and depend on factors other than the physical state.

The study of fluids and their properties dates back to the time of Archimedes (285–212 B.C.), who developed the displacement principle, and to Roman hydraulic engineers, who managed to design and construct extensive water supply systems with only a rudimentary understanding of the flow–friction relationship. Daniel Bernoulli (1738) and Leonhard Euler (1755) developed the equations of motion and the energy relationships that are used today (and bear their names). In the nineteenth century D’Alembert, Navier, Stokes, Reynolds, and Prandtl advanced the science of fluid flow by exploring the laws of motion, the two flow regimes (turbulent and laminar), and boundary-layer phenomena. The similarities between liquids and gases allow the use of equations and formulas developed by hydraulic engineers to be adapted to the study of airflow. Thus it should not be disconcerting to the ventilation

designer to hear expressions such as “wetted perimeter.” Most of the theory behind industrial ventilation is rooted in fluid mechanics, and many of the terms, definitions, and equations are borrowed from the research and practice of that discipline.

2.1 AIRFLOW

Air movement can be *restrained* or *unrestrained*, the former referring to air moving in a conduit (duct or pipe) and the latter involving air moving in a large space (room, building, or outdoors). The industrial ventilation designer will encounter both situations, although the properties pertaining to restrained flow are of greater importance. A thorough understanding of the basic laws governing fluid flow is valuable to the ventilation engineer so that the design equations are properly interpreted and implemented, even though the actual design of most systems can follow a straightforward approach. For the purposes of this chapter, the following assumptions will be made:

- In most ventilation systems, air can be considered to be incompressible; that is, its density will not vary appreciably from point to point within a system.
- Environmental parameters will deviate only slightly from a temperature of 68°F (20°C) and a pressure of 1 atm (1.01×10^5 Pa). These values will be termed *standard conditions* in this chapter.
- Air is a homogeneous fluid; its composition is spatially and temporally consistent.

Exceptions to these assumptions will be noted. Knowledge of a fluid’s density, pressure, and temperature is required to describe a resting fluid adequately. When considering fluid motion, additional properties, such as velocity, viscosity, and frictional energy losses, become important. Each of these parameters is discussed in the following sections.

2.2 DENSITY

One important property of a fluid is its *density*, a measure of the amount of mass in a unit volume. The density of dry air ρ_{air} at standard conditions is 0.075 lbm/ft³ (1.2 kg/m³).* It is helpful to express the density in the same units as those used in other ventilation measurements. The density of any gas, including air, is a function

*The unit lbm, pound-mass, is a measure of mass, not weight. The corresponding weight measure is the pound-force lbf or pound lb. Under normal effects of gravity on earth, if an object has a mass of 1 lbm, it will weigh 1 lbf. The general relationship between these units derives from Newton’s first law: force is equal to the product of mass and acceleration. When the force is weight, the acceleration is that due to gravity, g . Thus weight is equal to the product of mass and g , which, in the English system of units traditionally used in ventilation, is 32.17 ft/s². Given the fact that under normal gravitational conditions, a 1-lbm object weighs 1 lbf, it can be seen that 1 lbf = 32.17 ft/s² (1 lbm). This relationship will be used at several points in this chapter.

of the temperature and pressure at which it exists. The formula relating these parameters is the *ideal gas law*:

$$\rho R_a T = P \quad (2.1)$$

where ρ = mass density

P = absolute pressure

T = absolute temperature

R_a = gas constant for air

Because pressure differences from point to point in a ventilation system are, with the exception of high-velocity/low-volume systems, rarely as large as 5% (on an absolute basis), the effects of pressure on the density of air are unimportant and can usually be ignored. Similarly, unless the air being handled has been heated or cooled significantly (a 50°F or 30°C change from room temperature is required to effect a 10% change in density), density changes due to temperature can also be ignored. If the airstream temperature is outside the range 20–120°F (–5–50°C), density corrections are appropriate.

2.3 CONTINUITY RELATION

A simple, yet often neglected or misunderstood principle of fluid flow in ducts requires that within the system, matter must be conserved. In other words, in a continuous circuit the same quantity of gas must flow throughout. Known as the *principle of continuity*, the *continuity relation*, or the *law of conservation of matter*, this can be represented mathematically as

$$\int \rho V_r dA = \text{constant} \quad (2.2)$$

where ρ = mass density of fluid

V_r = velocity of fluid at an axial position r in the conduit

A = cross-sectional area where the velocity is measured

This means that if the density and velocity of the airstream were measured at all points in a cross section of the conduit, the integral of the product ρV_r is constant, regardless of location. With the assumption that the density of the air is constant throughout the conduit and the definition of the average velocity at any cross section V in the conduit to be

$$V = \frac{1}{A} \int V_r dA \quad (2.3)$$

Equation 2.2 then reduces to

$$\rho VA = \text{constant throughout system} = M \quad (2.4)$$

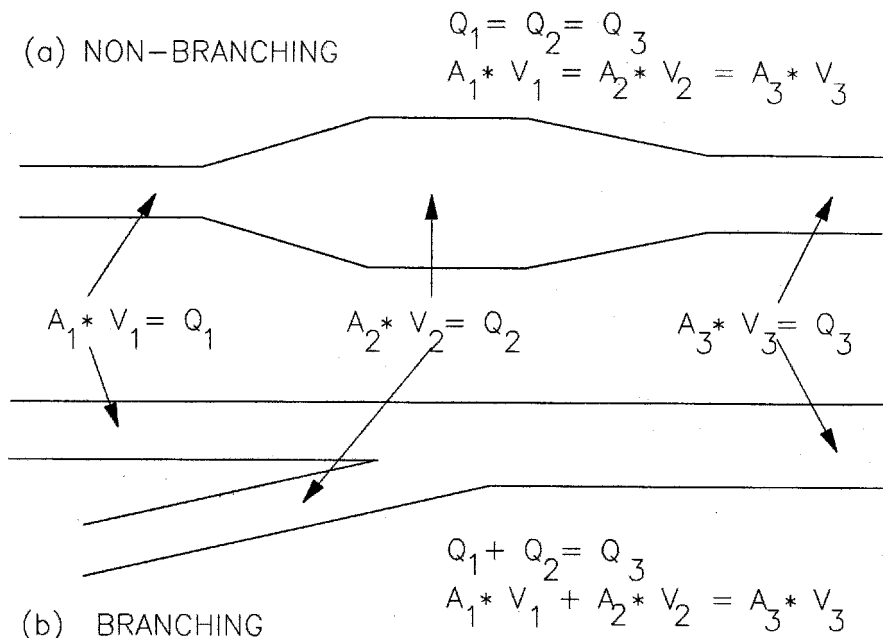


Figure 2.1 In a nonbranching system (a), the continuity relation for incompressible flow requires that the flow be constant at all points. When the duct diameter increases ($A_2 > A_1$), the velocity must decrease ($V_2 < V_1$). Conversely, when the diameter decreases ($A_3 < A_2$), the velocity must increase accordingly ($V_3 > V_2$). Since $Q_1 = Q_2 = Q_3$, then $A_1 V_1 = A_2 V_2 = A_3 V_3$. In a branching system (b), the continuity relation requires that the flow in a main (Q_3) be equivalent to the sum of the flow in the submains ($Q_1 + Q_2$). Similarly, the area-velocity products can be summed ($A_1 V_1 + A_2 V_2 = A_3 V_3$).

where M is the *mass flow*. This equation can be rearranged to

$$\frac{M}{\rho} = VA = Q = \text{constant throughout system} \quad (2.5)$$

or

$$V_1 A_1 = Q_1 = V_2 A_2 = Q_2 \quad (2.6)$$

where Q is the *volumetric flow*.* At all points in a nonbranching system, the flow rate Q , the product of the average velocity V across any cross section and the area A of the duct at that cross section, is the same (Fig. 2.1a). In a branching system, the flows in parallel submains and branches must be added to determine the flow in the resulting main duct (Fig. 2.1b).

*The subscripts are used to denote positions along the length of the conduit. It is conventional to use lower numbers to indicate upstream locations. Thus the fluid is assumed to be flowing from position 1 toward position 2.

2.4 PRESSURE

A second fundamental property of air is *pressure*, the force per unit area being exerted normal to that area. Pressure is also defined as the energy per unit volume. *Atmospheric pressure* results from the weight (force) of the air mass above us and is usually measured in reference to a total vacuum (zero pressure). When a pressure is measured in this manner, it is referred to as *absolute pressure*. Because the air pressures in a ventilation system differ only slightly from atmospheric, it can be useful to measure them relative to atmospheric pressure rather than with respect to zero. In these cases, pressure is termed *gage* (or *gauge*) *pressure*.

This is somewhat analogous to measuring temperature on a relative scale (Fahrenheit or Celsius) rather than an absolute scale (Rankine or Kelvin), with one important difference. In the case of pressure, the ambient reference is not constant. It varies as a result of elevation and meteorological conditions. As an example, when one measures pressure in automobile or bicycle tires, one is measuring gage pressure. This gage pressure is the difference between the internal tire environment and the ambient atmosphere. The barometric pressure is an absolute pressure. It is the difference between ambient and a total vacuum. In ventilation measurements, pressure differences between the atmospheric environment and the internal system environments are more important than the absolute magnitudes. Therefore, gage pressure is most commonly specified and reported.

2.4.1 Pressure Units

Four sets of units are commonly used to quantify pressure. If a vertical column of air measuring 1 square inch were to be weighed at sea level under standard conditions, one would find that there are 14.7 lbf of air in the volume extending from the ground through the atmosphere. Thus the air pressure at sea level is 14.7 pounds per square inch (psi). This absolute pressure is often referred to as *standard atmospheric pressure*. Often, a “g” or “a” is appended to the unit psi to differentiate between gage and absolute pressure. Under standard conditions, 14.7 psia = 0 psig. The psi unit is most often used when describing rather large pressure differences.

A second unit results from the common use of an instrument for measuring absolute pressure, the mercury (Hg) barometer. This device consists of an evacuated tube inverted in a pool of mercury (Fig. 2.2). Atmospheric pressure, exerting itself on the open pool, forces the mercury to rise in the column. At sea level, under “normal” weather conditions, the column would rise 29.92 in. above the surface of the open pool. The common unit of measurement of pressure is *inches of mercury*, abbreviated as “in. Hg”, and standard atmospheric pressure is 29.92 in. Hg. The unit is actually a surrogate for pressure and is often referred to as a unit of “pressure head”.

A third unit commonly used in ventilation measurements is the *inch of water*, (in. H₂O). If the barometer described above were filled with water instead of mercury, the column would rise to a height of 407 in., due to the difference in density between mercury and water. Inches of mercury and inches of water are measurement-related units of pressure. Gage pressures are often expressed in these units because they can

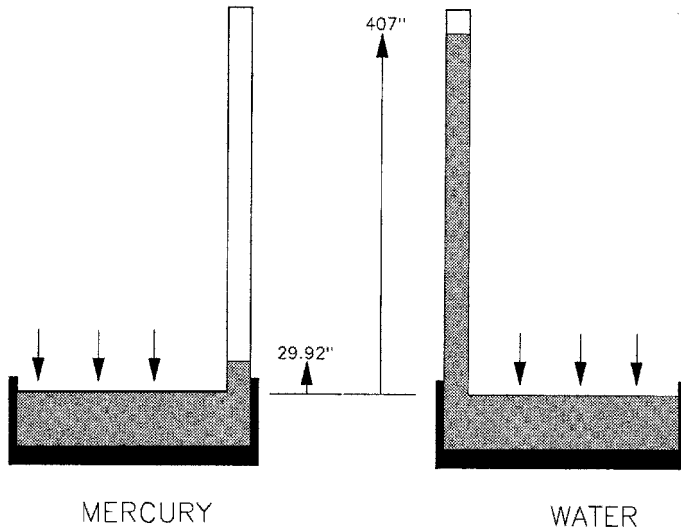


Figure 2.2 The absolute pressure of air can be measured by inverting an evacuated tube in a pool of liquid (shown here using both mercury and water). Because of the density differences between the liquids, the columns rise to different heights above the pool surfaces. At standard atmospheric pressure (1 atm), a column of mercury will rise 29.92 in. while a column of water will reach an elevation of 407 in.

be measured directly using either unit with a fluid-filled manometer. In reality, these are not actually pressure units but are surrogates for the pressure exerted by a column of fluid. They are *head units*, as shown in a later section.

The unit of pressure in the International System of Units (SI) is the *pascal* (Pa). The pascal is equal to 1 newton per square meter. Conveniently, 1 atm is equal to 1.01×10^5 Pa. Thus 14.7 psi, 29.92 in. Hg, 407 in. H_2O , and 1.01×10^5 Pa are equivalent quantities for atmospheric pressure under standard conditions.

Pressures existing in a ventilation system are nearly always measured and expressed as inches of water rather than mercury, to facilitate accurate determination of small pressure differences. On a manometer it is visually much easier to measure 1.4 in. H_2O than the equivalent 0.1 in. Hg. Some commercially available manometers use fluids less dense than water, yet are scaled to read directly in in. H_2O . These provide even better resolution of small pressure differences than do water-filled manometers.

2.4.2 Types of Pressure

Pressure, a measure of force per unit area, is also equivalent to energy per unit volume, since energy is the product of force and distance. In still air, pressure is omnidirectional and can be calculated from the ideal gas law, $P = \rho RT$. This hydrostatic pressure is associated with the *potential energy* of the fluid. However, because the ventilation engineer is concerned primarily with air in motion, other pressures must be considered. These pressures are associated with the *kinetic energy* of the moving fluid stream and are subject to different measurement techniques.

The *static pressure* (p_s) of a moving airstream represents the component associated with the potential energy. It is exerted equally in all directions, regardless of the direction or magnitude of flow. It is a function of the density and the temperature of the gas and exists in both moving and nonmoving bodies of air. The pressure measured by an automobile or bicycle tire gage is static pressure. In a ventilation system, it is pressure that tends to either burst (when greater than ambient) or collapse (when less than ambient) the duct. The static pressure is nearly always measured relative to ambient conditions and is therefore a gage pressure.

Velocity pressure (p_v) is associated with the kinetic energy of the moving airstream and is exerted only in the direction of flow. While it, like the static pressure, is affected by the gas density and temperature, p_v is primarily a function of the airstream velocity. If the air is not moving, $p_v = 0$. The velocity pressure is measured by mathematically or mechanically subtracting the static pressure from the total pressure (defined below). Velocity pressure is an absolute pressure; it cannot have a negative value.

The *total pressure* (p_t) reflects the combined static and velocity components and is measured as the pressure exerted in the direction of flow. While the total and static pressures can be either negative or positive with respect to ambient conditions, the velocity pressure must always be positive. The total pressure must always be greater than the static pressure for a moving fluid and equal to the static pressure for a non-moving fluid. In ventilation measurements, total and static pressures are nearly always measured relative to atmospheric while velocity pressure is usually measured by directly comparing total pressure and static pressure, as shown in Fig. 2.3. The standard procedure for determining these pressures is to measure p_s with a pressure tap perpendicular to the direction of airflow and p_t with an impact tube placed parallel to flow such that the moving air impinges directly on the opening. The two pressures, p_t and p_s , are measured with manometers and the velocity pressure is determined by subtracting the latter from the former. If one manometer is used to compare p_t and p_s simultaneously, the difference in the levels of the two legs of the manometer is the velocity pressure. The procedure is explained in detail in Chapter 3.

2.5 HEAD

Although we always use pressure in our discussions, the concept of *head* is encountered occasionally, so its relationship to pressure is introduced here. Fluid head was first used in describing liquid flow where gravity was used as the driving force. Total head h_t is a measure of the total energy of the fluid per unit weight:

$$h_t = \frac{p}{\rho g} + \frac{V^2}{2g} + z \quad (2.7)$$

where p = static pressure

ρ = fluid density

V = average fluid velocity

g = acceleration due to gravity

z = elevation (above a reference point)

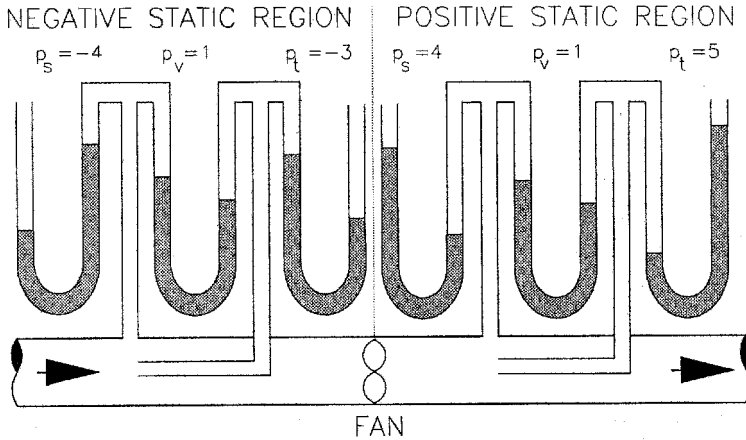


Figure 2.3 The relationships between total (p_t), velocity (p_v), and static (p_s) pressures are shown for both the negative- and positive-pressure situations. On the negative-pressure or suction side of the fan, the static and total pressures must both be negative, while the velocity pressure is always positive. On the positive-pressure side, the total and static pressures are positive with respect to ambient.

The individual terms in the equation, the pressure head $p/\rho g$, the velocity head $V^2/2g$, and the elevation head z , each has the unit of length of fluid. Given that head denotes energy per unit weight of fluid in motion and energy is measured in foot-pounds (ft-lbf), it can be seen that head would be in terms of ft-lbf/lbf, or simply, feet. The velocity head is the kinetic energy per unit weight, the pressure head is the potential energy (due to pressure differences) per unit weight, and the elevation head is the potential energy (due to gravity) per unit weight. For example, the kinetic energy E_k of a body is defined as

$$E_k = \frac{1}{2}mV^2 \quad (2.8)$$

where m is the mass and V is the velocity. Dividing both sides of this equation by the mass and then converting the mass m to weight by multiplying by the acceleration due to gravity g , we obtain

$$\frac{E_k}{mg} = \frac{V^2}{2g} = \text{velocity head} \quad (2.9)$$

Similarly, the static pressure p_s is the potential energy per unit volume v :

$$p_s = \frac{E_p}{v} \quad (2.10)$$

The density was defined as the mass per unit volume, hence

$$p_s = \frac{\rho E_p}{m} \quad (2.11)$$

The weight w is the product of the mass m and g :

$$p_s = \frac{g\rho E_p}{w} \quad (2.12)$$

or

$$\frac{p}{\rho g} = \frac{E_p}{w} \quad (2.13)$$

Thus, the static pressure head is the potential energy per unit weight.

Equation 2.7 can be simplified by (1) assuming a constant elevation at reference (i.e., $z = 0$), and (2) multiplying both sides of the equation by the product of the fluid density ρ and acceleration due to gravity g , so that

$$\rho gh_t = p + \rho \frac{V^2}{2} \quad (2.14)$$

These terms are now pressure terms, with

$$\rho gh = \text{total pressure } (p_t)$$

$$p = \text{static pressure } (p_s)$$

$$\rho V^2/2 = \text{velocity pressure } (p_v)$$

Thus pressure is equivalent to the product of head, density, and the acceleration due to gravity.

2.6 ELEVATION

In simplifying Eq. 2.7, elevation differences in the system were ignored. The elevation term z is significant only when the density of the fluid stream differs from that of the surroundings. Expressed in pressure units with the elevation term included, Eq. 2.7 becomes

$$\rho gh_t = p + \rho \frac{V^2}{2} + \rho gz \quad (2.15)$$

Under standard conditions, the density of air is 0.075 lbm/ft³ (1.2 kg/m³). Each foot of elevation difference at sea level represents a static pressure change of 0.014 in. H₂O (3.5 Pa). (This rate of change is not linear with elevation, due to the variation in density.) However, because this change occurs both inside and outside an air-handling system, any inside pressure measurements made relative to outside would not reflect it. For example, a 70-ft rise in elevation would at first seem to introduce a 1 in. H₂O pressure differential. However, there is an accompanying change in atmospheric (ambient) pressure external to the system. Since the reference atmosphere also “loses” 1 in. H₂O pressure, any measurement of system p_s or p_t made relative to ambient will not be affected by the elevation.

If the fluid being moved in the system has a density different from that of the external environment, elevation changes may be important. As shown in Fig. 2.4,

two 80-ft chambers are filled with gases of different densities. The chambers have rigid bottoms and walls while the tops are flexible, impermeable membranes so that the pressure at the top of each column is identical with the surroundings. The gases are introduced into the chambers so that the pressure at the top is balanced with ambient. The gas inside the first chamber (GAS₁) has a density twice that of air ($\rho_1 = 0.15 \text{ lbm/ft}^3$), while the density of the gas in the second chamber (GAS₂) is the same as that of air (0.075 lbm/ft^3).

If the atmospheric pressure at a height of 80 ft was 406 in. H₂O, the pressure at 10 ft would be 407 in. H₂O. Inside the GAS₂ chamber, the absolute pressures would be the same as ambient: 407 in. H₂O at 10 ft and 406 in. H₂O at 80 ft. Because static pressure is measured with respect to ambient, p_s at both heights is zero. For this situation, where the system fluid density is the same as ambient fluid density, the elevation term can be ignored. In the other chamber, however, the elevation aspect becomes important. Although the absolute pressure at the 80-ft mark is the same as that of the second column, the absolute pressure at the 10-ft point of the column 1 is higher, 408 in. H₂O. The relative, or gage, static pressure at 80 ft is 0; at 10 ft it is 1 in. H₂O. In the case of fluids with densities different from those of air, the elevation pressure term can be quite important and should not be ignored when there are system inlets and outlets that have significant vertical separation.

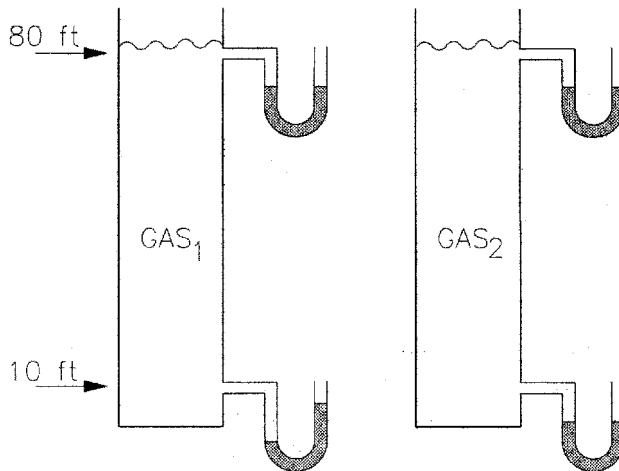


Figure 2.4 The importance of the elevation term is shown for fluids with different densities. Two 80-ft-high chambers have rigid bottoms and walls while the tops are flexible, impermeable membranes that act as weightless pistons. Gases with different densities are introduced into the chambers so that the pressure at the top is balanced with ambient. The gas introduced into the first chamber (GAS₁) has a density twice that of air, while the density of the gas in the second chamber (GAS₂) is the same as that of air. If the atmospheric pressure at a height of 80 ft is 406 in. H₂O, the pressure at 10 ft would be 407 in. H₂O. Inside the GAS₂ chamber, the absolute pressures would be the same as ambient: 407 in. H₂O at 10 ft and 406 in. H₂O, at 80 ft. Measured with respect to ambient, p_s at both positions is zero. Inside the GAS₁ chamber the absolute pressure at the 80-ft position is the same as ambient, but at the 10-ft location, it is higher, 408 in. H₂O. The relative, or gage, static pressure at 80 ft is 0; at 10 ft it is 1 in. H₂O.

2.7 PRESSURE RELATIONSHIPS

As stated previously, the velocity pressure is a function of the velocity and fluid density:

$$p_v = \rho \frac{V^2}{2} \quad (2.16)$$

Rearranging gives us

$$\begin{aligned} V^2 &= \frac{2p_v}{\rho} \\ &= \frac{2p_v}{0.075 \text{ lbf/ft}^3} \\ &= \frac{2p_v}{1.2 \text{ kg/m}^3} \end{aligned}$$

Since 1 lbf = (32.17 ft/s²)lbf, we obtain

$$V^2 = p_v \left[\frac{(2)(32.17)(3600)}{0.075} \right] \frac{\text{ft}^4\text{-s}^2}{\text{min}^2\text{-s}^2\text{-lbf}}$$

Replacing the real pressure unit lbf/ft² with the commonly used head unit in. H₂O, where 1 in. H₂O is the head corresponding to a pressure of 5.2 lbf/ft²*, we obtain

$$\begin{aligned} V^2 &= p_v \left[\frac{(2)(32.17)(3600)(5.2)}{0.075} \right] \frac{\text{ft}^4}{\text{min}^2\text{-ft}^2\text{-in. H}_2\text{O}} \\ &= 1.6 \times 10^6 p_v \frac{\text{ft}^2}{\text{min}^2\text{-in. H}_2\text{O}} \\ V &= 4000 \sqrt{p_v} \end{aligned} \quad (2.17)$$

where the velocity pressure is measured in in. H₂O and the velocity is expressed in feet per minute (fpm). This equation is very handy for determining velocity from velocity pressure measurements made at standard conditions.

A similar derivation in metric units produces the metric equivalent of Eq. 2.17:

$$V = 1.29 \sqrt{p_v} \quad (2.17a)$$

where the velocity pressure is measured in Pa and the velocity in m/s.

The relationships between velocity, velocity pressure, and static pressure are derived from *Bernoulli's equation*, which states, in terms of head, that fluids flowing

*Recalling that 14.7 psi = 407 in. H₂O, then

$$\begin{aligned} 1 \text{ in. H}_2\text{O} &= (14.7 \text{ lbf/in}^2)/407 \\ &= (0.0361 \text{ lbf/in}^2)(12 \text{ in./ft})^2 \\ &= 5.2 \text{ lbf/ft}^2 \end{aligned}$$

from point 1 to point 2 obey the formula

$$\frac{p_1}{g\rho_1} + \frac{V_1^2}{2g} = \frac{p_2}{g\rho_2} + \frac{V_2^2}{2g} + \text{losses}_{1-2} \quad (2.18)$$

where p_1, p_2 = static pressures at points 1 and 2

ρ_1, ρ_2 = densities at points 1 and 2

V_1, V_2 = average velocities at points 1 and 2

g = acceleration due to gravity

losses_{1-2} = head losses due to friction and turbulence between points 1 and 2

The head losses represent the conversion of potential energy to heat, which in a ventilation system serves no beneficial purpose. This form of the equation assumes that no work is being done on the system (i.e., no input of energy in the form of a fan or blower between points 1 and 2) as well as no changes in elevation. Assuming that the density is constant ($\rho_1 = \rho_2 = \rho$), then Eq. 2.18, now expressed in pressure units by multiplying all terms by ρg , is

$$p_1 + \rho \frac{V_1^2}{2} = p_2 + \rho \frac{V_2^2}{2} + \rho g(\text{losses}_{1-2}) \quad (2.19)$$

The first term on either side is the static pressure; the second is the velocity pressure; and the last, $\rho g(\text{losses}_{1-2})$, represents the *change* in total pressure. Equation 2.19 can be rewritten as

$$p_{s,1} + p_{v,1} = p_{s,2} + p_{v,2} + \Delta p_t \quad (2.20)$$

The relationships between total, static, and velocity pressure can be addressed by considering the simple system shown in Fig. 2.5. There is a reduction in the cross-sectional area of the duct on the intake side of the fan, where the static pressure would be negative (with respect to ambient). Assuming that the only losses in the system are due to friction and ignoring the losses associated with the shock in the abrupt reduction, the graphical representation of the pressures in the system is as shown.

While the static and total pressures drop through the system, the velocity pressure remains constant within each section. The increase in velocity pressure at the transition from the larger section to the smaller section results from the change in velocity, which is a function of the flow Q and the duct area A . Replacing V with Q/A in the velocity-to-velocity pressure relationship (Eq. 2.17) yields

$$p_v = \left(\frac{Q}{4000A} \right)^2 \quad (2.21)$$

and its metric equivalent

$$p_v = \left(\frac{Q}{1.29A} \right)^2 \quad (2.21a)$$

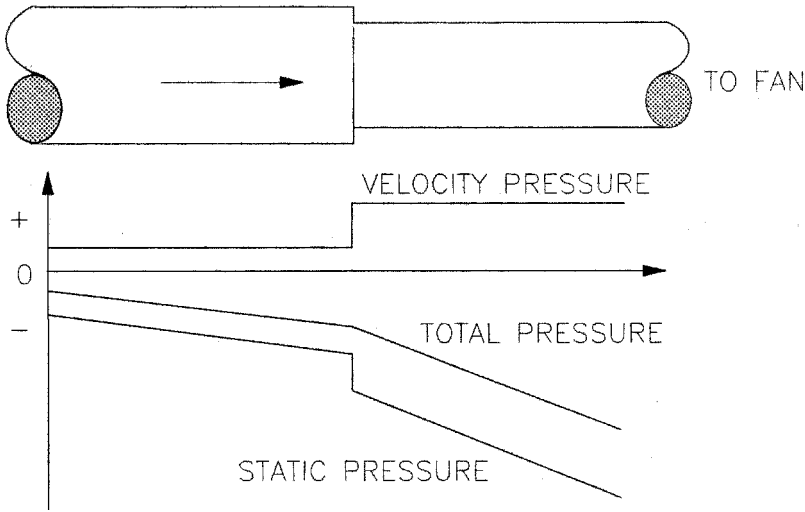


Figure 2.5 The relationships between the three pressures (static, velocity, and total) are shown for a converging system. As the cross-sectional area decreases, the velocity and velocity pressure increase, since $V = Q/A$ (the continuity relation) and the velocity is proportional to the square root of the velocity pressure. The frictional losses through the duct are shown as a gradually sloping line when the velocity is low and a more severely sloping line when the velocity increases in the smaller duct. The slope of the line is proportional to p_v . The total pressure is the arithmetic sum of p_v and p_s . Therefore, the increase in p_v at the abrupt reduction is accompanied by a decrease in p_s so that there is no sudden change in p_t . (The losses associated with turbulent shock are not shown.)

Since Q is constant throughout a nonbranching system (due to the conservation of mass), for a given flow, the change in velocity pressure is dependent solely on the change in the cross-sectional area between two points in that system. If the area is constant, then p_v is constant. If the area changes, p_v must also change, as

$$p_{v,2} = p_{v,1} \left(\frac{A_1}{A_2} \right)^2 \quad (2.22)$$

2.7.1 Reynolds Number

Before considering the causes of losses associated with flow through the system, an understanding of the two types of flow, laminar and turbulent, is helpful. *Laminar flow* (also known as *streamline* or *viscous flow*) refers to the parallel streamlines that gas molecules are observed to follow at low velocities. There is no lateral or radial mixing of the fluid in laminar flow. As the velocity increases, the flow becomes more chaotic and considerable cross-current mixing occurs. At higher velocities, the streamlines disappear altogether and the flow becomes fully *turbulent*.

While the specific transition point between laminar and turbulent flow is difficult to define, it is known to be dependent on the density, viscosity, and velocity of the fluid as well as the geometry of the conduit within which the fluid is moving. These factors are combined in a term developed by Osborne Reynolds and known as the

Reynolds number (Re), which is computed as

$$\text{Re} = VD \frac{\rho}{\mu} \quad (2.23)$$

where V = average velocity of the fluid

ρ = density of the fluid

μ = viscosity of the fluid

D = diameter of the conduit

If a consistent set of units is used (e.g., $[D] = \text{ft}$, $[V] = \text{ft/s}$, $[\rho] = \text{lbm/ft}^3$, and $[\mu] = \text{lbm/ft-s}$), the Reynolds number is dimensionless. In general, if the Reynolds number for a given flow regime is less than 2000, the flow will probably be laminar. If Re is greater than 4000, the flow will be turbulent. When $2000 < \text{Re} < 4000$, the type of flow is less predictable, depending on other factors, such as obstructions or directional changes in flow. Because the relationship between static pressure losses and velocity depends on the type of flow encountered, the derivation of a general formula requires one to know whether normal ventilation systems operate in the laminar or turbulent flow regions. To gain a better appreciation of the relationship between velocity and Reynolds number for air, Eq. 2.23 can be rearranged to

$$VD = \text{Re} \frac{\mu}{\rho} \quad (2.24)$$

The viscosity of air at standard conditions is $1.2 \times 10^{-5} \text{ lbm/ft-s}$ and the density is 0.075 lbm/ft^3 . Substituting these values into Eq. 2.24 yields

$$\begin{aligned} VD &= \left[\frac{(1.2 \times 10^{-5} \text{ lbm/ft-s})(60 \text{ s/min})}{0.075 \text{ lbm/ft}^3} \right] \text{Re} \\ &= 9.6 \times 10^{-3} \text{ Re ft}^2/\text{min} \\ &= 1.5 \times 10^{-5} \text{ Re m}^2/\text{s} \end{aligned} \quad (2.25)$$

For air at standard conditions, turbulent flow will exist when

$$\begin{aligned} 4000 &< \text{Re} \\ &< \frac{VD}{9.6 \times 10^{-3} \text{ ft}^2/\text{min}} \end{aligned}$$

or,

$$VD > 40 \text{ ft}^2/\text{min} \quad (0.06 \text{ m}^2/\text{s}) \quad (2.26)$$

Thus any flow with a velocity–diameter product greater than $40 \text{ ft}^2/\text{min}$ ($0.06 \text{ m}^2/\text{s}$) would be turbulent. Because industrial ventilation systems typically operate at velocities greater than 1000 fpm (5 m/s) and duct diameters are usually at least 0.25 ft

(75 cm), it is unlikely that laminar flow would be encountered. There may be certain, isolated cases (some air-cleaning devices operate at very low velocities) where laminar conditions must be considered. Nevertheless, as most industrial ventilation system display the turbulent regime, turbulent flow will be assumed in the determination of pressure losses.

2.8 LOSSES

As a fluid moves through a system, it will encounter resistance to flow. This resistance will result in decreases in static and total pressure throughout the system, which the air-moving device (fan) will be expected to overcome. These pressure drops, or losses, represent the conversion of potential energy into heat (first law of thermodynamics), which is nonproductive in a ventilation system. This resistance can arise from two general mechanisms: (1) friction associated with shearing stresses and turbulence within the duct, and (2) shock from sudden velocity (speed or direction) changes or flow separation at elbows, branches, and transitions.

2.8.1 Frictional Losses

Frictional pressure losses result from “rubbing” the fluid against the walls of the conduit as well as against itself. The magnitude of these losses depends primarily on the type of flow regime (laminar or turbulent) in the system. The system displayed in Fig. 2.6 shows the velocities at different radial positions across the duct. The lengths of the arrows indicate the relative velocities at that point. At the edge of the duct, next to the wall, there is an extremely thin boundary layer of stagnant air, the thickness of which depends on Re . The air velocity at the rigid boundary is zero. In the center of the duct, the air is moving at its maximum velocity. Between these two points, there is a velocity gradient that depends on the flow regime. In laminar flow, this gradient introduces shear stresses that produce frictional losses. In both laminar and turbulent flow, the gradient at the wall produces shear stresses.

If only turbulent flow is considered (the predominant flow in ventilation systems), the velocity profile is flat in the center of the duct and sharp near the boundary, at

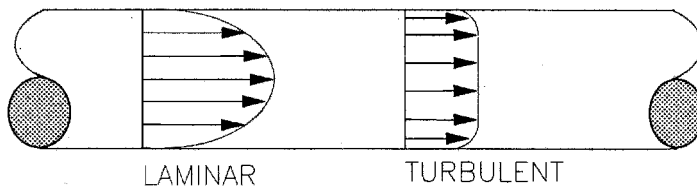


Figure 2.6 Flow velocity profiles of laminar ($Re < 2000$) and turbulent ($Re > 4000$) flow regimes. The turbulent flow profile is nearly uniform across the radius, whereas the laminar profile is more parabolic.

which point it drops rapidly to zero. This sharp gradient at the edge produces a large shear stress. This wall–fluid shear is more pronounced in turbulent flow, leading to a larger energy loss than in laminar flow. The chaotic flow also introduces shear stresses within the fluid as the slow- and fast-moving streams are continually being intermixed.

The pressure loss associated with frictional energy losses (conversion to heat) is given by the *Darcy–Weisbach relation*, in pressure terms:

$$\begin{aligned}\Delta p_f &= f \frac{L}{D} \left(\rho \frac{V^2}{2} \right) \\ &= f \frac{L}{D} p_v\end{aligned}\quad (2.27)$$

where Δp_f = pressure loss due to friction

f = friction factor

L = length of conduit

D = diameter of conduit

Values of the friction factor depend on the Reynolds number and, in turbulent flow, the roughness of the conduit interior wall. In laminar flow, we obtain

$$f = \frac{64}{\text{Re}} \quad (2.28)$$

Because Re is linear with velocity, the frictional pressure loss in *laminar* conditions is also linear with velocity.

For turbulent flow, the relationship is more complicated. Values of f are usually obtained from the Moody chart (Fig. 2.7), which provides friction factors as a function of Re and relative roughness of the conduit. As can be seen from this chart, at high Re and high relative roughness (a region known as *fully rough flow*), the friction factor becomes independent of Re . In the transition between fully rough flow and laminar flow, the curves for determining f are complex. Regardless of the origin of the friction *factor*, the friction *loss* is expressed as Eq. 2.27, with the loss proportional to the velocity pressure. In practice, this equation and the Moody chart are not directly used by the designer of ventilation systems. Instead, charts and nomograms have been developed for air passing through the standard, galvanized ductwork commonly used. Correction factors can be used to compensate for duct materials with different roughnesses. Alternatively, the designer can use data supplied by the duct manufacturer. To obtain approximate values for the term (fp_v/D) , which represents the pressure drop per length of duct the designer is referred to manufacturer's charts. The values provided by these charts have been adjusted from the theoretical equations based on empirical data. This term is used in the rarely applied design technique known as the *equivalent foot method* as mentioned in Chapter 8.

A second approach to system design, known as the *velocity pressure method*, employs the term f/D , which represents the frictional pressure loss, in pressure drop per velocity pressure per length of duct. When multiplied by the velocity pressure in

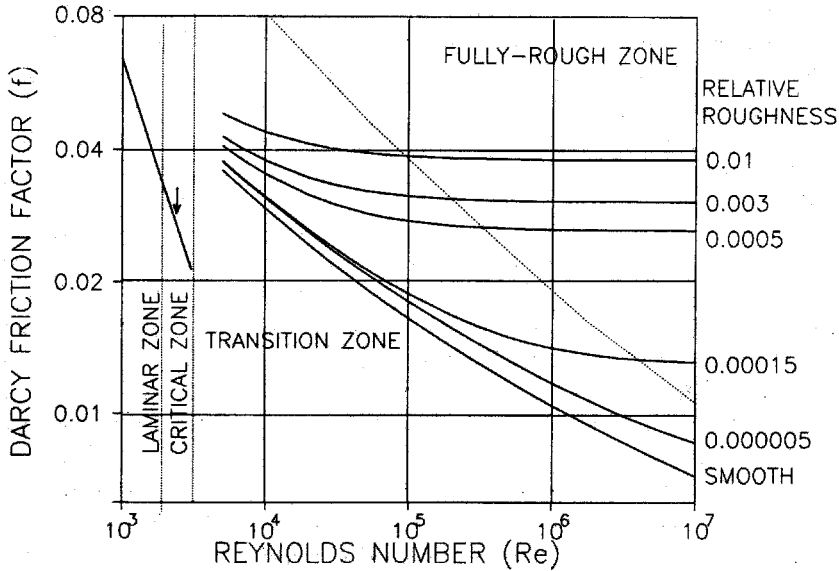


Figure 2.7 The Moody chart relates the friction factor to the Reynolds number and the relative roughness. For laminar flow conditions, the factor is dependent on Re and independent of relative roughness. In fully rough flow, the friction factor becomes independent of Re , depending only on relative roughness. Between these flow regimes, f depends on both parameters.

the duct section and the duct length, this provides the expected pressure drop. Values for f/D are presented in Figs. 5-19a and b of the *Ventilation Manual*. Although more details regarding these two design methods are provided in subsequent chapters, the reader should remember that the pressure drop due to friction through straight ducts is a function of roughness, diameter, length, and velocity (or velocity pressure).

2.8.2 Shock Losses

A second type of energy loss results from turbulence or “shock” in the fluid stream, which causes a violent mixing of the fluid and subsequent eddy formation. These disturbances are usually associated with redirection of flow or sudden changes in the duct size that consequently cause drastic velocity changes. The well-established velocity profiles are distorted and pressure losses result. These shock losses are also associated with merging airstreams. While the shock losses are highly variable, depending on the geometry of the system where the turbulence occurs, they are consistent in their dependence on the velocity pressure.

A second cause of shock loss is the flow separation observed primarily in contractions and expansions. Separation occurs when the primary fluid stream no longer follows the wall and breaks away, leaving irregular eddies in the wake region (Fig. 2.8). Reconsidering the earlier example (Fig. 2.5), the losses due not only to friction but also those resulting from the shock caused by the sudden contraction are

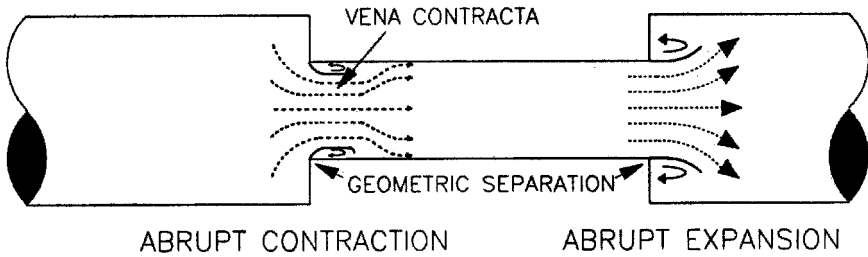


Figure 2.8 Flow separation is shown for contractions and expansions. There are energy (pressure) losses associated with this separation that are part of the shock losses for the fitting. A tapered fitting reduces the separation and thus the loss.

included (Fig. 2.9). As before, the velocity pressure changes only as a result of the decrease in area and subsequent increase in velocity. However, the total pressure decreases as a result of that portion of the loss in static pressure associated with the shock losses at the point of the velocity transition. For a sudden contraction such as this, the magnitude of the loss is proportional to the velocity pressure in the smaller section $p_{v,2}$ according to the formula

$$\Delta p_{\text{loss}} = K p_{v,2} \quad (2.29)$$

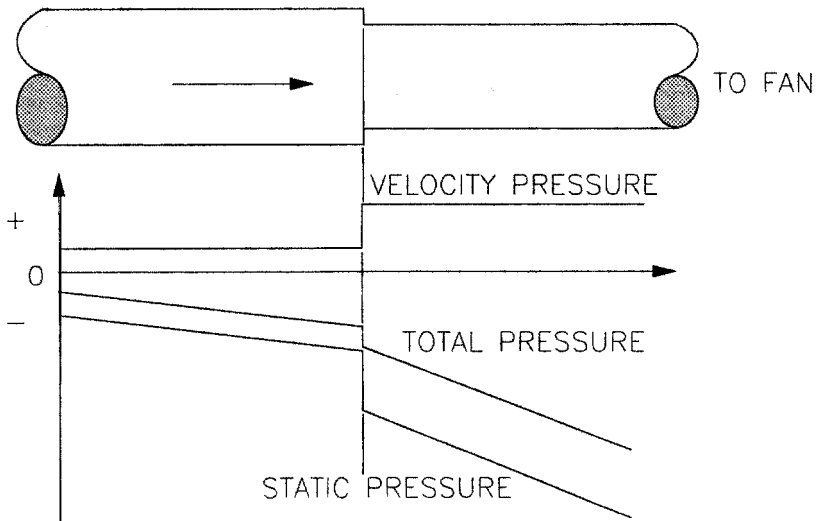


Figure 2.9 This is the same system as shown in Fig. 2.5, but the losses incurred due to “shock” at the transition are incorporated. The velocity pressure is not affected, but the static and total pressures both reflect the loss as a sudden drop. The extent of the loss is a function of the ratio of the areas and the velocity pressure.

where K is primarily a function of the ratio of the duct areas (A_2/A_1) and taper angle according to Fig. 5-18 of the *Ventilation Manual*. In addition to the shock loss associated with the duct size change, there is also the static pressure reduction required to boost the velocity pressure from $p_{v,1}$ to $p_{v,2}$. The static pressure difference for a fitting can thus be described as

$$\Delta p_s = -(\Delta p_{\text{loss}} + \Delta p_v) \quad (2.30)$$

where $\Delta p_s = p_{s,2} - p_{s,1}$ and $\Delta p_v = p_{v,2} - p_{v,1}$. The static pressure is reduced by the sum of the loss at the fitting and the velocity pressure change. The loss associated with the velocity pressure change is often referred to as an *inertial* loss. Shock losses occur at nearly every disturbance in the system, including hood entries, branch entries, reductions, expansions, elbows, and takeoffs. Most of the guidelines to reduce the magnitude of the transition static pressure loss involve reducing the severity of the disturbance.

2.9 LOSSES IN FITTINGS

The pressure loss encountered in straight ducts was shown to be dependent on the velocity pressure, the duct diameter and length, and the friction factor. Most of the losses encountered in other parts of a ventilation system (e.g., expansions, contractions, elbows, hood entries, and branch entries) are also proportional to the velocity pressure and are treated as such by expressing them as

$$\Delta p_{\text{loss}} = K \frac{\rho V^2}{2} = K p_v \quad (2.31)$$

The value of K depends primarily on the type and geometry of the fitting under consideration. Tables containing nominal values for most types of fittings can be found in the *Ventilation Manual*.

2.9.1 Expansions

The expansion of the cross-sectional area of a duct may be either abrupt or tapered (Fig. 2.10). The latter reduces the losses that result from flow separation. In either case, as the air emerges from the smaller duct section into the larger, the velocity is reduced. The impact of the faster-moving airstream on the slower one and the flow separation lead to shock losses. The Borda loss equation for expansions states that the total pressure loss depends on the square of the difference between the velocities in the two sections:

$$\Delta p_{\text{loss}} = \frac{\rho(V_1 - V_2)^2}{2} \quad (2.32)$$

where Δp_{loss} = drop in total pressure

V_1 = velocity in smaller (upstream) section

V_2 = velocity in larger (downstream) section

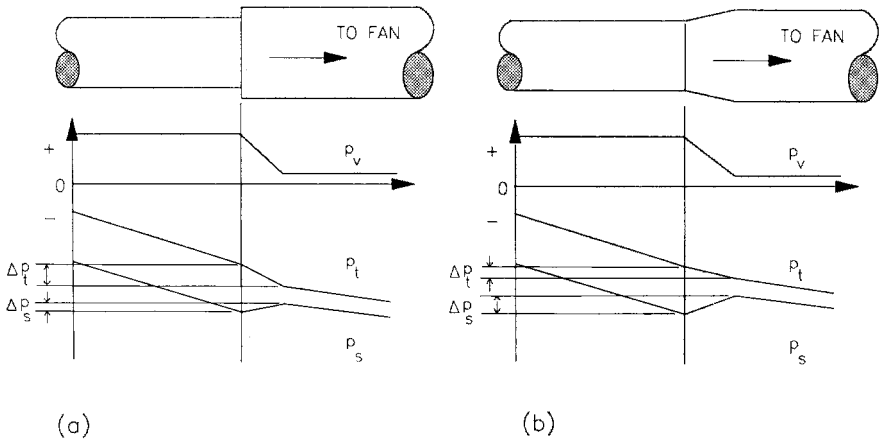


Figure 2.10 In an abrupt expansion (a), the velocity, and the resulting velocity pressure, decrease in accordance with the continuity equation, although some flow separation does occur. The magnitude of the decrease is in proportion to the ratio, r , of the areas. When the velocity pressure drops, some of the energy is regained as static pressure while the remainder is lost to turbulent shock. The quantity regained is shown as Δp_s while the frictional loss is Δp_f . The rate of static pressure (and total pressure) loss in the larger section is less than that in the smaller section. This is because the loss rate is proportional to the velocity pressure. When the velocity pressure decreases, the loss rate does as well. In the tapered expansion (b), the static pressure regain is larger because the gradual widening decreased the flow separation. [These pressure profiles apply to the case where the expansion is on the negative-pressure side of the air-moving device (AMD). If the expansion were on the outlet side, the total and static pressure profiles would be positive, not negative, but they would have the same shapes.]

The continuity relation requires that $A_1 V_1 = A_2 V_2$, so

$$\begin{aligned}\Delta p_{\text{loss}} &= \frac{\rho}{2} \left(V_1 - \frac{A_1}{A_2} V_1 \right)^2 \\ &= p_{v,1} \left(1 - \frac{A_1}{A_2} \right)^2 \\ &= p_{v,1} (1 - r)^2\end{aligned}\quad (2.33)$$

where r is the ratio of the areas (A_1/A_2). The change in velocity pressure, a portion of which will be “regained” as static pressure, is simply

$$\Delta p_v = p_{v,2} - p_{v,1} \quad (2.34)$$

Recalling Eq. 2.22, we have

$$\begin{aligned}\Delta p_v &= r^2 p_{v,1} - p_{v,1} \\ &= p_{v,1} (r^2 - 1)\end{aligned}\quad (2.35)$$

In the ideal case, all of the velocity pressure loss would be recaptured as a static pressure regain, leaving the total pressure loss close to zero.

$$\begin{aligned}
 \Delta p_s &= -(\Delta p_{\text{loss}} + \Delta p_v) \\
 &= -[p_{v,1}(1-r)^2 + p_{v,1}(r^2-1)] \\
 &= p_{v,1}2r(1-r)
 \end{aligned} \tag{2.36}$$

The efficiency of the expansion, defined as the ratio of the static pressure regain (a “negative” loss) and the velocity pressure loss, is a measure of the extent of regain:

$$\begin{aligned}
 \text{Efficiency} &= \frac{\Delta p_s}{\Delta p_v} \\
 &= \frac{p_{v,1}2r(1-r)}{p_{v,1}(1-r^2)} \\
 &= \frac{2r(1-r)}{(1-r)(1+r)} \\
 &= \frac{2r}{1+r}
 \end{aligned} \tag{2.37}$$

Efficiency therefore decreases as the ratio decreases, with a value of 100% at $r = 1$ (no expansion) and a value of 0% at $r = 0$ (a duct delivering air into a large room, for example).

Tapered expansions are used to reduce the extent of the shock by decreasing the flow separation and improve the efficiency of the static pressure regain. The pressure losses in tapered expansions are dependent on the angle of the expansion as well as the ratio of the initial and final cross-sectional areas. A table of values for the static regain in tapered expansions is provided in the *Ventilation Manual*, Fig. 5-18.

2.9.2 Contractions

A duct contraction, like an expansion, can be either sudden or gradual, with the latter being more efficient (Fig. 2.11). When the cross-sectional area decreases, the velocity (and the velocity pressure) must increase in accordance with the continuity relation. An accompanying decrease in static pressure occurs to accommodate the velocity pressure increase and the losses due to the shock losses. As with any fitting involving velocity changes, the general form of the equation describing the static pressure decrease is

$$\Delta p_s = -(\Delta p_{\text{loss}} + \Delta p_v) \tag{2.30}$$

Hood Entries. A hood entry (as opposed to a branch entry) is a special type of contraction, where the room is considered to be the larger section and the duct the

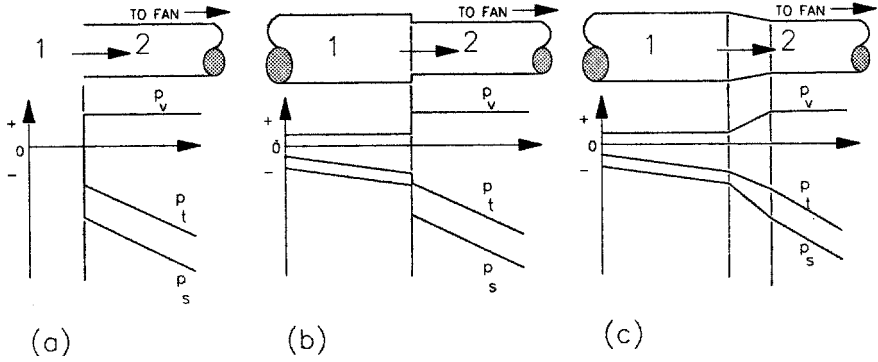


Figure 2.11 Three types of contraction are shown: an entry, an abrupt in-line contraction, and a tapered in-line contraction. At the entry (a), the three pressures (p_v , p_s , and p_t) are assumed to be zero. As the air enters the system, the static pressure must be sufficient to accelerate the air up to duct velocity as well as handle any energy loss associated with the entry. The latter loss is known as the hood entry loss (h_e), as shown. Similarly, for an abrupt in-line contraction (b), the static pressure must accommodate the increased velocity pressure and the transitional frictional losses. These frictional losses can be reduced by using a gradual, tapered fitting (c).

smaller, as shown in Fig. 2.11a. The static pressure differential between the room and the duct is called the entry loss h_e and the total static decrease is given by

$$\Delta p_s = -(h_e + \Delta p_v) \quad (2.38)$$

Because both room and duct static pressures are measured relative to ambient,

$$\Delta p_s = p_{s,2} - 0 = p_{s,2} \quad (2.39)$$

Similarly, because the room air has no velocity,

$$\Delta p_v = p_{v,2} - 0 = p_{v,2} \quad (2.40)$$

Equation 2.38 reduces to

$$p_{s,h} = -p_{s,2} = p_v + h_e \quad (2.41)$$

where the hood static pressure is $p_{s,h}$ and the duct velocity pressure is simply $p_v = p_{v,2}$. Because the hood static pressure is traditionally expressed as a positive value even though it is a negative gage pressure, the definition of $p_{s,h} = p_{s,2}$ accounts for this. As with all other losses in turbulent conditions, the hood entry loss h_e is treated as being directly proportional to the velocity pressure

$$h_e = F_e p_v \quad (2.42)$$

where F_e is the hood entry loss *factor*. Combining Eqs. 2.41 and 2.42 gives

$$p_{s,h} = p_v(1 + F_e) \quad (2.43)$$

The hood entry loss factor depends on the geometry of the entry. The coefficient of entry C_e is a dimensionless measure of this geometry and is calculated as the ratio of the actual flow observed in the duct at some hood static pressure to the maximum hypothetical flow possible at the same static pressure. This maximum flow would occur under the ideal conditions of no entry loss ($F_e = 0$, $h_e = 0$). In this case, all of the static pressure loss is converted into velocity pressure, so that $p_{s,h} = p_v$. In other words,

$$C_e = \frac{Q_{\text{actual}}}{Q_{\text{ideal}}} \quad (2.44)$$

Recalling Eqs. 2.6, 2.17, and 2.44, and setting $F_e = 0$ for Q_{ideal} , we obtain

$$C_e = \frac{4000A\sqrt{p_v}}{4000A\sqrt{p_{s,h}}} \quad (2.45)$$

$$= \sqrt{\frac{p_v}{p_{s,h}}} \quad (2.46)$$

For Q_{actual} , $p_v = p_{s,h}/(1 + F_e)$,

$$\begin{aligned} C_e &= \sqrt{\frac{p_{s,h}}{p_{s,h}(1 + F_e)}} \\ &= \sqrt{\frac{1}{1 + F_e}} \end{aligned} \quad (2.47)$$

Solving for F_e yields

$$F_e = \frac{1 - C_e^2}{C_e^2} \quad (2.48)$$

Typical values for C_e are provided in Fig. 2.12, ranging from 0.98 for a bell-mouthed inlet to 0.72 for a plain, unflanged duct opening.

In-Line Contractions. Contractions occurring within the duct can be abrupt (Fig. 2.11*b*) or gradual (Fig. 2.11*c*). The general form of Eq. 2.30 is used because the velocity pressure in the larger, upstream section is not zero and the static pressure in that section is no longer equivalent to ambient:

$$\Delta p_s = -(\Delta p_{\text{loss}} + \Delta p_v) \quad (2.30)$$

The loss term for the tapered contraction is given as

$$\Delta p_{\text{loss}} = L\Delta p_v \quad (2.49)$$

while for the abrupt contraction it is

$$\Delta p_{\text{loss}} = Kp_{v,2} \quad (2.50)$$


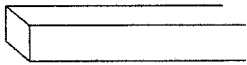
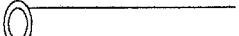
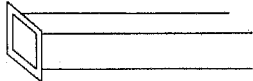
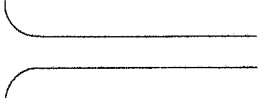
		COEFFICIENT OF ENTRY (C_e)	ENTRY LOSS FACTOR (F_e)
PLAIN		0.72	0.93
			
FLANGED		0.82	0.49
			
BELL MOUTH		0.98	0.04

Figure 2.12 Some typical hood entries and the associated coefficients of entry and entry loss factors. More specific data can be found in the *Ventilation Manual*.

Values of L and K are given on Fig. 5-18 of the *Ventilation Manual*. The tapered loss factor L is a function of the taper angle, while the abrupt loss factor K is dependent on the ratio of the two areas. Any angle greater than 60° is considered an abrupt contraction. In designing a system, abrupt contractions should be avoided because of their inefficiency in converting static pressure into velocity pressure, primarily as a result of the flow separation and resultant eddy formation.

2.9.3 Elbows

The pressure loss encountered as the airstream passes through an elbow (Fig. 2.13) is approximated in ventilation system design as

$$\Delta p_{\text{loss}} = K_{90} \frac{\theta}{90} p_v \quad (2.51)$$

where K_{90} is the loss factor for a 90° elbow and θ is the angle of the bend, in degrees. Because the loss is treated as being directly proportional to the angle (a 30° elbow exhibits one-third the loss of a 90° elbow), tables of K values are usually provided only for right-angle elbows ($\theta = 90^\circ$). For round ducts, K_{90} is a function solely of the elbow aspect ratio (R/D), as shown in Fig. 2.13. For rectangular ducts, both the elbow aspect ratio, R/D , and the duct aspect ratio, W/D , are important. Values of K_{90} for both round and rectangular ducts are provided on Fig. 5-16 of the *Ventilation Manual*.

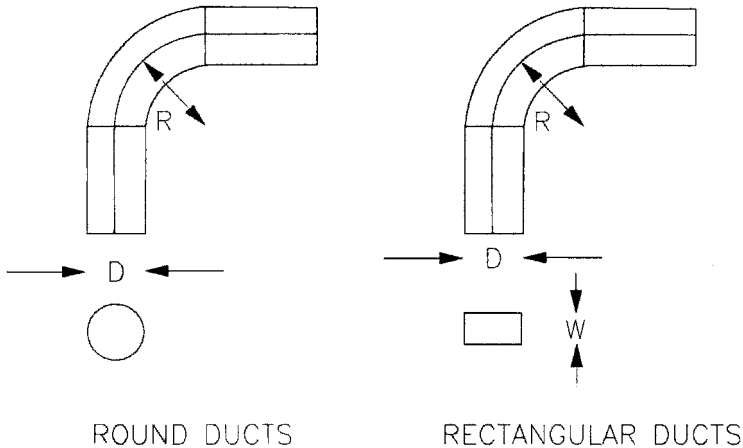


Figure 2.13 The frictional loss factor associated with elbows is dependent on the elbow aspect ratio for round ducts and both the elbow aspect ratio and the duct aspect ratio for rectangular ducts. The elbow aspect ratio is simply R/D , where R is the radius of curvature and D is the duct diameter. The duct aspect ratio is given by W/D , where W is the width of the duct. A table of elbow loss factors is provided as Fig. 5-16 of the *Ventilation Manual*.

Although the standard practice is to assume that the loss is proportional to θ , this is not completely accurate. However, because the actual loss depends on a number of other factors, including the length of straight run immediately prior to the elbow, this approximation is usually adequate.

2.9.4 Branch Entries (Junctions)

As the air in a branch enters a main duct (Fig. 2.14), there are turbulence losses which, in the design process, are assumed to occur in the branch and are therefore proportional to the velocity pressure there, not the velocity pressure in the main. The loss is calculated as

$$\Delta p_{\text{loss}} = K p_v \quad (2.52)$$

with values of K provided in the *Ventilation Manual*, Fig. 5-17, for angles between 10 and 90°. As with elbows, higher values of K are associated with the wider angles. The loss is associated with the entering airstream and therefore the velocity pressure in the branch is used in the calculation. If there is a significant difference in velocities between the resulting combined airstream and either of the merging streams, the change in velocity pressure would be accompanied by a change in static pressure. In the design process, this difference is treated as an “other loss.”

A frequent situation presented to a ventilation designer is the connection of a branch running perpendicular to the main duct (Fig. 2.15). A simple tee fitting, producing a

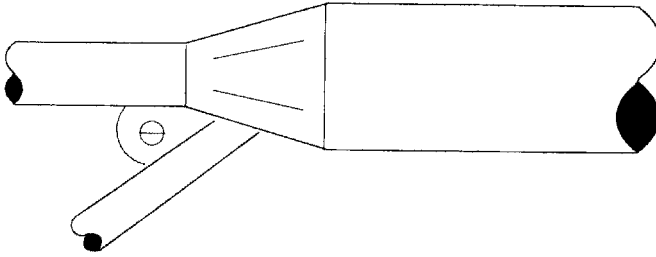


Figure 2.14 In a branch entry, the static pressure loss attributable to the fitting is attributed to the entering branch and is proportional to the velocity pressure there. The loss can be reduced by maintaining a small angle of entry.

right-angle entry, would induce a static pressure loss equal to $1.0p_v$ (*Ventilation Manual*, Fig. 5-17; $\theta = 90^\circ$). If, however, the designer uses the combination of a 60° elbow and a 30° entry, the pressure loss is reduced to

$$\left(\frac{60^\circ}{90^\circ}\right)(0.27)p_v + 0.18p_v = 0.36p_v \quad (2.53)$$

The designer should avoid entry angles of greater than 45° , with 30° being a better choice.

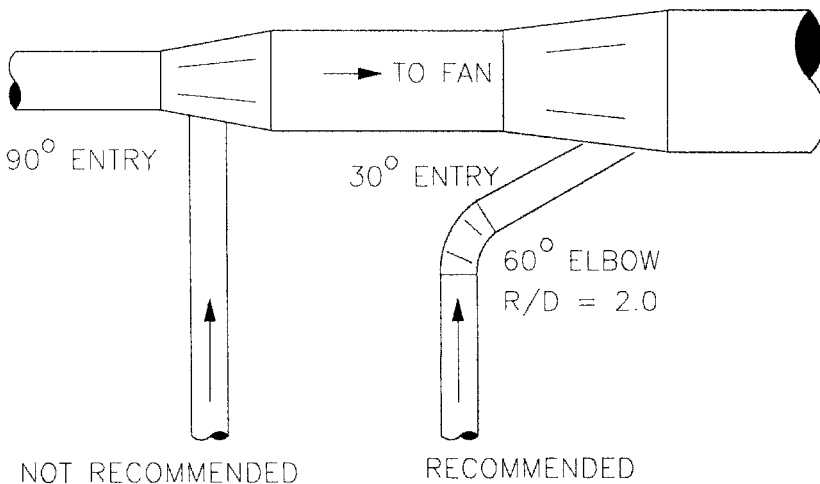


Figure 2.15 As a branch joins a perpendicular main, the use of a 90° branch entry is discouraged in favor of a 60° elbow combined with a 30° entry. The static pressure loss associated with the elbow–entry combination is substantially less than that of a 90° entry.

2.10 SUMMARY

This chapter should have provided the reader with an appreciation for the theory behind the behavior of moving air. With this background, some of the mystery surrounding the origins of the tables, nomograms, and procedures used to design these systems should be dispelled. An understanding of many of the relationships presented, especially those between velocity, static, and total pressure and between velocity pressure and velocity, is critical to the design and testing of effective ventilation systems.

LIST OF SYMBOLS

A	area
C_e	coefficient of entry
D	diameter
E_k	kinetic energy
E_p	potential energy
f	friction factor
F_e	hood entry loss factor
g	gravitational constant
h_e	hood entry loss
h_t	total head
K	loss coefficient
L	length, distance
m	mass
M	mass flow
p	pressure
p_s	static pressure
$p_{s,h}$	hood static pressure
p_t	total pressure
p_v	velocity pressure
Q	volume flow
r	ratio of cross-sectional areas
R	radius of curvature
R_a	gas constant for air
Re	Reynolds number
T	temperature
v	volume
V	average velocity
W	width (of rectangular duct)
z	elevation above reference datum
ρ	density (mass/volume)
θ	angle (of elbow, branch, entry)

PROBLEMS

Note: Problems requiring reference to the *Ventilation Manual* include the notation [Ref Man].

- 2.1** If the density of a gas doubles at constant temperature, by what factor does the absolute pressure increase?

Answer: 2

- 2.2** The average velocity in a 6-in.-diameter duct is 1500 ft/min. If the duct diameter is reduced to 4 in. and the airflow remains constant, what is the new average duct velocity?

Answer: 3,380 ft/min

- 2.3** The average velocity in a 30-cm-diameter duct is 12 m/s. If the duct diameter is increased to 50 cm and the airflow remains constant, what is the new average duct velocity?

Answer: 4.3 m/s

- 2.4** The airflow through a 15-in.-diameter duct is 3000 ft³/min. What is the average duct velocity?

Answer: 2440 ft/min

- 2.5** The average velocity in a 50-cm square duct is 15 m/s. What is the airflow?

Answer: 3.8 m³/s

- 2.6** Convert the following velocities to the corresponding velocity pressure: (a) 4790 ft/min; (b) 13.26 m/s; (c) 66 ft/s; (d) 51,700 cm/min.

Answers:

- (a) 1.43 in. H₂O
- (b) 106 Pa
- (c) 0.98 in. H₂O
- (d) 45 Pa

- 2.7** Convert the following velocity pressures to the corresponding velocities: (a) 0.07 in. H₂O; (b) 1.39 in. H₂O; (c) 335 Pa; (d) 1.23 cm H₂O.

Answers:

- (a) 1060 ft/min
- (b) 4720 ft/min
- (c) 24 m/s
- (d) 2780 ft/min

- 2.8** The velocity pressure at the center of a 14-in.-diameter duct is 1.84 in. H_2O . If the duct diameter is increased to 20 in. and the flow held constant, what is the new velocity pressure?

Answer: 0.44 in. H_2O

- 2.9** Air is flowing through an 8-in.-diameter duct at an average velocity of 4100 ft/min. (a) What is the flow Reynolds number? (b) A 10-cm duct at 6.16 m/s?

Answers:

(a) 285,000

(b) 40,800

- 2.10** Air is flowing through a 1-cm-diameter tube at a velocity of 8.2 cm/s. What is the flow Reynolds number?

Answer: 54

- 2.11** In Problems 2.9 and 2.10, what are the likely flow regimes in ventilation systems and the sampling lines used with personal air sampling pumps?

- 2.12** The following pressures are measured in different ventilation ducts. Calculate the missing value.

$$(a) \quad p_s = 2.7 \text{ in. } H_2O \quad p_v = 0.81 \text{ in. } H_2O \quad p_t = ?$$

$$(b) \quad p_s = -3.6 \text{ in. } H_2O \quad p_v = 1.32 \text{ in. } H_2O \quad p_t = ?$$

$$(c) \quad p_t = -4.1 \text{ in. } H_2O \quad p_v = 1.07 \text{ in. } H_2O \quad p_s = ?$$

$$(d) \quad p_t = -1.21 \text{ kPa} \quad p_s = -1.87 \text{ kPa} \quad p_v = ?$$

$$(e) \quad p_t = 980 \text{ Pa} \quad p_v = 520 \text{ Pa} \quad p_s = ?$$

Answers:

(a) 3.5 in. H_2O

(b) -2.3 in. H_2O

(c) -5.2 in. H_2O

(d) 0.66 kPa

(e) 460 Pa

- 2.13** Air is flowing through a 16-in.-diameter duct at a rate of 7000 ft³/min. At this airflow, the frictional loss factor is 0.012 p_v per foot of duct. What is the static pressure loss when the air flows through 50 ft of this duct?

Answer: 1.0 in. H_2O

- 2.14** Air is flowing through a 70-cm-diameter duct at a velocity of 15 m/s. At this velocity, the frictional loss is 0.0225 p_v per meter of duct. What is the static pressure loss when the air flows through 75 m of this duct?

Answer: 230 Pa

- 2.15** A 26-in.-diameter duct is carrying an airflow of 18,000 ft³/min. What is the static pressure loss across 80 ft of this duct? [Vent Man]

Answer: 0.86 in. H₂O

- 2.16** Air is flowing through a 4-in.-diameter duct at an airflow of 500 ft³/min. The 4-in.-diameter duct is connected to a 6-in.-diameter duct through a tapered expansion with a taper angle of 15°. If the static pressure entering the expansion is -3.18 in. H₂O, what is the static pressure leaving the expansion? [Vent Man]

Answer: -2.02 in. H₂O

- 2.17** Air is flowing through an exhaust hood into an 8-in.-diameter duct at a rate of 1500 ft³/min. If the hood entry loss factor is 0.25, what is the hood static pressure?

Answer: 1.44 in. H₂O

- 2.18** Air is flowing into a 20-in.-diameter duct through an attached exhaust hood. If the airflow is 9800 ft³/min and the hood static pressure is 1.97 in. H₂O, what is the hood entry loss?

Answer: 0.73 in. H₂O

- 2.19** Air is flowing through an exhaust hood into a 12-in.-diameter duct. (a) If the duct velocity pressure is 0.82 in. H₂O and the hood coefficient of entry is 0.61, what is the hood static pressure? (b) What is the hood entry loss?

Answers:

(a) 2.2 in. H₂O

(b) 1.38 in. H₂O

- 2.20** Air is flowing through an exhaust hood into a 60-cm-diameter duct at a rate of 3.1 m³/s. If the hood coefficient of entry is 0.35, what is the hood static pressure?

Answer: 590 Pa

- 2.21** Air is flowing at a rate of 4000 ft³/min into a hood connected to a 12-in.-diameter duct. If the hood static pressure is 2.37 in. H₂O,

(a) What is the coefficient of entry?

(b) What is the hood entry loss factor?

(c) What is the hood entry loss?

Answers:

(a) 0.83

(b) 0.45

(c) 0.73 in. H₂O

- 2.22** Air is flowing through a 16-in.-diameter duct at a rate of $6500 \text{ ft}^3/\text{min}$. What is the static pressure loss in traversing a four-piece stamped elbow with $R/D = 2$? [Vent Man]

Answer: 0.32 in. H_2O

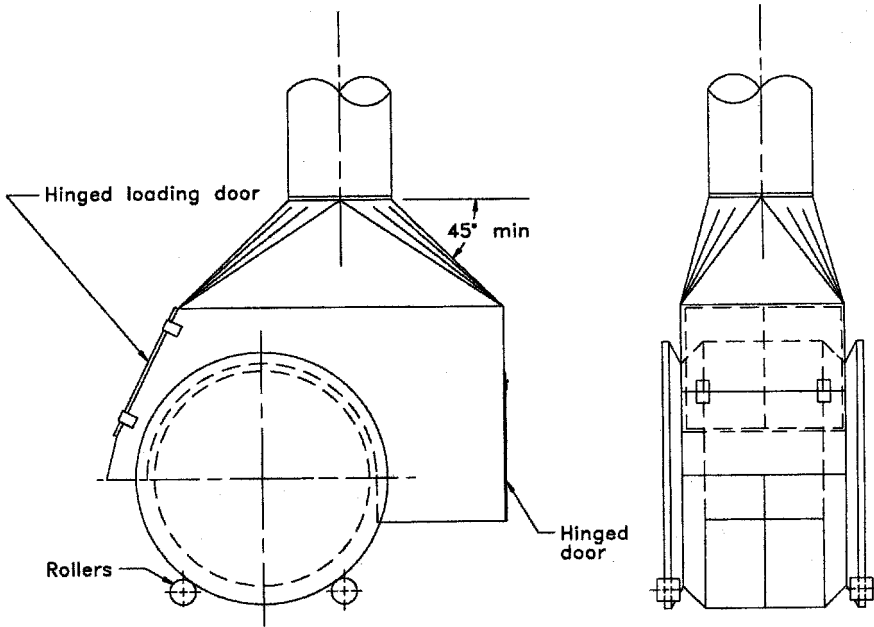
- 2.23** A 4-in.-diameter branch duct is entering a main at an angle of 30° . If the airflow through the branch is $230 \text{ ft}^3/\text{min}$, what is the branch entry loss? [Vent Man]

Answer: 0.08 in. H_2O

AIRFLOW MEASUREMENT TECHNIQUES

In this chapter we cover the methods available for the measurement of velocity, airflow rate, and certain system pressures under field conditions. After a ventilation system is designed and installed, airflow measurements are required to determine whether the system is performing according to the design; that is, whether the minimum critical velocities and airflows proposed in the design have been achieved in the installation (Fig. 3.1). There are other reasons why airflow measurements are made. In many cases, ventilation systems for the control of airborne contaminants must meet minimum standards established by various regulatory agencies. Periodic airflow measurements also provide a maintenance history of the ventilation system and highlight conditions that require correction. Finally, the measurement and inventory of the total exhaust rate are necessary to evaluate the adequacy of replacement air.

In most exhaust systems airflow is most conveniently measured by determining the average air velocity at a point in the system where the cross-sectional area is known. The airflow is then calculated as the product of the area and average velocity. As shown in Fig. 3.2, the common velocity measurement locations in ventilation systems are the face of the hood or a suitable duct location. Methods for measuring velocity at these locations are given principal attention in this chapter. A second method of airflow measurement utilizes total flow devices such as orifice and venturi meters. Since these devices have little application in measuring airflow in industrial ventilation systems and are covered adequately in other publications, they are given limited attention in this chapter.



$$Q = 400 \text{ cfm/ft}^2 \text{ of opening}$$

$$\text{Minimum duct velocity} = 3500 \text{ fpm}$$

$$h_e = 1.78 VP_s + 0.25 VP_d$$

Figure 3.1 As shown in the hood illustration plate for a melting furnace from the *Ventilation Manual* (2001), all basic design elements of the hood, including (1) geometry, (2) exhaust rate, (3) minimum duct velocity, and (4) entry loss are clearly identified. (From American Conference of Governmental Industrial Hygienists (ACGIH®), *Industrial Ventilation: A Manual of Recommended Practice*, 24th Edition. Copyright 2001. Reprinted with permission.)

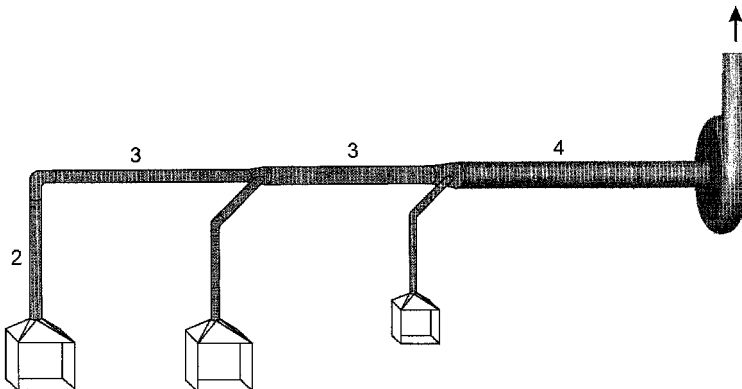


Figure 3.2 Ventilation measurements are commonly made (1) at the face of booth-type hoods, (2) just downstream of a hood at a branch location, (3) in the main to define hood exhaust rate by difference, and (4) in the main duct to define total system airflow.

In addition to the coverage of the measurement of air velocity and system pressures, attention is given the application of visual tracers to qualitatively define airflow patterns outside of exhaust hoods.

3.1 MEASUREMENT OF VELOCITY BY PITOT-STATIC TUBE

Recalling Eq. 2.17, the relationship between velocity pressure and the velocity of air is

$$V = 4000 \sqrt{p_v}$$

where velocity is expressed in feet per minute (fpm) and the velocity pressure is in in. H₂O. In SI units the velocity is in meters per second (m/s), the velocity pressure in pascals (Pa), and the expression is (again recalling Eq. 2.17a)

$$V = 1.29 \sqrt{p_v}$$

The velocity pressure can be measured as the difference between total pressure and static pressure using permanently mounted fittings at a fixed duct location. This technique is used occasionally in industry for continuous monitoring of airflow in a critical branch or main duct (Fig. 3.3). However, for general measurement purposes, the Pitot-static tube is the most widely used device. An integral combination of Pitot tube for measurement of total pressure and a static pressure measurement element, the Pitot-static tube can be inserted into the duct at a convenient location for direct measurement of velocity pressure (Fig. 3.4).

Although global standardization has made great headway since the mid-1990s, multiple Pitot-static tube designs continue to be in use. Until the mid 1900s both tapered and hemispherical Pitot-static tube nose designs were in use, and both

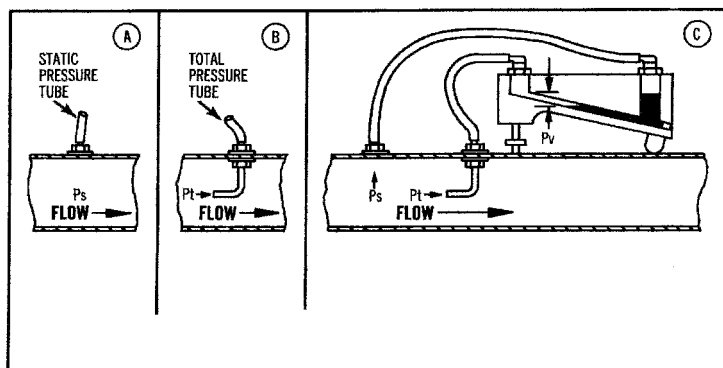


Figure 3.3 Fixed location total and static pressures are measured individually and velocity pressure is obtained by difference on an inclined manometer. (Courtesy of Dwyer Instruments, Inc.)

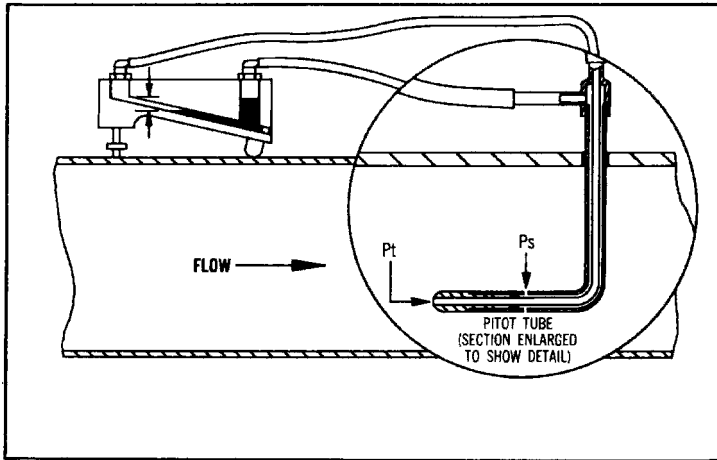


Figure 3.4 The total pressure probe of the Pitot–static tube consists of an inner tube that is positioned to point upstream and parallel to airflow. A second tube is sleeved over this tube to form an inner volume sealed on both ends and provided with a second manometer tap. This tube has a series of eight small holes drilled around its perimeter at a specified distance from the nose of the tube to measure static pressure. The velocity pressure, or the difference between total and static pressures, can be measured with the Pitot–static tube by connecting the two Pitot–static taps to a manometer. A common problem with the Pitot–static tube in dusty industries is the plugging of the static and total pressure holes. This frequently occurs when the hole for the Pitot–static tube is drilled in the bottom of a duct conveying particles with inadequate transport velocity. The Pitot–static tube must be pushed through the settled dust, and it frequently plugs. Blowing through the tubing taps usually clears the holes in the tube. If high dust loadings occur in the duct and frequent plugging occurs, a special Pitot–static tube with larger holes can solve the problem. (Courtesy of Dwyer Instruments, Inc.)

were assigned k factors of 1.0. In the 1950s it was shown that both designs could produce boundary-layer effects along the length of the probe with a magnitude dependent on the Reynolds number and airflow turbulence. A modified ellipsoidal nose was designed by the UK National Physical Laboratory to eliminate these effects while reducing the impact on the k factor from small changes in the nose profile due to manufacturing variations and damage during use. This new design, called the *modified ellipsoidal Pitot–static tube*, is now specified in the British Standards (BSI, 1992) while the hemispherical design continues to be the standard in the United States (ASHRAE, 2001). The minor differences in the performance of these designs as noted in the laboratory pale in importance to the potential errors in field studies where the observer may be on a ladder 20 ft (6.10 m) in the air positioning the Pitot–static tube for the traverse and attempting to read an inclined manometer in a poorly illuminated background. It is important to note that since the Pitot–static tube is considered a primary standard, it is used to calibrate other velocity measuring devices.

3.1.1 Pressure Measurements

A critical element in the effective use of the Pitot-static tube in industrial ventilation work is the pressure measuring device. There are many instruments available for measuring the low pressures encountered in industrial ventilation systems, each of which has its advantages and limitations. In most situations, the ventilation engineer or industrial hygienist will be measuring differential or relative pressure. Therefore, barometric instruments designed to determine absolute pressure are not covered in this chapter; for information on these devices, the reader is referred to other sources (ASHRAE, 2001).

The simplest and most reliable pressure indicator to be used with the Pitot-static tube is the vertical manometer, which consists of two connected columns of liquid, usually water, oil, or mercury. Since each column is connected to a distinct atmosphere, the difference in heights of the two columns is a direct indicator of differential pressure between those atmospheres. The vertical manometer used with water can be accurately read as low as 0.50 in. H_2O (125 Pa), the velocity pressure equivalent of 2832 fpm (14.42 m/s). Frequently duct velocities are below this velocity, so a more sensitive manometer must be used. The vertical manometer can be modified to improve readability at low pressures by tilting it at an angle so that a small pressure change will result in a longer deflection of the fluid meniscus. The inclined twin-leg manometer with a slope of 10 : 1 can be accurately read as low as 0.05 in. H_2O (12.46 Pa) corresponding to a velocity of 896 fpm (4.55 m/s). The advantage of the inclined manometer is its simplicity and the fact that it can be constructed in the laboratory from standard glass tubing and a wooden wedge. The difficulty encountered in its use is the problem in leveling the two legs and ensuring a 10 : 1 inclination plane.

The commercially available single-leg, inclined manometer is a solution to the difficulties encountered with the double-leg, inclined manometer described above. In this unit, one leg is replaced by a fluid reservoir, while the reading leg is a takeoff from the reservoir (Fig. 3.5a). The reading leg may be positioned at a fixed inclination (i.e., 10 : 1), as in the case of this device, or it may be adjustable, affording a wide measurement range. In the United States, the most common manometer in industrial ventilation fieldwork has a both a vertical and an inclined leg to measure both velocity pressures and system total and static pressures (Fig. 3.5b) over a wide range.

The discussion has referenced a water-filled manometer; in fact, the commercial manometers available in the United States use special red gage oil with a specific gravity of 0.826. This oil will deflect approximately 20% farther than water under the same pressure, thus increasing the readability of the instrument. This fluid has an additional advantage in that a well-defined meniscus is formed and the fluid “clears” or seeks a stable reading quickly. For high-pressure measurements, for example, those made on high-velocity/low-volume systems where total and static pressures are encountered in the range of 1–10 in. Hg (2.54–25.4 cm Hg), an electronic transducer-based instrument is appropriate.

Any change in manometer fluid must be noted so that the subsequent pressure readings can be adjusted for density. In an emergency, water can be substituted in a

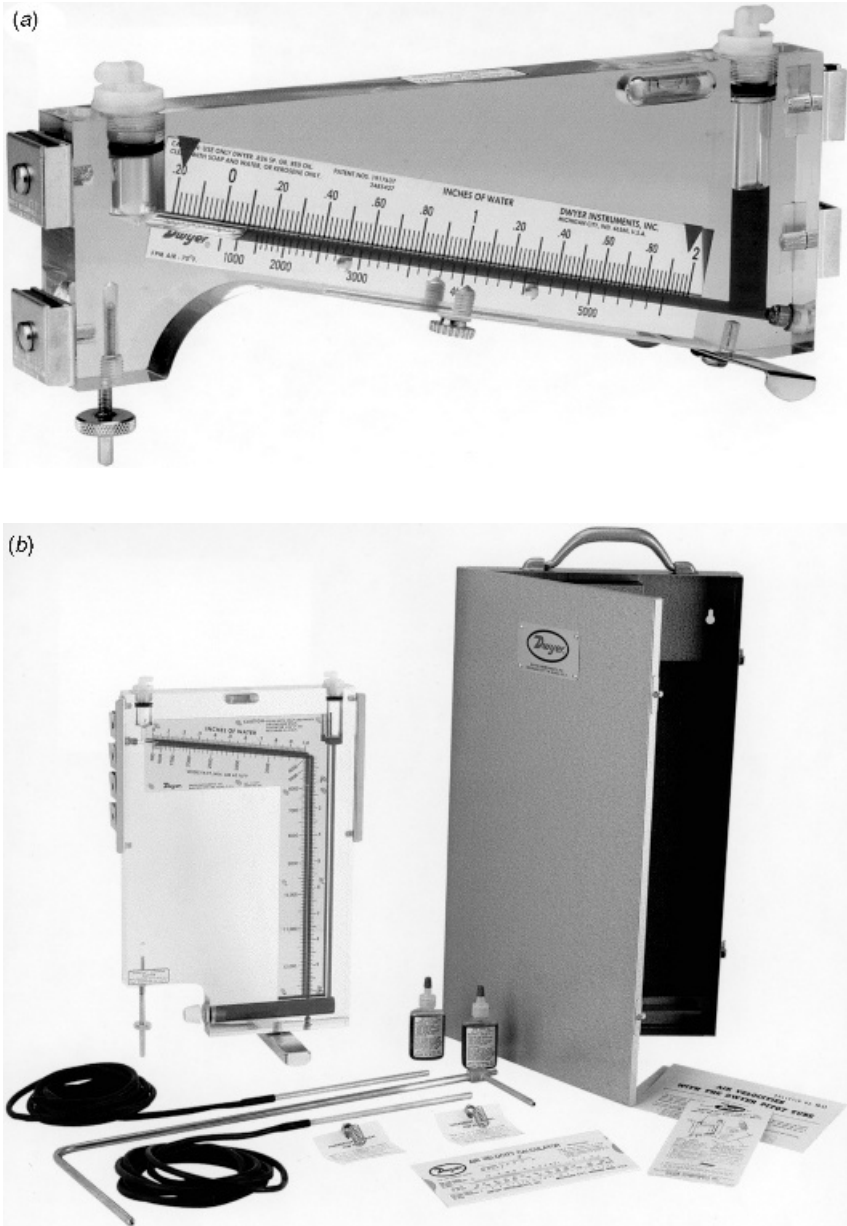


Figure 3.5 (a) Inclined manometer. If the duct velocity is 1000 fpm (5.08 m/s), the observed velocity pressure will be 0.07 in. H_2O (17.44 Pa), a pressure that can be accurately measured with this inclined manometer. (Courtesy of Dwyer Instruments, Inc.) (b) Inclined/vertical manometer. Since static and velocity pressures will frequently exceed the range of the inclined manometer, a combination inclined/vertical manometer is most convenient for fieldwork. Total and static system pressures may be read up to 10 in. (25.4 cm) H_2O on the vertical leg of this manometer. (Courtesy of Dwyer Instruments, Inc.)

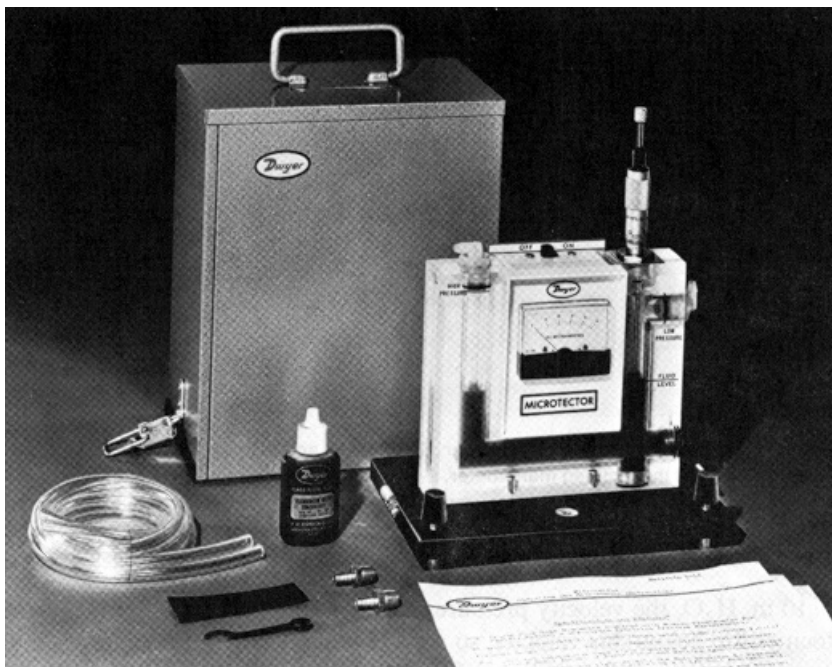


Figure 3.6 Hook gage micromanometer with electronic sensing that can be read to ± 0.00025 in. H_2O (0.06 Pa). (Courtesy of Dwyer Instruments, Inc.)

manometer designed for another fluid. Unless circumstances dictate otherwise (i.e., excessive loss of fluid), the use of other fluids in an oil manometer is strongly discouraged.

For measurements as low as 0.001 in. H_2O (0.25 Pa) corresponding to a velocity of 130 fpm (0.66 m/s), a number of fluid-based micromanometers are available (Fig. 3.6). Although widely utilized in the laboratory, these devices are not suitable for field investigations. A detailed description of these devices is presented by Ower and Pankhurst (1977).

In addition to the liquid-filled manometers, both mechanical and electronic-based pressure sensors are now widely used in the United States. A popular mechanical device is based on a diaphragm sensor, which is displaced under differential pressure driving a linkage connected to a meter display (Fig. 3.7). Electronic micromanometers are now available with microprocessor-based instruments for direct reading and averaging of pressure and velocity measurements in the field (Fig. 3.8). Devices of this type have definite advantages in the field, but unlike fluid-filled manometers, they are not primary standards, so frequent calibrations against a liquid manometer are important.

The most effective solution to the measurement of air velocities below 500 fpm (2.54 m/s) in a clean airstream may be the use of one of the heated devices to be



Figure 3.7 Magnehelic devices are available for a range of pressures and are useful for measuring velocity pressures as low as 0.05 in. H_2O (12.46 Pa). These sensors are convenient for field use in that they do not require leveling, are easily zeroed, and do not use fluids. Since they are not primary standards they do require periodic calibration, but this is easily done with a conventional manometer. These devices are commonly used to monitor airflow continuously at individual hoods using the hood static suction measurement technique described in Section 3.5. (Courtesy of Dwyer Instruments, Inc.)

described later in this chapter. A second solution to the measurement of low air velocities is to use a special type of Pitot-static tubes that provides a reading that is some multiple of the velocity pressure. Since this device is not a primary standard, it must be calibrated under the conditions of use. As a result, this special design is used in the laboratory but sees little application in field measurements.

3.1.2 Velocity Profile in a Duct

The measurement of airflow in a branch, submain, or main duct is based on a careful measurement of both the cross-sectional area of the duct at the measurement location and the mean velocity of air moving through the duct at that point.

The velocity profile in a duct has been described in Chapter 2. As air moves through the duct, the velocity at the surface of the duct is zero. As one moves away from the duct wall, the velocity increases, first as a very thin laminar flow layer of air and then to a turbulent zone. The velocity gradient is at first very rapid and then becomes asymptotic. The characteristic profile in a relatively smooth duct at constant temperature and pressure depends solely on Reynolds number. The relationship between the velocity at a given point and the centerline velocity (Ower and Pankhurst, 1977) is presented by the *power law*



Figure 3.8 Microprocessor-based system using electronic pressure transducer for direct Pitot-static velocity measurements as shown here with averaging and storage capability. The transducer has a measurement range from -15 to 15 in. H_2O (3735 Pa). A belt-mounted printer permits one person to conduct and record all measurements. (Courtesy of TSI Inc.)

$$\frac{v_r}{v_c} = \left(1 - \frac{r}{a}\right)^m \quad (3.1)$$

where r = radius of point

a = internal radius of duct

v_r = velocity at radius, r

v_c = velocity at duct centerline

m = exponent that varies with the Reynolds number corresponding to the centerline velocity as shown in Table 3.1

The characteristic velocity profile represented by Eq. 3.1 is noted only in fully developed flow (Fig. 3.9).

It would be useful to determine the mean velocity from a single centerline velocity measurement and it would appear feasible from the well-defined velocity profile shown in Fig. 3.9. Indeed, the relationship between centerline velocity, average duct velocity, and Reynolds number has been defined in some detail as shown in Fig. 3.10. However, in field measurements this approach is rarely useful for the reasons discussed below and is to be discouraged in favor of a full Pitot-static tube traverse to be discussed in Section 3.1.3.

As noted in Fig. 3.9, the ideal fully developed velocity profile is observed only in a long duct run of undisturbed flow. This is an unusual situation in industry, where long,

Table 3.1 Value of Exponent m in Eq. 3.1

Reynolds Number at Duct Centerline	Exponent, m
1.27×10^4	0.168
2.49×10^4	0.156
6.10×10^4	0.141
1.20×10^5	0.130
2.37×10^5	0.120
5.84×10^5	0.109
1.16×10^6	0.101

straight runs are rarely encountered and system fittings such as elbows, entries, expansions, and contractions are numerous. The velocity profile downstream of an elbow is distorted by the inertial “throw” of the air to the far wall as the air changes direction. The aspect ratio of the elbow and the duct velocity determine the observed profile. The characteristics of the velocity profile just downstream of the elbow are difficult to predict, as is the distance of straight pipe necessary to reestablish a reasonable profile. Branch entries also cause major disturbances of the velocity profile in the main downstream of the entry. The effect of this disturbance varies with the angle of entry of the branch, the ratio of the velocity in the branch to the main duct, and the volumes flowing in the two ducts. In many field situations it takes a distance of 8–10 duct diameters before the profile is acceptable for a Pitot–static measurement. Frequently, the branch-to-branch inlet distance is much less than this. In such cases a Pitot–static tube traverse is conducted in the individual branch and the branch flow is added to the flow in the main duct to obtain the total system flow downstream of the branch entry.

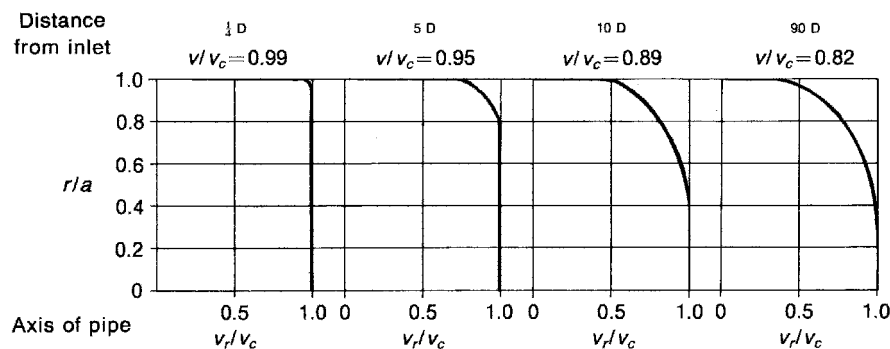


Figure 3.9 Velocity profile in a duct at distances from one-quarter to 90 pipe diameters downstream from a flared inlet opening showing progression to fully developed turbulent flow, where V_r , velocity at radius r ; V_c , velocity at axis; V , mean velocity; a , full internal radius. [From E. Ower and R. C. Pankhurst (1977), *The Measurement of Air Flow*. Used with permission of Pergamon Press.]

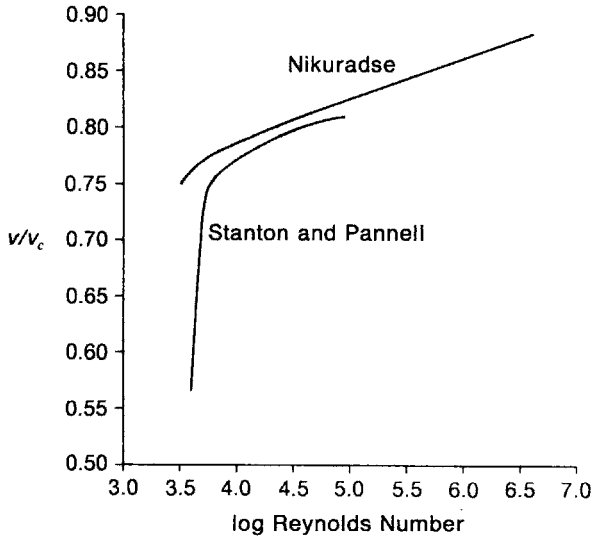


Figure 3.10 Relationship of average duct velocity to centerline velocity in smooth circular duct for various Reynolds numbers, where V , mean velocity; V_0 , velocity at axis. [From E. Ower and R. C. Pankhurst (1977), *The Measurement of Air Flow*. Used with permission of Pergamon Press.]

Expansion and contraction fittings are less likely than other common duct fittings to cause a serious distortion of the velocity profile. A low angle of expansion or contraction will present little velocity profile modification, and in many cases, a sharp contraction may improve the velocity profile.

As a result of these effects, if the Pitot-static tube traverse is done immediately downstream of duct fittings, the traverse profiles may be severely skewed. Few quantitative data on this issue were available until the work of Guffey and Booth (1999). These authors explored the influence of upstream fittings including plain duct openings, branch inlets, 90° elbows and two elbows rotated 90° on the traverse profile (Figs. 3.11 and 3.12). The authors show that if two 10-point perpendicular traverses are done, even as close as four duct diameters downstream of the disturbance, the deviations in airflow from ideal conditions seldom exceed 5%. The authors' work also supports the use of the conventional recommendation that if only a single traverse can be done, the traverse should be completed at a point more than $7D$ (i.e., seven duct diameters) downstream of the fitting to ensure accurate results.

No generalizations can be made about the velocity profiles at Pitot-static tube locations downstream of exhaust hoods since the velocity profile is defined by the geometry of the hood. The profile may be reasonably good a few diameters downstream of the hood if the hood has a symmetric tapering design; however, the profile may be difficult to assess for a hood with a tangential delivery to the branch duct.

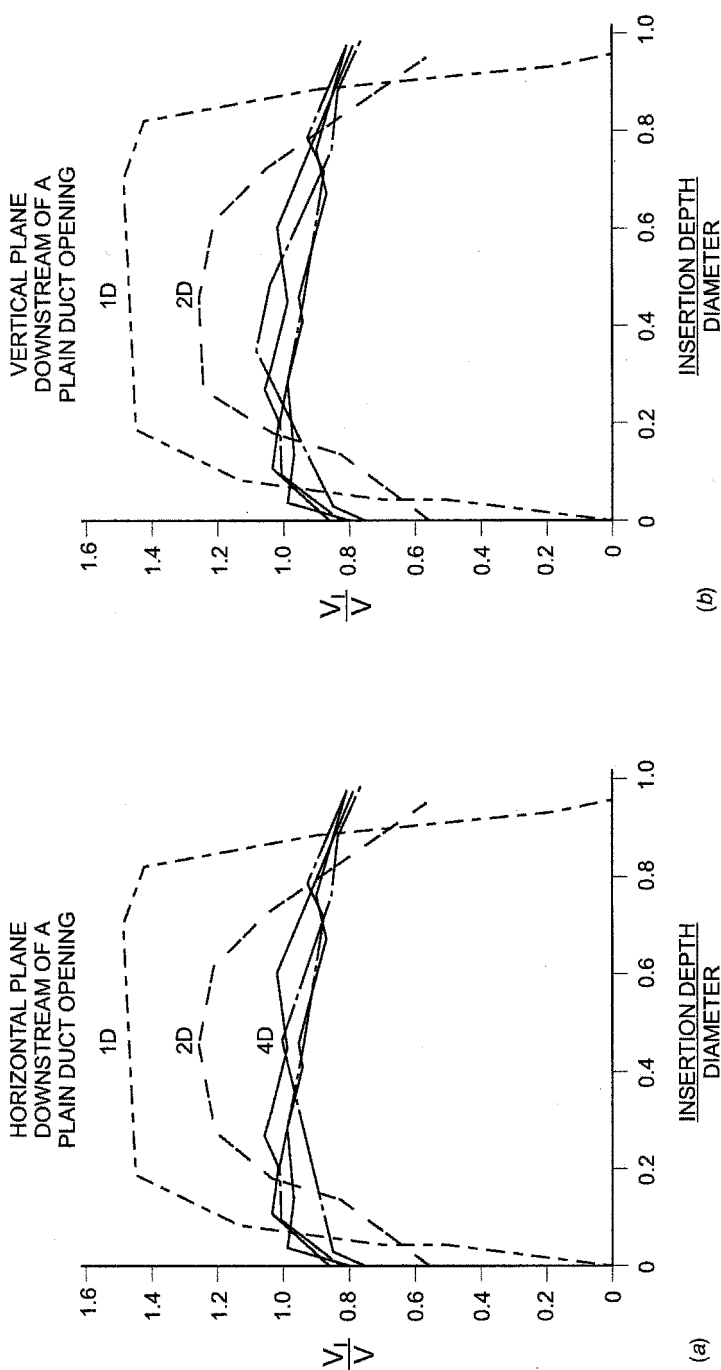


Figure 3.11 Velocity profile in a duct with a sharp-edged opening measured downstream in (a) a horizontal plane and (b) a vertical plane (From American Conference of Governmental Industrial Hygienists (ACGIH®), *Industrial Ventilation: A Manual of Recommended Practice*, 24th Edition. Copyright 2001. Reprinted with permission.)

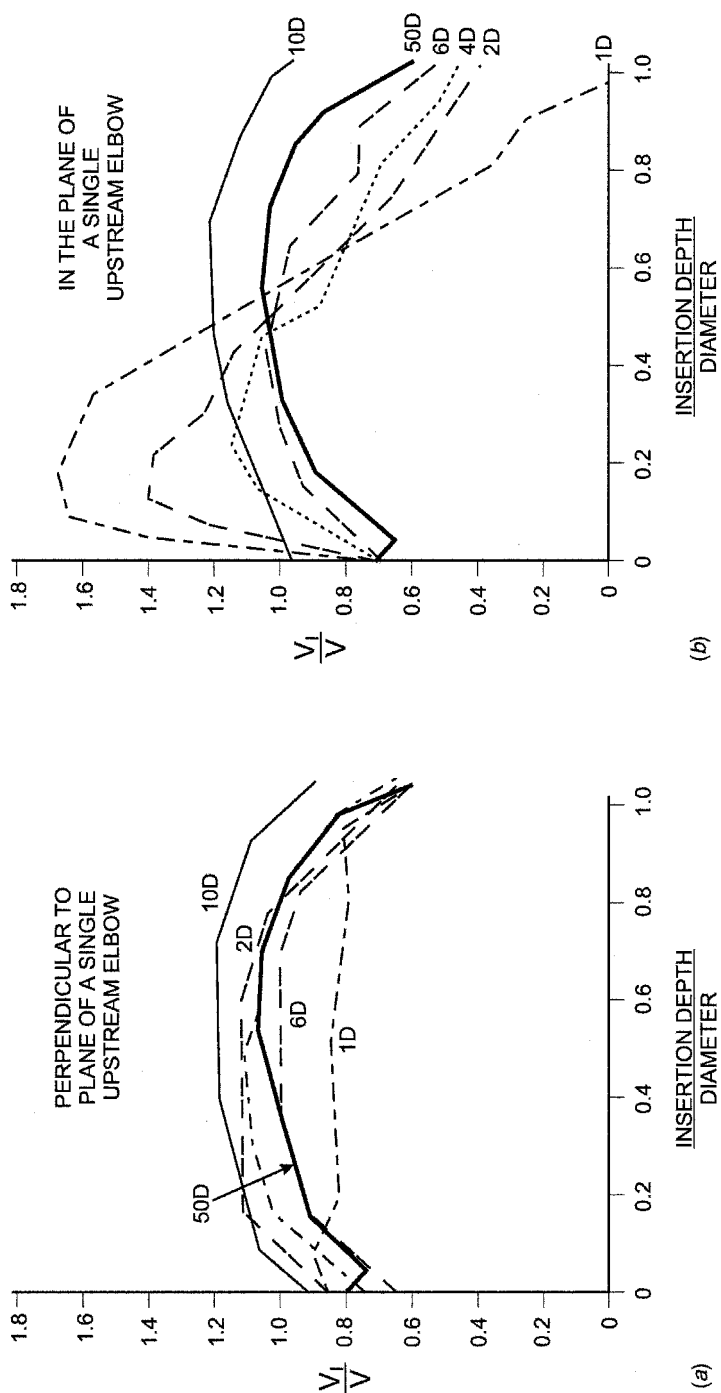


Figure 3.12 Effect of a single 90° elbow on the velocity profile in a duct measured (a) perpendicular to the plane of upstream elbow and (b) in the plane of the elbow at on 50° diameters downstream of the elbow (From American Conference of Governmental Industrial Hygienists (ACGIH®), *Industrial Ventilation: A Manual of Recommended Practice*, 24th Edition. Copyright 2001. Reprinted with permission.)

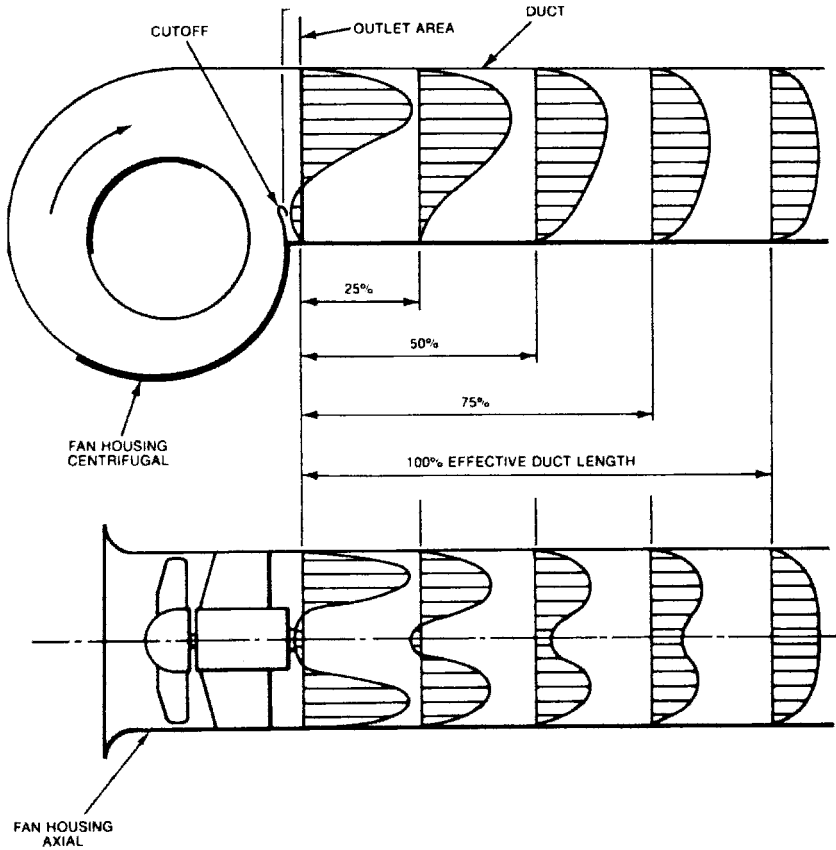


Figure 3.13 Velocity profiles at discharge from centrifugal blower (top) and from axial flow blower (bottom). (Reproduced through the courtesy of Air Movement and Control Association, Inc.)

It is extremely difficult to obtain a reasonable assessment of the velocity profile immediately downstream of a fan. In systems served by a centrifugal blower the velocity gradient across the duct increases dramatically, due to the throw from the impeller tip (Fig. 3.13). If the fan discharges to a duct run and there is access to the duct at some distance downstream, a reasonable traverse is possible. If the fan discharge is vertical, access may be difficult. In such cases Pitot-static measurements are best made on the suction or negative-pressure side of the fan. The discharge from axial flow fans (especially roof exhausters) may be accessible for measurement, but the velocity profile across the discharge face is quite uneven (Fig. 3.13). With roof exhausters, the flow actually reverses near the centerline of the air mover. It is common practice to estimate the delivery of these low-static roof exhausters by noting the pressure at the inlet to the fan and then estimating airflow from the manufacturer's catalog as described in Chapter 10.

3.1.3 Pitot-Static Traverse

Round Duct. The discussion in Section 3.1.2 should make it obvious that the mean duct velocity cannot be defined by taking one Pitot-static tube measurement; rather, multiple measurements must be made of velocity pressure at specific points across a duct diameter to determine the mean velocity.

Until recently the Pitot-static tube measurement points were defined by the tangential method as defined by Ower and Pankhurst (1977). "The duct is divided into n zones of equal area consisting of one central circular zone and $(n - 1)$ annular zones by circles of radii $r_1, r_2, r_3, \dots, r_n$: and it is assumed the mean velocity in each zone is obtained by measurement at the radius which divides the zones into two parts of equal area." A more accurate measurement grid, now accepted by the American Society of Heating Ventilating and Air Conditioning Engineers (ASHRAE, 2001) and presented in the 24th edition of the Ventilation Manual (ACGIH, 2001), is the log-linear method. In this method of defining the measurement points, the duct is divided into annular rings and a central circular zone of equal area; however, the measuring points are not at the center of area of each zone but at points where the mean zone velocities occur based on equations proposed by Winternitz and Fischl (1957). The traverse grid points defined by this log-linear method are shown in Fig. 3.14 and Table 3.2 for 4, 6, 8, and 10 measuring points.

Winternitz and Fischl (1957) compared the log-linear and tangential methods under conditions that exist in field studies, namely, where duct flow is not fully developed and an irregular velocity profile is encountered. Ower and Pankhurst (1977), reflecting on the author's conclusions, state "The four-point log-linear method was inferior, the six-point was about equivalent, and the eight-point and ten-point were superior, all by comparison with the ten-point tangential method. The

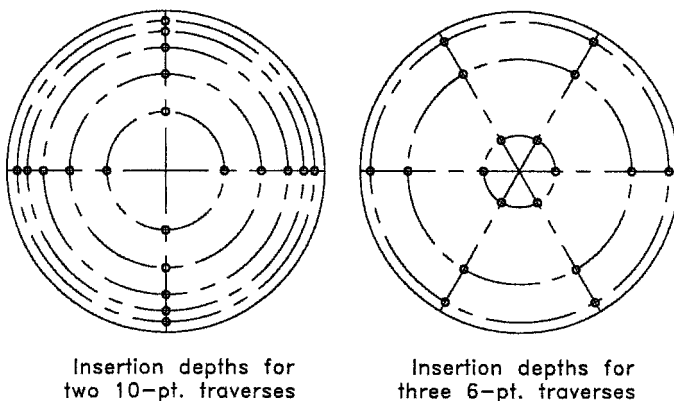


Figure 3.14 Log-linear method for establishing measurement points for a Pitot-static traverse of a round duct. In this method, commonly used in the United States, the immersion depth from the duct wall is expressed as a fraction of the pipe diameter as shown in Table 3.2.

Table 3.2 Pitot–Static Traverse Measurement Locations for Round Duct using the Log–Linear Rule

Number of Points per Diameter	Distance from Wall in Duct Diameters										
4	0.043	0.290	0.710	0.957	—	—	—	—	—	—	—
6	0.032	0.135	0.321	0.679	0.865	0.968	—	—	—	—	—
8	0.021	0.117	0.184	0.345	0.665	0.816	0.883	0.979	—	—	—
10	0.019	0.076	0.153	0.217	0.361	0.639	0.783	0.847	0.924	0.981	—

ten-point log-linear traverse, which has been specified by the British Standards Institute for Class A accuracy, resulted in a mean-square error of about 0.5% percent or about one-half that of the ten-point tangential method.”

In field measurements the velocity pressure is noted from the manometer for each point of the traverse, the velocity at each point is calculated from the velocity pressure, and the velocities are averaged to obtain the average duct velocity. A common error made by the inexperienced investigator is the averaging of the velocity pressures.

Rectangular Duct. One observes similar variations in velocity across the rectangular duct as noted with round duct, and multiple readings across a traverse plane must be taken to get a reasonable measurement of the mean velocity. Until the 1990s the center of equal areas approach method (AABC, 1989) was the industrial hygiene standard for traversing rectangular ducts. However, ASHRAE has adopted the log Chebyshev procedure (ASHRAE, 2001). This method requires a minimum of 25 velocity pressure measurements and the provision that the distance between points not exceed 6 in. (15.24 cm) as shown in Fig. 3.15 and Table 3.3. Additionally, the guidelines state “for the velocity distribution to be *acceptable*, 75% or more of the velocity measurements must be greater than 1/10 of the maximum velocity of that profile. A further statement is made for a more rigorous profile. If one wishes to qualify a distribution as *ideal* 80–90% of the velocity measurements must be greater than one-tenth of the maximum velocity at that profile. The *ideal* qualification is not appropriate for industrial hygiene fieldwork so it will not be discussed in this text. It may, however, be necessary to achieve that quality in a laboratory study.”

Klassen and House, (2001) have evaluated the relative accuracy of the log Chebyshev method and the equal area traverse methods for measurement of airflow in rectangular ducts. In a limited laboratory study with a single duct size and airflow rate and limited geometry, the two methods produce results with excellent agreement with a reference airflow measured with a primary standard. The authors state that due to the limited geometry and airflow the results of the study cannot be generalized. Since the ACGIH *Ventilation Manual* uses the log Chebyshev method for rectangular duct and equal area linear method for round duct, these measurement locations will be followed in this text.

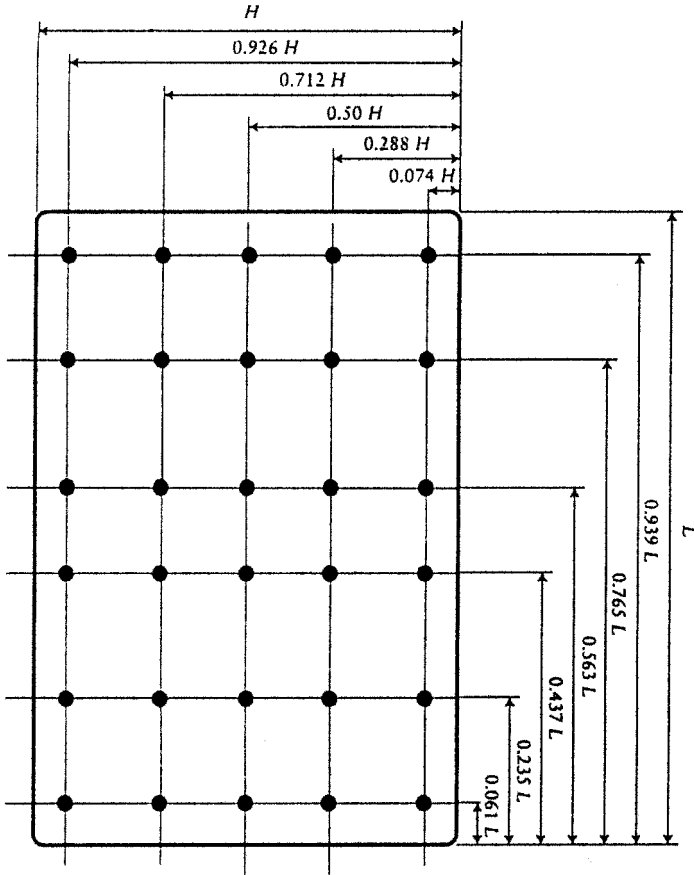


Figure 3.15 Log Chebyshev procedure for establishing Pitot-static traverse points for rectangular duct as shown in Table 3.2.

Table 3.3 Pitot-Static Traverse Measurement Locations for Rectangular Duct using the Log Chebyshev Rule

Number of Measurement Points per Traversing Line	Distance from Wall in Duct (l/L or h/H)										
5	0.074	0.288	0.500	0.712	0.926	—	—	—	—	—	—
6	0.061	0.235	0.437	0.563	0.765	0.939	—	—	—	—	—
8	0.046	0.175	0.342	0.400	0.600	0.658	0.825	0.954	—	—	—
10	0.037	0.141	0.263	0.338	0.456	0.544	0.662	0.737	0.859	0.963	—

Source: Airflow (1997).

3.1.4 Application of the Pitot–Static Tube and Potential Errors

Ower and Pankhurst (1977) provide a detailed review of potential errors in the use of the Pitot–static tube first noting errors associated with possible mechanical interference between the Pitot nose and the duct wall. In the 10-point traverse in a round duct using the log-linear protocol, the first and last measurement points are located 0.019 times the duct diameter away from the duct wall (Table 3.2). Therefore, the smallest duct in which a 10-point traverse can be conducted without the Pitot tube bumping into the duct is one in which 0.019 times the duct diameter equals one-half the outside Pitot–static tube diameter. It follows that for the standard U.S. Pitot with a diameter of 0.312 in. (0.79 cm) the smallest duct that can be traversed without mechanical interference is 8 in. (20.32 cm); for a 0.125 in. (0.48 cm) probe diameter the smallest is a 3-in. (7.62-cm)-diameter duct.

The authors then go on to note the errors due to the velocity gradient across the duct and the close proximity of the head of the Pitot–static tube to the inner duct wall at the first and final measuring point of the traverse. On the basis of limited studies the authors state that the errors due to these two effects are less than 0.5% if the ratio of the duct to Pitot–static tube outside diameters are limited to 35–40. If the standard U.S. standard Pitot–static tube is used [diameter of 0.312 in. (0.79 cm)], its use would be limited to ducts larger than 11 or 12 in. (27.94 or 30.48 cm). For smaller duct sizes the 0.125-in. (0.32-cm)-diameter Pitot–static tube must be used to minimize errors.

Detailed studies of errors due to misalignment of the pitot head with airflow done on a range of Pitot tube designs have shown that errors in pitch and yaw are most significant in the measurement of static pressure and rather minor for total pressure. First, a definition of yaw and pitch is appropriate. If the Pitot traverse is in a horizontal duct run an attitude of pitch would result in orientation of the nose of the Pitot–static tube either above or below the duct centerline; in this horizontal traverse, *yaw* is defined as an orientation that would place the nose to the left or right of the duct centerline. Ower and Pankhurst (1977) state that if the head of the probe is misaligned by 15°, there is a 5% reduction in static pressure from that noted with perfect alignment. The error in velocity pressure can be deduced from knowledge of the individual effects on static and total pressure from misalignment. The effects vary greatly dependent on nose design; for the hemispherical nose, which is commonly used in the United States, a misalignment of 15–20° results in a velocity pressure error of 3–5%. Angular misalignment of this magnitude is easily noted by observation in the field. To minimize this error in the field and for rigorous laboratory studies a holding fixture has been proposed by Guffey (1990). For an comprehensive review of all potential errors in the use of the Pitot–static tube the reader is referred to Ower and Pankhurst (1977), ASHRAE (2001), and Goodfellow and Tahti (2001).

The large Pitot–static tube requires a $\frac{3}{8}$ -in. (0.95-cm) hole (Table 3.4) for insertion in the duct wall; the small tube requires a $\frac{3}{16}$ -in. (0.48 cm) hole. An insulated duct requires a larger access hole depending on the thickness of the insulation. The fate of the small holes drilled in the duct for insertion of the Pitot–static tube requires some

Table 3.4 Leak through $\frac{3}{8}$ -in. Pitot–Static Hole at Various Static Pressures

Static Pressure		Leak Rate	
in. H ₂ O	Pa	cfm	m ³ /s × 10 ⁴
1.0	249	0.39	1.8
2.0	498	0.57	2.7
4.0	996	0.84	4.0
6.0	1494	1.01	4.7
7.8	1942	1.23	5.8

discussion since it is frequently of great concern to plant personnel. If the measurements are made inside a building downstream of the fan, that is, on the positive-pressure side of the fan, it is obvious that the holes should be sealed to prevent air contaminants from escaping to the workplace. On the suction side of the fan, this is not necessary since only a small leak inward will occur (Table 3.2). However, plant personnel frequently insist that such holes be taped over or plugged.

The major advantage of the Pitot–static tube is that it is a primary standard and does not require calibration; indeed, it is used to calibrate orifice and venturi meters and direct-reading instruments. The major disadvantage of the Pitot static tube is that it cannot be used at velocities below 1000 fpm (5.08 m/s) unless special manometers are used.

3.2 MECHANICAL DEVICES

3.2.1 Rotating Vane Anemometers

The rotating vane anemometer (RVA), used widely in mining and to a lesser extent in general industry, has proved useful in airflow measurements. Introduced in the 1920s, this device, shown in its simplest form in Fig. 3.16, uses a lightweight rotating vane as the sensor. This windmill is supported by low-friction bearings that permit it to rotate at a speed proportional to air velocity. In the conventional RVA design shown in Fig. 3.16, the impeller drives a mechanical transmission to provide a reading of the linear feet of air, which have passed through the instrument in a given time. If the elapsed time of the observation is noted, one can easily calculate the velocity of the air stream by dividing the linear feet of air displayed on the meter face by the elapsed time. The vane design, type of bearings, and readout system define the operating characteristics of the device.

Since the early 1990s, a number of new RVA designs have been introduced that make this device more attractive to the practitioner. A digital readout and integral timer improve the ease of use in field measurement. Low-friction bearings and counters based on photoelectric or capacitance sensors have improved the low-velocity performance of the device (Figs. 3.17*a* and 3.17*b*).



Figure 3.16 The conventional rotating vane anemometer (Birams type) consists of an aluminum vane impeller with a mechanical gear train driving a series of three dials that read 100, 1000, and 10,000 ft (30.5, 305.0, and 3050.0 m). The instrument is equipped with a zero-reset lever and a lever to activate the instrument. This unit has a 4-in. (10-cm)-diameter frame and has a useful range of 100–5000 fpm (0.51–25.5 m/s). It is available from several manufacturers. (Courtesy of Davis Instrument Manufacturing Co.)

These instruments are available in a range of sizes based on 1-, 3-, 4-, and 6-in. (2.54-, 7.62-, 10.16-, and 15.24-cm) diameter impellers. The size defines the operating range. The larger the diameter, the greater the available starting torque for a given velocity. Larger instruments are thus more sensitive and able to measure lower velocities, although they have a limited upper range. The small-diameter instruments are useful at high velocities. The 3- and 4-in. (7.62- and 10.16-cm) devices are by far the most common with a useful velocity range of approximately 100–5000 fpm (0.51–25.00 m/s).

The performance characteristics of several 4-in. (10.16-cm)-diameter RVAs are shown in Table 3.5. Minimum starting speed is in the range of 60 fpm (0.30 m/s) for a conventional 4-in. (10.16-cm)-diameter device with a mechanical readout and bronze bearings. The response is not linear until approximately 100–125 fpm (0.51–0.64 m/s), when the calibration does become linear for the balance of the useful range of this specific instrument. The manufacturer normally provides a calibration for each instrument. The response of newer devices with ball bearings and nonmechanical counters exhibits improved instrument sensitivity at low velocities with lower starting and stopping speeds.

The instrument is commonly used to measure velocity at hood faces, exhaust grilles, supply registers, and mine roadways. To minimize errors, the cross-sectional area of the anemometer must be small compared to the area of the opening. In general, it is not useful for duct measurements. If used to measure the velocity at a duct opening, the diameter of the duct should be at least 6 times the diameter of the instrument to maintain errors less than 1%.

The RVA measures the velocity at the axis of the instrument. Therefore, if a 4-in. (10.16-cm) RVA is to be used to measure mean velocity by a traverse across the duct



Figure 3.17 A new generation of electronic-based rotating vane anemometers has improved range and accuracy. (a) This series of instruments is available with a 4-in. (100-mm) or a 1.4-in. (35-mm) rotating vane sensor in an integral design as shown or with a telescopic probe head. It displays average, maximum, and minimum values; calculates flow; and is available with data logging capability. (Courtesy of TSI, Inc.) (b) This anemometer has a 2.83-in. (72-mm) rotating impeller with a ball bearing suspension and a 39-in. (1-m) cable and records maximum, minimum, and average values with recall functions. It has a built in serial interface with optional data acquisition software and data logger for subsequent analysis. (Courtesy of Extech Instrumentation Corp.)

face, the minimum ratio of duct diameter to RVA diameter is 15 for a 6-point traverse and 26 for a 10-point traverse (Ower and Pankhurst, 1977).

The instrument can be used in either a fixed-point survey or a hand traverse mode (Fig. 3.18). The timing of the RVA reading is conducted in two ways. The most accurate method is to position the instrument at the measurement point and allow it to come up to speed. A stopwatch is used to note the time for a given number of revolutions on the dial or for a counter interval on the newer digital instruments. The linear speed can then be easily calculated. A second technique, which (although not as accurate) is probably suitable for most field measurements, involves positioning the instrument, permitting it to come to speed and then actuating the counter for a given period, usually 2–4 min. At the end of this interval, the counter is turned off,

Table 3.5 Performance of Rotating Vane Anemometers

RVA Model	Readout	Bearings	Starting Speed		Stopping Speed	
			fpm	m/s	fpm	m/s
1	Gear train	Bronze	63	0.32	54	0.27
2	Gear train	Ball	23	0.12	18	0.09
3	Gear train	Jewel	61	0.31	67	0.34
4	Magnetic	Ball	60	0.31	40	0.20

the linear feet passed through the RVA are noted, and the velocity is calculated. In any case, no reading should be taken for less than 100 s or an instrument reading of less than 160 ft (48.77 m), and two readings should be taken at each location (Ower and Pankhurst, 1977).

Teale (1958) has identified the following sources of error in using the rotating vane anemometer.

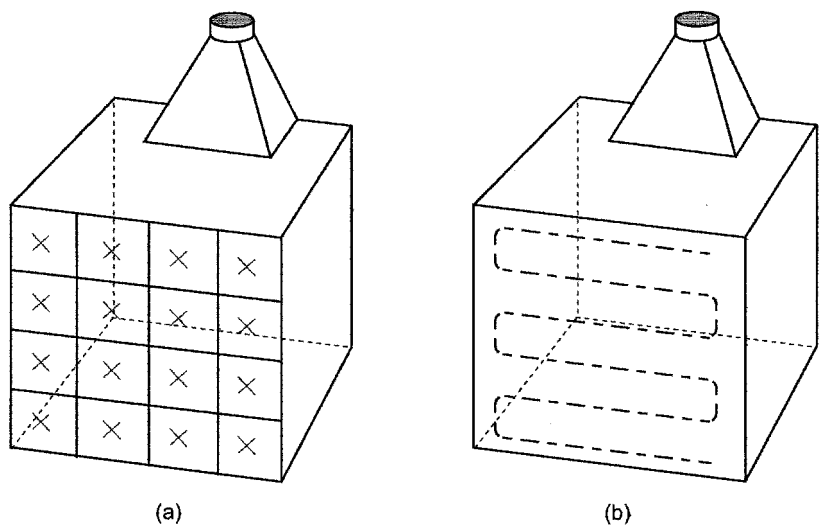


Figure 3.18 Two techniques are used to conduct velocity measurements with the rotating vane anemometer. (a) The cross-sectional area to be measured can be divided into equal areas and the measurement taken at the center of each area. The velocities are then averaged to obtain the average velocity at the plane of the opening. This fixed-point technique requires an assessment of the area geometry and assignment of measurement locations. It also requires a series of individual timed measurements; for a large opening this may be rather time consuming. (b) The second technique is to conduct a running traverse at the opening for a given period of time. This procedure requires some judgment in pacing the traverse, and it may be necessary to make more than one traverse to achieve a traverse speed that will permit equal velocity weighing over the entire area and completion at an assigned time. The traverse procedure is, in general, more convenient and faster than the fixed-point technique. Comparison of the two techniques has shown the traverse technique to be the more accurate while the fixed-point method is more precise.

- The conditions under which the field tests were conducted do not represent those under which the device was calibrated.
- Errors in averaging in the fixed-point survey may be due to errors in the measurement of the small areas. In the traverse method, errors may result from failure to cover equal distances in the same time interval.
- Measuring the cross-sectional area being evaluated is subject to error.
- The presence of the observer in the test field may influence the readings.
- Variations in velocity across the measurement plane during the period of measurement can affect the results.

Detailed investigations of the systematic errors in using early conventional RVAs with mechanical readout have been performed by Ower and Pankhurst (1977), Swirles and Hinsley (1954), and Teale (1958). Since the vane anemometer is directional, it must be aligned with the plane of the opening being measured, or an error will occur (Fig. 3.19). The magnitude of this error depends on the angle of incidence or yaw. It is evident that one must exceed an angle of 10° before a 1% error in indicated velocity is noted; a 30° yaw will result in a 10% error.

A second systemic error may occur if the traversing velocity is large compared to the true stream velocity being measured. Again, although the Teale (1958) study is restricted to early designs of RVAs, it is obvious from Fig. 3.20 that if one maintains a traversing velocity less than 20% of the true stream velocity, the measurement error will be less than 5%. The 4-in. (10.16-cm) RVA has limited application below 100 fpm (0.51 m/s), so that a traverse velocity of 20 fpm (0.10 m/s) or less ensures minimal error due to traverse speed.

Occasionally, an airflow stream is encountered that pulsates; that is, the air velocity varies with time. Since the RVA has a poor time response due to the inertia of the vane sensor, the correct mean velocity under pulsating flow may not be obtained. Under conditions of sinusoidal flow, the instrument overestimates the true velocity. The error is shown in Fig. 3.21 for two conventional instruments; if the amplitude of pulsation is $\pm 20\%$ of the true mean velocity, the instrument will overestimate the true velocity by less than 1%.

The modified airflow pattern created by the presence of the observer may be significant with the RVA. Mounting the instrument on a rod using the threaded mounting surface available on some instruments can minimize this effect. The required separation distance has not been thoroughly investigated; however, a minimum distance of 2 ft (0.62 m) will usually be adequate.

If used properly, the RVA will permit direct measurement of air velocity in field investigations with an accuracy of $\pm 5\%$ of the true velocity. The RVA does have a bearing suspension that is subject to damage; the lightweight vanes may also be corroded by air contaminants encountered in the field. For these reasons the device should be calibrated periodically. A major fault of the RVA is its poor response at low velocities. Also, if the device is used for measurement of supply and exhaust openings, corrections must be applied for the effect of the grille. These corrections should be validated for the particular grille or register in a laboratory test as shown in Fig. 3.22.

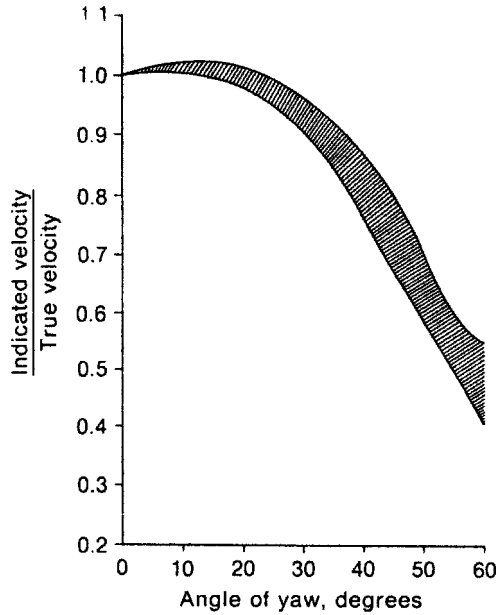


Figure 3.19 Effect of misalignment of rotating vane anemometer on accuracy. If the rotating vane is not aligned normal to the direction of airflow, an error may be noted. Ower has shown this error to be insignificant up to an angle of 20°. The effect of four early RVA designs is depicted here. Data are not available on the new instruments shown in Fig. 3.17; however, it is likely that similar results will be observed. [Adapted from Teale (1958).]

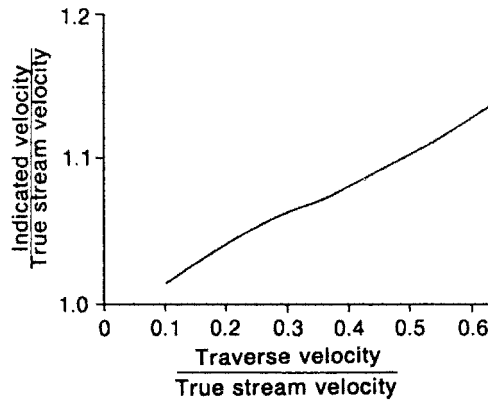


Figure 3.20 Movement of the rotating vane device while traversing a hood opening to determine the average face velocity results in an error. For the conventional Biram-type instrument the error is approximately 10% if the traversing speed is one-half the true air velocity. [Adapted from Teale (1958).]

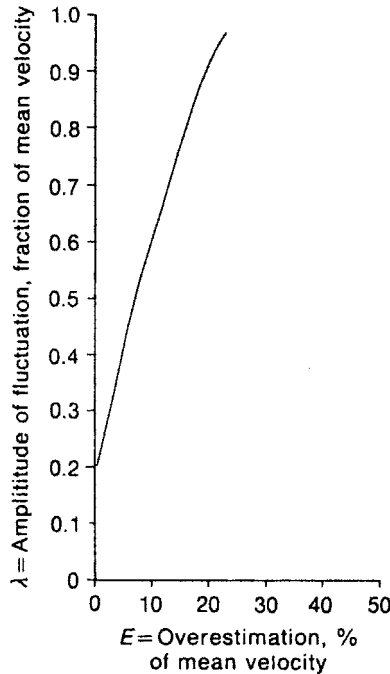


Figure 3.21 Teale has shown that a vane anemometer positioned in a fluctuating stream will give readings higher than the mean speed. The performance of the Biram-type instrument shown in this figure indicates that the amplitude of velocity fluctuations must exceed 50% before errors of 8 to 10% are encountered. This range of fluctuation is rarely encountered in industrial ventilation systems. [Adapted from Teale (1958).]

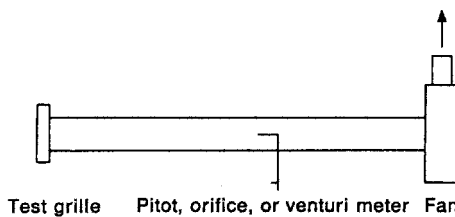


Figure 3.22 If a rotating vane anemometer is used to measure velocity at an HVAC supply or exhaust grille, a correction factor must be applied when calculating airflow. The correction factors available from the manufacturer apply to pressure and suction openings with specific geometry and net area. Frequently, grilles or registers are encountered that do not meet these specifications. If a number of locations must be measured, the correction factor should be evaluated in the laboratory. A Pitot tube traverse can be used to measure a set airflow or an orifice or Venturi meter can be utilized. The product of the velocity at the face of the grille or register measured with the RVA and the gross area is the indicated airflow. The ratio of the actual airflow measured by Pitot-static tube, or flowmeter, and the indicated airflow from the RVA is equal to the correction factor applicable to this specific grille.

3.2.2 Deflecting Vane Anemometers (Velometer)

The sensor for the deflecting or swinging vane anemometer (Velometer) consists of a lightweight vane positioned in a rectangular duct and mounted on a balanced taut-band suspension (Fig. 3.23). Air from the probe passes through the instrument, striking the vane and causing an angular deflection that is proportional to air velocity. The cross-sectional area of the tunnel in which the vane moves expands, providing increased clearance at high velocities.

The original instrument design had a series of probes or fittings, which were attached to the inlet side of the instrument and restricted the airflow by varying degrees. Each fitting had a separate calibration, and the velocity scale for each probe was identified on the dial face. This rather confusing arrangement was changed to a new design with a basic series of three probes, all of which are read on the same scale (Fig. 3.24). With the new design it is not necessary to calibrate each probe for a given instrument.

The principal application of this device is to measure air velocity in the plane of large hood openings using the low-velocity probe (Fig. 3.24*b*). In this configuration the meter has a range of 30–300 fpm (0.15–1.52 m/s). The manufacturer claims an

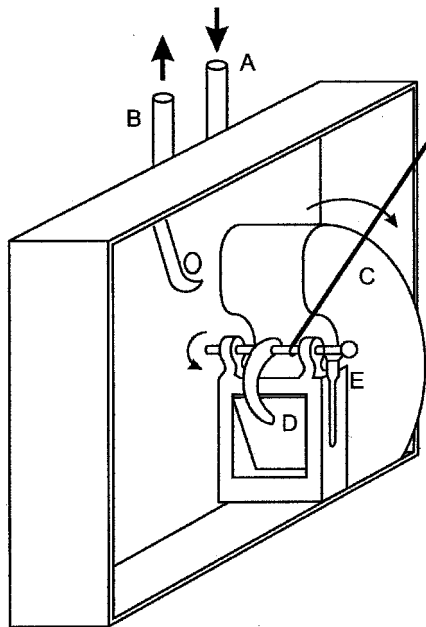


Figure 3.23 Construction of the swinging vane anemometer showing the sensing element. The two probe connections A and B penetrate the instrument case. Probe A is connected to the sensor tunnel casing E, and probe B communicates to the interior of the case. Air moving through probe A strikes vane D, causing a rotation of the counterweighted needle C, which displays the air velocity on the meter face. The air passing through the sensor tunnel exits through probe B.



Figure 3.24 (a) The basic swinging vane instrument (Alnor Model 6000). Applications include (b) a low-velocity probe for air velocity measurements in plane of hood opening or (c) a Pitot probe with a diameter of $\frac{1}{2}$ in. (1.27 cm). Since it does not have the 90° bend of the pitot, it requires only a slightly oversized hole. The advantage of this probe is that the velocity may be read directly from the meter. The device is not a primary standard and requires calibration by a standard Pitot–static tube. Also shown is (d) a probe for measuring delivery from diffusers. By measuring the diffusers throat velocity the delivery can be calculated using the manufacturer's k factor. (Courtesy of Alnor Instrument Company a Division of TSI, Inc.)

accuracy of 15% of full scale. With the low-velocity probe, the cross-sectional area of this instrument is 0.12 ft^2 (0.01 m^2). The instrument cannot be used for small openings, due to the change in effective hood area that occurs and the possible change in calibration due to the airflow geometry.

Other special probes are available for this instrument. A double-opening Pitot–static tube provides the same pressure output for a given velocity as does the standard Pitot–static tube. In effect, the manufacturer has forced the instrument to respond to the basic flow equation of the Pitot–static tube. A probe is also available for evaluating flow from HVAC (heating, ventilation, air conditioning) air supply diffusers. The diffuser throat velocity is measured with this probe, and the noted velocity is multiplied by the diffuser manufacturer's calibration factor to obtain airflow. The proper placement of the probe in the throat is critical for accurate measurements. For extensive balancing of airflow through supply diffusers, the use of the swinging vane anemometer with the canopy device shown in Fig. 3.25 is a more accurate technique. A simple adaptation of the vertical deflecting vane anemometer concept is shown in Fig. 3.26, and a simple horizontal vane deflecting device is shown in Fig. 3.27.

Few data are available on the accuracy and precision of the swinging vane anemometer. The response of the standard instrument has been investigated by Purtell (1979), and



Figure 3.25 Canopy device, that can be positioned over the HVAC diffuser and directs the supply air past a swinging vane instrument. The device is calibrated directly in cfm (m^3/s). This procedure is more accurate than the probe technique, which measures diffuser throat velocity. (Courtesy of TSI, Inc.)



Figure 3.26 A simple and inexpensive adaptation of the swinging vane anemometer designed to monitor face velocity at simple hood openings. (Courtesy of Alnor Instrument Company a Division of TSI, Inc.)



Figure 3.27 Horizontal deflecting vane anemometer. (Courtesy of Bacharach, Inc.)

these studies indicate that the accuracy below 100 fpm (0.51 m/s) is poor. Since these calibrations were done on an earlier instrument they should be used with caution. When used with the low-velocity probe, precise alignment with direction of airflow is not necessary; the deviation from the true velocity is minimal up to 20° . The instrument has a visually fast response time for field application; indeed, one must average readings in pulsating flow fields. The effect of flow pulsation on accuracy of measurement has not been explored. Special correction factors must be utilized for calculation of flow through grilles and registers.

3.2.3 Bridled Vane Anemometers

The sensor of this air-velocity device (Fig. 3.28) is a constrained windmill-type impeller whose angle of rotation is proportional to air velocity. The range of the instrument from 50 to 100 fpm (0.25 to 0.50 m/s) is determined by the spring used to establish the counterrotational torque on the impeller. The device is equipped with a

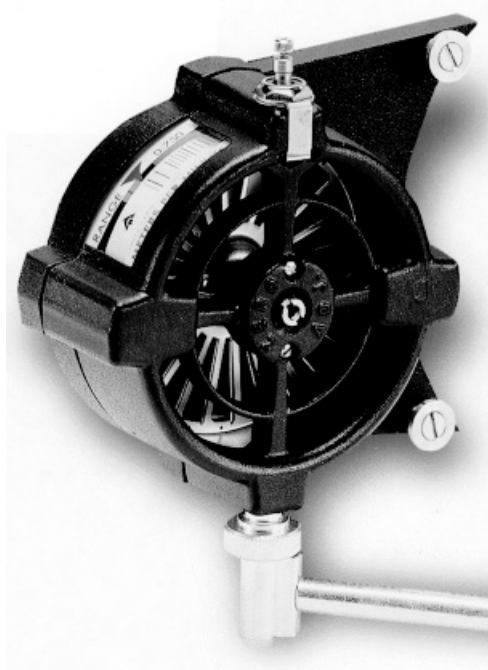


Figure 3.28 The bridled vane anemometer is a convenient device for remote measurement of velocity at grille and register openings using a reach rod. (Courtesy of Bacharach, Inc.)

brake mechanism that fixes the impeller at its maximum angular position to provide an instantaneous reading. The indicated velocity is read directly as the position of a pointer on a scale on the perimeter of the instrument housing. Performance data on this instrument have not been published; however, it is a convenient device for approximate measurements of HVAC grilles and registers.

3.3 HEATED-ELEMENT ANEMOMETERS

The large number of heated-element air velocity sensors now available commercially are based on the original hot-wire anemometry work by King (1914). These devices operate by virtue of the fact that a heated element placed in a flowing airstream will be cooled and the rate of cooling is proportional to the velocity of air movement. The introduction of a variety of heated sensors, including wires, thermistors, thermocouples, and films, coupled with advances in methods of evaluating the cooling rate, have added an important dimension to airflow measurement. These heated-element anemometers have attractive performance at low velocities, a range that is difficult to measure with the mechanical devices discussed in Section 3.2. The basic design and operating features of the family of heated devices can be described by reviewing the hot-wire device. King showed

that the heat loss from electrically heated wires in a moving fluid stream can be described by the following equation

$$H = kT + (2\pi k S \rho d v)^{0.5} T \quad (3.2)$$

where H = rate of heat loss per unit length of wire

d = diameter of wire

T = temperature of wire above ambient air temperature

K = thermal conductivity of fluid

S = specific heat at constant volume of fluid

ρ = density of fluid

v = velocity of fluid

For a given wire operating at the same elevated temperature in the same fluid, this equation becomes

$$H = A + Bv^{0.45} \quad (3.3)$$

where A and B are constants for a given instrument. For a more detailed discussion of this phenomenon, the reader is referred to Ower and Pankhurst (1977).

The simple heated-wire sensor may be a fine platinum or nichrome wire less than 0.01 in. (0.25 cm) in diameter with an operating temperature of 250–700°F (121–370°C), depending on the velocity to be measured. In the original instrument the cooling of the element in the velocity field was measured as a change in resistance of the heated element. In later designs the heated element is maintained at a constant temperature. As heat is lost from the element, additional current is required to maintain it at a constant temperature. The current is monitored as a measure of air velocity, with the normal response shown in Fig. 3.29. To permit the application of these devices over a wide temperature range, a reference sensor shielded from air movement is mounted in the probe.

The simple heated-wire sensor described above provides a powerful tool for velocity studies and is still in wide use today. However, the heated-wire element is fragile and the calibration of the instrument may change as a result of aging of the wire. A more suitable instrument for industrial field studies is the shielded-element device. In this device the wire or other heated element is placed inside small, thin-walled tubing, or a fine-wire coil is coated with a rigid plastic coating. In both cases the sensor is rugged and quite acceptable for field applications. Because of its mass and shielding, this device may have poor response time compared to the simple heated-wire device. Although they are not suitable for resolving rapid changes in velocity required in studies of turbulence, they are quite suitable for industrial ventilation work.

In addition to heated wires, other sensors have been applied to industrial anemometry (Fig. 3.30). One popular approach is a sensor based on the deposition of a metallic coating, often platinum, on an insulating form. The performance of this sensor follows the same basic law described by King and has a response time

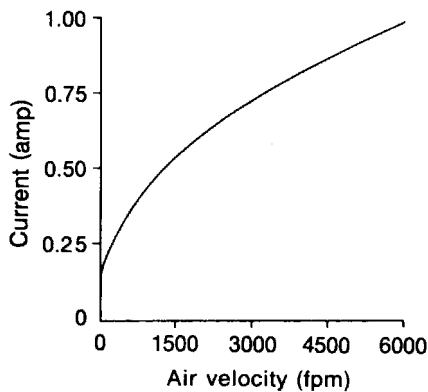


Figure 3.29 Output of a hot-wire device, demonstrating its nonlinear response.

similar to the shielded heated wire. Other instruments utilize thermistors or thermocouples as the sensing agent in a constant-current operating mode. The thermistor sensor heated to 200–400°F (93–204°C) is especially attractive since it has a much greater change in resistance per unit change in temperature than do other sensors. These instruments also utilize a reference junction so that reasonable



Figure 3.30 A simple heated-element anemometer for field use. Available in digital or analog readout and in English (U.S. Customary) or SI units. (Courtesy of Alnor, Instrument Co., a Division of TSI, Inc.)

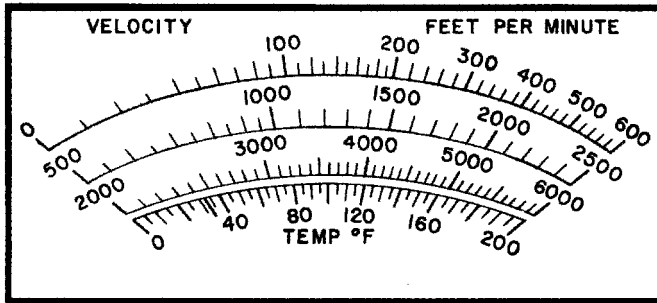


Figure 3.31 Nonlinearity of a heated-element anemometer as shown by the meter display of a standard instrument.

excursions in air temperature will not introduce an error over the range of 20–150°F (4–66°C).

The heated airflow sensors have excellent response at low velocities. With the exception of the heated wire the probes are fairly rugged, although all may be damaged by exposure to corrosive chemicals. The probe output is not linear, and field instruments thus have good sensitivity at low velocities and rather poor sensitivity at high velocities (Fig. 3.31). Linearizing electronics may be obtained, but this is seldom necessary in industrial ventilation fieldwork. Short battery life is the chronic difficulty with all battery-powered systems, including heated anemometers. The probes may or may not be directional, depending on their geometry. As with all airflow measuring devices other than the Pitot–static tube, these devices also require periodic maintenance and calibration.

Given the limitations above, the heated sensor instruments are extremely valuable instruments and are useful in studies of local exhaust ventilation, comfort, heat stress, and HVAC systems.

3.4 OTHER DEVICES

3.4.1 Vortex Shedding Anemometers

If an obstruction is placed in an airflow path, a discrete vortex forms just downstream of the obstruction. The pressure pulse that is formed by the new vortex at one side of the obstruction prevents formation of a vortex on the other side until the initial vortex is downstream. A series of vortices is generated and moves down the “vortex street.” The frequency of vortex generation is a function of air velocity and can be used as the basis of an air-velocity meter.

A number of different design approaches have been considered for a field instrument. In one design the vortex shedding rate is sensed by a thermistor array downstream of the obstruction. Each vortex causes rapid cooling of the heated thermistor, which results in an instantaneous change in resistance with a pulsed signal whose

frequency is directly proportional to air velocity. In another approach placing another obstruction directly after the first stabilizes the vortex shedding phenomena. The vibrations of the second obstruction caused by each individual vortex are sensed by a strain gage in the link between the two obstructions. Again, the vortex frequency is directly proportional to air velocity. A third technique uses an ultrasonic sensing system, which couples excellent sensitivity with a linear response. Although a vortex shedding anemometer is not available for field studies at this time, the field engineer should evaluate any new products of this type because of its many advantages.

3.4.2 Orifice Meters

The orifice meter (Fig. 3.32) is designed as a sharp-plate restriction in the duct and provides a means of accelerating flow and creating a static pressure drop between the upstream static tap and the downstream tap at the vena contracta. The flow through the orifice is proportional to the square root of the orifice pressure differential. The orifice plate can be sized to provide a given pressure drop at the anticipated flow. Unfortunately, the pressure loss across an orifice meter may constitute 40–90% of the orifice pressure differential. Particles and corrosive chemicals transported in many industrial exhaust systems may erode the plate necessitating frequent orifice replacement and calibration. For these reasons the orifice meter is rarely used for flow measurements in general industry exhaust systems; however, it has been noted in nuclear industry glovebox installations.

3.4.3 Venturi Meters

In a Venturi meter, the entrance contraction and the exit expansion are defined by the geometry shown in Fig. 3.33. Because of the gradual contraction and subsequent reenlargement, the conversion from static pressure to velocity pressure and then back to static pressure is accomplished more efficiently than in the orifice meter and the pressure loss is reduced significantly. The Venturi meter, although more efficient than the orifice meter, still has a loss of 10–20% of the Venturi differential pressure and is rarely used in general industry local exhaust ventilation

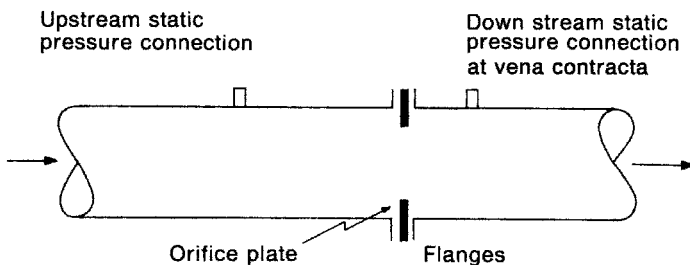


Figure 3.32 Orifice meter for measurement of airflow quantity.

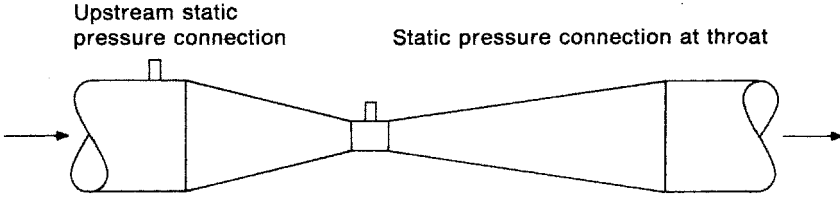


Figure 3.33 Venturi meter for measurement of airflow quantity.

systems, due to its initial cost, maintenance, and operating cost. If either the orifice or venturi meters are considered for field application, they should be constructed following design specifications (ASHRAE, 2001).

3.5 HOOD STATIC PRESSURE METHOD

As described in Chapter 2, one of the major energy losses in a local exhaust ventilation system is the entry loss as the air moves into the hood and duct. Recalling Eq. 2.41, the hood static pressure $p_{s,h}$ measured just downstream of the hood (Fig. 3.34) can be expressed as

$$p_{s,h} = h_e + p_v$$

where p_v is the velocity pressure in the duct and h_e represents the losses attributable to turbulence in the hood and transition (hood entry loss).

If the hood geometry were ideal, turbulent losses would not occur and the hood static pressure would be totally converted to velocity pressure. However, for even the best aerodynamic form possible, there are still turbulent losses. The aerodynamic quality of a hood is identified by the coefficient of entry C_e , defined as the ratio of the actual airflow at a given static pressure at the hood to the theoretical airflow that would occur if the total static pressure were available as velocity pressure

$$C_e = \frac{Q_{\text{actual}}}{Q_{\text{ideal}}} \quad (2.44)$$

$$C_e = \frac{4000A\sqrt{p_v}}{4000A\sqrt{p_{s,h}}} \quad (2.45)$$

$$C_e = \frac{\sqrt{p_v}}{\sqrt{p_{s,h}}} \quad (2.46)$$

and rearranging Eqs. 2.44 and 2.45 yields

$$Q_{\text{actual}} = 4000A_h\sqrt{p_{s,h}} \times C_e \quad (3.4a)$$

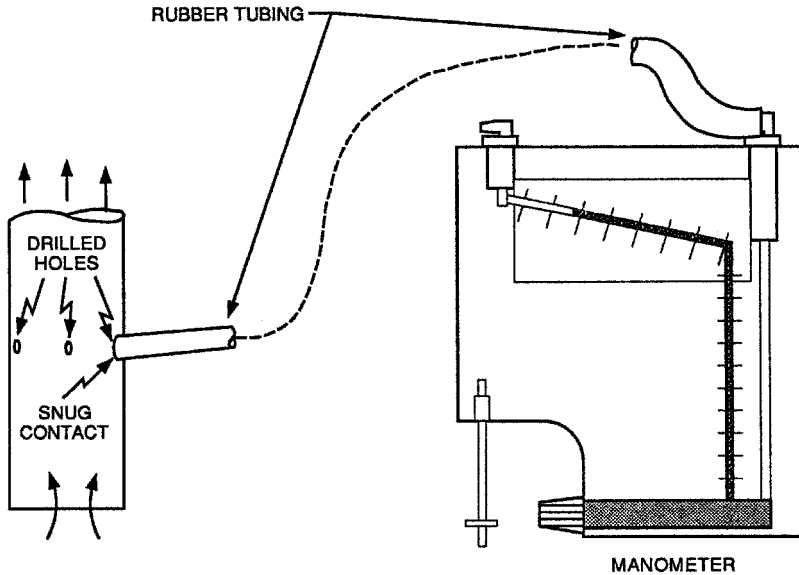


Figure 3.34 Hood static pressure method. In using this technique in the field, care must be given to the correct placement of the static tap. A deburring tool should be used to prepare the tap for measurement. The use of screens at the hood face to prevent debris from entering the hood confuses the measurement. The screen presents an element whose resistance varies as the screen plugs. Since this resistance is not a part of the entry loss factor, it is not included in the coefficient of entry. If the screen cannot be cleaned, it should be removed. Frequently, there is an elbow or other fitting directly after the hood. This fitting may be a part of the normal hood geometry, and if so, it is included in the published coefficient of entry. If not, a correction must be made in the flow rate calculations to account for this added resistance to flow.

Or in SI units

$$Q_{\text{actual}} = 1.29 A_h \sqrt{p_{s,h}} \times C_e \quad (3.4b)$$

Values of C_e have been developed for many hoods, as shown in the *Ventilation Manual*. It follows that the airflow through a standard hood with an assigned coefficient of entry can be calculated by the simple measurement of the duct area and the static pressure in the duct downstream of the hood. This technique is reasonably accurate for standard hoods and can be accomplished in a fraction of the time of other techniques. It is especially useful for measuring airflow through a group of identical hoods, such as a line of grinding or buffing wheels.

The principal difficulty with this system is the accuracy of the C_e values available to the field engineer. The published values for simple hoods such as a sharp entry or a flanged opening are quite accurate and can be used without reservation. For more complex hoods, such as grinding wheel hoods, small differences in construction may modify published entry loss values. In such cases, if the application warrants it, the hood may be tested in the laboratory to validate the C_e value. In the field, one can

determine the airflow rate by a Pitot–static tube traverse, note the duct area, measure the static pressure at the hood, and solve for C_e .

3.6 CALIBRATION OF INSTRUMENTS

With the exception of the Pitot–static tube, all air velocity measuring devices discussed in this chapter require periodic calibration. Instruments should be checked when received from the manufacturer, calibrated at regular intervals, and recalibrated when abused in the field.

The required frequency of calibration depends on both the history of instrument use and the criticality of the application. Shipment of an instrument from a central laboratory to various plants may subject the instrument to serious shock in handling. Instruments shipped as luggage are also subjected to vibration and shock. Industrial applications in hostile chemical environments may damage the basic suspension of a mechanical device or the probe and associated electronics of heated devices. Dusty environments such as foundries or mineral crushing plants are especially harmful to mechanical devices. If several persons use the instruments, the variation in the knowledge and experience of the practitioner must be considered in establishing a time schedule for calibration.

Given this range of applications, how often should such devices be calibrated? If the device is used infrequently (e.g., once a month) and by a single trained person, annual calibration is probably adequate. If the device is used frequently (e.g., once a week), if the environment is harsh, if several persons use the instrument, or if the device is used for critical applications, monthly calibration may be required.

It is difficult for the occasional user of an instrument working in an isolated industrial setting to calibrate anemometers. The devices may be returned to the manufacturer or a consulting laboratory, but this takes time and the instrument may be needed at the plant site. A backup instrument may be the answer to this dilemma. If a large number of instruments must be calibrated frequently and short turnaround is critical, it may be worthwhile to purchase a calibration tunnel facility of the type shown in Fig. 3.35. A number of manufacturers now offer portable calibration units. Some of these calibration test sections are quite small and are acceptable for thermoanemometer probes but not for devices of large cross section such as rotating vane anemometers and swinging vane anemometers.

In an industrial plant setting the user may wish to fabricate an in-plant calibration facility as described in the *Ventilation Manual* (ACGIH, 2001). These facilities use either a variable-speed or fixed-speed fan with a bypass to move air through initially through a large-area test tunnel and then directly to a small-area duct section. In this approach large instruments can be placed directly in the tunnel section and instruments with small sensors such as thermal anemometers can be tested either at low velocities in the tunnel section or the duct section for higher velocities. Conventionally, a Venturi meter calibrated with a Pitot–static tube is placed between the duct test section and the fan to monitor airflow and to establish the desired velocity in the test sections. This type of calibration system can also be used



Figure 3.35 A calibration tunnel designed for small probes such as heated elements. (Courtesy of TSI, Inc.)

to determine the calibration factor for swinging vane anemometers probes used to measure the delivery from HVAC diffusers (Section 3.3.2) and the coefficient of entry for hoods tested by the hood static pressure technique (Section 3.5).

Every effort should be made to measure air velocity accurately. Manufacturer claims of accuracy of $\pm 2\%$ of full scale are probably unrealistic for field instruments. Since design calculations are usually not better than $\pm 5\%$, an accuracy of $\pm 5\%$ is sufficient for a field instrument.

3.7 OBSERVATION OF AIRFLOW PATTERNS WITH VISIBLE TRACERS

This chapter is devoted to the measurement of air velocity, airflow rate, and system pressures with a variety of instrumental techniques in a field setting. Although these methods are critical in the evaluation of exhaust ventilation systems, practitioners frequently complement these procedures with visual tracers to qualitatively define the velocity, direction, and patterns of air movement. In the hands of an experienced ventilation engineer, these tracers offer valuable insight into the contaminant release and its transport through the workspace.

3.7.1 Tracer Design

In select cases where small particles are released from the operation, the generated contaminant can be used to track air movement due to the scattering of light by small particles in the dust cloud. This field technique, shown in Fig. 3.36a, although rarely practiced in the United States, has been used with great success by investigators in the United Kingdom to assist in the design of exhaust hoods for the ceramics industry and in other applications (BOHS, 1987) (HSE, 1997). If care is taken in setting up the viewing station, the dust release pattern and the movement of air conveying the dust to the workplace are clearly portrayed as shown in Fig. 3.36b.

This dust lamp procedure is not effective for all particle clouds. For these particle releases and for most gases and vapors, one must rely on visual tracers released by the investigator. The ideal tracer is one that will provide a persistent, well-defined, visible track of air movement using simple equipment that can be easily set up in the field at low cost. Also the tracer must not present a health hazard to workers nor interfere in any way with product manufacture and quality.

The tracers, which can be released and followed visually, have been evaluated by Maynard et al. (2000) as noted in Table 3.6. The most widely used tracers for small release rates are the “smoke tubes,” a misnomer since the released tracer is a fume, not smoke. In one design, a solid substrate packed in a glass tube is coated with an oleum reactant. Other manufacturers use stannic chloride and titanium tetrachloride as the reactant. In all cases a simple squeeze bulb passes ambient air containing water vapor over the coated granules, releasing a dense white cloud consisting primarily of either sulfuric or hydrochloric acid fume depending on the reactant design. Studies of a stannic chloride based tube (Lenhart and Burroughs, 1993) indicate a fume median diameter of 0.3–0.6 μm with a geometric standard deviation of approximately 2.0. The persistent white cloud from these tubes is a respiratory irritant and corrosive to metal. These properties limit its use somewhat, although Jensen et al. (1998) have shown that the stannic chloride tube can be used prudently in a hospital environment to explore negative-pressure zones and airflow patterns without exceeding exposure values for the corrosive particulate.

Four additional tracers worthy of comment were not considered by Maynard et al. (2000). Dry ice–water is used by the semiconductor industry where particle release in the cleanrooms of the fabrication bays is not permitted for product quality reasons (SEMI, 2000). Although a very simple procedure, the technique requires the storage of dry ice and the generation rate of the tracer is difficult to control by the investigator. The semiconductor industry also uses a water fog generator for airflow pattern mapping. A third tracer, not covered in Table 3.6, is Borozin powder. In this system a hand-powered gun releases a highly visible cloud of zinc stearate. A fourth technique has been introduced to provide a smoke tube that is not a respiratory irritant (Drager, 1995). An ampoule containing a glycerol-base material liquid is heated in a battery-powered gun and a visible smoke is released. The manufacturer states the unit is designed for the HVAC practitioner to help determine (1) the direction and dispersion of air currents, (2) the relative speed of the air movement, and (3) the pressure differential between spaces.

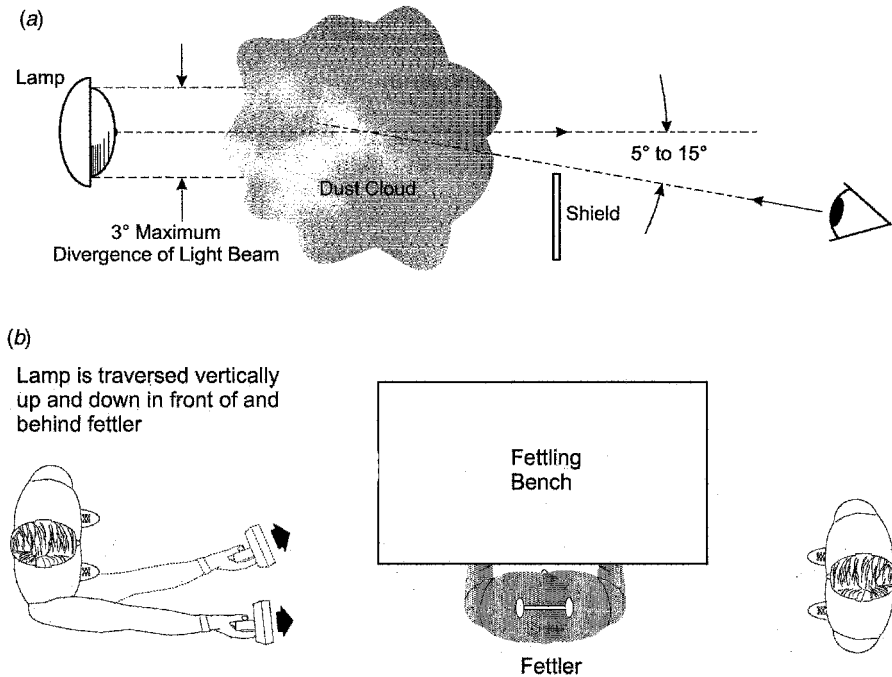


Figure 3.36 (a) The principle of operation is as follows. A bright parallel beam of light projects through the area where the investigator suspects a dust cloud is present. The observer shields his or her eyes from the main beam of the light by means of a piece of card held in position with a floor stand, or by using the worker's body or a convenient piece of machinery as a shield. The dust cloud should be observed looking up the beam toward the source of illumination and against a darker background, such as a portable curtain or large piece of black card. Sunlight and other sources of bright light present need to be suppressed and the aim should be to observe at some 5–15° off the centerline of the beam to pick up the most intense scattering. Dense clouds of some size and concentration are made visible with the dust lamp under normal lighting conditions but to see small clouds, for instance, leaks, or trace the extended movement of a cloud as much as possible, the background ambient lighting needs to be suppressed. Simply turning off the lights, blocking out light from immediately adjacent windows, and using a black curtain as a dark background are often sufficient to get good observations, although extreme measures such as turning off all the lights, blocking all the windows, or perhaps returning on the night shift may be called for on occasions to get maximum sensitivity. As with the use of smoke tracers mentioned earlier, use of a video camera greatly enhances the value of this technique. (BOHS, 1987, Courtesy of British Occupational Hygiene Society.) (b) A pedestal grinder with poor local exhaust ventilation demonstrates the use of the dust lamp to show the movement of the dust cloud. The grinder is working on firebrick to intensify the forward light scattering from the escaping dust. (BOHS, 1987, Courtesy of British Occupational Hygiene Society.)

In the conclusion of their comprehensive review Maynard et al. (2000) state, "Until a viable alternative is designed for the smoke tube it remains the most versatile choice for routine use in the workplace to monitor airflow patterns and assess control."

In applications where high tracer generation rates are required, such as tracking the reentry of contaminants from exhaust stacks, a variety of candles and canisters

Table 3.6 Visual Tracers for Observation of Airflow

Technique	Advantages	Disadvantages
Smoke tubes	Simple method; inexpensive; good for low-velocity localized flows	Irritant, toxic, corrosive smoke; low yield
Smoke pellets	Inexpensive and suitable for some workplace applications	Uncontrollable, acrid smoke; not intrinsically safe
Smoke canisters	Simple operation; high yield	Uncontrollable smoke generation; long dispersal time
Ammonium chloride	Simple smoke generation; potentially highly controllable	Corrosive, toxic precursors; precursor carryover possible
Metallic chlorides	Simple smoke generation method	Corrosive substance; toxic smoke not suitable for outside cabinets
Heated-element smoke generator (theatrical)	Inexpensive to run; high yield; nontoxic smoke (vegetable oils or glycerol/water-based mixtures)	Difficult to control; unsuitable for small-scale air movements; long dispersal times; not portable
Heated-element smoke generator (laboratory)	Inexpensive to run; high yield; degree of control	Not suitable for occupied workplaces; acrid smoke (mineral oils); highly specialized; not portable
Heated-element smoke generator (portable)	Nontoxic smoke (vegetable oils or glycerol/water-based mixtures); portable, detectable	Potential problems in the field with blockage and battery charge; not as compact as a smoke tube
Natural density bubbles	Nontoxic tracer	Expensive and bulky equipment; not portable; bubbles not as visible as some smokes
Water mist (ultrasonic nebulizer)	Nontoxic tracer	Expensive and bulky equipment; not portable; bubbles not as visible as some smokes
Water mist (pneumatic nebulizer)	Nontoxic tracer	Bulky equipment; not portable; bubbles not as visible as some smokes
Dry ice–water	Nontoxic; suitable for semiconductor facilities; no residual and no particles formed	Procurement of dry ice may be difficult; uncontrollable generation rate
Borozin powder	Designed for use with a powder gun to generate a cloud of zinc stearate that is highly visible	Limited generation rate; requires special gun

Source: Adapted from Maynard et al. (2000).

and smoke generators are available. Close coordination with production, facilities engineering and the fire authorities is necessary if these devices are used to ensure the tests can be conducted safely and will not be disruptive to employees and neighbors. As noted above, the tracer should also be cleared with production to ensure that product contamination does not occur.

3.7.2 Application of Visible Tracers

Design of Ventilation System. In the initial design phase of a local exhaust ventilation system, visual tracers are helpful in identifying the contaminant release point and the dispersal dynamics of the contaminant. Critical assessment of the release points is necessary to ensure that the proposed hood design and its placement will provide an opportunity to capture the contaminant at a reasonable airflow while minimizing physical interference with the worker.

Direct observation of the characteristics of the release may also be helpful to the designer in the choice of hood type. If the contaminant release is both compact and directional, as in the case of a metal furnace operation with a buoyant plume, one may take advantage of the effectiveness of a receiving hood. If an exterior hood is chosen, the discharge of a blowing airstream from a man cooler or a HVAC system directly at the hood position can be disruptive. A tracer study may help define the direction and impact of such drafts on the collection efficiency of the planned hood, and approaches such as using baffles can be considered to reduce the impact of the draft.

Finally, studies have shown that the position of the worker at the hood may result in the formation of vortex eddies downstream of the worker resulting in contaminant loss from the hood (Flynn et al., 1991). If recognized in the predesign tracer studies, changes in workstation layout may be devised to minimize this effect.

Acceptance of a New System. Once a system is installed and before detailed velocity and airflow measurements are conducted as a basis for acceptance by the plant, a visual tracer study is common practice. As an example, a preliminary tracer study on a plating tank equipped with lateral slot exhaust showed the system did not provide adequate capture velocity at the most distant contaminant release point. This “quickie” study showed that the fan had been wired incorrectly and as a result the fan rotation was backward and the airflow was approximately one third the design value. Discovery of this defect early in the evaluation stage eliminated a time consuming series of Pitot-static tube traverses.

Education. The value of visual tracers in the education of the worker in the proper use of a ventilation system is one tracer application that is frequently overlooked. Industrial hygienists are well acquainted with the difficulty in instructing welders in the proper use of portable exhaust hoods (elephant trunks) used for control of welding fume. Smoke tracers can be used to show the welder that the “sphere of influence” of a portable hood is limited and the hood will work effectively only if the welder locates the exhaust hood close to the arc as he moves along the weldment.

Maintenance. A continuing problem in granular crushing plants is the proper installation and maintenance of the multiple exhausted enclosures at the conveyor-belt transfer points. The physical pounding these hoods take so frequently results in leakage at seams and fittings. The smoke tube is an excellent way to periodically check the integrity of all seams as one part of a well-designed maintenance program.

The reentry of contaminants in an exhaust stream discharged at roof level to an air supply system is one of the most difficult problems to solve in laboratory and industrial settings. In this case, capture of 100% of the tracer is achieved by releasing it deep inside the hood suspected to be the source of the reentry contaminant. A roof observer can visually track the discharge plume from the stack to identify the offending air inlet. If the trouble spot is located, the exhaust and entry ports must be decoupled in some way (see Chapter 15).

A critical control in hospitals, laboratories, and industrial cleanrooms is the maintenance of differential pressures across the facility to prevent the flow contamination into or out of critical zones. In some cases these zone pressures are monitored continuously by instrumentation, in other facilities visual tracers are used weekly to ensure compliance.

Air Velocity. Rarely can smoke tracers be used to approximate the velocity of movement, but this can be done in mines with straight runs of roughly consistent cross-sectional area. A small pulse of tracer is released at an initial point; knowing the area of the passageway and the time for the tracer to traverse a measured distance, one can calculate air velocity and airflow rate.

LIST OF SYMBOLS

a	duct radius
C_e	coefficient of entry
D	duct diameter
d	wire diameter
H	heat loss
h_e	hood entry loss
$p_{s,h}$	hood static pressure
p_v	velocity pressure
Q	airflow
r	radius at measurement point
S	specific heat of fluid
T	temperature above ambient
V	average velocity
v_r	velocity at radius, r
v_c	velocity at duct centerline
ρ	density (mass/volume)

REFERENCES

- Associated Air Balance Council. *National Standards*, 5th ed., Volume Measurements, AABC, Washington, DC, 1989.
- Airflow Inc., Technical Topic I 004, *Traverse Techniques for Air Duct Measurement*, High Wycombe, Buckinghamshire, UK, 1997.
- American Conference of Governmental Industrial Hygienists (ACGIH), Committee on Industrial Ventilation, *Industrial Ventilation: A Manual of Recommended Practice*, 24th ed., ACGIH, Cincinnati, OH, 2001.
- American Society of Heating, Refrigeration and Air Conditioning Engineers (ASHRAE), *Handbook of Fundamentals*, ASHRAE, Atlanta, 2001.
- British Occupational Hygiene Society (BOHS), Technical Guide No. 7, *Controlling Airborne Contaminants in the Workplace*, H&H Consultants Ltd., Leeds, UK, 1987.
- British Standards Institute, *Methods for the Measurement of Fluid Flow in Closed Conduits—Methods Using Pitot-Static Tubes*, B.S. 1042, Section 2.1, BSI, London (identical to ISO 3966-977), 1983.
- Flynn, M. R., and C. T. Miller, "Discrete Vortex Methods for the Simulation of Boundary Layer Separation Effects on Worker Exposure," *Ann. Occup. Hyg.* **35**:35–50 (1991).
- Goodfellow, H., and E. Tahti, eds, *Industrial Ventilation Design Guidebook*, Academic Press, San Diego, CA, 2001.
- Guffey, S. E., "Simplifying Pitot Traverses," *Appl. Occup. Environ. Hyg.* **5**:95–100 (1990).
- Guffey, S. E., and D. W. Booth, "Comparison of Pitot Traverses Taken at Varying Distances Downstream of Obstructions," *Am. Ind. Hyg. Assoc. J.* **60**:165–174 (1999).
- Health & Safety Executive, *The Dust Lamp, a Simple Tool for Observing the Presence of Airborne Particles*, HSE Books, Suffolk, UK, 1997.
- Jensen, P. A., C. S. Hayden, G. E. Burroughs, and R. T. Hughes, "Assessment of the Health Hazards Associated with the Use of Smoke Tubes in Healthcare Facilities," *Appl. Occup. Env. Hyg.* **13**(3):172–176 (1998).
- King, L. V., "On the Convection of Heat from Small Cylinders in a Stream of Fluid," *Phil. Trans. Soc.* **A214**:373 (1914).
- Klaassen, C. J., and J. M. House, "Equal Area vs. Log Tchebycheff," *HPAC Eng.* 31–35 (March 2001).
- Lenhart, S. W., and G. E. Burroughs, "Occupational Health Risks Associated with the Use of Irritant Smoke for Quantitative Fit Testing of Respirators," *Appl. Occup. Env. Hyg.* **8**(9):745–750 (1993).
- Maynard, A., J. Thompson, J. R. Cain, and B. Rajan, "Air Movement Visualization in the Workplace: Current Methods and New Approaches," *Am. Ind. Hyg. Assoc. J.* **61**:51–55 (2000).
- Ower, E., and R. C. Pankhurst, *The Measurement of Air Flow*, Pergamon Press, Oxford, 1977.
- Purtell, L. P., *Low Velocity Performance of Anemometers*, National Bureau of Standards, Report No. NBSIR 79-1759, Washington, DC, 1979.
- Semiconductor Equipment and Materials International (SEMI), *Book of Semi Standards 0200, Facility Standards and Safety Guidelines Volume*, SEMI, Mountain View, CA, 2000.
- Swirls, J., and F. B. Hinsley, "The Use of Vane Anemometers in the Measurement of Air Flow," *Trans. Inst. Min. Eng.* **113**:895 (1954).

Teale, R., "The Accuracy of Vane Anemometers," *Colliery Eng.* 239–246 (June 1958).
 Winternitz, F. A. L., and C. F. Fischl, "A Simplified Integration Technique for Pipe Flow Measurement," *Water Power* 9:225 (1957).

MANUFACTURERS OF AIRFLOW MEASURING INSTRUMENTS

Airflow Developments Ltd., Lancaster Road, High Wycombe, Buckinghamshire HP 12 3QP, UK
 (www.airflow.com).
 Alnor Instrument Company, 7555 North Linder Avenue, Skokie, IL 60077, (800) 424-7427
 (www.alnor.com).
 Bacharach Inc., 621 Hunt Valley Circle, New Kensington, PA 15068-7074, (800) 736-4666
 (www.bacharach-inc.com).
 Davis Instrument Inc., 4701 Mount Hope Drive, Baltimore, MD 21215, (800) 368-2516
 (www.davis.com).
 Dwyer Instruments, Inc., P.O. Box 373, Michigan City, IN 46360 (www.dwyer-inst.com).
 Extech Instruments, 285 Bear Hill Road, Waltham, MA 02451, (781) 890-7440
 (www.extech.com).
 Shortridge Instruments, Inc., 7855 E. Redfield, Scottsdale, AZ 85260, (480) 991-6744
 (www.shortridge.com).
 TSI, Inc., 500 Cardigan Road, P.O. Box 64394, St. Paul, MN 55164, (800) 777-8356
 (www.tsi.com).

MANUFACTURERS OF SMOKE TUBES

Mine Safety Appliances, Co., *Ventilation Smoke Tubes* (5645), Mine Safety Appliances Co.,
 Pittsburgh, PA, 1994.
 National Draeger, Inc., *Air Current Tubes* (CH25301), National Draeger, Inc., Pittsburgh, PA,
 1995.
 Sensidyne, Inc., *Air Flow Indicator Tubes* (0501), Sensidyne, Inc., Pittsburgh, PA, 1993.

PROBLEMS

Note: Problems 3.1–3.3 require reference to the *Ventilation Manual*.

- 3.1** Compute the airflow in a 14-in. round duct based on the average duct velocity determined from a 10-point Pitot–static traverse. The individual velocity pressures noted as one progressed across the duct were 07, 0.11, 0.17, 0.22, 0.39, 0.41, 0.38, 0.29, 0.13, and 0.11 in. H₂O.
- Identify the insertion depths for the 10-point traverse.
 - From the given velocity pressure data, calculate the velocity at the individual points and the duct average velocity.
 - Calculate the airflow in the duct.

Answers:

- (a) Measurement points based on a log-linear traverse: 0.27, 1.08, 1.08, 2.14, 3.04, 5.05, 7.0, 8.95, 10.96, 11.9, 12.9, and 13.7 in.
- (b) The velocities corresponding to the 10 velocity pressures are 1070, 1328, 1651, 1879, 2501, 2564, 2469, 2157, 1444, and 1328 fpm. The average velocity is 1839 fpm.
- (c) The airflow in the duct is 1960 cfm.

- 3.2** Compute the airflow in a 356-mm round duct based on the average duct velocity determined from a 10-point Pitot-static traverse. The individual velocity pressures in pascals noted as one progressed across the duct were 17.4, 27.4, 42.3, 54.8, 97.1, 102.1, 94.7, 72.2, 32.4, and 27.4
- (a) Identify the insertion depths for the ten point traverse.
 - (b) From the given velocity pressure data calculate the velocity at the individual points and the duct average velocity.
 - (c) Calculate the airflow in the duct.

Answers:

- (a) Measurement points in millimeters based on a log-linear traverse: 9, 29, 52, 81, 122, 234, 276, 304, 327, and 347.
- (b) The velocities in meters per second corresponding to the 10 velocity pressures are 5.4, 6.76, 8.41, 9.57, 12.74, 13.06, 12.57, 10.98, 7.35, and 6.76. The average velocity is 9.36 m/s.
- (c) The airflow in the duct is 0.93 m³/s.

- 3.3** A hood static pressure measurement is used to determine the airflow through a simple hood. The duct has a diameter of 12 in., and the coefficient of entry of the hood is 0.60. The hood static pressure is 1.6 in H₂O. What is the airflow in cfm?

Answer: 2384 cfm

- 3.4** A hood static pressure measurement is used to determine the airflow through a simple hood. The duct has a diameter of 60 cm, and the coefficient of entry of the hood is 0.72. The hood static pressure is 600 Pa. What is the airflow in m³/s?

Answer: 6.43 m³/s

- 3.5** Which of the following instruments measures time averaged velocity?
- (a) Rotating vane anemometer
 - (b) Pitot-static tube
 - (c) Swinging vane anemometer
 - (d) Thermoanemometer

- 3.6** Which of the following instruments does not require periodic calibration in normal use?
- (a) Rotating vane anemometer
 - (b) Pitot–static tube
 - (c) Swinging vane anemometer
 - (d) Thermoanemometer
- 3.7** Which of the following instruments is not appropriate for measuring the face velocity of a laboratory chemical hood?
- (a) Rotating vane anemometer
 - (b) Pitot–static tube
 - (c) Swinging vane anemometer
 - (d) Thermoanemometer
- 3.8** Which of the following instruments would you use to measure airflow through a 4-in.-diameter duct where the velocity is likely to be less than 500 fpm? Why?
- (a) Rotating vane anemometer
 - (b) Pitot–static tube
 - (c) Swinging vane anemometer
 - (d) Thermoanemometer
- 3.9** Draw a sketch of a Pitot–static tube and explain its principle of operation. What is its primary advantage in making velocity measurements? What is its primary disadvantage?

GENERAL EXHAUST VENTILATION

General exhaust ventilation (GEV), also known as *dilution ventilation*, differs from *local exhaust ventilation* (LEV) in the manner in which the contaminants are removed from the workplace as well as the equipment employed. As discussed in Chapter 1, LEV is based on the principle of contaminant collection and removal at the emission source, thereby preventing it from entering the internal building environment. In practice, complete capture and removal is rarely achieved with LEV, resulting in partial release into the workplace air. General ventilation relies on *dilution* to minimize contaminant concentrations. As workplace air is removed by mechanical systems, it is replaced by outside air entering the building, either through replacement-air systems or simply through openings in the building. As this clean air enters the workplace, it mixes with and dilutes the contaminated air, resulting in lowered concentrations. In designing or evaluating a GEV system, it is assumed that all the material released from the process will enter the workplace air. Therefore, a sufficient quantity of clean air must be introduced to dilute the concentration to an acceptable level.

The primary element in a general ventilation system is an exhaust fan or blower, usually a propeller-type unit mounted in the ceiling or wall. A GEV system does not include hoods and extensive *exhaust* ducting, although the system for supplying replacement air may be quite sophisticated. Replacement air is often provided by *natural ventilation*, which is simply air movement through openings in the building shell (windows, cracks, or roof ventilators) driven by pressure and thermal differences as well as by wind. Rather than relying on the uncontrolled infiltration of replacement air, equipment capable of providing clean, conditioned air through properly designed

and positioned ducts and diffusers should be included. The design of appropriate replacement-air systems is covered in Chapter 12.

The basic concept governing general exhaust ventilation design is that sufficient air must be provided to prevent the contaminant concentration from exceeding a specified “unsafe” level at any location at which a person could be exposed. This design must incorporate knowledge of

- Physical properties of the contaminant
- Contaminant generation rate
- Health hazard guidelines (e.g., threshold limit value)
- Relative positions of contaminant generation points, work areas, and air supply and exhaust points
- Existing ventilation (natural and mechanical)

One common use of general exhaust ventilation is to prevent the accumulation of flammable gases or vapors at concentrations that would represent a hazardous condition. For these situations, the “safe” concentration is usually specified as 10% of the *lower flammable limit* (LFL) of the vapor in question. Because this concentration (10% of LFL) is nearly always well above any health hazard guidelines (e.g., threshold limit values, permissible exposure limits, maximum allowable concentrations), this approach is restricted to areas where worker exposure would be brief and intermittent, such as drying ovens and storage tanks. The method can also be employed in storage rooms as well as production areas to prevent vapor buildup in the event of a leak or spill.

4.1 LIMITATIONS OF APPLICATION

General exhaust ventilation should be considered as an acceptable method of environmental workplace control only after gaining a thorough understanding of both the situation to be controlled and the limitations of GEV. Often, one or more factors will preclude the use of general ventilation. An initial consideration is the *physical nature* of the material. Is it present as a gas, vapor, or particulate (dust, mist, or fume)? General ventilation is usually not considered appropriate for the control of particulate contaminants, for a number of reasons. Because air velocities associated with general exhaust are low, large particles will not be transported efficiently from their point of generation to an exhaust point; they are likely to settle out and present a housekeeping problem. A second limitation is that the proper design of a GEV system requires reasonable knowledge of the contaminant generation rate, a parameter that is often difficult to determine for processes producing particulate emissions. Third, many processes that generate particulate emissions do so on a sporadic basis, so that the generation rate, even if known, is not constant. Unless the GEV system is designed to handle the peak emissions, occasional excursions above the target concentration will occur. The final and most

important reason is that particulate contaminants are often produced and released in a small area, making it much more desirable, for both health and economic reasons, to use local exhaust ventilation.

These arguments do not necessarily apply to gaseous contaminants. Nearly all gases and vapors disperse homogeneously in air and so move with the air through the workplace; they do not “settle out” at low air velocities. Second, the contaminant generation rate can often be determined using simple mass balance calculations. In a number of processes, particularly continuous ones, vapors are generated at known and fairly constant rates. Such processes might also involve contaminant release over a large area. For example, a material applied to a product at one point in the manufacturing process may continue to be a source of vapors after removal from the point of application. A solvent-based paint sprayed on a workpiece will continue to dry after it is removed from the locally exhausted spray booth. The evaporating solvents from such processes may require additional control by general exhaust ventilation if they are not controlled adequately by an LEV system in the drying area.

One method for estimating contaminant release rates is to determine the “loss” of material during a time period and assume that all of this loss reflects evaporation into the workplace. Consider, for example, an electroplating shop in which $\frac{1}{2}$ gallon of trichloroethylene (TCE; density = 1.5 g/ml) must be added to a continuously operating wet degreaser every 8-h shift to account for solvent loss. In this shop, local exhaust ventilation is not used to control the degreaser emissions. Because concentrations are most often expressed in metric units, the first task is to convert gallons of TCE into milligrams:

$$m = \left(\frac{1}{2} \text{ gal}\right) \left(3785 \frac{\text{ml}}{\text{gal}}\right) \left(1.5 \frac{\text{g}}{\text{ml}}\right) \left(1000 \frac{\text{mg}}{\text{g}}\right)$$

$$= 2.8 \times 10^6 \text{ mg}$$

Next, determine the loss rate by averaging the loss over the 8-h workshift:

$$\frac{m}{t} = \frac{2.8 \times 10^6 \text{ mg}}{480 \text{ min}} = 5800 \frac{\text{mg}}{\text{min}}$$

For this degreaser, operating continuously, the average generation rate of TCE would be 5800 mg/min.

Given that the contaminant can be efficiently conveyed by slow-moving air, that the generation rate is known and stable, and that the area over which the material is potentially released is quite large and thus ill suited to LEV, the toxicity of the material in relation to its generation rate remains to be considered. How much air will be necessary to reduce the concentration to a safe level? Is it feasible to remove, and supply, this quantity of air? These questions can be answered with the following quantitative approach to predicting airborne concentrations.

4.2 EQUATIONS FOR GENERAL EXHAUST VENTILATION

To facilitate calculations using equations for predicting GEV performance, several simplifying assumptions must be made.

- There is perfect mixing in the room.
- The generation rate is constant.
- The dilution air contains negligible amounts of the contaminant.
- The contaminant is introduced into the workplace solely through process generation.
- The contaminant is removed from the workplace solely through general exhaust ventilation.

The first assumption, that of perfect mixing, applies both spatially and temporally. Perfect mixing means that when the contaminant is released, it completely and immediately mixes throughout the room. It means that the replacement air completely and immediately mixes, as well. Although this, as well as the other assumptions, can never be satisfied in real-life conditions, appropriate adjustments can be made to the equations describing the ideal case to accommodate most deviations. In practice, while the problem of imperfect mixing creates dilemmas for the designer in calculating the system capacity, the concentration gradients can actually be used to optimize the effectiveness of the GEV system.

To calculate the airborne concentration C of a substance as a function of time t , the generation rate G , the ventilation rate Q , and the room volume V (Fig. 4.1) must be known or estimated. Any change in concentration ΔC during a time period Δt is due to addition of material to the room air through process generation and/or removal

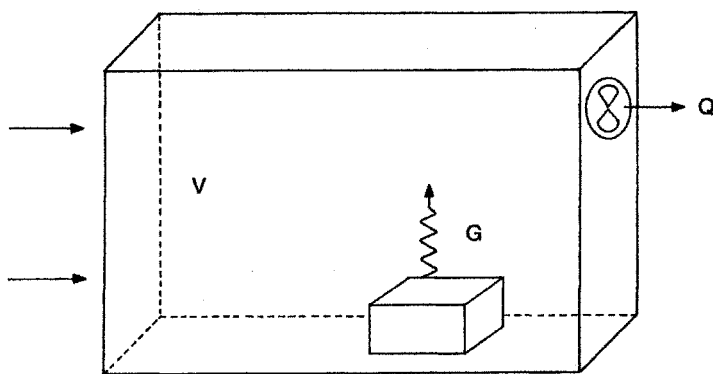


Figure 4.1 The workplace is represented as a simple box, with a single process generating contaminants at a mass rate G . The volume of the room is V and air is being removed with the general exhaust system at a volumetric rate Q . No replacement-air system is shown, so it is assumed that natural infiltration is providing the replacement air.

of material by exhaust ventilation. The amount of material introduced during the time period Δt is equal to $G \Delta t$, while the amount removed is $QC \Delta t$. Thus the net change in the total amount of contaminant present in the space ΔM is

$$\Delta M = G \Delta t - QC \Delta t \quad (4.1)$$

This change can also be expressed in terms of a change in the air concentration ΔC by dividing both sides of the equation by the volume V :

$$\begin{aligned} \Delta C &= \frac{\Delta M}{V} \\ &= \frac{G \Delta t}{V} - \frac{QC \Delta t}{V} \end{aligned} \quad (4.2)$$

Expressed in the form of a differential equation, we have

$$\begin{aligned} dC &= \frac{G}{V} dt - \frac{QC}{V} dt \\ &= \frac{G - QC}{V} dt \end{aligned} \quad (4.3)$$

or

$$\frac{V}{G - QC} dC = dt \quad (4.4)$$

The change in concentration from any time t_1 to a later time t_2 can be obtained by integration:

$$V \int_{C_1}^{C_2} \frac{1}{G - QC} dC = \int_{t_1}^{t_2} dt \quad (4.5)$$

Integrating yields

$$\begin{aligned} -\frac{V}{Q} \ln \left(\frac{G}{V} - \frac{QC_2}{V} \right) - \frac{-V}{Q} \ln \left(\frac{G}{V} - \frac{QC_1}{V} \right) &= t_2 - t_1 \\ \ln \frac{G - QC_2}{G - QC_1} &= -\frac{Q}{V} (t_2 - t_1) \\ \frac{G - QC_2}{G - QC_1} &= \exp \left[-\frac{Q}{V} (t_2 - t_1) \right] \\ C_2 &= \frac{1}{Q} \left\{ G - (G - QC_1) \right. \\ &\quad \left. \times \exp \left[-\frac{Q}{V} (t_2 - t_1) \right] \right\} \end{aligned} \quad (4.6)$$

Equation 4.6 can be used to calculate the concentration C_2 at any time t_2 if the concentration C_1 at an earlier time t_1 is known. This is the general equation describing concentration change (either buildup or decay) as a function of time, generation rate, room volume, and ventilation rate. Several specific cases produce simplified forms of the general equation.

Case I ($C_1 = 0$ at $t_1 = 0$, $G > 0$). If the initial concentration is assumed to be zero, the resulting concentration at any time t is given by

$$C = \frac{G}{Q} \left[1 - \exp \left(\frac{-Qt}{V} \right) \right] \quad (4.7)$$

where the contaminant is being generated at a rate G for the time t and the air is being exhausted at a rate Q .

Case II ($t \gg t_1$, $G > 0$). As seen in Fig. 4.2, when contaminant generation first starts, the concentration rises rapidly and then levels off. After sufficient time, the exponential term of Eq. 4.7, $\exp(-Qt/V)$, approaches zero and the concentration asymptotically approaches a maximum steady-state concentration C_{\max} given by

$$C_{\max} = \frac{G}{Q} \quad (4.8)$$

At this point, the material is being removed from the room at the same rate as it is being introduced. This can also be seen by setting the net mass change ΔM equal to zero in Eq. 4.1, since steady state means no change in concentration.

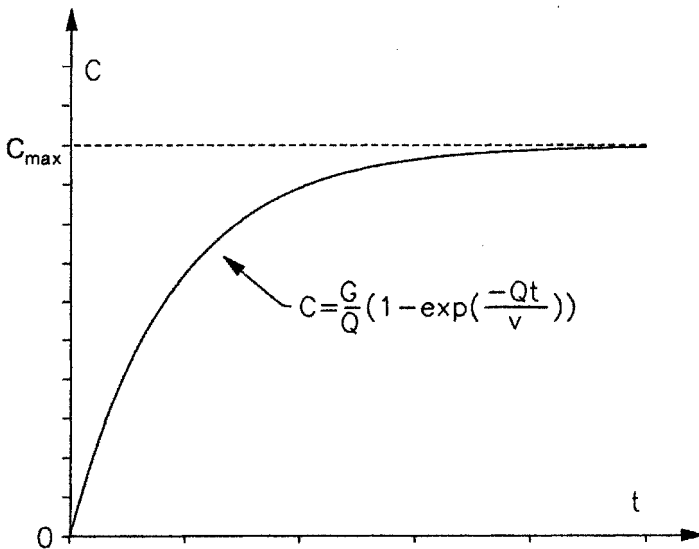


Figure 4.2 The general shape of the curve corresponding to Eq. 4.7 is shown. The concentration C asymptotically reaches a steady-state concentration C_{\max} . This graph assumes that the concentration was zero $t = 0$.

Rearranging Eq. 4.1 for this special case will also produce Eq. 4.8. The steady-state equation does not depend on the room volume. Room size will affect how quickly the steady-state concentration is achieved, but not the magnitude of the final concentration.

Case III ($G = 0$). For intermittent sources, the decrease in concentration when generation stops can be calculated by setting $G = 0$ in Eq. 4.6

$$C_2 = C_1 \exp \left[\frac{-Q}{V} (t_2 - t_1) \right] \quad (4.9)$$

As shown in Fig. 4.3, the concentration decreases exponentially after generation stops, approaching zero asymptotically. If generation resumes again at time t_2 , Eq. 4.6 can be used to calculate subsequent concentrations.

Purge time, defined as the time necessary to reduce the concentration to a specified level on cessation of the generation source, can also be calculated. The purge time is often measured in *half-lives* ($t_{1/2}$) referring to the amount of time required to reduce the concentration by 50% ($C_2 = 0.5C_1$) once the generation of contaminant has stopped ($G = 0$). After two half-lives ($2t_{1/2}$), the concentration has been reduced to 25% of the original level, after $3t_{1/2}$ it has been reduced to 12.5%, and so on. The half-life is a function of the room volume and the ventilation rate. Let $t_2 - t_1 = t_{1/2}$ in Eq. 4.9:

$$\frac{C_2}{C_1} = \exp \left(\frac{-Qt_{1/2}}{V} \right) \quad (4.10)$$

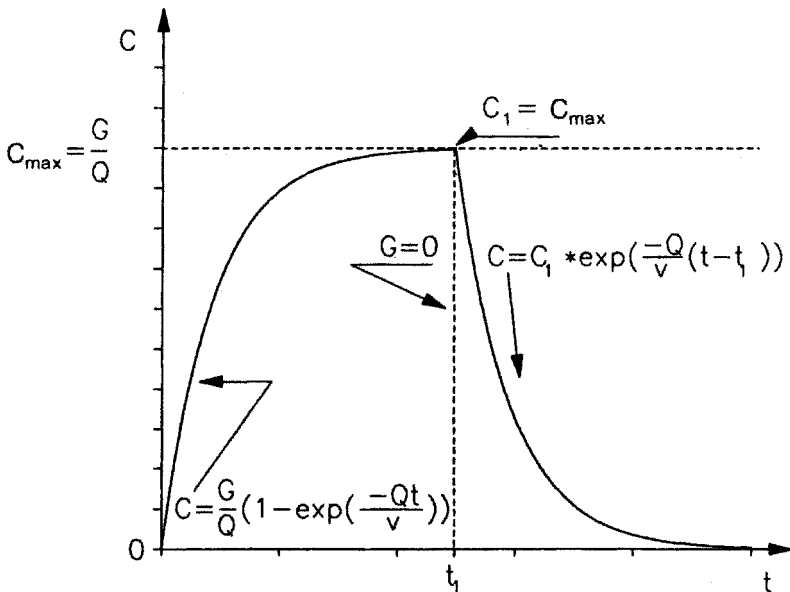


Figure 4.3 If the generation rate ceases ($G = 0$) at time t_1 , the concentration declines according to Eq. 4.9.

After time $t_{1/2}$, $C_2 = 0.5 C_1$:

$$\begin{aligned}\frac{0.5 C_1}{C_1} &= \exp\left(-\frac{Qt_{1/2}}{V}\right) \\ t_{1/2} &= -\frac{V}{Q} \log_e 0.5 \\ &= 0.693 \frac{V}{Q}\end{aligned}\quad (4.11)$$

There are five useful equations for describing the general case and the special situations. The general equation describes the change in concentration with time (Eq. 4.6). The special cases are

1. Concentration buildup from an initial value of zero (Eq. 4.7)
2. Steady-state concentration (Eq. 4.8)
3. Rate of concentration decrease after generation cessation (Eq. 4.9)
4. Rate of purging, or half-life (Eq. 4.11)

If the degreaser described previously is used intermittently during the workshift, these equations can be used to construct a temporal concentration profile. For example, consider a process that operates for the first 45 min of every hour during the first 4 h of the 8-h shift, for the next 2 h continuously, and then not at all for the last 2 h. When the degreaser is not in use, the employees have been instructed to cover it. It is located in a 30,000-ft³ room that has a wall-mounted fan exhausting 3000 cfm. The concentration is negligible ($C = 0$) at the start of the shift.

To determine the concentration at any time during the shift, Eqs. 4.6, 4.7, and 4.9 are used. Equation 4.7 is used to predict concentrations during the first 45 min; Eq. 4.9 is used for the next 15 min, when the generation stops. Equation 4.6, the general equation, must be used to calculate the next period, because the initial concentration is not zero as it was at the start of the shift. The concentrations for the remainder of the shift can be calculated using Eq. 4.6 while TCE is being released and Eq. 4.9 when it is not. The resulting profile is shown in Fig. 4.4. The steady-state concentration can be determined graphically from Fig. 4.4 or by using Eq. 4.8. First, airflow is changed to metric units:

$$\begin{aligned}Q &= \left(3000 \frac{\text{ft}^3}{\text{min}}\right) \left(0.0283 \frac{\text{m}^3}{\text{ft}^3}\right) \\ &= 85 \text{ m}^3/\text{min}\end{aligned}$$

Then, solving for the concentration C_{\max} given

$$\begin{aligned}C_{\max} &= \frac{G}{Q} \\ &= \frac{5800 \text{ mg/min}}{85 \text{ m}^3/\text{min}} \\ &= 68 \text{ mg/m}^3\end{aligned}\quad (4.8)$$

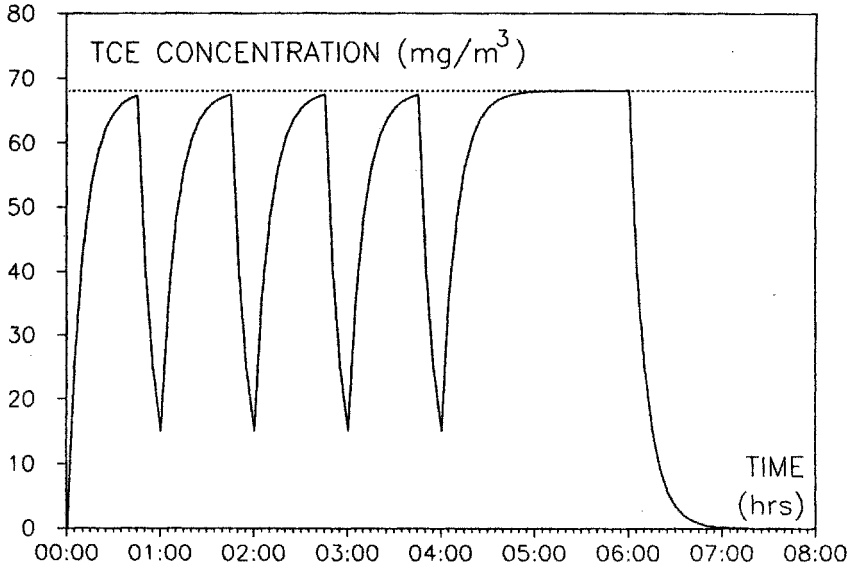


Figure 4.4 For the degreaser operating on an intermittent basis, the concentration profile will change over time. To determine the increase in concentration when the emission begins, Eq. 4.7 is used when the initial concentration is zero and Eq. 4.6 is used when it is not. To determine the decay curve, Eq. 4.9 is used. The concentration is seen to approach the steady-state concentration, 68 mg/m^3 , after approximately 45 min.

The half-life $t_{1/2}$ is useful for predicting the decay rate on cessation of generation. From Eq. 4.11, each half-life is

$$t_{1/2} = 0.693 \frac{V}{Q} = 0.693 \frac{30,000 \text{ ft}^3}{3000 \text{ ft}^3/\text{min}} \approx 7 \text{ min}$$

For example, after 14 min ($2t_{1/2}$), the concentration would be

$$68 \text{ mg/m}^3 \times \frac{1}{2} \times \frac{1}{2} = 17 \text{ mg/m}^3$$

From the steady-state concentration equation, the minimum ventilation rate Q_{\min} necessary to maintain the concentration at a target level C_{\max} can be calculated as

$$Q_{\min} = \frac{G}{C_{\max}} \quad (4.12)$$

If the target concentration C_{\max} were 80 mg/m^3 , then

$$\begin{aligned} Q_{\min} &= \frac{5800 \text{ mg/min}}{80 \text{ mg/m}^3} \\ &= 72.5 \frac{\text{m}^3}{\text{min}} \times \frac{35.3 \text{ ft}^3}{\text{m}^3} \\ &= 2560 \text{ ft}^3/\text{min} \quad (1.2 \text{ m}^3/\text{s}) \end{aligned}$$

As stated at the beginning of this section, the derivation of these formulas relied on several assumptions. Because these assumptions are rarely met, this design flow Q_{\min} must be adjusted to accommodate variations in generation rate, inadequate mixing, worker position, and other appropriate safety factors, as discussed below.

Often, the rate of air exchange E in general ventilation systems is measured in terms of room air changes per hour (ACH) with a unit of inverse hours (h^{-1}). The number of ACH is obtained by dividing the volumetric flow Q by the volume of the ventilated workspace V :

$$E = \frac{Q}{V} \quad (4.13)$$

The inverse hour unit for E arises when the flow unit is m^3/h (or ft^3/h) and the volume unit is m^3 (or ft^3).

The air exchange rate is a ventilation rate that has been normalized by the room volume. Air exchange rates when expressed in this manner are often used (and misused) to compare ventilation rates of workplaces with different volumes. A comparison is appropriate when the equation describing the concentration can be simplified by eliminating the individual Q and V terms, and replacing them with E . This is only feasible for the purge rate (Eqs. 4.9 and 4.11). In these cases, the (Q/V) term can be replaced with E , leaving no dependence on Q or V alone. However, the steady-state concentration (Eq. 4.8) is a function of the generation and ventilation rates and is independent of the room volume. Therefore, the volume-normalized unit would be inappropriate for purposes of comparison. To compare anticipated steady-state concentrations, only the generation and volumetric rates for the two situations need be known. The room volumes are unimportant. Similarly, when considering the concentration buildup ($G > 0$), the equations describing the change in concentration contain not only a (Q/V) term, but also contain the flow term Q , alone. Attempting to simplify Eq. 4.6 or 4.7 by replacing the (Q/V) term with E would not help, since the flow must still be known.

4.3 VARIATIONS IN GENERATION RATE

If the variations in the contaminant generation rate are less than 20%, they are usually ignored. Similarly, if the periodicity of the variation is small, those variations can be safely overlooked. However, when lengthy, pronounced duty cycles are present, the possibility of transient excess exposures must be considered. For example, if a process emits a contaminant at a rate G for one hour out of every two, with no emissions during the second hour, it would usually be inappropriate to use an average emission rate of $0.5G$ because this would provide inadequate control during the periods of peak emission.

If the system cannot be designed to provide higher exhaust rates during periods of emission, the most prudent approach to this problem is to assume, for design purposes, that the generation rate is constant at a level equal to the maximum rate observed during the cycle. Although this will result in more than adequate ventilation

during most of the workshift, it will assure that the intermittent emissions will not produce concentrations above the target level. If the period of contaminant release is brief compared to the period of nonrelease, as might be the case with some batch processes, excursions above the target level might be allowable. This would depend on the toxicity of the material, the frequency of release, the duration of the release, and the projected exposure concentrations, both during the peak emission episodes as well as the intervening periods.

In some situations, the distance between the point of release and the employees' work stations can be used effectively to "average out" the peaks. Unfortunately, in many operations the release of emissions is associated directly with the presence of the workers. For example, emission of solvent vapors from a degreasing tank is often caused by the operator-attended removal of wet parts. Similarly, the opening of a dryer-oven door may produce a brief, yet intense material release. During this phase of the process, an operator standing nearby often receives a considerable exposure. However, if a process can be modified to avoid human involvement during peak emissions, the amount of air being handled by the general exhaust system might safely be reduced.

4.4 MIXING

The mechanisms governing dispersal of airborne material in buildings are not well understood. The equations developed in Section 4.2 assume that the mixing of both the contaminant and the clean replacement air into the workplace environment was complete and instantaneous, although this is never attained. Two approaches have been taken in attempts to accommodate, in the theoretical treatments, the inherent lack of ideal mixing encountered in the real world.

The industrial ventilation engineers traditionally incorporate into the equations a multipurpose safety factor K that addresses the imperfect mixing as well as other variables such as material toxicity, seasonal changes in natural ventilation, reduced operating efficiencies of ventilation systems, process cycle and duration, worker location, number of workers exposed, location and number of contaminant release points, and other circumstances affecting worker exposure (Soule, 1978). This K factor is introduced at the last stage of the steady-state calculation (Eq. 4.8), so that the desired amount of dilution air is now provided as

$$Q_a = KQ_i = K \frac{G}{C} \quad (4.14)$$

where Q_i = air exhaust rate under ideal conditions

Q_a = air exhaust rate under actual conditions

K = multipurpose safety factor (dimensionless)

The range of values traditionally cited for K is 3–10 (ACGIH, 2001), although experimental validation is lacking. Moreover, a rigorous method to choose the proper value has yet to be developed.

As noted above, it is conventional to aggregate all of the various factors into a single K factor. However, it is more appropriate to examine individually each of the reasons for adjusting the design ventilation rate. At the least, the physical mixing should be considered apart from the safety and health issues mentioned above. The adequacy of the mixing would be included in a mixing factor K_m while a safety factor K_s would incorporate the toxicity of the material, the number of workers, and so on. The multipurpose factor K would be the product of K_m and K_s . The mixing factor K_m could be used to calculate expected concentrations, given knowledge of generation rates, recirculation rates, air cleaner removal efficiencies, and outdoor concentrations. However, virtually no work has been conducted to characterize the parameters affecting and describing mixing rates in large, well-ventilated spaces. Given this lack of knowledge, the ability to choose and assign an appropriate mixing and safety factor remains a very uncertain art, not a science.

4.5 INLET/OUTLET LOCATIONS

Because the physical mixing factor K_m is dependent on the locations of the exhaust outlets and supply inlets, these must be specified in the design process, bearing in mind that judicious selection will result in both a cleaner workplace and cost savings. In the derivation of the equations describing steady-state conditions, it was assumed that the concentration was homogeneous throughout the workplace; that is, the contaminant was evenly distributed. Of course, there will always be a concentration gradient. The concentration will be higher near the emission sources and lower near the replacement air inlets, a fact of some importance in the design phase for two reasons. First, the location of workers relative to the source must be considered. The closer the workers are to the point of generation, the greater their exposure is likely to be. This should be addressed in selection of the safety factor K_s . Second, the differences in concentration can be used to provide more effective removal of the contaminant by adapting certain concepts from local exhaust ventilation. If the point of exhaust is located as close to the point of release as possible, the rate at which material is removed from the workplace QC will actually increase, thus providing lower overall concentrations throughout the workplace. This premise rests, of course, on the reasonable assumptions that the highest concentrations are encountered near the source.

Consider the simplified case illustrated in Fig. 4.5, where one source emits material at a generation rate G . The concentration near the source C_s will be higher than the background room concentration C_r . There is an intermediate zone, with concentration C_i . Although this approach will assume only these three, somewhat distinct, zones, in real life there are no clear delineations between them. Rather, there would be continuous concentration gradient as one moved farther from the source. For illustrative purposes, however, one can consider these three regions in which $C_s > C_i > C_r$.

One common approach to locating the exhaust outlet is to place the fan in the ceiling, with little or no regard for its position relative to the three regions (source,

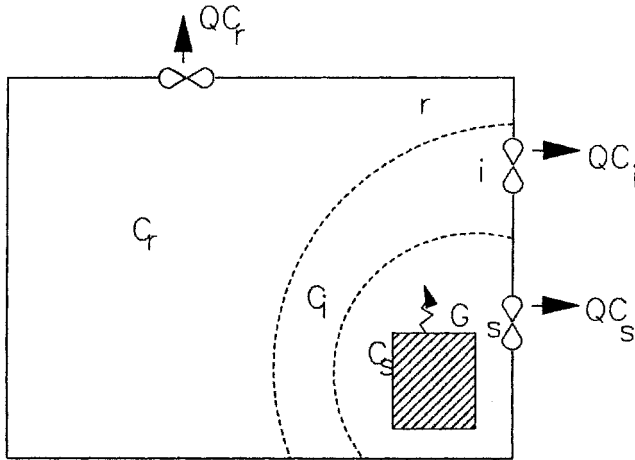


Figure 4.5 The three regions (source, s ; intermediate, i ; and room, r) are shown. If the exhaust fan pulls air from the general room region, the mass rate of contaminant removal is given as QC_r . If the fan is located in the intermediate zone, the pollutant is removed at a faster rate QC_i , since $C_i > C_r$. Even more effective removal can be achieved by locating the exhaust fan near the source, so that the removal rate is QC_s , which is greater than QC_r .

intermediate, or room). Therefore, it is usually exhausting air from the room region, removing the contaminant at a rate QC_r . Note, however, that by locating the fan in the intermediate region where the concentration is higher than the background concentration, more effective contaminant removal is achieved, since the material is now being removed at a rate QC_i , which is greater than QC_r . It follows that moving the exhaust point into the source region will provide yet more effective removal. “Spot” ventilation, as this is frequently termed, is a hybrid, with attributes of both general and local ventilation systems. Although the equations describing general exhaust no longer apply, the desirability of LEV-like systems is clearly apparent. It is seen, therefore, that the effectiveness of a GEV system can be increased by locating the exhaust point as close as possible to the point of contaminant release.

4.6 OTHER FACTORS

A consideration mentioned earlier is the location of the workers. Obviously, personal exposures should be minimized. By locating the exhaust and replacement air points strategically, it is possible to establish an airflow pattern that will draw contaminated air away from the employees. The practice of moving contaminated air through populated regions of the plant should be avoided if at all possible. Rather, the system should be designed to move air from clean areas into dirty areas. If this is not possible, the suitability of GEV should be reconsidered.

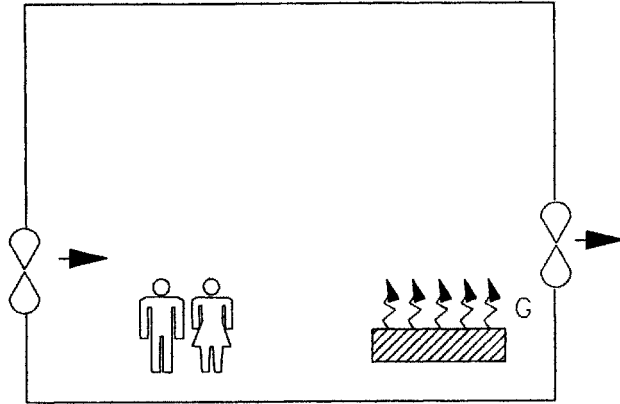


Figure 4.6 Providing clean, tempered air to the populated areas of the workplace and exhausting dirty air directly from the process area is good practice. This discourages intrusion of the contaminated air into the populated zone. The supply air should be properly conditioned and a system for delivery (i.e., fans, ducts, diffusers) should be designed.

The locations of the supply air inlets are dictated by logic similar to that used to locate the exhaust outlets. Given that the tempered replacement air is cleaner than the general room air, this air should be delivered directly into the area populated by employees before passing through the contaminated zone. This has a twofold effect. Not only does it provide clean, fresh air for the workers but also discourages intrusion of dirty air into this zone. This helps to establish and maintain a pattern of flow within the plant, as shown in Fig. 4.6. This supply air requires conditioning and a system for delivery (i.e., fans, ducts, diffusers). Guidelines for replacement air systems are provided in Chapter 12.

The provision of adequate replacement air is a critical aspect of GEV system design. Propeller-type fans, which are often used as wall or ceiling exhaust fans, suffer substantial degradation in performance at even small negative static pressures (see Chapter 10). Therefore, if a sufficient quantity of replacement air is not provided, the building will come under negative pressure (with respect to the outdoors) and the exhaust fans will not perform as expected. Natural ventilation patterns in the building should also be considered. Open doors, windows, roof ventilators, and so on, will affect both the quantity and patterns of airflow. Temperature differences in the plant may also induce air movement. Natural dilution ventilation is highly dependent on seasonal characteristics as well as other factors such as window opening and door propping. The potential for interaction between natural and mechanical ventilation must be considered in the design phase, as well as during testing after installation and routinely thereafter.

If possible, the amount of natural ventilation should be measured. This can be accomplished by using tracer gas decay techniques. It is important to know the extent of natural ventilation because the reduction in concentration is not linearly

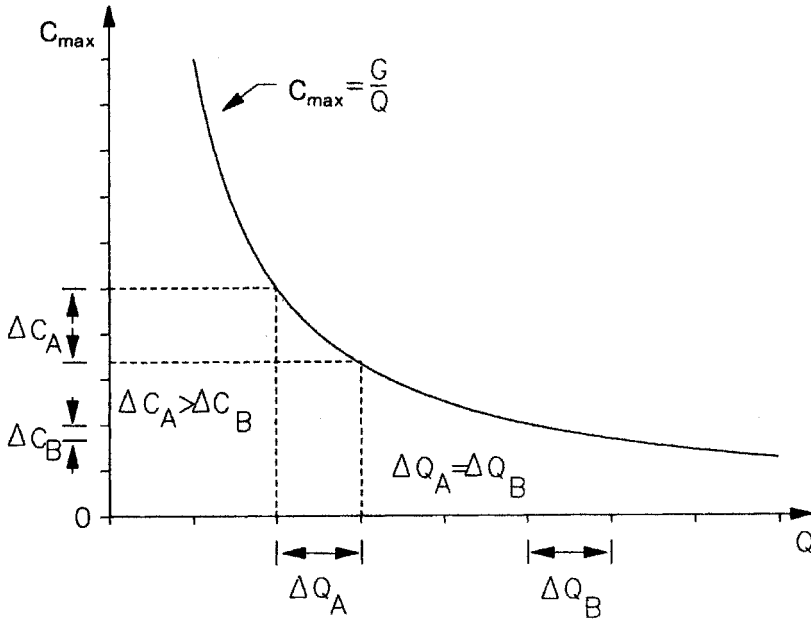


Figure 4.7 The steady-state concentration C_{\max} is shown as a function of the exhaust rate Q assuming a constant generation rate G . The extent of concentration reduction to a lower steady-state level is a function of the change in Q and the existing Q . At low exhaust rates, small increases can produce substantial decreases in concentration. For example, ΔQ_A produced a large concentration decrease ΔC_A . However, at a higher Q , the same increase in Q will produce only minor decreases in C . Even though ΔQ_B is the same as ΔQ_A , the change in concentration attributable to the former ΔC_B is much less than ΔC_A . The efficiency of additional general ventilation is highly dependent on existing ventilation.

proportional with increasing ventilation rate, as illustrated in Fig. 4.7, and by the steady-state equation (Eq. 4.8). At low ventilation rates, a small increase in Q will have a marked effect on the concentration. If a building has little existing ventilation (either naturally or from other ventilation systems), the introduction of a mechanical GEV system is likely to have real benefits in lowering in-plant concentrations. However, if the present ventilation rates are high, any further decrease in concentration will require substantial amounts of exhaust air.

Consider a warehouse with propane forklift trucks producing indoor workplace carbon monoxide concentrations of 100 ppm, in which a concentration reduction to 40 ppm is to be accomplished with the introduction of a new GEV system. The generation rate G and mixing factor K are assumed to be constant. Rearranging Eq. 4.14 yields

$$C_1 = K \frac{G}{Q_1}$$

$$C_2 = K \frac{G}{Q_1 + Q_2}$$

where $C_1 = 100$ ppm CO

$C_2 = 40$ ppm CO

Q_1 = actual natural (existing) ventilation rate

Q_2 = actual mechanical (additional) ventilation rate

Rearranging and combining gives us

$$C_1 Q_1 = C_2 (Q_1 + Q_2) \quad (4.15)$$

$$= C_2 Q_2 + C_2 Q_1$$

$$Q_2 = \frac{C_1 - C_2}{C_2} Q_1$$

$$= \frac{60}{40} Q_1$$

$$= 1.5 Q_1 \quad (4.16)$$

If there was an initial airflow of 10,000 cfm (4.7 m³/s) through the warehouse, the GEV system should be designed to move an additional 15,000 cfm (7.0 m³/s). However, if Q_1 was already 50,000 cfm (23.3 m³/s), the system would be required to handle 75,000 cfm (35.0 m³/s), a fivefold increase over the 15,000-cfm (7.0 m³/s) figure. Thus, without knowing the contaminant generation rate G for a process, the amount of air required to reduce the concentration to a target level from an existing concentration can be calculated using Eq. 4.16 if the existing ventilation rate is known.

4.7 COMPARISON OF GENERAL AND LOCAL EXHAUST

Although this chapter has emphasized the theory and design of GEV systems, the problems associated with this form of environmental control need discussion. Although it does have valid applications, GEV is too often used as a quick and dirty alternative to LEV, based on its low capital cost, simple design, and easy installation. There are several serious deficiencies associated with GEV, however.

There may be adverse health consequences of GEV compared with alternative control methods, primarily LEV. By allowing the contaminants to be released into the workplace air, personal exposure to the contaminant will always occur, albeit at a nominally “safe” level. Local exhaust ventilation, on the other hand, has the *potential* of capturing the contaminants at the point of release, thereby eliminating worker exposure. Second, the amount of air handled by a GEV system will always be greater than that of a LEV system designed to control the same process (see Chapter 6). Since all of the exhausted air should be replaced with clean, tempered air, the costs of operating a replacement-air system for the GEV system will be substantially more than for a LEV system. Third, the problem of cleaning the exhaust air must be

addressed. It is easier and less expensive to clean the small volume of highly contaminated air produced by a LEV system than a large volume of less-contaminated air resulting from a GEV system. In general, capital and operating costs for air-cleaning devices are proportional to the quantity of air being handled, rather than the total amount of contaminant being removed.

In summary, a general exhaust ventilation system should be considered as a primary means of environmental control only if

- The workers will not be exposed to excessive concentrations.
- A LEV system is not feasible or is inappropriate.
- The contaminant is not highly toxic.
- The contaminant will be transported effectively to the exhaust point.
- The costs of supplying replacement air will not be excessive.
- Existing ventilation rates are relatively low.

This generally limits the use of GEV to widely distributed sources of gaseous or vapor-phase contaminants such as solvent vapors.

LIST OF SYMBOLS

C	concentration
E	air exchange rate
G	generation rate
K	multipurpose safety factor
K_m	mixing factor
K_s	safety factor
m, M	mass
Q	volume flow
t	time
$t_{1/2}$	half-life
V	volume

REFERENCES

- American Conference of Governmental Industrial Hygienists, Committee on Industrial Ventilation, *Industrial Ventilation, A Manual of Recommended Practice* 24th ed., ACGIH, Lansing, MI, 2001, p. 2–4.
- Soule, R. D., “Industrial Hygiene Engineering Controls,” in *Patty’s Industrial Hygiene and Toxicology*, 3rd ed., Vol. 1, G. D. Clayton and F. E. Clayton, eds., Wiley, New York, 1978, pp. 786–787.

PROBLEMS

- 4.1** A vapor-phase degreaser emits solvent vapors at a rate of $2.1 \text{ ft}^3/\text{min}$. It is located in a room with dimensions of $20 \times 40 \times 10 \text{ ft}$, and the room has a fan exhausting air at a rate of $7000 \text{ ft}^3/\text{min}$. Assume a mixing factor of 6.
- (a) What is the maximum vapor concentration in the room?
 - (b) What is the vapor concentration in the room after 5 minutes of operation?

Answers:

- (a) 1800 ppm
- (b) 1780 ppm

- 4.2** A chemical process emits ammonia gas from a vent into the work room at a rate of $1.5 \times 10^{-3} \text{ m}^3/\text{s}$. The threshold limit value (TLV) for ammonia is 25 ppm. The room dimensions are $15 \times 12 \times 9 \text{ m}$. Assume a mixing factor of 2.
- (a) What general exhaust ventilation airflow is required to ensure that the ammonia concentration does not exceed its TLV?
 - (b) Is the use of general exhaust ventilation a satisfactory control technique for this operation? Explain your answer.

Answers:

- (a) $120 \text{ m}^3/\text{s}$

- 4.3**
- (a) What is the vapor generation rate G in cfm, if 0.5 gal of toluene is evaporated uniformly over an 8-h shift? [Vent Man]
 - (b) What airflow is required to hold the maximum concentration of toluene to 10 ppm? Assume a mixing factor of 2.

Answers:

- (a) $0.031 \text{ ft}^3/\text{min}$
- (b) $6300 \text{ ft}^3/\text{min}$

HOOD DESIGN

The key concept underlying local exhaust ventilation is the capture of airborne contaminants at the source. The system should be designed to capture air containing the contaminants given off by the process being ventilated. In many instances this is an extremely difficult task, and the success or failure depends on the exhaust hood design.

An exhaust hood is defined to be a suction source in an exhaust system through which air moves from the ambient environment, carrying with it any contaminant generated or released from the process or piece of equipment served by that suction source. Hoods can range in design from a plain opening at the end of a duct to a complex enclosure surrounding an entire process. Past studies and common sense tell us that the specific design of an exhaust hood is the most important element in the success or failure of any exhaust system.

The critical elements of any exhaust hood are its geometry (which determines the airflow patterns in the vicinity of the hood), its location relative to the process, and the amount of air being moved through it. These factors determine *how much* air is being removed from the vicinity of the process and *from where* the air is drawn. If a sufficient quantity of air is being removed from regions where the contaminant is released, those contaminants will be captured by the exhaust system with high efficiency. If any of the three elements are deficient, however, exhaust flow will not be provided at the point of generation in sufficient quantity to ensure contaminant capture.

A considerable portion of the *Ventilation Manual* (2001) is devoted to the design of exhaust hoods. References in this and following chapters to “VS numbers” refer to specific design plates in Chapter 10 of the *Ventilation Manual*. Detailed guidelines

concerning hood shape, airflow, and hood energy loss are presented for a wide range of specific operations; these are useful, but specific designs should always be used with care. Their routine application may lead to installed systems which have poor contaminant capture efficiencies. These potential deficiencies can be traced to many factors, such as shortcomings in the design plates, excessive cross-draft conditions, and processes that differ from the design assumed in the plate. Circumstances under which the guidelines must be tempered with sound engineering judgement are discussed in this chapter. Hood designs for several specific processes are discussed in Chapter 6.

5.1 CLASSIFICATION OF HOOD TYPES

Hemeon (1963) was perhaps the first to describe a simple scheme to categorize hood designs. He concluded that all local exhaust hoods fall into three categories: enclosures, exterior hoods, and receiving hoods. The classification of a hood into one of these categories is useful, since the design procedure to be followed is different for each. The key element in classifying hoods is the *location* of the hood relative to the point of contaminant generation or escape. The relative location of hood with respect to source helps to determine the amount of airflow needed for effective capture. The design process for each hood type is discussed in the following sections.

5.1.1 Enclosures

If a hood is designed so that the contaminants are released from the process *inside* the hood, it is classified as an *enclosure* (Fig. 5.1). This type of hood generally is the most desirable from the ventilation engineer's point of view, since the contaminants are always contained inside the boundaries of the hood. Effective control of emissions

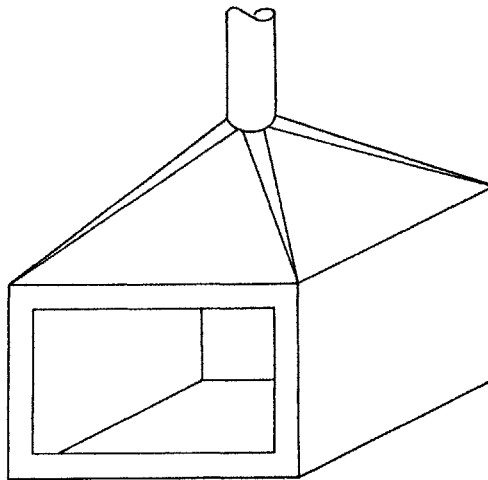


Figure 5.1 Enclosing hood.

is much easier in this case than for exterior-type hoods (to be described in Section 5.1.2), where the exhaust airflow must “reach out” and capture the contaminated air as the contaminant is generated.

Enclosing hoods can be further categorized, depending on the completeness of the enclosure provided. Complete enclosures are typified by gloveboxes (Fig. 5.2a); the process/work is conducted entirely inside the exhaust hood. This type of hood offers the greatest protection to the user, since the possibility of worker exposure to air contaminants in a well-designed hood during normal operation is negligible. It also conserves energy, since of the three basic hood types this design requires the least amount of airflow to ensure adequate control. An exhaust airflow is chosen sufficient to create a slight negative pressure inside the enclosure; this ensures that contaminated air will not escape from the enclosure.

Generally, gloveboxes and other similar enclosures are provided with a designed air inlet so that a small continuous airflow is maintained in the absence of leaks. This airflow can be filtered at the inlet if the interior of the box must be maintained in a clean condition. Gloveboxes frequently are specified when handling highly toxic chemicals. In such cases it is usually necessary to provide a high-efficiency air-cleaning system for the exhaust air (see Chapter 11).

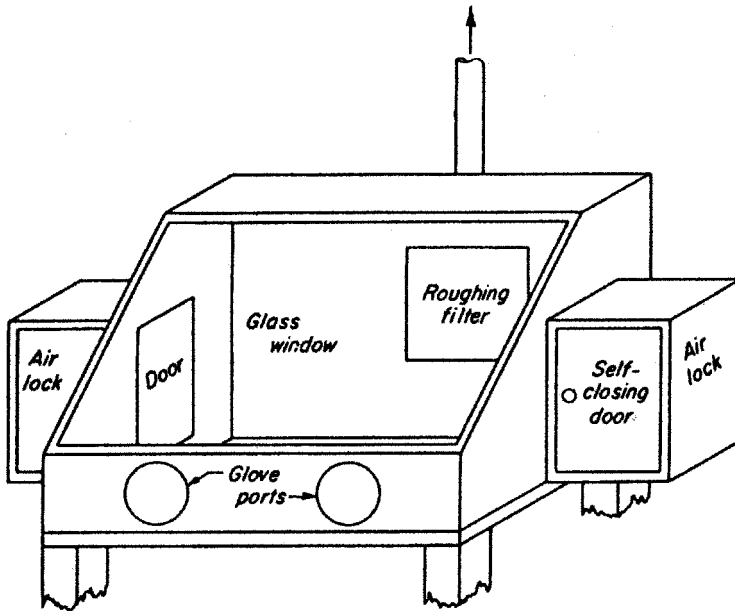
The principal problem with using complete enclosures is the lack of access to the process. For this reason, complete enclosures are used only for the most hazardous exposures, where product cleanliness must be assured, or where the process is completely automated and no worker access is required. An example of the latter is the flat deck screen hood pictured in Fig. 5.2b; obviously, instances where complete enclosures are feasible will be limited in most industries.

Booths, the second subcategory of enclosures, are simply enclosures with one side partially or completely open to provide access. Common examples are hoods used for abrasive cutoff sawing (Fig. 5.3a) and spray painting (Fig. 5.3b). Booths are classified as enclosures because the contaminant release takes place inside the hood itself, as it does with gloveboxes and other complete enclosures. Although the contaminants are generated inside the hood, the presence of one open side gives rise to the possibility of contaminant escape through this opening. To prevent this, a sufficiently high air velocity must be maintained through the open area (called the *hood face*) to preclude the loss of any of the contaminants from the hood due to internally generated air currents or external eddies. The specification of this *minimum face velocity* is a major part of the design process for booths.

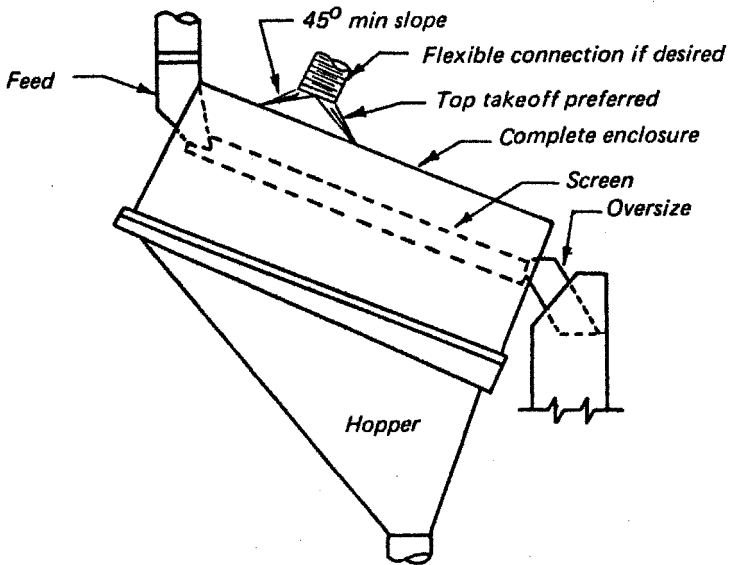
Tunnels (Fig. 5.4), the third type of enclosing hood, are similar to booths, except that they have two open faces for process flow or access. The contaminants are still given off inside the hood, but now two routes of escape exist. As with booths, it is the face velocity of the air drawn in through the openings that determines the hood capture efficiency.

5.1.2 Exterior Hoods

The basic difference between an enclosing hood and an exterior hood is that the latter does not surround the contaminant at the point of release. The contaminant is



(a)



(b)

Figure 5.2 Examples of enclosing hoods: (a) glovebox; (b) flat deck screen hood. [After Hagopian and Bastress (1976).]

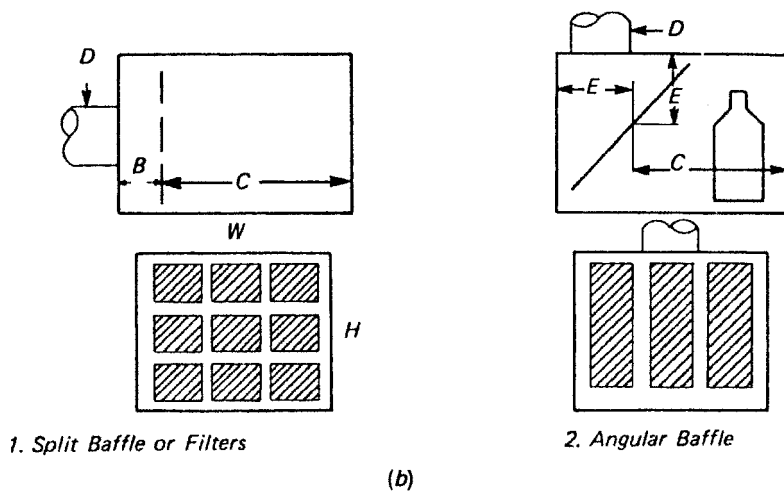
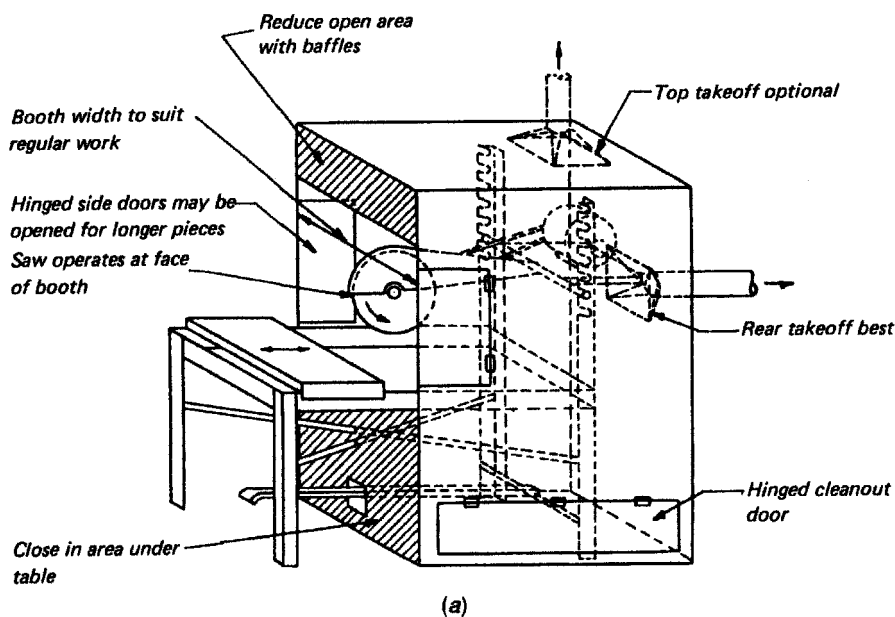


Figure 5.3 Examples of booth-type enclosures: (a) abrasive cutoff saw hood; (b) spray painting hood. [After Hagopian and Bastress (1976).]

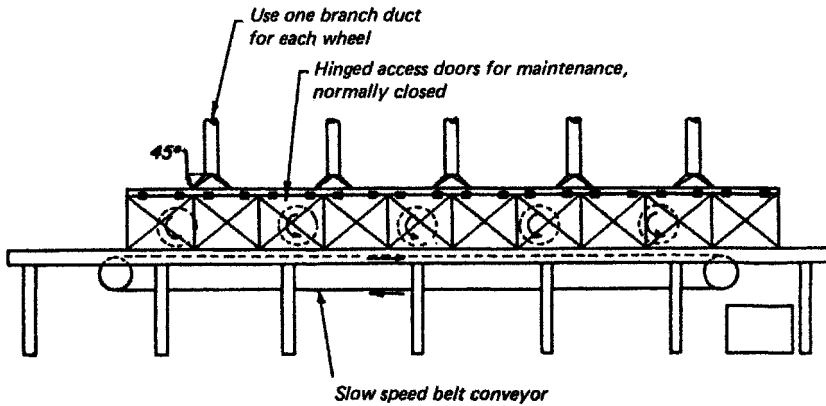


Figure 5.4 Straight-line multiple buffing, an example of a tunnel-type enclosure. [After Hagopian and Bastress (1976).]

given off *outside* the hood and must be *captured* by the hood rather than allowed to escape to the general plant atmosphere. A typical exterior hood is the portable welding hood (Fig. 5.5).

With an exterior hood the contaminant is captured by the movement of air past the point of generation into the hood. This air movement is caused by the exhaust system fan, which draws air from the duct connecting the hood to the fan. This creates

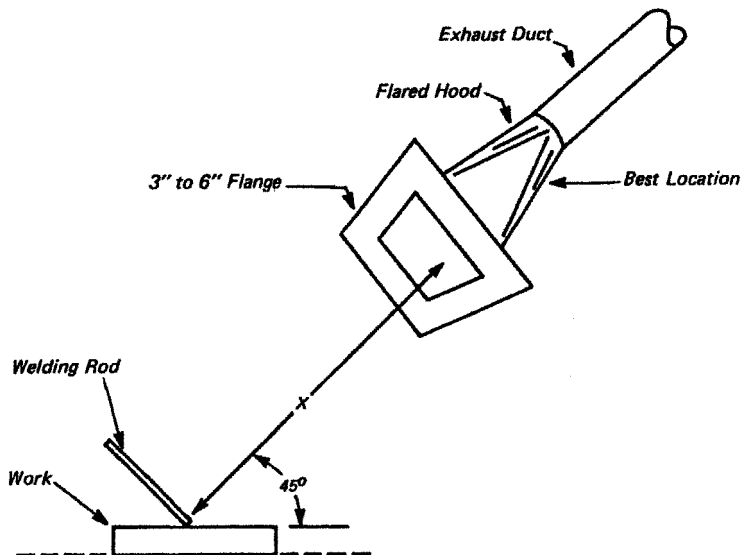


Figure 5.5 Movable welding hood, an example of an exterior hood. [After Hagopian and Bastress (1976).]

a partial vacuum at the hood, causing air to flow from outside the hood to replace the air that has been drawn into the duct system. If the contaminants are given off into the air that enters the hood, they will be captured by the exhaust system.

In many cases process access requirements necessitate the use of exterior hoods, which inherently are less desirable than enclosing hoods. With enclosing hoods, contaminants are given off directly into the hood and not into the general workplace atmosphere. The process creating the contaminants and the exhaust system can be thought of as a closed system, and if this system is working properly the worker is never exposed. The exterior hood suffers greatly in comparison to such a closed system, since the contaminant is first *released* into the air surrounding the process and then the air containing the contaminant is *captured* by the exhaust system. Unfortunately, many adverse effects can occur between generation and capture.

External hoods are susceptible to extraneous air movements that can disrupt the airflow patterns between the point of contaminant release and the exhaust hood. Such air currents are ubiquitous; almost any room experiences random air movements with velocities of at least 30–50 fpm (0.15–0.25 m/s) when no overt sources of air movement are present (as a point of reference, 100 fpm is approximately equal to 1 mile per hour). In industrial facilities, where numerous sources of air movement exist, severe cross-draft conditions may completely disrupt the performance of exterior hoods. Cross-drafts are discussed extensively in the following section covering exterior hood design.

Exterior hoods have other problems in addition to cross-drafts. Since the contaminants are released into the air surrounding the process and then captured, it is possible for a worker to be in the path between the contaminant source and the hood, and be exposed to the contaminants before they are captured. Consider a worker at an open-surface tank, which is exhausted by an overhead, or canopy, hood, as shown in Fig. 5.6a. As part of the job the worker must lean over the tank to insert and remove

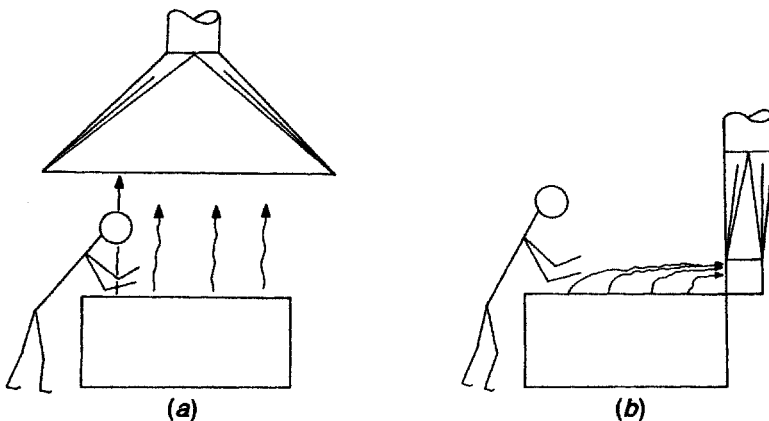


Figure 5.6 Airflow patterns for hoods used on an open-surface tank: (a) canopy hood; (b) slot hood.

objects, and in so doing is exposed to the contaminants being generated. In this case, even if the hood is capturing 100% of the contaminants being released, the worker would still be exposed. A better design for the exhaust hood on this process might be the slot hood shown in Fig. 5.6*b*, which creates an airflow pattern that bypasses the worker's breathing zone. This concept is discussed in detail later in this chapter.

5.1.3 Receiving Hoods

Receiving hoods are exterior hoods designed to take advantage of some aspect of the contaminant generation process to assist in moving the contaminant from the source to the hood. If the contaminant is released in a preferential direction, the exhaust hood is positioned to take advantage of this preferential motion and "receive" the contaminant. Most exterior hoods have to "reach out" and direct the contaminant into the hood with exhaust air; in receiving hoods the contaminants "ride with" the exhaust air into the hood.

The two properties of contaminant release that are commonly utilized in receiving hoods are particle momentum and thermal updrafts. Certain processes, such as the grinding shown in Fig. 5.7, propel particles into the air with a considerable amount of momentum. Grinding wheel exhaust hoods (Fig. 5.7*a*) are designed to intercept the particles as they are thrown off; if the hood cannot be placed in the path of particle travel (Fig. 5.7*b*), it is much more difficult to "turn" the particle by air movement and direct it into the hood. A detailed discussion of the design of grinding wheel hoods is included in Section 5.4.2.

Thermal drafts can be powerful forces directing contaminants upward. This can often be used to advantage when designing exhaust hoods for hot processes, such as canopy-type hoods (Fig. 5.8). The hood in Fig. 5.8*a* is exhausting a room-temperature process, while the hood in Fig. 5.8*b* is exhausting a hot process. Since there are no external forces directing contaminants into the exhaust hood for the room-temperature process, this hood is an *exterior* hood and as such must create sufficient air velocity by *exhaust air alone* to capture the contaminants evolved at the tank surface. The heated process, on the other hand, creates a thermal updraft that *carries* the contaminants toward the hood. In this case the canopy hood acts as a receiving hood. The discussion in Section 5.4.1 will demonstrate that canopy-type receiving hoods may be effective, but canopy hoods are poor exterior hoods.

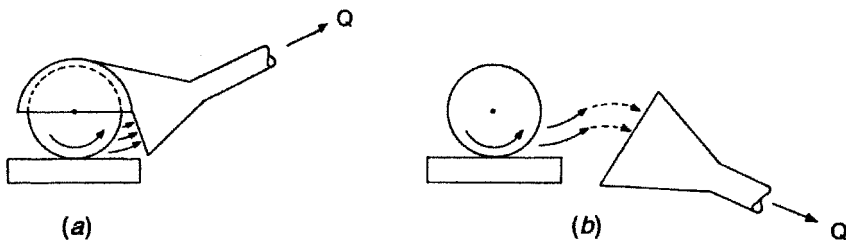


Figure 5.7 Grinding wheel hood types: (a) receiving hood; (b) exterior hood.

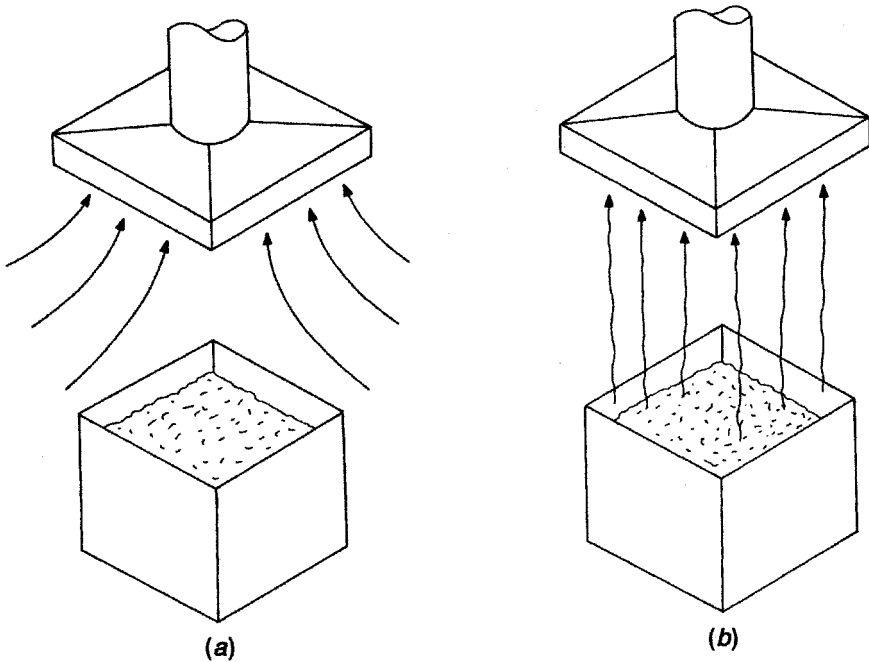


Figure 5.8 Airflow into a canopy hood: (a) hood over a room-temperature process; (b) hood over a heated process.

5.1.4 Summary

The discussion above should convince the reader of the desirability of using enclosing-type hoods whenever possible. The basic idea when designing an exhaust system is to use a hood that encloses each process as completely as possible, consistent with necessary access by personnel and materials. In many cases this hood selection and design process relies on the engineering judgment and common sense of the ventilation designer. The process to be ventilated should be observed closely whenever possible to determine what access is required by the worker, material transport, and the process equipment. The worker should be consulted and the possible interactions between the proposed exhaust system and the process should be discussed. An exhaust hood can then be designed that encloses the process as completely as possible but that is not looked upon by the worker as an interference with effective task performance.

5.2 DESIGN OF ENCLOSING HOODS

With an enclosing hood the contaminant, by definition, is given off *inside* the hood. The important considerations in designing such a hood are to ensure that the contaminant

is actually given off inside the hood and to *keep* it inside the hood at all times. The process creating the contaminant and the exhaust system should be thought of as a closed system that contains the contaminant at all times; the worker is positioned outside this closed system and thus has no possible exposure to the contaminant.

In most practical applications a complete enclosure is not possible. The contaminant may be given off inside the physical dimensions of the hood, but openings exist in the hood to allow necessary access to the process. In these cases sufficient exhaust must be provided so that adequate inward velocity is created through all such hood openings to prevent the escape of any contaminant.

The abrasive blasting cabinet (VS-80-02), one example of a true enclosure, illustrates the limitations entailed by requiring an exhaust system to enclose a process completely. The cabinet is extremely effective in controlling worker exposure to air-borne contaminants, but imposes severe limitations on the worker's interaction with that process.

Most enclosing-type hoods fall into one of two subcategories, booths and tunnels. A booth (Fig. 5.3) is an enclosure with one open side, while a tunnel (Fig. 5.4) has two open sides. Each meet the definition of an enclosure, since the contaminants are still released within the confines of the hood itself. Booths are probably the most common type of enclosure found in industry; examples include the paint spray booth (VS-75-01, 75-02, 75-05), the swing grinder booth (VS-80-16), and the laboratory hood (VS-203). Tunnels are used typically to enclose material transfer or conveying operations such as conveyor belts (VS-306), screens (VS-99-01), and straight-line automatic buffing (VS-80-33).

In designing enclosures, the important consideration is *face velocity*, in this case defined as the average velocity through all hood openings that penetrate the enclosure. Thus, in looking at the simple booth of Fig. 5.3, the face velocity V_f (in fpm or m/s) is given as

$$V_f = \frac{Q}{A_f} \quad (5.1)$$

where Q is the total airflow through the hood (in cfm or m^3/s) and A_f is the total cross-sectional area of the hood openings (in ft^2 or m^2). The design of enclosing-type hoods must concentrate on (1) fitting the hood to the process so that the enclosure is as complete as possible, and (2) selecting an airflow through the hood which will result in a face velocity of sufficient magnitude to ensure that contaminants cannot escape the hood.

The first of these steps, the fitting of the hood itself, is probably the most important consideration for ensuring good control. The design process to be followed cannot, unfortunately, be described in detail, since it depends largely on the specific process being controlled. General guidelines for designing enclosures are available, but the specific details are best left to the ventilation designer. The following basic rules apply:

1. Make the enclosure as complete as possible. This reduces the total area of the openings through which exhaust air must be drawn, thus minimizing the airflow required for contaminant control.

2. Include design features to ensure that airflow is evenly distributed across the openings. This is especially important with large open areas, such as those associated with paint spray booths. If such booths are designed to be very shallow, as shown in Fig. 5.9a, the average face velocity (Eq. 5.1) may be adequate but the airflow will be poorly distributed. Since much of the air will flow in near the center of the booth face, which is the path of least resistance, the velocity near the edges of the booth face will be inadequate.

To ensure an even distribution of exhaust air, steps must be taken to equalize the resistance to airflow across all areas of the hood face. To accomplish this, the following design features, singly or in combination, can be applied:

1. Make the booth deeper (Fig. 5.9b). The *Ventilation Manual* (VS-75-01, 75-02) recommends that the depth of the booth be at least 75% of the booth face height or width, whichever is larger.
2. Use a baffle. Examples of a solid baffle, an angular baffle, and a split baffle are shown in Fig. 5.9c. The dimensions for such baffles are given in VS-75-01 for large hoods and VS-75-02 for small hoods. Baffle design is also pictured in Fig. 3-13 of the *Ventilation Manual*.
3. Use filters. Filters or other air-cleaning devices are commonly used in paint spray and other operations for air pollution control purposes. When placed at the rear of the booth (Fig. 5.9d), they provide relatively high resistance to airflow and thus serve to even out the air distribution. In fact, such devices, unless properly designed and maintained, are more effective as air distributors than as air cleaners (see Chapter 11).

Once a basic enclosing hood configuration is selected, all that remains is to calculate the airflow Q required to ensure contaminant control. The important quantity for system design purposes is Q , but the important quantity for control is the average face velocity V_f . In most applications, face velocities in the range 100–200 fpm are sufficient. It is important to realize that velocities that are too high can be just as detrimental to good hood performance as velocities that are too low. For example, velocities greater than 150 fpm at the face of laboratory hoods have been known to create serious problems (Chapter 7). High air velocities can disrupt experiments being carried out in the hood (as, for example, when a Bunsen burner or other combustion source is being used).

The presence of the operator introduces additional difficulties. Standing in front of the hood, the operator creates an obstruction to airflow; if the air flows past the operator at too great a velocity, eddies can be created between the operator and the hood opening. Such turbulent eddies can entrap contaminants given off inside the hood and carry them out of the hood. These types of problems can be minimized by the selection of the proper fume hood face velocity, as discussed in Chapter 7.

Recommended face velocities for enclosures used on many processes are given in the *Ventilation Manual*. In many cases, a range of velocities is specified. For these cases, and where a standard design is not available, the designer must pick a specific

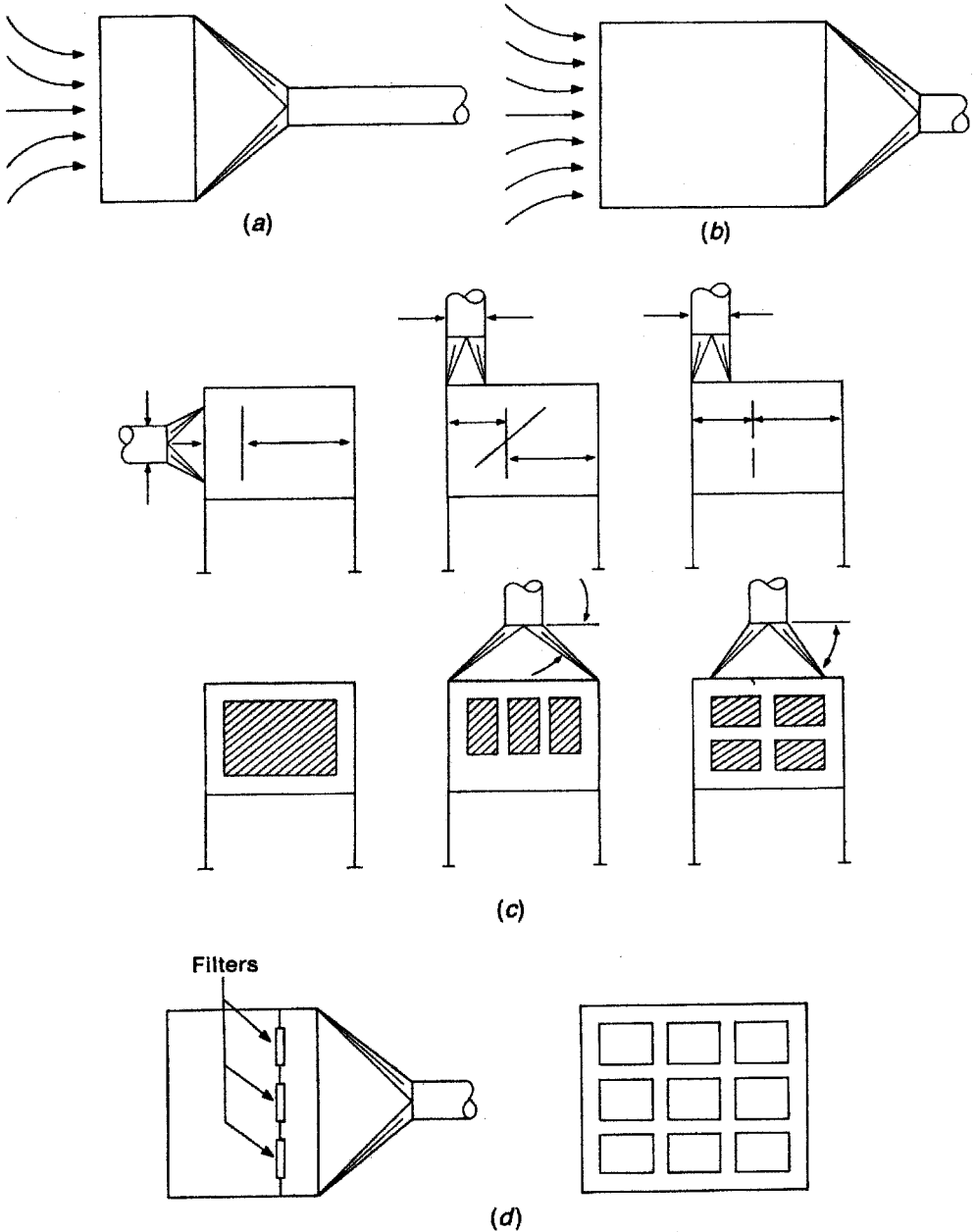


Figure 5.9 Airflow distribution in booths: (a) if the booth is too shallow, poor distribution results; (b) distribution can be improved by making the booth deeper; (c) baffles can be used to help distribute airflow [after Hagopian and Bastress (1976)]; (d) filters are also effective.

velocity within the recommended range. The following factors should be considered in making such a selection:

1. The presence of disruptive cross-drafts requires the use of higher face velocities. Cross-drafts are usually thought of as being disruptive to the performance of exterior hoods, but they can also affect the performance of booths and tunnels.
2. The collection of highly toxic materials requires a more conservative design to ensure positive control. A lower permissible exposure limit for the material being collected would indicate a higher face velocity (within the recommended range).
3. Material-handling systems can cause induced airflows that must be overcome by increased hood face velocities. This is discussed in Chapter 6.

5.3 DESIGN OF EXTERIOR HOODS

As stated earlier, exterior hoods are inherently less satisfactory than enclosing hoods as collection devices. Since such hoods must “reach out” and capture contaminated air beyond the boundaries of the hood, it is extremely important that they be designed properly. Poor design invariably ensures that contaminants will escape in significant quantities into the workplace, causing worker exposure.

The three elements of critical importance in designing exterior hoods are the capture velocity to be created at the point of contaminant release, the airflow through the hood required to create the capture velocity outside the hood, and the physical shape and location of the hood itself. Each is discussed separately.

5.3.1 Determination of Capture Velocity

Capture velocity is defined to be the air velocity at the point of contaminant release sufficient to “capture” the contaminants and carry them into the exhaust hood. The proper selection of the capture velocity is of critical importance in the design of exterior hoods. The air velocities created by an exterior hood are imposed on a complex airflow pattern which is always present due to other sources of air movement, such as replacement air, perimeter infiltration, and process-induced airflow. The capture velocity must be large enough to overcome any other air velocity patterns at the point of contaminant release so that the resultant airflow is from the release point to the exhaust hood.

These points can be illustrated by the simple example shown in Fig. 5.10. A plain round duct exhausts a process at a distance x directly in front of the opening. For simplicity the contaminant is assumed to be released as a point source. The exhaust induces an airflow at point x with a velocity $V_c(x)$ (the relationship between the amount of air flowing Q and the velocity induced at x is developed in the next section).

Under the assumption that no other air movement exists in the vicinity of x , the air is completely still when the local exhaust hood is not operating. Under these

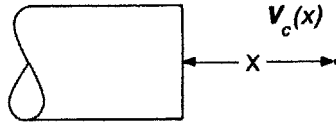


Figure 5.10 Unflanged round exterior hood used to capture contaminants at distance x .

circumstances the operation of the exhaust hood will induce an airflow at point x that will be directed into the exhaust hood. The capture velocity $V_c(x)$ can take any value at all; in the absence of other air currents, the actual velocity is irrelevant since all air passing point x will eventually be drawn into the exhaust hood.

Such a condition is not realistic, of course. In any practical situation extraneous airflows will exist at point x . The simplest such situation is a uniform cross-draft parallel to the hood face, as shown in Fig. 5.11. If the cross-draft has a velocity $V_d(x)$ at point x and the exhaust system is operating, the total velocity of the air at point x is now the vector sum of the capture velocity and the cross-draft velocity:

$$V(x) = V_c(x) + V_d(x) \quad (5.2)$$

In this case, whether or not the contaminant is drawn into the exhaust hood depends on the relative magnitudes of V_c and V_d and the distance x from the release point to the hood opening.

This example illustrates the critical importance of cross-drafts to the performance of exterior hoods. In the complete absence of cross-drafts, any exterior hood will capture all contaminants given off in its vicinity. It is the action of cross-drafts and other air motions in the workplace that degrade the performance of exterior hoods and make their design particularly difficult. For each operation being exhausted, a capture velocity must be selected to overcome the action of expected extraneous airflow patterns and direct the resultant velocity vector into the exhaust hood.

The performance of exterior hoods in the presence of crossdrafts is the subject of considerable research (Conroy et al., 1988; Conroy, 1988; Dalrymple, 1986;

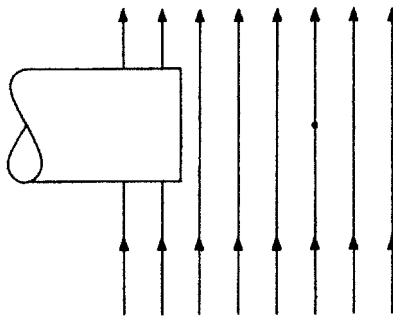


Figure 5.11 Unflanged round exterior hood in a uniform cross-draft parallel to the hood face.

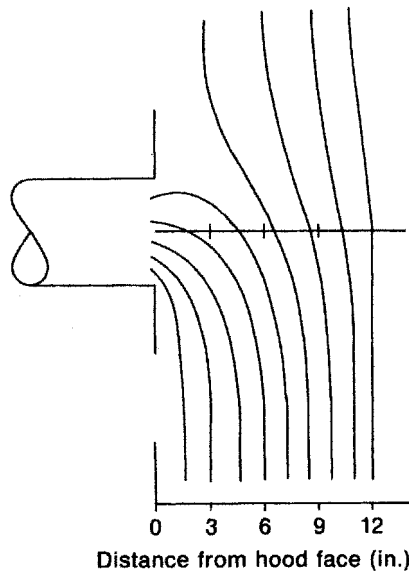


Figure 5.12 Airflow patterns in the vicinity of a 6-in. flanged circular hood exhausting 100 cfm in the presence of a 100-fpm cross-draft.

Ellenbecker et al., 1983; Fletcher and Johnson, 1986; Flynn and Ellenbecker, 1985, 1986, 1987; Jansson, 1980, 1985; Regnier et al., 1986). For example, Flynn and Ellenbecker have developed a method to predict the airflow patterns into flanged circular hoods in the presence of uniform cross-drafts. As an example, the airflow pattern into a 6-in. flanged circular hood exhausting 100 cfm ($0.05 \text{ m}^3/\text{s}$) in the presence of a 100-fpm (0.5 m/s) cross-draft is shown in Fig. 5.12. The zone of influence of the hood is defined by the pattern of streamlines present. Any contaminants given off in an area where streamlines converge on the exhaust hood will be carried by the exhaust air into the hood and captured; any contaminants given off outside this area will likewise escape the hood. For the case shown in Fig. 5.12, the capture efficiency of the hood along the x axis might be expected to follow a step function (Fig. 5.13a). In actual practice, turbulent diffusion will act on the contaminant as it travels toward the hood, and the capture efficiency would be expected to follow a sigmoidal curve (Fig. 5.13b). Capture efficiency is discussed in more detail in Chapter 13.

Given the overriding importance of cross-drafts, the novice ventilation designer might think that the selection of a capture velocity for a specific application is relatively straightforward; one simply measures or estimates the cross-draft and selects a capture velocity sufficient to overcome it. It is unfortunate that the “real world” does not operate in such a straightforward manner. Experimental and theoretical work to quantify the effect of cross-drafts on hood capture efficiency, of the type described above and in Chapter 13, is in its infancy. Until considerably more work is done, the selection of capture velocities sufficient to overcome extraneous airflows will remain an art rather than a science. Our inability to quantify existing airflow patterns and the

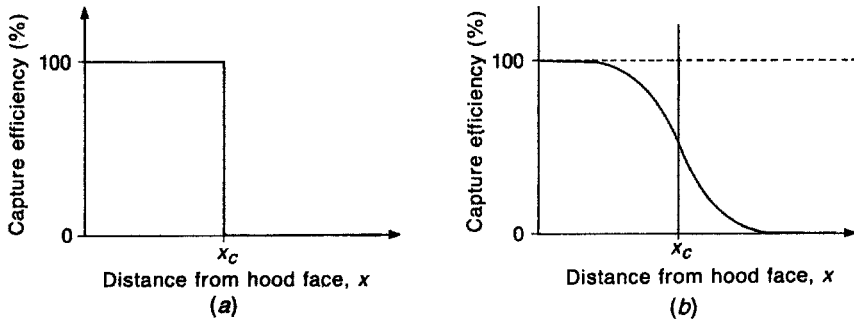


Figure 5.13 Hood capture efficiency versus distance from hood face: (a) theoretical, no turbulence; (b) actual, with turbulence.

effect of a new exhaust system on those patterns limits the estimation of hood performance to an approximation. Given this, current design procedures result in capture velocities specified in a manner that acknowledges, either implicitly or explicitly, the uncertainties in the design process.

The selection of a capture velocity is covered in less than one page in the *Ventilation Manual*. The essential information is given in Table 3-1 of that volume, reproduced here in its entirety as Table 5.1. This table was adapted directly from Brandt (1947), and has seen little change in the last 57 years. Four categories, or ranges, of capture velocity are given. A particular category is selected based on a qualitative estimate of both cross-draft magnitude and velocity of contaminant release; no quantitative guidelines are given to help the designer select a category.

Within each category, a range of capture velocities is specified. Rules of thumb to assist in selecting a value from that range describe how much *room for error* should be allowed when the exhaust hood is operated; in other words, they are an attempt to estimate the importance of ensuring complete contaminant capture for the operation in question. Selection of capture velocities at or near the lower end of each range in essence means that some escape of contaminants will be allowed, while selection from the upper end is an attempt to ensure complete capture.

Some difficulties in using this table should be obvious. The range of capture velocities presented is enormous, with the highest velocity being a factor of 40 greater than the lowest. Several critical terms meant to help in the selection of a value within this wide range are qualitative and almost cryptic. For example, the system designer must decide whether the contaminants are released into “quiet” air, “moderately still” air, air with “rapid air motion,” or air with “very rapid air motion”; none of these terms are defined or quantified. Many other critical terms (e.g., size of hood, toxicity, active generation, room air currents favorable to capture) are similarly undefined. What if the process releases contaminants at high velocity into still air, or at low velocity into rapidly moving air? No hint is given as to the value to be selected under these conditions.

Table 5.1 Range of Capture Velocities

Condition of Dispersion of Contaminant	Examples	Capture Velocity (fpm)
Released with practically no velocity into quiet air	Evaporation from tanks; degreasing, etc.	50–100
Released at low velocity into moderately still air	Spray booths; intermittent container filling; low-speed conveyor transfers; welding; plating; pickling	100–200
Active generation into zone of rapid air motion	Spray painting in shallow booths; barrel filling; conveyor loading; crushers	200–500
Released at high initial velocity into zone of very rapid air motion	Grinding; abrasive blasting, tumbling	500–2000

In each category above, a range of capture velocity is shown. The proper choice of values depends on several factors:

<i>Lower End of Range</i>	<i>Upper End of Range</i>
1. Room air currents minimal or favorable to capture	1. Disturbing room air currents
2. Contaminants of low toxicity or of nuisance value only	2. Contaminants of high toxicity
3. Intermittent, low production	3. High production, heavy use
4. Large hood—large air mass in motion	4. Small hood—local control only

Source: ACGIH *Industrial Ventilation*, 24th Edition.

Inexperienced ventilation designers may thus find it difficult to use this table properly in the selection of capture velocity for exterior hoods. The designer has two approaches to making this critical design decision. Design plates for selected operations are specified in the *Ventilation Manual*. This approach has the effect of allowing the author of the design plate to select the capture velocity. The second approach is to choose what is thought to be a conservatively high value of capture velocity.

Both approaches have disadvantages. The indiscriminate use of design plates may not properly take into account specific characteristics of the application, such as cross-drafts, which are greater than the design plate was meant to overcome. An attempt to use an overly conservative capture velocity introduces two distinct possibilities. The value may not be conservative enough, in which case the hood capture efficiency may be low, or the capture velocity may be much higher than actually required. In the latter case the hood will have high capture efficiency, but the amount of air exhausted will be excessive and energy will be wasted. These possibilities are discussed in more detail in Chapter 13. In any case, the selection of a capture velocity remains the weakest part of the design procedure for an exterior hood.

5.3.2 Determination of Hood Airflow

The next step in designing an exterior hood is to select an airflow through the hood that will give the desired capture velocity at the furthest point of contaminant generation. To do this it is necessary to understand the airflow patterns that exist around an exhaust hood of the type being used.

Comparison of Blowing and Exhausting Air. A look at the different velocity patterns of blowing and exhausting air will illustrate the difficulties encountered in trying to use an exhaust hood to “reach out” and capture contaminants. The simple exhaust system shown in Fig. 5.14 will be used for illustration; it consists of a fan and plain rectangular outlets and inlets. The air being blown from a plain duct opening forms a jet that persists for a long distance from the opening.

The *ASHRAE Fundamentals Handbook* (2001) describes four distinct zones in a jet. The first two, an initial zone and a transition zone, are relatively short, extending about 12 duct diameters from the outlet. The third zone, called the zone of fully established turbulent flow, extends quite far, from 25 to 100 duct diameters. In this zone the velocity of a jet of air at a distance x from a plain round opening is

$$V(x) = \frac{KQ}{x\sqrt{A_f}} \quad (5.3)$$

where K = a dimensionless constant

Q = airflow at the opening, cfm (m^3/s)

A_f = cross-sectional area of the opening, ft^2 (m^2)

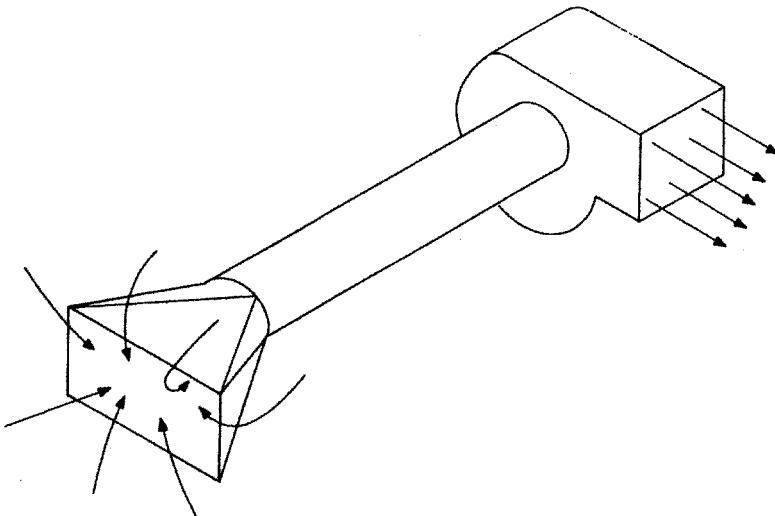


Figure 5.14 Simple exhaust system, showing both blowing and exhausting air.

For a round opening, Hemeon (1963) states that K is equal to 2. Solving Eq. 5.1 for Q and substituting for Q and K in Eq. 5.3 gives an expression for the velocity at a distance x as a fraction of the face velocity V_f :

$$\frac{V(x)}{V_f} = \frac{2\sqrt{A_f}}{x} \quad (5.4)$$

Substituting the diameter of the opening D for the area gives the following equation:

$$\frac{V(x)}{V_f} = \frac{1.8D}{x} \quad (5.5)$$

In the fully established turbulent zone, the velocity falls off linearly in front of a jet. The influence of the jet can be felt at some distance from the opening. From Eq. 5.5, the jet will still have 10% of its face velocity [$V(x) = 0.1V_f$] at a point 18 duct diameters downstream ($x = 18D$).

The characteristics of a jet can be contrasted with those of a source of suction, such as an exhaust hood. In the simple exhaust system shown in Fig. 5.14, the blower is the energy source that causes air to move; it does this by transferring air molecules from the downstream duct to the upstream duct. The act of physically removing air molecules from the downstream duct causes a partial vacuum to be created inside the duct. Air molecules move from outside the duct to fill this partial vacuum, and it is this motion that constitutes the airflow into the hood.

The ventilation system designer intends to create a velocity at some point *in front of* the hood opening in order to capture contaminants. Unfortunately, the air that moves into the hood opening to fill the partial vacuum does so from *all* directions, not only from directly in front. Some of the air actually enters the hood from *behind* the opening (Fig. 5.14). This means that the velocity of the entrained air falls off very rapidly with distance from the hood face. It would be desirable for the airflow into the hood to be highly directional, as in a jet, but the aerodynamic behavior of a suction source does not conform to this wish.

Theoretical Considerations for Exhausting Air. The relationship between velocity, airflow, and distance from the source of suction must be known if a hood is to be designed to attain a desired capture velocity at a particular location in front of the hood. This relationship can best be understood by first considering a hood with vanishingly small dimensions, so that it becomes a point source of suction (Fig. 5.15). This point source will draw air equally from all directions; if the amount of air being exhausted is Q , the velocity of the air at any distance x will be given by the simple formula

$$V(x) = \frac{Q}{A} \quad (2.6)$$

where A is the area through which the air is flowing. In this case the area is simply the surface of a sphere with radius x , so that

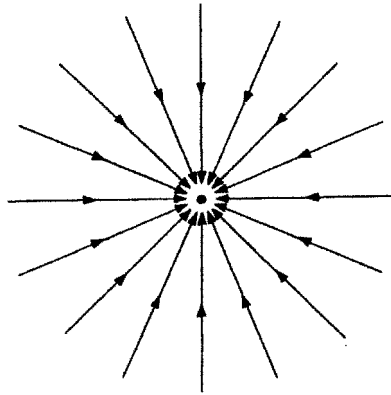


Figure 5.15 Streamlines into a point source of suction.

$$V(x) = \frac{Q}{4\pi x^2} \quad (5.6)$$

In theory, the velocity is inversely proportional to the square of the distance from the hood.

Experimental Determination of Capture Velocities. The simple inverse-square relationship demonstrated in Eq. 5.6 is valid only for (hypothetical) point sources of suction. Actual sources of suction vary from this model in two ways. The suction is applied over finite area (the hood face area A_f), and the hood and duct take up part of the physical space surrounding the point of suction, so the suction cannot operate over the surface of an entire sphere. Real-world considerations such as these have hindered the development of theoretical predictions of capture velocities in front of exhaust hoods.

This question was first investigated empirically in a series of experiments performed at the Harvard School of Public Health by Joseph Dalla Valle (1930), who measured the velocity contours and streamlines created in front of several basic hood shapes operated under suction. He studied flanged and unflanged square hoods, round hoods, and rectangular hoods with aspect ratios (i.e., hood width divided by hood length) ranging from 0.75 to 0.33. This work generated a large quantity of data concerning the nature of airflow patterns in front of these simple hood shapes; typical examples of his results are shown in Fig. 5.16, taken from his thesis. Shown are the measured velocity contours and streamlines in front of a plain 8-in. square opening (Fig. 5.16a) and a similar plot for the same hood with a 5-in. flange installed (Fig. 5.16b).

The centerline velocity for the unflanged hood decreases rapidly with distance from the hood face. The velocity is reduced to 50% of the face velocity at $x = 2.25$ in., and falls to 10% of the face velocity at $x = 8$ in., or one duct diameter. The reduction in velocity with distance is much more severe at locations off the centerline; for

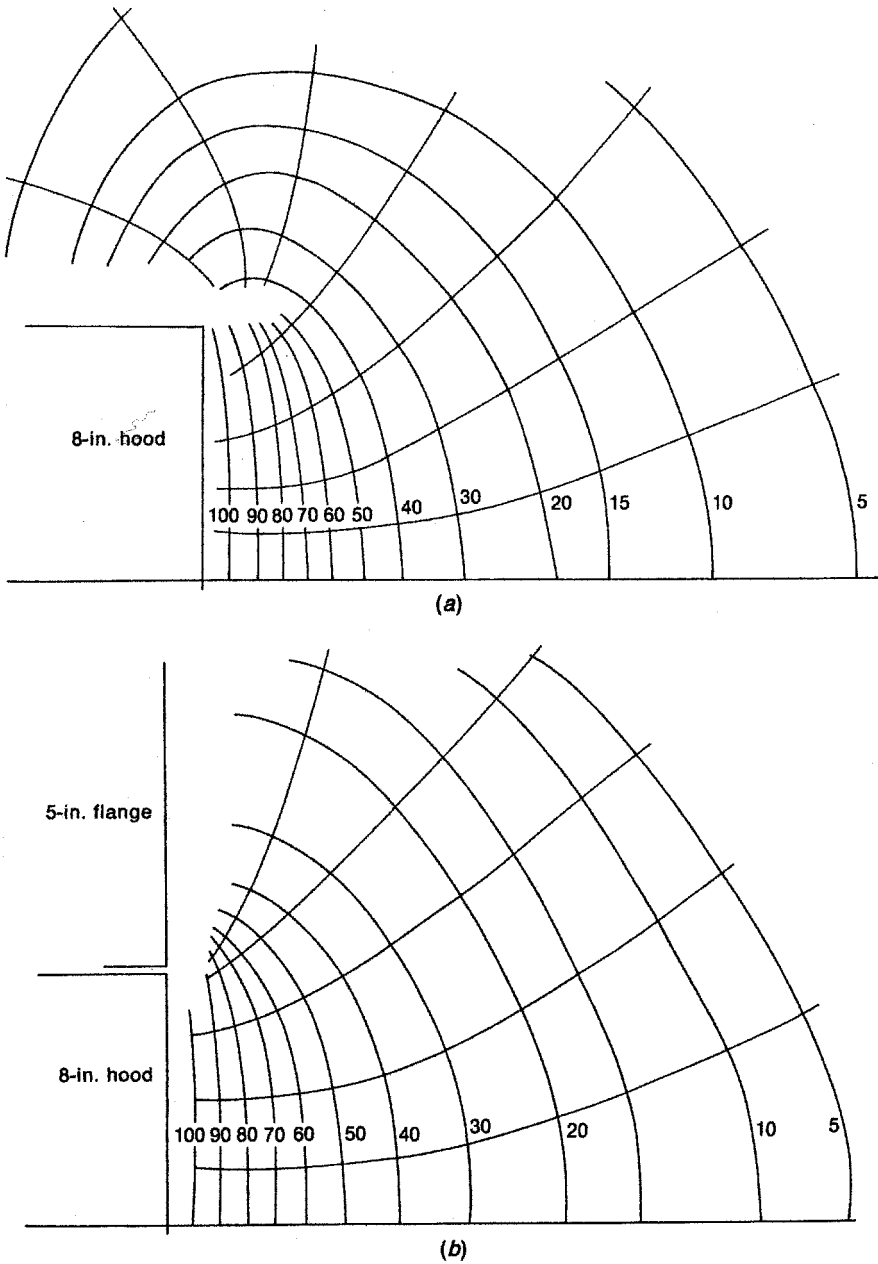


Figure 5.16 Typical equal velocity contours and streamlines measured by DallaValle (1930): (a) unflanged 8-in. square opening; (b) same hood with a 5-in. flange installed.

example, along the edge of the duct the velocity falls to the 50% value at a distance of 1.25 in. in front of the hood and falls to 10% at 6.75 in. Note also the flow of air from *behind* the hood.

The improvement in performance gained by the addition of the flange is apparent in Fig. 5.16*b*. Air is now prevented from flowing from behind the hood; since the same total amount of air is flowing it must now all enter from in front of the hood. This improves the “reach” of the hood, so that the centerline velocity falls to 10% of the face velocity at a distance of 9 in. rather than 8 in. as occurred without the flange. In general, flanges should be used on all exterior-type exhaust hoods to gain maximum benefit from the air being exhausted.

The data described above, which were collected by Dalla Valle over 70 years ago, still form the basis for the design of exterior exhaust hoods. Empirical formulas were developed that fit the data collected along the centerline of each basic hood type. When all the data for unflanged hoods were examined, it was found (Dalla Valle, 1952) that the best fit was obtained by using the formula

$$V(x) = \frac{Q}{10x^2 + A_f} \quad (5.7)$$

The velocity of air into an unflanged exhaust hood at any distance x along the centerline in front of the hood, for a given airflow Q and hood face area A_f can be calculated with Eq. 5.7. This equation is valid for round hoods, square hoods, and rectangular hoods with aspect (i.e., width to length) ratios greater than 0.2.

This empirical formula is similar to the theoretical equation developed for a point source of suction (Eq. 5.6). Both include the inverse-square relationship between velocity and distance, with slightly differing constants (10 versus 4π); the empirical formula also includes the effect of the hood area, which, of course, is zero for the idealized point source.

To obtain the normalized velocity at any distance in front of the opening, Eqs. 5.1 and 5.7 can be combined:

$$V(x) = \frac{V_f A}{10x^2 + A_f}$$

Rearranging gives us

$$\frac{V(x)}{V_f} = \frac{A}{10x^2 + A_f} \quad (5.8)$$

The normalized velocity equations for blowing air (Eq. 5.4) and exhausting air (Eq. 5.6) are compared in Fig. 5.17 for a 1-ft-diameter round duct. The data have been plotted on log-log paper because of the drastic difference in performance at the two ends of the exhaust system. The blowing air forms a jet that still has 10% of its initial velocity at a distance of almost 20 duct diameters from the duct face. In contrast, the velocity of the air being drawn into the duct falls off very rapidly, reaching 10% of the face velocity in less than one duct diameter and 1% in about three duct diameters.

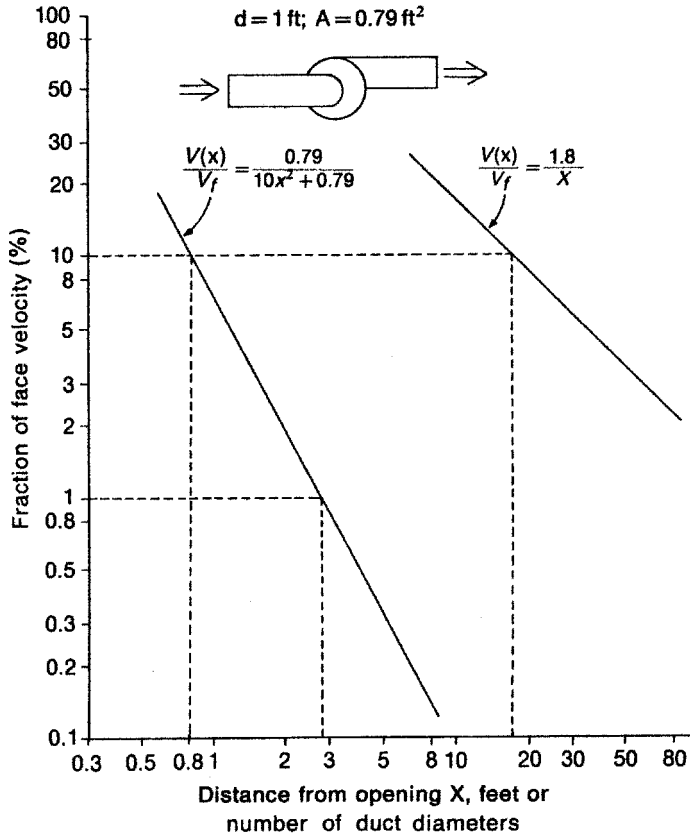


Figure 5.17 Comparison of air velocity patterns for blowing and exhausting air for a round duct 1 ft in diameter.

An equation similar to Eq. 5.8 has been developed to take into account the effect of the flange on the velocity characteristics in front of an exterior hood. Dalla Valle (1952) found that the following equation best fit his data for flanged hoods:

$$V(x) = \frac{Q}{0.75(10x^2 + A_f)} \quad (5.9)$$

In normalized form, we obtain

$$\frac{V(x)}{V_f} = \frac{A}{0.75(10x^2 + A_f)} \quad (5.10)$$

These equations illustrate the effect the flange has in increasing the “reach” of the hood; for a given value of airflow Q , the capture velocity at any distance x is increased by a factor of $1/0.75$, or 1.33. It should be emphasized that these are empirical

formulas, not ones developed from theory. Since DallaValle, several investigators have conducted further studies into the performance of round, square, and rectangular hoods. Garrison (1981, 1983a, 1983b; Garrison and Byers, 1980a, 1980b) measured the centerline velocities in front of a large number of hoods operated at high face velocities (so-called low-volume/high-velocity hoods) and developed empirical formulas relating V/V_f as a function of the relative distance x/D or x/W , where D is the hood diameter for round hoods and W is the width of square, rectangular, and slot hoods. He studied both flanged and unflanged hoods, and developed separate equations for each hood type.

Fletcher (1977, 1978, 1982; Fletcher and Johnson, 1982) performed similar studies but only on unflanged hoods. He developed a single empirical equation which accounts for hood shape by incorporating the hood width-to-length ratio.

Flynn and Ellenbecker (1985, 1986, 1987) developed equations for airflow into flanged circular hoods. Their approach differed from previous work in two respects: (1) the equations were derived theoretically from fluid mechanics rather than from empirical correlations; and (2) the equations describe the entire flow field, not just velocity along the hood centerline.

Two different models were developed. One, the so-called exact solution, rests on the assumption that potential flow theory describes the flow field in front of an exhaust hood. This assumption is valid at all points except near the hood face, where the model does not predict velocities well. The second model, the so-called approximate solution, modifies the first to improve prediction near the hood face. Figure 5.12 illustrates a typical flow field predicted by the approximate solution model.

The equations used in all of these models to predict centerline velocity for round, square, and rectangular hoods, both flanged and unflanged, are presented in the Appendix to this chapter. The equations are given in dimensionless form for ready comparison with each other and with empirical data. One such comparison is shown in Fig. 5.18, which compares the centerline velocities predicted by the various models with Dalla Valle's data for a round 8-in. flanged slot hood exhausting 100 cfm. All of the models are seen to predict centerline velocities very well; Flynn and Ellenbecker's theoretical model predicts velocity slightly better than do the empirical models at intermediate distances ($0.4 < V/V_f < 0.1$) and has the additional advantage of predicting the entire flow field and not just centerline velocities.

Capture Velocities in Front of Slot Hoods. Slot hoods (Fig. 5.19a) are rectangular hoods with aspect ratios less than 0.2. Such hoods were studied by Leslie Silverman (1941, 1942a, 1942b, 1943) at the Harvard School of Public Health in the early 1940s as a follow-on to Dalla Valle's work. The behavior of slot hoods is fundamentally different from that of rectangular or round openings; this difference can be demonstrated both theoretically and experimentally.

A slot hood can be modeled in the ideal case by a line source of suction (Fig. 5.19b). Here the velocity falls off with distance as a function of the surface area of a cylinder. Ignoring the cylinder ends, the area of a cylinder is given by

$$A_c = 2\pi Lx \quad (5.11)$$

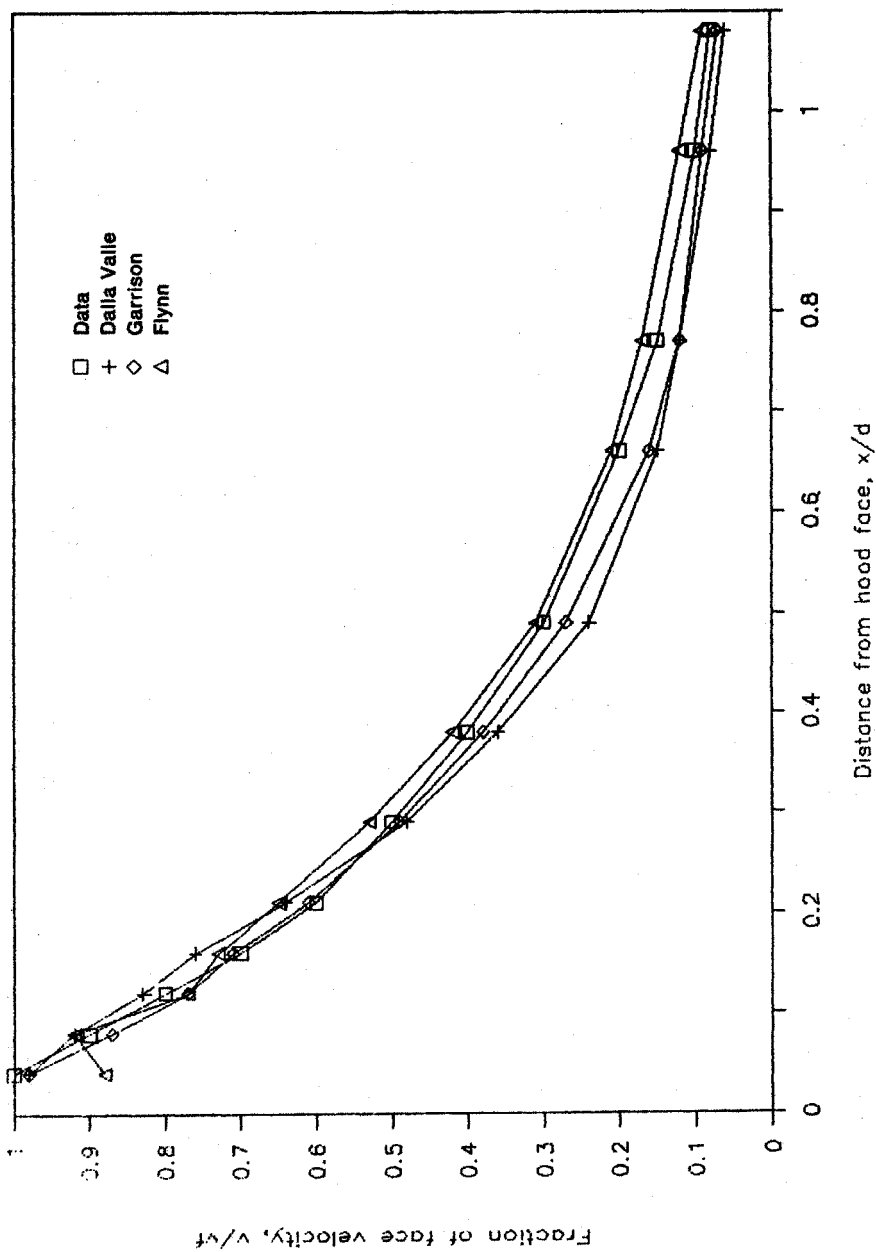


Figure 5.18 Comparison of models predicting centerline velocity as a function of distance for an 8-in. flanged circular hood. [Data from DallaValle (1930).]

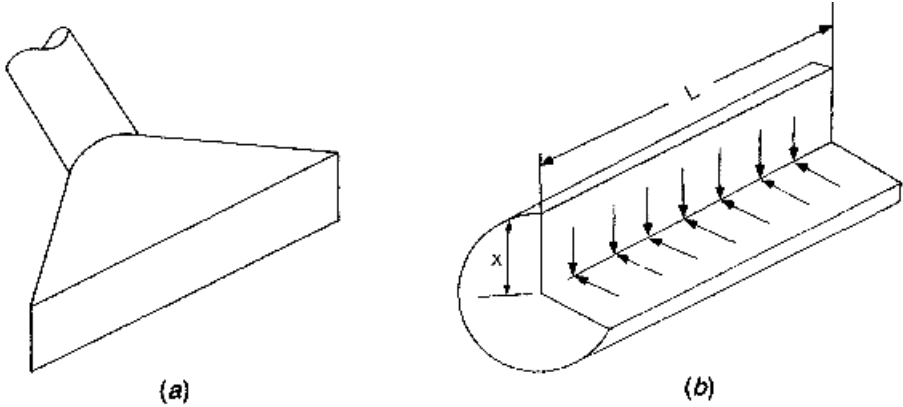


Figure 5.19 (a) Simple slot hood; (b) modeling a slot as a line source of suction.

where L is the length of the cylinder and x is the radius. If the hypothetical line source of suction is inducing an airflow Q , the velocity at a distance x is then

$$\begin{aligned} V(x) &= \frac{Q}{A_c} \\ &= \frac{Q}{2\pi Lx} \end{aligned} \quad (5.12)$$

Velocity is thus inversely proportional to distance for a line source of suction; this is an improvement over the point source (Eq. 5.6), where velocity falls off as the square of the distance. For a constant Q , however, the velocity at a point in front of a line source of suction is also a function of the length of the source L . Such sources of suction are useful only for contaminant sources which have an appreciable linear dimension, such as open-surface tanks.

Silverman (1943) measured velocity contours in front of several configurations of slot hoods, and derived empirical formulas relating capture velocity to airflow and distance. For unflanged slot hoods, the data were best fit by the following formula:

$$V(x) = \frac{Q}{3.7Lx} \quad (5.13)$$

and for flanged hoods,

$$\begin{aligned} V(x) &= \frac{Q}{0.75(3.7Lx)} \\ &= \frac{Q}{2.8Lx} \end{aligned} \quad (5.14)$$

These equations are similar to those predicted by theory, differing only by a constant factor (i.e., 3.7 vs. 2π).

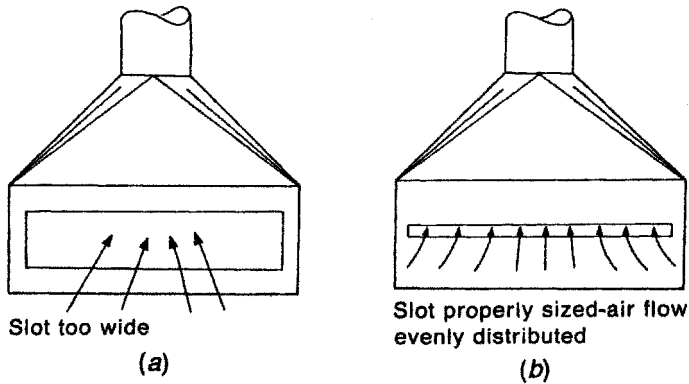


Figure 5.20 Principles of slot design: (a) if the slot is too wide, most of the air will flow through the center of the slot; (b) narrowing the slot causes the airflow to distribute evenly.

In designing a slot hood, it is desirable to use a slot that is relatively narrow, so that the airflow entering the hood is distributed relatively evenly over its length. The principles involved are illustrated in Fig. 5.20. If the slot on this hood is too *wide*, the air will enter the hood primarily through the *center* of the slot, near the transition from the plenum to duct. Narrowing the slot will place a high-resistance element in series with the low-resistance plenum; since the pressure drop across the opening must be equal at all locations, the high resistance of a narrow slot will tend to even out the airflow along the length, ensuring uniform flow across the tank being ventilated.

It is possible, of course, to make the slot *too* narrow, causing an excessive pressure drop. Practical experience has shown that a slot sized to give a slot velocity of 1000–2000 fpm (5–10 m/s) will provide good airflow distribution while avoiding excessive pressure drop. This is the velocity range prescribed in the design sections of the *Ventilation Manual*.

Recognizing that the average slot velocity V_s and width w are fixed by design considerations, Eqs. 5.13 and 5.14 can be rewritten to obtain normalized forms. In this case

$$\begin{aligned} Q &= V_s A_s \\ &= V_s Lw \end{aligned} \quad (5.15)$$

where A_s is the slot area selected to give the desired slot velocity. Substituting and rearranging yields

$$V(x) = \frac{V_s Lw}{3.7 Lx} \quad (5.13)$$

$$\frac{V(x)}{V_s} = \frac{w}{3.7x} \quad (5.16)$$

and for flanged hoods

$$\frac{V(x)}{V_s} = \frac{w}{2.8x} \quad (5.17)$$

Other investigators have also studied slot hoods. The work of Fletcher and Garrison described previously also included slot hoods, and Conroy et al. (1988) have extended the work of Flynn and Ellenbecker to this subject. Centerline velocity equations for each slot model are also presented in the Appendix. Silverman's model predicts an infinite velocity at the hood face, and so is not accurate in this area. For x/w values greater than 1, all the models predict similar velocities. Fletcher's model can only be used for unflanged hoods, while that of Conroy et al. can only be used for flanged hoods but has the advantage of predicting the entire flow field.

5.3.3 Exterior Hood Shape and Location

The basic principle behind shaping and locating an exterior hood is to make it as much like an enclosing hood as is physically possible. A complete enclosure is always the preferred design. Deviations from this ideal are caused by "real world" considerations, such as worker or material access. Frequently, the designer must be satisfied with a partial enclosure, which is of course superior to a purely exterior hood. Examples of partial enclosures abound; they can be as simple as the inclusion of baffles at the ends of a welding bench (Fig. 5.21a, VS-90-01 416), or as complicated as a double side-draft hood around a foundry shakeout (Fig. 5.21b, VS-20-02).

Partially enclosing an exterior hood reduces the effects of cross-drafts and directs the exhaust airflow from the point of contaminant release toward the exhaust hood. To the extent that an exterior hood can be partially enclosed, the amount of airflow needed to capture all contaminants will be reduced.

5.4 DESIGN OF RECEIVING HOODS

Most receiving hoods fall into one of two categories, canopy hoods for heated processes and hoods for grinding and other material finishing operations. Each is a special category of exterior hood, where the contaminant capture is assisted by a property of the contaminated gas stream. The recommended design procedure is different for each of these hood types, so they will be described separately.

5.4.1 Canopy Hoods for Heated Processes

The design of ventilation systems for heated processes was studied and described extensively by Hemeon (1963). Goodfellow (1985) also discusses the subject in detail and presents design data for several heated processes. A version of Hemeon's equations is presented in summary form in Chapter 3.9 of the *Ventilation Manual*; there are also several design plates for specific hot processes. The *Industrial Ventilation*

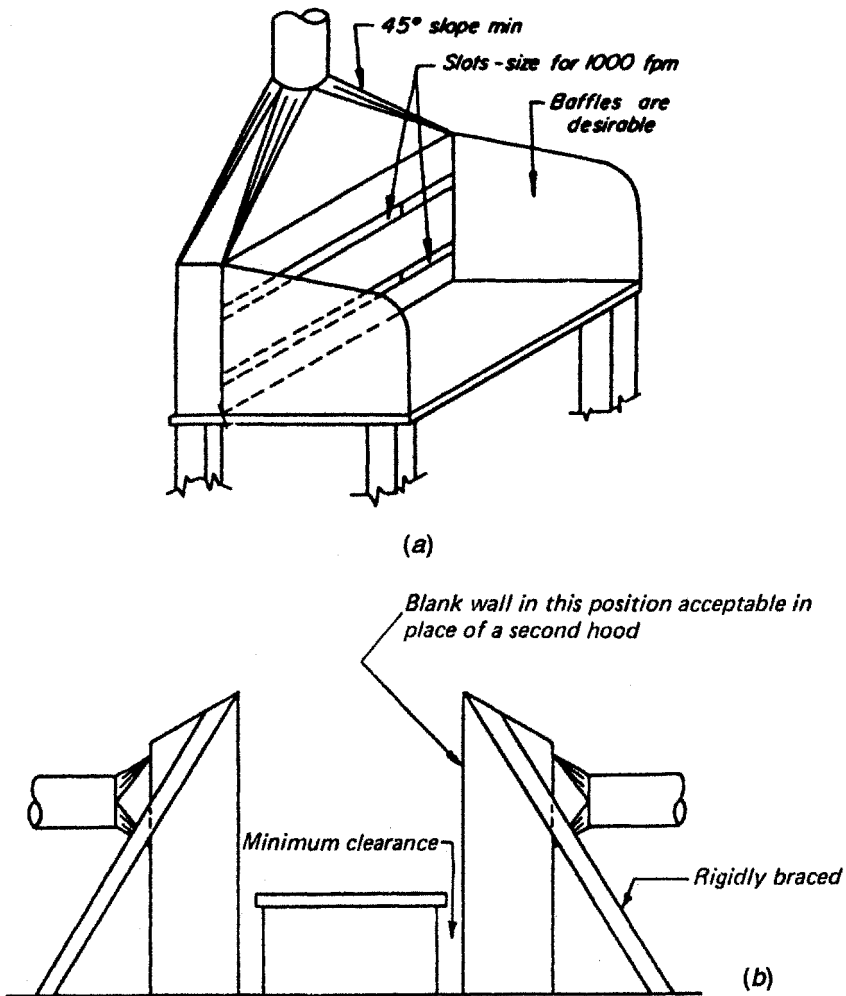


Figure 5.21 Partially enclosing exterior hoods: (a) welding bench with end baffles; (b) double side-draft foundry shakeout hood. [After Hagopian and Bastress (1976).]

Design Guidebook (Goodfellow and Tahti, 2001) summarizes recent analytical and numerical modeling [computational fluid dynamics (CFD); see Chapter 14] studies. Basic principles for design are presented here; the reader who needs more information is referred to Hemeon (1963) and Goodfellow (1985).

Thermal Updrafts from Heated Sources. The principle underlying the operation of canopy receiving hoods is the capture of the thermal updraft created by a heated process; the contaminants are presumed to be contained in this heated airstream, so the capture of the air transported by the chimney effect or thermal head will ensure

the efficient capture of the contaminants. A canopy hood used over a cold process, on the other hand, is an exterior hood; since the contaminants are not carried into the hood by the thermal head, the contaminants must be drawn into the hood by creating a sufficient capture velocity.

The difference between heated and unheated processes is illustrated in Fig. 5.22. For a room-temperature process (Fig. 5.22a), the canopy hood can be considered to be a booth with four open faces of dimension xy surrounding the process. Sufficient

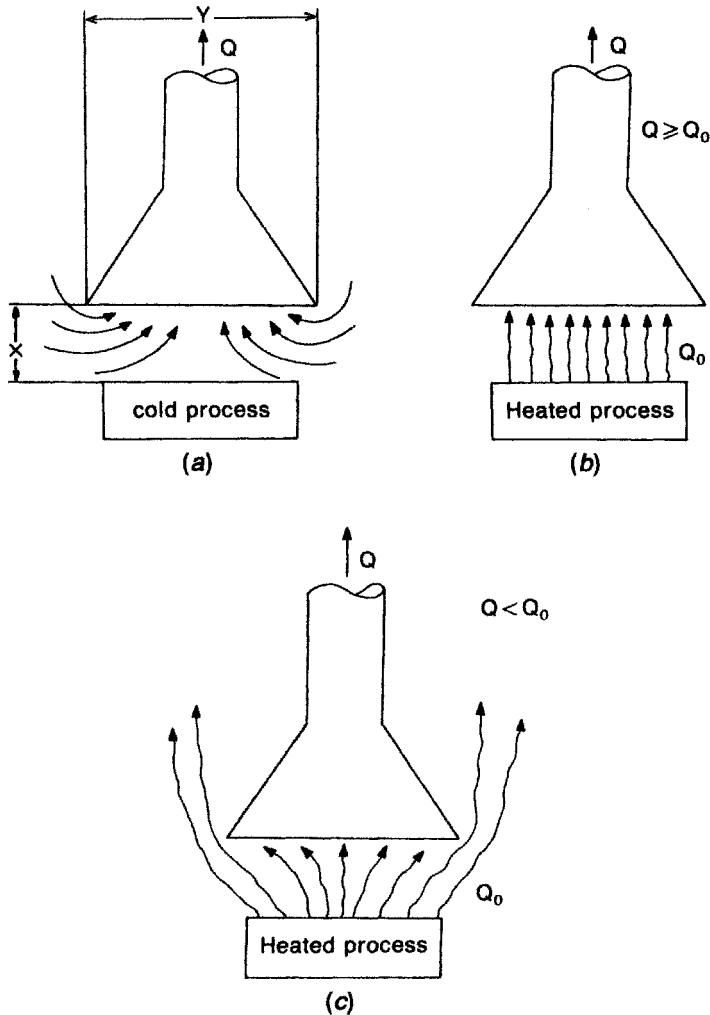


Figure 5.22 Comparison of canopy hoods used for heated and cold processes: (a) airflow patterns for a cold process, where the hood acts as an exterior hood; (b) airflow patterns for a heated process, where the induced airflow Q_h causes the hood to act as a receiving hood; (c) spillover for a heated process with $Q < Q_h$.

inward velocity must be developed across each face to ensure that the contaminants are drawn into the hood. The contaminants given off by a heated process are carried into the hood by the buoyancy of the exhaust gas (Fig. 5.22*b*). The required exhaust airflow in this case is governed by the rate at which heated air is given off by the process; if the hood is properly sized and positioned, the exhaust airflow Q must be selected to be greater than the rate Q_h at which hot gas is generated. If this condition is not met, some of the heated air will “spill over” the edges of the canopy hood and escape (Fig. 5.22*c*).

Required Airflow for Heated Processes. The principal design consideration for canopy hoods, then, is the determination of Q_h . Hemeon (1963) and Goodfellow (1985) have considered this problem in detail. The amount of airflow set in motion by a heated body Q_h is a function of the body's heat loss rate, which in turn is a function of the body's size, surface characteristics, and surface temperature relative to ambient temperature. The induced airflow rises and mixes turbulently with the surrounding air; it is also affected by any cross-drafts that might be present. The relative importance of these effects depends on the receiving hood location.

Hemeon distinguishes between low canopy hoods, which are located within about 3 ft (1 m) of the heated surface, and high canopy hoods, which are located higher. The design of low hoods is much simpler since turbulent mixing and cross-draft interaction are less extensive than with high hoods. Low hoods are generally preferred because they can capture a higher percentage of the contaminants with a much lower required airflow than can high hoods. If high hoods must be used, Goodfellow presents design equations and examples of proper design.

The design and use of slot hoods for heated sources is much more difficult than for room-temperature sources, due to the necessity of calculating the required capture velocity to overcome the buoyant plume. The design procedure for open-surface tanks discussed in Chapter 6 includes provisions for elevated liquid temperature; in general, the exhaust volumes specified by this procedure are much higher than those required for a canopy hood.

5.4.2 Hoods for Grinding Operations

Receiving hoods used in grinding and other finishing operations are quite different in concept from the canopy hoods described above. The property assisting in the transport of the contaminants to the hood is the momentum imparted to the particles by the grinding process. The hood is positioned and sized to “catch” the particles created by the grinding process, which are “thrown” with some momentum toward the hood (Fig. 5.23). Since the hood does not have to “reach” as far to capture the contaminant, the capture velocity can be supplied at some distance which is less than x , the separation between the wheel and the hood. The airflow required, using DallaValle's equations, would be less than if the particle throw were not taken into account. If these equations are used, the designer must estimate the new distance x' at which the capture velocity must be created (Fig. 5.23). This distance is given by

$$x' = x - S \quad (5.18)$$

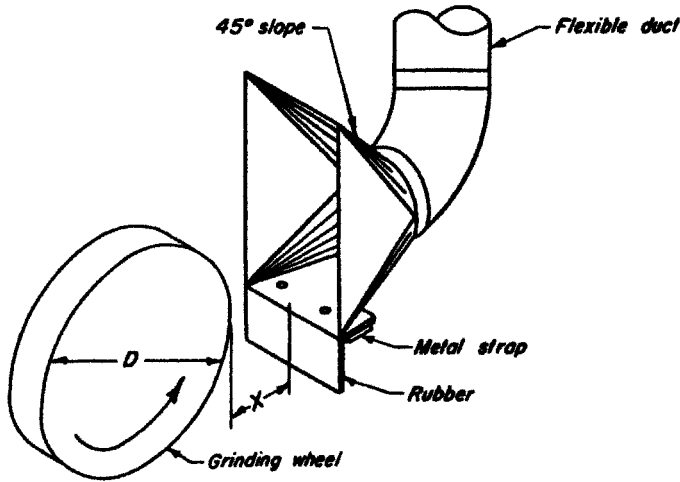


Figure 5.23 Receiving hood used for grinding. [After Hagopian and Bastress (1976).]

where S is the particle stopping distance, defined as the distance a particle ejected into still air at an initial velocity will travel in decelerating to rest due to drag forces.

Hinds (1982) has calculated stopping distances for different-sized particles for the case of an initial velocity of 2000 fpm (10 m/s) (Table 5.2). These data illustrate the difficulty in “throwing” even fairly large particles an appreciable distance in still air. Any particles that are in the inhalable range (i.e., $d_p < 10 \mu\text{m}$) should be considered immovable in still air, so for industrial hygiene purposes it should always be assumed that $x = x'$. Larger particles, which may present a housekeeping problem if not captured, may travel appreciable distances and hood designs for such processes need to take this into account.

Although aerosol particles cannot travel a considerable distance in still air, the high-velocity projection of such particles into still air can *induce* an airflow similar to that caused by falling particles (Chapter 6). Hemeon (1963) investigated this phenomenon and concluded that significant amounts of air would be entrained only for large particles ($d_p > 1000 \mu\text{m}$).

Table 5.2 Particle Stopping Distances for an Initial Velocity of 2000 fpm (10 m/s)

Particle Diameter (μm)	Stopping Distance (cm)
0.01	2.0×10^{-6}
0.1	6.8×10^{-5}
1.0	3.6×10^{-3}
10	0.23
100	12.7

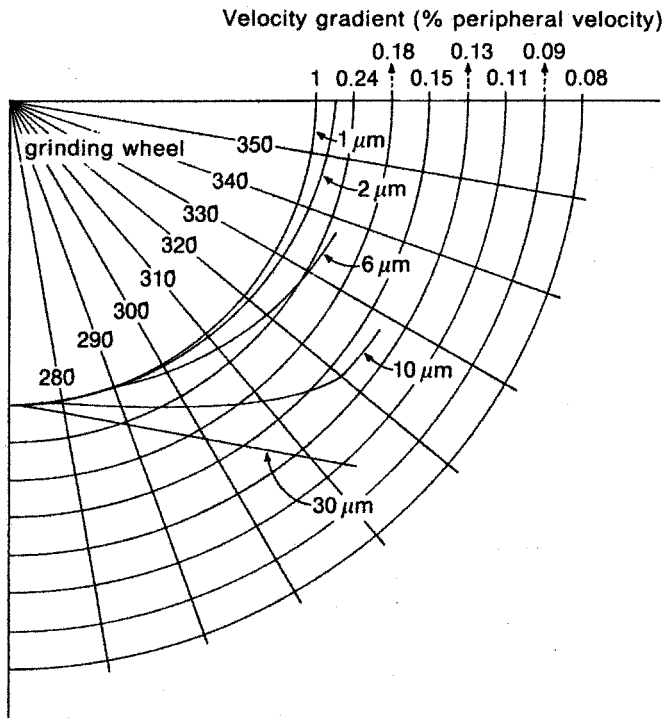


Figure 5.24 Particle trajectories around grinding operations.

As part of a study of ventilation requirements for grinding operations (Bastress et al., 1974), detailed particle trajectories around these operations were modeled. A typical result of this effort is shown in Fig. 5.24. The behavior of particles can be divided into three categories, depending on particle diameter. Small particles ($d_p < 3 \mu\text{m}$) travel around the periphery of the wheel and thus are not “thrown” toward the exhaust hood. Large particles ($d_p > 30 \mu\text{m}$) are thrown in a nearly straight trajectory toward the exhaust hood, and thus are easily captured. Particles in the intermediate size range ($3 \mu\text{m} < d_p < 30 \mu\text{m}$) follow an intermediate trajectory that carries them some distance toward the hood and facilitates capture.

It is apparent from this analysis that the grinding wheel hood does act as a receiving hood for large particles but not for small, respirable ones. Such particles must be collected by creating a sufficiently high capture velocity near the surface of the grinding wheel. Bastress et al. (1974) found that respirable particles were not captured efficiently by typical grinding wheel exhaust systems and escaped to the workplace in the vicinity of the worker’s breathing zone. For example, the study found that about 20% of the respirable particles generated when grinding mild steel escaped the exhaust system even when large airflows were employed (Fig. 5.25). Nonetheless, the standard hood designs recommended in the *Ventilation Manual*, while not 100% efficient at capturing respirable particles,

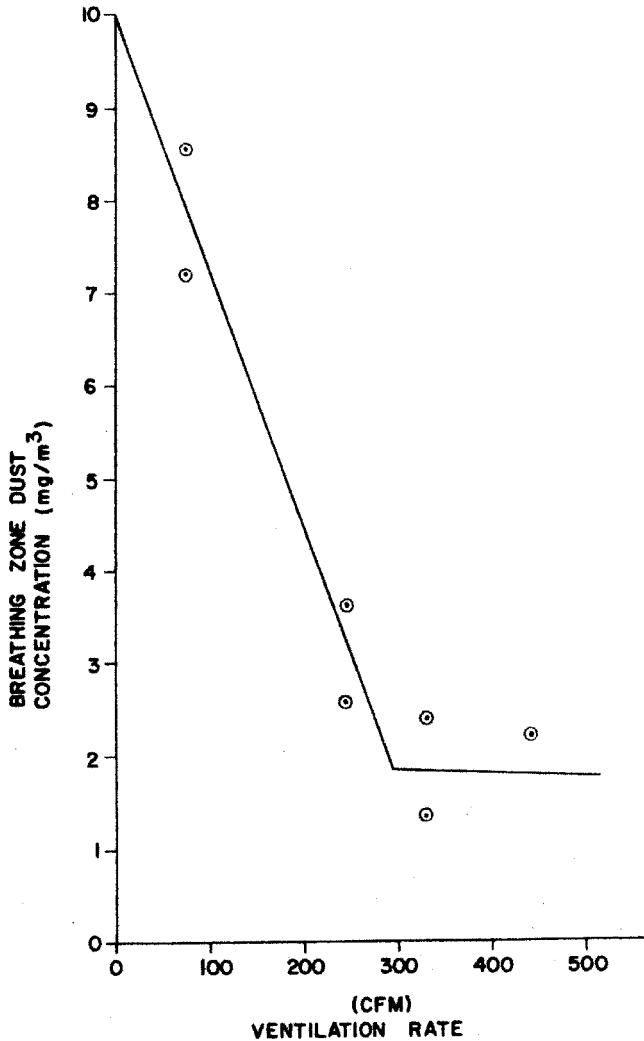


Figure 5.25 Typical performance characteristics of a ventilation system used in conjunction with a pedestal grinder.

were sufficient to provide worker protection at or below the threshold limit values for total and respirable inert dust.

5.5 EVALUATION OF HOOD PERFORMANCE

After installation, the performance of exhaust hoods should be evaluated to confirm that (1) the airflow through the hood is equal to the design airflow, and (2) the hood

is capturing the contaminants given off by the process that it is controlling. Because these issues more accurately assess the performance of the entire exhaust system rather than the exhaust hood alone, they are addressed in detail in Chapter 13.

LIST OF SYMBOLS

A	area
A_c	cylinder surface area
A_f	hood face cross-sectional area
A_s	slot area
D	duct diameter
d_p	particle diameter
K	constant in Eq. 5.3
L	cylinder length
Q	airflow
Q_h	airflow induced by a heated process
V	velocity
S	particle stopping distance
V_c	capture velocity
V_d	cross-draft velocity
V_f	hood face velocity
V_s	slot velocity
W	hood width
w	slot width
x	distance, length
y	distance, length

REFERENCES

- American Conference of Governmental Industrial Hygienists, Committee on Industrial Ventilation, *Industrial Ventilation*, 24th ed., ACGIH, Lansing, MI, 2001.
- American Society of Heating, Refrigerating and Air Conditioning Engineers, 2001 *ASHRAE Handbook—Fundamentals*, ASHRAE, Atlanta, GA, 2001.
- Bastress, E., J. Niedzwecki, and A. Nugent, *Ventilation Requirements for Grinding, Buffing, and Polishing Operations*, U.S. Department of Health, Education, and Welfare, National Institute for Occupational Safety and Health, Publication No. 75-107, Washington, DC, 1974.
- Brandt, A., *Industrial Health Engineering*, Wiley, New York, 1947.
- Conroy, L., M. Ellenbecker, and M. Flynn, "Prediction and Measurement of Velocity into Flanged Slot Hoods," *Am. Ind. Hyg. Assoc. J.* **49**(5):226-234 (1988).
- Conroy, L., *Capture Efficiency of Flanged Slot Hoods under the Influence of a Uniform Crossdraft*, doctoral thesis, Harvard School of Public Health, Boston, 1988.
- DallaValle, J., *Studies in the Design of Local Exhaust Hoods*, doctoral thesis, Harvard School of Public Health, Boston, 1930.

- DallaValle, J., *Exhaust Hoods*, Industrial Press, New York, 1952.
- Dalrymple, H. L., "Development and Use of a Local Exhaust Ventilation System to Control Fume from Hand Held Soldering Irons," *Proc. 1st Int. Symp. Ventilation for Contaminant Control*, Oct. 1–3, 1985, Toronto, Canada, H. G. Goodfellow, ed., Elsevier, New York.
- Ellenbecker, M., R. Gempel, and W. Burgess, "Capture Efficiency of Local Exhaust Ventilation Systems," *Am. Ind. Hyg. Assoc. J.* **44**(10):752–755 (1983).
- Esman, N., D. Weyel, and F. McGuigan, "Aerodynamic Properties of Exhaust Hoods," *Am. Ind. Hyg. Assoc. J.* **47**(8):448–454 (1986).
- Fletcher, B., "Centreline Velocity Characteristics of Rectangular Unflanged Hoods and Slots under Suction," *Ann. Occup. Hyg.* **20**:141–146 (1977).
- Fletcher, B., "Effect of Flanges on the Velocity in Front of Exhaust Ventilation Hoods," *Ann. Occup. Hyg.* **21**:265–269 (1978).
- Fletcher, B., "Centreline Velocity Characteristics of Local Exhaust Ventilation Hoods," *Am. Ind. Hyg. Assoc. J.* **43**(8):626–627 (1982).
- Fletcher, B., and A. Johnson, "Velocity Profiles around Hoods and Slots and the Effects of an Adjacent Plane," *Ann. Occup. Hyg.* **25**(4):365–372 (1982).
- Fletcher, B., and A. Johnson, "The Capture Efficiency of Local Exhaust Ventilation Hoods and the Role of Capture Velocity," *Proc. 1st Int. Symp. Ventilation for Contaminant Control*, Oct. 1–3, 1985, Toronto, Canada, H. G. Goodfellow, ed., Elsevier, New York, 1986.
- Flynn, M., and M. Ellenbecker, "The Potential Flow Solution for Air Flow into a Flanged Circular Hood," *Am. Ind. Hyg. Assoc. J.* **46**(6):318–322 (1985).
- Flynn, M., and M. Ellenbecker, "Capture Efficiency of Flanged Circular Local Exhaust Hoods," *Ann. Occup. Hyg.* **30**(4):497–513 (1986).
- Flynn, M., and M. Ellenbecker, "Empirical Validation of Theoretical Velocity Fields into Flanged Circular Hoods," *Am. Ind. Hyg. Assoc. J.* **48**(4):380–389 (1987).
- Garrison, R., "Centerline Velocity Gradients for Plain and Flanged Local Exhaust Inlets," *Am. Ind. Hyg. Assoc. J.* **42**(10):739–746 (1981).
- Garrison, R., "Velocity Calculation for Local Exhaust Inlets—Empirical Design Equations," *Am. Ind. Hyg. Assoc. J.* **44**(12):937–940 (1983a).
- Garrison, R., "Velocity Calculation for Local Exhaust Inlets—Graphical Design Concepts," *Am. Ind. Hyg. Assoc. J.* **44**(12):941–947 (1983b).
- Garrison, R., and D. Byers, "Static Pressure and Velocity Characteristics of Circular Nozzles for High Velocity/Low Volume Exhaust Ventilation," *Am. Ind. Hyg. Assoc. J.* **41**(11):803–811 (1980a).
- Garrison, R., and D. Byers, "Static Pressure, Velocity, and Noise Characteristics of Rectangular Nozzles for High Velocity/Low Volume Exhaust Ventilation," *Am. Ind. Hyg. Assoc. J.* **41**(12):855–863 (1980b).
- Goodfellow, H. (1985), *Advanced Design of Ventilation Systems for Contaminant Control*, Elsevier, New York.
- Goodfellow, H., and E. Tahti, eds., *Industrial Ventilation Design Guidebook*, Academic Press, San Diego, 2001.
- Hagopian, J., and E. Bastress, *Recommended Industrial Ventilation Guidelines*, Arthur D. Little, Inc., Contract No. CDC-99-74-33, U.S. Department of Health, Education, and Welfare, Public Health Service, Centers for Disease Control, National Institute for Occupational Safety and Health, Cincinnati, OH, Jan. 1976.

- Hemeon, W., *Plant and Process Ventilation*, 2nd ed., Industrial Press, New York, 1963.
- Hinds, W., *Aerosol Technology: Properties, Behavior, and Measurement of Airborne Particles*, Wiley, New York, 1982.
- Jansson, A., "Capture Efficiencies of Local Exhausts for Hand Grinding, Drilling and Welding," *Staub-Reinhalt. Luft* (English ed.), **43**(3):111–113 (1980).
- Jansson, A., *Description of Air Movement Outside a Circular Exhaust Opening without Flange* (in Swedish), Undersökningsrapport No. 36, 1985.
- Regnier, R., R. Braconnier, and G. Aubertin, "Study of Capture Devices Integrated into Portable Machine-Tools," *Proc. 1st Int. Symp. Ventilation for Contaminant Control*, Oct. 1–3, 1985, Toronto, Canada, H. G. Goodfellow, ed., Elsevier, New York, 1986.
- Silverman, L., "Fundamental Factors in the Design of Lateral Exhaust Hoods for Industrial Tanks," *J. Ind. Hyg. Toxicol.* **23**(5):187–266 (1941).
- Silverman, L., "Centerline Velocity Characteristics of Round Openings under Suction," *J. Ind. Hyg. Toxicol.* **24**(9):259–266 (1942a).
- Silverman, L., "Velocity Characteristics of Narrow Exhaust Slots," *J. Ind. Hyg. Toxicol.* **24**(9):267–276 (1942b).
- Silverman, L., *Fundamental Factors in the Design of Exhaust Hoods*, doctoral thesis, Harvard School of Public Health, Boston, 1943.

APPENDIX: EXTERIOR HOOD CENTERLINE VELOCITY MODELS

Applicable Range	Equation	Equation Number
<i>Round Hoods, Unflanged</i>		
DallaValle $0 < \frac{x}{D} < \infty$	$\frac{V}{V_f} = \frac{1}{12.7(x/D)^2 + 1}$	(5.19)
Fletcher $0 < \frac{x}{D} < \infty$	$\frac{V}{V_f} = \frac{1}{10.9(x/D)^2 + 1}$	(5.20)
Garrison $0 < \frac{x}{D} < 0.5$	$\frac{V}{V_f} = 1.1(0.06)^{x/D}$	(5.21)
$0.5 \leq \frac{x}{D} \leq 1.5$	$\frac{V}{V_f} = 0.08 \left(\frac{x}{D} \right)^{-1.7}$	(5.22)
<i>Round Hoods, Flanged</i>		
DallaValle $0 < \frac{x}{D} < \infty$	$\frac{V}{V_f} = \frac{1}{9.6(x/D)^2 + 0.75}$	(5.23)

APPENDIX (Continued)

Applicable Range	Equation	Equation Number
Flynn (approximate)		
$0 < \frac{x}{D} < \infty$	$\frac{V}{V_f} = \frac{\sqrt{3}\varepsilon^2}{2(3-2\varepsilon^2)^{1/2}}$ <p style="text-align: center;">where $\varepsilon^2 = \frac{1}{4(x/D)^2 + 1}$</p>	(5.24)
Flynn (exact)		
$0 < \frac{x}{D} < \infty$	$\frac{V}{V_f} = \frac{1}{8(x/D)^2 + 1}$	(5.25)
Garrison		
$0 < \frac{x}{D} < 0.5$	$\frac{V}{V_f} = 1.1(0.07)^{x/D}$	(5.26)
$0.5 \leq \frac{x}{D} \leq 1.5$	$\frac{V}{V_f} = 0.10\left(\frac{x}{D}\right)^{-1.6}$	(5.27)
<i>Square Hoods, Unflanged (side = a)</i>		
DallaValle		
$0 < \frac{x}{a} < \infty$	$\frac{V}{V_f} = \frac{1}{10(x/a)^2 + 1}$	(5.28)
Fletcher		
$0 < \frac{x}{a} < \infty$	$\frac{V}{V_f} = \frac{1}{8.6(x/a)^2 + 0.93}$	(5.29)
Garrison		
$0 < \frac{x}{a} < 0.5$	$\frac{V}{V_f} = 1.07(0.09)^{x/a}$	(5.30)
$0.5 \leq \frac{x}{a} \leq 1.5$	$\frac{V}{V_f} = 0.10\left(\frac{x}{a}\right)^{-1.7}$	(5.31)
<i>Square Hoods, Flanged</i>		
DallaValle		
$0 < \frac{x}{a} < \infty$	$\frac{V}{V_f} = \frac{1}{7.5(x/a)^2 + 0.75}$	(5.32)
Garrison		
$0 < \frac{x}{a} < 0.5$	$\frac{V}{V_f} = 1.07(0.11)^{x/a}$	(5.33)
$0.5 \leq \frac{x}{a} \leq 1.5$	$\frac{V}{V_f} = 0.12\left(\frac{x}{a}\right)^{-1.6}$	(5.34)

APPENDIX (Continued)

Applicable Range	Equation	Equation Number
Flynn (exact)		
$0 < \frac{x}{D} < \infty$	$\frac{V}{V_f} = \frac{1}{6.3(x/a)^2 + 0.25}$	(5.35)
<i>Rectangular Hoods, Unflanged ($0.2 < w/L < 1$)</i>		
DallaValle		
$0 < \frac{x}{w} < \infty$	$\frac{V}{V_f} = \frac{1}{10(x^2/wL) + 1}$	(5.36)
Fletcher		
$0 < \frac{x}{w} < \infty$	$\frac{V}{V_f} = \frac{1}{8.58\alpha^2 + 0.93}$	(5.37)
	$\alpha = \frac{x}{(wL)^{1/2}} \left(\frac{w}{L} \right)^{-\beta}$	
	$\beta = 0.2 \left[\frac{x}{(wL)^{1/2}} \right]^{1/3}$	
Garrison ^a		
At $w/L = 0.5$:		
$0 < \frac{x}{w} < 0.5$	$\frac{V}{V_f} = 1.07(0.14)^{x/w}$	(5.38)
$0.5 \leq \frac{x}{w} < 1.0$	$\frac{V}{V_f} = 0.18 \left(\frac{x}{w} \right)^{-1.2}$	(5.39)
$1.0 \leq \frac{x}{w} \leq 2.0$	$\frac{V}{V_f} = 0.18 \left(\frac{x}{w} \right)^{-1.7}$	(5.40)
At $w/L = 0.25$:		
$0 < \frac{x}{w} < 0.5$	$\frac{V}{V_f} = 1.07(0.18)^{x/w}$	(5.41)
$0.5 \leq \frac{x}{w} < 1.0$	$\frac{V}{V_f} = 0.23 \left(\frac{x}{w} \right)^{-1.0}$	(5.42)
$1.0 \leq \frac{x}{w} \leq 2.5$	$\frac{V}{V_f} = 0.23 \left(\frac{x}{w} \right)^{-1.5}$	(5.43)
<i>Rectangular Hoods, Flanged</i>		
DallaValle		
$0 < \frac{x}{w} < \infty$	$\frac{V}{V_f} = \frac{1}{7.5x^2/wL}$	(5.44)

APPENDIX (*Continued*)

Applicable Range	Equation	Equation Number
Conroy (exact)		
$0 < \frac{x}{w} < \infty$	$\frac{V}{V_f} = \frac{1}{2\pi[0.25 + (x/w)^2]^{1/2} [0.25 + (x/L)^2]^{1/2}}$	(5.45)
Garrison		
For $w/L = 0.5$:		
$0 < \frac{x}{w} < 0.5$	$\frac{V}{V_f} = 1.07(0.17)^{x/w}$	(5.46)
$0.5 \leq \frac{x}{w} < 1.0$	$\frac{V}{V_f} = 0.21\left(\frac{x}{w}\right)^{-1.1}$	(5.47)
$1.0 \leq \frac{x}{w} \leq 2.0$	$\frac{V}{V_f} = 0.21\left(\frac{x}{w}\right)^{-1.6}$	(5.48)
For $w/L = 0.25$:		
$0 < \frac{x}{w} < 0.5$	$\frac{V}{V_f} = 1.07(0.22)^{x/w}$	(5.49)
$0.5 \leq \frac{x}{w} < 1.0$	$\frac{V}{V_f} = 0.27\left(\frac{x}{w}\right)^{-0.9}$	(5.50)
$1.0 \leq \frac{x}{w} \leq 3.0$	$\frac{V}{V_f} = 0.27\left(\frac{x}{w}\right)^{-1.4}$	(5.51)
<i>Slot Hoods, Unflanged</i>		
Silverman		
$0 < \frac{x}{w} < \infty$	$\frac{V}{V_s} = 0.27\left(\frac{x}{w}\right)^{-1.0}$	(5.52)
Garrison		
$0 < \frac{x}{w} < 0.5$	$\frac{V}{V_s} = 1.07(0.19)^{x/w}$	(5.53)
$0.5 \leq \frac{x}{w} < 1.0$	$\frac{V}{V_s} = 0.24\left(\frac{x}{w}\right)^{-1.0}$	(5.54)
$1.0 \leq \frac{x}{w} \leq 3.5$	$\frac{V}{V_f} = 0.24\left(\frac{x}{w}\right)^{-1.2}$	(5.55)

APPENDIX (Continued)

Applicable Range	Equation	Equation Number
Fletcher		
$0 < \frac{x}{w} < \infty$	$\frac{V}{V_s} = \frac{1}{8.58\alpha^2 + 0.93}$	(5.56)
	$\alpha = \frac{x}{(wL)^{1/2}} \left(\frac{w}{L} \right)^{-\beta}$	
	$\beta = 0.2 \left[\frac{x}{(wL)^{1/2}} \right]^{1/3}$	
<i>Slot Hoods, Flanged</i>		
Silverman		
$0 < \frac{x}{w} < \infty$	$\frac{V}{V_s} = 0.36 \left(\frac{x}{w} \right)^{-1.0}$	(5.57)
Garrison		
$0 < \frac{x}{w} < 0.5$	$\frac{V}{V_s} = 1.07(0.22)^{x/w}$	(5.58)
$0.5 \leq \frac{x}{w} < 1.0$	$\frac{V}{V_s} = 0.29 \left(\frac{x}{w} \right)^{-0.8}$	(5.59)
$1.0 \leq \frac{x}{w} \leq 4.0$	$\frac{V}{V_s} = 0.29 \left(\frac{x}{w} \right)^{-1.1}$	(5.60)
Conroy (exact)		
$0 < \frac{x}{w} < \infty$	$\frac{V}{V_s} = \frac{1}{2\pi[0.25 + (x/w)^2]^{1/2}[0.25 + (x/L)^2]^{1/2}}$	(5.61)

^a Empirical coefficients were calculated only at $w/L = 0.5$ and $w/L = 0.25$.

PROBLEMS

- 5.1** (a) What airflow is required to give a capture velocity of 150 ft/min at a distance 8 in. from the center of a 6-in.-diameter unflanged round opening?
- (b) If a flange is added to the opening, what airflow would then be required to give the same capture velocity?
- (c) A flanged slot hood, 5 ft long, has an airflow of 1500 ft³/min. What is the capture velocity of this hood at a distance of 15 in. in front of the slot?

Answers:

- (a) 700 cfm
- (b) 520 cfm
- (c) 86 fpm

5.2 An exhaust hood is attached to a 14-in.-diameter round duct. The hood static pressure is 2.3 in. H_2O , and the hood entry loss is 1.1 in. H_2O .

- (a) What is the duct velocity pressure?
- (b) What is the hood entry loss factor?
- (c) What is the average velocity in the 14-in.-diameter duct?
- (d) What is the airflow through the system?

Answers:

- (a) 1.2 in. H_2O
- (b) 0.92
- (c) 4390 fpm
- (d) 4690 cfm

- 5.3** (a) A portable flanged rectangular hood is being used to exhaust a welding operation. If the hood dimensions are 5×7 in. and the welding is being performed at a distance of 7 in. from the hood face, what airflow is required to give a capture velocity of 200 ft/min at the welding location?
- (b) Instead of using the portable hood described in part (a), a welding bench is used with a slot hood running the length of the back of the bench (the hood plenum serves as a flange for the hood). If the bench is 3.5 ft long and 21 in. deep (front to back), what airflow is required to maintain a capture velocity of 200 ft/min at the front edge of the bench?

Answers:

- (a) 550 cfm
- (b) 3490 cfm

5.4 For each of the following hoods, determine the required airflow, slot velocity, and dimensions (where appropriate), duct velocity, duct diameter, hood entry loss factor, and hood static pressure. Assume standard conditions. [Vent Man]

- (a) Grinding wheel hood, 12-in.-diameter, 2 in. width, good enclosure, tapered takeoff, rotating speed = 2500 rpm.
- (b) Bench hood for welding, bench 3 ft long.
- (c) Small paint booth, booth face area 3×3 ft, baffles to distribute airflow, for air paint spraying.
- (d) Open-surface tank used for chromium stripping in a hydrochloric acid bath, tank 3 ft long \times 18 in. wide, lateral hood with upward plenum.

(e) Chemical laboratory hood for general use, vertical sash, sash opening 4 ft wide.

5.5 The following table shows measurements taken for five different hoods, connected to a straight run of duct. In each case, the pressure measurements were taken four to six duct diameters downstream from the hood. Fill in the blanks in the table.

Hood No.	1	2	3	4	5
Q , ft ³ /min	4000	4000	4000	4000	4000
V , ft/min			2000		
p_s , in. H ₂ O		-2.40		-0.98	
p_r , in. H ₂ O	-1.20			-0.08	
p_v , in. H ₂ O	1.00				0.43
F_e		1.67		0.09	
h_e , in. H ₂ O		1.50			1.27
C_e	0.67		0.80		

HOOD DESIGNS FOR SPECIFIC APPLICATIONS

The hood designs in Chapter 10 of the *Ventilation Manual* cover a range of industrial operations and include recommendations on hood geometry, airflow or critical control velocity, duct velocity, and entry loss. Caution is necessary in applying these designs to a specific plant operation since there may be plant-to-plant differences in industrial processes such that an exhaust system that is effective at one facility may not work at another. The ventilation designer must use knowledge of the specific materials in use at the plant, production rate, work practices, and special production requirements to modify the *Ventilation Manual* hood designs where appropriate.

In this chapter we cover the application of hood design data on selected industrial operations chosen because they are commonly encountered in general industry and may present potential occupational health risk to workers if air contaminants released from the process are not controlled effectively. In the case of electroplating, effective design data are available but their applications are frequently poor due to difficulty in interpreting the design data in Chapter 10 of the *Ventilation Manual* or in modifying the data to fit a related process. Painting and welding are included in this discussion because of their widespread application in industry. Material transfer operations are covered in the *Ventilation Manual*, but the designer should be aware of an alternative design technique, the induced airflow method, which complements the *Ventilation Manual* design approach. Chemical processing operations are given little attention in the *Ventilation Manual* and semiconductor gas cabinet ventilation design is not covered in detail in any source book.

6.1 ELECTROPLATING

There are numerous metal treatment and coating operations associated with the electroplating industry. Normally, these processes are conducted in open-surface tanks and the toxic air contaminants released by the process must be controlled by local exhaust ventilation techniques. The local exhaust design data on open-surface tanks presented in Chapter 10 of the *Ventilation Manual* define hood geometry and airflow required for effective contaminant control and are the culmination of over seven decades of research and field experience. In the early twentieth century, open-surface tanks were frequently placed on an outside plant wall and exhausted by a wall fan. Early ventilation designs also favored open-canopy hoods; however, the deficiencies of these hoods limit their application in modern plants. Two hood types, enclosing hoods and lateral exhaust hoods, offer effective control of air contaminants released from open-surface tanks. The design of both hood types is discussed below.

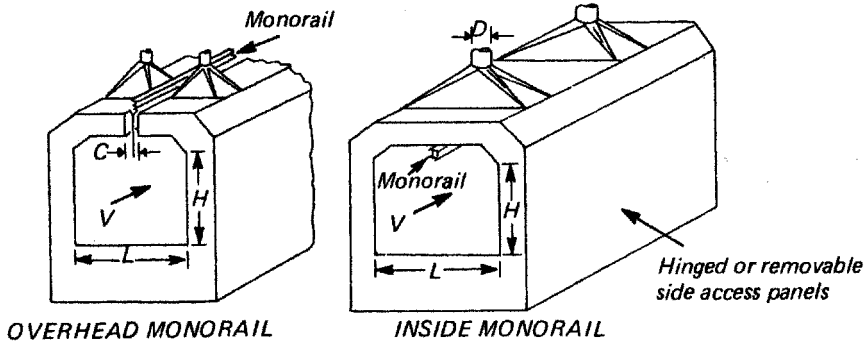
6.1.1 Hood Design

As noted in Chapter 10 of the *Ventilation Manual*, enclosing hoods are preferred for many industrial operations since they permit efficient containment of toxic air contaminants with minimum airflow. The principal difficulty with this design is that the hood may restrict access to the operation. An enclosing hood with a conveyor access slot and open ends (Fig. 6.1a) finds wide application in automated plating operations; in a job shop with manual transfer of parts from tank to tank an enclosing hood with an open-front face may be acceptable (Fig. 6.1b).

The open-face area of an enclosing hood must be defined accurately in the design phase so that airflow can be calculated. A commitment must be obtained from production management on the planned degree of enclosure that will minimize airflow yet will not interfere with operations. Frequently, enclosing hood systems are properly designed and installed but are rendered useless when operating personnel remove a portion of the enclosure to gain access to the tank for the transfer of parts.

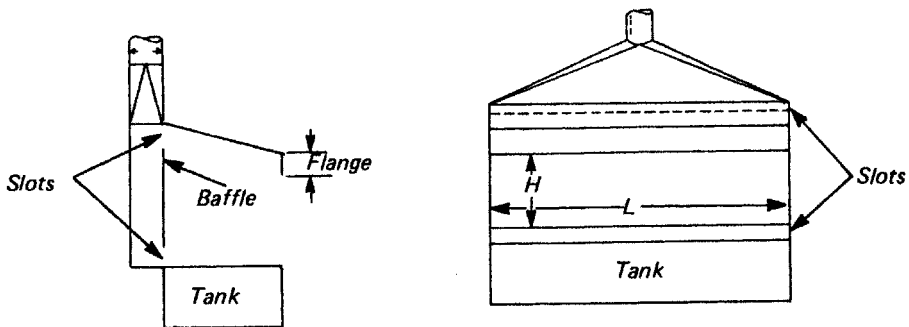
The three exhaust hoods in Figs. 6.2 and 6.3 are characterized as lateral exhaust hoods since they are designed to provide a horizontal sweep of air across the surface of the tank to convey the toxic air contaminants to the hood. This is the most popular open-surface tank hood in electroplating job shops; the operator has access to the tank contents from three or four sides, thus permitting easy movement of parts from one tank to another.

An important feature of the hoods with an upward plenum (Fig. 6.2) is that the fishtail taper from hood to duct provides a baffle to shield the tank from room drafts that can interfere with hood capture efficiency. The lip or perimeter slot exhaust hood (Fig. 6.3) requires that external baffles be installed or the tank must be positioned against a wall to provide equivalent shielding from interfering drafts.



Q = exhaust volume, cfm, equals AV
 H = height of rectangular opening, feet
 L = length of opening, feet
 A = area of openings in enclosure
 = $2HL$ + area of monorail slot
 V = minimum face velocity, fpm
 Duct velocity = 1500 fpm (7.62 m/s) minimum
 Entry loss = entry loss factor for tapered hood \times duct VP
 Make C , L , and H only large enough to pass work and hanger

Figure 6.1 (a) Enclosing hood in an electroplating shop with two open ends for material transport by conveyor.



Q = exhaust volume, cfm, equals AV
 H = height of open area, feet
 L = length of open area, feet
 A = area of openings in enclosure, sq ft, equals LH
 V = minimum face velocity, fpm
 Duct velocity = 1500 fpm (7.62 m/s) minimum
 Slot velocity = 2000 fpm (10.16 m/s) minimum
 Entry loss = 1.78 slot VP plus entry loss factor for tapered hood \times duct VP

Figure 6.1 (b) Enclosing hood with an open front face, which is acceptable for manual transfer of parts.

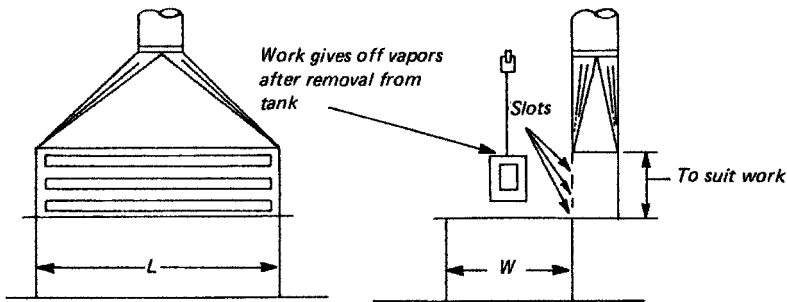


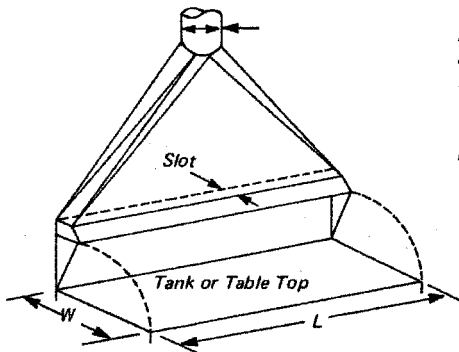
Figure 6.2 (a) So-called "pickling hood" with a slotted plenum. The parts removed from the tank can be positioned in front of this hood for collection of toxic air contaminants.

Q = exhaust volume, cfm (m^3/s), equals qLW

L = tank length, feet

W = tank width, feet (meters)

q = cfm/sq ft ($\text{m}^3/\text{s}/\text{m}^2$) tank area to maintain minimum capture velocity



Duct velocity = 1500 fpm (7.62 m/s) minimum

Slot velocity = 2000 fpm (10.16 m/s) minimum

Entry loss = 1.78 slot VP plus entry loss

factor for tapered hood x duct VP

W/L not over 2 to 1.

Maximum length of transition piece = 4 ft (1.22 m).

Use more than one for longer hoods.

Hood may be raised 6 inches (0.15 m) to allow for pipes over edge of tank. Gap should be baffled.

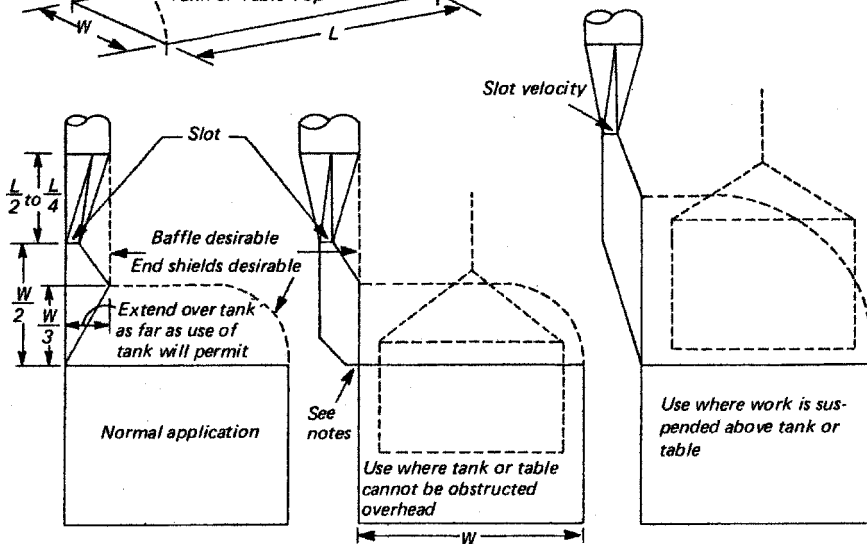
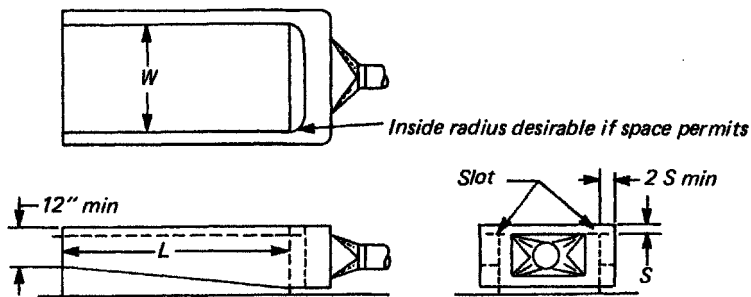


Figure 6.2 (b) Common fishtail hood on tanks with a width-to-length ratio of less than 0.5.



Q = exhaust volume, cfm (m^3/s), equals qLW

L = tank length, feet (m)

W = tank width, feet (m)

q = cfm/sq ft ($\text{m}^3/\text{s}/\text{m}^2$) tank area to maintain minimum capture velocity

Duct velocity = 1500 fpm (7.6 m/s) minimum

Slot velocity = 2000 fpm (10.2 m/s) minimum

Entry loss = 1.78 slot VP plus entry loss factor for tapered hood \times duct VP

Figure 6.3 Lateral exhaust hood with an end takeoff.

6.1.2 Airflow

The preliminary layout for an electroplating shop presented to the ventilation designer will include tank size, approximate location, tank contents, operating temperature, and materials of construction. As noted above, if the facility is highly automated, semienclosed hoods (Fig. 6.1) may be specified by the designer to provide efficient control of toxic air contaminants at minimal airflow. Job shop operations requiring direct tank access may use one of the hoods shown in Fig. 6.2 or 6.3. Tank width-to-length ratio has a critical impact on the minimum airflow necessary to control toxic air contaminants effectively. If the tank width is less than 3 ft, a lateral exhaust hood exhausting from one side of the tank may be adequate. A wider tank may require lateral slot exhaust from both sides of the tank (VS-70-01B), a center-line exhaust (*Ventilation Manual*, VS-10-01C), or a push-pull system (*Ventilation Manual*, VS-70-10, 11).

The choice of hood type will have a significant influence on the airflow necessary to provide control of toxic air contaminants released from the tank. A rational approach to calculating the required airflow on open-surface tank operations has evolved since the 1930s. Through the 1940s, the exhaust airflow for electroplating tanks was based on a fixed airflow per unit tank area (cfm/ft^2) ($\text{m}^3/\text{s}/\text{m}^2$). The criterion varied with the agency or authority. During this period the New York Department of Industrial Hygiene specified 120 cfm/ft^2 (0.06 $\text{m}^3/\text{s}/\text{m}^2$) for electroplating tanks handling toxic chemicals and operating at temperatures below 160°F (71°C).

The first step toward a more rational design approach occurred with the publication of American National Standards Institute (ANSI) Standard Z9.1 in 1957. This

Table 6.1 Determination of Hazard Potential Class

Hazard Potential	Hygienic Standards		Flash Point
	Gas or Vapor (ppm)	Mist (mg/m ³)	
A	0–10	0.00–0.1	—
B	11–100	0.11–1.0	Under 100°F (40°C)
C	101–500	1.1–10	100–200°F (40–95°C)
D	Over 500	Over 10	Over 200°F (95°C)

standard proposed that the airflow per unit tank area be based on a two-part code that defines the hazard potential of the bath contents and the likelihood of release of the contents to the work environment. The first part of the code is the hazard potential classification (A through D); it is a rating based on the toxicity and the fire and explosion characteristics of the bath contents (Table 6.1). Classifications are chosen based on the accepted exposure standards for the most toxic bath component and the flash point for the bath. The higher of the two hazard potential classes is used in the design.

The second part of the code (classes 1 through 4) describes the potential for release of toxic air contaminants to the workplace based on tank operating temperature, evaporation rate, and gassing rate (Table 6.2). Gassing rate applies to electrolytic baths such as those encountered in plating and alkaline cleaning. In an electrolytic bath not all energy goes into the transfer of metal from the bath to the part. A portion of the energy, depending on bath efficiency, causes dissociation of water with hydrogen gas released at the cathode and oxygen at the anode. The gas bubbles produced in this fashion rise and burst at the surface of the bath, generating mist of the bath contents, which may be inhaled by the worker. Volatile bath contents may also be released when the bath is heated. Finally, air agitation used to improve

Table 6.2 Determination of Classification for Rate of Vapor, Gas, and Mist Evolution

Rate	Liquid Temperature [°F (°C)]	Degrees below Boiling Point [°F (°C)]	Relative Evaporation ^a	Gassing
1	Over 200 (95)	0–20 (0–10)	Fast	High
2	150–200 (65–95)	21–50 (11–25)	Medium	Medium
3	94–149 (35–65)	51–100 (25–50)	Slow	Low
4	Under 94 (35)	Over 100 (50)	Nil	Nil

^aRelative evaporation rate is determined according to the method described by A. K. Doolittle in *Ind. Eng. Chem.* **27**:1169 (1939), where time for 100% evaporation is as follows: fast, 0–3 h; medium, 3–12 h; slow, 12–50 h; nil, more than 50 hours. For classification of specific contaminants, see Occupational Safety and Health Administration (1985), 29 CFR 1910. 1000 Washington, DC.

Table 6.3 Minimum Capture Velocity for Tank

Class	Enclosing Hood Face Velocity [fpm, (m/s)]		Lateral Exhaust Capture Velocity fpm, (m/s)
	One Open Side	Two Open Sides	
A-1, and A-2	100 (0.50)	150 (0.75)	150 (0.75)
A-3, B-1, B-2, and C-1	75 (0.38)	100 (0.50)	100 (0.50)
B-3, C-2, and D-1 ^a	65 (0.33)	90 (0.45)	75 (0.38)
A-4, C-3, and D-2 ^a	50 (0.25)	75 (0.38)	50 (0.25)
B-4, C-4, D-3, ^a and D-4	General room ventilation required		

^aWhere complete control of hot water is desired, design as next highest class.

product quality may generate a coarse mist. Using the technique shown in Table 6.2, the bath is assigned a numerical class based on the ability of the tank contents to be released to the workroom.

The combined hazard potential–contaminant evolution rate classification is used to choose the appropriate design capture velocity for a given operation and tank geometry (Table 6.3). The exhaust airflow is then calculated based on the required design velocity, the hood type, and the tank width-to-length ratio (Table 6.4), where width is the distance the hood must pull the air.

Table 6.4 Minimum Exhaust Airflow per Unit Tank Area for Lateral Exhaust Hoods

Required Minimum Capture Velocity [fpm, (m/s)] (from Table 6.3)	Cubic Feet per Minute per Square Foot (cubic meters per second per square meter) to Maintain Required Minimum Capture Velocities at Following Tank Width (W)/Tank Length (L) Ratios				
	0.0–0.09	0.1–0.24	0.25–0.49	0.5–0.99	1.0–2.0
Hood along one side or two parallel sides of tank when one hood is against a wall or baffle; also for a manifold along tank centerline					
50 (0.25)	50 (0.25)	60 (0.30)	75 (0.38)	90 (0.45)	100 (0.50)
75 (0.38)	75 (0.38)	90 (0.45)	110 (0.55)	130 (0.65)	150 (0.75)
100 (0.50)	100 (0.50)	125 (0.63)	150 (0.75)	175 (0.88)	200 (1.00)
150 (0.75) ^a	150 (0.75)	190 (0.95)	225 (1.10)	250 (1.27)	250 (1.27)
Hood along one side or two parallel sides of free standing tank not against wall or baffle					
50 (0.25)	75 (0.38)	90 (0.45)	100 (0.50)	110 (0.55)	125 (0.63)
75 (0.38)	110 (0.55)	130 (0.65)	150 (0.75)	170 (0.85)	190 (0.95)
100 (0.50)	150 (0.75)	175 (0.88)	200 (1.00)	225 (1.20)	150 (1.30)
150 (0.75) ^a	225 (1.10)	250 (1.27)	250 (1.27)	250 (1.27)	250 (1.27)

^aWhere specified the minimum exhaust airflow of 250 (1.27) will not achieve a capture velocity of 150 (0.75) but is considered adequate for control.

The ANSI approach described above results in a 16-step tank classification scale ranging from A1 (highest capture velocity) to D4 (lowest capture velocity). Although the procedure was a step forward, it did require familiarity with the open-surface tank processes, and for this reason many designers continued to use the earlier simple criteria of airflow per unit tank area.

In 1953 the New York State Division of Industrial Hygiene published a series of tables that encouraged the use of the ANSI rating approach. These tables covered the common electroplating processes and included information on the component of the bath released, physical form of the contaminant, rate of gassing, and tank operating temperature. The designer could take these data and use Tables 6.1 and 6.2 to assign a hazard potential–release rate classification for each individual open-surface tank and from that classification, choose an appropriate airflow. The New York tables were published in the *Ventilation Manual* in 1958. The tables have since been simplified by assigning the specific classification for each of the listed open-surface tank processes using the procedures described above (*Ventilation Manual*, Tables 10.70.6, 10.70.7, and 10.70.8).

Once the proper hazard potential–release rate class is assigned for a given tank process, the designer specifies the critical design velocity. For enclosing hoods (Fig. 6.1) the design velocity is the face velocity at the hood opening. The design velocity for lateral exhaust hoods (Figs. 6.2 and 6.3) is the capture velocity obtained from Table 6.3. For consistency in nomenclature, the authors believe the design velocity on lateral exhaust hoods should be identified as a capture velocity since it is that velocity that must be established at the point of the tank furthest from the hood to overcome air currents and capture the contaminated air, causing it to flow into the hood hence the difference in nomenclature in this volume and *Industrial Ventilation*.

The information on minimum tank capture velocity (Table 6.3) is adapted from *Ventilation Manual*, Table 10.70.3, with the elimination of the data for canopy hoods. It is strongly recommended that canopy hoods *not* be used for ventilation control of open-surface tanks. The *Ventilation Manual* states canopy hoods should not be used for tanks with highly toxic materials in locations where drafts are unavoidable, or where the worker must bend over the tank or process. A conservative approach is recommended; since tanks are frequently converted from one use to another, it is prudent not to utilize canopy hoods on any open-surface tank, hence their omission from Table 6.3.

Once the critical design velocity is identified, Table 6.4 is used to choose the appropriate minimum exhaust airflow. The minimum exhaust rate depends on the type of hood selected for the process and the width-to-length ratio of the tank. A review of Table 6.4 shows that airflow can be minimized by utilizing as small a tank as possible, keeping the width-to-length ratio low and using hoods with integral baffles or installing baffles or shields to prevent drafts. The push–pull concept (*Industrial Ventilation* VS-78-10.11) is an effective approach to the exhaust of wide-surface tanks that would be difficult to handle with conventional lateral exhaust. In a push–pull system, a pressurized air supply plenum positioned at the lip at one side of the tank blows a uniform jet of air across the tank and conveys the contaminant to

a collecting hood on the other side of the tank. Although this design can be effective, the authors have encountered a number of poor installations that have placed the operators at risk. Happily, since the early 1990s the design base for push-pull systems has been scrutinized, and the results of laboratory and plant experimental studies combined with mathematical modeling of the flow pattern provides improved design insight (Goodfellow and Tahti, 2001).

A ventilation system for a plating shop is designed in Chapter 9. The procedure for calculating the exhaust rate on the tanks in this sample problem using the *Ventilation Manual* is shown in Problem 6.1.

6.2 SPRAY PAINTING

Spray painting by air atomization results in the exposure of workers to vapors of the volatile components of the vehicle and catalyst and to paint mist consisting of binder, fillers, and pigments. Engineering control is usually accomplished with ventilated spray booths that are classed as simple partial enclosures. These booths are frequently used for control of other industrial processes, including weighing and mixing of chemicals, solvent cleaning, and coating operations. Due to their widespread use, the designer should be acquainted with the types of paint spray hoods and their application. The discussion in this section is limited to ventilation control for conventional spray painting of liquid paint. Powder coating, the dry electrostatic application of a paint powder containing all components of liquid paint except the vehicle, is not discussed in this section. Although not well documented, there is apparently minimal risk of exposure in powder coating due to the passive release of the powder from the application gun and the form of the airborne contaminant. To date there has been no comprehensive study on the required ventilation for powder coating operations.

6.2.1 Hood Design

More than two dozen companies in the United States manufacture paint spray hoods ranging from small benchtop units widely used in the jewelry industry to room-sized booths for painting automobiles and locomotives. Each vendor has a standard line of hoods with numerous design options. The hoods are designed to provide a lateral flow of clean air past the breathing zone of the operator with a uniform velocity distribution across the hood face, thereby minimizing worker exposure to toxic air contaminants. Downdraft hoods are installed in heavy industry for painting large, irregular-shaped objects such as castings, cars, trucks, and locomotives.

The conventional spray booth is a heavy-gage sheet metal enclosure with one open face (Fig. 6.4). The side panels and roof may have openings to allow a conveyor to bring the parts directly to the spray area. This feature is especially important in automated painting operations. The choice of hood size is obviously dependent on the size of the parts to be painted. It is important that the face area of the hood be large enough so that the part being painted does not block airflow through the hood face,

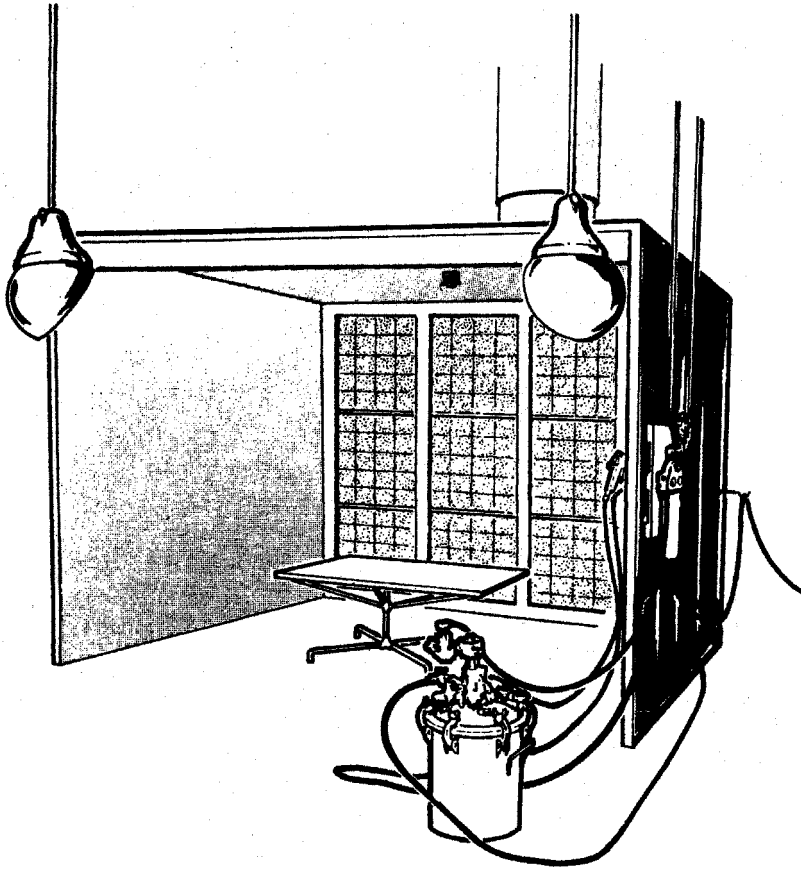


Figure 6.4 Main features of a conventional spray booth.

which might result in poor capture efficiency. Geometry of the parts to be painted frequently requires a holding fixture or a turntable for complete spray coverage; the booth must be sized to accommodate this equipment.

Booth depth is critical to good performance since it helps to ensure a flat velocity profile at the hood face with resulting effective capture of toxic air contaminants (Chapter 5). Rebound from flat surfaces sprayed in a shallow booth may escape capture; a deep booth will assist in the recovery of such contaminants (Fig. 6.5).

Air cleaning on spray booths is usually limited to removal of paint mist with little attention given to solvents. Sheet metal baffles hung at the rear of the hood are the simplest approach to improvement in air distribution (Fig. 6.6). Baffles are simple to install and clean, and they present minimal resistance to airflow. DallaValle (1952) recommends the number of baffles to be used and their spacing as a function of cross section of the individual booth (Table 6.5). In addition to providing a flat velocity profile at the face of the hood, baffles remove a small portion of the coarse paint spray mist.

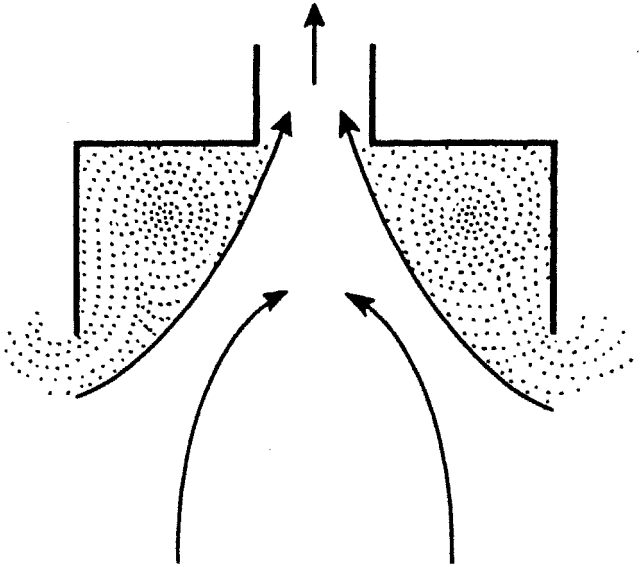


Figure 6.5 Hood depth is a critical design element. With a shallow booth leakage occurs from eddies as shown in this plan view.

A bank of disposable particle filters mounted in the rear of the hood provides a rear plenum and helps to establish a uniform velocity at the hood face. The filter medium is usually a coarse fibrous medium with a collection efficiency of less than 50% against overspray from conventional air-atomized paint. As these filters are coated with paint, their resistance will increase and airflow will drop off. Performance should be monitored continuously and filters should be changed periodically. Filter life may be extended by providing baffles in front of the filters to provide minimal collection of coarse paint mist.

The most effective air-cleaning approach for removal of paint mist while providing a good velocity profile in the hood is the water-wash booth (Fig. 6.7). These booth designs vary but usually include a water-wash curtain, countercurrent sprays, and impingement plates for removal of water mist. It is stated that these systems are relatively effective against paint mist; however, no data are available on their performance. These simple water-wash booths are not effective for removal of the organic vapors encountered in painting.

The efficiency of a short-throat, concurrent-flow wet scrubber used with a down-draft paint spray booth has been evaluated by Chan et al. (1986) against a high-solids base coat and a clear-coat enamel paint mist generated by air-atomization spray guns and rotary atomizers. The base coat paint mist generated by air atomization had a mass median aerodynamic diameter (MMAD) ranging from 4.7 to 6.6 μm depending on gun pressure; the MMAD of the clear-coat paint generated by a rotary atomizer varied from 20 to 35 μm as the unit was operated at various rotational speeds.

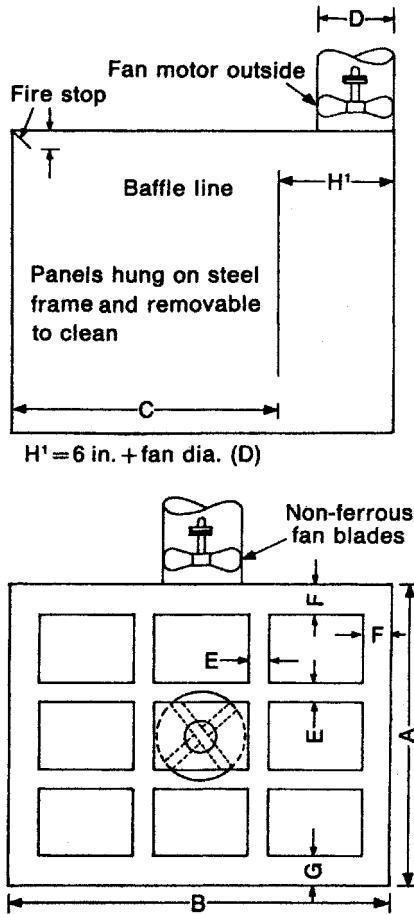


Figure 6.6 Hood baffles for air distribution. [From DallaValle (1952).]

Table 6.5 Spray Booth Baffle Design
(Refer to Fig. 6.6)

Booth Cross-Sectional Dimensions, $A \times B^a$ [ft (m)]	No. of Panels, D	Spacing [in. (cm)]		
		Between Panels, E	Top and Side, F	Bottom, G
3×3 (0.9 \times 0.9)	1			
$6\frac{1}{2} \times 4$ (2.0 \times 1.2)	3	4 (10)	6 (15)	12 (30)
$6\frac{1}{2} \times 6$ (2.0 \times 1.8)	4	4 (10)	6 (15)	12 (30)
$6\frac{1}{2} \times 8$ (2.0 \times 2.4)	6	4 (10)	10 (25)	12 (30)
$6\frac{1}{2} \times 10$ (2.0 \times 3.0)	9	6 (15)	10 (25)	18 (46)
9×12 (2.7 \times 3.7)	9	8 (20)	12 (30)	18 (46)
12×14 (3.7 \times 4.3)	12	8 (20)	18 (46)	24 (60)

^aFor booths of dimensions not shown, use the nearest size in the table for number and spacing of baffles.

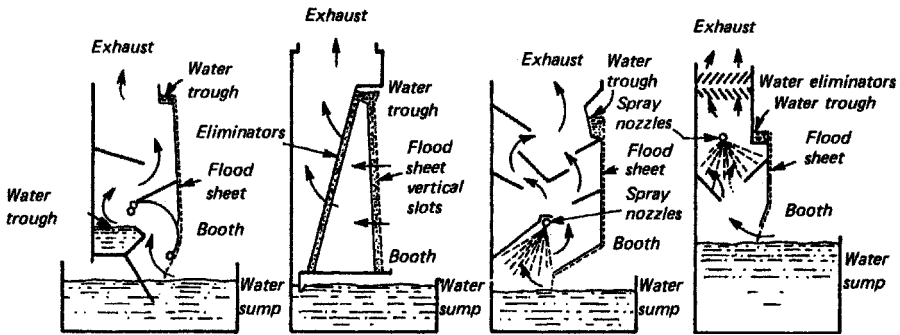


Figure 6.7 Typical water-wash spray booth designs.

The collection efficiency of this one-stage wet scrubber was greater than 90% for particles with a MMAD greater than $2\text{ }\mu\text{m}$. The authors stressed the importance of optimizing the spray operating conditions to minimize the generation of mist less than $2\text{ }\mu\text{m}$ in size.

6.2.2 Airflow

The choice of paint spray booth face velocity and therefore airflow varies with authority; a comparison of the *Ventilation Manual* and ANSI/OSHA requirements is shown in Table 6.6. The designer is cautioned that these criteria may not be adequate to protect against paint containing heavy metals such as lead and cadmium or catalyst systems used in epoxy or urethane paints. Once the appropriate face velocity is

Table 6.6 Ventilation Requirements per Unit Face Area of Spray Booths cfm/ft^2 ($\text{m}^3/\text{s}/\text{m}^2$)

	ACGIH		ANSI OSHA	
	Air Spray	Airless	Air Spray	Airless/ Electrostatic
Bench-type spray booth	150 ^a –200 ^b (0.76–1.02)	100 ^a –125 ^b (0.51–0.64)	150 ^c –200 ^d (0.76–1.02)	100 (0.51)
Large spray booth Walk-in	100 ^e (0.51)	60 (0.31)	100 ^c –150 ^d (0.51–0.75)	—
Operator outside	100–150 (0.51–0.75)	60–100 (0.31–0.51)	100 ^c –150 ^d (0.51–0.75)	—
Autospray paint booth	100 (0.51)	60 (0.31)	—	—

^aBooth cross section less than 4 ft^2 (0.37 m^2).

^bBooth cross section more than 4 ft^2 (0.37 m^2).

^cCross-drafts up to 50 fpm (0.26 m/s).

^dCross-drafts up to 100 fpm (0.51 m/s).

^e75 fpm (0.38 m/s) for very large, deep booth (operator may require an approved respirator).

chosen, the open area consisting of the booth face and any openings for conveyor access must be calculated.

Installation and proper operating practice are important in obtaining good performance from a paint spray booth. The following practices are important in controlling exposure:

- Minimize the distance between the paint spray nozzle and the part.
- Select spray conditions to generate particles with a diameter greater than $12\mu\text{m}$ to minimize overspray.
- Use extension arms on the spray gun to provide access to voids in workpiece.
- Apply robotic methods to the operation where possible to eliminate the worker at the booth.
- Stand to the side of the piece being sprayed.

Replacement air must be introduced in sufficient quantities to satisfy the exhaust requirements of the spray booth. Frequently, the air supply must be provided with endpoint filtration to minimize surface imperfections in the paint. The location and type of diffuser for replacement air are important considerations to booth performance and control of product quality. Although it is generally good practice to have replacement air introduced at some distance from the hood (see Chapter 12), this is not so in the case of paint spray booths. Travel distance will increase the potential for particle pickup and contamination of the painted surface. Proper placement of the booth is necessary. Hood placement in corners frequently results in nonsymmetrical flow and a poor velocity profile at the face. Spray booths should not be placed near receiving or shipping doors, where disruptive drafts may exist.

It is important to select the correct fan, as described in Chapter 10. A fan is frequently supplied as a part of the paint spray booth package. Such fans are usually chosen based on a short duct run, no elbows or transitions, and direct discharge to outdoors. Since this is rarely the case in practice, the fan-booth system may not be matched and proper airflow will not be obtained when the installation is completed. A fan delivering 5000 cfm ($2.36\text{ m}^3/\text{s}$) at $\frac{1}{8}$ in. H_2O (31.14 Pa) may deliver only 3500 cfm ($1.65\text{ m}^3/\text{s}$) at 1.0 in. H_2O (249.1 Pa) when the usual additional resistance is encountered. It is good practice to size and purchase a fan separately based on total system loss calculations.

Although the design of the spray painting hood is important, faulty work practices can degrade the performance of any hood with resulting worker exposure to air contaminants. As an example, when spraying small parts in a job shop, the operator commonly places the freshly sprayed part on a rack just behind him (her). The air moving to the hood first flows past the drying rack where highly volatile solvents evaporate from the parts. This solvent laden air then moves to the breathing zone of the operator resulting in significant solvent exposures. Also, simple changes in worker position at the face of a spray hood can have a dramatic effect on hood performance and potential for worker exposure (Flynn et al., 1996). In a tracer gas study at a large hood, the authors showed that changing the operators position from

of the problem with dozens of potential dust release points at each step of the process. For a comprehensive review of the myriad approaches to dust control in material handling, the reader is referred to Smandych et al. (1998). The authors chronicle the technologies for dust control on conveying, storing, processing, packaging, and feeding operations in addition to providing an overview of dust collection and suppression techniques. The discussion in this chapter will focus on a alternative procedure for the calculation of exhaust rates at material transfer points.

The *Ventilation Manual*, in a series of design plates, recommends exhaust rates for bucket elevators, conveyors, bins, hoppers, and loading stations based on the hood open area, belt width, and speed, bin volume, and screen area. In the authors' experience the recommended airflows based on these design plates may be insufficient for effective dust control. The induced-air concept is introduced in this section to complement the *Ventilation Manual* design data. This concept provides a fundamental understanding of the dust generation and release mechanism in material-handling operations and introduces a rational local exhaust design base for such installations.

Initial attempts at dust control at granular transfer points were based on the use of enclosing hoods with a selected face velocity at all open areas. This approach was typified by early New York State codes, which required 150–200 cfm/ft² (0.76–1.02 m³/s/m²) at all hood openings. In many installations these recommendations did not provide adequate control. Vendors of packaged systems proposed designs based on 400–500 cfm/ft² (2.03–2.54 m³/s/m²) at all hood openings. Frequently, this approach did result in improved control at the difficult transfer points, but in many cases it resulted in overdesign at other points. The second general design approach as cited in the *Ventilation Manual* in the VS-50 series of design plates specifies a given cfm/ft² through all hood openings, with the total airflow not less than a second design criterion such as conveyor-belt width, bin volume, or of screen area. Although this approach is the accepted design practice in the United States, it has not been thoroughly validated in the field.

A number of investigators have pointed out that installed systems based on the face velocity approach frequently do not result in effective control because this design procedure does not anticipate the quantity of air induced into the system. Pring (Pring et al., 1949) was one of the first investigators to demonstrate that falling granular material draws air from the top of a system enclosure and forces it out the bottom, carrying dust with it. If the system component such as a bin, is tight, the induced air will reverse its path and carry the entrained dust back through the upstream opening as shown in Fig. 6.9. Hemeon (1963) also studied this problem and found that the maximum air volume induced into such a system is proportional to

- The cube root of the mass rate of solids flowing
- The cube root of the specific gravity of solids
- The cube root of the particle diameter
- The two-thirds power of the solids cross-sectional area
- The two-thirds power of the falling distance

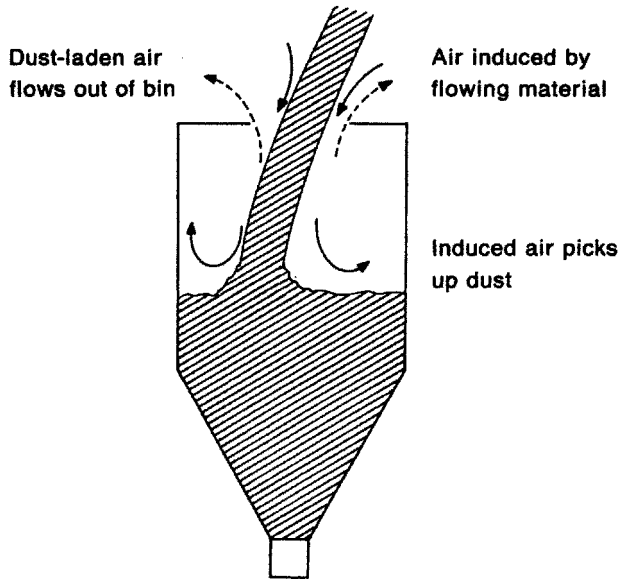


Figure 6.9 Induced-air concept showing how air induced into a bin from flowing granular material results in contamination of the workplace.

Although this information is of value in identifying those system parameters influencing the magnitude of the induced air, it did not provide a useful design approach. A laboratory investigation conducted by Dennis (1954) of the airflow induced by falling granular material in material-handling operations led to the following empirical equation of induced airflow by Anderson (1964):

$$Q_i = 10.0 A_u \left(\frac{RS^2}{D} \right)^{1/3} \quad (6.1)$$

where Q_i = induced airflow, cfm

A_u = open area of the enclosure upstream of the dump location, ft

R = material flow rate, tons/h

S = height of fall of material, ft

D = average particle diameter, ft ($D > 1/8$ ft)

The use of this design formula for a series of material transfer points is shown in Figs. 6.10 through 6.14. Anderson (1964) has provided examples of the differences between exhaust volumes calculated by the conventional face velocity and this induced air method. The total system airflow derived from the induced-air method may not differ greatly from that specified by the *Ventilation Manual* approach. However, the induced-air approach has the advantage that it can assist in identifying the locations that warrant control and the exhaust rate necessary to minimize the release of dust. It is therefore prudent to calculate the required exhaust for granular transfer

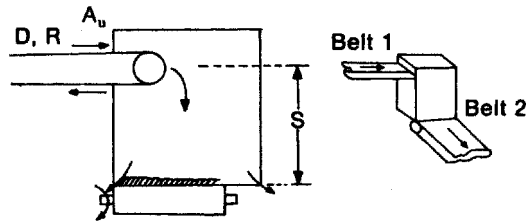


Figure 6.10 Induced air, belt to belt, chute to chute.

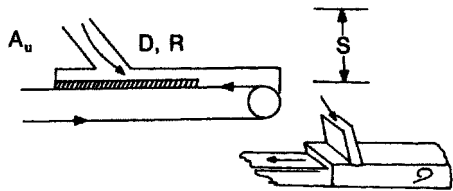


Figure 6.11 Induced air, chute to belt.

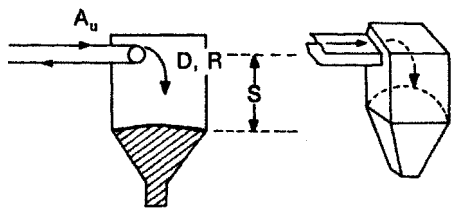


Figure 6.12 Induced air, belt to bin.

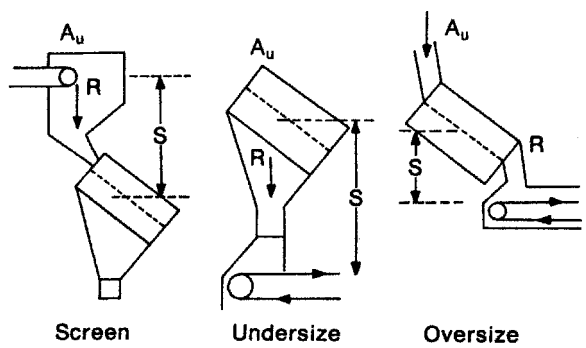


Figure 6.13 Induced air, screens.

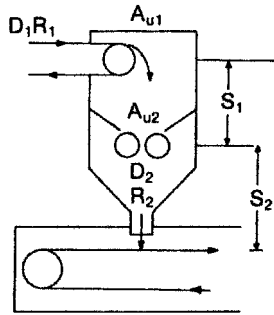


Figure 6.14 Induced air, crusher.

points by both the *Ventilation Manual* and the induced-air methods and select the larger value for the design.

A common operation in handling dry granular material is the bagging of the final product in 50–100-lb (22.7–45.4-kg) paper bags. This operation is one of the dustiest encountered in broad industry and the most difficult to control since effective reduction in worker exposure depends not only on excellent installed local exhaust but also the observance of rigorous work practices by the operator. Bagging operations studied at the NIOSH Pittsburgh Research Laboratory have resulted in a number of ventilation control innovations (Cecala et al., 2000). Dust exposures at bag filling operations range from 1 to 5 mg/m³ with standard ventilation controls. The exposures were reduced 80–90% using a dual-bag nozzle system that reduces product blowback as pressure builds up in the bag. The authors also evaluated a bag clamp that reduced product blowback during filling.

A fresh approach by the NIOSH team to reduce dust concentrations in pallet loading of bags is the use of a clean-air island served by 6000–10,000 cfm (2.83–4.72 m³/s) of recirculated air. In two test applications the island provided reductions of 98 and 86% in the operator's exposure with exposures concentrations noted to be below 0.04 mg/m³. A push pull exhaust ventilation system at a bag pallet loading workstation reduced air concentrations from 0.82 to 0.2 mg/m³. The push air nozzle delivered 120 cfm (0.06 m³/s) at a discharge velocity of 1200 fpm (6.10 m/s) with a capture hood operating at 2500 cfm (1.20 m³/s). Another ventilation innovation investigated by the NIOSH group that provided positive results included a “bottom to top” general dilution ventilation system.

6.4 WELDING, SOLDERING, AND BRAZING

The required ventilation controls for welding operations vary greatly depending on the welding process utilized, the composition of the base metal, the coating on the base metal, and the degree of confinement existing in the welding area. Prior to World War II the majority of welding was done by the shielded metal arc (SMA) welding process (Fig. 6.15). Using this technique the welder is exposed to respirable

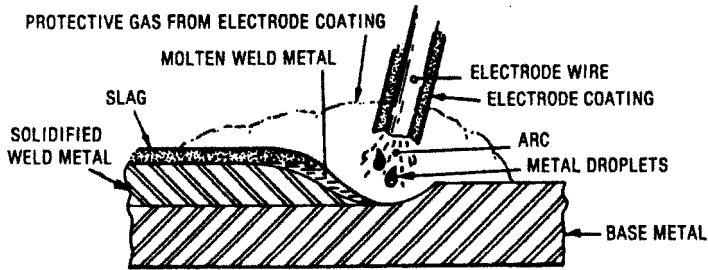


Figure 6.15 Shielded metal arc (SMA) welding. The consumable electrode used in this process is coated with a flux that has a variety of functions, including forming a gas to shield the molten weld metal. The arc is established manually by the welder, who feeds the electrode into the work area. This process, commonly used on mild steels, may generate large quantities of metal fume from the electrode and base metal and gases from the vaporization of the welding rod coating.

metal particles in the form of the oxides of iron and other alloy metals present in the welding plume, concentrations of various contaminants released from the rod and its coating, and minor quantities of ozone and nitrogen dioxide fixed by the arc. Low-hydrogen electrodes are used on selected alloys; the coatings on these electrodes contain soluble fluorides which release hydrogen fluoride and particles of soluble fluoride salts which are respiratory irritants and cause systemic effects.

Technical innovation in welding engineering in the 1940s and 1950s to improve welding quality resulted in the development of techniques to blanket the arc with an inert gas, thereby preventing defects in the weldment. Two methods, tungsten inert-gas (TIG) shielded arc welding (Fig. 6.16) and metal inert-gas (MIG) shielded arc welding (Fig. 6.17), frequently result in worker exposures to metal fume and toxic gases, such as ozone, nitrogen dioxide, and carbon monoxide. In a fourth technique,

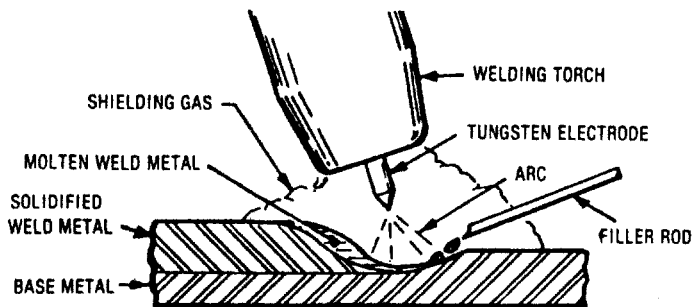


Figure 6.16 Tungsten inert-gas (TIG) shielded arc welding. In this process the arc is established between the workpiece and a nonconsumable tungsten electrode. A filler rod is fed into the weld separately by the welder. Shielding gas such as argon or helium blankets the welding area. This process is used on special alloys and on more critical work on lighter sections than SMA. Airborne contaminants include relatively low metal fume concentrations from the variety of alloys, steels, and nonferrous materials welded with this technique; significant ozone concentrations may occur in poorly ventilated workstations.

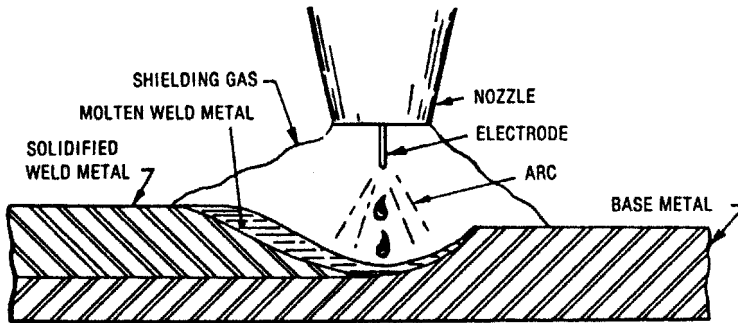


Figure 6.17 Metal inert-gas (MIG) shielded arc welding. The arc is established with a consumable electrode and the inert shielding gas flowing from an annular space in the gun blankets the weldment. This process is frequently used at high current densities for a variety of metals, including steels and aluminum. High ozone concentrations are generated, especially when welding aluminum with argon as the shielding gas.

submerged arc welding (Fig. 6.18), the arc is shielded by granular flux which presents minimal air contamination and normally does not warrant local exhaust ventilation. Plasma welding (Fig. 6.19) operates at still higher current densities than TIG and MIG techniques, resulting in concurrent increases in the generation of toxic air contaminants. Associated arc processes such as cutting, gouging, and flux-cored welding also require greater attention to the control of welding exposures.

Processes similar to welding such as soldering and brazing may require ventilation to control contaminants such as volatilization products from filler rod or solder, thermal degradation products of the flux, and carbon monoxide and oxides of nitrogen generated by gas torch operations.

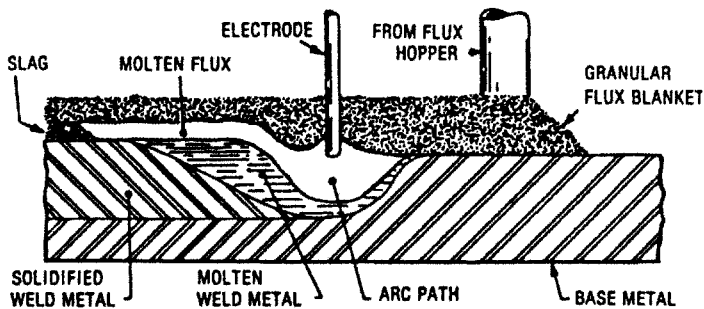


Figure 6.18 Submerged arc welding (SAW). This process does not normally require local exhaust ventilation. SAW is used to weld heavy sections of steel plate such as in shipbuilding; the consumable electrode establishes an arc under a granular flux which provides the shield. The flux does degrade, and minimal concentrations of soluble fluoride particles and hydrogen fluoride gas may be generated.

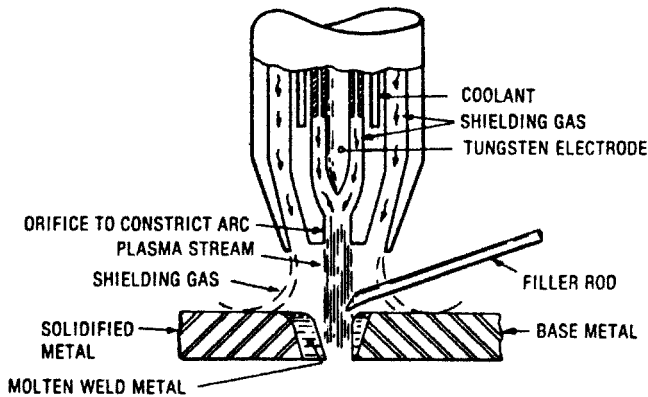


Figure 6.19 Plasma arc welding (PAW). In this welding equipment the gun has both an inerting stream of argon and a separate orifice stream of argon. The orifice gas is placed under high voltage and results in a highly ionized gas stream or plasma with arc temperatures in excess of 60,000°F. This process can be used for a variety of metals, including titanium, stainless steels, aluminum, and refractory metals. Because of the ozone, nitrogen dioxide, and metal fume exposures, this process requires local exhaust ventilation.

Familiarity with each welding process is necessary to design the most effective ventilation system. An overview of these processes and the principal airborne contaminants which must be controlled is presented in Table 6.7.

In a comprehensive review of ventilation control on welding operations by Hagopian and Bastress (1976), air contaminants generated during welding operations were grouped by toxicity into three classes (Table 6.8). The suitability of various ventilation techniques and the minimum exhaust ventilation rates for each approach were assigned based on the contaminant class as shown in Table 6.9.

In this summary, general exhaust ventilation is not included as one of the candidate methods of control. The application of general exhaust for welding can be criticized in many ways. Since design criteria have not been validated, the installations rarely provide suitable control and empirical upgrading frequently is required. In addition, the airflows required for effective general exhaust designs make for very high operating costs. These limitations have been outlined in Chapter 4 and are reinforced by Hagopian and Bastress (1976). One of the local exhaust ventilation methods listed in Table 6.9 usually is feasible for control.

Of the four local exhaust ventilation methods listed in Table 6.9, the technique most frequently applied to welding is the freely suspended open hood (Fig. 6.20). In this system an exterior hood attached to a flexible duct is provided with a positioning system to permit the welder to move the hood close to the welding point. As noted in Fig. 6.20, the required airflow is modest if the hood can be positioned within 6 in. (15 cm) of the weldment. Obviously, this approach requires the cooperation of the welder to position the hood and achieve good control. Multiple workstations can utilize either a central system or a series of individual systems. Since 1975, a number of manufacturers have provided packaged systems consisting of a hood, flexible duct,

Table 6.7 Potential Hazards from Welding^a

Hazard	Welding Process						
	SMA ^b	Low Hydrogen	GTA ^c	GMA ^d	Submerged	Plasma	Gas
Metal fumes	M-H	M-H	L-M	M-H	L	H	L-M
Fluorides	L	H	L	L	M	L	L
Ozone	L	L	M	H	L	H	L
Nitrogen dioxide	L	L	L	M	L	H	H
Carbon monoxide	L	L	L	L, H if CO ₂	L	L	M-H
Decomposition of chlorinated HC	L	L	M	M-H	L	H	L
Radiant energy	M	M	M-H	M-H	L	H	L
Noise	L	L	L	L	L	H	L

^aHazard codes: L, low; M, medium; H, high.^bShielded metal arc welding.^cGas tungsten arc.^dGas metal arc.

positioner, fan, and air cleaner. The air cleaner is usually a high-efficiency particle filter or an electrostatic precipitator (Chapter 11). If aluminum is welded, the electrostatic precipitator may not be suitable since the electrodes can become coated with an insulating coat of aluminum oxide. Depending on the application, these packaged systems may be used in a recirculation mode. The freely suspended hood approach is commonly used in maintenance and repair shops where it can reach both a welding bench area and a portion of the shop floor if large equipment must be welded.

Production and maintenance welding operations on small parts can be accomplished at a small workstation provided with rear-slot ventilation (Fig. 6.21). This is

Table 6.8 Contaminant Classification for Welding

Contaminant Class	Classification Criteria	Example Materials
I	Dusts, fumes, and mists with exposure limits of 5 mg/m ³ and above; gases and vapors with exposure limits of 100 ppm and above	Iron oxide
II	Dusts, fumes, and mists with exposure limits of 0.1 mg/m ³ and above (up to 5 mg/m ³); gases and vapors with exposure limits of 1 ppm and above (up to 100 ppm)	Fluorides; carbon monoxide; nitrogen dioxide
III	Dusts, fumes, and mists with exposure limits below 0.1 mg/m ³ ; gases and vapors with exposure limits below 1 ppm	Beryllium; mercury; ozone; cadmium

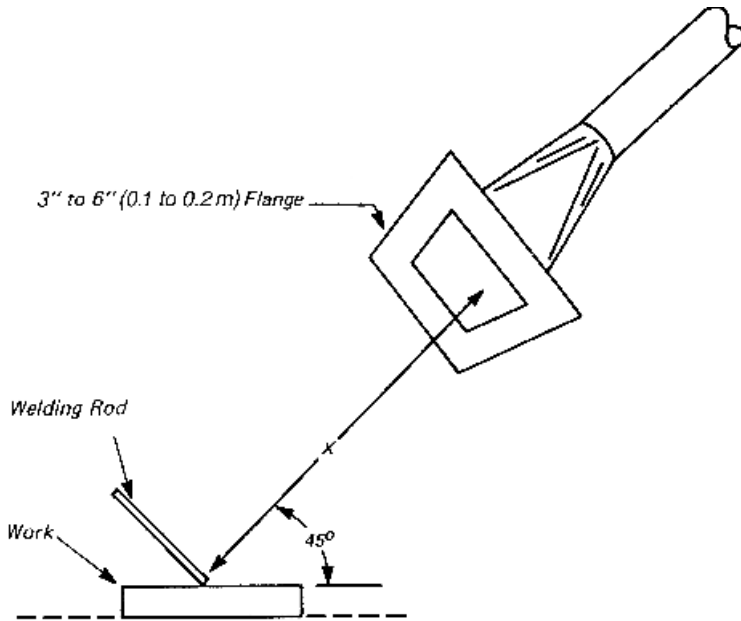
Sources: After Hagopian and Bastress (1976).

Table 6.9 Ventilation Requirements for Various Welding Techniques and Contaminant Class

Operation	Low-Volume/ High-Velocity			Enclosing Hood
	Freely Suspended Open Hood	Rear-Slot Table	Gun-mounted Hood	
Gas welding	Classes I and II—100-fpm (0.51 m/s) capture velocity Class III—not recommended	Classes I and II—100-fpm (0.51-m/s) capture velocity Class III—not recommended	Not applicable	Classes I and II—100-fpm (0.51-m/s) face velocity Class III—150-fpm (0.76-m/s) face velocity
Torch brazing and soldering	Classes I and II—100-fpm (0.51 m/s) capture velocity Class III—not recommended	Classes I and II—100-fpm (0.51-m/s) capture velocity Class III—not recommended	Not applicable	Classes I and II—100-fpm (0.51-m/s) face velocity Class III—150-fpm (0.76-m/s) face velocity
Shielded metal arc welding	Classes I and II—100-fpm (0.51 m/s) capture velocity Class III—not recommended	Classes I and II—100-fpm (0.51-m/s) capture velocity Class III—not recommended	Not applicable	Classes I and II—100-fpm (0.51-m/s) face velocity Class III—150-fpm (0.76-m/s) face velocity
Plasma arc welding and submerged arc welding	Classes I and II—100-fpm (0.51 m/s) capture velocity Class III—not recommended	Classes I and II—100-fpm (0.51-m/s) capture velocity Class III—not recommended	Not applicable	Classes I and II—100-fpm (0.51-m/s) face velocity Class III—150-fpm (0.76-m/s) face velocity
Gas shielded-arc welding and flux-cored arc welding	Classes I and II—100-fpm (0.51 m/s) capture velocity Class III—not recommended	Classes I and II—100-fpm (0.51-m/s) capture velocity Class III—not recommended	Classes I and II—exhaust rate to be determined by manufacturer or user Class III—not recommended	Classes I and II—100-fpm (0.51-m/s) face velocity Class III—150-fpm (0.76-m/s) face velocity

Oxygen cutting, arc cutting, and gouging	Not recommended	Not recommended	Not applicable	Classes I and II—100-fpm (0.51-m/s) face velocity Class III—150-fpm (0.76-m/s) face velocity Class I—125-fpm (0.64-m/s) face velocity
Thermal spraying	Class I—200-fpm (1.02 m/s) face velocity with operation at face of hood Classes II and III—not recommended	Not recommended	Not applicable	Classes II and III—200-fpm (1.02-m/s) face velocity

Source: After Hagopian and Bastress (1976).



$$Q = K(10 X^2 + A)V_x$$

Q = exhaust volume, cfm (m^3/s)

X = distance from center of hood face to farthest point of contaminant release, ft (m)

A = hood face area (not including flange), sq ft (m^2)

V_x = minimum capture velocity, fpm (m/s)

K = 1.0 for unflanged hood; 0.75 for flanged hood

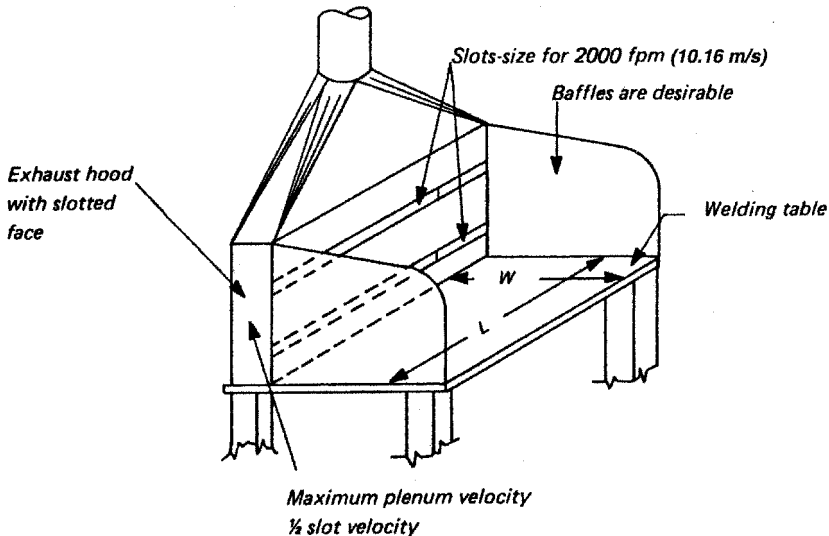
Entry loss = entry loss factor for tapered hood \times duct VP

Duct velocity = 2000 fpm (10.2 m/s) minimum

Figure 6.20 Movable hood to be positioned by welder. [From Hagopian and Bastress (1976).]

an attractive approach since the welder need not position a hood for effective control. As discussed in Chapter 5, the hood should be provided with side baffles to minimize the effects of cross-drafts and improve collection of contaminants. Such stations frequently are used to weld long sections of pipe, strap, and angle, and welders often object to the interference presented by side baffles. This problem can be eliminated by providing slotted baffles, hinged side baffles, or heavy fabric side drapes. This rear-slot welding station is also an effective design for soldering and brazing operations.

A third local exhaust technique, a low-volume/high-velocity hood, applicable to both TIG and MIG processes, is shown in Fig. 6.22. This technique, providing effective capture at a minimal airflow, employs an exhausted annular ring around the welding head. The exhaust airflow varies depending on the manufacturer and the



Q = exhaust volume, 350 cfm/ft
(0.54 m³/s/m) of hood length

W = table width, ft maximum 24 in. (600 mm)

L = table length

Entry loss = 1.78 slot VP
plus entry loss factor

Duct velocity = 2000 fpm (10.16 m/s)
minimum

Figure 6.21 Rear-slot bench exhaust suitable for welding and brazing of small parts. [From Hagopian and Bastress (1976).]

specific operation, but the usual range of 50–100 cfm (0.25 to 0.50 m³/s) is approximately 10% that of the freely suspended open hood. There is some reluctance on the part of welders to use this technique since the exhaust may strip the shielding gas from the welding point unless care is taken in setting the exhaust rate.

If extremely toxic metals are processed, the best approach is to use an enclosing hood. In practice, this may be a welding bench placed in a modified paint spray booth. The downdraft table (Fig. 6. 23) is a local exhaust hood designed principally for gas and arc cutting processes. The metal slab to be cut is placed on the table and the metal fume is pulled downward. Large molten droplets fall to the plenum and the fume is exhausted from the box plenum. The choice of a canopy hood for a welding station is a common mistake in industry. These hoods are not acceptable for control of toxic air contaminants for the reasons discussed in Chapter 5.

6.5 CHEMICAL PROCESSING

Although no other industrial setting presents the range of contaminant generation points and the variety of air contaminants encountered in the chemical processing

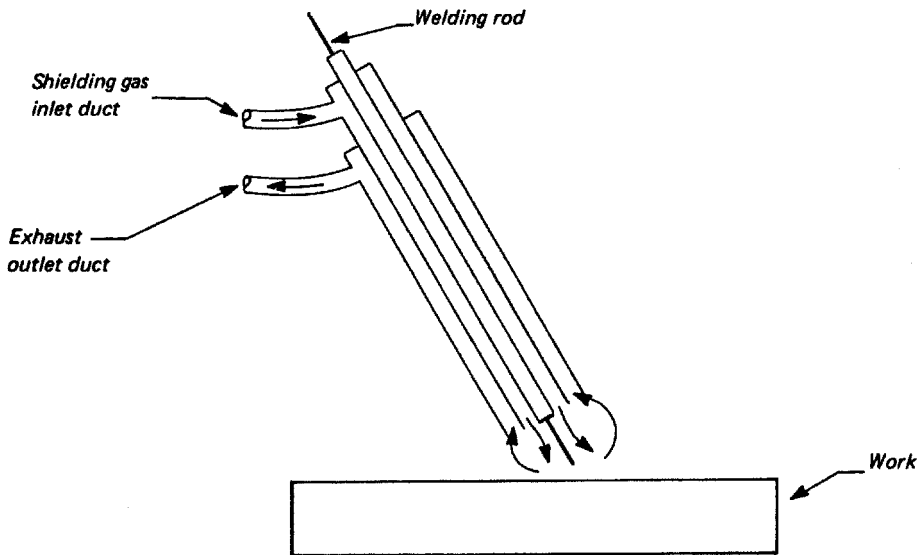


Figure 6.22 Low-volume/high-velocity exhaust for inert-gas shielded process. [From Hagopian and Bastress (1976).] Exhaust flow requirements must be determined for each welding operation and welding gun configuration by experimental testing with air contaminant sampling and analysis.

industry, standard ventilation designs are available for only a limited number of operations. In this section common operations in a batch chemical processing plant are reviewed and the possible approaches to ventilation control are discussed.

6.5.1 Chemical Processing Operations

A batch processing plant may synthesize several dozen chemicals in production scales ranging from tens to hundreds of thousands of kilograms per year (Fig. 6.24). Starting materials include granular chemicals, chemicals in liquid form such as solvents, and reactive gases. Granular materials utilized in small quantities are usually received in drums and may require preweighing of batches. This material frequently can be ordered in prill or flake form to minimize dusting. Regardless of material form, the weighing station normally warrants local exhaust hooding to control dust (Fig. 6.25). Granular chemicals used in large quantities are delivered to the plant by truck, railroad bulk cars, or transporters and may be transferred by pneumatic conveying directly to the mix or reaction vessel or to storage bins for later transfer to the vessel. This bulk transfer is usually performed in enclosed systems with minimal release of dust to the environment.

Liquid reagents may also be transported in bulk for tank storage at the plant, or, if used in small quantities, by drums held in special storage areas. Bulk solvents are frequently received at a loading dock equipped with a piping manifold for flexible

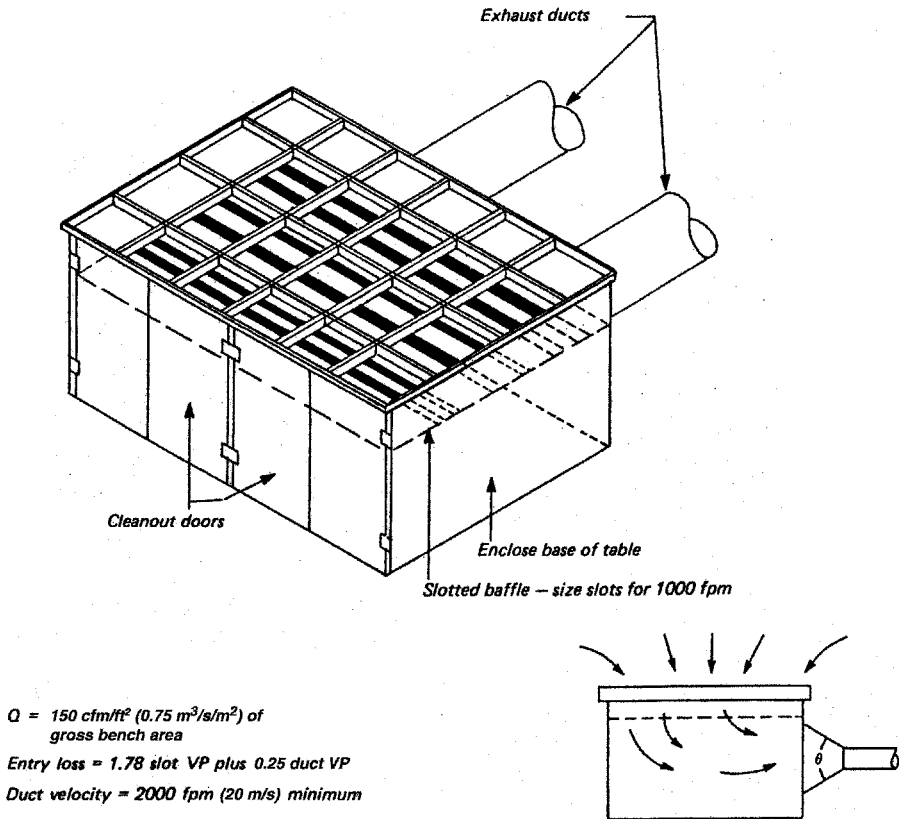


Figure 6.23 Downdraft cutting table for gas cutting or plasma operations. [From Hagopian and Bastress (1976).]

hose transfer from truck or train to tank storage. Investigators have demonstrated that significant exposure to volatile liquids may occur during making up and draining of transfer lines. Even though this work is usually done outdoors, ventilation control may be necessary.

The first major in-plant processing equipment requiring ventilation control is the reaction vessel. As an example, consider the batch process for the synthesis of a dye, illustrated in Fig. 6.24. The various chemicals are added in a carefully planned manner to the reactor. Liquid is added by closing all vessel ports and valves and placing the reactor under vacuum. The liquid is then transferred from a storage tank to the reactor in an enclosed piping system with negligible exposure to workers.

Granular material is frequently added to the vessel. In large production operations the granular chemical may be pneumatically conveyed directly from storage bin to the vessel. In the more common batch process shown in Fig. 6.24, it is added manually through a vessel charging port or manway. In this case, two exposures can

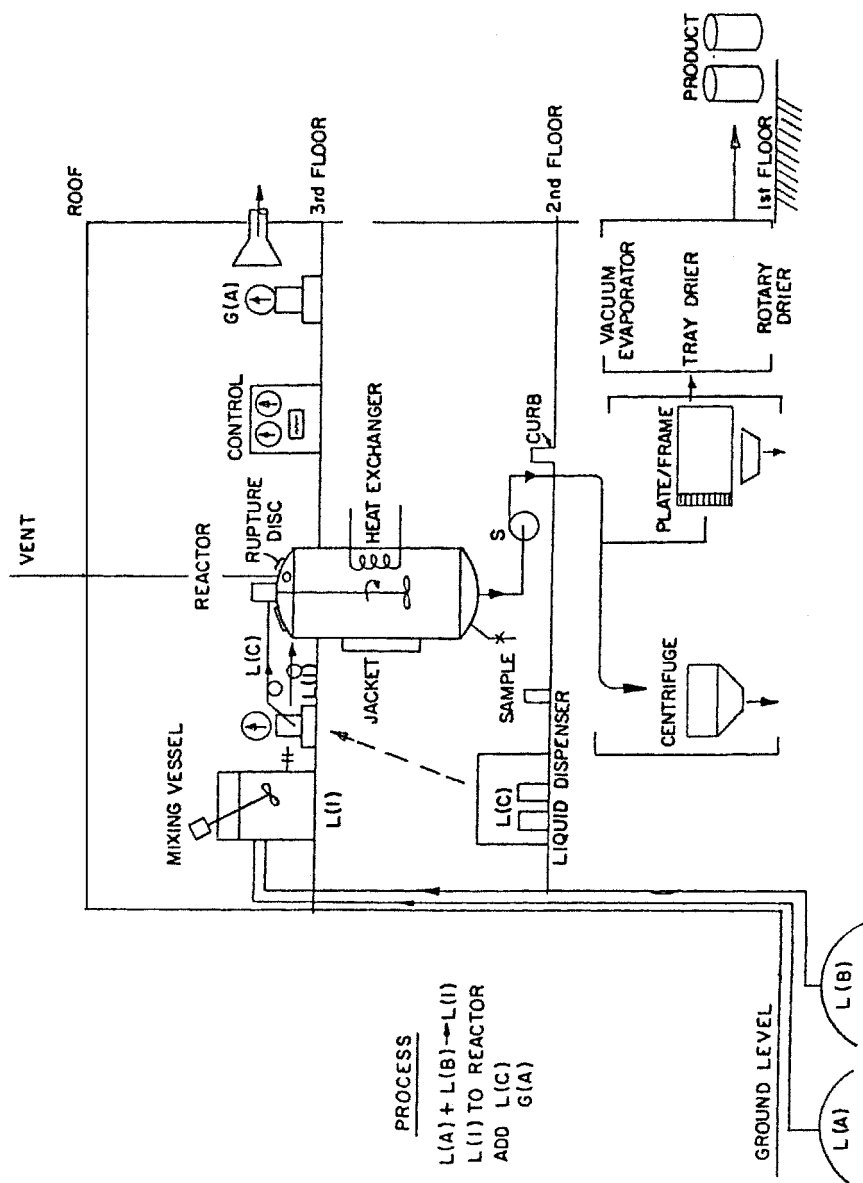


Figure 6.24 Chemical processing plant for batch processing (L, liquid; G, granular; S, suspension).

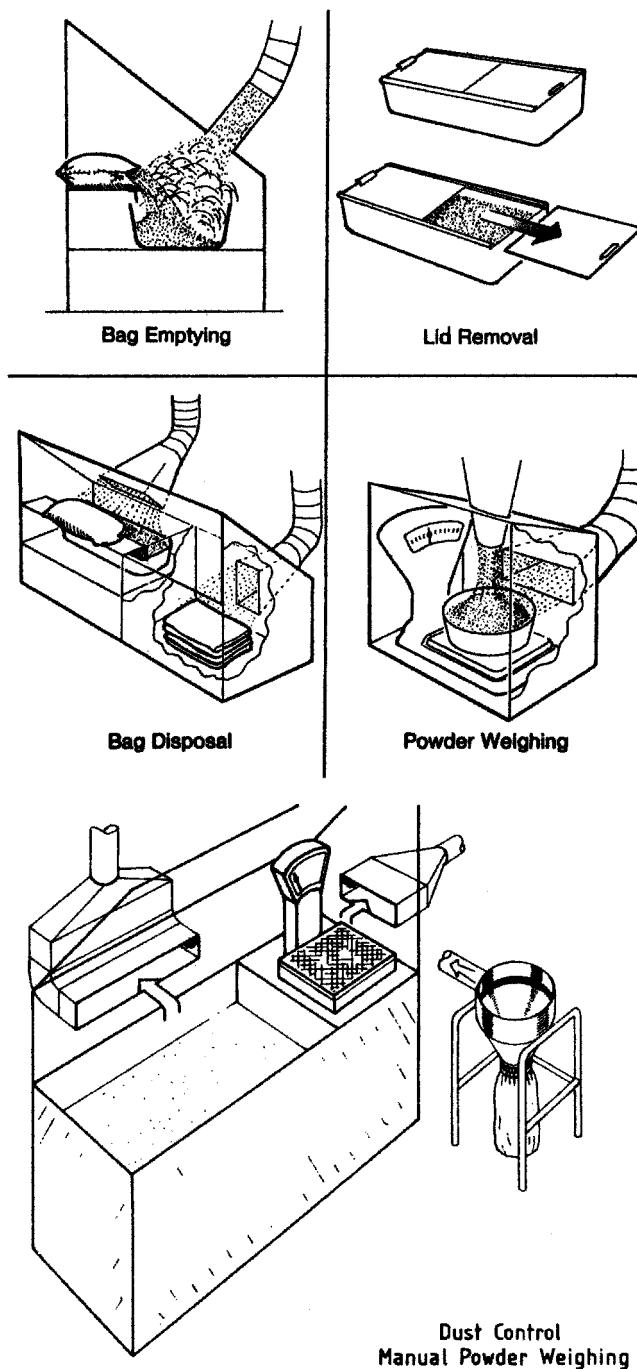


Figure 6.25 Weigh station dust control. [Reproduced with permission from *Annals of Occupational Hygiene* (1980).]

occur. Dumping the granular material into a reactor already charged with liquid solvent can induce airflow into the vessel, with the resulting displacement of particles and solvent-laden air into the workplace. This is an important exposure point and must be controlled by local exhaust ventilation. The usual approach is an exterior hood positioned at the charge port whose geometry and airflow permit effective capture of both solvent vapors and respirable dust (Fig. 6.26). Collection efficiency of well-designed hoods of this type is greater than 95% as measured by tracer studies by the authors.

Small quantities of solvent may be added to the reactor from a drum using a drum pump that discharges to the reactor through an open access port. Exposure to chemical vapors can occur both during preparatory mounting of the pump in the drum and as the wetted wand is removed from the drum when pumping is completed. There are two approaches to ventilation control during such operations. A bung hole exhaust hood may be positioned on the drum (Fig. 6.27) or a partial enclosure for the drum can be positioned adjacent to the reactor. The latter approach usually is more effective.

Periodically, samples must be taken from the reactor to check on the status of the reaction or as a final product quality check. This is frequently done by opening an access port on the top of the reactor and using a dipstick with a sampling cup. Although there is potential exposure from the headspace contaminants in the reactor and the vapor from the sample, exposures are usually negligible when the reactor is equipped with charge port ventilation as described above. Headspace exposure can also be controlled by placing the reactor under vacuum, causing an inward flow of air through the charge port. A second sampling technique involves the use of a special sampling line positioned near the bottom of the reactor. This sampling location

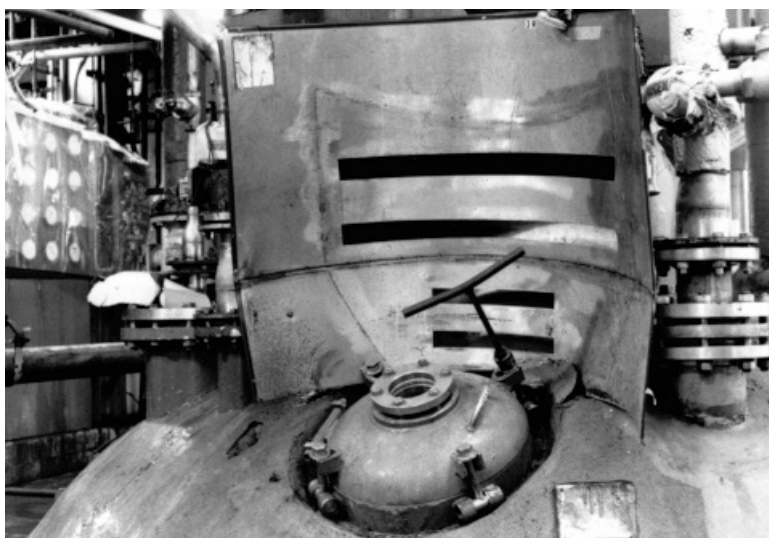


Figure 6.26 Reactor charge port ventilation. (Q varies from 1000 to 2000 cfm (5 to 10 m/s), depending on size, $C_e = 0.60$.)

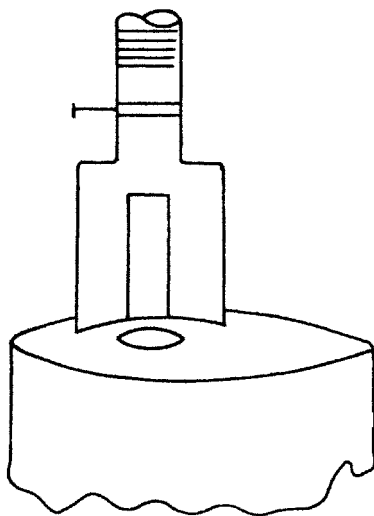


Figure 6.27 Drum bung hole exhaust. ($Q = 150$ cfm ($0.07 \text{ m}^3/\text{s}$), $C_e = 0.50$.)

should be equipped with a small exhausted enclosure (Fig. 6.28), as described in VS-15–30.

The final product, in our example a suspended particle, is now ready to be recovered from the reaction fluid. As shown in Fig. 6.29, three common techniques available to perform this function are the Neutsche filter, the centrifuge, and the plate and frame filter. Each of these operations results in potential exposure due to the residual solvents; the latter two require special attention.

If a centrifuge is used, the suspension in the reactor is pumped to the centrifuge, where it flows into a spinning basket lined with a filter pad (Fig. 6.30). The particles are trapped on the filter as the solvent flows through the filter and is pumped to a holding tank. The cake on the inner surface of the basket is washed serially with fresh solvent sprayed through the spray header. If the solvent presents a fire and explosion hazard, the centrifuge cavity is flushed with nitrogen or carbon dioxide. When the cake is completely washed a plow scrapes it from the basket surface and the recovered product drops to a container. Worker exposure to solvent occurs when the access doors are opened to scrape the basket manually or to inspect the condition of the basket filter. A secondary exposure occurs at the product collection drum or bin.

It is difficult to achieve control at the access port on the top of the centrifuge. One possibility is to pull sweep air through the centrifuge using the line to the holding tank. If this is not possible, an exterior hood must be installed at the access port as shown in Fig. 6.31. Solvent vapor control at the product collection drum can be accomplished by a barrel exhaust station.

The second technique in common use for recovery of the product is a plate and frame filter. Available in a variety of designs, the conventional system utilizes a number

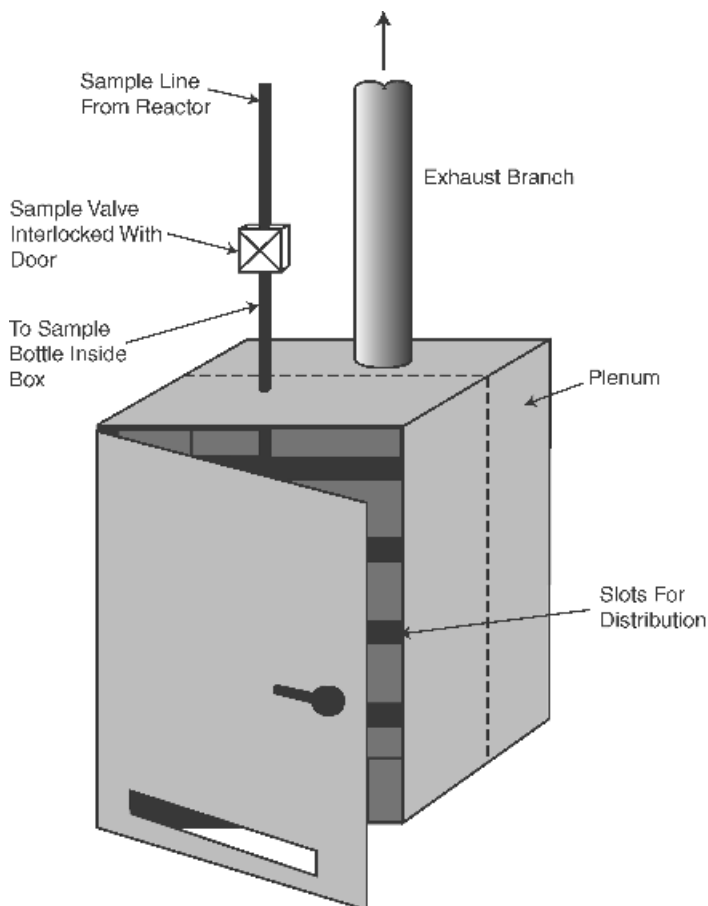


Figure 6.28 Sampling hood.

of filter pads placed in parallel to arrest the particles. The suspension in the reactor is pumped to the plate and frame filter, the particles are collected on the filter, and the stripped solvent is directed to a holding tank. The plate and frame process also permits the washing of the collected product with clean solvent or water. When the washing is completed the plate clamping pressure is released and the plates are separated. The product cake, still wet with solvent, is manually scraped from the plates and drops to a recovery cart (Fig. 6.32). During this process the solvent evaporated from the wet cake results in significant air concentrations in the workplace, which require ventilation control.

Effective control of solvent vapors from plate and frame filters is extremely difficult. One approach utilizes a top exhausted plenum with a perimeter plastic curtain or horizontal sliding sash, which must be positioned by the operator for effective control (Fig. 6.33). If adequate overhead space is not available for the plenum, two

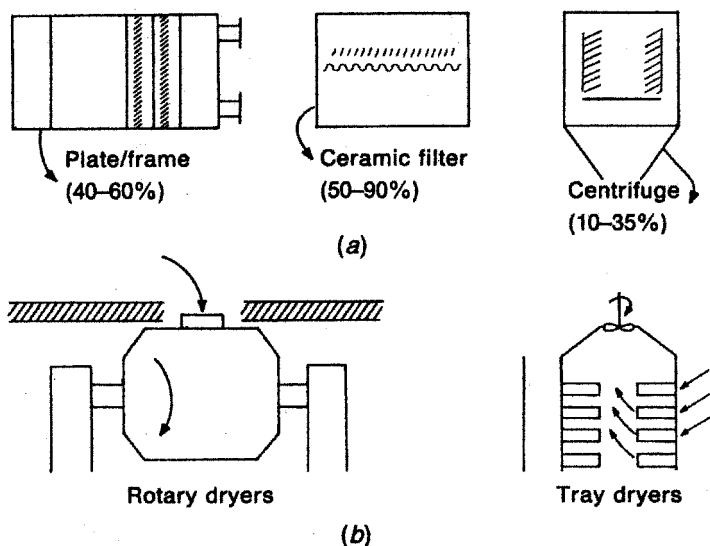


Figure 6.29 (a) Filtration and (b) drying techniques. The percent residual solvent in the wet cake is shown for each of the three filtration methods.

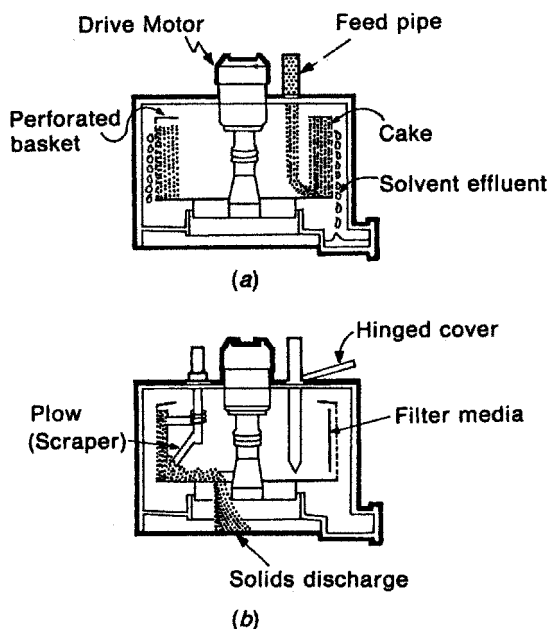


Figure 6.30 Details of basket centrifuge during two major operational steps: (a) active filtration; (b) removal of product. The product is also frequently removed manually with a small spade working through the hinged cover.

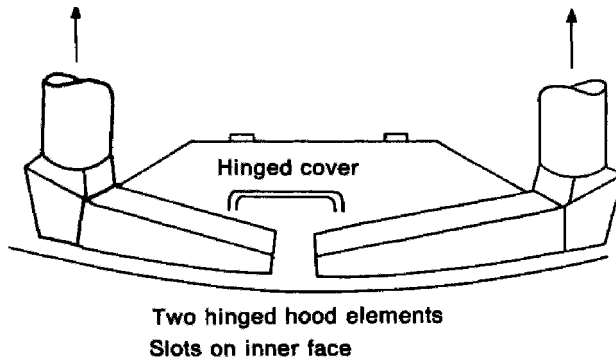


Figure 6.31 Exhaust hood for centrifuge hinged cover at access door. [$Q = 250$ cfm ($0.12 \text{ m}^3/\text{s}$) per leg, $C_e = 0$, 60.]

fishtail hoods can be positioned at the ends of the press (Fig. 6.34). Again, the effectiveness of control depends on proper positioning of the curtains by the operators to ensure proper airflow past the operator breathing zone.

Drying of the product cake in a batch operation is normally accomplished by a tray dryer, a conical dryer, or a fluidized-bed dryer. Loading of each operation involves a solvent exposure; unloading may result in an exposure to respirable dust during packaging and transport.



Figure 6.32 Dropping product from plate and frame filter.



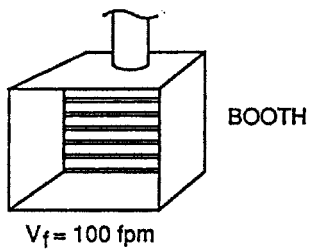
Figure 6.33 Ventilation of plate and frame filter enclosure based on rigid sliding panels or plastic curtains.

6.6 SEMICONDUCTOR GAS CABINETS

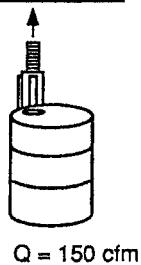
A variety of highly toxic gases, including arsine and phosphine, are used in semiconductor manufacturing operations. The gases are normally dispensed from pressurized cylinders through a pressure regulating manifold. The principal control for minimizing the potential for worker exposure to these gases in the event of a leak during storage and dispensing operations is an exhausted enclosure. These enclosures, known in the semiconductor industry as gas cabinets, fulfill the definition of an enclosing-type hood and should provide a high level of control with minimum airflow. It should be noted that gas cabinets are designed for control of fugitive emissions and not violent release of total gas cylinder contents (SEMI, 2000).

Manufacturers make standard gas cabinets to house up to four gas cylinders. The gas cylinder is positioned in the cabinet and connected to a panel-mounted manifold that permits accurate flow metering of the gas to the various fabrication operations.

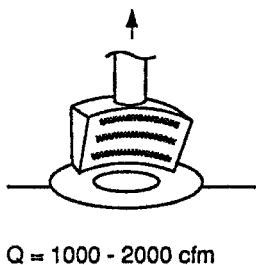
REACTIVE CHEMICAL DISPENSING



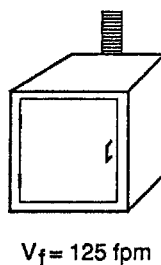
DRUM BUNG HOLE



REACTOR CHARGE PORT



SAMPLING HOOD



CENTRIFUGE

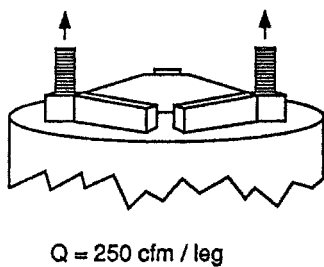


PLATE & FRAME

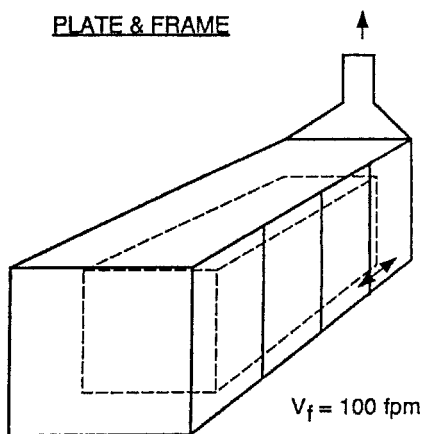


Figure 6.34 Summary of exhaust ventilation for chemical processes.

The major structural variables in the design of the gas cabinet are the air inlet and outlet configurations. In the conventional gas cabinet design, air sweeps through an opening in the bottom of the door and exhausts through a straight-duct takeoff at the top of the cabinet. The inlet is usually a series of slots in the door and may include mounting for a “roughing” particle filter, which acts as a diffuser.

Although these hoods are widely used in industry, there are few published data on their performance, nor has a method of defining optimum design been published. Furthermore, the air flows specified by various manufacturers may be quite different for similar equipment. Recognizing this deficiency, the authors used a tracer gas to evaluate the performance of gas cabinets (Forster and Burgess, 1986). The study evaluated optimum gas cabinet geometry and exhaust airflow for these cabinets.

A two-cylinder test gas cabinet equipped with a variety of inlet and outlet configurations and accommodations for a range of cylinder sizes was made available for this study from Matheson Gas Products, Inc. (Fig. 6.35). The cabinet is provided with a full-length front door used to change cylinders; pressure regulation and other adjustments are done through an access port to minimize the potential for personnel exposure to the toxic gas.

The test cabinet was provided with three interchangeable inlet air configurations: (1) a plain slotted inlet in the door, (2) a perforated plate inlet in the base of the cabinet, and (3) a diffuser inlet in the door. The perforated bottom plate inlet was included

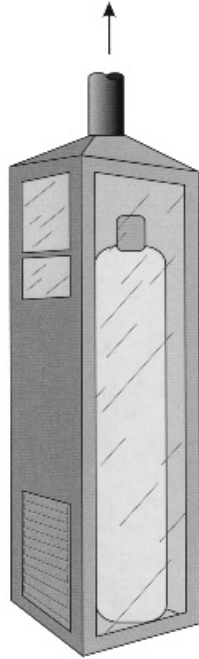


Figure 6.35 Two-cylinder test gas cabinet showing front door with access port, diffuser air inlet at base of door, shallow cone exhaust, and clear side panels for flow visualization studies.

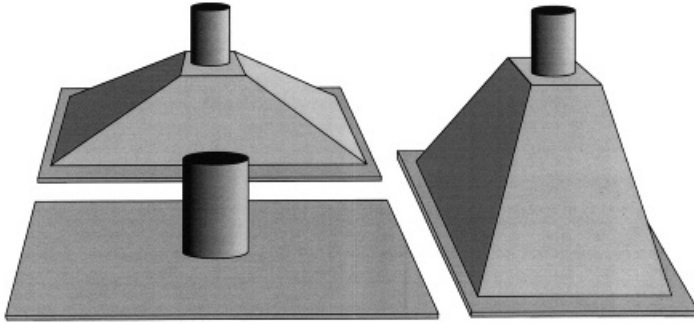


Figure 6.36 Three air exhaust outlets for mounting on top of test cabinet. Left front is flat, left rear is shallow cone, and right is deep cone.

to test the theory that a “piston” flow of air through a perforated bottom plate to a takeoff at the top would provide excellent clearance of any fugitive gas leakage.

The conventional gas cabinet for semiconductor gases has a flat exhaust duct takeoff, a geometry that may encourage corner eddies and possibly increase clearance time. To minimize these effects, conical exhausts have been considered in cabinet design. Shallow and deep exhaust cones representing more conventional aerodynamic design were tested in addition to the flat exhaust takeoff (Fig. 6.36).

6.6.1 Entry Loss

The coefficients of entry (C_e) calculated at various flow rates for each of the different inlet and exhaust configurations are shown in Table 6.10. The air inlet geometry was found to have a major effect on the coefficient of entry, while differences in outlet geometry had little effect on entry loss. Specifically, C_e for the slot inlet ranged from 0.44 to 0.47, while the best values of 0.68–0.75 were obtained with the diffuser and perforated base inlets.

Table 6.10 Coefficient of Entry C_e for Gas Cabinet inlet and Outlet Configurations

Inlet	Outlet	Coefficient of Entry, C_e
Slot	Flat	0.44
	Shallow cone	0.47
	Deep cone	0.47
Diffuser	Flat	0.70
	Shallow cone	0.75
	Deep cone	0.72
Perforated base	Flat	0.68
	Shallow cone	0.72
	Deep cone	0.72

Source: Forster and Burgess (1986).

6.6.2 Optimum Exhaust Rate

In a series of tests to define the minimum airflow exhaust rate to maintain control, a tracer gas was released at a rate of 1.9 lpm (liters per minute) from a critical leak location inside the cabinet. The downstream concentration of the tracer gas was measured continuously at the sampling port in the exhaust duct. When the system had stabilized and a steady downstream concentration had been established, the leak was stopped and the time noted on the chart recorder. The decay of the downstream concentration was then used to define the performance of the system. For these tests, the time of decay to 5% of the original concentration was used to evaluate performance.

The clearance time data for the various test configurations without cylinders in place are summarized in Fig. 6.37. These data demonstrate several points:

- The slotted inlet consistently takes longer to clear a leak than do the other two inlets.
- The clearance time for all three inlets is reduced significantly by increasing the airflow from 150 to 250 cfm (0.07 to 0.12 m³/s) for this two-cylinder cabinet.
- For the perforated plate and the diffuser inlet, little improvement in performance is gained by increasing the airflow to 350 cfm (0.17 m³/s).
- There is little difference in the performance of the perforated baseplate and the diffuser front at 250 and 350 cfm (0.12 and 0.17 m³/s).
- The exhaust configuration has little bearing on clearance time.

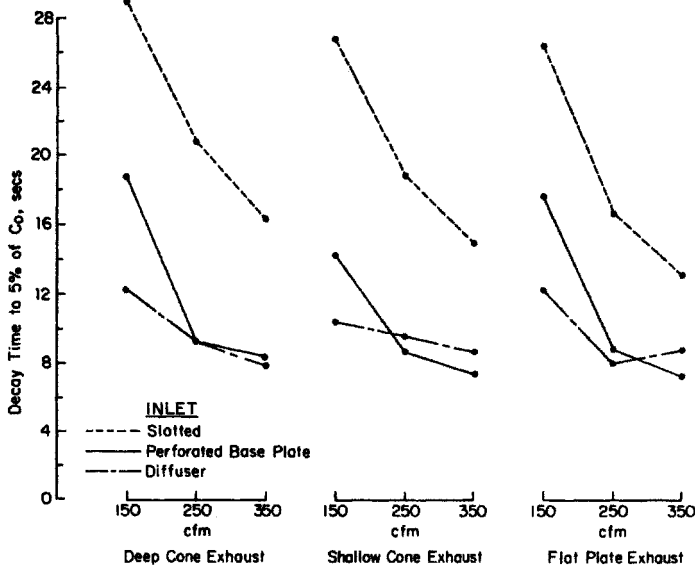


Figure 6.37 Clearance times of three test inlets for each test configuration without cylinders (150 cfm = 0.07 m³/s; 250 cfm = 0.12 m³/s; 350 cfm = 0.17 m³/s).

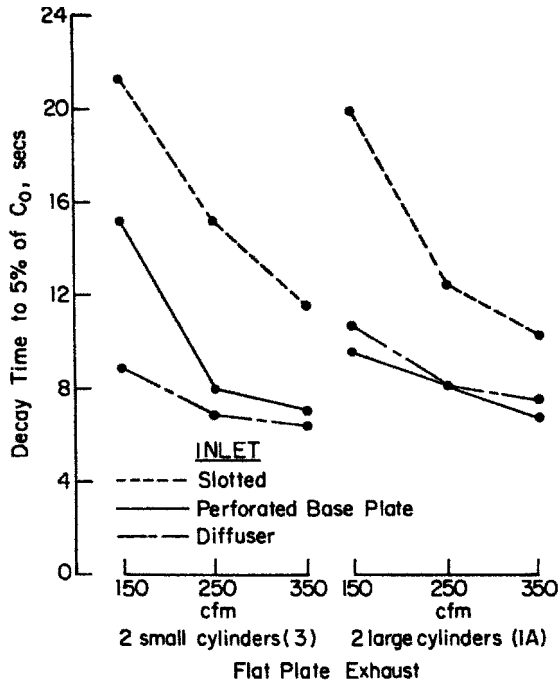


Figure 6.38 Clearance times of three test inlets for flat plate exhaust with small and large cylinders (150 cfm = $0.07 \text{ m}^3/\text{s}$; 250 cfm = $0.12 \text{ m}^3/\text{s}$; 350 cfm = $0.17 \text{ m}^3/\text{s}$).

The clearance time for the gas cabinet was also evaluated with either two 60-cm or two 130-cm cylinders in place. The results of this testing with the flat plate and shallow cone exhausts are presented in Figs. 6.38 and 6.39. The deep cone was not evaluated since it did not demonstrate an advantage over the shallow cone in the previous tests. These results demonstrate the same trends as the data generated with no cylinders in place, thereby validating the earlier findings. Therefore, a diffuser inlet in the bottom of the cabinet door with an exhaust rate of 250 cfm ($0.12 \text{ m}^3/\text{s}$) for a two-cylinder cabinet is recommended.

6.7 LOW-VOLUME/HIGH-VELOCITY SYSTEMS FOR PORTABLE TOOLS

The low-volume/high-velocity capture system *Industrial Ventilation* VS-40-20 uses an extractor hood designed as an integral part of the tool or positioned very close to the operating point of the cutting tool. The hood is empirically designed to provide high capture velocities, frequently greater than 10,000 fpm (50 m/s), at the contaminant release point. This velocity may frequently be achieved at airflows less than 50 cfm ($0.02 \text{ m}^3/\text{s}$) by employing a small hood face area.

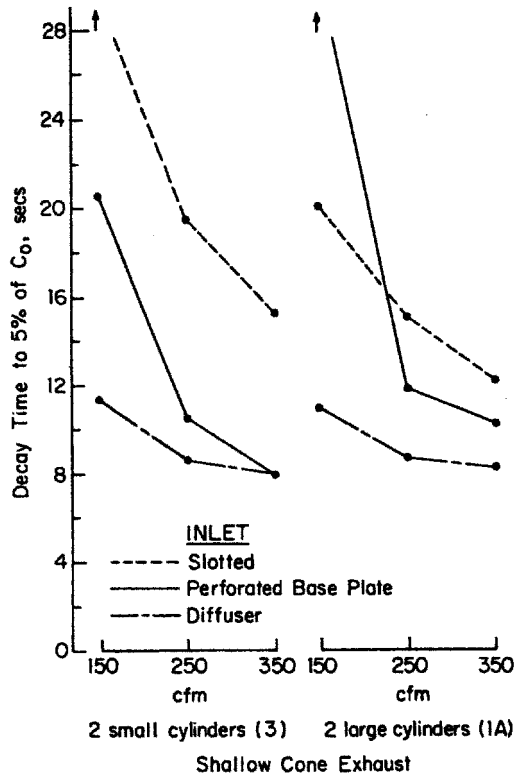


Figure 6.39 Clearance times of three test inlets for shallow cone exhaust with small and large cylinders (150 cfm = $0.07 \text{ m}^3/\text{s}$; 250 cfm = $0.12 \text{ m}^3/\text{s}$; 350 cfm = $0.17 \text{ m}^3/\text{s}$).

This approach was applied in the 1950s in the United States for the control of highly toxic materials such as beryllium released from machining operations (Chamberlin, 1959). Although application on machine tools has continued to this date, the major impetus in the acceptance of low-volume/high-velocity systems has resulted from its application to portable tools pioneered in the United Kingdom and the Scandinavian countries since 1965. It is now widely used on at job sites, buffing and grinding operations at widely dispersed plant operations, and pneumatic drilling in mining and quarrying.

There are a number of advantages to this ventilation control technique. The collection system is an integral part of the tool and does not rely on the operator to position an exhaust hood close to the work for proper control each time the work position is changed. In addition, the exhaust airflows required to achieve the high collection efficiency are frequently 10% of that required with conventional exterior hoods. Due to the expense of conditioning replacement air in northern latitudes, this has great cost reduction potential in a plant containing a large number of workstations. Finally, this may be the only feasible approach for the control of highly toxic air contaminants

in operations where conventional workstations with local exhaust ventilation cannot be installed (Fig. 6.40).

It might appear on first glance that an additional advantage to the system is reduced air mover operating cost. This turns out not to be the case since the energy cost to operate an air mover is proportional not only to airflow but also to total resistance (Chapter 10). In low-volume/high-velocity systems the airflow is, as noted above, frequently reduced by a factor of 10, but the system resistance may be increased tenfold; hence the air horsepower is approximately the same as that for a conventional system and the cost of operating the air mover will be approximately the same.

The principal disadvantages of this system are the high initial cost of the high static pressure air mover and the customized exhaust nozzles and the associated equipment, high noise levels caused by the air moving through the restricted area of the nozzle at high speed, and the propensity for high-vacuum hoods to pick up small tools and material placed close to the inlet. When used on portable tools the operators complain of the additional weight and bulk of the suction hose.

The design of a low-volume/high-velocity system is largely empirical and is based on a general understanding of the release mechanism of the air contaminant. The extractor hood is connected to the exhaust system with a length of high-resistance flexible duct that permits its use on a portable tool and allows latitude for movement of movable work beds on fixed machine tools. The flexible duct is connected to the main duct, which is a heavy-walled, smooth-bore tubing with no inner surface discontinuity. Because conventional pipe or tubing would quickly erode on a particle collection application due to the abrasive action of debris carried by the high-velocity airstream, the main tubing must be equipped with large sweep elbows and low-angle entries. As a result of static charge accumulation, the flexible hose at the tool must be conductive and staticproof.

In the United Kingdom the extractor hoods are designed so that a hood static pressure of 5 in. Hg (16,950 Pa) will provide the necessary airflows (U.K. Department of Employment, 1974). Typical system losses downstream of the hood due to the flexible hose, smooth duct, and air cleaner are 5–7 in. Hg (16,950–23,730 Pa), for a total system static pressure requirement of 10–12 in. Hg (33,900–40,680 Pa). A single tool can, therefore, be operated by a suitable vacuum cleaner; a multihood system requires the greater power of a multistage turbine fan or a positive-displacement blower.

The design of the typical low-volume/high-velocity systems in the United States is also empirical; the recommended minimum extraction volumes in Table 6.11 are approximately three to four times those recommended in the United Kingdom (Stephenson and Nixon, 1987). The extractor hood static pressure is claimed to be 6 in. Hg (20,340 Pa) by one U.S. manufacturer and the *Ventilation Manual* cites pressures in the range 7–14 in. Hg (23,730–47,460 Pa). The design procedure used by one manufacturer of these systems is noted in Example 6.2 and Fig. 6.41 (Stephenson and Nixon, 1987). The nozzle entry loss is obtained from a chart and combined with the losses due to the flexible hose, the air cleaner, and the system tubing running to the multistage turbine. Since the system operates at nearly one-half an atmosphere, air volumes must be corrected to standard conditions.

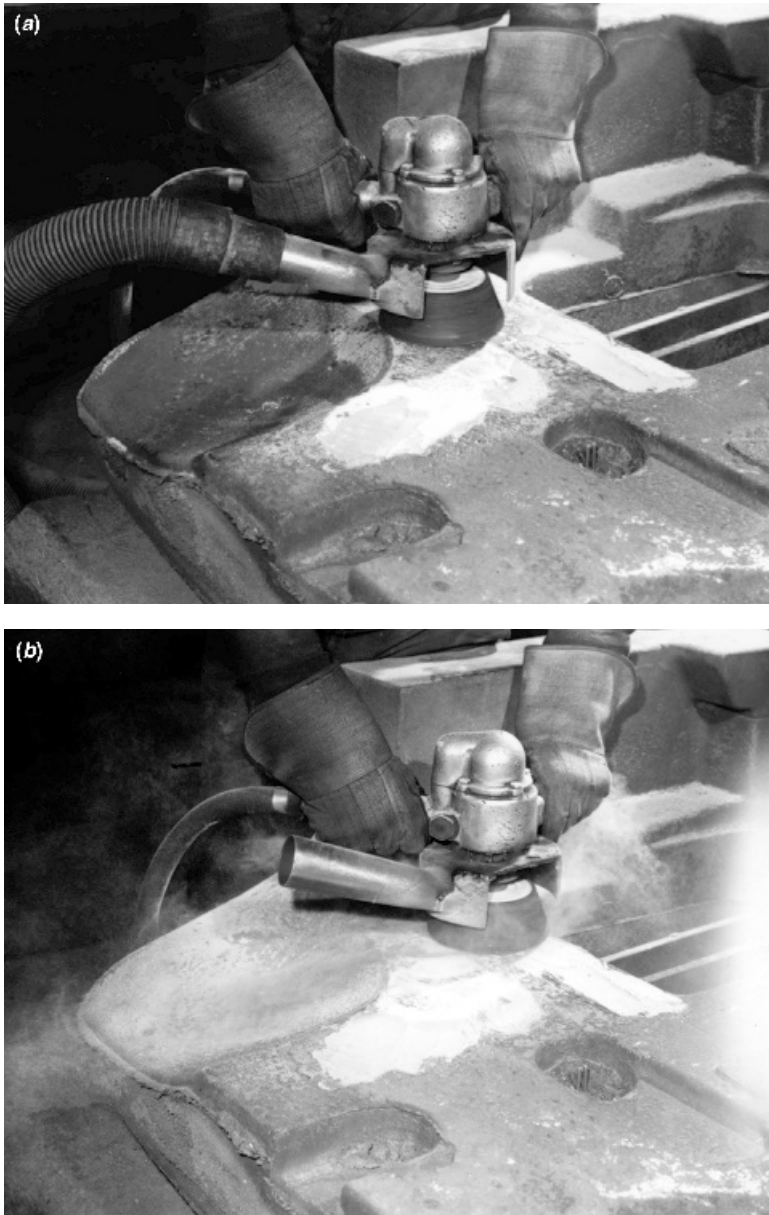


Figure 6.40 (a) The effectiveness of a low volume/high-velocity hood on a cup grinder is shown in a foundry operation. (b) When the suction hose is removed from the cup grinder, the dust released from the operation is visible.

Table 6.11 Minimum Volumes and Hose Sizes^a

Hand Tool	CFM	Plastic Hose Inside Diameter (in.)
Disk sander		
3 in.—10,000 rpm	125	1
7 in.—5,000 rpm	200	2
9 in.—2,500 rpm	200	2
Vibratory pad sander—4 × 9	150	1½
Router		
½ in.—50,000 rpm	125	1½
¾ in.—30,000 rpm	150	1½
1 in. Cutter—20,000 rpm	150	1½
Belt sander 3 in.—4,000 rpm	125	1½
Pneumatic chisel	125	1½
Radial wheel grinder	150	1½
Surface die grinder, ¼ in.	125	1½
Cone wheel grinder, 2 in.	150	1½
Cup stone grinder, 4 in.	200	2
Cup-type brush, 6 in.	250	2
Radial wire brush, 6 in.	175	1½
Hand wire brush—3 × 7	125	1½
Rip-out knife	175	1½
Rip-out cast cutter	150	1½
Saber saw	150	1½
Swing frame grinder—2 × 18	600	3
Saw abrasive, 3 in.	150	1½

^aBased on low production requirement with ideal pickup hoods and branch static at 6 in. Hg (20,340 Pa). Metric conversions: 125 cfm (0.06 m³/s); 150 cfm (0.07 m³/s); 175 cfm (0.08 m³/s); 200 cfm (0.09 m³/s); 250 cfm (0.12 m³/s); 600 cfm (0.28 m³/s).

Source: Stephenson and Nixon (1987).

The performance of low-volume/high-velocity systems has been evaluated by American (Burgess and Murrow, 1976; Garrison and Byers, 1980a, 1980b, 1980c), British (Dalrymple, 1986), and French (Regnier et al., 1986) investigators. These studies indicate high collection efficiencies on a variety of particulate contaminants using air volumes in the same range as those cited in the *Ventilation Manual*. The application of LVHV systems on portable sanding tools is increased rapidly and studies of its efficacy on dust control on automobile body, aircraft composites, and woodworking have been numerous. Little attention, however, has been given its application on fixed machine tools where it has great potential.

In addition to their use on particle control for portable tools, these systems have been applied to other air contaminants, such as soldering and welding fumes (as noted previously in this chapter). Since the metal fume contaminant is released at low velocity, excellent control can be achieved with very low airflows. Dalrymple (1986) describes a soldering application where pyrolysis products of solder fluxes can be captured with high efficiency at flows of 1–2 cfm.

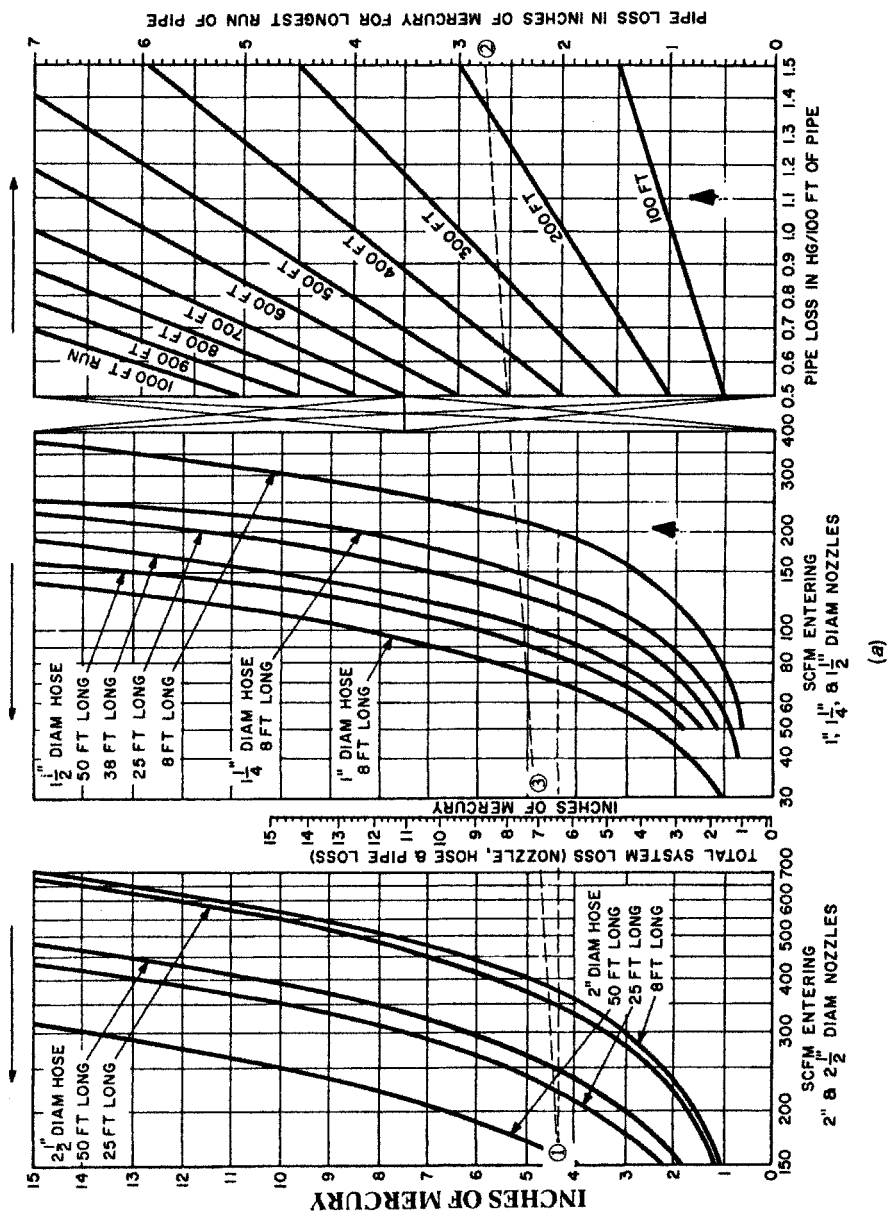


Figure 6.41 (a) Design procedure for low-volume/high-velocity system. (Courtesy of Hoffman Air and Filtration Systems.)

(a)

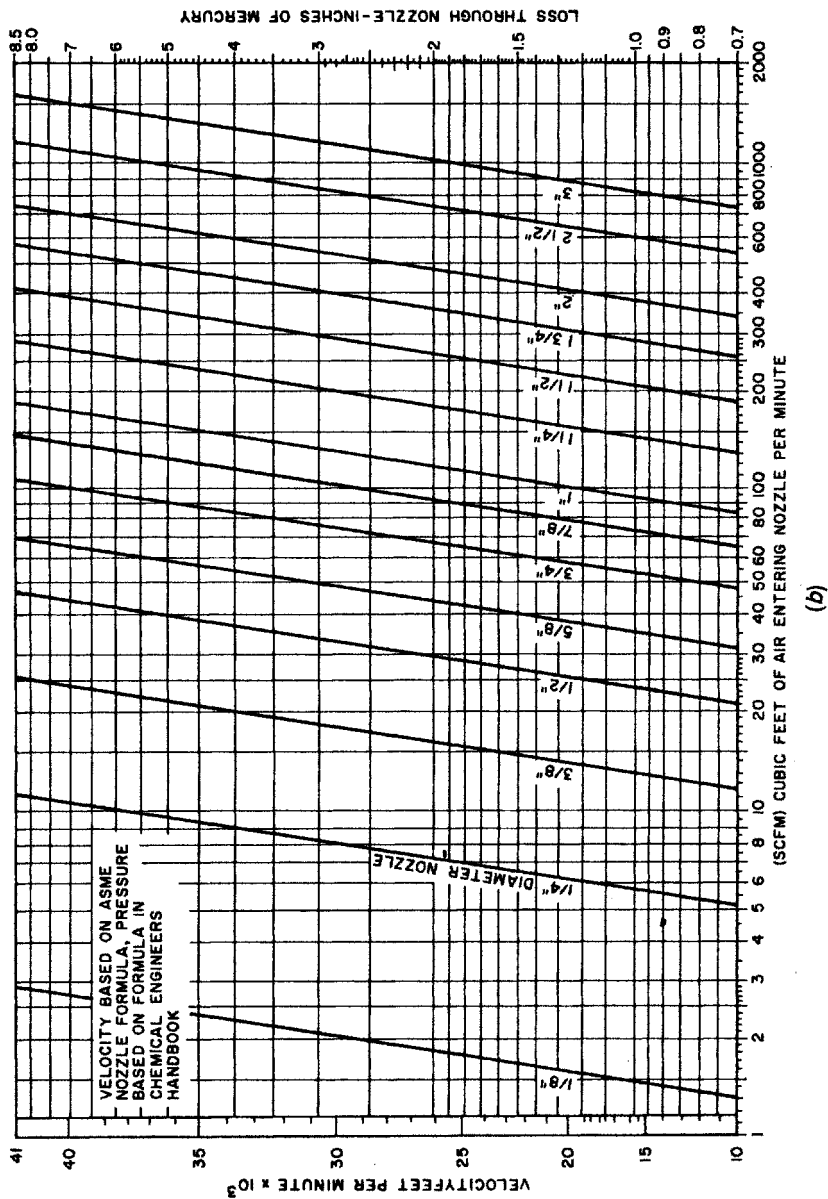


Figure 6.41 (b) Design procedure for low-volume/high-velocity system. (Courtesy of Hoffman Air and Filtration Systems.)

Recently, there has been a movement to design machine tools to take advantage of the low-volume/high-velocity concept. One application on a milling machine utilizes a hollow milling cutter exhausted at 50 cfm with a hood static pressure of 7.5 in. Hg. In this system the milling cutter is mounted in a hollow spindle drive to which is attached the vacuum source and filter. This system is now used in the United States for milling “proof” board made of Styrofoam and machining structural plastic materials.

EXAMPLE 6.1 CALCULATION OF EXHAUST RATE FOR OPEN-SURFACE TANKS

Example 6.1a Calculation of Exhaust Rate for Open-Surface Tanks in Example 9.2

(1)	(2)	(3)	(4)	(5)				(6)	(7)	(8)
Tank	Solution	Temp- erature (°C)	Class	Tank Dimensions				V Capture (fpm)	Minimum Rate (cfm/ft ²)	Q (cfm)
				L	W	W/L	A			
1	Hot water	200	D-1	3	2	0.67	6	75	130	780
2	Cr strip	130	C-3	$2\frac{1}{3}$	2	0.86	$4\frac{2}{3}$	50	90	420
3	Acid Cu	110	B-3	6	$3\frac{1}{2}$	0.58	21	75	130	2730
4	Cr plate	115	A-1	4	3	0.75	12	150	250	3000
5	Ni plate	70	B-2	4	3	0.75	12	100	175	2100
6	Alkaline cleaner	200	C-1	5	2	0.40	10	100	150	1500

Column 1 gives tank identification numbers to be used in Example 9.2

Column 2 shows contents of the plating tanks and *column 3* shows operating temperature specified by the customer. Tank 1, hot water; 2, chromium strip (alkaline); 3, bright acid, copper plate; 4, chromium plate (acid); 5, nickel plate (sulfate); 6, alkaline cleaner.

Column 4 gives the hazard potential evolution rate class, obtained from various tables in the *Ventilation Manual* as shown below.

Column 5 has tank dimensions, given to the designer by customer.

Column 6 is obtained from Table 10.70.3

Column 7 is obtained from Table 10.70.4

Column 8 equals column 7 \times column 5A.

Tank	Table	Special Conditions	Class
1	10.70.5	Complete collection of steam	D-1
2	10.70.8		C-3
3	10.70.7	Higher temperature range	B-3
4	10.70.7		A-1
5	10.70.7		B-2
6	10.70.6	Higher temperature range	C-1

Example 6.1b Calculation of Exhaust Rate for Open-Surface Tanks in Example 9.2—metric version

(1)	(2)	(3)	(4)	(5)				(6)	(7)	(8)
Tank	Solution	Temp- erature (°C)	Class	Tank Dimensions				V Capture (m/s)	Minimum Rate (m³/s per m²)	Q (m³/s)
				L	W	W/L	A			
1	Hot water	93	D-1	0.91	0.61	0.67	0.56	0.38	0.65	0.36
2	Cr strip	55	C-3	0.71	0.61	0.86	0.43	0.25	0.45	0.20
3	Acid Cu	43	B-3	1.83	1.07	0.58	1.96	0.38	0.65	0.27
4	Cr plate	46	A-1	1.22	0.91	0.75	1.11	0.75	1.27	1.41
5	Ni plate	21	B-2	1.22	0.91	0.75	1.11	0.50	0.88	0.98
6	Alkaline cleaner	93	C-1	1.52	0.61	0.40	0.93	0.50	0.75	0.70

Column 1 gives tank identification numbers to be used in Example 9.2

Column 2 shows contents of the plating tanks and *column 3* shows operating temperature specified by the customer. Tank 1, hot water; 2, chromium strip (alkaline); 3, bright acid, copper plate; 4, chromium plate (acid); 5, nickel plate (sulfate); 6, alkaline cleaner.

Column 4 gives the hazard potential evolution rate class, obtained from various tables in the *Ventilation Manual* as shown below.

Column 5 has tank dimensions, given to the designer by customer.

Column 6 is obtained from Table 10.70.3

Column 7 is obtained from Table 10.70.4

Column 8 equals column 7 \times column 5A.

Tank	Table	Special Conditions	Class
1	10.70.5	Complete collection of steam	D-1
2	10.70.8		C-3
3	10.70.7	Higher temperature range	B-3
4	10.70.7		A-1
5	10.70.7		B-2
6	10.70.6	Higher temperature range	C-1

EXAMPLE 6.2 DESIGN OF A LOW-VOLUME/HIGH-VELOCITY EXHAUST SYSTEM

Example 6.2: Calculation. Determine the inlet-cfm (ICFM) and suction in inches of mercury existing at the exhaust inlet, where

1. The distance from the most remote inlet valve to the inlet of the exhaust pipework with due allowance for fittings is 250 ft.
2. The piping loss in the system is assumed at 1.1 in. Hg per 100 ft of pipe.
3. There are 10 hoses in simultaneous operation on the entire system.

4. Each hose is $1\frac{1}{2}$ in. in diameter, 8 ft long, with $1\frac{1}{4}$ -in.-ID nozzle.
5. Each nozzle will draw in 200 cfm.
6. A separator (bag filter) loss of 1 in. Hg is assumed.
7. The installation is at 400 ft above sea level.

Using Fig. 6.41a, locate 200 cfm along bottom scale of center graph, rise to curve representing $1\frac{1}{2}$ -in.-diameter 8-ft-long hose and move horizontally to the far left scale and read out 4.34 in. Hg and mark as point 1. Locate 1.10 in. Hg loss per 100 ft of pipe value along the bottom of the right-hand graph and rise vertically to the sloping line representing 250 ft run; move horizontally to the right and read out 2.75; mark as point 2. Connect points 1 and 2 with a straight line and readout 7.09 (point 3). (Note: This problem and its solution are provided by courtesy of Hoffman Air and Filtration Systems Division of Gardner Denver Co. Since the solution is based on monograms from Stevenson and Nixon (1987), which are only available in English units, a metric solution is not presented.)

Using Fig. 6.41b, locate a point representing 200 cfm along the bottom of the scale and rise vertically, stopping first at the sloping line representing a $1\frac{1}{2}$ -in. nozzle. Move horizontally to the right scale and read out 0.94 in. Hg, continue vertically to the sloping line representing a $1\frac{1}{4}$ -in.-nozzle and move horizontally to the right scale and read out 2.85 in. Hg.

System loss with $1\frac{1}{2}$ -in.-diameter nozzle	7.09
less $1\frac{1}{2}$ in. nozzle loss	-0.94
	<hr/>
	6.15
plus $1\frac{1}{4}$ in. nozzle loss	2.85
	<hr/>
Total loss in nozzle, hose, and piping	9.00 in. Hg

To this value add 1 in. Hg separator loss, making a total suction S of 10 in. Hg at the exhaustor inlet.

$$\begin{aligned}
 \text{ICFM} &= \frac{N(\text{SCFM/hose})B}{B-S} \quad \text{where } N = \text{number of hose} \\
 &\quad B = \text{barometric pressure, in. Hg} \\
 &\quad S = \text{static pressure, in. Hg.} \\
 &= \frac{10 \times 200 \times 29.92}{29.92 - 10.00} = 3004 \\
 &= 3004 \text{ cfm at 10.0 in. Hg suction at exhaustor inlet}
 \end{aligned}$$

LIST OF SYMBOLS

A_u	open area of the enclosure upstream at dump location
C_e	coefficient of entry

D	average particle diameter
L	tank length
Q	airflow
Q_i	airflow induced by falling granules
R	material flow rate
S	height of fall
W	tank width

REFERENCES

- American National Standards Institute, *Standard for Spray Finishing Operations*, ANSI Z9.3-1994, ANSI, New York, 1994.
- Anderson, D. M., "Dust Control by Air Induction Technique," *Ind. Med. Surg.* **34**:168 (1964).
- Burgess, W. A., and J. Murrow, "Evaluation of Hoods for Low Volume-High Velocity Exhaust Systems," *Am. Ind. Hyg. Assoc. J.* **37**:546 (1976).
- Cecala, A. B., R. F. Timko, and E. D. Thimons, "Methods to Lower the Dust Exposure of Bag Machine Operators and Bag Stackers," *Appl. Occup. Env. Hyg.* **15**:751-765 (2000).
- Chamberlin, R., "The Control of Beryllium Machining Operations," *Arch. Ind. Health*, **19**(2):231 (Feb. 1959).
- Chan, T. L., J. B. D'Arcy, and R. M. Schreck, "High-Solids Paint Overspray Aerosols in a Spray Painting Booth: Particle Size Analysis and Scrubber Efficiency," *Am. Ind. Hyg. Assoc. J.* **47**:411 (1986).
- Dalla Valle, J. M., *Exhaust Hoods*, Industrial Press, New York, 1952.
- Dalrymple, H. L., "Development and Use of a Local Exhaust Ventilation System to Control Fume from Hand Held Soldering Irons," *Proc. 1st Int. Symp. Ventilation for Contaminant Control*, Oct. 1-3, 1985, Toronto, Canada, H. D. Goodfellow, ed., Elsevier, Amsterdam, 1986.
- Dennis, R. (1954), personal communication.
- Flynn, M. R., B. D. Lackey, and P. Muthedath, "Experimental and Numerical Studies on the Impact of Work Practices Used to Control Exposures in Booth-Type Hoods," *Am. Ind. Hyg. Assoc. J.* **57**:469-475 (1996).
- Forster, F., and W. A. Burgess, *Proc. 1st Int. Symp. Ventilation for Contaminant Control*, Oct. 1-3, 1985, Toronto, Canada, H. D. Goodfellow, ed., Elsevier, Amsterdam, 1986.
- Garrison, R. P., and D. H. Byers, "Noise Characteristics of Circular Nozzles for High Velocity/Low Volume Exhaust Ventilation," *Am. Ind. Hyg. Assoc. J.* **41**:713 (1980a).
- Garrison, R. P., and D. H. Byers, "Static Pressure and Velocity Characteristics of Circular Nozzles for High Velocity/Low Volume Exhaust Ventilation," *Am. Ind. Hyg. Assoc. J.* **41**:803 (1980b).
- Garrison, R. P., and D. H. Byers, "Static Pressure, Velocity, and Noise Characteristics of Rectangular Nozzles for High Velocity/Low Volume Exhaust Ventilation" *Am. Ind. Hyg. Assoc. J.* **41**:855 (1980c).
- Goodfellow, H., and E. Tahti, eds, *Industrial Ventilation Guidebook*, Academic Press, San Diego, 2001.
- Hagopian, J. H., and E. K. Bastress, *Recommended Industrial Ventilation Guidelines*, U.S. Department of Health, Education, and Welfare, National Institute for Occupational Safety and Health, Publication No. 76-162, Washington, DC, 1976.

- Hemeon, W. C. L., *Plant and Process Ventilation*, 2nd ed., Industrial Press, New York, 1963.
- Occupational Safety and Health Administration, OSHA Standard 29, CFR 1910.94, 1910.107, Washington, DC, 1985.
- Pring, R. T., J. F. Knudsen, and R. Dennis, "Design of Exhaust Ventilation for Solid Materials Handling," *Ind. Eng. Chem.* **41**:2442 (1949).
- Regnier, R., R. Braconnier, and G. Aubertin, "Study of Capture Devices Integrated into Portable Machine-Tools," *Proc. 1st Int. Symp. Ventilation for Contaminant Control*, Oct. 1–3, 1985, Toronto, Canada, H. D. Goodfellow, ed., Elsevier, Amsterdam.
- Smandych, T. S., M. Thompson, and H. Goodfellow, "Dust Control for Material Handling Operations: A Systematic Approach," *Am. Ind. Hyg. Assoc. J.* **58**:139–146 (1998).
- Stephenson, R. L., and H. E. Nixon, *Design of Industrial Vacuum Cleaning Systems and High Velocity, Low Volume Dust Control*, Hoffman Air & Filtration Systems, Inc., New York, 1987.
- Semiconductor Equipment and Materials International, SEMI S2-0200, *Environmental, Health and Safety Guideline for Semiconductor Manufacturing Equipment*, Mountain View, CA, 2000.
- U.K. Department of Employment, Her Majesty's Factory Inspectorate (1974), *Dust Control, The Low-Volume High-Velocity System*, Technical Data Note 1 (2nd rev.), H.M. Factory Inspectorate, London.

CHEMICAL LABORATORY VENTILATION

Early attempts to exhaust noxious air contaminants from chemical laboratory operations were crude. Chemists conducted their experiments near a window or door to disperse air contaminants. Later a storage cupboard was converted to a work area and equipped with an exhaust stack to provide natural ventilation. Some improvement in control was gained by using burners in the hood to achieve convective air movement. These workstations were first provided with mechanical ventilation in the late nineteenth century and the first proprietary laboratory hoods were manufactured shortly after the turn of the century. Principal design innovations to improve contaminant capture and containment have occurred since 1950.

In this chapter the benchtop hood used in chemical laboratories will be identified as a “laboratory hood,” “chemical laboratory hood,” or “laboratory chemical hood,” terms widely used in the United States. Drawing on the history of the evolution of the laboratory hood, the terms “fume hood” and “laboratory fume cupboard” are widely used in the European Community and to a lesser degree in the United States. This inconsistency with accepted occupational hygiene nomenclature is resolved in the British Standards (BSI, 1994) by redefining fume as consisting of gas, vapor, and particulate contaminants.

At this time the laboratory hood remains the primary ventilation control device in teaching, material control, and research laboratories. In this chapter attention will be given to the chemical laboratory hood, the integration of the hood into the total ventilation scheme, and the effective utilization of the hood by laboratory personnel. Limited attention will be given chemical storage hoods, auxiliary supplied

hoods, and ductless hoods. A number of other special hoods, including walk-in hoods, hoods open on more than one side, radiological and microbiological hoods, will not be discussed since these hoods are described elsewhere (DiBerardinis et al., 2001).

7.1 DESIGN OF CHEMICAL LABORATORY HOODS

The design evolution of the modern “bench-type” laboratory hood will be traced. The engineer must understand the reason for the principal features of the standard laboratory hood to properly design an effective chemical laboratory ventilation system.

7.1.1 Vertical Sliding Sash Hoods

The first laboratory hoods took the form of the simple exhausted storage cabinet shown in Fig. 7.1; these hoods are classified as partial enclosures using the definitions presented in Chapter 5. The size and geometry of these early laboratory hoods varied greatly; in most cases, however, the exhaust stack takeoff was at the top of the hood. Because of this geometry the velocity profile across the face of the hood was poor and the efficiency of containing air contaminants released in the hood varied greatly depending on the release point.

The first major improvement to this simple hood was the addition of a vertical sliding sash (Fig. 7.2). The tempered or laminated safety glass sash slides out of the way while the apparatus is set up and during manipulation. When access is not required the sash is partially or totally closed to improve contaminant containment efficiency, dilute in-hood flammable air contaminants below explosion limits and to protect the operator from chemical splashes or projectiles from minor explosions or exothermic reactions.

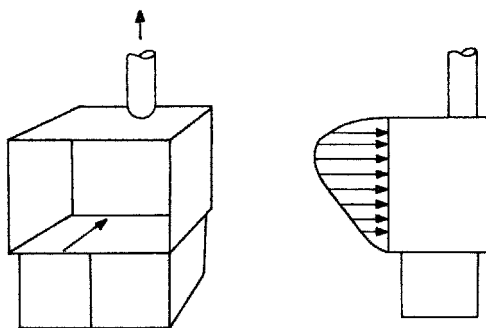


Figure 7.1 Simple exhausted box or enclosure with a top “takeoff.” This laboratory hood provides a dedicated workspace but rather poor ventilation control. Since most of the air enters the top half of the hood, the velocity profile is not uniform. A rear takeoff would improve the velocity profile, but that geometry requires more space and is rarely used in laboratory hoods.

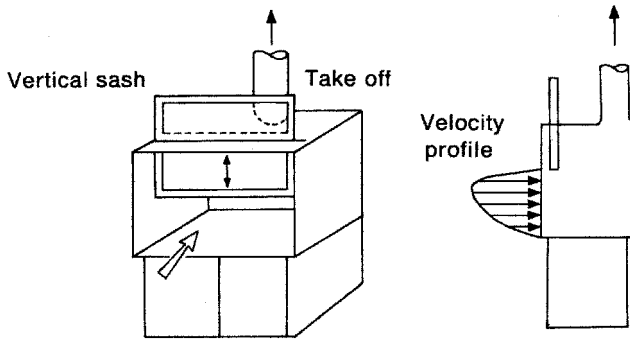


Figure 7.2 The addition of a vertical sliding sash permits variable face area and velocity. In early designs the sash projected through a slot in the top of the hood and leakage could occur under high contaminant generation rates. In later designs the sash slides into a pocket or the hood bonnet and this leakage path is eliminated.

With the sash in the upper position, the velocity can vary greatly across the face of the hood, and hood containment efficiency may be poor. A simple modification to flatten the velocity profile is the introduction of a rear baffle with slots (Fig. 7.3). In initial designs a single slot was located at the work surface; although this provided a flat horizontal velocity profile at the work surface, it did not improve the vertical velocity profile. Improvement in the vertical profile was obtained by adding a second adjustable slot in the upper bonnet of the hood. The flattening of the velocity profile with this slot geometry permits the face velocity at all locations to be maintained relatively constant with the sash wide open. The number of slots required to achieve a

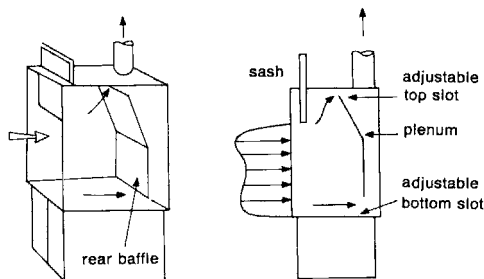


Figure 7.3 The plenum slot arrangement introduced in the 1930s provided a flat velocity profile across the face of the hood. Slots sized for 1000–2000 fpm (5.08–10.16 m/s) presented a resistance element, which resulted in even distribution of airflow along the length of the slot (see Chapter 5). Normally, the bottom and top slots are adjustable and the intermediate slots are fixed. The slots must be set at the optimum position when installed and maintained in that position unless conditions change. A perforated plate defining the plenum is an alternative to the slots, although manufacturers hesitate to provide this option since it would plug with dust and require periodic cleaning. With proper slot dimensions a velocity profile at the hood face is obtained with variations around the mean velocity of less than 10%. Such a flat velocity profile will ensure consistent collection efficiency across the face of the hood.

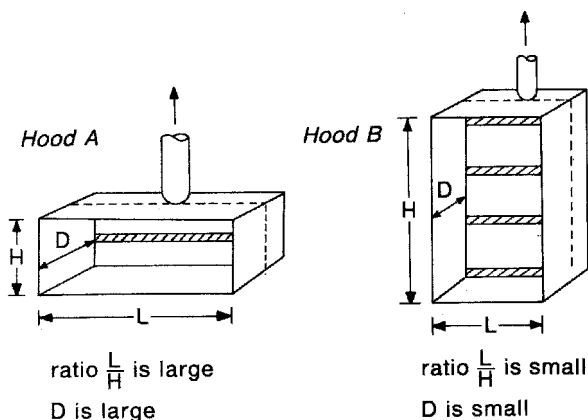


Figure 7.4 Hood A is a deep hood with minimum height and may require only one of two slots for proper airflow distribution across the hood face. A large shallow walk-in hood such as hood B requires multiple slots to produce a uniform face velocity.

reasonable velocity profile depends on the hood geometry and slot placement (Fig. 7.4). The impact on hood performance of additional slots has not been studied thoroughly; it is possible that poorly designed intermediate slots may contribute to contaminant “roll,” with resulting leakage at the face. Although on first view it would appear the slots should be adjustable many experienced designers object, stating this invites manipulation of the slot configuration by the individual chemist, which may result in malfunction of the hood.

In general, the sash and the rear baffle have resulted in improved hood performance. However, when the sash is in a lowered position the air inside the hood may have a characteristic rollback toward the face of the hood, which can be visualized with smoke (Fig. 7.5). In a poorly designed hood, contaminant may escape from the face of the hood by this mechanism.

With the introduction of the vertical sash, an additional problem was presented to the hood designer. As the sash is pulled down, the face area is decreased and the face velocity is increased. This increased velocity may be disruptive to open flames,

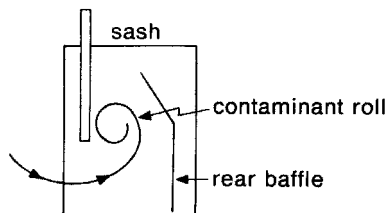


Figure 7.5 The characteristic roll noted behind the sash in a conventional hood may result in loss of contaminant to the workplace.

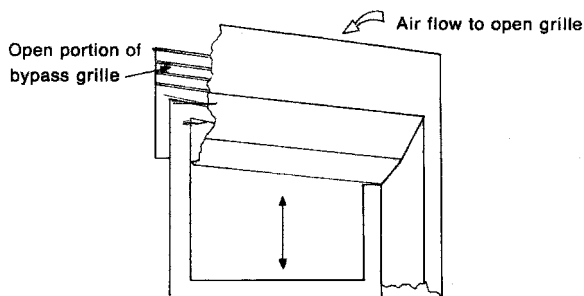


Figure 7.6 A simple bypass or bleeder hood ensures that a critical face velocity limit of 300 fpm (1.52 m/s) is not exceeded when the sash is down. As the sash is lowered, there is an increase in face velocity until the upper edge of the sash uncovers the bypass grille, permitting air to enter the hood. The face velocity then remains relatively constant until the bottom sash stop is reached. Manufacturers have various designs to provide this bypass feature. In all cases the bypass grille should provide line-of-sight protection against debris generated by explosions in the hood.

sensitive balances, filter aids, and certain chemical operations. A screen must be placed over the slots to prevent materials from being swept from the work surfaces to the duct. To resolve this problem the bypass hood (Fig. 7.6) was introduced in the 1950s. In this design when the sash is in its upper position it covers the bypass opening and the total exhaust passes through the face opening at the design velocity. As the sash is pulled down, at the point the sash is approximately one-third closed the bypass grille is uncovered and a fraction of the exhaust is pulled through the bypass with the fraction increasing as the sash approaches a closed position. This design ensures the face velocity does not significantly increase and the total exhaust volume of the bypass hood remains constant at all sash positions thereby simplifying the design of the laboratory supply system. The design of the bypass grille and its housing are important to ensure that when the sash is closed a minimum airflow must still be established through the hood to meet fire protection standards, usually 50 cfm per foot of hood width ($0.08 \text{ m}^3/\text{s}$ per m of hood width) or 20% of the wide open sash airflow, whichever is greater (NFPA, 2000).

Modifying the entry to improve the airflow pattern at the hood face completed the evolution of the contemporary hood. Studies by Schulte et al. (1954) at the Los Alamos Scientific Laboratory revealed that the square vertical posts and front edge of the work surface of the standard hood generated a slight vena contracta at the hood face. The resulting turbulent eddies caused flow reversal and impaired the capture efficiency of the hood. To minimize this problem, the corner posts were “softened” by an airfoil section, as shown in Fig. 7.7. Although this change had a negligible effect on the coefficient of entry, it did reduce contaminant loss by boundary eddies. The turbulent losses at the front edge of the work surface or sill were reduced with a displaced airfoil section (Fig. 7.7). A well-designed hood with all of these design features is shown in Fig. 7.8. European investigators have shown that the sash handles may also have a major effect on contaminant loss (Saunders et al., 1994), and hood designers are now adding a sash airfoil to improve performance.



Figure 7.7 The turbulent eddies at the hood corner posts can be minimized by modifying the hood inlet geometry. An ideal corner post would have the form of a bell mouth. In practice this is frequently approximated with a simple angled detail, which is inexpensive to fabricate and install, but effectively minimizes the entrance eddies and improves contaminant control at the entrance to the hood. Although the same simple geometry used on the corner posts could be used to improve the entrance geometry at the front lip of the work surface, a more effective approach is the displaced airfoil. This element breaks turbulent eddies, provides a well-defined airflow path to sweep the hood work surface when the sash is down, and may be used to define the minimum working distance from the face of the hood. The space between the work surface and the airfoil should be large enough so that the operator can pass through tubing and electrical cables.

7.1.2 Horizontal Sliding Sash Hoods

In the basic laboratory hood described above, the chemist can choose a convenient workspace at the hood face by adjusting the vertical position of the sliding sash. This goal can also be achieved by horizontal sliding panels positioned on tracks at the hood face (Fig. 7.9). Although available for several decades, horizontal sliding sash hoods have only recently (as of the 1990s) gained popularity since they provide an effective means of minimizing face area, with a resulting reduction in airflow and operating cost. In addition to minimizing face area, an advantage claimed for the horizontal sliding sash hood is the availability of the panel as a shield to protect against splashes and small explosions. Detractors of horizontal sliding sash hoods claim that the chemist frequently rejects this design since it requires different work practices than those associated with the traditional vertical sash hood. If not accepted, the sash may be removed by laboratory personnel, resulting in an unsafe hood. A combined vertical/horizontal sash hood can resolve this issue.

The experience of a large university, well experienced in the installation and operation of over 1200 chemical laboratory hoods, is a success story in how one can



Figure 7.8 A modified constant volume/by-pass vertical sliding sash hood that incorporates the various design features, including airfoil elements, bypass feature, and multiple rear slots. (Courtesy of Fisher Hamilton LLC.)

achieve acceptance of horizontal hoods by a group of research chemists. Changes in the occupancy density of a new research building resulted in an unplanned increase in the number of hoods, which taxed the existing exhaust and supply system capacity. It was decided to install 150 combined vertical–horizontal hoods, which, because of their low exhaust requirements, could be serviced by the existing capacity. Prior to the final design decisions and installation, three test hoods were installed. The chemists were encouraged to use these hoods and comment on the design. The “test drive” was favorable, and the 150 hoods were installed with excellent results. The engineers feel that the availability of the three test hoods was critical in the acceptance of the horizontal sash hoods.

4 horizontal sliding sash
2 tracks



Sash placement options

No. 1



No. 2



No. 3



(a)



Figure 7.9 Horizontal sliding sash laboratory hood (a) sash placement options on an 8-ft (2.5m) hood, which can reduce the required airflow by 50% and (b) a modern horizontal moving sash hood with bypass detail. (Courtesy of Fisher Hamilton Industries LLC.)

A vertical sash hood has one sharp edge, the bottom of the sash, which will cause a rolling eddy in the back of the sash. In the horizontal sliding sash hood, air may pass two or more vertical sharp-edged entrance elements. In the vertical sliding sash hood the edge turbulence may occur with the sash up, away from the point of contaminant generation, and the effect of the eddy may be minimized. In the horizontal sliding sash system the vertical turbulence is generated along the full height of the sash and, therefore, through the zone where the contaminant is generated. This may result in significant loss of contaminant from the hood. The eddies formed at the edges of both vertical and horizontal sashes can be minimized by an airfoil element similar to that shown in Fig. 7.7.

The horizontal sliding sash designs vary; the principal differences is the width and number of panels and the number of tracks. A minimum panel width of 18 in. (0.46 m) is recommended to minimize this edge effect. However, ANSI (2003) states if a panel is to be used as a safety shield it shall not be more than 14 in. (0.36 m) wide. In all cases an airfoil should be mounted on the sill.

7.1.3 Auxiliary Air Supply Hoods

The auxiliary air supply hood, also known as a supply air or compensating hood, is designed to minimize the quantity of conditioned replacement air to be supplied to the laboratory space during the cooling season. The principal application of this hood is in laboratories with severe air demand that cannot be met by the existing system or in locations where there is an extreme summer conditioning load. The system, shown in Fig. 7.10, may be purchased as a complete hood system or as a canopy system for retrofitting conventional hoods. It is designed for application on a vertical sliding sash hood, although it can be used on a horizontal sliding sash system. When used with a horizontal sliding sash hood, it does not realize its full energy conservation potential and may cause additional turbulence around the hood face. In this design, rather than taking 100% of the total hood exhaust from the room, a minimum of 35–40% is removed from the laboratory space, and up to 60–65% of the exhaust is outside air delivered directly to the face of the hood through a canopy. The economy is realized in the summer season since unconditioned outside air or partially conditioned air may be used for the major portion of the exhaust. In the winter this fraction must be heated to room temperature to eliminate operator complaints and to minimize condensation problems in the hood.

If convenient, the canopy supply can be secondary air, that is, air that has been conditioned and must normally be exhausted for general ventilation needs. In any case the supply must be delivered to the outside face of the hood through a well-designed canopy. Typically, the canopy is provided with an egg crate grille to more closely approach laminar flow across the hood face. Designs that provide air directly to the hood cavity should not be considered since they are disruptive, pressurize the hood, and will cause loss of contaminant to the room.

A well-designed auxiliary-air-supplied hood reduces air-conditioning costs and improves hood capture efficiency (Chamberlin and Leahy, 1978; ANSI, 2003). The disadvantages of this hood include higher initial cost and maintenance due to the additional



Figure 7.10 A well-designed auxiliary air supply hood with a bypass detail. The outside air is introduced through a canopy designed to provide a laminar flow pattern that blankets the hood face and blends with room air as it enters the hood. The hood is designed to provide air at room temperature during the heating season; unconditioned air is supplied during cooling periods, thereby saving air-conditioning costs for the air supplied through the canopy. An additional advantage is less well known. When a person stands in front of a laboratory hood, a slight negative pressure is created between his or her body and the hood, causing turbulence and loss of contaminant from the hood. The auxiliary air supply fills this space, eliminates turbulence, and improves containment efficiency. (Courtesy of Fisher Hamilton Industries LLC.)

replacement air system, the possible introduction of airborne dust into the laboratory, discomfort to operators during winter conditions unless the air is tempered, disturbance of the exhaust velocity profile at the hood face with poor canopy designs, condensation in the hood in high humidity environments, and the possible hazard that exists in a poorly designed system if the exhaust fan fails and the auxiliary air fan continues to operate. Although these objections can be resolved through appropriate system design, they do demonstrate the complexity of the auxiliary air supply system. One facility requirement that frequently cannot be met is the overhead space required for the air supply duct and the auxiliary air plenum.

7.2 FACE VELOCITY FOR LABORATORY HOODS

A discussion of face velocity for a laboratory hood may seem unnecessary since extensive advice is available on face velocity of industrial hoods. However, experience has shown special attention must be given to face velocity criteria for laboratory hoods due to their unique application, the range of toxic chemicals handled, and the siting of the hood in the laboratory.

By definition, the laboratory hood is an enclosure with an adjustable front-access panel. Face velocity is a critical design element for a laboratory hood. Capture velocity, the velocity established outside the physical boundary of a hood to capture the contaminated air, is often incorrectly used to identify face velocity. "Face area" denotes the working opening at which the design face velocity shall be achieved. Other terms, such as "sash opening" or "door area," are used interchangeably with face area. The design airflow is based on the average face velocity and the hood design face area with the vertical or sliding sash configuration. If the sash is constrained to a restricted position by mechanical means that cannot be bypassed without an alarm being activated, that restricted face area may be used in defining the minimum airflow. As noted earlier in this chapter, the hood airflow must meet the minimum fire protection standards when the sash is closed. If the hood is the only source of general ventilation in the laboratory that minimum airflow must be also be provided with the sash closed (NFPA, 2000).

The standard opening height for a bench-mounted, vertical sliding sash hood is 30 in. (0.76 m), although a range of 26–36 in. (0.66–0.91 m) may be encountered. Individual laboratories interested in minimizing energy costs have found that an opening height as low as 20 in. (0.51 m) may be acceptable for normal laboratory work. In this configuration, the full standard opening height of 30 in. (0.76 m) is available during equipment setup; the reduced height is used during the chemical procedure.

A major investigation of laboratory hood face velocity was completed by Schulte et al. (1954). Hughes (1980) summarized 20 literature citations for the period 1950–1980 and subsequent studies on face velocity are reviewed in Goodfellow and Tahti (2001). These three reviews show that recommendations for face velocity for chemical laboratory hoods may be proposed in three specific forms. The first approach provides a rational format to calculate the face velocity for a specific chemical used in a given laboratory environment (Peterson, 1959). This calculation requires the user to consider a range of critical variables influencing the containment of the contaminant by the hood. In the second approach graded classes or quality of hoods are established and a minimum face velocity is specified for each class. The classifications may be based (1) on the application realm with some inferred level of risk (Coleman, 1951); (2) solely on the toxicity of the chemicals handled in the hood (Brief et al., 1963); or (3) on a classification scheme that includes consideration of the toxicity of the chemical and the laboratory geometry. The third approach utilizes a single recommended face velocity for all hoods in the belief that the minimum face velocity necessary to overcome background air movement in the laboratory will control any chemical air contaminant in a well- designed hood (Schulte et al., 1954).

Although the response to these approaches introduced over several decades has varied, general trends have emerged. The comprehensive chemical-by-chemical procedure provides extensive insight into hood performance design criteria; however, it has not been widely accepted, probably because of its complexity. Many laboratories have used the broad classification schemes, but critics of this approach state that it is difficult to anticipate the chemicals and procedures to be used in laboratory hoods even on a short-term basis. This procedure also limits hood use to selected chemicals, thus complicating laboratory operation and supervision. By far the most common procedure for setting minimum face velocities is the third approach, the use of a single face velocity that will permit application of the hood for a range of chemical activities and laboratory environments.

The recommended face velocities from these approaches have ranged widely. The minimum velocity needed to overcome diffusion of gases and vapors from the hood is 20 fpm (0.10 m/s) (Ettinger et al., 1968). During the 1950s, when the classification schemes were popular, a wide range of velocities from 50 to 150 fpm (from 0.26 to 0.76 m/s) was widely cited. A velocity of 100 fpm (0.51 m/s) emerged during the 1960s under the single-value approach and was widely supported until 1980. It can be shown that 100 fpm (0.51 m/s) provides control for most chemicals handled in industrial laboratories using the rational design procedure proposed by Peterson (1959). This velocity also has been demonstrated to overcome the disruptive air movement generated by a chemist working at a hood (Schulte et al., 1954). For these reasons 100 fpm (0.51 m/s) is still thought to constitute a good general design value.

The energy constraints instituted in the mid-1970s provided an impetus to investigate methods to minimize hood operating cost by lowering the total quantity of exhaust air. One obvious approach is to reduce face velocity and as a result the widely accepted design face velocity of 100 fpm (0.51 m/s) has been under attack. Investigators have demonstrated that face velocities as low as 60 fpm (0.30 m/s) are adequate for containment if an aerodynamic hood is used in a nearly ideal setting and the operator follows rigorous work practices. Critics of this approach agree that reasonable control may be achieved under ideal conditions with such low face velocities, but contend that it is difficult to provide such operating conditions in a "real world" laboratory.

This philosophy is clearly reflected in the design guidelines for new laboratories presented in the 24th edition of the *Ventilation Manual* (VS 35-01), which recommends a face velocity of 80–100 fpm (0.41–0.51 m/s) based on the air supply flow path and the uniformity of the hood face velocity. The lower face velocity reflects an optimum environment. The working distance behind the sash must be kept to a maximum and replacement air must be introduced through perforated ceiling panels or by grilles or diffusers that result in a the "throw" velocity at the hood face of less than 30–50 fpm (0.02–0.26 m/s). Furthermore, air movement from doors, windows, and traffic must be minimized, as should the amount of apparatus in the hood.

Although there continues to be disagreement on the minimum face velocity needed for laboratory hoods, most investigators agree that increasing the face velocity above 120 fpm (0.61 m/s) will not improve capture efficiency, and at velocities above 150 fpm

(0.76 m/s) hood performance may actually be diminished as a result of turbulence at the hood face. The anticipated operating characteristics at face velocities from 60 to greater than 150 fpm (0.31–0.76 m/s) are described in ANSI (2003).

For effective containment there must be a uniform velocity across an aerodynamically designed laboratory hood face. Acceptable variations in face velocity for actual conditions in a working laboratory with the sash in maximum open position are cited as being equal to or less than 10% (ACGIH, 2001) or below 90% or above 120% of the acceptable face velocity (ANSI, 2003).

Although face velocity is an important predictor of performance, it is not the only one. Other factors to be discussed later in this chapter that may have a major impact on containment include hood design, facility layout, cross-drafts, air distribution, and pedestrian traffic. This assertion is echoed by participants in the 1998 Howard Hughes Medical Institute Workshop, who state “face velocity alone is not a good predictor of containment” (DiBerardinis et al., 2003).

7.3 SPECIAL LABORATORY HOODS

The laboratory hoods described above are valuable general-purpose control devices in the modern chemical laboratory. This hood provides a physical barrier to contain spills, splashes, and mild overpressure accidents and a modest face velocity will contain air contaminants released from chemical operations. Although it has these impressive features, the laboratory hood should not be considered the only ventilation control available in chemistry laboratories. Standard procedures such as evaporation, distillation, and digestion are routinely conducted in laboratories, and a range of local exhaust hoods are available for these operations. A selection of these special-purpose hoods, which have the advantages of low initial cost, low airflow, and excellent capture efficiency, are described below.

Specimen digestion using strong oxidizers such as perchloric acid is frequently encountered in settings ranging from biological to metallurgical laboratories. This procedure requires excellent containment and air cleaning to ensure that violent reactions do not occur. Organic materials cannot be used in the hood or duct construction, and spray nozzles must be installed to wash down the ductwork hood, and fan to prevent the buildup of unstable perchlorates (*Ventilation Manual*, VS-35-03). A hood used for perchloric acid digestion must be committed to this activity exclusively. Silverman and First (1962) designed a scrubber for perchloric acid digestion that is placed directly in a standard laboratory hood. After cleaning, the scrubber exhaust stream is discharged to the laboratory hood exhaust stream. An integral scrubber effective against perchloric acid has also been described by Renton and Duffield (1986).

A routine procedure in chemical laboratories is paper chromatography. In this process a paper sheet onto which the liquid sample has been placed is placed in a large jar in a solvent-saturated environment for the development of the chromatograph. The changing of samples results in release of the solvent vapors to the air. Again, this work could be done in a conventional laboratory hood, but it can be

controlled more efficiently by utilizing a portable exterior hood placed directly behind the jar during transfers (Brief et al., 1963). This design provides excellent control using modest airflows of 250–300 cfm (0.12–0.14 m³/s). The savings in installation and operating cost utilizing this special hood over the conventional laboratory hood are impressive.

A common procedure in material control laboratories is the evaporation of a large number of samples. Rather than conducting this procedure in a chemical laboratory hood, it can be controlled more efficiently by spot local exhaust as described in the *Industrial Ventilation* (VS-35-40). A more difficult chemical laboratory procedure to control is distillation or reaction equipment mounted on a large rack with the potential for release of air contaminants at multiple locations. A “walk-in hood” can be provided for control, but the penalty of limited accessibility and large exhaust volumes must be accepted. An alternative approach is to mount the equipment in the open and provide one or more flexible “drops” that can be positioned at critical release points. Normally a 3-in. (7.62-cm)-diameter flexible duct with an exhaust volume of 200 cfm (0.09 m³/s) is adequate to control all except major accidental releases. Finally, for maximum control of contaminants a totally enclosed hood is now available for this application.

7.4 LABORATORY EXHAUST SYSTEM FEATURES

7.4.1 System Configuration

Whether to use a separate fan for each hood or to manifold a number of hoods together to be served by a single fan in a balanced system is one of the first major decisions to be made in the design of a laboratory ventilation system. Each installation must be considered separately. A third option is the use of individual fans on hoods with discharge to a collection plenum serviced by a high-volume booster dilution fan.

Single-Hood System. The “one-hood/one-fan” system might at first glance seem desirable. This approach provides ultimate flexibility for the individual operator and the manager of the laboratory. The chemist can control a total system deciding when to turn it on or off. Furthermore, the individual hood is available for use during off-shift periods. If a classification scheme has been used to choose the hood face velocity, the hood can be upgraded to a higher classification by changing fan speed or installing a new fan to achieve a higher face velocity. If air cleaning is necessary on the total hood exhaust stream, the additional resistance to airflow presented by the air cleaner may be handled by a change in sheave size or air mover. If a need arises for a new specialty hood such as a perchloric acid digestion hood, a one-hood system can be modified and committed to this service without compromising other hood applications. The design of such systems is simple and a modular design can be used throughout the facility. If maintenance is necessary, the system can be shut down and the activities of only one operator will be disrupted.

The disadvantages of a one-hood/one-fan system include higher initial cost and additional space requirement for multiple ducts and fans. If there are several hoods in one laboratory and one hood is shut down, lack of replacement air may cause backflow to the laboratory through the duct of the inoperative hood into the laboratory. At best, this may cause temperature extremes in the vicinity of the hood; at worst, if the duct terminated at a location where contaminated air is present, it could introduce toxic air contaminants into the laboratory. The installation of backflow dampers to prevent this should be discouraged since these devices will frequently fail in the closed position. Finally, due to the hood usage factor it is difficult to design a suitable supply system for the “one hood-one fan” approach.

Central System. A central system utilizing one fan serving a number of hoods in a balanced ventilation design can be used as long as the air contaminants released from the various hoods are compatible. There are anecdotal stories of serious fire, explosion, or health hazards resulting from the mixing of two chemistry laboratory hood exhaust streams; however, the authors are not personally aware of such incidents. This favorable history is probably due to the low concentrations of contaminants commonly present in hood exhaust streams. There are other more serious disadvantages to a central system. If the fan serving multiple hoods fails, all hoods served by the system are out of commission and backflow may occur from one laboratory to another. The initial cost of a central system may be lower than that of a family of single-hood systems, although balanced design of such a system takes more engineering skill and committed maintenance. Since all hoods in a central system operate continuously, the replacement-air system can be a fixed-flow design to respond to the total system needs.

Collection and Dilution Systems. A hybrid system that has gained some favor in Europe because of its potential to provide high dilution rates and excellent dispersal of stack effluent from a single point source, is the collection and dilution system (BOHS, 1992). In this system the individual fans servicing a hood do not discharge directly to air but rather to a large plenum or manifold that is serviced by a high-flow, low static fan. The single, tall stack with high-velocity discharge enhances the dispersal of contaminants as compared to multiple individual hood exhausts. The authors have no experience with this system and hesitate to recommend it.

7.4.2 Construction

If the single-unit (one hood—one fan) design approach is chosen, the hoods should not be purchased with an integral fan mounted at the hood since this configuration places the duct run under positive pressure and leakage of contaminated air into occupied spaces may occur. Additionally, integral fans provided with laboratory hoods are usually low-static, direct-drive fans and cannot handle the resistance to airflow presented by long duct runs.

In any system the fan should be positioned so that the duct run inside the building is under negative pressure. This normally means a roof-mounted fan for a multistory

building or a roof or ground-level fan for a single story building. If a short portion of the duct run inside a building must be under positive pressure, the duct should have welded seams, flanged joints with gaskets, or joints sealed with an impervious material.

Fans for large laboratories using the single-hood systems are frequently placed in a roof penthouse dedicated to mechanical services. Such placement keeps the fans out of the weather and encourages maintenance. However, this practice may present a risk to maintenance personnel in case of duct failure downstream of the fan within this penthouse. The penthouse should be provided with dilution ventilation, and all joints on duct runs under positive pressure inside the penthouse should be sealed.

A range of construction materials has been introduced to perform under specific environments. Although stainless steel is a common hood sheathing material, one now notes mild steel panels coated with polyvinyl chloride, polyethylene or powder coating paints. Solid plastic construction materials are rigid polyvinyl chloride, polypropylene, and composites based on amino and epoxide resins. Powder coating with epoxy paints is also popular. The application of asbestos-based material has disappeared, although one may encounter exposures during renovation and removal of old hoods. Materials of construction for laboratory systems are discussed in detail elsewhere (DiBerardinis et al., 2001).

The initial duct run from the hood should be designed with an elbow close to the hood to prevent material from falling back into the hood. If the hood is to handle condensable vapor, the first few lengths of duct should be pitched to a drainage point and the drain trapped. All longitudinal seams on the horizontal duct runs should be positioned on the top of the duct.

The duct should normally be sized for a velocity of 1000–2000 fpm (5.08–10.16 m/s). If high particle loadings are encountered in laboratory systems, higher duct transport velocities are required. Space constraints in service chases may also require small duct sizes with corresponding high duct velocities.

The choice of fan will depend on the type of system in use. Axial flow fans, because of their low cost, straight-through geometry, and ease of installation, frequently serve single-hood systems. This choice precludes the many advantages of a centrifugal fan, including the flexibility of fan speed change. Large systems serving multiple hoods are normally equipped with centrifugal blowers because of their ruggedness and high performance. Fan impellers can be fabricated of polyvinyl chloride, fiberglass-reinforced polyester, or steel with an impervious plastic coating. If flammable gases or vapors or explosive dusts are encountered, an aluminum, bronze, or fiberglass-reinforced polyester impeller may be required. Occasionally, a serious corrosion problem exists that cannot be handled by fan construction materials. In this case an ejector may be the air mover of choice.

Reentry of odorous or toxic air contaminants from exhaust stacks is a chronic problem in many industrial and academic chemical laboratories. The design data provided in Chapter 15 (Section 15.5) will help minimize this problem, but ultimately only appropriate air and gas cleaning can eliminate it. The conventional industrial approach to air cleaning is to direct the entire hood exhaust stream through the air cleaner. This approach is not effective for the general-purpose laboratory hood since the exhaust

stream has very low concentrations of contaminants in a relatively large airflow. Such systems are not amenable to air cleaning. The most successful approach to this problem is to direct the low-volume release from the reaction underway in the hood to an air-cleaning unit in the hood before it is released to the main hood exhaust. Most general chemistry laboratories handle 0.10–1 molar quantities. The contaminant release rates, presuming a 20-min reaction time, are therefore in the range 0.1–1.0 lpm. Acidic and alkaline air contaminants can be scrubbed in simple packed columns, and other streams can be treated as described in Chapter 11.

The air-cleaning technology evolved since the early 1950s in the respiratory protection field may also be applied to such small streams. A range of adsorbents and absorbents available as cartridges, chin canisters, and chest canisters may be effective against certain off-gas streams. Unfortunately it is difficult to convince the chemist that air cleaning or “scrubbing” of the contaminant stream before it is released to the hood exhaust is worthwhile. The recent interest in “green chemistry” by the chemical research and teaching community may support this approach in the future.

7.5 FACTORS INFLUENCING HOOD PERFORMANCE

A number of factors that influence the field performance of the laboratory hood must receive the attention of the design engineer. One set of factors relates to the physical location of the hood and other elements in the laboratory, which may disrupt airflow at the hood face. In addition, the performance of the hood depends on its proper use by the chemist. Although the latter issue is beyond the responsibility of the engineer, the impact of the chemist’s work practices on hood performance must be considered.

7.5.1 Layout of Laboratory

Doorways. A pedestrian door positioned close to the face of a laboratory hood may seriously impair hood performance. A door opened in a normal fashion acts as an air mover. If swung open in a 90° arc in 2 s, a door 30 in. (0.76 m) × 80 in. (2.03 m) has an edge speed of approximately 200 fpm (1.02 m/s) and displaces room air at a rate of 1200 cfm (0.57 m³/s). This effective pumping rate is approximately equal to the airflow through a 5-ft hood with a sash height of 30 in. (0.76 m) operating with a face velocity of 100 fpm (0.51 m/s). Saunders (1994) states that the air velocity induced by a door opening adjacent to a hood face ranges from 175 to 450 fpm (from 0.90 to 2.29 m/s).

Positioned near a hood, such a door can therefore temporarily induce an airflow across the hood face equivalent to the hood exhaust, disrupting the airflow pattern and sweeping contaminant from the hood. It is therefore important that hoods be positioned some distance from laboratory access doors. If it is absolutely necessary that a door be positioned near a hood, using a door governor to ensure a low opening and closing speed can minimize its disruptive effects. Another solution is to restrict access to the laboratory through the critical door. Door placement is also important in ensuring a safe means of egress. Since a hood may be the site of a

fire, explosion, or toxic chemical spill, it is obvious that the egress route should not be past the hood.

Pedestrian Traffic. Walking past a hood can affect its performance, and this should be reflected in the laboratory layout. Walking while wearing a buttoned lab coat sweeps out a cross-sectional area of approximately 10–20 ft². At a slow walking speed of 2.3 mph (mi/h) or 200 fpm (1.02 m/s), 2000–4000 cfm (0.95–1.89 m³/s) is displaced. This is equivalent to the exhaust of an 8-ft-long laboratory hood with a 30-in. (0.76-m) sash opening operating at a 100 fpm (0.51 m/s) face velocity. If a person walks in front of a laboratory hood, this induced air movement of 260–450 fpm (1.34–2.29 m/s) (Saunders, 1994) can result in escape of contaminant from the hood. To minimize this problem, a free zone should be established 1 m from the hood face, which should be entered only by the chemist (BSI, 1994).

Windows. Most laboratories are air-conditioned, and windows, if available, will have permanently closed sashes. However, if it is possible to open a window in a laboratory, an outdoor wind gust of as little as 3–5 mph [300–450 fpm (1.52–2.29 m/s)] across the hood face can be quite disruptive resulting in contaminant loss from the hood.

Equipment. The optimum performance of a laboratory hood occurs when the movement of air in front of the hood approaches laminar flow in a direction perpendicular to that of the hood face. Placement of laboratory benches, hoods, and partitions can interfere with this airflow. To minimize this interference, it is wise to adopt the minimum clearances shown in Table 7.1 (BSI, 1994)

Another important feature of the laboratory, which affects hood performance, is the introduction of replacement air. The basics of replacement-air systems described in Chapter 12 applies to laboratory settings; however, because of the tight layout of hoods and the variability in hood use, the difficulty in achieving adequate air supply without interference of hood performance due to drafts at the hood face is extremely difficult. In many cases conventional grilles and diffusers cannot be positioned without resulting

Table 7.1 Minimizing Airflow Disturbances at Hood Face

Critical Architectural Feature	Minimum Distribution of Feature from Hood Face	
	Feet	Meters
Common pedestrian walkway	3.3	1.0
Opposite bench used by chemist	4.9	1.5
Opposite hood used by chemist	9.8	3.0
Opposing wall	6.6	2.0
Adjoining wall	1.0	0.3
Doorway	3.3/4.9	1.0/1.5

Source: Adapted from BSI (1994).

in severe drafts; the only solutions are perforated walls or ceiling supply panels. Rarely can one achieve in an operating laboratory the low velocity flow path from supply to hood face achieved in the manufacturer's test room. Equally difficult is the provision of pressure differentials between laboratory spaces and ancillary offices that are frequently required to be satisfied by the exhaust/supply system.

A basic rule is to introduce the air at the maximum possible distance from the hood and permit it to sweep through the laboratory to achieve maximum effective general ventilation. Another good rule is to maintain the discharge velocity from air supply grilles below 400 fpm (2.03 m/s), and ensure that the velocity caused by the grille or diffuser does not exceed 30–50 fpm (0.15–0.26 m/s) at the hood face. As noted above, if the laboratory is small, replacement air can be introduced through a perforated ceiling plenum at velocities of 70–100 fpm (0.36–0.51 m/s). Such a system ensures excellent mixing in the laboratory space and will minimize disruptive effects at the hood face. If introduced just in front of the hood, it will provide some of the advantages of the auxiliary air supply hood.

7.5.2 Work Practices

Even if the basic hood design is excellent and is placed in a “sheltered” location in the laboratory, it may still “spill” contaminants unless properly used. Although the engineer will not have primary responsibility for proper hood use, the impact of poor work practices on hood performance should be understood. One common poor work practice is the use of the hood as a chemical storage cabinet (Fig. 7.11). Typically, a large number of chemical bottles are placed deep in the hood against the lower exhaust slot. Blocking this slot causes the airflow balance between the lower and upper slots to be disrupted and hood performance to suffer. Separate storage cabinets should be provided to eliminate storage in the laboratory hood. A flammable liquid storage cabinet requires an exhaust flow of only 50 cfm (0.02 m³/s). Storage can also be provided in an exhausted base cabinet under the hood. A hood shelf can be installed above the bottom slot if it is absolutely necessary to keep large numbers of bottles in the hood however, shelves should not be constructed inside of the hood on side panel.

Another disruptive work practice is the storage of miscellaneous boxes of supplies or equipment in the hood. If a large piece of equipment such as an oven, blender, or hotplate must be in the hood, it should be positioned to minimize disruption of the hood velocity profile. The equipment should be placed deep in the hood on legs or blocks to raise it 1–2 in. (25–50 mm) so that the bottom slot of the hood will not be blocked (BSI, 1994). The equipment should also be positioned so that the minimum cross-sectional area is normal to the direction of airflow.

Depth of the working area is an important hood performance variable. For example, in industrial ventilation systems the larger the paint spray booth or the deeper the work location in the hood, the lower the required face velocity. These same guidelines apply to laboratory hoods. If work is done directly at the face, a contaminant may escape the hood and not be recaptured. If the maneuver is repeated deep in the hood, the ability to contain the contaminant in the hood is improved. It may therefore be possible to reduce face velocity in a chemical laboratory hood if a deep working depth

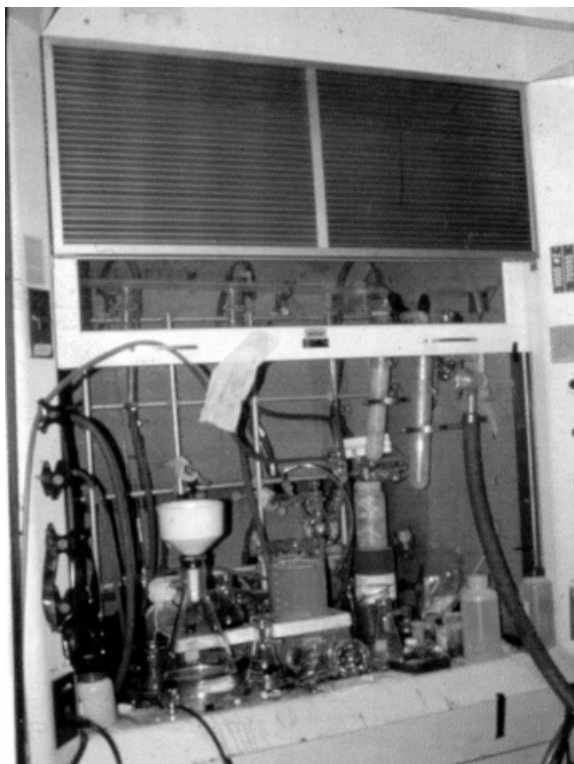


Figure 7.11 An example of a cluttered hood that will impair hood performance.

is acceptable. However, the chemist should be warned not to lean into the hood, or the advantages of a deep hood will be negated. The proper working depth can be designated by identifying the desired position on the laboratory hood work surface with tape, placing a physical lip on the work surface, or using an airfoil section that extends into the hood and thus physically defines the minimum working depth. Work practices have an important impact on the ability of the hood to contain the contaminant as noted in comprehensive standards (BOHS, 1992). This Standard recommends that (1) all equipment be set up in the hood chamber before active work is started and (2) the equipment be placed a minimum of 6 in. (150 mm) back from the sash and no closer than 2 in. (50 mm) from the back slot.) These practices result in a restrictive work area and are frequently disregarded by the chemist.

The convective head produced by a heat-generating apparatus placed in the hood can overwhelm the exhaust system and impair hood performance. Schulte et al. (1954) found that three 1200-W electric hotplates operating in a hood were acceptable, but that four Bunsen burners operating in a 4-ft hood resulted in air temperatures in the upper part of the hood 38°C above room temperature. The resulting convective velocities were disruptive to effective contaminant collection and containment, and a tracer smoke released in the hood during this temperature excursion escaped to the room

through openings in the bypass mechanism. Although several investigators have noted this effect since that time, the most comprehensive study is by Johnston et al. (2000). This study used three types of laboratory burners to establish a range of thermal loads. A standard containment test (ASHRAE, 1995) using a sulfur hexafluoride tracer was used to assess the impact of the thermal load on hood performance. Each increase in the thermal load of 10,000 Btu/h (British thermal units per hour; 2931 W) over a test range of 69,342 Btu/h (20,324 W) resulted in an increase of 4 ppm in the air concentration of the tracer at the breathing zone of the test manikin. The three test burners used to develop the heat load and their maximum capacities were an economy burner at 5000 Btu/h (1465 W), a Meeker burner at 10,000 Btu/h (2931 W), and a blast burner at 40,000 Btu/h (11,724 W). The authors state that similar quantitative studies are needed on hotplates, ovens, water baths, and other heat-producing laboratory devices in order to establish operating parameters for safe hood usage.

Brief et al. (1963) states that the application of electric heaters should be restricted to 100 W/ft of hood length to minimize this thermal effect. If there is a high heat load in the hood, the top slot should be adjusted to draw a greater share of the airflow.

As noted earlier, the chemist should place all equipment and supplies in the hood before starting a procedure, since manipulation during the chemical procedure may result in contaminant escape. It is also good practice to close the sash as far as possible, thereby approaching a complete enclosure and minimizing loss of contaminant. Greenley et al. (2000) state that "in training chemists on proper work practices lowering the sash should be stressed as being the major factor in reducing hood leakage." When closed, the sash is also a barrier that can offer protection from spray, splashes, and minor explosions.

7.6 ENERGY CONSERVATION

The rapidly escalating energy cost has called attention to the cost of laboratory ventilation. A standard 5-ft hood installed in an air-conditioned laboratory in the Boston area and operating continuously (8760/h per year) at a face velocity of 100 fpm (0.51 m/s) costs approximately \$4500 per year to operate at 2002 energy prices. If an industrial or academic laboratory complex has 100 such hoods, the annual operating cost to run the fans and heat and cool the replacement air is \$450,000. The four approaches to minimizing this cost are to reduce the operating time, limit the air quantity being exhausted from each hood, recover heat from exhaust air, and recirculate the conditioned air back to the laboratory after appropriate air cleaning.

7.6.1 Reduce Operating Time

There are several reasons for operating laboratory hoods 24 h a day, 7 days a week in research and educational facilities:

- Personnel might work in the laboratories any time of the day or night, on weekends, or on holidays.

- Hazardous chemicals are frequently stored inside the hood overnight when the hood is not being used.
- Some untended reactions are left ongoing in the hood for extended periods.
- The exhaust hood frequently provides the minimum general ventilation for the space and establishes the required pressure difference between spaces.

Even given these reasons, a number of major laboratories have found that hoods can be shut off at least 50% of the time with significant savings. Since the hoods are not operated continuously, alternative ventilated storage space must be provided for selected chemicals. The storage space may be a flammable-liquid storage cabinet meeting National Fire Protection Association requirements. Nonflammable hazardous liquids can be placed in a separately exhausted storage cabinet, an exhausted storage area under the laboratory hood, or in a specially designed chemical storage box (DiBerardinis et al., 2001).

It is important to note that in reducing the hood operating time, the air balance within the laboratory and the building may be compromised. Buildings frequently have one supply system for a group of laboratories. It is difficult to maintain laboratories at negative pressure with respect to corridors when the exhaust rate varies as a result of changes in hood utilization. Variable-air-volume supply systems that match the quantity of air exhausted can be used to handle this replacement-air problem (DiBerardinis et al., 2001).

7.6.2 Limit Airflow

By design, the required laboratory hood airflow is based on the presumption that the sash is wide open and that the operator will utilize the hood in this position with the maximum open-face area for critical work some fraction of the time. On a vertical sash hood this face area is usually the width of the hood work surface, multiplied by the height of the hood opening with the sash fully raised. Limiting the vertical sash travel can reduce the maximum opening and thus the airflow. Laboratory fume hood sashes commonly open to a height of 30 in. (0.76 m), but if sash height is limited to 20 in. (0.51 m), a height many chemists find acceptable, the amount of air being exhausted can be reduced by 33% while maintaining the required face velocity.

This restricted opening may present a problem to the chemist while installing equipment, in that it may be difficult to reach the upper part of the hood. This problem can be resolved by equipping the hood with an alarm system. If the sash is raised above 20 in. (0.51 m) for short periods to allow setting up apparatus, an audiovisual alarm is activated to let the hood user know that the hood is not in a safe operating mode. If the sash must be positioned above 20 in. (0.51 m) for long periods, the audible alarm can be temporarily disarmed. The alarm should have a memory so that it will reset if the sash is still raised after some time period. As soon as the sash is lowered below the proper height, the alarm is reset and is available to respond the next time the hood sash is raised above the proper height. If a reaction is not running, the exhaust can be reduced to a minimum rate that will control any chemicals left in the

hood while providing the minimum general exhaust ventilation of the laboratory space through the opening at the sill airfoil detail.

The most aggressive systems approach to energy management is the variable-air-volume (VAV) laboratory hood. In its simplest form the position of the hood sash is sensed and the required exhaust rate is provided to achieve 100 fpm (0.5 m/s) or any other specified design face velocity. The exhaust rate is tracked, and a VAV control box delivers a matching supply of conditioned air to the hood site. This approach can be extended to multiple hoods in a laboratory with the exhaust/supply controls and a system with multiple hoods on a single fan. The advantage of this approach is that balance is achieved and operating costs of the exhaust/supply systems are reduced. However, as noted by DiBerardinis et al. (2001), a major disadvantage is that the system controls require more sophisticated service and maintenance than traditional maintenance operators are normally trained to apply. The reader is referred to DiBerardinis et al. (2001) for a detailed review of the VAV approach.

As described previously, the exhaust airflow can be reduced with a horizontal sliding sash. In the typical case illustrated in Fig. 7.9, a maximum of one-half of the normal opening of the 8-ft hood is available; an energy savings of 50% in operating cost is realized. As mentioned earlier, a potential problem with this approach is the poor acceptance by hood users. To reach every part of the hood, the individual sash elements must be moved horizontally, which may provoke the chemist to remove the sashes, thus creating an unsafe condition. Some method of monitoring is necessary to ensure that horizontal sashes are used correctly.

The use of special local exhaust hoods to reduce airflow has also been discussed previously. The major disadvantage of this approach is that such hoods are restricted to specific tasks and cannot be used for general laboratory purposes. In addition, special local exhaust hoods do not provide the protection of a chemical laboratory hood in terms of containment of spills or protection from small explosions or fires.

Auxiliary air supply hoods draw only 30–50% of the hood exhaust from the laboratory space. A slight economic advantage occurs during the heating season since the outside air entering the hood from the canopy must only be heated to 55°F (12°C), not to the room supply psychrometric state point. However, significant savings in cooling cost may be realized in the summer season since the air delivered directly from the hood canopy must only be cooled within 20°F of room temperature. In the latter case, however, the chemist must accept the discomfort from the warm air envelope in the front of the hood.

The search for a hood design that will permit effective containment at face velocities below 100 fpm with a resulting reduction in hood operating costs has continued since the 1970s. One of the unique approaches to improve containment (Ljundqvist et al., 1989) is the deliberate induction of either a horizontal or vertical vortex in the hood chamber. The vortex entrains the contaminant and the vortex spirals to an exhaust location at the hood edge where the stream is removed from the hood. Although this design is discussed in the European literature, to the author's knowledge no hoods of this design have been installed in the United States.

In the United States a 7-year program has been underway at the Lawrence Berkeley National Laboratory to develop a high-performance hood with a goal to

reduce laboratory hood airflow requirements by 50–70% (LBNL, 2001). At the time of this publication, advanced prototypes have been tested at operating laboratories with positive results. The hood uses a push–pull concept with a series of small fans delivering air to supply plenums at the top and bottom of the hood sash opening. Exhaust ports are positioned up at the back and top of the hood. The designers envision this air curtain separating the chemist from the contaminant released inside the hood. If one assumes that there are 750,000 hoods in the United States, LBNL estimates the operating cost at \$3.2 million. Assuming a 75% market penetration of this hood, the designers estimate that \$1.2 billion could be saved annually.

7.6.3 Design for Diversity

The issue of diversity in laboratory design, not well understood by many, is clearly defined by DiBerardinis et al. (2001):

Diversity refers to designing and operating a system at a lesser capacity than the sum of all the included facilities when running at peak demand. With respect to laboratory chemical hoods, diversity can be thought of as the expected percentage of full flow demand on a manifolded system in active use at any time. A system using 70% of the peak demand is said to operate at 70% usage factor or 70% diversity. A system that is designed with full flow capacity for all hood is designed for 100% diversity.

Applying diversity to the design of laboratory exhaust systems, in our example designing the system for 70% of the peak demand, results in major reductions in both installation and operating cost. The issues one faces in a design based on diversity are covered elsewhere, but it is becoming a popular approach in laboratory energy conservation (ANSI, 2003; DiBerardinis et al., 2001).

7.6.4 Heat Recovery

The major issues in attempting to recover energy from any industrial exhaust airstream are considered in Chapter 12. The heat recovery systems frequently employ a heat exchanger in the exhaust airstreams. The application of this type of system must be based on a building-by-building evaluation. This may not be a particularly useful technique for laboratory spaces since the laboratory exhaust stream may contain corrosive or reactive contaminants, which will damage the heat recovery system.

7.6.5 Ductless Laboratory Hoods

Portable laboratory hoods with an integral enclosure, fan, and a filter/activated-charcoal bed permitting direct return of air to the laboratory workplace were introduced in the 1970s. Manufacturers claim that these hoods provide good contaminant control while conserving operating costs since replacement air is not needed. This concept is attractive to laboratory management since there is a chronic need for additional exhausted workstations in laboratories with space limitations and without adequate replacement

air to handle a conventional hood. In addition, the initial cost of these recirculating laboratory hoods is less than the total cost of a small conventional laboratory hood, including the initial hood cost, hood installation, and the provision of replacement air.

Investigations of the performance of ductless hoods indicate that caution should be exercised before purchasing them for conventional laboratories (ANSI, 2003). A hazard evaluation and analysis is necessary as described in ANSI Z-9.7 (1998) since the hoods are recirculating air from the work site. Such hoods should be considered only for laboratories where the chemicals in use are well defined and for which the manufacturer's sorbent bed is known to be effective.

The most serious objection to the recirculating laboratory hood is that the operator does not know when the sorption bed is depleted. For this reason, these hoods should not be used for toxic air contaminants which do not have adequate warning properties unless a suitable air monitor is installed to monitor breakthrough of the bed. One manufacturer provides a system that releases an offensive odorant when the bed is depleted and breakthrough occurs. Other manufacturers provide a back-up filter with a space between it and the main filter. This design permits routine testing of breakthrough of the main filter bed.

As discussed, there are several alternatives that apply to energy conservation in the use of laboratory hoods. In most cases a combination of the alternatives described above may be required, particularly in new buildings. In the renovation of older buildings, it may be difficult to apply these methods, and each situation will have to be evaluated on a case-by-case basis. In any energy conservation approach a primary concern is the effect of each alternative on laboratory safety. In addition, the effect on HVAC systems of the building must be evaluated. Also, any restrictions placed on the use of the hood must be acceptable to the laboratory personnel. The last caution requires a detailed education and training program for laboratory personnel. This program should include information on how laboratory chemical fume hoods operate; what restrictions, if any, are being placed on their use; and how this may affect work in the area.

7.7 PERFORMANCE OF LABORATORY HOODS

Quantitative measurement of hood containment is now practiced using a variety of gaseous tracers (ASHRAE, 1995; BSI, 1994). The tracer is released at multiple points or from a single diffuser positioned inside the hood. The tracer escaping from the laboratory hood is collected at the front face of the hood using a multiple point sampling grid or a probe mounted in a manikin head. The challenge gas in the ASHRAE Standard 110 test is sulfur hexafluoride, and the concentration of the tracer in the outside hood sample is measured with an electron capture detector. The protocol in this standard is suitable for testing the containment of a hood in (1) an ideal test room without drafts or cross-currents, (2) an empty laboratory space with an operating HVAC system, and (3) in an actual working laboratory setting. Other test protocols have been proposed for use in field surveys in working laboratories to evaluate hoods in normal use (DiBerardinis et al., 1991).

In a workshop on laboratory hoods held in 1998 and sponsored by the Howard Hughes Medical Institute, 24 experts on laboratory chemical hoods reviewed the state of knowledge on a number of issues including hood performance testing (DiBerardinis et al., 2003). The experts acknowledged that the ASHRAE Standard 110 test is of importance to hood designers; however, they emphasized that one cannot transfer the results of the test to the calculation of operational exposure of the chemist. Specifically, they did not feel that the containment factors developed in the test could be used to calculate a hood protection factor. Further, there was general agreement that conventional personal air sampling is the only valid method to measure the exposure of the chemist.

7.8 GENERAL LABORATORY VENTILATION

Laboratory hoods not only perform as local exhaust hoods but also provide general exhaust ventilation in the space. Such general ventilation is necessary to establish comfort conditions and provide dilution ventilation for any minor contamination generated outside the hood. Guidelines for general ventilation for chemical laboratories are covered in detail in other sources (DiBerardinis et al., 2001).

REFERENCES

- American Conference of Governmental Industrial Hygienists (ACGIH), *Industrial Ventilation, Manual of Recommended Practice*, 24th ed., ACGIH, Cincinnati, OH, 2001.
- American National Standards Institute, *American National Standard for Laboratory Ventilation*, American National Standards Institute (ANSI) Z9.5-2003, AIHA, Fairfax VA, 2003.
- American National Standards Institute (ANSI), *American National Standard for the Recirculation of Air from Industrial Process Exhaust Systems*, ANSI/AIHA Z9.7-1998, Fairfax, VA, 1998.
- American Society of Heating, Refrigeration and Air-Conditioning Engineers (ASHRAE), *Methods of Testing Performance of Laboratory Fume Cupboards*, ANSI/ASHRAE 110-1995, ASHRAE Inc., Atlanta, GA, 1995.
- Brief, R. S., F. W. Church, and N. V. Hendricks; "Design and Selection of Laboratory Hoods," *Air Eng.* 5:70 (1963).
- British Occupational Hygiene Society, BOHS Technology Committee Working Group, *Laboratory Design Issues*, Technical Guide No. 10, H&H Scientific Consultants Ltd, Leeds, UK, 1992.
- British Standards Institute (BSI), *BS 7258 Standard for Laboratory Fume Hood, Parts 1-4*, British Standards Institute London, 1994.
- Chamberlin R. I., and J. E. Leahy, *Laboratory Fume Hood Standards Recommended for the U.S. Environmental Protection Agency, Report on Contract No. 68-01-4661*, EPA, Washington, DC, 1978.
- Coleman, H. S., *Laboratory Design: National Research Council Report on Design, Construction and Equipment of Laboratories*, Reinhold, NY, 1951.
- DiBerardinis, L., M. W. First, and R. E. Ivany, "Field Results of an In-Place, Quantitative Performance Test for Laboratory Fume Hoods," *Appl. Occup. Env. Hyg.* 6:227-231 (1991).

- DiBerardinis, L., J. S. Baum, M. First, G. T. Gatwood, and A. Seth, *Guidelines for Laboratory Design: Health and Safety Considerations*, 3rd ed., Wiley, New York, 2001.
- DiBerardinis, L. et al., "Report of Howard Hughes Medical Institute Workshop on the Performance of Laboratory Chemical Hoods," *Am. Ind. Hyg. Assoc. J.* 63 (2003).
- Ettinger, H. J., M. W. First, and R. N. Mitchell, "Industrial Hygiene Practices Guide: Laboratory Hood Ventilation," *Am. Ind. Hyg. Assoc. J.* 29:611–617 (1968).
- Goodfellow, H., and E. Tahti, eds, *Industrial Ventilation Guidebook*, Academic Press, San Diego, 2001.
- Greenley, P. L., C. E. Billings, L. J. DiBerardinis, R. W. Edwards, and W. E. Barkley, "Containment Testing of Laboratory Hoods in the As-Used Condition," *Appl. Occup. Env. Hyg.* 15(2):209–216 (2000).
- Hughes, D., *A Literature Survey and Design Study of Fume Cupboards and Fume Dispersal Systems*, Occupational Health Monograph No. 4, Science Reviews Ltd., Leeds, UK, 1980.
- Johnston, J. D., S. J. Chassin, B. W. Chesnovar, and D. R. Lilliquist, "The Effects of Thermal Loading on Laboratory Fume Hood Performance," *Appl. Occup. Env. Hyg.* 15:863–868 (2000).
- Lawrence Berkeley National Laboratory, (LBNL), *The Berkeley Hood. Progress Report and Research Status: 1995–2001*, LBNL, Berkeley, CA, Oct. 2001.
- Ljungqvist, B., and C. Waring, "Some Observations on Modern Design of Fume Cupboards," *Proc. 2nd Int. Symp. on Ventilation for Contamination Control*, Sept. 1988, J. H. Vincent, ed., Pergamon, London, 1989, pp. 83–88.
- National Fire Protection Association (NFPA), *National Fire Protection Standard*, NFPA 45, 2000 Edition, National Fire Protection Association, Quincy, MA, 2000.
- Peterson, J. E., "An Approach to a Rational Method of Recommending Face Velocities for Laboratory Hoods," *Am. Ind. Hyg. Assoc. J.* 24:259–266 (1959).
- Renton, R., and G. Duffield, "Preliminary Evaluation of an Integral Scrubber/ Fume Hood Design For Control of Noxious Vapors," *Proc. 1st Int. Symp. on Ventilation for Contaminant Control*, Oct. 1–3, 1985, Toronto, Canada, H. D. Goodfellow, ed., Elsevier, Amsterdam, 1986.
- Saunders, C. J., A. E. Johnson, and B. Fletcher, "Flow in the Region of Fume Cupboard Sash Handles," *Proc. 1st Int. Symp. on Ventilation for Contaminant Control*, Stockholm, Arbeteoch Hals, 1994, pp. 264–269.
- Schulte, H. F., E. C. Hyatt, H. S. Jordan, et al., "Evaluation of Laboratory Fume Hoods," *Am. Ind. Hyg. Assoc. J.* 15:195–202 (1954).
- Silverman, L., and M. W. First, "Portable Laboratory Scrubber Unit for Perchloric Acid," *Am. Ind. Hyg. Assoc. J.* 23:462–472 (1962).

PROBLEMS

Note: You are preparing a memorandum on laboratory health and safety to be sent to all chemists in your R&D division. Prepare an outline of the coverage to be given each of the following topics.

- 7.1** What are the features of a modern chemical laboratory hood used to ensure a flat velocity profile at the face of the hood?

- 7.2** A number of architectural and HVAC features may impact adversely on the velocity profile at the hood face. What are they?
- 7.3** An older laboratory wing has 30-year-old “single pass” hoods, which malfunction because of inadequate replacement air. These hoods will be replaced by auxiliary air supply hoods. Describe the advantages and disadvantages of this type of hood for the chemists.
- 7.4** In a new R&D building a decision has been made to install horizontal sliding sash hoods. Until this time only vertical sliding sash hoods have been used. Introduce this concept to the chemist and describe its correct use.
- 7.5** Several laboratories in the R&D group work with TBTX, a chemical with an obnoxious odor and an olfactory threshold of 0.01 ppb. In one procedure 900 ml/min is released to the hood over a 4-h period. Offer advice on how the chemists can minimize odor complaints from neighbors.
- 7.6** One R&D group located in Natchez has 200 hoods. Briefly note the options available to reduce HVAC operating costs from these hoods.
- 7.7** Management had decided to use recirculating hoods on a special operation at a laboratory located in Ohio. Outline a series of operating guidelines for these hoods.
- 7.8** The chemical laboratory hoods in an advance projects group are cluttered with large containers of solvent and other chemicals. Describe the impact of this storage on the performance of the hoods and outline solutions to the problem.

DESIGN OF SINGLE-HOOD SYSTEMS

Tens of thousands of new or redesigned local exhaust ventilation (LEV) systems are installed annually in U.S. industry. It is estimated that the total capacity of these new systems approaches 50 million cfm with an installation cost of \$250 million and an annual operating cost of \$100 million. The majority of these systems are designed by personnel who have little training in this field and who do not consider rigorous engineering design to be necessary. As a result, a large fraction of existing LEV systems are not effective in protecting worker health. The availability of source information such as the ANSI Standard (ANSI, 2001), the ACGIH *Ventilation Manual* (ACGIH, 2001), a self-study companion to the manual (Burton, 2001), and computer design programs for both hand-held calculators and personal computers have improved this situation somewhat. However, a large group of plant engineering and health and safety professionals remain uninformed or believe that the design of LEV systems is not in their purview. Chapters 8 and 9 are intended to provide a basic understanding of the importance of engineering design and to introduce the available design techniques.

In this chapter local exhaust ventilation systems will be designed for single-hood systems using the *velocity pressure* design method. The velocity pressure method had been in widespread use for about 50 years; its popularity results from the ease of initial calculation and the ability to redesign system elements when necessary. The concept that all turbulent and frictional losses are directly proportional to the velocity pressure provides a rational basis to the method that can be readily understood by the novice designer.

In the first edition, an alternative design procedure called the *equivalent foot method* was described. This method was developed before the velocity pressure method. At the time the first edition was published, both methods were presented in the *Ventilation Manual*, but the velocity pressure method was given as the preferred one. In the interim, the equivalent foot method fell further from favor, and is no longer presented in the *Ventilation Manual*. Since the velocity pressure method has clear advantages and is used by virtually everyone, the equivalent foot method has been dropped from this edition.

Other changes in the design procedure since the first edition include the inclusion of density correction in the ACGIH *Velocity Pressure Calculation Sheet*, and the widespread availability of design programs for the personal-computer. These are included in the material presented in Chapters 8 and 9.

8.1 DESIGN APPROACH

The standard design procedure is a five-step process that relies on the design information in Chapter 5 of the *Ventilation Manual*.

Step 1: Choose Hood Geometry. A great deal of hood design information for common industrial operations is contained in Chapter 10 of the *Ventilation Manual*. Processes unique to certain industries (e.g., semiconductor manufacturing) may not be covered adequately, however, and the designer must go to other sources. In some cases, the system designer must develop a hood design for a unique operation.

Step 2: Calculate the Required Airflow. The hood airflow specified in the design plate is an integral part of any hood design. The specification may be a given airflow or an airflow calculated from a specified face or capture velocity. The design data in the *Ventilation Manual* are usually supported by observed performance of the hood in an industrial setting.

Step 3: Specify the Minimum Duct Velocity. Duct transport velocity information is also included in the design plate specifications. If the hood is to be used for gases and vapors, a duct velocity of 1500–2000 fpm (8–10 m/s) is usually specified; if particles are to be conveyed, the minimum transport velocity is 3500–4500 fpm (18–23 m/s).

Step 4: Choose a Duct Size. The size of a round duct is chosen to provide the required minimum duct velocity for the given airflow. The maximum duct cross-sectional area is obtained by dividing the airflow by the minimum velocity. Choosing the standard duct diameter with the next smaller area will assure that the minimum velocity is met. The actual duct velocity is then calculated based on the duct area and air flow.

Step 5: Lay out the Duct Run. The layout in the plant is chosen to minimize energy loss due to straight duct runs and elbows while observing the space constraints of both architectural and equipment obstructions. Frequently, several optional

layouts must be considered, and plant engineers and process managers must be consulted. One important consideration is the location of the stack. Two problems commonly arise. First, reentry of exhausted contaminants must be avoided; this is discussed in detail in Chapter 15. The second problem concerns the necessity to penetrate the roof or a building wall; the location of such penetrations must be carefully considered and coordinated with building managers.

Step 6: Calculate Energy Losses. Once the duct layout is defined, the frictional and turbulent losses due to air flowing through the system can be determined from equations, charts, or tables. These static pressure losses may be calculated directly, or as multiples of velocity pressure that are later converted to static pressure; the second option is the method used in the *Ventilation Manual*.

8.2 DESIGN OF A SIMPLE ONE-HOOD SYSTEM (BANBURY MIXER HOOD)

The first system design example is a hood for a Banbury mixer (Fig. 8.1) used in the rubber and plastics industries to mix the elastomeric material with accelerators, antioxidants, antiozonants, pigments, plasticizers, and vulcanizing agents. The “feeding” or “charging” of these granular materials to the Banbury is a dusty operation and requires

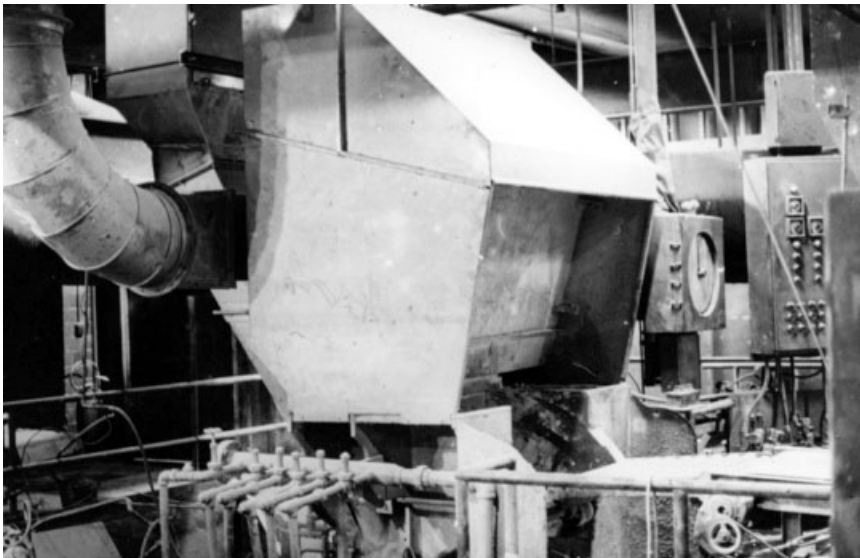


Figure 8.1 The Banbury mixer is used to mix rubber and plastic stock with various additives. This is a view of the charging platform on the upper level where the stock and additives are fed to the mixer. After feeding, the charging door closes, a ram seals the chamber, and the material is mixed. When mixing is completed, the bottom dump door opens and the blended material drops to a mill positioned directly under the Banbury on the lower level.

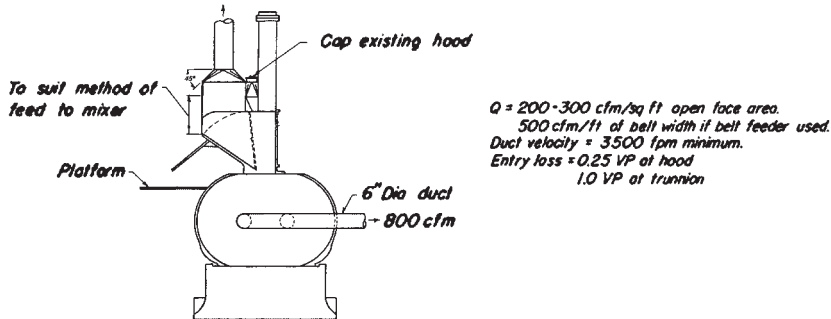


Figure 8.2 This design plate of a Banbury mixer provides the engineer with the four key design elements: (1) design and placement of hood, (2) minimum airflow to achieve control, (3) minimum duct velocity, and (4) hood entry loss. (From *Ventilation Manual*, VS-60-10. Used by permission of Committee on Industrial Ventilation, ACGIH, Lansing, MI.)

excellent local exhaust ventilation. The accepted technique as described in *Ventilation Manual* VS-60-10 is a partial enclosure over the charging port (Fig. 8.2). Two additional small hoods are usually provided to handle dust escaping from the dust rings at the ends of the trunnion. In this example, only the charge port will be provided with ventilation. The ventilation system to be designed consists of a hood, fan, and connecting ductwork. The goals of the design process are the determination of the minimum airflow required (cfm) and the total resistance to airflow (in. H_2O) for this system. These design data can then be used to select an appropriate fan using the techniques described in Chapter 10.

Step 1: Choose Hood Geometry. The design data presented in Fig. 8.2 will be used to develop the system design for the hood on the Banbury mixer.

Step 2: Calculate the Required Airflow. On inspection, the Banbury mixer is found to be fed manually, not by belt. In addition, there are no serious drafts from doors, windows, or traffic. Based on this information, a minimum exhaust of 200 cfm/ft² of open face area (equivalent to a face velocity of 200 fpm) is chosen. If the Banbury were located near a receiving door and serious drafts occurred or if drafts resulted from pedestal-type cooling fans, the higher value of 300 fpm from VS-60-10 would be chosen. A belt feeder would require 500 cfm/ft² of opening. As shown in Fig. 8.3, the hood is 5 ft wide and 4 ft high, so the airflow is calculated as

$$\begin{aligned}
 Q &= VA \\
 &= 200 \frac{\text{ft}}{\text{min}} (5 \text{ ft} \times 4 \text{ ft}) \\
 &= 4000 \text{ ft}^3/\text{min}
 \end{aligned}
 \tag{2.5}$$

Step 3: Specify the Minimum Duct Velocity. The minimum duct velocity recommended in VS-60-10 is 3500 fpm.

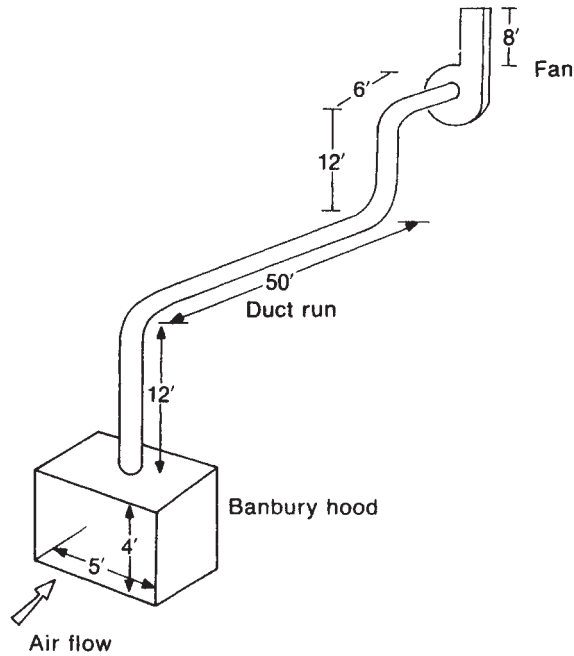


Figure 8.3 Layout of the Banbury, duct, and fan. The hood face is 5 ft wide and 4 ft high, and the duct lengths are indicated. The sources of static pressure loss in this system include the hood entry loss, the inertial loss, the frictional loss of straight duct, and the losses due to elbows.

Step 4: Choose a Duct Size. The maximum allowable duct area is found by dividing the airflow by the minimum duct velocity:

$$\begin{aligned}
 A &= \frac{Q}{V} \\
 &= \frac{4000 \text{ ft}^3/\text{min}}{3500 \text{ ft}/\text{min}} = 1.14 \text{ ft}^2
 \end{aligned}$$

Any duct with an area smaller than 1.14 ft^2 and conveying 4000 cfm will satisfy the minimum duct velocity requirement of 3500 fpm. From Table 8.1 the round duct with a cross-sectional area just smaller than 1.14 ft^2 is a 14-in. duct, with an area of 1.069 ft^2 . The actual duct velocity and the associated velocity pressure must be calculated since they are needed in this design process. The velocity is

$$\begin{aligned}
 V &= \frac{Q}{A} \\
 &= \frac{4000 \text{ ft}^3/\text{min}}{1.069 \text{ ft}^2} = 3740 \text{ ft}/\text{min}
 \end{aligned}$$

Table 8.1 Choosing the Correct Duct Diameter^a

Diameter (in.)	Area		Circumference	
	in. ²	ft ²	in.	ft
12	113.1	0.7854	37.70	3.142
13	132.7	0.9218	40.84	3.403
14	153.9	1.069	43.98	3.665
15	176.7	1.227	47.12	3.927
16	201.0	1.396	50.26	4.189
17	226.9	1.576	53.41	4.451
18	254.4	1.767	56.55	4.712
19	283.5	1.969	59.69	4.974
20	314.1	2.182	62.83	5.236
21	346.3	2.405	65.97	5.498

^aSee *Ventilation Manual* for complete data.

The associated velocity pressure is

$$\begin{aligned}
 p_v &= \left(\frac{V}{4000} \right)^2 \\
 &= \left(\frac{3740}{4000} \right)^2 \\
 &= 0.87 \text{ in. H}_2\text{O}
 \end{aligned} \tag{2.17}$$

Step 5: Lay out the Duct Run. The chosen duct layout is shown in Fig. 8.3. The duct rises 12 ft to the underside of the plant ceiling, turns 90° to run 50 ft along the ceiling, turns 90° again and runs 12 ft to penetrate the roof, turns 90°, and runs 6 ft to the fan located on the roof. Also included is an 8-ft stack running from the fan.

Step 6: Calculate Energy Losses. The energy losses occurring in simple systems such as this have been discussed in detail in Chapter 2. As noted in that discussion, both the turbulent losses due to changes in direction and velocity of airflow and the frictional losses due to the air flowing in the duct are directly proportional to the velocity pressure. For this reason, each loss can be expressed as a loss factor times the velocity pressure in the duct. The losses in the Banbury hood design expressed in inches of water will be calculated in this fashion.

Hood Static Pressure in the Duct. As described in Chapter 2, the hood static pressure as measured in the duct just downstream of the hood consists of the hood entry loss and the acceleration factor (one velocity pressure):

$$p_{s,h} = p_v + h_e \tag{2.41}$$

where $p_{s,h}$ = hood static pressure (in. H₂O)

p_v = velocity pressure (in. H₂O)

h_e = hood entry loss (in. H₂O)

Table 8.2 Velocity Pressure Chart^a

p_v (in. H ₂ O)	V (fpm)
0.82	3622
0.83	3644
0.84	3666
0.85	3688
0.86	3709
0.87	3731
0.88	3752
0.89	3774
0.90	3795
0.91	3816

^aSee *Ventilation Manual* for complete data.

The hood entry loss h_e is usually specified as the hood entry loss factor F_e multiplied by the velocity pressure:

$$h_e = F_e \times p_v \quad (2.42)$$

so that

$$p_{s,h} = p_v(1 + F_e) \quad (2.43)$$

The entry loss factor F_e for the Banbury hood is 0.25 as shown in Fig. 8.2. Equation 2.43 can now be used to calculate the hood static pressure:

$$\begin{aligned} p_{s,h} &= p_v(1 + F_e) \\ &= p_v(1 + 0.25) \\ &= 1.25 p_v \end{aligned}$$

This hood static pressure must be established in the system to provide an airflow of 4000 cfm through this hood.

Duct Friction. The frictional loss due to the 4000 cfm flowing through the 14-in.-diameter duct can also be expressed as a product of a loss factor and the velocity pressure. As shown in Fig. 8.3, the length of straight duct upstream of the fan is $12 + 50 + 12 + 6 = 80$ ft, and there is an additional 8 ft downstream of the fan. Since air flowing through a duct exhibits the same frictional losses whether the duct is upstream or downstream of the fan, the total duct run of 88 ft can be considered as a unit.

The frictional loss of straight duct expressed as velocity pressure is obtained from Fig. 8.4. The intersection of the 4000 cfm airflow and the 14-in. duct diameter curves is found and the corresponding loss for each foot of duct is $0.0155 p_v$. Since the Banbury system has 88 ft of straight duct, the loss is

$$88 \text{ ft} \times 0.0155 \frac{p_v}{\text{ft}} \quad \text{or} \quad 1.36 p_v$$

Alternatively, the loss per foot can be calculated using the equation in Fig. 5-19 of the *Ventilation Manual*:

$$p_{s,f} = 0.0307 p_v \frac{V^{0.533}}{Q^{0.612}}$$

where D is the duct diameter (in.). In this case

$$\begin{aligned} p_{s,f} &= 0.0307 p_v \frac{3740^{0.533}}{4000^{0.612}} \\ &= 0.0155 p_v \end{aligned}$$

Elbow Losses. The turbulent loss in elbows is also directly proportional to velocity pressure; typical loss factors are shown in Fig. 8.5. More recent data have been developed by Durr et al. (1987).

Elbows are typically made out of sections of straight duct, or stamped smooth, as shown in Fig. 8.5. The larger the radius of curvature R and the larger the number of sections, the lower the turbulent loss. Stamped elbows are much more expensive than sectional elbows, so they typically are not specified. In addition, large sweep elbows are expensive to fabricate and take up valuable space, so elbows in most local exhaust ventilation systems are specified to be of 4 or 5-piece construction with a radius of curvature equal to 1.5 or 2.0 duct diameters (D). Elbows with an $R/D = 1.5$ and 4-piece construction will be used for the Banbury and all of example designs. The 14-in.-diameter elbow thus has a sweep radius of 21 in. and the turbulent loss in one elbow is $0.27 p_v$ (Fig. 8.5). Since there are three 90° elbows, the total elbow loss is $0.81 p_v$.

The total frictional and turbulent loss for the hood and duct elements in the Banbury mixer exhaust system is as follows:

Hood entry loss h_e	$0.25 p_v$
Acceleration (inertial loss) p_v	$1.00 p_v$
Straight duct frictional loss $p_{s,f}$	$1.36 p_v$
Elbow loss	$0.81 p_v$
<hr/>	
Total static pressure loss (p_s)	$3.42 p_v$

The velocity pressure was previously calculated to be 0.87 in. H_2O ; therefore the actual static pressure required to move 4000 cfm through this system is

$$p_s = (3.42) (0.87 \text{ in. H}_2\text{O}) = 2.98 \text{ in. H}_2\text{O}$$

Use of Calculation Sheet for Example 8.1. The detailed procedure employed above is useful for demonstrating the individual steps necessary to calculate static pressure losses. However, it is much too laborious and inconvenient for routine calculation, especially for the complex multibranch systems to be considered in Chapter 9. The

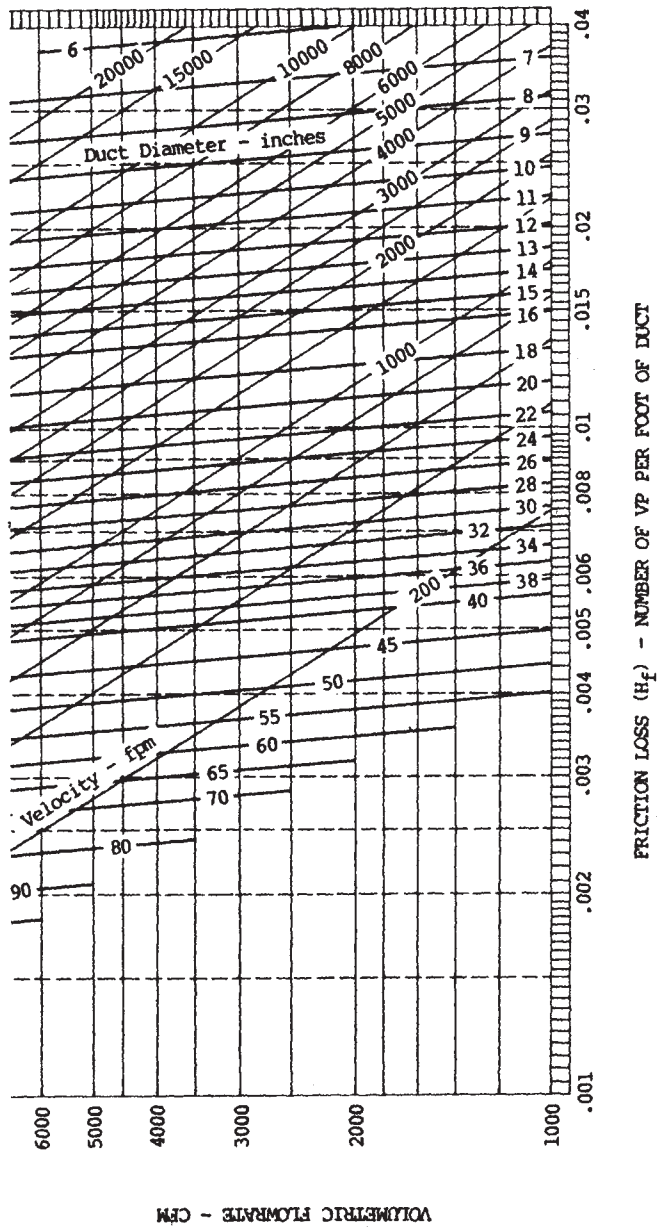


Figure 8.4 Frictional loss of straight duct, using the velocity pressure method. (From Ventilation Manual, Fig. 5-19.)

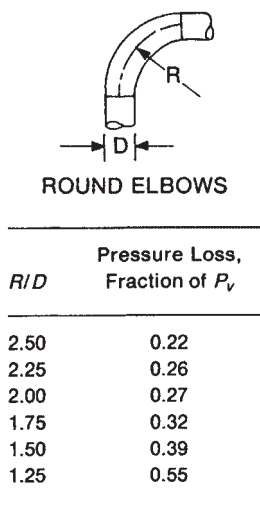


Figure 8.5 Geometry of a 90° elbow showing duct diameter (D), the radius of curvature (R), and typical loss factors for given R/D values. See *Ventilation Manual* for complete data.

calculation sheet provided in the *Ventilation Manual* provides a convenient format to organize the design process. The Banbury mixer hood design is repeated in Example 8.1 using a version of the calculation sheet that has been simplified to eliminate extraneous information. A more complete version will be presented in Chapter 9.

In the design of a complex local exhaust system it is important to use a consistent method of identifying the various hoods and duct sections. The *Ventilation Manual* uses the convention shown in Fig. 8.6. Each hood is assigned a number and each duct junction or transition is assigned a letter. A hood-to-junction or junction-to-junction duct run represented by a two-character combination (e.g., 1A, AB) is used to label the duct section under design. Each column in the calculation sheet corresponds to one section of duct.

8.3 DESIGN OF A SLOT HOOD SYSTEM FOR A DEGREASING TANK

Because of the toxicity of chlorinated hydrocarbon solvents used in degreasers, it is common practice to install a lateral slot hood on degreasing tanks (Fig. 8.7). The value of such a slotted hood in providing effective exhaust distribution over the tank surface has been discussed in Chapter 5. The hood entry loss for such hoods is more complex than for simple hoods due to this slot, the plenum, and the duct transition.

8.3.1 Loss Elements in a Complex Hood

The entry loss in a slotted hood depends on the relationship between the slot and duct velocity and the geometry of the plenum. A general view of the slot, plenum, and duct transition is shown in Fig. 8.8.

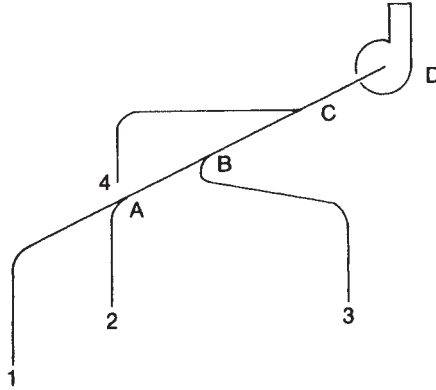


Figure 8.6 Nomenclature for major duct elements in a local exhaust ventilation system. Hoods are identified by a number and junctions by a letter.

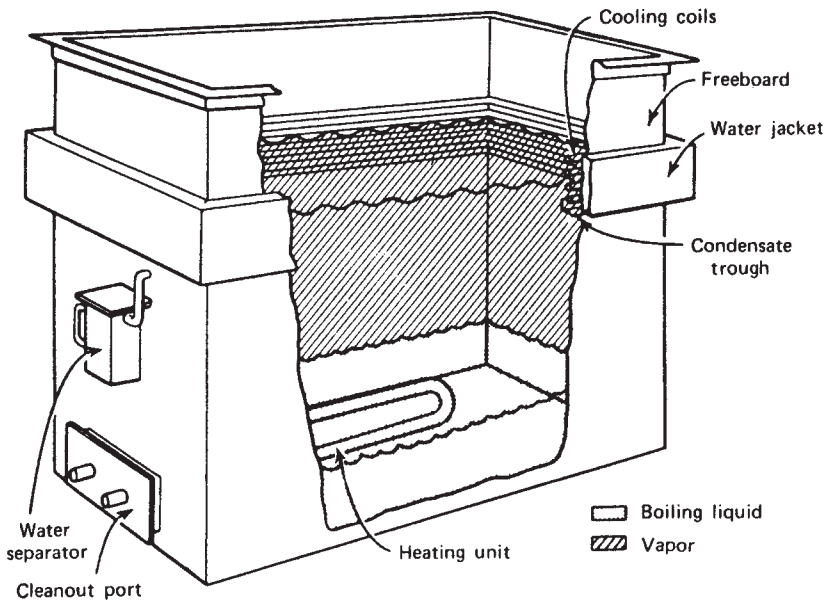


Figure 8.7 The solvent in a vapor-phase degreaser is heated with steam or electricity and a dense vapor is formed which fills the tank. The tank is equipped with a cold-water condenser jacket. The hot vapor condenses on the jacketed side of the tank and runs back into the sump. When parts are lowered into the vapor cloud, the hot solvent vapor condenses on the cold parts and strips off the oily residue, which drops to the tank bottom. Fugitive losses from the tank are commonly controlled with lateral slot exhaust hoods. (From J. A. Murphy, *Surface Preparation and Finishes for Metals*. Copyright 1971. Used with permission of McGraw-Hill Book Company.)

The hood entry loss for a slot hood has two components, the entry loss through the slot itself ($h_{e,s}$) and the entry loss in the transition from the plenum to the duct ($h_{e,d}$). Mathematically, we have

$$h_e = h_{e,s} + h_{e,d} \quad (8.2)$$

The air velocity and velocity pressure through a slot hood changes as it passes through the slot $p_{v,s}$, the plenum $p_{v,p}$, and finally into the duct $p_{v,d}$. For the general case in which the slot velocity is high, there is a residual plenum velocity $p_{v,p}$ (Fig. 8.8) which is reaccelerated to the duct velocity $p_{v,d}$. The required velocity pressure is

$$p_v = p_{v,s} + (p_{v,d} - p_{v,p}) \quad (8.3)$$

The hood static pressure

$$p_{s,h} = p_v + h_e \quad (2.41)$$

is obtained by combining Eqs. 8.2 and 8.3:

$$p_{s,h} = p_{v,s} + (p_{v,d} - p_{v,p}) + h_{e,s} + h_{e,d} \quad (8.4)$$

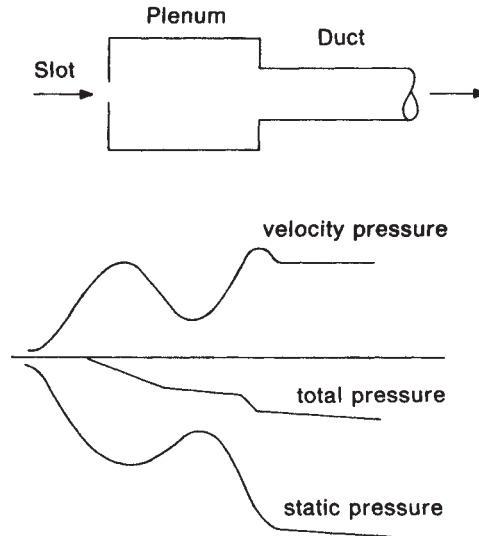


Figure 8.8 Pressures in slot hoods including velocity pressure at slot $p_{v,s}$, velocity pressure at plenum $p_{v,p}$, and velocity pressure at duct $p_{v,d}$.

If the duct velocity is greater than the slot velocity ($p_{v,d} > p_{v,s}$)

- For a shallow plenum ($p_{v,p}$ is approximately equal to $p_{v,s}$)

$$p_{s,h} = p_{v,d} + h_{e,s} + h_{e,d} \quad (8.5)$$

- For a deep plenum ($p_{v,p}$ is approximately zero)

$$p_{s,h} = p_{v,s} + p_{v,d} + h_{e,s} + h_{e,d} \quad (8.6)$$

If the duct velocity is less than the slot velocity ($p_{v,d} < p_{v,s}$)

- For a shallow plenum ($p_{v,p}$ is approximately equal to $p_{v,s}$) and both $p_{v,p}$ and $p_{v,s}$ are greater than $p_{v,d}$

$$p_{s,h} = h_{e,s} + h_{e,d} + p_{v,s} \quad (8.7)$$

(no credit for static regain, $p_{v,d} - p_{v,s}$)

- For a deep plenum ($p_{v,p}$ is approximately zero)

$$p_{s,h} = p_{v,s} + p_{v,d} + h_{e,s} + h_{e,d} \quad (8.8)$$

For the most common case, a shallow plenum hood where the duct velocity is greater than the slot velocity, the hood static pressure is

$$p_{s,h} = h_{e,s} + h_{e,d} + p_{v,d} \quad (8.9)$$

If the slot is modeled as a sharp-edged orifice, the slot entry loss is

$$h_{e,s} = 1.78 p_{v,s} \quad (8.10)$$

The plenum-to-duct entry loss is

$$h_{e,d} = F_{e,d} \times p_{v,d} \quad (8.11)$$

where $F_{e,d}$, the plenum-to-duct entry loss factor, depends on the taper angle of the transition. Values are given in *Ventilation Manual*, Fig. 5-15.

As an example, if the included taper angle for a round duct is 120°

$$h_{e,d} = 0.25 p_{v,d} \quad (8.12)$$

substituting Eqs. 8.10 and 8.12 into Eq. 8.2 gives the hood entry loss

$$h_e = 1.78 p_{v,s} + 0.25 p_{v,d}$$

and the hood static pressure from Eq. 8.2 is thus

$$p_{s,h} = 1.78 p_{v,s} + 1.25 p_{v,d} \quad (8.13)$$

8.3.2 Degreaser Hood Design Using Velocity Pressure Calculation Sheet (Example 8.2)

The system design using the velocity pressure calculation sheets is shown in Fig. 8.9 and Example 8.2. The duct design for the degreasing tank is conducted in a fashion similar to the Banbury hood. The slot loss is calculated using lines 15–21 on the standard velocity pressure method calculation sheet.

The design process indicates that the system will provide 1500 cfm with a static pressure loss of 1.15 in. H₂O. The selection of an 11-in.-diameter duct in solution A provided the minimum duct velocity of 2000 fpm specified in Fig. 8.9 for this example. Maintaining a minimum duct velocity is important in a system handling particles since dust settling in the duct should be avoided. In a system conveying gases or vapors the duct velocity is less important and lower velocities can be chosen if space is available for the larger duct. The energy reduction in going to a lower duct velocity can easily be calculated. The use of the next larger duct (12 in.) in solution B (in Example 8.2) reduces the duct velocity from 2270 fpm to 1910 fpm. This modest reduction in velocity will result in the pressure loss dropping from 1.15 in. H₂O to 0.85 in. H₂O.

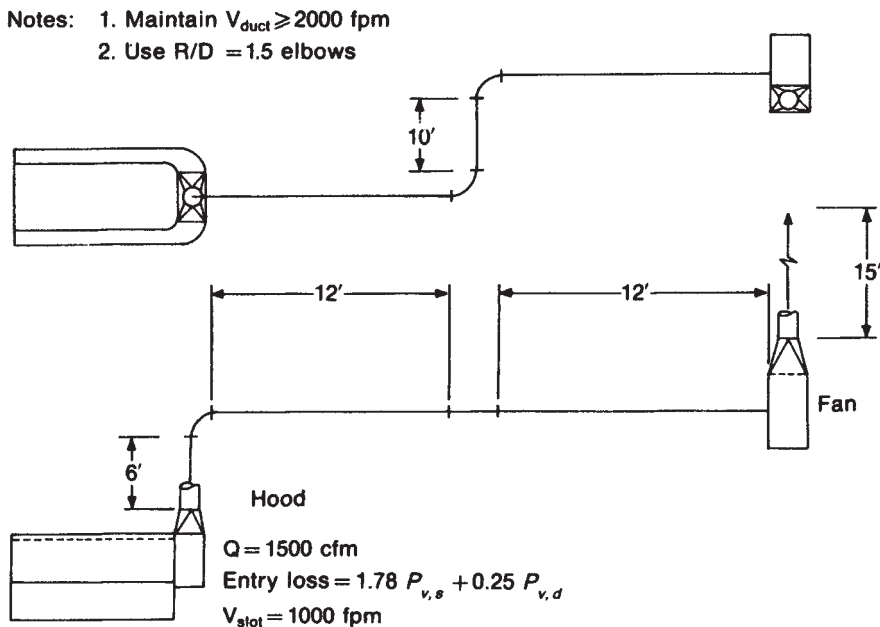


Figure 8.9 Design plate for a vapor-phase degreaser.

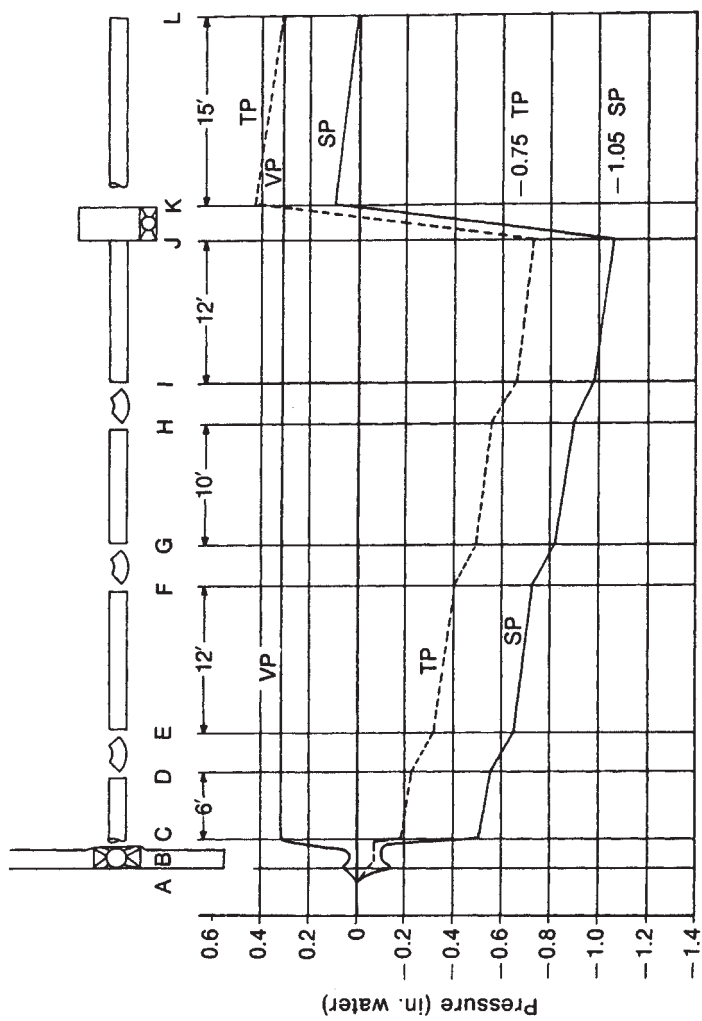


Figure 8.10 Plot of duct pressures for vapor-phase degreaser system using 11-in. duct.

8.4 PRESSURE PLOT FOR SINGLE-HOOD SYSTEM

The pressures existing in a duct run were defined in Chapter 2. Velocity, static, and total pressures for the degreasing tank system (using the 11-in. duct) can be plotted as shown in Fig. 8.10.

The most convenient approach to calculating the pressures at any point in the system is first to calculate the velocity pressure for each duct element. An 11-in.-diameter duct is used in the system, so the velocity pressure of 0.32 in. H₂O exists throughout the duct portion of the system. The velocity pressure at the slot can be calculated, but the velocity change in the plenum can only be approximated. The individual frictional and turbulent losses are calculated for each system element shown in Fig. 8.9 and added incrementally starting with a static pressure of 0 in. H₂O at the hood to obtain the static pressure at each benchmark. The total pressure at each benchmark is then calculated based on $p_t = p_v + p_s$. As illustrated, the total pressure line is parallel to the static pressure line and offset by an amount equal to the velocity pressure. Connecting the fan inlet and outlet pressures (shown as *J-K*) is a graphic presentation of the function of the fan as a static pressure generator.

LIST OF SYMBOLS

A	area
D	diameter
F_e	hood entry loss factor
$F_{e,d}$	duct entry loss factor
h_e	hood entry loss
$h_{e,d}$	entry loss for transition plenum to duct
$h_{e,s}$	entry loss for hood slot
p_s	static pressure
$p_{s,h}$	hood static pressure
p_t	total pressure
p_v	velocity pressure
$p_{v,d}$	duct velocity pressure
$p_{v,p}$	plenum velocity pressure
$p_{v,s}$	slot velocity pressure
Q	airflow
R	radius of curvature
V	average velocity

EXAMPLE 8.1 BANBURY MIXER SYSTEM DESIGNED BY THE VELOCITY PRESSURE METHOD

Simplified velocity pressure method calculation sheet*

1		Duct segment identification			1A			
3	Q	Standard volumetric flow rate		scfm	4000			
4	V_t	Minimum transport velocity		fpm	3500			
9	A_t	Target duct area	3÷4	ft ²	1.14			
10	d	Selected duct diameter		inches	14			
11	A	Selected duct area		ft ²	1.069			
12	V_d	Duct velocity	3+11	fpm	3740			
13	VP_d	Duct velocity pressure	Eq. 2.21	in. H ₂ O	0.87			
15	A_s	Slot area		ft ²				
16	F_s	Slot loss coefficient						
17		Acceleration factor		0 or 1				
18	V_s	Slot velocity	8+15	fpm				
19	VP_s	Slot velocity pressure	Eq. 2.21	in. H ₂ O				
20		Slot loss in VP	16 + 17					
21		Slot static pressure	20 × 19	in. H ₂ O				
22	F_h	Duct entry coefficient			0.25			
23		Acceleration factor		0 or 1	1			
24		Duct entry loss in VP	22 + 23		1.25			
25		Duct entry loss	24 × 13	in. H ₂ O	1.09			
26		Other losses		in. H ₂ O				
27	SP_h	Hood static pressure	21 + 25 + 26	in. H ₂ O	1.09			
28	l	Straight duct length		ft	88			
29	H_f	Duct friction factor	Eq. 8.1		0.0155			
30		Number of 90° elbows			3			
31	F_{el}	Elbow loss coefficient	Fig. 8.5		0.27			
32	F_{en}	Branch entry coefficient						
33		Special fitting coefficient						
34	h_f	Duct friction loss in VP	28 × 29		1.36			
35		Elbow loss in VP	30 × 31		0.81			
36		Branch entry loss in VP	32					
37		Duct loss in VP	33 + 34 + 35 + 36		2.17			
38		Duct loss	37 × 13	in. H ₂ O	1.89			
39		Other losses		in. H ₂ O				
42		Duct pressure loss	27 + 38 + 39	in. H ₂ O	2.98			

*This form is adapted from the ACGIH Ventilation Calculation Sheets: Velocity Pressure Method. Copies of blank forms suitable for design calculations can be purchased from the American Conference of Governmental Industrial Hygienists, Kemper Woods Center, 1330 Kemper Meadow Drive, Cincinnati, OH 45240-1634, customerservices@acgih.org.

Example 8.1 Design Notes for Calculation Sheet

General Comments. All velocities are rounded to the nearest 10 fpm, and all pressures are rounded to the nearest 0.01 in. H₂O.

Line 3: The design airflow for each duct segment should be entered in this line. The entry for a single-hood system such as the Banbury mixer is the minimum design airflow for the hood, as determined in step 2 in Section 8.1.

Line 9: The target duct area is determined by dividing the required airflow by the minimum duct transport velocity. This is the *maximum* duct area allowed, since any larger area will result in a duct velocity below the required minimum.

Line 10: The duct diameter selected is the diameter with an area just smaller than that calculated on line 9.

Line 12: The actual duct velocity is calculated by dividing the required airflow by the duct area.

Line 13: The duct velocity pressure is calculated using Eq. 2.21.

Lines 15–21: Entries are required in these lines only if the system includes a complex hood, that is, one with slots. Since the Banbury hood is not a slotted hood, this part of the calculation form does not apply to this example.

Line 22: The hood entry loss is obtained from design plate VS-60-10.

Line 23: The air entering the hood must be accelerated to the duct velocity; therefore, 1 is entered on this line.

Lines 24–27: The hood entry loss is calculated by summing the duct entry loss coefficient and the acceleration factor and multiplying by the duct velocity pressure, as per Eq. 2.43:

$$p_{s,h} = p_v(1 + F_e) = 0.87(1.0 + 0.25) = 1.09 \text{ in. H}_2\text{O}$$

Line 28: The length of straight duct is determined from plan and elevation views of the system. It is standard practice to use centerline distances and round off to the nearest foot. The additional distance represented by elbows is not included.

Line 29: The duct friction factor can be calculated (e.g., using Eq. 8.1) or obtained from graphs (e.g., Fig. 8.4, or *Ventilation Manual*, Fig. 5-19).

Line 31: The elbow loss coefficient can be obtained from Fig. 8.5 or *Ventilation Manual*, Fig. 5-16.

Line 32: This loss element is used only for multiple-hood systems.

Line 34: The friction loss factor is expressed as the product of the total duct length and friction factor.

Line 35: The elbow loss factor is expressed as the product of the number of 90° elbows and the elbow loss coefficient.

Line 38: The duct static pressure loss, in in. H₂O, is determined by summing the duct loss factors and multiplying by the duct velocity pressure.

Line 42: The static pressure loss in the system is determined by summing the hood static pressure loss and the duct static pressure loss.

EXAMPLE 8.2 DEGREASER SYSTEM DESIGNED BY THE VELOCITY PRESSURE METHOD

Simplified velocity pressure method calculation sheet*

1		Duct segment identification			Solution A	Solution B
3	Q	Standard volumetric flow rate		scfm	1500	1500
4	V_t	Minimum transport velocity		fpm	2000	2000
9	A_t	Target duct area	3+4	ft ²	0.75	0.75
10	d	Selected duct diameter		inches	11	12
11	A	Selected duct area		ft ²	0.6600	0.7854
12	V_d	Duct velocity	3+11	fpm	2270	1910
13	VP_d	Duct velocity pressure	Eq. 2.21	in. H ₂ O	0.32	0.23
15	A_s	Slot area		ft ²	1.5	1.5
16	F_s	Slot loss coefficient			1.78	1.78
17		Acceleration factor		0 or 1	0	0
18	V_s	Slot velocity	8+15	fpm	1000	1000
19	VP_s	Slot velocity pressure	Eq. 2.21	in. H ₂ O	0.06	0.06
20		Slot loss in VP	16 + 17		1.78	1.78
21		Slot static pressure	20 × 19	in. H ₂ O	0.11	0.11
22	F_h	Duct entry coefficient			0.25	0.25
23		Acceleration factor		0 or 1	1	1
24		Duct entry loss in VP	22 + 23		1.25	1.25
25		Duct entry loss	24 × 13	in. H ₂ O	0.40	0.29
26		Other losses		in. H ₂ O	0	0
27	SP_h	Hood static pressure	21 + 25 + 26	in. H ₂ O	0.51	0.40
28	l	Straight duct length		ft	55	55
29	H_f	Duct friction factor	Eq. 8.1		0.0220	0.0159
30		Number of 90° elbows			3	3
31	F_{el}	Elbow loss coefficient	Fig. 8.5		0.27	0.27
32	F_{en}	Branch entry coefficient			0	0
33		Special fitting coefficient			0	0
34	h_f	Duct friction loss in VP	28 × 29		1.21	0.87
35		Elbow loss in VP	30 × 31		0.81	0.81
36		Branch entry loss in VP	32		0	0
37		Duct loss in VP	33 + 34 + 35 + 36		2.02	1.68
38		Duct loss	37 × 13	in. H ₂ O	0.65	0.39
39		Other losses		in. H ₂ O	0	0
42		Duct pressure loss	27 + 38 + 39	in. H ₂ O	1.16	0.79

*This form is adapted from the ACGIH Ventilation Calculation Sheets: Velocity Pressure Method. Copies of blank forms suitable for design calculations can be purchased from the American Conference of Governmental Industrial Hygienists, Kemper Woods Center, 1330 Kemper Meadow Drive, Cincinnati, OH 45240-1634, customerservices@acgih.org.

Example 8.2 Design Notes for Calculation Sheet

General Comments

Lines 3 and 4: Required airflow and minimum transport velocity obtained from Fig. 8.9.

Lines 10–13: Solution A meets the required minimum transport velocity strictly, while Solution B illustrates the effect of allowing the velocity to fall just below the required minimum.

Line 15: The slot area is selected to give the desired slot velocity (line 18). Selection of slot velocity is discussed in Chapter 5.

Lines 17 and 23: The acceleration factor must be taken on one of these lines, depending on the relative velocities in the slot and in the duct (see Section 8.3.1). In this case, since the duct velocity is higher than the slot velocity, 0 is entered in line 17 and 1 is entered in line 23.

Line 20: Obtained from Fig. 8.9.

Line 21: The static pressure loss through the slot is determined from the product of the slot entry loss coefficient and the slot velocity pressure, Eq. 8.10.

Line 22: This is the entry loss coefficient for the transition from the plenum to the duct, obtained from Fig. 8.9.

Line 27: For a complex hood, the hood static pressure is the sum of the static pressure loss through the slot and the static pressure loss for the transition from the plenum to the duct, Eq. 8.13.

Line 28: From Fig. 8.9, the total duct length is $6 + 12 + 10 + 12 + 15 = 55$ ft.

REFERENCES

- American Conference of Governmental Industrial Hygienists, Committee on Industrial Ventilation, *Industrial Ventilation*, 24th. ed., ACGIH, Cincinnati, OH, 2001.
- American National Standards Institute, *Fundamentals Governing the Design and Operation of Local Exhaust Systems*, ANSI Standard Z9.2-2001, ANSI, New York, 2001.
- Burton, D. J., *Companion Study Guide to Industrial Ventilation: A Manual of Recommended Practice*, ACGIH, Cincinnati, OH, 2001.
- Burton, D. J., *Hemeon's Plant and Process Ventilation*, 3rd ed., Industrial Press, New York, 1999.
- Durr, D., N. Esmen, C. Stanley, and D. Weyel, "Pressure Drop in Elbows," *Appl. Ind. Hyg.* 2:57 (1987).

APPENDIX: METRIC VERSION OF EXAMPLE 8.1

Simplified velocity pressure method calculation sheet—metric version*

1		Duct segment identification		1A			
3	Q	Standard volumetric flow rate		m ³ /s	1.89		
4	V_t	Minimum transport velocity		m/s	17.5		
9	A_t	Target duct area	3+4	m ²	0.108		
10	d	Selected duct diameter		mm	350		
11	A	Selected duct area		m ²	0.096		
12	V_d	Duct velocity	3+11	m/s	18.8		
13	VP_d	Duct velocity pressure	Eq. 2.21	Pa	211		
15	A_s	Slot area		m ²			
16	F_s	Slot loss coefficient					
17		Acceleration factor		0 or 1			
18	V_s	Slot velocity	8+15	m/s			
19	VP_s	Slot velocity pressure	Eq. 2.21	Pa			
20		Slot loss in VP	16 + 17				
21		Slot static pressure	20 × 19	Pa			
22	F_h	Duct entry coefficient		0.25			
23		Acceleration factor		0 or 1	1		
24		Duct entry loss in VP	22 + 23		1.25		
25		Duct entry loss	24 × 13	Pa	264		
26		Other losses		Pa			
27	SP_h	Hood static pressure	21 + 25 + 26	Pa	264		
28	l	Straight duct length		m	26.8		
29	H_f	Duct friction factor	Eq. 8.1	0.050			
30		Number of 90° elbows		3			
31	F_{el}	Elbow loss coefficient	Fig. 8.5	0.27			
32	F_{en}	Branch entry coefficient					
33		Special fitting coefficient					
34	h_f	Duct friction loss in VP	28 × 29	1.35			
35		Elbow loss in VP	30 × 31	0.81			
36		Branch entry loss in VP	32				
37		Duct loss in VP	33 + 34 + 35 + 36	2.16			
38		Duct loss	37 × 13	Pa	456		
39		Other losses		Pa			
42		Duct pressure loss	27 + 38 + 39	Pa	720		

*This form is adapted from the ACGIH Ventilation Calculation Sheets: Velocity Pressure Method. Copies of blank forms suitable for design calculations can be purchased from the American Conference of Governmental Industrial Hygienists, Kemper Woods Center, 1330 Kemper Meadow Drive, Cincinnati, OH 45240-1634, customerservices@acgih.org.

PROBLEMS

8.1 What are the hood entry loss factor and minimum duct velocity for the hoods used for the following equipment or operation? [Vent Man]

- (a) Finishing granite with a swing grinder
- (b) Carpentry shop radial arm saw

- (c) Chemical plant bag filling operation
- (d) High-toxicity metal milling
- (e) Soldering radiators in an automobile repair shop

Answers:

- (a) 0.25, 3500 ft/min
- (b) 3.5, 4000 ft/min
- (c) 0.25, 3500 ft/min
- (d) 0.35, 3500 ft/min
- (e) 0.25, 3000 ft/min

8.2 A bench used for welding is 4 ft long and 2 ft wide. It is furnished with a slot hood designed according to the specifications in VS-90-01. [Vent Man]

- (a) What duct diameter should be connected to the hood?
- (b) Using this diameter duct, what is the hood static pressure?
- (c) If 50 ft of this duct is connected to the hood, what is the static pressure at the end of the duct furthest from the hood?

Answers:

- (a) 11 in.
- (b) 0.80 in. H_2O
- (c) 1.10 in. H_2O

DESIGN OF MULTIPLE-HOOD SYSTEMS

The design technique for a single-hood system is straightforward, and a collection of single-hood systems provides the ultimate in flexibility for the user. However, single-hood systems do have many drawbacks, and it is usually more economical to group a series of hoods into a system with a single fan. Such multiple-hood systems can be designed in a variety of ways, depending on the application.

A key goal in the design of multiple-hood systems is establishment of the proper airflow at each hood. This is attained by a combination of two factors. The correct *total* flow through the system is obtained by selection of the proper fan; this process is discussed in Chapter 10. The proper *distribution* of the flow among the various hoods is obtained by balancing the airflow resistance of the hoods and their associated duct work. The process by which such balance is obtained is the subject of this chapter.

9.1 APPLICATIONS OF MULTIPLE-HOOD SYSTEMS

The most common application for a multiple-hood system is a manufacturing facility with a number of workstations that release the same airborne contaminant. Buffing and polishing lines are examples of this application. All workstations are provided with identical hoods exhausted at the same airflow and ducts are designed for a minimum transport velocity.

Another example is a foundry cleaning room, where the air contaminants released from the process include fused-silica sand and metal particles. Since the individual operations and equipment differ from station to station, the hood geometry and exhaust rate will vary. It is common practice to group these hoods in a multiple-hood system since the same contaminants are generated on each operation and one air cleaner can be used. Such a system will be designed in this chapter.

Grouping exhaust hoods into one system for operations that produce different airborne contaminants can present design and operational difficulties. As an example, assume that a series of hoods in a metal finishing shop handles noncorrosive gases and vapors. However, one hood exhausts a stripping tank releasing a corrosive acid mist. If the latter hood is included in a multiple-hood system, the entire system must be constructed of corrosion-resistant material. In this case, the solution may be to group all hoods handling noncorrosive air contaminants in one system and install a single-hood system constructed of materials appropriate for the corrosive bath. The grouping of hoods handling high concentrations of noncompatible or reactive materials is also poor practice, due to the potential for violent reaction.

In the foregoing examples of multiple-hood systems it was assumed all hoods are exhausted continuously. In many cases this may not be necessary. Each process may operate for a small fraction of the total shift and the operating times may be scattered throughout several shifts. Operating all hoods continuously will waste energy. One obvious solution is to install a separate hood-fan system for each process. Another approach is to utilize a multiple-hood system but equip each hood with a blast gate or damper that is opened only when the operation is underway. The required system exhaust capacity can be determined by a time study of all operations. Such an approach works when gases and vapors are to be conveyed; it frequently fails when particles are handled since variable airflows make it difficult to maintain proper transport velocities. A plenum exhaust system (*Ventilation Manual*, Chapter 5) is another technique available for this application. This system maintains a minimum transport velocity in the branches, but the low-velocity main or plenum acts as a settling chamber requiring periodic cleanout.

Several other cautions should be advanced. The installation of multiple-hood systems to provide exhaust for operations located in different departments under different supervision should be avoided if possible. Just as it is difficult to share production tooling, it is difficult to share local exhaust ventilation capacity. Another precaution should be observed during the system design phase. If a particular hood design is tentative because the hood shape and exhaust rate have not been validated, the hood should be a candidate for a separate fan. The reason is that extensive retrofitting of that hood might be necessary, possibly causing disruption of the rest of the system.

The permanence of the plant operations to be exhausted is critical to the successful design and operation of a large multiple-hood system. If frequent changes in process and equipment occur, large multiple-hood systems should be avoided. Modifications of existing multiple-hood systems to add hoods to the system without engineering review is one of the most flagrant problems encountered in local exhaust ventilation systems and frequently results in malfunctioning of the total system.

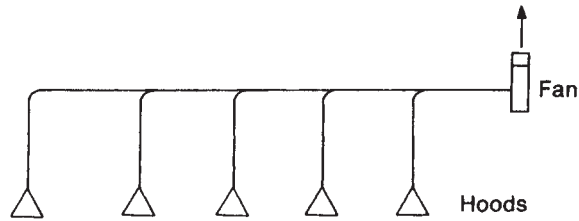


Figure 9.1 Multiple-hood system on similar operations with balance obtained by choice of duct size and airflow.

9.2 BALANCED DESIGN APPROACH

The process of obtaining the proper airflow distribution among hoods is termed *balancing*. Balancing is achieved either by the static pressure balance method or by the use of blast gates. In both approaches the desired flow through each branch and sub-main is obtained by providing the necessary static pressure and airflow resistance at each junction.

In the static pressure balance method (Fig. 9.1) the required static pressure at each junction is obtained by the choice of hood entry loss, duct size, and other resistance elements. If the design is executed properly and the appropriate fan is installed, the static pressures established in the design will be achieved and the required airflow will occur at each hood. This design approach is the preferred one and will be followed in this chapter.

In the blast gate balancing process, static pressures equal to or in excess of that required to maintain the desired flows are selected at each junction in the system. Blast gates are installed on each branch and are adjusted in the field to provide the branch resistance associated with the desired airflow (Fig. 9.2). An excellent critique of the two balancing methods by Caplan (1983) indicates the serious limitations in the blast gate method and describes why the static pressure balance method is preferred. A brief comparison of the two balancing methods is provided in Table 9.1.

A third system design procedure (Fig. 9.3) can be used on a multiple-hood system when the individual hoods are used intermittently. In this procedure the blast

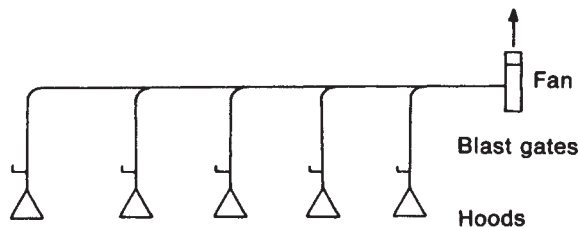


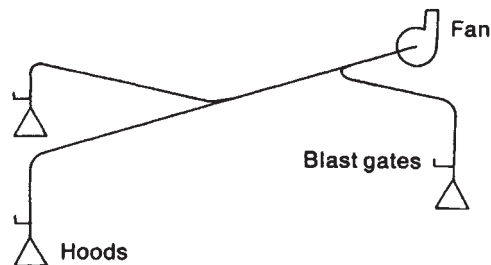
Figure 9.2 Multiple-hood system with adjustable blast gates used to obtain balance and correct airflow through each hood.

Table 9.1 Comparison of Balancing Methods

Balance without Blast Gates	Balance with Blast Gates
Air volumes cannot easily be changed by workers	Air volumes may be changed relatively easily
Little flexibility for future equipment changes or additions	Greater degree of flexibility for future changes or additions
Choice of exhaust volumes for a new operation may be incorrect	Improperly estimated exhaust volumes can be corrected
No unusual duct erosion or deposits in duct	Partially closed blast gates may cause erosion to slides, changing airflow, and may cause dust accumulations; ductwork may plug if the blast gate adjustments are tampered with
Design calculation is more time-consuming than blast gate method	Design calculations are relatively brief
Total air volumes are slightly greater than design air volume due to corrected airflows	Balance may be achieved with design air volume
Poor choice of “branch of greatest resistance” will show up in design calculations	Poor choice of “branch of greatest resistance” may remain undiscovered; in such case the branch of greater resistance will be “starved”
Layout of system must be in complete detail and installations must exactly follow layout	Allowance for variations in duct location to avoid obstructions or interferences not known at time of layout

Source: Adapted from ACGIH *Industrial Ventilation Manual*.

gates are not used for balancing but are merely on–off valves. This process requires that the designer define the utilization time of the various processes, and the system is designed to provide the necessary airflow through a limited number of hoods. It is obvious that if the blast gates on more than the specified hoods are open at one time the system will malfunction. The best way to prevent this is to interlock the operation with the hood dampers and use controls to restrict the number of operations that can be conducted at one time. It may be possible to operate such systems without

**Figure 9.3** Multiple-hood system with on–off blast gates to activate hood only when needed.

elaborate controls if the users are informed of the operating instructions and are diligent about closing dampers on hoods not in use.

A conventional multiple-hood system has a main duct run with individual branches joining the main at several locations. The design of multiple-hood systems is conducted in the same manner as the single-hood systems (Chapter 8). The individual branches can be viewed as single-hood systems and the main as a network of these simple systems. The designer defines the frictional and turbulent energy losses incurred by air flowing through each branch at the desired flow up to the junction at the submain or the main. An additional energy loss not encountered in the one-hood system is incurred as the branch enters the main duct. The goal in the static pressure balance design approach is to match the static pressure required by each branch with that available at the main where the branch enters. If these static pressures are matched and a fan of suitable capacity is provided, the design airflow will be drawn through the hood.

To optimize the design it is prudent to evaluate the product of airflow and total resistance for a number of different layouts of duct and fan. In each case the design should be started with the branch of highest resistance, since this tends to simplify the design procedure. The choice of this branch is frequently obvious, but the following guidelines may be helpful in choosing the design starting point:

- If hoods and exhaust airflows are all similar, the branch farthest from the fan is probably the one with the highest resistance.
- A hood with a combination of high entry loss and high airflow is a good candidate for the branch of highest resistance.
- A branch with high duct velocity may require the greatest static pressure.
- The use of long runs of flexible duct for hood mobility will frequently result in the branch of maximum resistance.

In any case, the static pressure balancing method is forgiving in this respect. If the branch of highest resistance is not chosen a priori, it will identify itself as the system is designed. This is not the case with the blast gate balancing method.

Once the branch of maximum resistance is chosen, the frictional and turbulent losses are calculated starting at the hood and proceeding to the first junction at the submain or main. The basic procedure is illustrated in Fig. 9.4. At the part of the system most distant from the fan, two branches join to form one end of the main (point A). The required static pressure in the first branch (1A) is calculated followed by the required static pressure in the second branch (2A). The two static pressures are then compared; if they differ, one of the branches will not have the proper airflow when the system is operated. This is true because only one static pressure can exist at point A. There are several design options available to balance these static pressures and obtain the desired airflows in both branches.

In the example, hood 1 requires an airflow of 2000 cfm and a static pressure at junction A of 0.8 in. H₂O. Hood 2 has a static pressure requirement of 0.95 in. H₂O at this junction to supply the required airflow of 500 cfm. In operation, the fan will

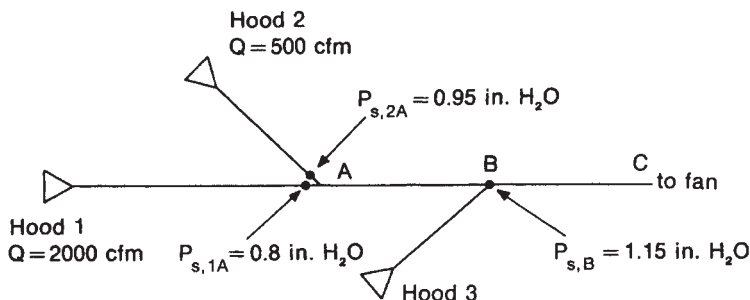


Figure 9.4 Branches 1A and 2A join at junction A. The design airflow and the total losses for the two runs are presented to permit the design of a balanced system.

supply only one value of static pressure to point A. If 0.8 in. H_2O is selected, hood 1 will have the proper airflow, but the design airflow of 500 cfm through hood 2 will not be attained. Since the duct velocity and airflow vary as the square root of static pressure, the flow through hood 2 will be $(500)(0.8/0.95)^{0.5} = 460$ cfm. Alternatively, the fan can be designed to provide 0.95 in. H_2O at point A. Now hood 2 will have the proper airflow, but hood 1 will have a new airflow of $(2000)(0.95/0.8)^{0.5}$ or 2180 cfm.

The three available options are to reduce the resistance in branch 2A, increase the resistance in branch 1A, or allow the increased flow in branch 1A. First, the design of hood 2 and its ductwork should be reviewed to determine if the resistance to airflow can be reduced. If the hood has a high entry loss, it might be replaced with a hood with a higher coefficient of entry. It might be possible to eliminate elbows. If the duct run is long and the duct velocity is high, it might be possible to increase the duct diameter, thereby reducing the duct velocity and resulting friction losses, but only if a minimum transport velocity is not required. In this example, hood 2 cannot be redesigned and the transport velocity in that branch must be maintained. Under this condition, redesign of branch 2A is not the solution.

The design of the hood 1 branch should now be reviewed. Since hood 2 cannot be changed, the static pressure in branch 1A must be increased to 0.95 in. H_2O to match that required by branch 2A. Boosting the required static pressure of the hood 1 branch can be accomplished in one of several ways. If the 2000 cfm airflow is to remain unchanged, the resistance to airflow must be increased. A high-loss hood could replace the original or a resistance element such as a blast gate could be installed in the duct. The duct size can also be reduced to increase duct velocity and frictional loss. A final alternative is to allow the increased airflow of 2180 cfm as calculated above. This option is selected here. The increased airflow might improve hood performance but has the disadvantage of increased operating cost. If an airflow is increased during this phase of the design process, it is designated as the corrected airflow.

The static pressure of 0.95 in. H_2O is defined as the governing static pressure or design point at junction A. In calculating the frictional loss from air flowing through the main (AB), the corrected flow of 2180 cfm from hood 1 is added to the 500 cfm through hood 2 to obtain the total airflow of 2680 cfm. The duct size and frictional

loss factor are obtained in the conventional way, and the static pressure loss for this segment is calculated as 0.2 in. H₂O. This static pressure is added to the governing static pressure at A (0.95 in. H₂O) to provide the required static pressure (1.15 in. H₂O) at junction B. The required pressure in branch 3B is then calculated and compared to the value at junction B. The design approach described above is then repeated for branch 3B and the final duct elements (BC) until the fan and outlet are reached.

In general, static pressures will not match perfectly at junctions. What is an acceptable balance at a junction, and what is the preferred design approach to correct this difference? The convention followed by most designers is to calculate the ratio of the two static pressures and follow the recommendations given in Table 9.2.

9.3 STATIC PRESSURE BALANCE METHOD

9.3.1 Foundry Cleaning Room System (Example 9.1)

A small foundry cleaning room will be used as an introductory multiple-hood design problem. This hypothetical foundry casts water-meter components from a brass alloy containing lead. After casting, the parts are taken to a shakeout operation, where the molding sand and core debris are removed. The parts are then cleaned in an abrasive blasting unit. Finally, the parts are “rough dressed” using a swing grinder, a belt sander, and a pedestal grinder. Since the alloy contains lead, the dust generated from these operations must be controlled using local exhaust ventilation.

A local exhaust ventilation system will be designed using the static pressure balancing method. This example requires balancing only by correcting airflow; duct resizing will be introduced as a balancing technique later in this chapter (Example 9.2).

Comments on the design are as follows:

- It is not necessary to use the *Ventilation Manual* VS design plates in this example, since the necessary design data are presented directly on Fig. 9.5.
- Because the system is designed for particle collection, a minimum velocity of 3500 fpm is chosen in this example. Beyond the air cleaner, the minimum

Table 9.2 Benchmarks for Balancing Multiple Hood Systems

If the Ratio of the Higher to Lower Static Pressure Is	Action
Less than 1.05	Acceptable; do not change flow in calculations; use higher static pressure as governing value
Between 1.05 and 1.20	Allow increased flow in branch of lowest static pressure; recalculate flow as $Q_{\text{corrected}} = Q_{\text{design}} \left(\frac{p_s \text{ of duct with higher loss}}{p_s \text{ of duct with lower loss}} \right)^{0.5}$
Greater than 1.20	Resize duct with lower static pressure

Notes:

1. Maintain duct velocity ≥ 3500 fpm up to filter; ≥ 2000 fpm beyond
2. Use $R/D = 2.0$ elbows & 30° entries

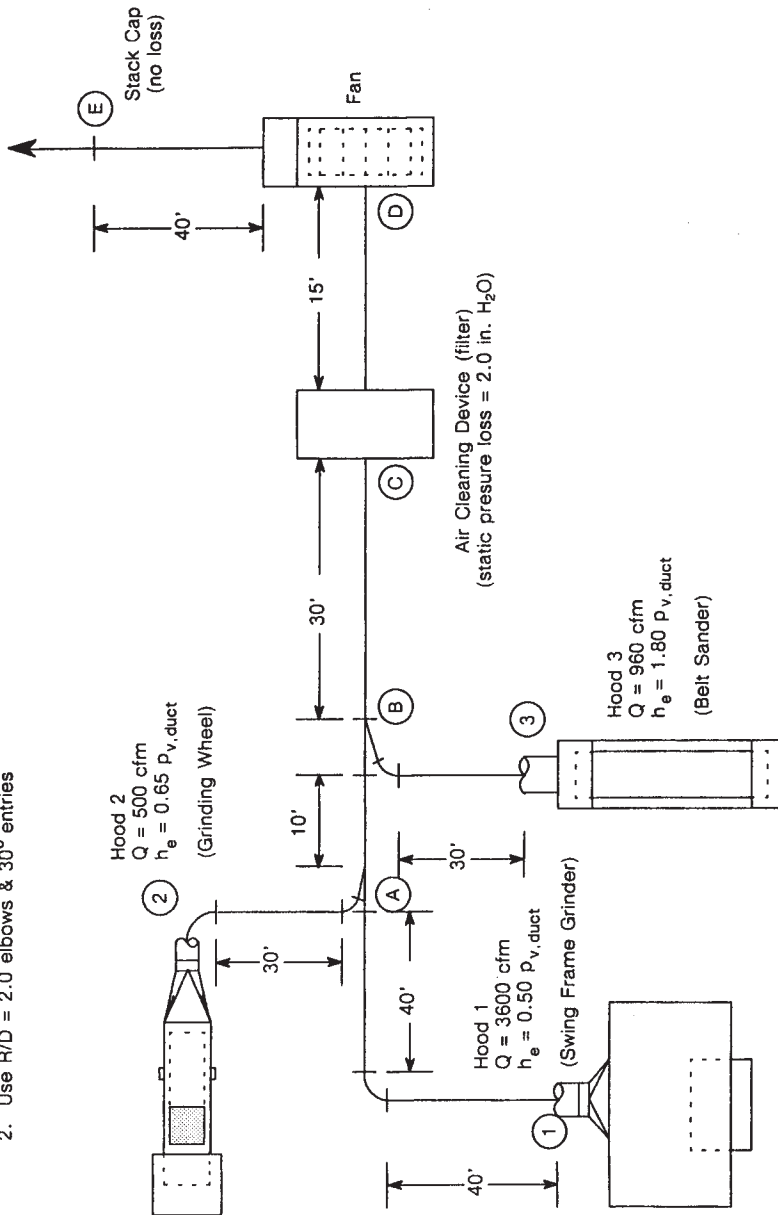


Figure 9.5 Layout of ductwork for local exhaust ventilation system in the foundry cleaning room.

velocity is reduced to 2000 fpm since particle transport is no longer required. This lower velocity allows for a larger duct diameter with lower frictional resistance losses.

- The resistance to airflow of the air cleaner normally is obtained from the manufacturer. In this example the static pressure loss incorporates all losses associated with the air cleaner, including turbulent losses at the entry to the filter, the resistance to airflow of the filter medium, and the transition from the air cleaner to the duct.
- The duct runs are all in one plane to simplify this introductory problem.
- All branch entries to the main are made at 30° angles. Preentry elbows on branches 2A and 3B must therefore be 60°.
- By convention, the loss due to a branch entry is included in the branch and not in the main.
- All hoods are simple hoods with a single loss factor, as shown in Fig. 9.5.

The calculation sheet for this problem is shown in Example 9.1. The solution of this design problem provides the following information, which is required for the effective installation, testing, and operation of this system:

1. Construction details, including duct layout and the number and type of special duct fittings in the installation.
2. Data for effective choice of the air mover including airflow and fan static pressure (see Chapter 10).
3. The hood static pressure that will exist if the desired hood airflow is achieved (line 27). Once the system is installed this pressure can be used to evaluate hood airflow, as discussed in Chapter 3.

9.3.2 Electroplating Shop (Example 9.2)

In Chapter 6 the common processes releasing air contaminants in electroplating operations were described and a variety of hood designs for effective control were presented. In Example 6.1 a technique described in the *Ventilation Manual* was used to calculate the minimum exhaust rate for a series of open-surface tanks in a small plating shop. This electroplating shop is shown in Fig. 9.6 and the exhaust rates for each tank are presented again in Table 9.3. These data are the basis for the design of a multiple-hood ventilation system using the static pressure balance method and the following design criteria.

- All tanks are provided with lateral slot exhaust using the upward plenum hood design (*Ventilation Manual*, VS 70-01). This design was chosen because it requires little floor space and the plenum provides an effective baffle. The hood entry loss is

$$h_e = 1.78p_{v,s} + 0.25p_{v,d}$$

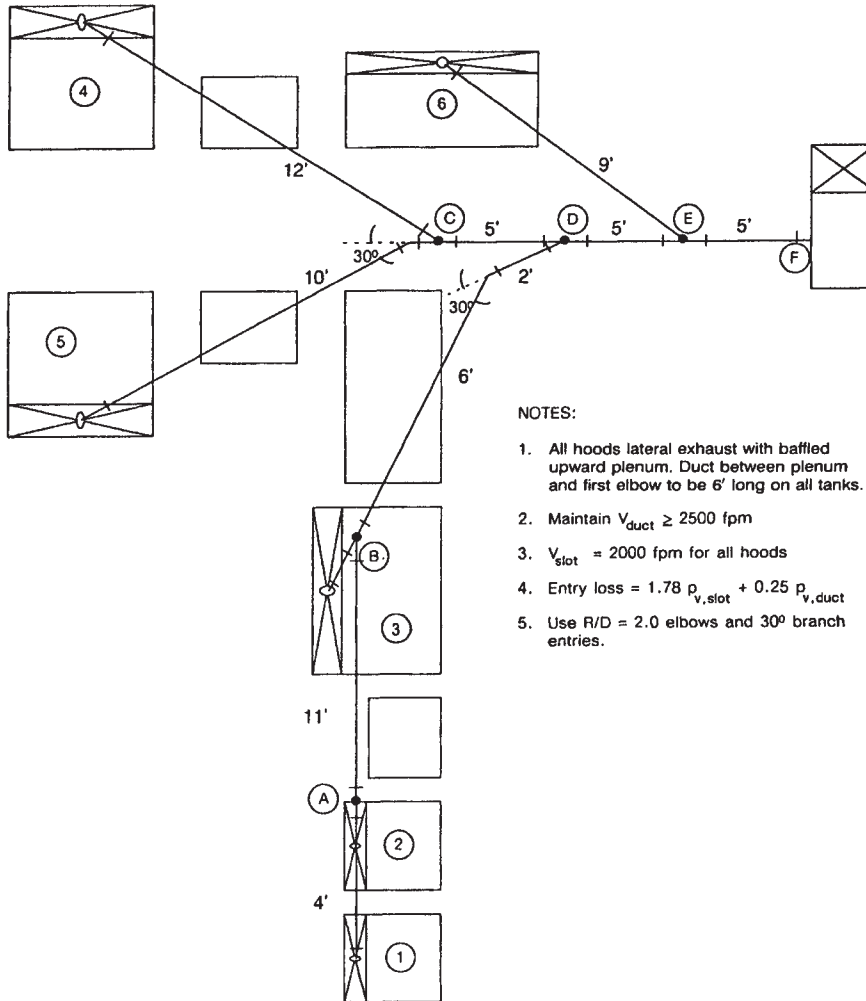


Figure 9.6 Layout of ductwork for local exhaust ventilation in the electroplating shop.

- All branches include a vertical run of 6 ft from the plenum to the elevation at which the horizontal main duct run will be made. This elevation was required to clear obstructions in the overhead.
- The minimum slot velocity is 2000 fpm. The fishtail design of the hood and the resistance presented by the slot ensure that the exhaust will be relatively constant along the length of the tank (see Chapter 5).
- In this system all 90° elbows are 4-piece and have an $R/D = 2.0$ and therefore a loss of $0.27p_v$. The layout of the duct in Fig. 9.6 shows the main running directly over the plenum so that the branches enter the main from the bottom. For this reason all entries except 1A will include a 60° elbow and a 30° branch entry.

Table 9.3 Exhaust Rates for Open-Surface Tanks in Example 9.2

Tank	Solution	Temperature (°C)	Class	Tank Dimensions			V Control (fpm)	Minimum Rate (cfm/ft ²)	Q (cfm)	A _s (ft ²)	Slot Width		Minimum Plenum Depth
				L	W	W/L					ft	in.	
1	Hot water	200	D-1	3	2	0.67	6	130	780	0.39	0.13	1.6	3.2
2	Cr strip	130	C-3	2½	2	0.86	4⅔	90	420	0.21	0.09	1.1	2.2
3	Acid Cu	110	B-3	6	3½	0.58	21	130	2730	1.36	0.23	2.7	5.4
4	Cr plate	115	A-1	4	3	0.75	12	150	3000	1.50	0.38	4.5	9.0
5	Ni plate	70	B-2	4	3	0.25	12	100	2100	1.05	0.26	3.1	6.2
6	Alkaline cleaner	200	C-1	5	2	0.40	10	150	1500	0.75	0.15	1.8	3.6

- All branch entries to main will be 30° and have a loss of $0.18p_v$.
- The submain duct run from hood 1 to junction D appears to present the greatest resistance to airflow; therefore, the sequence of calculations chosen is 1A, 2A, AB, 3B, BD, 4C, 5C, CD, DE, 6E, EF, and stack.
- Table 9.3 is based on Example 6.1 and has been expanded to show the technique used to design the slot and plenum as recommended in the *Ventilation Manual*.

9.4 BLAST GATE BALANCE METHOD

In this design technique the engineer chooses the hood that represents the maximum resistance to flow as the initial point in calculating losses. The system is designed from hood to first junction. At that point the design airflow from hood 1 is added to the airflow from hood 2, the main is sized, and losses are calculated for the section up to the main, where the branch from hood 3 enters the main. When hood 3 joins the main, its design airflow is added to the total of hoods 1 and 2 and the main is sized and losses calculated up to the next branch entry.

Accumulating static pressure losses in this manner assures that if the branch with maximum resistance is properly chosen for the start of the calculation, the static pressure in the main at any junction will be greater than that needed by the entering system branch. The desired airflow distribution can then be achieved by adjusting the blast gates provided on all hoods to adjust the required branch static pressure to equal the static pressure in the main.

This procedure is not as straightforward as it sounds, since the adjustment of a blast gate in one branch will affect the flow in adjacent branches. It is thus necessary to adjust all blast gates in a trial-and-error method until the proper balance is attained. Prior to the design of a system by the blast gate balance method the designer is encouraged to review the limitations of this technique (Caplan, 1983).

9.5 OTHER COMPUTATIONAL METHODS

Chapters 8 and 9 have dealt mainly with the manual design of balanced ventilation systems using the velocity pressure method. Although useful in introducing the design process and for the occasional design problem, the manual calculation sheet method is time-consuming. Since the mid-1970s a number of computer programs for the design of systems have been introduced in the open literature and by engineering consultants and manufacturers. One type of design program has been developed for the programmable hand calculator (Barritt, 1978; Malchaire, 1981; Shotwell, 1984). These have the merit of simplicity and are easily used in the field but may not have advanced features, such as automatic rebalancing. More recently, spreadsheet programs for personal computers have been applied to ventilation design using the velocity pressure method (Rennix, 1987; Koshland and Yost, 1987; Temple Systems, 1999). These powerful programs permit design of complex systems, optimization of design, and correction for nonstandard air.

266 DESIGN OF MULTIPLE-HOOD SYSTEMS

The widespread application of computer technology to ventilation system design will continue, and the person doing routine designs should take advantage of the speed and power of these programs.

LIST OF SYMBOLS

A	area
A_s	slot area
D	duct diameter
h_e	hood entry loss
L	length of tank
$p_{v,d}$	duct velocity pressure
$p_{v,s}$	slot velocity pressure
R/D	ratio of elbow sweep radius to diameter
Q	airflow
$Q_{\text{corrected}}$	corrected airflow
Q_{design}	design airflow
p_s	static pressure
T	temperature
V	average velocity
W	width of tank

EXAMPLE 9.1 FOUNDRY CLEANING ROOM DESIGNED BY STATIC PRESSURE BALANCE METHOD

Velocity pressure method calculation sheet (Part 1)*

1		Duct segment identification			1A	2A	AB	3B
2	T	Dry-bulb temperature						
3	Q	Standard volumetric flow rate		scfm	3600	500	4300	960
4	V_i	Minimum transport velocity		fpm	3500	3500	3500	3500
5	m_{H_2O}	Pounds of water per minute		#H ₂ O/min				
6	m_{da}	Pounds of dry air per minute		#da/min				
7	df	Density factor	Eq. 2					
8	Q_{act}	Actual volumetric flow rate	Eq. 3	acfm				
9	A_i	Target duct area	3+4	ft ²	1.03	0.14	1.23	0.27
10	d	Selected duct diameter		inches	13	5	14	7
11	A	Selected duct area		ft ²	0.922	0.136	1.069	0.267
12	V_d	Duct velocity	3+11	fpm	3910	3670	4020	3590
13	VP_d	Duct velocity pressure	Eq. 5	in. H ₂ O	0.95	0.84	1.01	0.80
14	h	Total heat	Branch balance	btu/#da				
15	A_s	Slot area		ft ²				
16	F_s	Slot loss coefficient						
17		Acceleration factor		0 or 1				
18	V_s	Slot velocity	8+15	fpm				
19	VP_s	Slot velocity pressure	Eq. 5	in. H ₂ O				
20		Slot loss in VP	16 + 17					
21		Slot static pressure	20 × 19	in. H ₂ O				
22	F_h	Duct entry coefficient			0.50	0.65		1.80
23		Acceleration factor		0 or 1	1.00	1.00		1.00
24		Duct entry loss in VP	22 + 23		1.50	1.65		2.80
25		Duct entry loss	24 × 13	in. H ₂ O	1.43	1.39		2.24
26		Other losses		in. H ₂ O				
27	SP_h	Hood static pressure	21 + 25 + 26	in. H ₂ O	1.43	1.39		2.24
28	l	Straight duct length		ft	80	30	10	30
29	H_f	Duct friction factor	Eq. 8		0.0165	0.054	0.0148	0.035
30		Number of 90° elbows			1	1.67		0.67
31	F_{el}	Elbow loss coefficient	Table 6		0.27	0.27		0.27
32	F_{en}	Branch entry coefficient	Table 7			0.18		0.18
33		Special fitting coefficient						
34	h_f	Duct friction loss in VP	28 × 29		1.32	1.62	0.148	1.05
35		Elbow loss in VP	30 × 31		0.27	0.45		0.18
36		Branch entry loss in VP	32			0.18		0.18
37		Duct loss in VP	33 + 34 + 35 + 36		1.59	2.25	0.148	1.41
38		Duct loss	37 × 13	in. H ₂ O	1.51	1.89	0.15	1.13
39		Other losses		in. H ₂ O				
40	VP_r	Resultant velocity pressure	Eq. 9	in. H ₂ O			1.04	
41		Loss from velocity increase	13 - 40 (if > 0)	in. H ₂ O				
42		Duct pressure loss	27 + 38 + 39 + 41	in. H ₂ O	2.94	3.28	0.15	3.37
43	SP_{gov}	Governing static pressure		in. H ₂ O	3.28	3.28	3.43	3.43
44	SP_{cum}	Cumulative static pressure		in. H ₂ O	2.94	3.28	3.43	3.37
45	Q_{corr}	Corrected volumetric flow rate	Eq. 10	acfm	3800			970
46	V_{corr}	Corrected velocity	45+11	fpm	4120			3630
47	VP_{corr}	Corrected velocity pressure	Eq. 5	in. H ₂ O	1.06			0.82

* This form is adapted from the ACGIH Ventilation Calculation Sheets: Velocity Pressure Method. Copies of blank forms suitable for design calculations can be purchased from the American Conference of Governmental Industrial Hygienists, Kemper Woods Center, 1330 Kemper Meadow Drive, Cincinnati, OH 45240-1634, customerservices@acgih.org.

Velocity pressure method calculation sheet (Part 2)

1		Duct segment identification			BC	CD	DE	FG
2	T	Dry-bulb temperature						
3	Q	Standard volumetric flow rate		scfm	5270	5270	5270	5270
4	V_i	Minimum transport velocity		fpm	3500		2000	2000
5	m_{H_2O}	Pounds of water per minute		#H ₂ O/min				
6	m_{da}	Pounds of dry air per minute		#da/min				
7	df	Density factor	Eq. 2					
8	Q_{act}	Actual volumetric flow rate	Eq. 3	acfm				
9	A_t	Target duct area	3+4	ft ²	1.51		2.64	2.64
10	d	Selected duct diameter		inches	16		22	22
11	A	Selected duct area		ft ²	1.396		2.64	2.64
12	V_d	Duct velocity	3+11	fpm	3780		2000	2000
13	VP_d	Duct velocity pressure	Eq. 5	in. H ₂ O	0.89		0.25	0.25
14	h	Total heat	Branch balance	btu/#da				
15	A_s	Slot area		ft ²				
16	F_s	Slot loss coefficient						
17		Acceleration factor		0 or 1				
18	V_s	Slot velocity	8+15	fpm				
19	VP_s	Slot velocity pressure	Eq. 5	in. H ₂ O				
20		Slot loss in VP	16 + 17					
21		Slot static pressure	20 × 19	in. H ₂ O				
22	F_h	Duct entry coefficient						
23		Acceleration factor		0 or 1				
24		Duct entry loss in VP	22 + 23					
25		Duct entry loss	24 × 13	in. H ₂ O				
26		Other losses		in. H ₂ O				
27	SP_h	Hood static pressure	21 + 25 + 26	in. H ₂ O				
28	l	Straight duct length		ft	30		15	40
29	H_f	Duct friction factor	Eq. 8		0.0125		0.0092	0.0092
30		Number of 90° elbows						
31	F_{el}	Elbow loss coefficient	Table 6					
32	F_{en}	Branch entry coefficient	Table 7					
33		Special fitting coefficient						
34	h_f	Duct friction loss in VP	28 × 29		0.375		0.14	0.37
35		Elbow loss in VP	30 × 31					
36		Branch entry loss in VP	32					
37		Duct loss in VP	33 + 34 + 35 + 36		0.375		0.14	0.37
38		Duct loss	37 × 13	in. H ₂ O	0.33		0.04	0.09
39		Other losses		in. H ₂ O		2.00		
40	VP_r	Resultant velocity pressure	Eq. 9	in. H ₂ O	0.98			
41		Loss from velocity increase	13–40 (if > 0)	in. H ₂ O				
42		Duct pressure loss	27 + 38 + 39 + 41	in. H ₂ O	0.33	2.00	0.04	0.09
43	SP_{gov}	Governing static pressure		in. H ₂ O				
44	SP_{cum}	Cumulative static pressure		in. H ₂ O	3.76	5.76	5.80	5.89
45	Q_{corr}	Corrected volumetric flow rate	Eq. 10	acfm				
46	V_{corr}	Corrected velocity	45+11	fpm				
47	VP_{corr}	Corrected velocity pressure	Eq. 5	in. H ₂ O				

Example 9.1 Design Notes for Calculation Sheet

General Comments. All velocities are rounded to the nearest 10 fpm, and all pressures are rounded to the nearest 0.01 in. H₂O. Lines 2, 5–8, and 14 are used only for nonstandard conditions; this example is at STP, so these lines are not used.

Line 9: “Target duct area” is the duct area corresponding to the minimum transport velocity; it is the maximum allowable duct area.

Line 10: The “Selected duct diameter” is the available duct diameter with a cross-sectional area closest to but not exceeding the “target duct area.”

Comments. Hood calculations are performed in lines 15–27; they are left blank for any duct segment without a hood. Lines 15–21 are used only for slot hoods or other compound hoods with two loss factors. Lines 28–39 are used to perform duct calculations; they are used for every duct segment. Lines 40–47 are used during the balancing process at a junction.

Branch 1A

Line 22: The duct entry coefficients are given in Fig. 9.5.

Line 23: The acceleration factor of $1p_v$ is taken on either line 17 or 23 for a slot hood; for a simple hood, as in this example, line 23 must equal 1.

Line 27: The hood static pressure, calculated here, is very useful for troubleshooting systems once they are built.

Line 37: The duct loss in this branch has two components: the friction loss through 80 ft of duct and one 90° elbow.

Line 38: The duct loss in velocity pressure is converted to actual duct loss in in. H₂O.

Line 42: The total static pressure loss in branch 1A is the sum of the hood static pressure and the static pressure loss in the duct.

Line 45: The corrected flow = $3600(3.28/2.94)^{1/2} = 3800$ cfm.

Lines 46–47: The velocity and velocity pressure corresponding to the corrected airflow are calculated here.

Branch 2A

Line 30: In this branch there are two elbows—one 90° elbow and one 60° elbow at the junction.

Line 32: By convention, the entry loss at a junction is taken in the branch entering at an angle rather than the main.

Line 37: In this case the duct loss has three components: the friction loss through 30 ft of duct, the loss in 1.67 elbows, and the entry loss.

Line 42: The static pressure required for branch 2A is 3.28 in. H₂O; since this is different from the 2.94 in. H₂O required for branch 1A, junction A must be balanced.

Line 43: The higher static pressure, in this case 3.28 in. H₂O, is always the governing static pressure.

Line 44: Calculate the static pressure ratio: $3.28/2.94 = 1.12$. Since this ratio is less than 1.2, it is necessary to correct the flow in branch 1A.

Main AB

Line 3: The total airflow in *AB* is the corrected airflow in branch 1A, 3800 cfm, plus the airflow in branch 2A, 500 cfm.

Lines 15–27: Since there is no hood in this duct segment, these lines are left blank.

Line 40: The resultant velocity pressure is calculated from the velocity pressures of the two ducts entering the junction.

Line 42: The only static pressure loss in this segment is the frictional loss through 10 ft of duct.

Line 44: The static pressure loss in branch *AB* is added to the governing static pressure at junction *A* to give the required static pressure at junction *B*: $3.28 \text{ in. H}_2\text{O} + 0.15 \text{ in. H}_2\text{O} = 3.43 \text{ in. H}_2\text{O}$.

Branch 3B

Line 45: Since the governing static pressure is for main *AB*, the flow in branch 3B is corrected.

Main BC

Line 3: The airflow in main *BC* is the flow in main *AB*, 4300 cfm, plus the corrected flow in branch 3B, 970 cfm.

Line 44: The static pressure at junction *C* equals the static pressure at junction *B* plus the static pressure loss in main *BC*.

Main CD

Line 39: The segment between junctions *C* and *D* constitutes the air cleaner. Its static pressure drop, 2 in. H₂O, is given in Fig. 9.5 and entered on line 39, “Other losses.”

Main DE

Line 4: Since the particles were removed in the air cleaner, the minimum duct transport velocity no longer needs to be observed. The velocity can be reduced to approximately 2000 cfm, with the actual duct diameter selected to match the fan inlet diameter (see Chapter 10).

Main EF

Line 44: The cumulative static pressure at junction *E* is the static pressure at the fan inlet, $p_{s,i}$ (see Fig. 10.9), and is actually a negative number (i.e., $-5.80 \text{ in. H}_2\text{O}$).

Main FG

Line 42: The static pressure loss in this segment is the loss in the stack and the calculated value, 0.09 in. H₂O, is the static pressure at the fan outlet, $p_{s,o}$, and is a positive value.

Line 44: The total static pressure required by the system, 5.89 in. H₂O, is the sum of the static pressure at the inlet to the fan, 5.80 in. H₂O, and the static pressure at the outlet from the fan, 0.09 in. H₂O.

EXAMPLE 9.2 ELECTROPLATING SHOP SYSTEM DESIGNED BY STATIC PRESSURE BALANCE METHOD

Velocity pressure method calculation sheet (Part 1)*

1		Duct segment identification		1A	2A	AB	3B(1)
2	T	Dry-bulb temperature					
3	Q	Standard volumetric flow rate	scfm	780	420	1240	2730
4	V_t	Minimum transport velocity	fpm	2500	2500	2500	2500
5	m_{H_2O}	Pounds of water per minute	#H ₂ O/min				
6	m_{da}	Pounds of dry air per minute	#da/min				
7	df	Density factor	Eq. 2				
8	Q_{act}	Actual volumetric flow rate	Eq. 3	acfm			
9	A_t	Target duct area	3+4	ft ²	0.31	0.17	0.50
10	d	Selected duct diameter		inches	7	5.5	9
11	A	Selected duct area		ft ²	0.267	0.165	0.442
12	V_d	Duct velocity	3+11	fpm	2920	2550	2810
13	VP_d	Duct velocity pressure	Eq. 5	in. H ₂ O	0.53	0.40	0.49
14	h	Total heat	Branch balance	btu/#da			
15	A_s	Slot area		ft ²	0.39	0.21	1.36
16	F_s	Slot loss coefficient			1.78	1.78	1.78
17		Acceleration factor		0 or 1	0	0	0
18	V_s	Slot velocity	8+15	fpm	2000	2000	2000
19	VP_s	Slot velocity pressure	Eq. 5	in. H ₂ O	0.25	0.25	0.25
20		Slot loss in VP	16 + 17		1.78	1.78	1.78
21		Slot static pressure	20 × 19	in. H ₂ O	0.45	0.45	0.45
22	F_k	Duct entry coefficient			0.25	0.25	0.25
23		Acceleration factor		0 or 1	1.00	1.00	1.00
24		Duct entry loss in VP	22 + 23		1.25	1.25	1.25
25		Duct entry loss	24 × 13	in. H ₂ O	0.66	0.50	0.50
26		Other losses		in. H ₂ O			
27	SP_h	Hood static pressure	21 + 25 + 26	in. H ₂ O	1.11	0.95	0.95
28	l	Straight duct length		ft	10	6	11
29	H_f	Duct friction factor	Eq. 8		0.037	0.049	0.016
30		Number of 90° elbows			1	0.67	1
31	F_{el}	Elbow loss coefficient	Table 6		0.27	0.27	0.27
32	F_{en}	Branch entry coefficient	Table 7			0.18	0.18
33		Special fitting coefficient					
34	h_f	Duct friction loss in VP	28 × 29		0.37	0.29	0.30
35		Elbow loss in VP	30 × 31		0.27	0.18	0.27
36		Branch entry loss in VP	32			0.18	0.18
37		Duct loss in VP	33 + 34 + 35 + 36		0.64	0.65	0.48
38		Duct loss	37 × 13	in. H ₂ O	0.34	0.26	0.24
39		Other losses		in. H ₂ O			
40	VP_r	Resultant velocity pressure	Eq. 9	in. H ₂ O		0.51	
41		Loss from velocity increase	13 – 40 (if > 0)	in. H ₂ O			
42		Duct pressure loss	27 + 38 + 39 + 41	in. H ₂ O	1.45	1.21	0.24
43	SP_{gov}	Governing static pressure		in. H ₂ O	1.45	1.45	1.71
44	SP_{cum}	Cumulative static pressure		in. H ₂ O	1.45	1.21	1.69
45	Q_{corr}	Corrected volumetric flow rate	Eq. 10	acfm	460	1250	Resize
46	V_{corr}	Corrected velocity	45+11	fpm	2790	2820	
47	VP_{corr}	Corrected velocity pressure	Eq. 5	in. H ₂ O	0.48	0.50	

*This form is adapted from the ACGIH Ventilation Calculation Sheets: Velocity Pressure Method. Copies of blank forms suitable for design calculations can be purchased from the American Conference of Governmental Industrial Hygienists, Kemper Woods Center, 1330 Kemper Meadow Drive, Cincinnati, OH 45240-1634, customerservices@acgih.org.

Velocity pressure method calculation sheet (Part 2)

1		Duct segment identification			3B(2)	3B(3)	BD	4C
2	T	Dry-bulb temperature						
3	Q	Standard volumetric flow rate		scfm	2730	2730	3980	3000
4	V_t	Minimum transport velocity		fpm	2500	2500	2500	2500
5	m_{H_2O}	Pounds of water per minute		#H ₂ O/min				
6	m_{da}	Pounds of dry air per minute		#da/min				
7	df	Density factor	Eq. 2					
8	Q_{act}	Actual volumetric flow rate	Eq. 3	acfm				
9	A_t	Target duct area	3÷4	ft ²			1.59	1.20
10	d	Selected duct diameter		inches	13	12	17	14
11	A	Selected duct area		ft ²	0.922	0.785	1.576	1.069
12	V_d	Duct velocity	3+11	fpm	2960	3480	2520	2800
13	VP_d	Duct velocity pressure	Eq. 5	in. H ₂ O	0.55	0.75	0.40	0.49
14	h	Total heat	Branch balance	btu/#da				
15	A_s	Slot area		ft ²	1.36	1.36		1.50
16	F_s	Slot loss coefficient			1.78	1.78		1.78
17		Acceleration factor		0 or 1	0	0		0
18	V_s	Slot velocity	8+15	fpm	2000	2000		2000
19	VP_s	Slot velocity pressure	Eq. 5	in. H ₂ O	0.25	0.25		0.25
20		Slot loss in VP	16 + 17		1.78	1.78		1.78
21		Slot static pressure	20 × 19	in. H ₂ O	0.45	0.45		0.45
22	F_h	Duct entry coefficient			0.25	0.25		0.25
23		Acceleration factor		0 or 1	1.00	1.00		1.00
24		Duct entry loss in VP	22 + 23		1.25	1.25		1.25
25		Duct entry loss	24 × 13	in. H ₂ O	0.69	0.94		0.61
26		Other losses		in. H ₂ O				
27	SP_h	Hood static pressure	21 + 25 + 26	in. H ₂ O	1.14	1.39		1.06
28	l	Straight duct length		ft	8	8	8	18
29	H_f	Duct friction factor	Eq. 8		0.017	0.019	0.013	0.016
30		Number of 90° elbows			1	1	0.33	1
31	F_{el}	Elbow loss coefficient	Table 6		0.27	0.27	0.27	0.27
32	F_{en}	Branch entry coefficient	Table 7				0.18	0.18
33		Special fitting coefficient						
34	h_f	Duct friction loss in VP	28 × 29		0.14	0.15	0.10	0.28
35		Elbow loss in VP	30 × 31		0.27	0.27	0.09	0.27
36		Branch entry loss in VP	32				0.18	0.18
37		Duct loss in VP	33 + 34 + 35 + 36		0.41	0.42	0.37	0.73
38		Duct loss	37 × 13	in. H ₂ O	0.23	0.32	0.15	0.36
39		Other losses		in. H ₂ O				
40	VP_r	Resultant velocity pressure	Eq. 9	in. H ₂ O			0.67	
41		Loss from velocity increase	13 - 40 (if > 0)	in. H ₂ O				
42		Duct pressure loss	27 + 38 + 39 + 41	in. H ₂ O	1.37	1.71	0.15	1.42
43	SP_{gov}	Governing static pressure		in. H ₂ O	1.69	1.71	1.86	1.42
44	SP_{cum}	Cumulative static pressure		in. H ₂ O	1.37	1.71	1.86	1.42
45	Q_{corr}	Corrected volumetric flow rate	Eq. 10	acfm	Resize			
46	V_{corr}	Corrected velocity	45÷11	fpm				
47	VP_{corr}	Corrected velocity pressure	Eq. 5	in. H ₂ O				

Velocity pressure method calculation sheet (Part 3)

1		Duct segment identification			5C	CD(1)	CD(2)	DE
2	T	Dry-bulb temperature						
3	Q	Standard volumetric flow rate		scfm	2100	5190	5190	9490
4	V_f	Minimum transport velocity		fpm	2500	2500	2500	2500
5	m_{H_2O}	Pounds of water per minute		#H ₂ O/min				
6	m_{da}	Pounds of dry air per minute		#da/min				
7	df	Density factor	Eq. 2					
8	Q_{act}	Actual volumetric flow rate	Eq. 3	acfm				
9	A_t	Target duct area	3+4	ft ²	0.84	2.08		3.80
10	d	Selected duct diameter		inches	12	19	17	26
11	A	Selected duct area		ft ²	0.785	1.969	1.576	3.687
12	V_d	Duct velocity	3+11	fpm	2670	2640	3290	2570
13	VP_d	Duct velocity pressure	Eq. 5	in. H ₂ O	0.45	0.43	0.68	0.41
14	h	Total heat	Branch balance	btu/#da				
15	A_s	Slot area		ft ²	1.05			
16	F_s	Slot loss coefficient			1.78			
17		Acceleration factor		0 or 1	0			
18	V_s	Slot velocity	8+15	fpm	2000			
19	VP_s	Slot velocity pressure	Eq. 5	in. H ₂ O	0.25			
20		Slot loss in VP	16 + 17		1.78			
21		Slot static pressure	20 × 19	in. H ₂ O	0.45			
22	F_h	Duct entry coefficient			0.25			
23		Acceleration factor		0 or 1	1.00			
24		Duct entry loss in VP	22 + 23		1.25			
25		Duct entry loss	24 × 13	in. H ₂ O	0.56			
26		Other losses		in. H ₂ O				
27	SP_h	Hood static pressure	21 + 25 + 26	in. H ₂ O	1.01			
28	I	Straight duct length		ft	16	5	5	5
29	H_f	Duct friction factor	Eq. 8		0.019	0.011	0.012	0.007
30		Number of 90° elbows			1.33			
31	F_{el}	Elbow loss coefficient	Table 6		0.27			
32	F_{en}	Branch entry coefficient	Table 7					
33		Special fitting coefficient						
34	h_f	Duct friction loss in VP	28 × 29		0.30	0.05	0.06	0.04
35		Elbow loss in VP	30 × 31		0.36			
36		Branch entry loss in VP	32					
37		Duct loss in VP	33 + 34 + 35 + 36		0.66	0.05	0.06	0.04
38		Duct loss	37 × 13	in. H ₂ O	0.30	0.02	0.04	0.02
39		Other losses		in. H ₂ O				
40	VP_r	Resultant velocity pressure	Eq. 9	in. H ₂ O			0.49	
41		Loss from velocity increase	13 - 40 (if > 0)	in. H ₂ O			0.19	
42		Duct pressure loss	27 + 38 + 39 + 41	in. H ₂ O	1.31	0.02	0.23	0.02
43	SP_{gov}	Governing static pressure		in. H ₂ O	1.42	1.86	1.86	1.96
44	SP_{cum}	Cumulative static pressure		in. H ₂ O	1.31	1.44	1.65	1.88
45	Q_{corr}	Corrected volumetric flow rate	Eq. 10	acfm	2190	Resize	5510	9690
46	V_{corr}	Corrected velocity	45+11	fpm	2780		3500	2630
47	VP_{corr}	Corrected velocity pressure	Eq. 5	in. H ₂ O	0.48		0.76	0.43

Velocity pressure method calculation sheet (Part 4)

1		Duct segment identification			6E(1)	6E(2)	EF	FG
2	T	Dry-bulb temperature						
3	Q	Standard volumetric flow rate		scfm	1500	1500	11,190	11,190
4	V_t	Minimum transport velocity		fpm	2500	2500	2500	2500
5	m_{H_2O}	Pounds of water per minute		#H ₂ O/min				
6	m_{da}	Pounds of dry air per minute		#da/min				
7	df	Density factor	Eq. 2					
8	Q_{act}	Actual volumetric flow rate	Eq. 3	acfm				
9	A_t	Target duct area	3+4	ft ²	0.60		4.48	4.48
10	d	Selected duct diameter		inches	10	9	28	28
11	A	Selected duct area		ft ²	0.545	0.442	4.276	4.276
12	V_d	Duct velocity	3+11	fpm	2750	3400	2620	2620
13	VP_d	Duct velocity pressure	Eq. 5	in. H ₂ O	0.47	0.72	0.43	0.43
14	h	Total heat	Branch balance	btu/#da				
15	A_s	Slot area		ft ²	0.75	0.75		
16	F_s	Slot loss coefficient			1.78	1.78		
17		Acceleration factor		0 or 1	0	0		
18	V_s	Slot velocity	8+15	fpm	2000	2000		
19	VP_s	Slot velocity pressure	Eq. 5	in. H ₂ O	0.25	0.25		
20		Slot loss in VP	16 + 17		1.78	1.78		
21		Slot static pressure	20 × 19	in. H ₂ O	0.45	0.45		
22	F_h	Duct entry coefficient			0.25	0.25		
23		Acceleration factor		0 or 1	1.00	1.00		
24		Duct entry loss in VP	22 + 23		1.25	1.25		
25		Duct entry loss	24 × 13	in. H ₂ O	0.59	0.90		
26		Other losses		in. H ₂ O				
27	SP_h	Hood static pressure	21 + 25 + 26	in. H ₂ O	1.04	1.35		
28	l	Straight duct length		ft	15	15	5	15
29	H_f	Duct friction factor	Eq. 8		0.024	0.027	0.007	0.007
30		Number of 90° elbows			1	1		
31	F_{el}	Elbow loss coefficient	Table 6		0.27	0.27		
32	F_{cn}	Branch entry coefficient	Table 7		0.18	0.18		
33		Special fitting coefficient						
34	h_f	Duct friction loss in VP	28 × 29		0.36	0.40	0.03	0.10
35		Elbow loss in VP	30 × 31		0.27	0.27		
36		Branch entry loss in VP	32		0.18	0.18		
37		Duct loss in VP	33 + 34 + 35 + 36		0.81	0.85	0.03	0.10
38		Duct loss	37 × 13	in. H ₂ O	0.38	0.61	0.01	0.04
39		Other losses		in. H ₂ O				
40	VP_r	Resultant velocity pressure	Eq. 9	in. H ₂ O				
41		Loss from velocity increase	13 – 40 (if > 0)	in. H ₂ O				
42		Duct pressure loss	27 + 38 + 39 + 41	in. H ₂ O	1.42	1.96	0.01	0.04
43	SP_{gov}	Governing static pressure		in. H ₂ O	1.88	1.96	1.97	2.01
44	SP_{cum}	Cumulative static pressure		in. H ₂ O	1.42		1.97	2.01
45	Q_{corr}	Corrected volumetric flow rate	Eq. 10	acfm	Resize			
46	V_{corr}	Corrected velocity	45 ÷ 11	fpm				
47	VP_{corr}	Corrected velocity pressure	Eq. 5	in. H ₂ O				

Example 9.2 Design Notes for Calculation Sheet**Column 1A**

Line 3: The design airflow for each hood is taken from Table 9.3.

Lines 15–21: Lateral slot exhaust hoods have a complex entry loss, as discussed in Section 8.3. Calculations for the first loss element, the slot, are entered on these lines.

Lines 22–27: Calculations for the second loss element, the transition from the plenum to the duct, are made here.

Line 15: The slot area is chosen to give the desired slot velocity:

$$A = \frac{Q}{V} = \frac{(780 \text{ ft}^3/\text{min})}{2000 \text{ ft/min}} = 0.39 \text{ ft}^2$$

Line 17: The acceleration factor of $1.0p_v$ must be entered either here or on line 23. If the slot velocity is higher than the duct velocity, it is taken here; if the duct velocity is higher than the slot velocity, as in this case, the acceleration factor is entered on line 23.

Line 28: The duct length consists of a 6-ft vertical riser and a 4-ft horizontal run.

Line 30: There is a 90° elbow at the top of each riser, except for hood 2.

Line 43: This entry is discussed under branch 2A below.

Column 2A

Line 32: Since branch 2A enters branch 1A, the entry loss is taken here.

Line 43: The governing static pressure at junction A, 1.45 in. H_2O , is entered in line 45 for both branches entering the junction.

Line 45: The required static pressure at junction A is 1.45 in. H_2O in branch 1 and 1.21 in. H_2O in branch 2. Since only one static pressure can exist at junction A, the higher value is selected as the controlling static pressure and the ratio of the two calculated:

$$\frac{P_{s, 1A}}{P_{s, 2A}} = \frac{1.45}{1.21} = 1.20$$

According to Table 9.2, this ratio is the highest value allowed without resizing the ducts. Therefore, the two duct sizes are accepted and the flow through branch 2A is corrected using the equation in Table 9.2:

$$Q_{\text{corrected}} = 420 \left(\frac{1.45}{1.21} \right)^{0.5} = 460 \text{ cfm}$$

This value is entered on line 45.

Lines 46 and 47: New values of velocity and velocity pressure are calculated corresponding to the new airflow in the branch.

Column AB

Line 3: The airflow in duct *AB* is the sum of the original flow in branch 1A (780 cfm) and the *corrected* flow in branch 2A (460 cfm).

Lines 15–27: Since there is no hood in this duct segment, these lines are blank.

Line 44: The additional static pressure loss in branch *AB* (0.24 in. H₂O) is added to the governing static pressure at junction A (1.45 in. H₂O) to give the cumulative static pressure at junction *B* (1.69 in. H₂O).

Column 3B(1)

Lines 42 and 44: The calculated static pressure loss in branch 3B (1.11 in. H₂O) is entered in line 42; since this branch starts at a hood, the cumulative static pressure is the same and is entered in line 44.

Line 45: The two values of cumulative static pressure at junction *B* are compared:

$$\frac{P_{s,AB}}{P_{s,3B}} = \frac{1.69}{1.11} = 1.52$$

Since this ratio is >1.20 , according to Table 9.2, the duct with the smaller static pressure must be resized. This is done in the next column.

Column 3B(2)

Line 1: When a duct is resized it is given the (2) designation.

Line 10: Since the static pressure loss in the branch must be increased, the duct diameter must be reduced. The next smaller duct diameter, 13 in., is tried. (An alternative approach would be to decrease the slot area, increasing the slot static pressure loss.)

Lines 42 and 44: The new static pressure loss at junction *B* is 1.37 in. H₂O.

Line 45: The new static pressure ratio is

$$\frac{P_{s,AB}}{P_{s,3B}} = \frac{1.69}{1.37} = 1.23$$

The ratio is still >1.20 ; therefore, the duct must be resized a second time.

Column 3B(3)

Line 10: The new duct diameter is 12 in.

Lines 42 and 44: The new static pressure is 1.71 in. H₂O.

Line 45: Now the flow in branch *AB* can be corrected:

$$Q_{\text{corr}} = 1240 \left(\frac{1.71}{1.69} \right)^{0.5} = 1250 \text{ cfm}$$

Column BD

Line 45: The losses in duct *BD* (0.15 in. H₂O) are added to the governing static pressure at junction *B* (1.71 in. H₂O) to obtain the cumulative static pressure at junction *D* (1.86 in. H₂O).

Columns 4C and 5C. The same procedure is used to balance junction *C*.

Column CD(1)

Line 45: Cumulative static pressures in duct *BD* (1.86 in. H₂O) and *CD* (1.44 in. H₂O) are compared, the ratio is >1.20, and duct *CD* must be resized.

Column CD(2)

Lines 40 and 41: With the decreased duct size, the velocity pressure in duct *CD* has increased significantly. Therefore, the resultant velocity pressure in the two ducts entering junction *C* is calculated using Eq. 5.6 of the *Ventilation Manual*. Since this resultant static pressure entering junction *C* (0.49 in. H₂O) is less than the static pressure leaving junction *C* (0.68 in. H₂O), an additional acceleration term must be applied, which is the difference between the two values (0.19 in. H₂O). This is entered on line 41 and added to the other losses in branch *CD*.

Line 45: The new static pressure ratio is <1.20, so the corrected airflow in duct *CD* can be calculated:

$$Q_{\text{corr}} = 5190 \left(\frac{1.86}{1.65} \right)^{0.5} = 5510 \text{ cfm}$$

Column DE

Line 3: The airflow in duct *DE* is the sum of the original flow in branch *BD* (3980 cfm) and the *corrected* flow in branch *CD* (5510 cfm).

Columns 6E(1) and 6E(2). The first design of branch *6E* once again results in an unbalanced junction, so it must be resized. The second duct size works, but now the static pressure in this branch governs and the flow in duct *DE* must be corrected:

$$Q_{\text{corr}} = 9490 \left(\frac{1.96}{1.88} \right)^{0.5} = 9690 \text{ cfm}$$

Column EF

Line 3: The total flow through the system can now be calculated as the flow through *6E* (1500 cfm) and the *corrected* flow in *DE* (9690 cfm).

REFERENCES

American Conference of Governmental Industrial Hygienists, Committee on Industrial Ventilation, *Industrial Ventilation Manual*, 24th ed., ACGIH, Lansing, MI, 2001.

- Barritt, S. L., "Duct Design by Programmable Calculator," *Heat./Piping/Air Cond.* (Dec. 1978).
- Caplan, K. J., "Balance with Blast Gates—a Precarious Balance," *Heat./Piping/Air Cond.* (Feb. 1983).
- Chen, S. Y. S., "Design Procedure for Duct Calculations," *Heat./Piping/Air Cond.* (Jan. 1981).
- Clapp, D. E., D. S. Groh, and J. D. Nenandic, "Ventilation Design by Microcomputer," *Am. Ind. Hyg. Assoc. J.* **43**:212 (1982).
- Guffey, S. E., "An Easier Calculation System for Ventilation Design," *Am. Ind. Hyg. Assoc. J.* **44**:627 (1983).
- Guffey, S., and J. Hickey, "Equations for Redesign of Existing Ventilation Systems," *Am. Ind. Hyg. Assoc. J.* **44**:819 (1983).
- Koshland, C. P., and M. G. Yost, "Use of a Spreadsheet in the Design of an Industrial Ventilation System," *Appl. Ind. Hyg.* **2**:204 (1987).
- Lynch, J. R., "Computer Design of Industrial Exhaust Systems," *Heat./Piping/Air Cond.* (Sept. 1968).
- Malchaire, J. B., "Design of Industrial Exhaust Systems Using a Programmable Calculator," *Ann. Occup. Hyg.* **24**:217 (1981).
- Rennix, C. P., "Computer Assisted Ventilation Design and Evaluation," *Appl. Ind. Hyg.*, **2**:32 (1987).
- Shotwell, H. P., "A Ventilation Design Program for Hand-Held Programmable Computers," *Am. Ind. Hyg. Assoc. J.* **45**:749 (1984).
- Temple Systems, Inc., *J. Square Duct 2.0, Industry Standard for Ventilation System Sizing and Balancing*, 1999.

ADDITIONAL READING

- Burton, D. J., *Companion Study Guide to Industrial Ventilation: A Manual of Recommended Practice*, ACGIH, Cincinnati, OH, 2001.

APPENDIX: METRIC VERSION OF EXAMPLE 9.1

Velocity pressure method calculation sheet (Part 1)—metric version*

1		Duct segment identification			1A	2A	AB	3B
2	T	Dry-bulb temperature						
3	Q	Standard volumetric flow rate		m ³ /s	1.70	0.50	2.49	0.45
4	V_t	Minimum transport velocity		m/s	17.5	17.5	17.5	17.5
5	m_{H_2O}	Kilograms of water per minute		kg H ₂ O/min				
6	m_{da}	Kilograms of dry air per minute		kg da/min				
7	df	Density factor	Eq. 2					
8	Q_{act}	Actual volumetric flow rate	Eq. 3	m ³ /s				
9	A_t	Target duct area	3+4	m ²	0.097	0.029	0.142	0.026
10	d	Selected duct diameter		mm	350	180	425	180
11	A	Selected duct area		m ²	0.096	0.025	0.142	0.025
12	V_d	Duct velocity	3+11	m/s	17.7	19.7	17.5	17.7
13	VP_d	Duct velocity pressure	Eq. 5	Pa	188	233	184	189
14	h	Total heat	Branch balance	J/kg da				
15	A_s	Slot area		m ²				
16	F_s	Slot loss coefficient						
17		Acceleration factor		0 or 1				
18	V_s	Slot velocity	8+15	fpm				
19	VP_s	Slot velocity pressure	Eq. 5	Pa				
20		Slot loss in VP	16 + 17					
21		Slot static pressure	20 × 19	Pa				
22	F_h	Duct entry coefficient			0.50	0.65		
23		Acceleration factor		0 or 1	1.00	1.00		
24		Duct entry loss in VP	22 + 23		1.50	1.65		
25		Duct entry loss	24 × 13	Pa	282	384		
26		Other losses		Pa				
27	SP_h	Hood static pressure	21 + 25 + 26	Pa	282	384		
28	l	Straight duct length		m	29.4	9.1	3.0	9.1
29	H_f	Duct friction factor	Eq. 8		0.052	0.116	0.041	0.117
30		Number of 90° elbows			1	1.67		0.67
31	F_{el}	Elbow loss coefficient	Table 6		0.27	0.27		0.18
32	F_{en}	Branch entry coefficient	Table 7			0.18		
33		Special fitting coefficient						
34	h_f	Duct friction loss in VP	28 × 29		1.26	1.06	0.12	1.06
35		Elbow loss in VP	30 × 31		0.27	0.45		0.18
36		Branch entry loss in VP	32			0.18		0.18
37		Duct loss in VP	33 + 34 + 35 + 36		1.53	1.69	0.12	1.42
38		Duct loss	37 × 13	Pa	288	394	22	268
39		Other losses		Pa				
40	VP_r	Resultant velocity pressure	Eq. 9	Pa				
41		Loss from velocity increase	13–40 (if > 0)	Pa				
42		Duct pressure loss	27 + 38 + 39 + 41	Pa	570	778	22	797
43	SP_{gov}	Governing static pressure		Pa	778	778	800	800
44	SP_{cum}	Cumulative static pressure		Pa	570	778	800	797
45	Q_{corr}	Corrected volumetric flow rate	Eq. 10	m ³ /s	1.99			
46	V_{corr}	Corrected velocity	45+11	m/s	20.7			
47	VP_{corr}	Corrected velocity pressure	Eq. 5	Pa	258			

*This form is adapted from the ACGIH Ventilation Calculation Sheets: Velocity Pressure Method. Copies of blank forms suitable for design calculations can be purchased from the American Conference of Governmental Industrial Hygienists, Kemper Woods Center, 1330 Kemper Meadow Drive, Cincinnati, OH 45240-1634, customerservices@acgih.org.

Velocity pressure method calculation sheet (Part 2)—metric version

1		Duct segment identification			BC	CD	DE	FG
2	T	Dry-bulb temperature						
3	Q	Standard volumetric flow rate		m^3/s	2.94	2.94	2.94	2.94
4	V_t	Minimum transport velocity		m/s	17.5		10.0	10.0
5	$m_{\text{H}_2\text{O}}$	Kilograms of water per minute		$\text{kg H}_2\text{O}/\text{min}$				
6	m_{da}	Kilograms of dry air per minute		$\text{kg da}/\text{min}$				
7	df	Density factor	Eq. 2					
8	Q_{act}	Actual volumetric flow rate	Eq. 3	m^3/s				
9	A_t	Target duct area	3+4	m^2	0.168		0.294	0.294
10	d	Selected duct diameter		mm	450		600	600
11	A	Selected duct area		m^2	0.159		0.283	0.283
12	V_d	Duct velocity	3+11	m/s	18.5		10.4	10.4
13	VP_d	Duct velocity pressure	Eq. 5	Pa	205		65	65
14	h	Total heat	Branch balance	J/kg da				
15	A_s	Slot area		m^2				
16	F_s	Slot loss coefficient						
17		Acceleration factor		0 or 1				
18	V_s	Slot velocity	8+15	fpm				
19	VP_s	Slot velocity pressure	Eq. 5	Pa				
20		Slot loss in VP	16 + 17					
21		Slot static pressure	20 + 19	Pa				
22	F_h	Duct entry coefficient						
23		Acceleration factor		0 or 1				
24		Duct entry loss in VP	22 + 23					
25		Duct entry loss	24 + 13	Pa				
26		Other losses		Pa				
27	SP_h	Hood static pressure	21 + 25 + 26	Pa				
28	I	Straight duct length		m	9.1		4.6	12.2
29	H_f	Duct friction factor	Eq. 8		0.038		0.028	0.028
30		Number of 90° elbows						
31	F_{el}	Elbow loss coefficient	Table 6					
32	F_{en}	Branch entry coefficient	Table 7					
33		Special fitting coefficient						
34	h_f	Duct friction loss in VP	28 + 29		0.35		0.13	0.34
35		Elbow loss in VP	30 + 31					
36		Branch entry loss in VP	32					
37		Duct loss in VP	33 + 34 + 35 + 36		0.35		0.13	0.34
38		Duct loss	37 + 13	Pa	72		8	22
39		Other losses		Pa		500		
40	VP_r	Resultant velocity pressure	Eq. 9	Pa				
41		Loss from velocity increase	13 – 40 (if > 0)	Pa				
42		Duct pressure loss	27 + 38 + 39 + 41	Pa	72	500	8	22
43	SP_{gov}	Governing static pressure		Pa				
44	SP_{cum}	Cumulative static pressure		Pa	872	1372	1380	1402
45	Q_{cor}	Corrected volumetric flow rate	Eq. 10	m^3/s				
46	V_{cor}	Corrected velocity	45+11	m/s				
47	VP_{cor}	Corrected velocity pressure	Eq. 5	Pa				

FANS AND BLOWERS

The fan is an extremely important part of any ventilation system, since it supplies the energy necessary to cause air movement. In a general exhaust ventilation system, the fan frequently *is* the ventilation system, since it is usually just installed in a wall or ceiling without ductwork. The fan used in a local exhaust ventilation (LEV) system, on the other hand, is an integral part of that *system*, and as such must be carefully selected to be compatible with the rest of the system. The network of hoods, ducts, and air cleaners in an LEV system offers a certain inherent resistance to airflow. The amount of air that actually flows through this resistance is a function of the fan attached to the system and the suction it provides to the exhaust system.

The definitions of “fan,” “blower,” and “compressor” can be the subject of some confusion. Jorgensen (1999) states:

Any device that produces a current of air by the movement of a broad surface can be called a fan. . . . Broadly speaking, the function of a fan is to propel, displace, or move the air or gas, while the function of a compressor is to increase the pressure, reduce the volume, or compress the air or gas. However, there is always some fluid movement through a compressor, and it is debatable whether that function is less important than the others listed. . . . Some other names for fans and compressors are: ventilator (generally restricted to a very-low-pressure-rise), exhaustor (used to signify that gases are being removed from something), and blower (used to signify that gases are being supplied to something).

In this book we call all such devices “fans.” Fans can be distinguished from compressors and vacuum pumps, which also move gases but at pressures significantly different from atmospheric (usually, many inches of mercury).

10.1 TYPES OF AIR MOVERS

All fans used in ventilation systems can be categorized into one of two types, depending on the nature of the airflow through the device. In axial flow fans the airflow is parallel to the axis of fan rotation, while centrifugal fans exhaust air radially. Sometimes it is necessary to move air without the use of a fan; one common way to do this is to use an air ejector.

10.1.1 Axial Flow Fans

Axial fans, also called “propeller” fans, find a wide variety of uses in industry. As the name implies, airflow in this type of fan is parallel to the axis of rotation—air does not have to change direction in passing through the fan. There are three basic types of axial fans, each with its special design details and proper area of application to industrial ventilation.

Propeller Fans. The simplest propeller fan, equipped with sheet metal blades, is the common air fan ubiquitous to homes, offices, and hot work environments (Fig. 10.1). The principal advantage of such fans is their ability to move large amounts of air; conversely, their principal disadvantage is their inability to move air

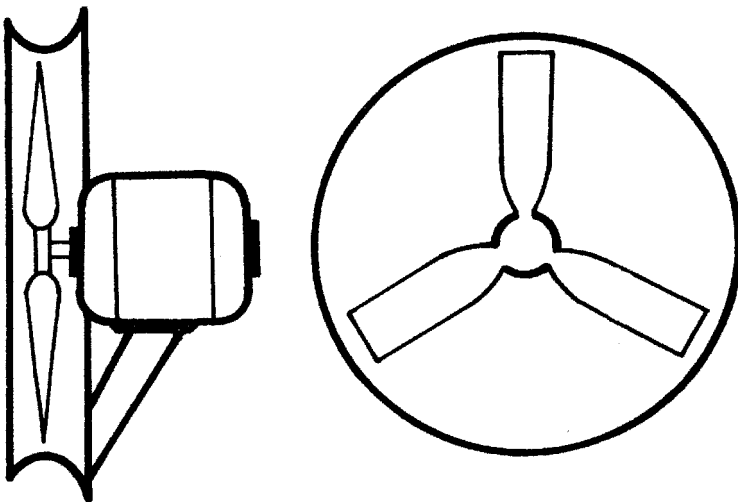


Figure 10.1 Propeller fan.

against any appreciable resistance. The amount of air that such fans can move is greatly reduced when the static pressure against that they are operating is increased to 0.5–1 in. H_2O (100–200 Pa). If the fan is specially designed with propellers with an airfoil cross section, it can operate in the range 1–2 in. H_2O (200–500 Pa), but no higher.

Despite this limitation, propeller fans are commonly used in industry; their most common use is as wall or ceiling fans in dilution ventilation systems. Since this type of fan cannot develop significant static pressure, care must be taken to supply adequate replacement air, or the fan will not be able to move the amount of air desired due to the negative pressure built up in the room (see Chapter 4). Their poor static pressure capability also precludes their use in local exhaust systems.

Tubeaxial Fans. Tubeaxial fans (Fig. 10.2) are propeller fans that have been modified so that they can be inserted into a duct. The close spacing between the blade tips and the housing improves efficiency and allows the development of greater static pressure than the simple propeller fan. The motor can be located either inside the duct for a direct-drive fan or outside the duct for a belt-driven fan. Such fans are designed to operate against low [0–3 in. H_2O (0–800 Pa)] static pressures, and thus have limited application in local exhaust ventilation systems. They are used primarily in simple one-hood systems where space is at a premium and system resistance is low, such as paint spray booths.

Vaneaxial Fans. Vaneaxial fans (Fig. 10.3) are tubeaxial fans that have been modified by the addition of air-directing vanes on the motor housing behind the fan blades. The vanes serve to reduce the whirl in the air as it exits the fan blades, which improves the fan efficiency and allows the development of increased static pressure. Such fans can operate at static pressures up to 10 in. H_2O (2000 Pa) and are thus suitable for use in local exhaust systems. They must be used with relatively clean air, and thus cannot transport dust-laden gas streams. Such fans are generally more

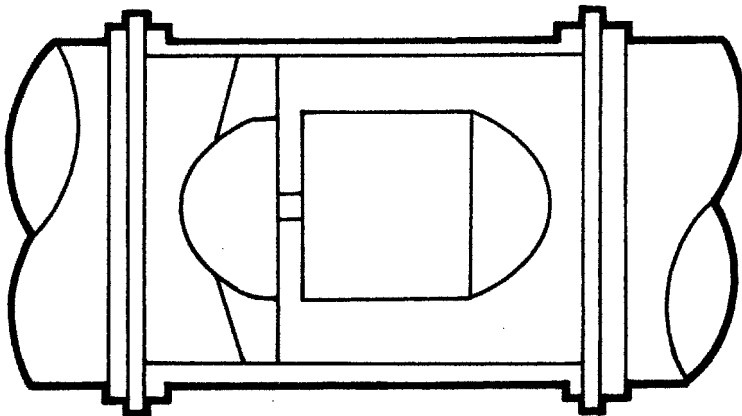


Figure 10.2 Tubeaxial fan.

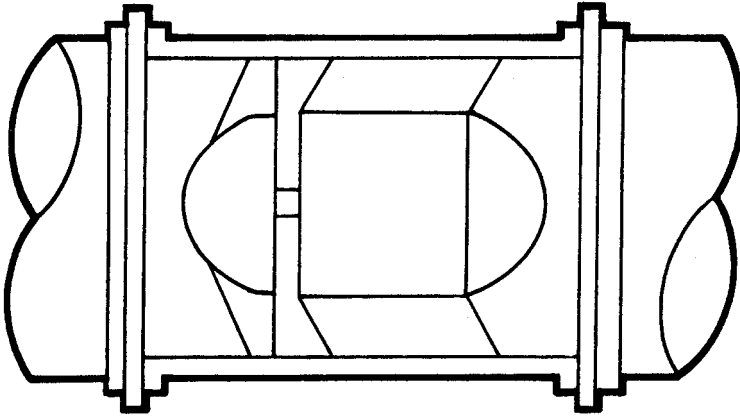


Figure 10.3 Vaneaxial fan.

expensive than a comparable centrifugal fan (see Section 10.1.2), and are usually employed only when space is at a premium.

10.1.2 Centrifugal Fans

Centrifugal fans are distinguished from axial fans in that the air leaves the rotating blades in the radial direction (i.e., perpendicular to the axis of rotation). A simple centrifugal fan is shown in Fig. 10.4. These fans are commonly divided into three performance and application categories, which are determined by the shape of the impeller.

Forward-Curved-Blade Fans. Forward-curved-blade fans are the common “squirrel cage” fans used widely for moving large amounts of air against low-to-moderate

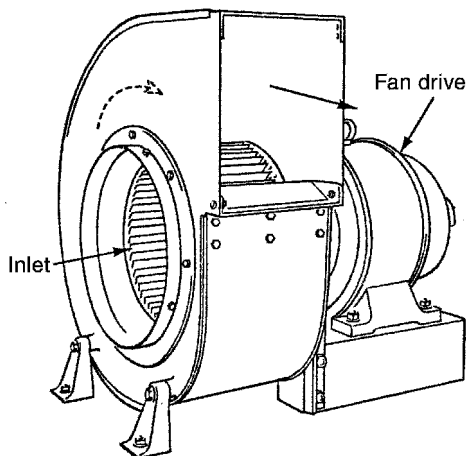


Figure 10.4 Centrifugal fan.

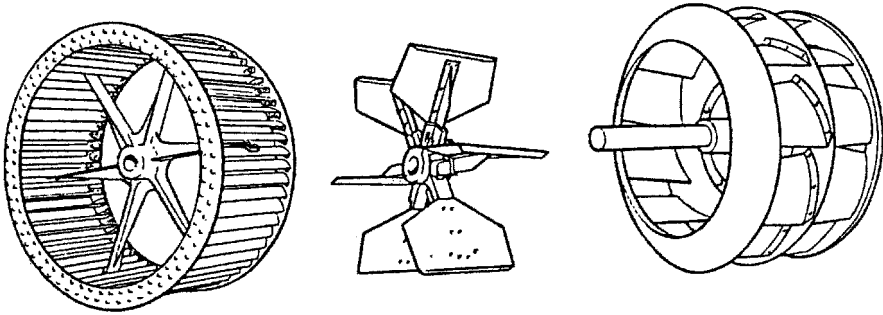


Figure 10.5 Centrifugal fan impellers: from left to right are forward curved, radial, and backward curved.

static pressures. This type of fan has many cup-shaped blades that accelerate the air to a high velocity at relatively low rotating speeds. The individual blades and impeller are stamped from sheet steel and assembled by spot welding, so that this design is much cheaper than the heavier impellers used in radial and backward-curved blade fans. The high air velocity at low rotating speed results in quieter operation, which is important for many air-moving applications.

This fan type has three main disadvantages; it has a low operating efficiency, it cannot develop a high static pressure, and it cannot be used in corrosive or erosive environments. These limitations preclude its use in most local exhaust systems; its most common use in industry is in air supply and exhaust for building HVAC systems.

Radial Blade Fans. Radial blade fans are the simplest, and least efficient, type of centrifugal fan. They are used whenever dusty air or highly corrosive contaminants must be moved, since the blades can be constructed as thick as necessary or replaced to withstand erosion or corrosion. The blades also tend to be self-cleaning, which minimizes dust deposition and subsequent imbalance. Since these fans are less efficient and more expensive than the types described below, they are usually used only for systems transporting dusty or corrosive air through the fan.

Backward-Curved-Blade Fans. Backward-curved-blade fans are the preferred choice for local exhaust systems where nondusty air is moved through the fan. This would be the case where the contaminants being exhausted are gases, or where particulate contaminants are being exhausted but an air-cleaning device is located upstream of the fan. This type of fan is more efficient than the radial blade type, thus reducing power requirements. It is not without its disadvantages, however. The backward curve of the blade means that the blade tip must have a higher velocity than the radial blade to impart the same velocity to the air; these fans must thus operate at higher rotating speeds than other centrifugal fans moving the same amount of air. This higher speed increases the stresses on the fan and results in a higher capital cost, although this is offset by the higher operating efficiencies attained by this design.

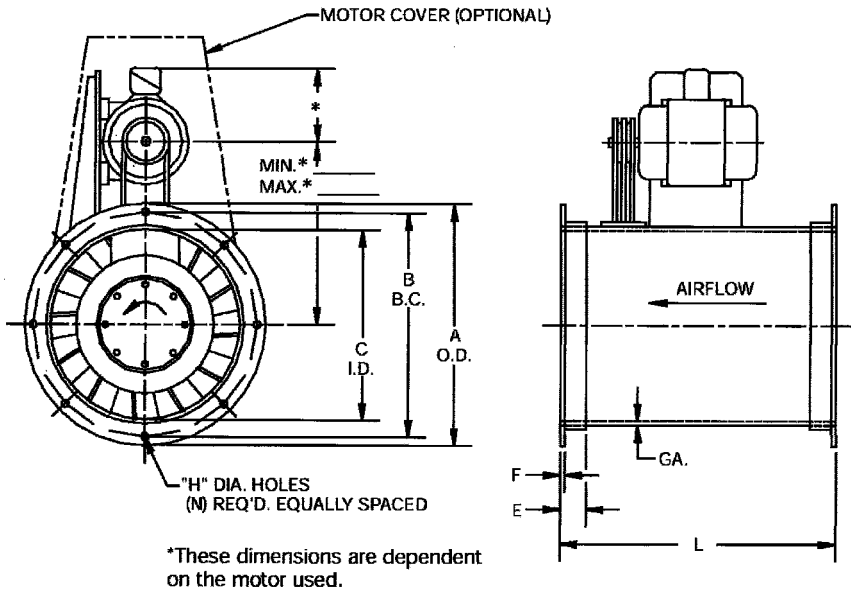


Figure 10.6 In-line centrifugal fan.

Miscellaneous Centrifugal Fans. Centrifugal fans can take several forms other than the classical “standalone” variety shown in Figs. 10.4 and 10.5. Examples of such fans are the roof fan and “upblast” roof fan used primarily for commercial kitchen range hood exhaust systems, and the “in-line” centrifugal fan (Fig. 10.6), which is mounted directly in the duct in a manner similar to tubeaxial fans, thus providing the space-saving advantages of an axial fan together with the static pressure capabilities of a centrifugal fan.

10.1.3 Air Ejectors

Air ejectors (also called *injectors* or *jet pumps*) are a means of moving air without having it pass through a fan. Typical designs are shown in Fig. 10.7a (a simple ejector) and Fig. 10.7b (a Venturi-type ejector). Airflow (secondary air) is induced in the large duct by jet action of the primary fluid leaving the nozzle at high velocity. The ejecting fluid can be water, steam, compressed air, or air from a fan; since the first three involve an excessive use of energy, the usual ejecting fluid is air from a fan.

Ejectors are inherently very inefficient devices, since much of the jet energy is employed in overcoming friction. The maximum efficiency attainable under optimum conditions is only 40%, while typical efficiencies in field conditions range from 15 to 25% (Jorgensen, 1999). Such low efficiencies limit ejector applications to those where for some reason the air cannot come in contact with the fan; examples would include gas streams that are extremely hot, sticky, corrosive, or explosive.

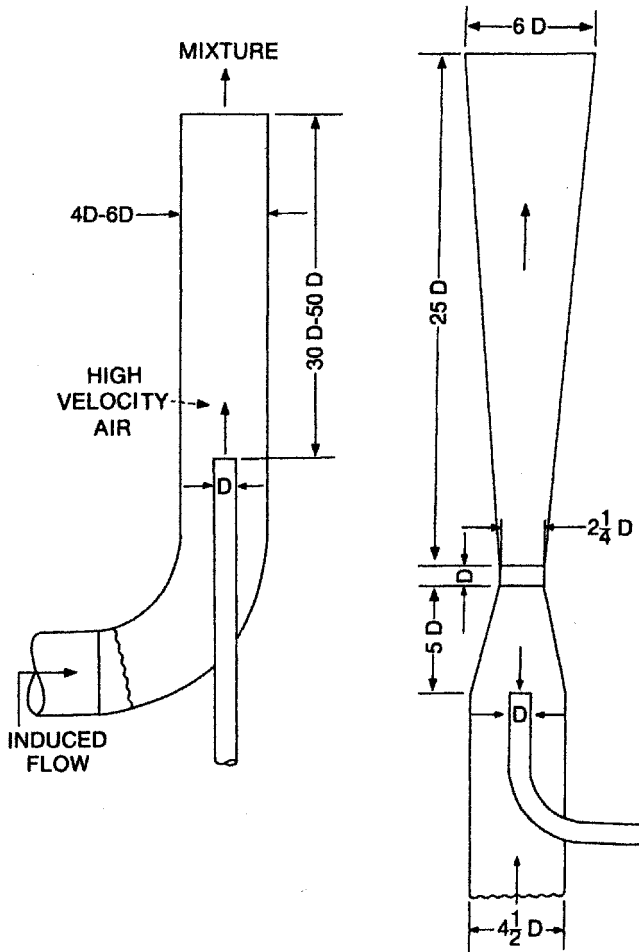


Figure 10.7 Ejectors: (a) simple design; (b) Venturi design.

10.2 FAN CURVES

A fan's operating characteristics can be described by reference to several important variables. These include the amount of air being moved by the fan (Q , cfm or m^3/s), the static pressure developed by the fan (P_s , in. H_2O or Pa), the fan efficiency (η), the fan rotating speed (N , rpm), and the power (H , hp or W) required to operate the fan. Empirical formulas have been developed relating these variables to each other; such formulas can be displayed both in tabular form, resulting in fan tables, or in graphical form, giving what are known as fan curves.

Manufacturers specify fan performance by means of fan tables, but the performance of various fan types is more easily visualized from the use of fan curves; we will start our discussion using fan curves and then relate the curves to fan tables. Since the

end result of using a fan is to deliver a certain amount of airflow to a desired location, it is most common to specify fan performance in terms of airflow. Fan curves then relate all of the other fan variables to airflow. Such curves thus have airflow as the abscissa and the other variables of interest plotted on the ordinate.

10.2.1 Static Pressure Curve

The basic performance of a typical radial blade fan is illustrated in Fig. 10.8a, which plots the amount of air moved by the fan versus the resistance to airflow offered by whatever system is attached to it. As would be expected, maximum airflow occurs when no resistance is presented to the fan; this is the so-called free delivery no pressure (FDNP) point. At the other extreme, no airflow occurs when the resistance is infinite (i.e., when the fan inlet or outlet is blocked completely). At this so-called static no delivery (SND) point, the blower develops its maximum static pressure, as shown by the curve. (In actuality, the static pressure increases slightly at very low airflow due to the inefficiency of fan operation in this zone.) The exact shape of the fan pressure curve between these two points depends on the specific fan design, but the curve shown is typical of a radial blade fan.

The static pressure plotted in this curve is called the *fan static pressure* (P_s). This quantity can be defined with the help of the simple exhaust system pictured in Fig. 10.9. To draw air through this system, the fan must develop a certain negative static pressure at the inlet ($p_{s,i}$) and a positive static pressure at the fan outlet ($p_{s,o}$). The total amount of static pressure that must be developed by the fan is thus

$$P_s = |p_{s,i}| + |p_{s,o}| \quad (10.1)$$

Fan static pressure is slightly different from the total static pressure needed to move air through the system. It is defined as

$$P_s = p_s - p_{v,i} \quad (10.2)$$

where $p_{v,i}$ is the velocity pressure of the air at the inlet to the fan. This somewhat arbitrary definition of fan static pressure arises from the standard definition of fan total pressure (P_t); a derivation of Eq. 10.2 is given in Jorgensen (1999).

Static pressure curves for backward-curved centrifugal, forward-curved centrifugal, and vaneaxial fans are shown in Figs. 10.8b, 10.8c, and 10.8d, respectively. Note the “dip” exhibited by the fan static pressure curves for the vaneaxial and, to a lesser extent, forward-curve blade centrifugal fans. This so-called “stall” zone is a region of unstable fan operation caused by aerodynamic conditions established when these fans are operated at airflows well below the maximum design airflows. Fan operation at or near the stall zone is to be avoided, since the flow will be unstable. This instability is demonstrated in Fig. 10.8d; at static pressure P_1 , three different airflows (Q_1 , Q_2 , Q_3) can be delivered. Such instability can result in considerable air pulsation and mechanical vibration. These fans should always be operated at airflows high enough to avoid the stall zone, on the downward slope of the fan static pressure curve.

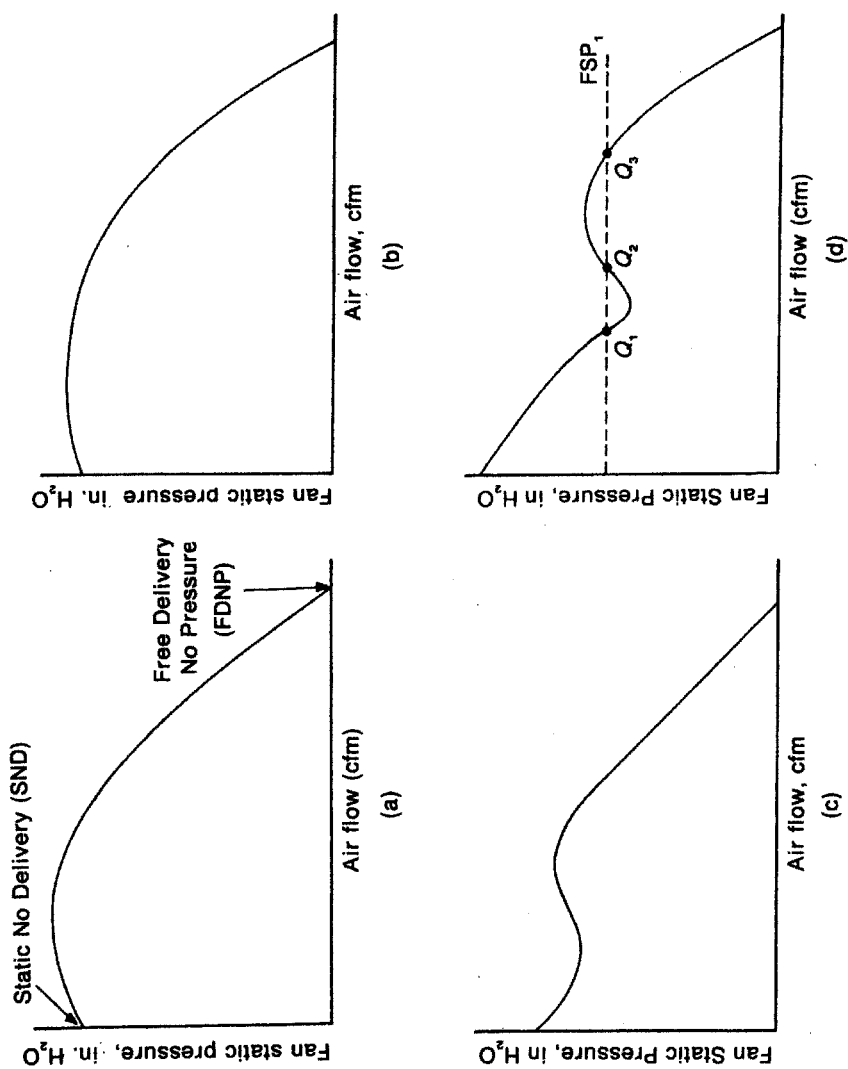


Figure 10.8 Fan static pressure curves: (a) radial blade; (b) backward-curved blade; (c) forward-curved blade; (d) vaneaxial fan.

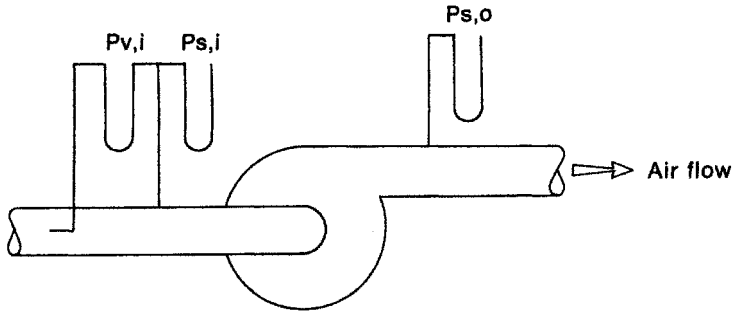


Figure 10.9 Fan pressures.

10.2.2 Power Curve

To develop the brake power curve and the mechanical efficiency curve that follows, we must first define the quantity moving air power (H_a). Air power is a measure of the work done by the fan and is thus defined as the amount of energy added to the moving air per unit time. In general, the work (W) done in moving an airflow Q across a pressure drop Δp is

$$W = (\Delta p)Q \quad (10.3)$$

If the pressure drop is given in pounds per square foot (psf) and the airflow is given in cfm, the work is calculated in the engineering units of foot-pounds per minute (ft-lb/min). To calculate fan air power, the change in pressure that must be used in the equation is the total pressure required to get air through the system, which is usually specified in inches of water. The following conversions can be used with Eq. 10.3 to obtain the desired relationship:

$$\begin{aligned} H_a(\text{hp}) &= \frac{p_t(\text{in. H}_2\text{O}) Q(\text{cfm})}{33,000[(\text{ft-lb/min})/\text{hp}] 0.192 [\text{in. H}_2\text{O}/(\text{lb/ft}^2)]} \\ &= \frac{p_t Q}{6343} \end{aligned} \quad (10.4a)$$

In the metric system the units are consistent, so the equation is simply

$$H_a = p_t Q \quad (10.4b)$$

This expression describes the amount of energy per unit time being transferred to the moving air. For purposes of designing the fan, however, we need to know the power requirements of the motor driving the fan. If the motor were 100% efficient at transferring energy to the fan blades, and if the fan were 100% efficient at transferring energy of rotation to energy in the moving air, the required motor power, designated by H_m , would be just equal to the air power.

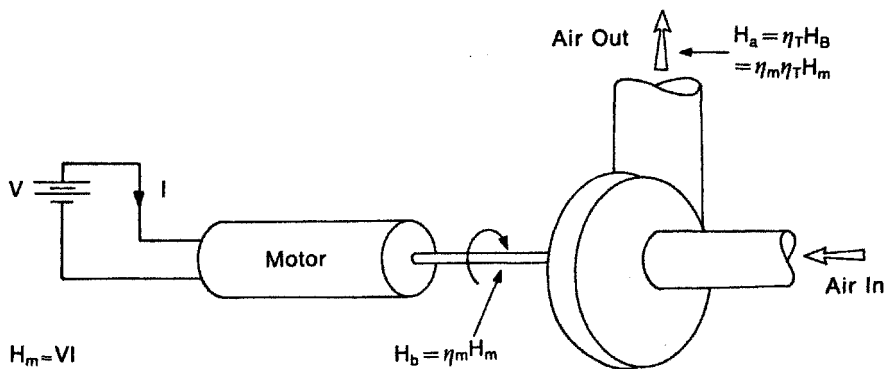


Figure 10.10 Fan-motor horsepower relationships.

Both of these energy transfers are, of course, less than 100% efficient, so that the motor power requirement is always considerably higher than the resulting air power. If the efficiency of the motor in converting electrical energy into rotating mechanical energy is designated by η_m and the efficiency of the fan in converting rotating energy into moving air is designated by η_T (standard fan terminology for total mechanical efficiency), we can picture the energy transformation process by Fig. 10.10.

The work done by the rotating fan is called the *fan brake power* (H_b). Mathematically, H_a and H_b are related by the simple equation

$$\begin{aligned} H_b &= \frac{H_a}{\eta_T} \\ &= \frac{p_t Q}{6343 \eta_T} \end{aligned} \quad (10.5a)$$

In metric units, this is

$$H_b = \frac{p_t Q}{\eta_T} \quad (10.5b)$$

The electrical horsepower required by the motor is

$$H_m = \frac{H_b}{\eta_m} \quad (10.6)$$

Combining Eqs. 10.5 and 10.6 gives the relationship between electrical power supplied to the fan and the resulting work done by the moving air:

$$H_a = H_m \eta_m \eta_T \quad (10.7)$$

Fan motor efficiency η_m is usually about 95%, so that brake power and motor power are nearly equal. Fan power requirements are usually specified in terms of brake power, and the user of fan tables should keep in mind that the motor power used will be slightly higher than the value specified.

This introduction to fan power terminology is a necessary prelude to an understanding of fan power curves. A typical brake power curve for a radial blade fan is shown in Fig. 10.11a. The curve does not intersect the origin, as predicted by Eq. 10.5, because the fan uses some energy to rotate the impeller even when shut tight so that no air flows. The power curve rises steadily with increasingly flow, reaching its maximum at free delivery (leading to the possibility that the motor may burn out if such a fan is operated under no load).

Similar curves are shown in Fig. 10.11b for a backward-curved blade fan, in Fig. 10.11c for a forward-curved blade fan, and in Fig. 10.11d for a vaneaxial fan. Note the downward curve of the brake power curve at high airflows for the backward-curved blade fan. This “load-limiting” characteristic is a desirable feature of this type of fan, since the power requirement does not climb to excessive levels when the fan is operated under low-resistance conditions.

10.2.3 Mechanical Efficiency Curve

Mechanical efficiency refers to the efficiency of the fan in transferring rotating mechanical energy to energy of moving air. Two different efficiencies, called *total* efficiency and *static* efficiency, are used in standard fan terminology.

Total efficiency η_T was defined in Eq. 10.5, rearranged here:

$$\eta_T = \frac{H_a}{H_b} \quad (10.5)$$

Substituting Eq. 10.4 into Eq. 10.5 gives

$$\eta_T = \frac{p_t Q}{6343 H_b} \quad (10.8a)$$

Note that this is simply Eq. 10.6, solved for total efficiency. In metric units, this is

$$\eta_T = \frac{p_t Q}{H_b} \quad (10.8b)$$

Note that total efficiency is defined in terms of the total pressure required by the fan. If static pressure is used in place of total pressure, a new efficiency, called the *static efficiency* (η_s), is defined as:

$$\eta_s = \frac{p_s Q}{6343 H_b} \quad (10.9a)$$

In metric units, this is

$$\eta_s = \frac{p_s Q}{H_b} \quad (10.9b)$$

Five parameters (static pressure, total pressure, horsepower, total efficiency, and static efficiency) can now be plotted as functions of airflow for any particular fan. Typical sets of fan curves for several types of blowers are shown in Fig. 10.12.

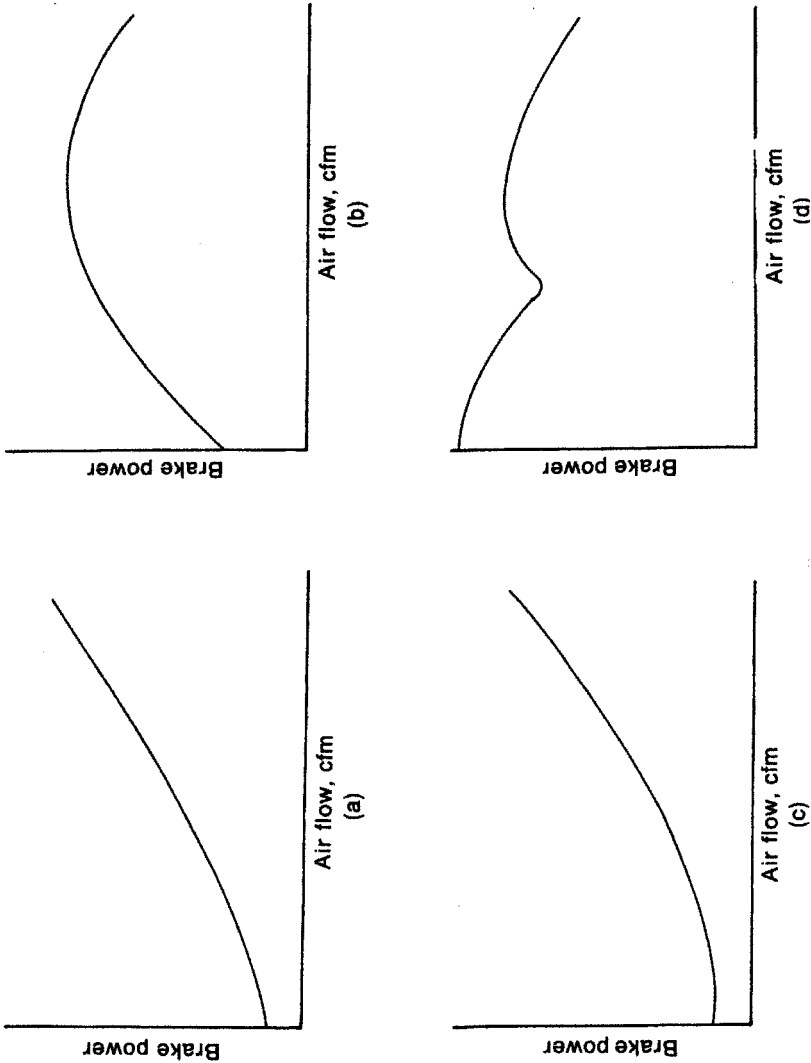


Figure 10.11 Typical fan power curves: (a) radial blade fan; (b) backward-curved blade fan; (c) forward-curved blade fan; (d) vaneaxial fan.

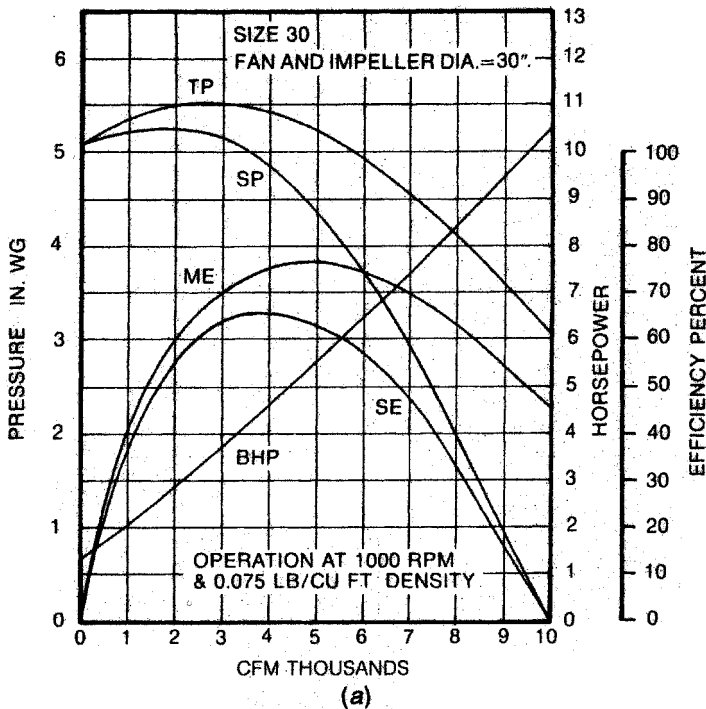
10.2.4 Fan Laws

Virtually all centrifugal fans are available in “families” of geometrically similar models, varying only in their size and thus their capacity for moving air. In addition, a particular fan can be operated over a wide range of rotating speeds, which also has the effect of changing the amount of air the fan can move. The changes in a fan’s operating characteristics corresponding to changes in fan size and/or rotating speed can be determined by using a series of equations that are known as the “fan laws.”

Effect of Rotating Speed. As a blade of a centrifugal fan rotates, it “picks up” a volume of air at the fan inlet and “throws” that same volume out of the fan outlet. Changing the fan rotating speed simply changes the rate at which parcels of air are picked up and thrown out, so that changes in fan rotating speed result in corresponding changes in airflow delivered by the fan. Mathematically, the first fan law can be written as

$$\frac{Q_1}{Q_2} = \frac{N_1}{N_2} \quad (10.10)$$

where N designates fan rotating speed.



FAN PERFORMANCE CURVE

Figure 10.12 Typical performance curves for several fan designs: (a) performance curve for radial centrifugal fan.

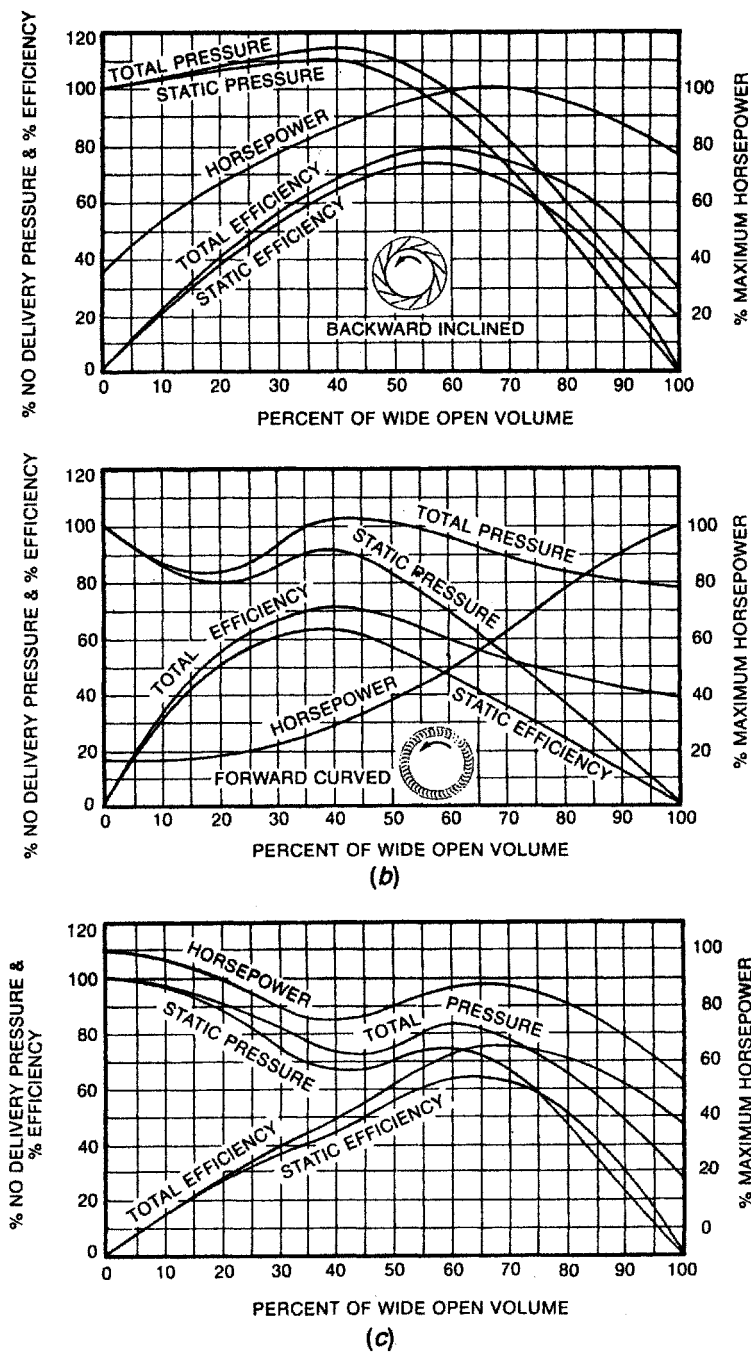


Figure 10.12 (b) Normalized curves for centrifugal fans; (c) normalized curve for an axial flow fan.

As discussed earlier, most of the static pressure losses in a ventilation system are proportional to air velocity squared. Since air velocity is directly proportional to airflow, and airflow is directly proportional to fan speed (Eq. 10.10), it follows that static pressure (and total pressure) varies as the square of the fan speed. This is the second basic fan law:

$$\frac{P_{s,1}}{P_{s,2}} = \frac{P_{t,1}}{P_{t,2}} = \left(\frac{N_1}{N_2}\right)^2 \quad (10.11)$$

Since brake power is directly proportional to total pressure and to airflow (Eq. 10.4), combining Eqs. 10.10 and 10.11 leads to the third basic fan law (i.e., power varies with the third power of fan speed):

$$\frac{H_{b,1}}{H_{b,2}} = \frac{P_{t,1}Q_1}{P_{t,2}Q_2} = \left(\frac{N_1}{N_2}\right)^3 \quad (10.12)$$

These relationships are exact only for the case where the pressure losses through all components of a ventilation system are proportional to the square of the velocity through that component. This is true for most components of typical systems, but the pressure loss through many air-cleaning devices increases more slowly (see Chapter 11). If the pressure loss through an air cleaner is a significant proportion of the total pressure loss in the system, these relationships will have to be modified and a more detailed procedure will have to be followed to determine the new system static pressure and power requirement when fan speed is changed.

Effect of Other Variables. Equations 10.10–10.12 describe the behavior of a particular fan when the airflow through that fan is changed. Basic references such as *Fan Engineering* (1999) and the *ASHRAE Handbook* (1985) present many additional fan laws that describe fan behavior when fan size and/or gas density are varied. The reader is referred to these sources for discussion of these laws.

10.2.5 Relationship between Fan Curves and Fan Tables

Graphically, changing the fan speed has the effect of shifting the static pressure curve, as illustrated in Fig. 10.13. For any given fan motor configuration, there thus exists a “family” of static pressure curves, where each curve corresponds to one fan rotating speed; each of these static pressure curves has a set of the other four curves (total pressure, horsepower, total efficiency, and static efficiency) associated with it, so a myriad of curves can be constructed for any given fan. Fan manufacturers have found it easier to present this wealth of data in the form of tables rather than a large set of curves.

A typical fan rating table for a backward-curved blade centrifugal fan is shown in Table 10.1. Each row of the table corresponds to one airflow, and each pair of two columns corresponds to one fan static pressure. The entries in the table show the fan rotating speed necessary to obtain each combination of Q and P_s , and the resulting brake power required to drive the fan. If entries from the table are selected for a constant rotating speed, a fan curve similar to those described above can be constructed. To illustrate this procedure, the entries closest to 600 and 800 rpm have

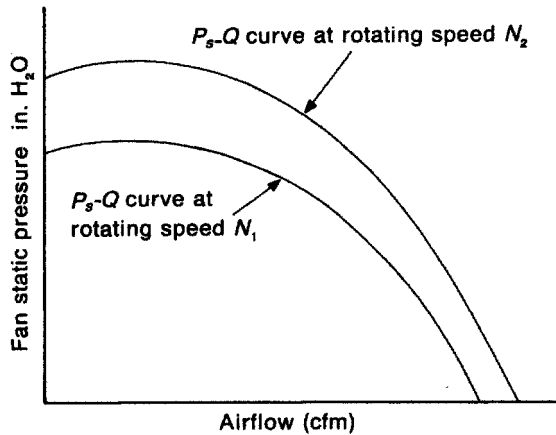


Figure 10.13 Effect of changing fan rotating speed N on static pressure–airflow curve. Increasing N has the effect of moving the curve upward.

been underlined in Table 10.1 and brought together in the first three columns of Table 10.2. Equation 10.7 can be used to calculate static efficiency for each set of conditions in Table 10.2; these values are shown in column 4.

The values in Table 10.2 can now be used to construct fan curves (Fig. 10.14) by plotting fan static pressure (Fig. 10.14*a*), brake power (Fig. 10.14*b*), and static efficiency (Fig. 10.14*c*) for the two rotating speeds. The effect of changing rotating speeds is clearly evident. Note that these curves constructed from an actual fan table resemble the generic fan curves for a backward-curved blade fan shown in Fig. 10.12. The static efficiency values are not normally included in a fan rating table; rather, the point of maximum efficiency for each value of static pressure is indicated by underlining or shading the appropriate value in the table. Thus in our example, according to Table 10.1, the point of maximum efficiency when operating at 4 in. H_2O fan static pressure is attained at a rotating speed of 553 rpm and an airflow of 9000 cfm; at 5 in. H_2O the maximum efficiency is attained at 626 rpm and 11,000 cfm. The maximum efficiency at 600 rpm should thus fall between 9000 and 11,000 cfm, as confirmed by Fig. 10.14*c*.

10.3 USING FANS IN VENTILATION SYSTEMS

A fan is always used as part of a ventilation system (in some simple dilution ventilation installations it *is* the ventilation system.) As such, an understanding of the interaction of the fan and the rest of the system is a crucial part of the system design. The proper fan type, size, and rotating speed must be selected to produce the desired system airflow.

10.3.1 General Exhaust Ventilation Systems

The fan usually used for general exhaust ventilation is the propeller-type axial fan. This fan is designed to move large volumes of air against low resistance, which is

Table 10.1 A Section from Typical Fan Rating Table

CFM	Outlet Velocity	1 in. S.P.		2 in. S.P.		3 in. S.P.		4 in. S.P.	
		rpm	hp	rpm	hp	rpm	hp	rpm	hp
4,000	867	273	0.88						
5,000	1084	<u>280</u>	<u>1.09</u>	383	2.24	466	3.48		
6,000	1301	291	1.33	388	2.63	469	4.04	539	5.53
7,000	1518	302	1.60	<u>396</u>	<u>3.05</u>	473	4.62	541	6.27
8,000	1735	315	1.91	406	3.52	480	5.23	546	7.04
9,000	1952	327	2.26	417	4.03	<u>489</u>	<u>5.89</u>	<u>553</u>	<u>7.85</u>
10,000	2169	340	2.65	429	4.59	500	6.61	561	8.71
11,000	2386	<u>353</u>	3.10	441	<u>5.21</u>	511	7.38	571	9.64
12,000	2603	<u>368</u>	<u>3.60</u>	<u>454</u>	<u>5.88</u>	522	8.22	582	10.6
13,000	2819	383	4.18	466	6.61	534	9.12	593	11.7
14,000	3036	398	4.83	479	7.39	547	10.1	<u>605</u>	12.8
15,000	3253	415	5.55	492	8.25	560	11.1	617	14.0
16,000	3470	431	6.36	506	9.19	572	12.2	630	15.3
17,000	3687	448	7.25	521	10.2	585	13.4	642	16.7
18,000	3904	465	8.24	536	11.4	<u>598</u>	14.7	655	18.1
19,000	4121	483	9.32	551	12.6	612	16.0	668	19.6
20,000	4338	501	10.5	567	13.9	626	17.5	680	21.2
21,000	4555	519	11.8	583	15.4	640	19.1	693	22.9
22,000	4772	537	13.2	<u>600</u>	16.9	655	20.8	707	24.8
23,000	4989	556	14.7	616	18.6	671	22.6	721	26.7
24,000	5206	575	16.4	633	20.4	687	24.6	736	28.8
25,000	5422	<u>593</u>	18.2	650	22.4	703	26.7	751	31.1
26,000	5639			668	24.5	719	28.9	766	33.4
27,000	5856			686	26.7	735	31.3	782	36.0
28,000	6073			703	29.0	752	33.8	<u>797</u>	38.6
29,000	6290			721	31.5	769	36.5	813	41.4
30,000	6507			740	34.2	786	39.3	830	44.4
31,000	6724			758	37.1	<u>803</u>	42.3	846	47.6
32,000	6941			777	40.1	821	45.4	863	50.9

what normally is required for general ventilation systems. The selection and installation of general ventilation fans is relatively simple and straightforward. Nonetheless, many such systems operate poorly, for a variety of reasons: the wrong size fan is selected, the fan is installed in the wrong location, insufficient replacement air is provided, and so on.

A properly designed general exhaust ventilation system will operate at static pressures very close to zero, so that the propeller fan can deliver its maximum airflow. The most common design flaw in such systems, however, is the absence of a proper replacement air system; if an amount of air equal to the exhaust airflow is not provided mechanically to the room being exhausted by a general exhaust ventilation system, the room will be “starved” for air and the exhaust fan will create a condition of negative

Table 10.2 Calculation of Fan Static Efficiencies for the Typical Fan of Table 10.1^a

P_s (in. H ₂ O)	Q (cfm)	H_B (hp)	n_s (%)
At 600 rpm			
1	25,000	18.2	2
2	22,000	16.9	41
3	18,000	14.7	58
4	14,000	12.8	69
5	7,000	8.0	69
At 800 rpm			
3	31,000	42.3	35
4	28,000	38.6	46
5	25,000	35.6	55
6	22,000	33.2	63
7	19,000	30.7	68
8	15,000	26.2	72
9	9,000	18.7	68

^aData in the first three columns were taken from Table 10.1 at constant fan rotating speeds of 600 and 800 rpm; fan static efficiencies were calculated using these values and Eq. 10.7.

static pressure in the room. The design of replacement air systems will be discussed in Chapter 12.

10.3.2 Local Exhaust Ventilation Systems

The proper selection of a fan to be used with a LEV system involves the matching of the fan characteristics to the exhaust system characteristics to obtain the desired airflow. In this regard the exhaust system can be looked on as a fixed resistance to airflow; the amount of air actually flowing through this resistance network depends on the characteristics of the exhaust fan being used. This might be made clearer by use of an electrical analogy (Fig. 10.15). The application of a voltage (V) to a network of resistors results in current flow through each of the network branches. The current through each individual branch (I_1 , I_2 , etc.) depends on the relative magnitude of each resistance, while the total current (I) depends on the overall resistance of the network. Similarly, the branches of a ventilation system can be thought of as representing a network of resistances to airflow. The pressure difference created by the fan is analogous to the voltage in an electrical circuit; the magnitude of this pressure difference, together with the overall resistance of the ventilation system, determines the total airflow (Q). The airflow in each branch is determined by the relative resistance to airflow presented by that branch.

This analogy may be useful to a point, but it is not perfect. In an electrical system it is usually possible to provide a constant voltage, but an exhaust fan develops a variable amount of pressure, as described by its fan curve. The first step in determining

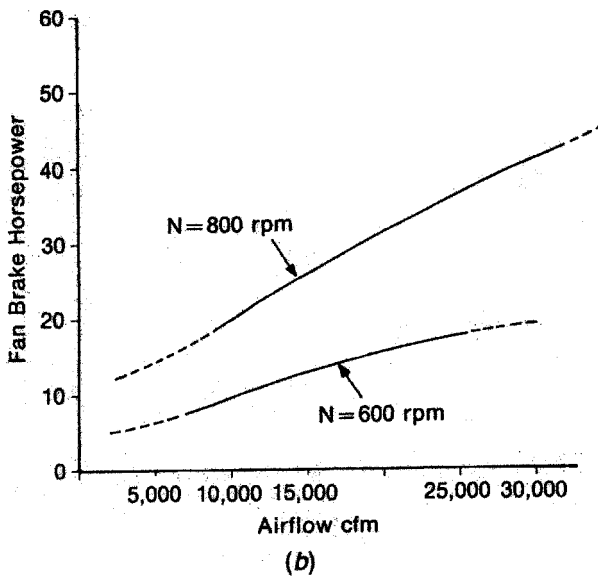
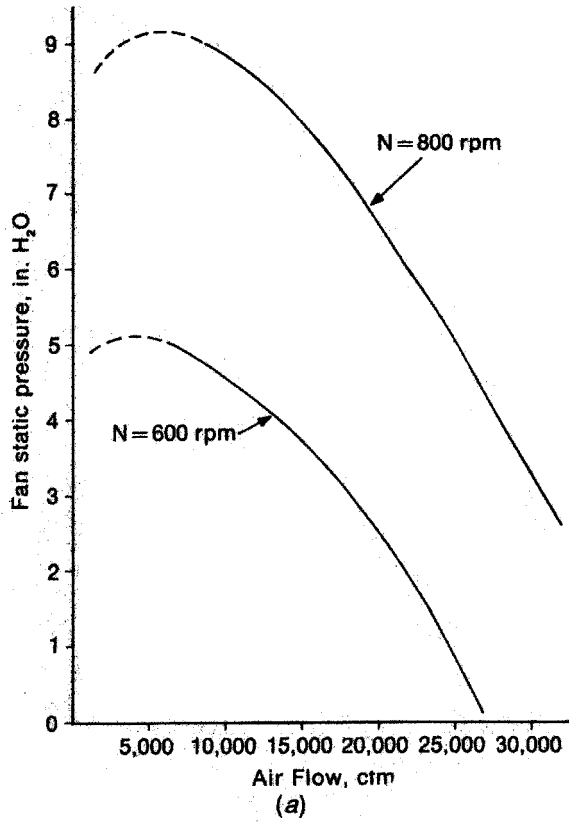


Figure 10.14 Performance curves for the fan of Table 10.1: (a) fan static pressure versus air flow; (b) brake horsepower versus airflow.

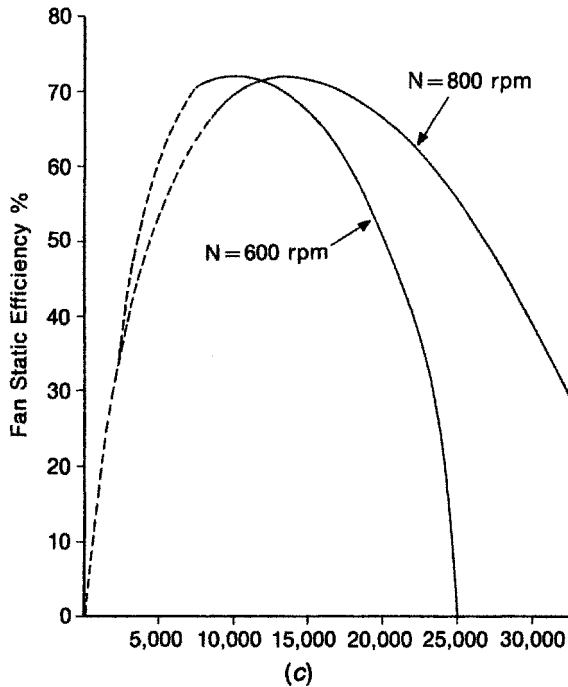


Figure 10.14 (c) Static efficiency versus horsepower.

the fan's actual operating point is to determine the resistance characteristics of the exhaust system.

Exhaust System Resistance Curve. Chapters 2, 8, and 9 developed the concept that the resistance to airflow of most elements in an exhaust system is proportional to the *square* of the average air velocity through that element. This is true for hoods, ducts, elbows, and miscellaneous other fittings. The principal exception to this rule of thumb is that of air-cleaning devices that might be used in the ventilation system; many of these have pressure drops that vary linearly with velocity and/or vary significantly over time for a constant velocity.

Ignoring air-cleaning devices for the moment, let us consider the airflow resistance of a typical exhaust system, the electroplating shop system designed in Chapters 6 and 9. As detailed in Example 9.2, the electroplating system requires an airflow of 11,230 cfm with a system static pressure of 1.71 in. H_2O . The velocity pressure at the inlet to the fan is 0.43 in. H_2O , so the fan static pressure is

$$\begin{aligned}
 P_s &= p_s - p_{v,i} \\
 &= 1.71 \text{ in. } H_2O - 0.43 \text{ in. } H_2O \\
 &= 1.28 \text{ in. } H_2O
 \end{aligned}
 \tag{10.2}$$

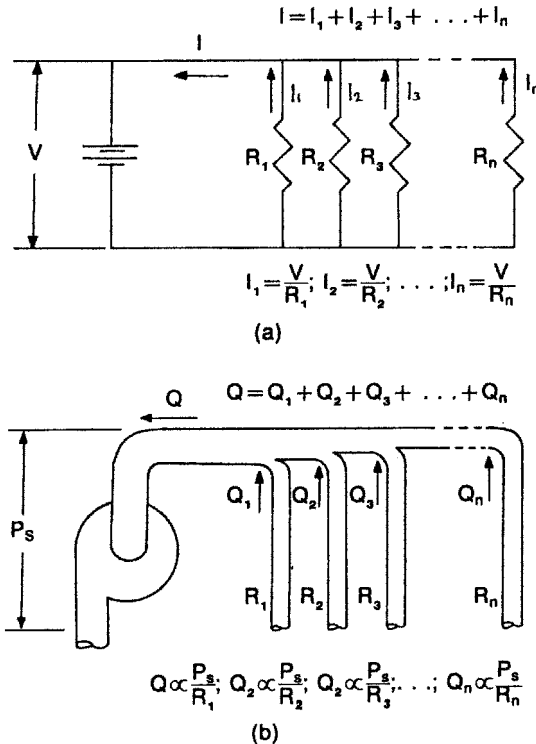


Figure 10.15 Analogy between an electrical network (a) and a local exhaust ventilation system (b). Voltage is analogous to fan static pressure, electrical resistance to airflow resistance, and current to airflow.

This system has the airflow–resistance relationship shown in Fig. 10.16. This so-called system resistance curve shows the second-power relationship between airflow and static pressure supplied by the fan; that is, to double the air from the design value of 11,230 cfm to 22,460 cfm, the fan static pressure would have to increase fourfold, from 1.28 in. H_2O to 5.12 in. H_2O .

Matching the Fan to the System. The system resistance curve specifies the airflow that will pass through this system for any value of static pressure applied by the fan; what remains in the design procedure is to select the fan that will supply the desired fan static pressure (1.28 in. H_2O) to give the desired airflow (11,230 cfm). The data in Table 10.1 suggest that the fan represented by this fan table might have performance in the proper range for this application; at 11,000 cfm between 1 and 2 in. H_2O the fan is operating near its maximum efficiency, as indicated by the underlined rpm values. The problem is to select the fan rotating speed that will supply 11,230 cfm at 1.28 in. H_2O .

To give an indication of what might happen, the system resistance curve (Fig. 10.16) and the fan static pressure curve at $N = 600$ rpm (Fig. 10.14) can be

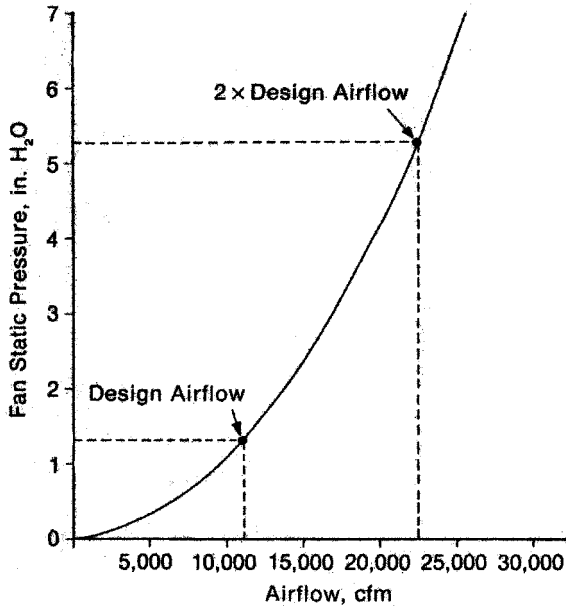


Figure 10.16 Static pressure required to induce different airflows for the electroplating local exhaust ventilation system designed in Chapter 6.

plotted on the same graph; the results are shown in Fig. 10.17. The fan curve describes the airflow that will be delivered by the fan at different static pressures required to overcome resistance to airflow, while the system curve describes the static pressure needed to overcome the resistance of this *particular* system at different airflows. It is evident that the curves intersect at one point, which is an airflow of 17,500 cfm and a fan static pressure of 3.2 in. H₂O. This is the only point common to the fan and to the exhaust system operating characteristics, so that if *this* fan is installed in *this* system of ducts and operated at *this* speed (600 rpm), 17,500 cfm of air will be exhausted and a fan static pressure of 3.2 in. H₂O will be developed.

This is considerably more airflow than is desired for the electroplating system. Recall that there is a *family* of fan static pressure curves, one for each rotating speed. Two of these curves ($N = 600$ rpm and $N = 800$ rpm) are given for the fan in Fig. 10.14a. It should be evident that *one* of these curves, and *one only*, passes through the desired operating point, *B* (see the dashed line in Fig. 10.17). A key part of the fan selection procedure is to choose the proper fan rotating speed to give the desired intersection point with the system resistance curve. This procedure is described in the next section.

If the proper fan curve is selected, 11,230 cfm of air will indeed flow at a fan static pressure of 1.28 in. H₂O. We have thus met the design requirements for the electroplating operation, and if the hoods and ducts have been designed properly and the proper airflow has been selected, the contaminants given off by the various electroplating tanks should be captured by the exhaust system.

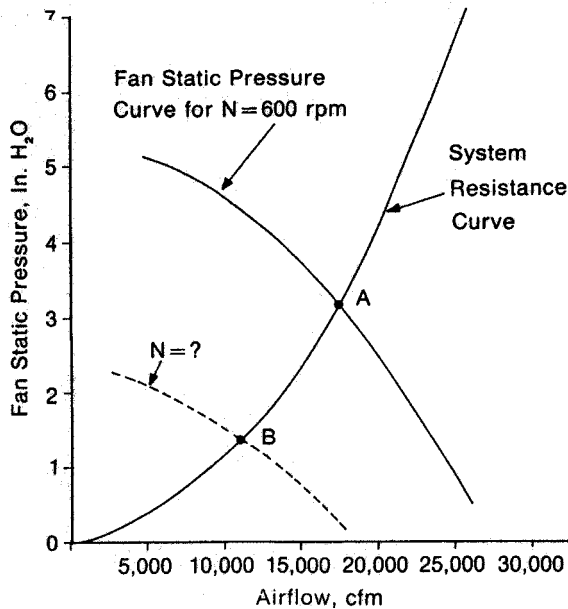


Figure 10.17 Fan static pressure curve at $N = 600$ rpm from Fig. 10.14 and system resistance curve from Fig. 10.16 plotted together. Note point of intersection (A) and desired operating point (B).

10.4 FAN SELECTION PROCEDURE

Once a desired fan operating point has been selected, it is necessary to select the proper fan, which, when inserted in the ventilation system, will furnish the desired combination of fan static pressure and airflow. The process to be followed when using a family of fan curves was described in Section 10.3; one simply selects the fan curve that intersects the system resistance curve at the desired operating point. What is usually available to the designer is not fan curves but a series of fan rating tables similar to that shown in Table 10.1. In this section we describe the procedure to be followed in selecting a fan from such a set of rating tables.

The first step is to select the *type* of fan to be used. In general, dilution ventilation systems will use axial flow fans, LEV systems moving particle-free air through the fan will utilize a backward-curved blade centrifugal fan, and LEV systems that require the fan to move particle-laden air will require a radial-blade centrifugal fan. Once the fan type is selected, it is necessary to consult fan catalogs that contain rating tables for that fan type.

The electroplating ventilation system will once again be used as an example of the procedure to be followed. This system moves particle-free air through a system of ducts, so a backward-curved centrifugal fan should be used. The fan data in Table 10.1 are taken from a catalog of such tables for a family of geometrically similar fans of a range of sizes. Information is given at the top of the table about the

dimensions of the particular fan being described; the fans are named according to the diameter of the fan inlet, which in our example is 29 in. (thus, fan size 429A). This particular series of fans ranges in size from 11-in. inlet diameter to 37-in. inlet diameter.

The first step in choosing a fan from this series is to attempt to match the fan inlet diameter to the diameter of the duct that will enter the fan, as determined by the system design procedure. The diameter of the final duct run for the electroplating design is 28 in. There is no fan in this series with an inlet diameter of 28 in., however; the closest values are 26 in. and 29 in. Since 29 in. is the closest to the desired value, it will be tried first.

Changing the final duct diameter has no effect on system airflow and negligible effect on system static pressure, but the change in velocity will affect the fan static pressure because of the change in inlet velocity pressure. The area of a 29-in. duct is 4.587 ft²; the inlet velocity is thus

$$\begin{aligned} V_i &= \frac{Q}{A} \\ &= \frac{11,230 \text{ ft}^3/\text{min}}{4.587 \text{ ft}^2} \\ &= 2450 \text{ ft/min} \end{aligned} \quad (2.5)$$

From Eq. 2.14, the corresponding inlet velocity pressure is

$$\begin{aligned} p_{v,i} &= \left(\frac{V_i}{4000} \right)^2 \\ &= 0.38 \text{ in. H}_2\text{O} \end{aligned} \quad (2.14)$$

Equation 10.2 can now be used to calculate the fan static pressure with a 29-in.-diameter inlet:

$$\begin{aligned} P_s &= p_s - p_{v,i} \\ &= 1.71 \text{ in. H}_2\text{O} - 0.38 \text{ in. H}_2\text{O} \\ &= 1.33 \text{ in. H}_2\text{O} \end{aligned} \quad (10.2)$$

Thus the fan static pressure (1.33 in. H₂O) has changed slightly from the value calculated during the system design procedure (1.28 in. H₂O).

Once a possible fan size is selected on the basis of the inlet diameter, the fan table must be checked to see if the desired combination of airflow and fan static pressure can be attained with this particular fan. Recall that an airflow of 11,230 cfm at a fan static pressure of 1.33 in. H₂O is required. In checking the fan table as reproduced in Table 10.1, these values are found to fall between the four entries enclosed in the square in the table; since some calculations will be performed on these numbers, they are reproduced in Table 10.3a. Table 10.3b shows the generalized nomenclature used in the equations that follow.

Table 10.3 Fan Interpolation from Rating Tables

(a) Example problem				
Airflow (cfm)	Fan Static Pressure			
	1.0 in. H ₂ O		2.0 in. H ₂ O	
	Rotating Speed (rpm)	Horsepower	Rotating Speed (rpm)	Horsepower
11,000	353	3.10	441	5.21
12,000	368	3.60	454	5.88

(b) General Nomenclature				
Airflow	Fan Static Pressure			
	$P_{s,1}$		$P_{s,2}$	
	Rotating Speed	Horsepower	Rotating Speed	Horsepower
Q_1	N_{11}	H_{11}	N_{12}	H_{12}
Q_2	N_{21}	H_{21}	N_{22}	H_{22}

A quick examination of Table 10.3 reveals that the required airflow is somewhere between the tabular values of 11,000 and 12,000 cfm, and the required fan static pressure is between the tabular values of 1 and 2 in. H₂O; the required fan rotating speed must thus be somewhere between 353 rpm, which would deliver 11,000 cfm at 1 in. H₂O, and 454 rpm, which would deliver 12,000 cfm at 2 in. H₂O. The proper fan operating speed is determined by linear interpolation between the tabular values.

Interpolation must be made between both the airflow values and the static pressure values. The resulting equation for fan operating speed is

$$N = N_{11} + \frac{P_{s,r} - P_{s,1}}{P_{s,2} - P_{s,1}} (N_{12} - N_{11}) + \frac{Q_r - Q_1}{Q_2 - Q_1} (N_{21} - N_{11}) \quad (10.13)$$

Similarly, the equation for required brake power is

$$H_b = H_{11} + \frac{P_{s,r} - P_{s,1}}{P_{s,2} - P_{s,1}} (H_{12} - H_{11}) + \frac{Q_r - Q_1}{Q_2 - Q_1} (H_{21} - H_{11}) \quad (10.14)$$

In this example

$$\begin{aligned}
 N &= 353 + \frac{1.33 - 1.0}{2.0 - 1.0} (441 - 353) + \frac{11,230 - 11,000}{12,000 - 11,000} (368 - 353) \\
 &= 353 + 0.33(88) + 0.23(15) \\
 &= 353 + 29 + 4 \\
 &= 386 \text{ rpm}
 \end{aligned}$$

and

$$\begin{aligned}
 H_b &= 3.10 + 0.33 (5.21 - 3.10) + 0.24 (3.60 - 3.10) \\
 &= 3.10 + 0.70 + 0.12 \\
 &= 3.92 \text{ hp}
 \end{aligned}$$

Finally, the static efficiency at the operating point can be calculated:

$$\begin{aligned}
 \eta_s &= \frac{p_s Q}{6343 H_b} & (10.9) \\
 &= \frac{(1.71)(11,240)}{(6343)(3.92)} \\
 &= 0.77
 \end{aligned}$$

The fan is thus operating at or near the point of maximum efficiency for this fan type (see Table 10.2 and Fig. 10.14*a*), so this size is an excellent choice for this application. If the efficiency had been lower, the next size fan in the series could have been tried, and a new operating point (rotating speed and horsepower) and efficiency calculated. The fan size that gives the maximum efficiency should be chosen for use.

LIST OF SYMBOLS

A	area
H	power
H_a	air power
H_b	brake power
H_m	motor power
N	fan rotating speed
P_s	fan static pressure
$P_{s,r}$	required fan static pressure
P_t	fan total pressure
P_s	system static pressure
$P_{s,i}$	static pressure at fan inlet
$P_{s,o}$	static pressure at fan outlet
$P_{v,i}$	velocity pressure at fan inlet
Q	airflow
Q_r	required airflow
V_i	velocity at fan inlet
W	work
Δ_p	pressure drop
η_m	electrical-to-mechanical energy conversion efficiency
η_s	fan static efficiency
η_T	fan total efficiency

REFERENCES

- American Society of Heating, Refrigerating and Air Conditioning Engineers, 2000 *ASHRAE Handbook—HVAC Systems and Equipment*, ASHRAE, Atlanta, GA, 2000.
- R. Jorgensen, ed., *Fan Engineering*, 9th ed., Howden, Inc., Buffalo, NY, 1999.

PROBLEMS

- 10.1** The static pressure loss in a local exhaust ventilation system is 3.78 in. H_2O , the velocity pressure in the duct entering the fan is 0.85 in. H_2O , and the velocity pressure in the duct exiting the fan is 0.66 in. H_2O . What is the fan static pressure?

Answer: 2.93 in. H_2O

- 10.2** A local exhaust system consists of a 6-in.-diameter round duct connected to the inlet of a centrifugal fan and an 8-in.-diameter round stack connected to the outlet of the fan. If the system static pressure is 9.10 in. H_2O and the fan static pressure is 8.22 in. H_2O
- (a) What is the average velocity in the inlet duct?
 - (b) What is the system airflow?
 - (c) What is the average velocity in the outlet duct?

Answers:

- (a) 3760 ft/min
- (b) 740 ft³/min
- (c) 2120 ft/min

- 10.3** A local exhaust ventilation system has a system static pressure loss of 6.55 in. H_2O , an airflow of 13,140 ft³/min, and a brake power of 17.6 hp. What is the fan static efficiency?

Answer: 0.77

- 10.4** A local exhaust ventilation system has a system static pressure drop of 2.37 kPa, an airflow of 3.65 m³/s, and a static efficiency of 65%. What brake power is the system drawing?

Answer: 13.3 kW

- 10.5** A fan is operating with a brake power of 11.7 kW and an air power of 7.2 kW. What is its total efficiency?

Answer: 0.62

- 10.6** A local exhaust ventilation system has a centrifugal fan with a 4-in.-diameter duct connected to its inlet and a 6-in.-diameter duct connected to its outlet.

The velocity pressure in the 4-in. duct is 0.93 in. H_2O , the static pressure at fan inlet is -4.81 in. H_2O , and the fan static pressure is 5.11 in. H_2O . What is the static pressure at the fan outlet?

Answer: 1.23 in. H_2O

- 10.7** A local exhaust ventilation system has a centrifugal fan rotating at 504 rpm. The airflow is $2.5 \text{ m}^3/\text{s}$, the system static pressure is 740 Pa, and the brake power is 2.8 kW. If the rotating speed is increased to 550 rpm, what are the new values for airflow, system static pressure, and brake power?

Answers: $Q_2 = 2.7 \text{ m}^3/\text{s}$, $P_{s,2} = 880 \text{ Pa}$, $H_{b,2} = 3.6 \text{ kW}$

- 10.8** A centrifugal fan is operating at a rotating speed of 770 rpm and is producing an airflow of $2400 \text{ ft}^3/\text{min}$, a system static pressure of 7.8 in. H_2O , and a brake power of 4.6 hp.

- (a) What rotating speed is required to double the airflow?
- (b) What effect does this increase have on static efficiency?

Answers:

- (a) $N_2 = 1540 \text{ rpm}$
- (b) Although both the static pressure and brake power increase dramatically, the efficiency remains constant.

- 10.9** A local exhaust system is constructed such that the airflow equals 1000 cfm when the system static pressure loss is 1 in. H_2O and the airflow equals 2000 cfm when the system static pressure loss is 4 in. H_2O . A forward-curved blade centrifugal fan with a static no delivery (SND) of 8 in. H_2O and a full delivery no pressure (FDNP) of 4000 cfm is connected to the system and is operating at a rotating speed of 523 rpm.

- (a) Draw the fan curve and the system curve on a graph and estimate the system operating point (airflow and static pressure). Assume for simplicity that the fan static pressure equals the system static pressure.
- (b) Assume that the fan speed has increased to 607 rpm. Draw a new fan curve and estimate the new system operating point.

AIR-CLEANING DEVICES

This chapter is not intended to be a comprehensive survey of air-cleaning devices used in conjunction with industrial ventilation systems. Such an effort would take a full volume in itself, and several such texts are available (Licht, 1980; Stern, 1977, 1986; Strauss, 1975; Theodore and Buonicore, 1982; Heinsohn and Kabel, 1999; Cooper and Alley, 2002). Rather, in this chapter we cover the aspects of air-cleaning device selection and design that are important considerations during the design of local exhaust ventilation systems.

The ventilation system designer must know what *type* of air cleaning device will be used with the system, its *dimensions*, the *configuration* of the inlets and outlets, and the *pressure drop* across the device. In addition, the designer must know if the device changes the psychrometric state point of the airstream in any significant way (e.g., by cooling it, thereby reducing the airflow). Each of these considerations is discussed in this chapter.

The importance of including an air-cleaning device as an integral part of the original ventilation system design cannot be overemphasized. Since a local exhaust ventilation system is being designed to collect a contaminant from the workplace, and this contaminant presumably presents some danger to the workers, it is usually not acceptable just to discharge the contaminant into the general environment. Not only does this trade an outdoor pollution problem for an indoor one, it also creates the potential for contaminant reentry into the workplace.

The air-cleaning device should always be included in the original ventilation system design rather than added on later. Certain characteristics, such as the pressure

drop across the device, its size and location, and its power requirements, must be taken into account during the ventilation system design phase.

11.1 CATEGORIES OF AIR-CLEANING DEVICES

The usual method of categorizing air cleaners is by type of contaminant being collected. Particles and gases or vapors require completely different collection mechanisms, and the devices used reflect this difference.

11.1.1 Particle Removers

The principal particle collection methods are gravity settling, centrifugation, filtration, electrostatic precipitation, and scrubbing. In this section we briefly describe the most common types of equipment incorporating these methods, concentrating on the characteristics that are important in selecting an air cleaner for a particular application.

Gravity Settling Devices. This type of device is the simplest available and has the most limited application. The simple horizontal flow gravity settling chamber (Fig. 11.1) operates by increasing the cross-sectional area of the duct, thereby reducing the gas velocity and increasing the particle residence time inside the settling chamber. Since airborne particles settle at a constant velocity due to the force of gravity, the device is designed to allow particles sufficient time to fall into the hoppers.

In theory, any particle size could be collected in a settling chamber by making the device sufficiently large to give the smallest particles time to fall out of the gas stream. In practical applications, such devices are limited to the collection of very large particles because of the low settling velocities of small particles. This limitation

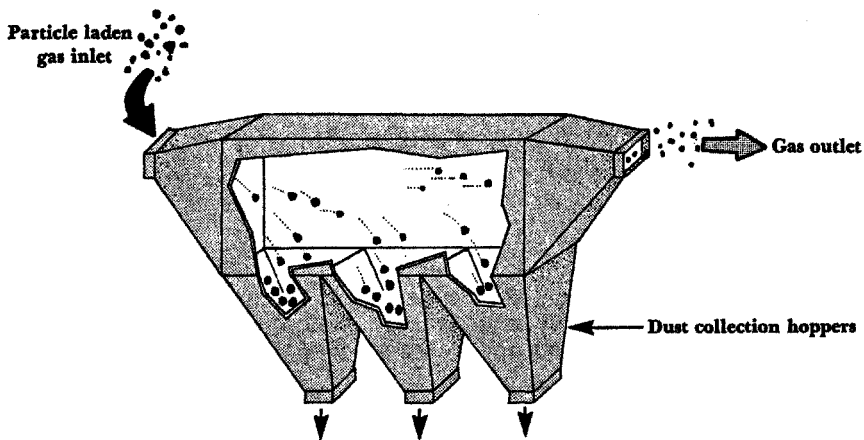


Figure 11.1 Gravity settling chamber.

Table 11.1 Terminal Settling Velocities of Particles with Selected Aerodynamic Diameters

Particle Diameter (μm)	Settling Velocity (cm/s)
0.01	0.000007
0.1	0.00008
1	0.004
5	0.08
10	0.3
20	1.2
50	7.5
100	25

is illustrated in Table 11.1, which lists theoretical gravitational settling velocities for a range of particle sizes.

It should be apparent that only particles with an aerodynamic diameter* larger than about $50\mu\text{m}$ will be collected efficiently in such a device. Inhalable and respirable particles are difficult to collect; gravity settlers are thus limited to applications where high concentrations of large particles are generated and present a housecleaning problem which is solved by collecting the particles in a local exhaust ventilation system.

Centrifugal Collectors. These devices, commonly called “cyclones,” are probably the most common air-cleaning device found in industry. This popularity is due to their simple construction, with no moving parts, which makes them inexpensive to buy and easy to maintain. An offsetting limitation, however, is the large amount of energy required to collect small particles.

Cyclones are similar to gravity collectors in concept, except that they use centrifugal force rather than gravity to separate particles from the airstream. In a conventional cyclone (Fig. 11.2) the air is introduced tangentially into a cylindrical body section and above a conical section leading to a hopper. The gas spins around the cylinder and particles are thrown toward the walls by centrifugal force. Particles that strike the walls fall into the hopper, while those too small to be influenced by the centrifugal force travel with the gas stream into the cone and back up through the outlet.

Since centrifugal forces can be achieved that are many times larger than that due to gravity, these devices can better collect small particles than can gravity settlers. As with gravity settlers, it is theoretically possible to collect particles of any size in cyclones; in practice, excessive energy requirements usually limit their use to particles with an aerodynamic diameter greater than $10\mu\text{m}$.

**Aerodynamic diameter* is defined as the diameter of the standard density (density of water, 1 kg/m^3) sphere that settles with the same velocity as the particle under question. Aerodynamic diameter is normally used when describing the properties of air-cleaning devices, since it normalizes for the effects of particle shape and density.

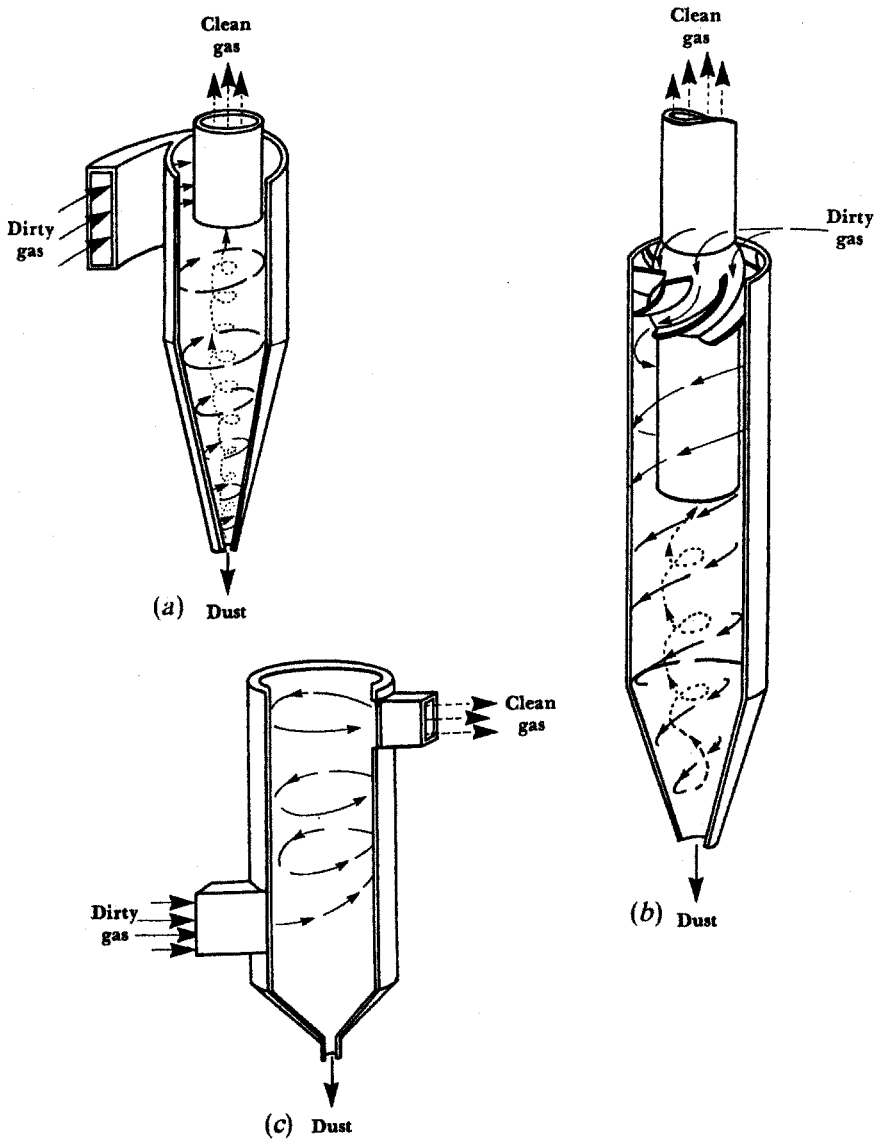


Figure 11.2 Types of cyclones: (a) top inlet; (b) axial inlet; (c) bottom inlet.

Cyclones are relatively compact devices and can be integrated into an exhaust system rather easily. Because of the particle-size limitations, they should be used primarily for the collection of nuisance dusts and as preseparators for other more efficient particle removal devices. They can collect both solid and liquid particles, but should not be used for sticky dusts or other materials that would not easily fall down the walls and be collected in the hopper. Cyclones can be made out of almost

any material and can thus be used to remove dusts from hot and/or corrosive gas streams.

Filters. As used in air-cleaning work, “filter” is the general name for three basic types of devices, *i.e.*, fibrous and granular (“media”) filters, high-efficiency particle air (HEPA) filters, and fabric filters. All three may be used in conjunction with local exhaust ventilation systems, but they have completely different characteristics and applications.

Media Filters. These devices are so named because they collect particles by their aerodynamic capture on individual filter elements throughout the depth of the filter medium. The most common media are various types of fibers and granules. Because these filters collect particles throughout the depth of the material, they are generally difficult to clean and reuse. Most fibrous filters, in fact, are designed to be thrown away after they are loaded with dust.

Media filters have two principal uses: as prefilters to remove large particles before a second-stage collector of greater efficiency, and as filters for dusts that cannot easily be collected and cleaned from other collectors. An example of the first use is the common furnace-type filter, which can collect only large particles and is thrown away after becoming loaded with dust. An example of the second type would be a deep-bed fibrous filter used to collect sticky particles.

HEPA Filters. HEPA filters (Fig. 11.3) are used wherever extremely high particle collection efficiency is required. Filters of this type are constructed of a filter paper that is folded to give a very high surface area to the filter. This construction lowers the filtration velocity, leading to the low pressure drop and high collection efficiency characteristic of this filter, but it makes the device impossible to clean. The close spacing between the folds makes the dust-holding capacity of these filters very low. The combination of lack of cleanability with low dust capacity limits the use of these filters to gas streams with very low dust loading. These filters originally were designed to remove radioactive particles from atmospheric air, and should be used only in gas streams where the concentration approximates those found in typical outdoor atmospheres (e.g., $50 \mu\text{g}/\text{m}^3$). Used under these conditions, a HEPA filter should operate at an acceptable pressure drop for at least several years before it must be replaced.

HEPA filters are used extensively wherever ultraclean air is needed, such as in hospital operating rooms and the cleanrooms used in electronics and pharmaceutical manufacturing. In these applications the HEPA filters are cleaning the supply air, rather than the exhaust. They are also used where emission levels must be very low, for example as a second-stage collector located downstream from a fabric filter that is collecting lead dust.

HEPA filters are becoming more common as fail-safe devices in exhaust air recirculation systems. Because they have such high inherent collection efficiency, they can serve as second-stage collectors to collect particles if the first stage fails, thus offering protection to the workers (see Chapter 12).

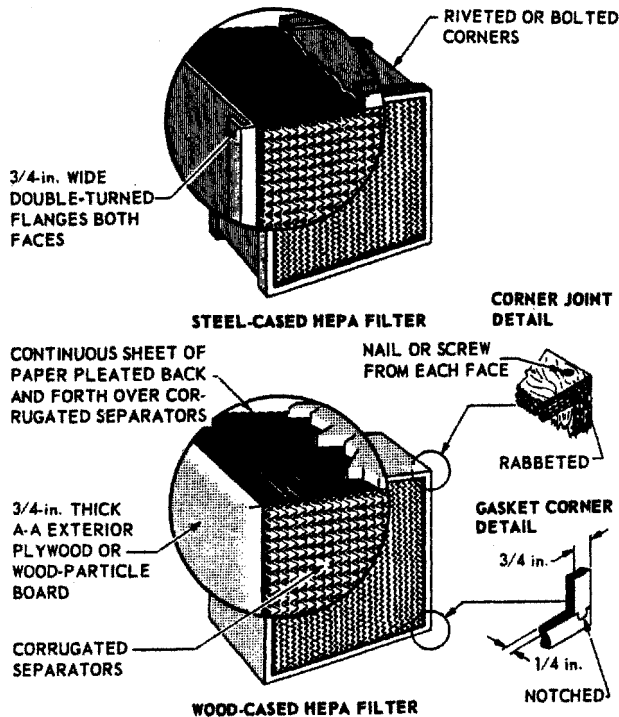


Figure 11.3 High-efficiency particulate air (HEPA) filter construction.

Fabric Filters. Fabric filters (Fig. 11.4) are by far the most common type of filter encountered in the industrial environment and the one most likely to be used in a local exhaust ventilation system. The filter itself consists of pieces of fabric sewn into cylinders or envelopes and mounted in a housing. During operation, exhaust air is drawn through the fabric by the fan; particles either collect in the fabric itself or in a dust cake on the fabric surface and are thus removed from the exiting exhaust stream.

As with other filters, fabric filters must eventually be cleaned. In fact, cleaning is so important that fabric filters are classified by the cleaning method used. The three most common cleaning methods are shaking, reverse airflow, and pulse jet air. Each of the three cleaning methods has different applications, which will be described briefly.

Shaking is the oldest and simplest method to clean a fabric filter. The tops of the bags are oscillated in either the horizontal or vertical direction; this motion flexes the fabric and causes the collected dust cake to be dislodged and fall into the hopper. Shaker-cleaned bags are generally constructed of woven fabrics, which collect the dust as a surface cake that is easily dislodged by the fabric flexion.

The shaking mechanism is usually motor driven and can be initiated either automatically (e.g., by sensing excess pressure drop) or manually whenever the operator decides cleaning is necessary. Small units may not employ a motor and are cleaned

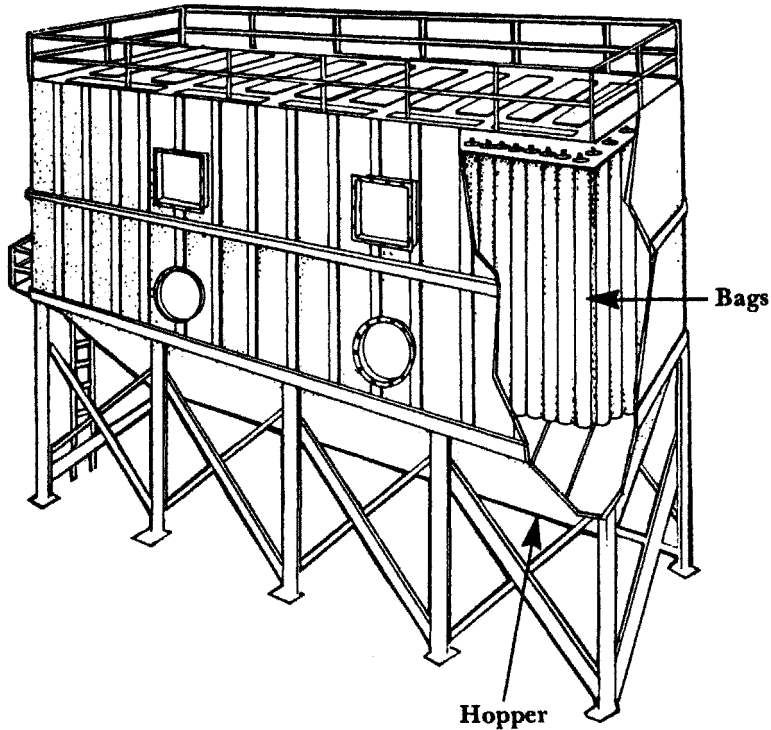


Figure 11.4 Typical pulse-jet baghouse.

instead by moving an external lever that oscillates the bags. Exhaust airflow must be shut down before a bag is shaken, to allow the dislodged dust to fall into the hopper. This means that either the process has to be shut down while the baghouse is cleaned, or the baghouse has to be divided into compartments so that one compartment can be isolated and shut down with dampers while the remaining compartments continue filtering the exhaust air. The first alternative is possible for intermittent operations or operations which produce so little dust that the baghouse can be cleaned once at the end of the workshift; most applications, however, will require a compartmentalized baghouse.

In some instances bag shaking is supplemented by a gentle reverse airflow through the fabric; this reverse flow helps to carry the dislodged dust away from the fabric and into the hopper. Reverse flow cleaning requires a system of dampers to shut off the main flow and open the reverse flow; this tends to complicate the baghouse design and operation and increases capital and operating costs. Consequently, reverse air cleaning is usually found only in rather large baghouses filtering a dust that is difficult to remove with shaking alone.

High-temperature filtration requires the use of specialized fabrics, such as fiberglass, which can withstand this severe environment. Woven fiberglass cannot tolerate shaking, so baghouses using these fabrics employ gentle reverse air cleaning without

shaking. Such systems usually require bags with special surface treatment to enhance the release of dust.

The last major fabric filter cleaning technique employs blasts of high-pressure air to remove collected dust. A typical system using this method, called *pulse jet cleaning*, is shown in Fig. 11.5. A short pulse of high-pressure compressed air is introduced into the top of the bag. This pulse travels down the bag, temporarily reversing flow through the fabric and flexing the bag outward. This sudden flexing dislodges dust from the outer surface of the fabric in the form of agglomerates, which fall toward the hopper. Cleaning pulses can either be applied at regular intervals by incorporating a timer or can be initiated by sensing excess pressure drop across the fabric.

Pulse jet cleaning requires the use of felted fabrics rather than woven ones, to withstand the violent motion induced by the pulses. Felted fabrics tend to collect dust throughout the depth of the felt rather than at the surface as a cake; this porous dust deposit is more difficult to remove than a surface deposit, so pulse jet cleaning is less efficient than the other methods and typically must be applied more often.

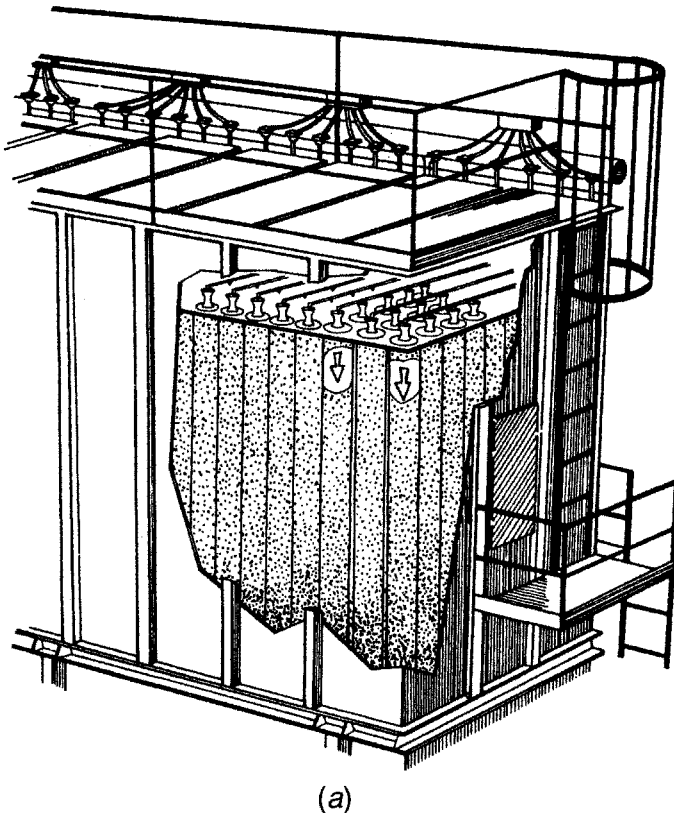


Figure 11.5 Typical reverse-pulse baghouse during cleaning cycle. (a) general view; (b) close up of pulse travelling down bag.

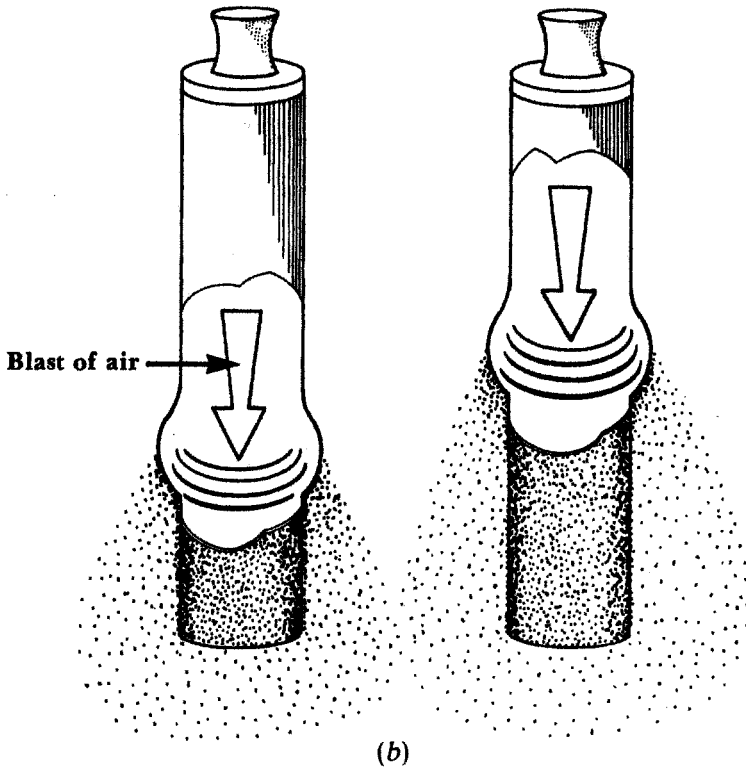


Figure 11.5 Continued.

Pulses can be applied to a bag either *on line*, where normal airflow is maintained through the system during cleaning, or *off line*, where a compartment is isolated from the exhaust flow during cleaning. Most pulse-jet systems use on-line cleaning; such systems constitute the simplest type of fabric filter since they require no moving parts, such as isolation dampers or shaking mechanisms. This is a big advantage from the point of view of maintenance, but naturally there are tradeoffs involved. On-line cleaning is not as effective at removing dust as off-line cleaning, since the exhaust airflow tends to redeposit dust onto the fabric after the pulse is over. Off-line cleaning allows the removed dust to fall into the hopper before filtration resumes, but requires the additional complication and expense of isolation dampers.

Electrostatic Precipitators. This class of air cleaner collects particles from an exhaust stream by three distinct steps. Particles are first imparted an electrical charge. Next, the charged particles are attracted toward and collected on grounded plates. Finally, the collected particles are removed from the collecting plates to a hopper. Precipitators are classified as *single-stage*, where the particle charging and collection occur in the same section of the device, and as *two-stage*, where the two actions take place in sequential sections.

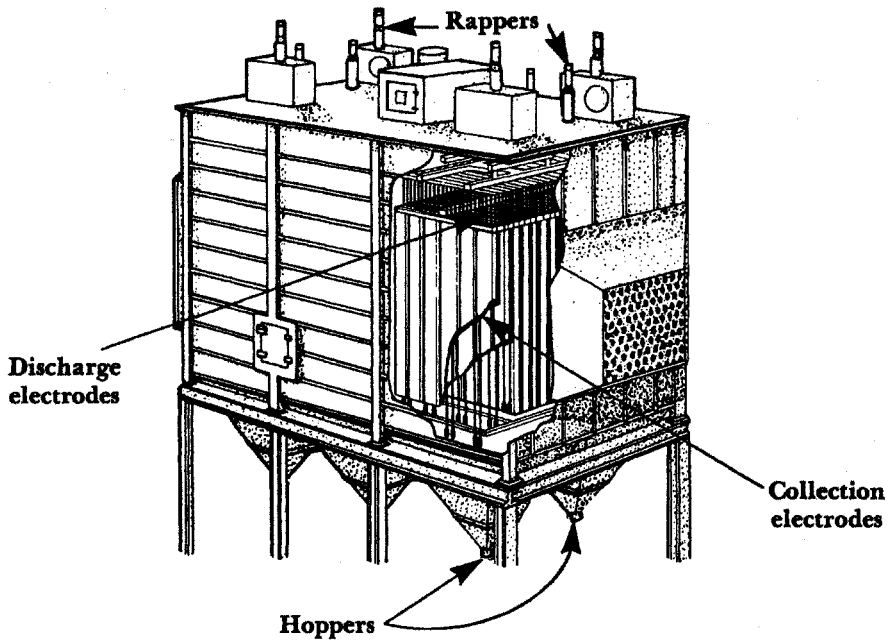


Figure 11.6 Typical single-stage electrostatic precipitators.

For economic reasons the application of single-stage precipitators (Fig. 11.6) is limited to large-volume gas streams, such as the exhaust from coal-fired power plants and cement kilns. Such devices will not generally be found on small, multihood local exhaust systems.

Two-stage precipitators (Fig. 11.7), on the other hand, are used for low-volume gas streams with relatively low dust loadings such as atmospheric dust removal in HVAC systems, smoke and fume removal from general room air, and on single-hood local exhaust systems. The ventilation system designer may encounter suitable applications for such devices from time to time.

Scrubbers. There are several device types that remove particles from a gas stream by contact with a liquid, but the most common is the venturi scrubber. Other scrubbers, such as gravity and centrifugal spray towers, self-induced spray scrubbers, and impingement plate and packed-bed scrubbers, have limited specialized applications for particle collection and are not described here.

The venturi scrubber (Fig. 11.8) is a very simple device, in both construction and operation. Exhaust gases are accelerated to high velocity through the throat of the Venturi, where water is introduced. The high-velocity gas shears the water stream into droplets and the high relative velocities cause particles to be collected on the droplets, primarily by impaction. The droplets are subsequently removed from the gas stream in a cyclone or entrainment separator.

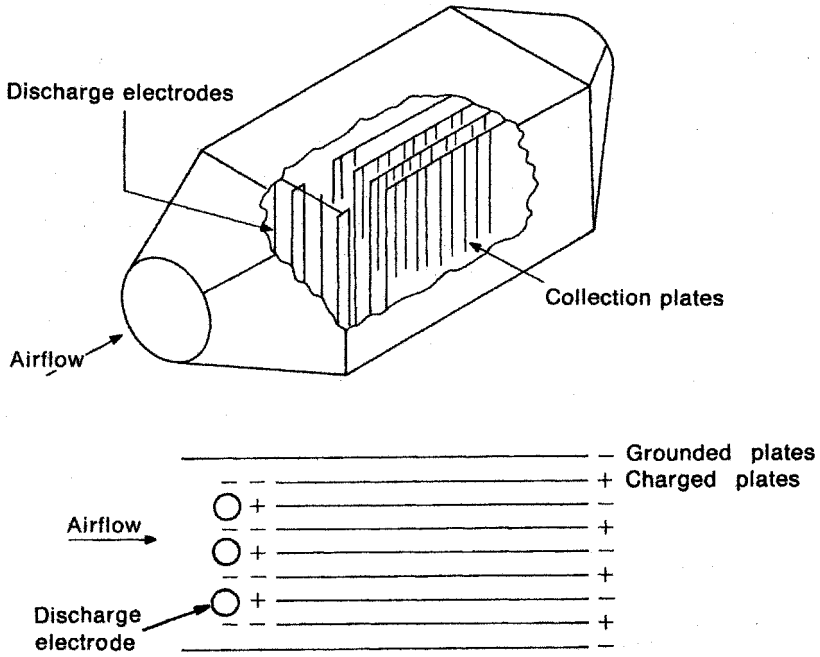


Figure 11.7 Typical two-stage electrostatic precipitator.

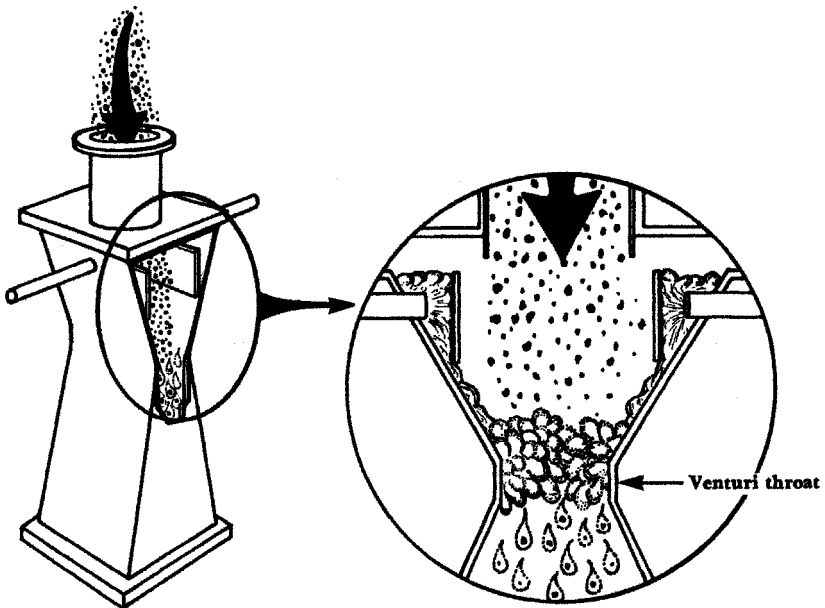


Figure 11.8 Typical Venturi scrubber.

Venturi scrubbers have several characteristics that make them useful in particular applications. They can collect particles from high-temperature gas streams, which are then cooled and washed at the same time. This type of scrubber can collect and neutralize corrosive gases and mists, and works well in situations that present a fire or explosion hazard. Venturi scrubbers are very compact because they operate at high gas velocities; they thus do not occupy much space in the plant.

There are inherent disadvantages to Venturi scrubbers which limit their application. The primary disadvantage common to all wet devices is the disposal of the waste liquid. The use of liquids creates other problems, such as corrosion, freezing in cold weather, and creation of a high-humidity exhaust gas stream.

Another important disadvantage is the high energy required to collect small particles. Like cyclones, Venturi scrubbers trade simple design for difficulty in collecting small particles; both devices require a very high velocity to collect these particles, which entails a high-pressure drop. Scrubbers require additional energy to accelerate the water droplets from rest to the gas velocity. This energy requirement easily outstrips that needed to accelerate the gas. The required pressure drop to operate a scrubber can exceed 60 in. H₂O (15 kPa) if small particles are to be collected.

The disadvantages inherent in Venturi scrubbers limit their use to applications where other device types have difficulty performing satisfactorily. These include the collection of acid mists and other corrosive liquid aerosols, high-temperature fumes such as those from incineration and foundry and steel furnaces, and sticky, viscous particles such as those found in asphalt production.

11.1.2 Gas and Vapor Removers

The selection of a method to remove gases and vapors from an exhaust stream is somewhat simpler than for particles. There are only three basic methods: absorption in a liquid, adsorption on a solid, and chemical reaction (including incineration) to change a harmful gas or vapor to one less so. With some exceptions for the third, each of these processes involves the diffusion of the gaseous molecules to a surface, where the various removal mechanisms take place. This dependence on a single collection mechanism is in marked contrast to the situation for particles, where a myriad of collection mechanisms operate to remove particles to surfaces. The selection and design of gas and vapor removers should thus present fewer problems than for particle removers.

Absorbers. Absorption involves the diffusion of gaseous molecules to the surface of a liquid, where they are removed by further diffusion into the bulk of the liquid. To be efficient, close contact must be made between the exhaust gas and the liquid. There are two techniques used in the design of practical absorbing devices to ensure such close contact: either the gas is passed through a continuous stream of the liquid or the liquid is dispersed as drops through the gas.

The two most common methods for passing gas through the liquid are plate towers and packed towers (Fig. 11.9). The plates in the former are perforated to allow liquid and gas to flow. The packing in the latter may take the form of simple broken rock or gravel, rings, saddles, or low-density material such as fibers or expanded

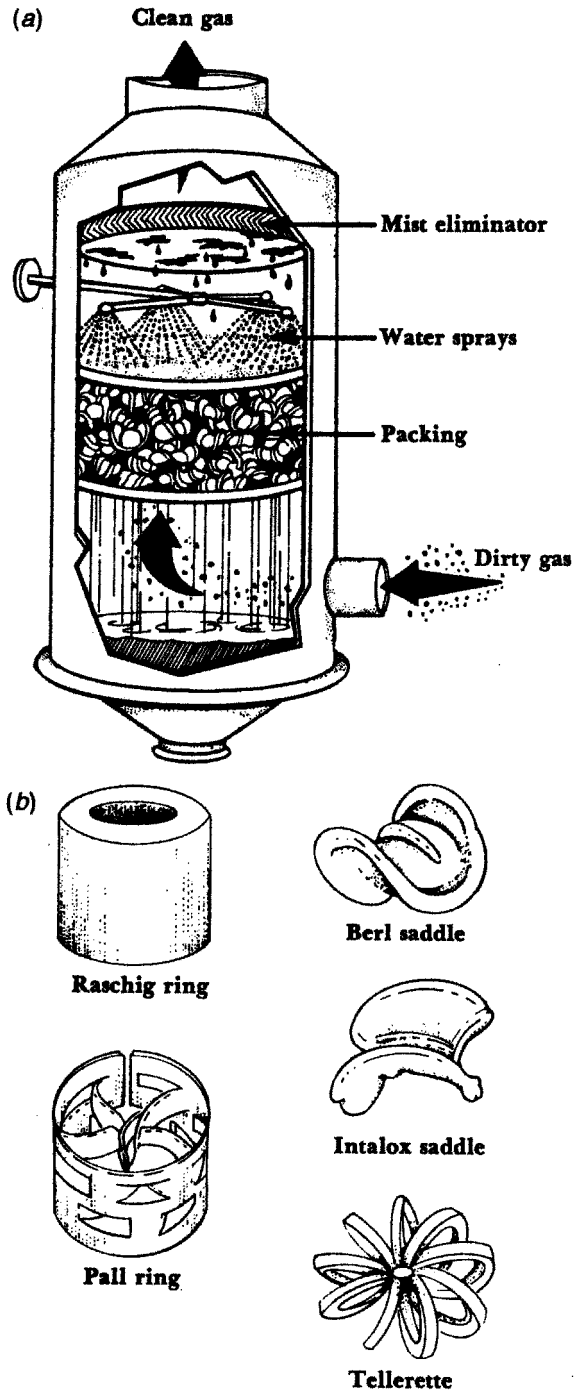


Figure 11.9 Simple packed tower: (a) tower design; (b) a sampling of typical packing materials.

metal. Complex shapes such as saddles are more expensive but spread the liquid over a larger effective surface area, thereby increasing collection efficiency for a given tower size, but entail additional capital cost over simpler materials.

The diameter of a tower is selected to give the desired gas velocity through the packing material. If the velocity is slowly increased a point will be reached where the gas has sufficient velocity to hold up the liquid and flooding will occur. Scrubbers are usually designed to operate at about 50–60% of the flooding velocity; this value and the total gas flow determine the cross-sectional area of the tower. The height of the tower is determined by the inherent efficiency of the device (“height of a transfer unit”) and the overall efficiency desired (“number of transfer units”).

Adsorbers. Adsorption is similar to absorption in that gas molecules are removed from an exhaust stream by diffusing to a surface—in this case, however, the surface is solid rather than liquid. The mechanisms by which molecules actually adhere to a solid surface are complex, making generalizations about the design of such devices difficult. In general, molecules are held to solid surfaces by physical forces, chemical reaction (chemisorption), or some combination of the two.

Adsorption proceeds in three steps. The first step, diffusion of the gas to the surface, is identical to the diffusion mechanism discussed for absorption. The second step is the penetration of the molecules to be collected into the pores of the adsorbing material. The third step is the actual adsorption of the molecule into the pore. The third step is very rapid compared to the first two, so it is the rate of diffusion to the surface and into the pores that determines the rate of adsorption in any particular case.

Turk (Stern, 1977) summarizes the factors that control the mass of material that can physically be adsorbed by a given mass of adsorbent.

- The concentration of the material in the space around the adsorbent
- The total surface area of the adsorbent
- The total volume of pores in the adsorbent whose diameters are small enough to facilitate condensation of gas being adsorbed
- The temperature
- The presence of other gases that may compete for sites on the adsorbent
- The characteristics of the molecules to be adsorbed (especially their molecular weight, electrical polarity, size, and shape)
- The electrical polarity of the adsorbent surface

Adsorbents are classified as *polar* or *nonpolar*, depending on the distribution of electrical charges on the surface at the molecular level. The only important nonpolar adsorbent is carbon, which presents an array of neutral atoms that create a homogeneous surface with no potential gradients. Carbon is very efficient at attracting nonpolar molecules in preference to polar ones; it is thus used extensively to collect nonpolar organic molecules (e.g., chlorinated hydrocarbons, alcohols). The form of carbon used for adsorption is activated carbon (also called *activated charcoal*), which consists of particles of carbon with a very large surface area.

Polar adsorbents are oxides, either of silicon (silica, in the form of silica gel, Fuller's earth, or diatomaceous earths) or metals (most commonly aluminum oxide). These adsorbents are used for the removal of polar molecules such as water vapor, ammonia, formaldehyde, sulfur dioxide, and acetone.

A third category of adsorbents are those that combine adsorption with chemical reaction. This is usually accomplished by the impregnation of activated carbon or alumina with a reagent or catalyst. There is a whole range of such reactions that can be used for the removal of specific gases and vapors. Examples include the impregnation of activated carbon with bromine for the removal of ethylene or other olefins by conversion to dibromide and the impregnation of activated alumina with potassium permanganate for the oxidation of formaldehyde.

Chemical Reaction Devices. One example of chemical reaction, chemisorption, was discussed under adsorption. The other common form of chemical reaction for the removal of gaseous constituents is oxidation, either by flame or by thermal oxidation with or without a catalyst. Both techniques are applicable when the gaseous pollutant can be oxidized. The ideal products of such oxidation of the pollutant are water vapor and either carbon dioxide (for organic material) or sulfur dioxide (for organic sulfides).

If the concentration of the contaminant gas in the exhaust stream is between the lower and upper explosive limits, it generally can be oxidized by direct combustion either in a flare or a direct combustion chamber. Such devices have to be carefully designed and operated, because of the inherent danger of explosion.

Oxidizable contaminants present in concentrations below the lower explosive limit can be removed by thermal oxidation in a device called an *afterburner*. Afterburners can be either *thermal*, where the contaminant is oxidized by heating in a flame, or *catalytic*, where preheated waste gas is oxidized on a catalyst at temperatures considerably lower than would be possible using thermal oxidation alone. The most popular catalyst is a finely divided precious metal, such as platinum or palladium, supported on another material, such as a crimped nickel-alloy ribbon or activated alumina. The catalytic converter used in automobiles is a common example of such a device.

Catalyst materials are expensive, but are usually employed in small amounts so that the additional cost of a catalytic afterburner over the thermal type is usually not excessive. In any case, the energy savings over the life of the device due to the lower oxidation temperature required would far exceed the additional capital cost. Additional savings can be incurred by recovering the waste energy.

11.2 MATCHING THE AIR-CLEANING DEVICE TO THE CONTAMINANT

11.2.1 Introduction

Possibly the most difficult step in solving an air-cleaning problem is the selection of the device type to be used. This is obviously a complex subject, and can be only summarized in this book. The reader is urged to consult texts on air cleaning such as those listed in the References.

Selection of the proper device type depends on a knowledge of certain basic information about both the contaminant to be removed and the carrier airstream. The most important information about the contaminant is, of course, its physical state. If it is a gas or vapor, further information concerning chemical species, temperature, concentration, and so on, will be required. Particle collection will require information on particle state (solid, liquid, sticky solid), size, shape, density, and surface properties, in addition to concentration in the exhaust stream.

The principal properties of interest concerning the exhaust stream itself are temperature, pressure, and total airflow. In addition, secondary properties such as gas composition, moisture content, combustibility, and viscosity are sometimes of importance.

Information about the contaminant and exhaust air can usually be obtained rather easily if the process is already in operation by sampling the exhaust stream. If it is a new process in the design stage, the required information may be available from another identical or similar plant. Information on many basic industrial operations is available in the literature, and these sources should be consulted (U.S. Environmental Protection Agency, 1973, 1978). For completely new processes, or the application of a new device type to an old process, it may be necessary to construct a pilot-scale air cleaner and test it either on a pilot version of the process or on a sidestream from the actual process to be cleaned.

11.2.2 Device Selection

Many generalizations about the suitability of air-cleaning devices for certain applications should be evident from the discussion in Section 11.1. Much of the basic information about collection device characteristics, summarized in Table 11.2, can be used as an aid in device selection.

There appears to be increased interest in the fractional collection efficiency of various types of control equipment for collecting particles of various sizes. This is particularly important for the control of respirable particles in the industrial environment. Experimental data concerning the fractional efficiency of various categories of particle collection equipment are summarized in Fig. 11.10.

Occasionally, two device types will be equally efficient at collecting the contaminant of interest. When this occurs, selection will depend on the relative annualized operating costs of the two devices. The components of this cost are the capital, operating, and maintenance costs associated with the equipment. Many times a system that is cheaper initially may have higher operating costs (i.e., higher pressure drop) or may be more difficult to maintain. All such factors should be considered carefully when selecting an air cleaner.

11.3 INTEGRATING THE AIR CLEANER AND THE VENTILATION SYSTEM

Previous sections of this chapter have discussed the characteristics of air-cleaning devices and the problems in choosing one for a specific application. In this section

Table 11.2 Collection Device Characteristics

Collection Device Type	Types of Contaminants	Typical Loading	Collection Efficiency	Pressure Drop (in. H ₂ O)	Initial Cost	Operating Cost	Serviceability (Durability)
<i>Particles</i>							
Inertial collectors							
Settling chambers, inertial separators, cyclones, dynamic (fan and separator)	Crushing, grinding, machining	0.1–100 g/m ³	High for $d_p > 10\ \mu\text{m}$	2–6	Low	Moderate	Good (erosion)
Filters							
Industrial cleanable cloth	All dry powders	0.1–20 g/m ³	High for $d_p > 0.1\ \mu\text{m}$	3–6	Moderate	Moderate	Good
Paper, deep-bed (HEPA)	Precleaned, atmospheric air	< 0.001 g/m ³	High for all sizes	1–6	Moderate	High	Fair to poor
Electrostatic precipitators							
Single-stage	Flyash, H ₂ SO ₄	0.1–2 g/m ³	High for $d_p > 0.1\ \mu\text{m}$	0.5–1	High	Low	Fair
Two-stage	Welding fume, cigarette smoke	< 1 g/m ³	High for $d_p > 0.1\ \mu\text{m}$	0.5–1	Moderate	Low	Good
Wet scrubbers							
Venturi scrubber	Chemical and metallurgical fumes	0.1–100 g/m ³	High for $d_p > 0.25\ \mu\text{m}$	20–80	Low	High	Good (corrosion)
Wetted baffles, wetted cyclone, wetted dynamic	Crushing, grinding, machining	0.1–100 g/m ³	High for $d_p > 2\ \mu\text{m}$	2–6	Moderate	Moderate	Good (corrosion)

Table 11.2 (Continued)

Collection Device Type	Types of Contaminants	Typical Loading	Collection Efficiency	Pressure Drop (in. H ₂ O)	Initial Cost	Operating Cost	Serviceability (Durability)
<i>Gases and Vapors</i>							
Packed-tower absorber	Inorganic gases (HCl, HF, SO ₂ , Cl ₂)	ppm to %	90–99%	4–12	Moderate	Moderate	Poor
Carbon bed (adsorbers)	Organic gases and vapors (odors)	ppb to %	95–99 + %	2–6	High	Moderate	Fair
Direct-flame incinerator	Organic gases and vapors (odors)	ppb to %	90–99	0.2	Low	Extremely high	Good
Catalytic converter	Organic gases and vapors (odors)	ppb to %	90–99	2–6	Moderate	High	Poor

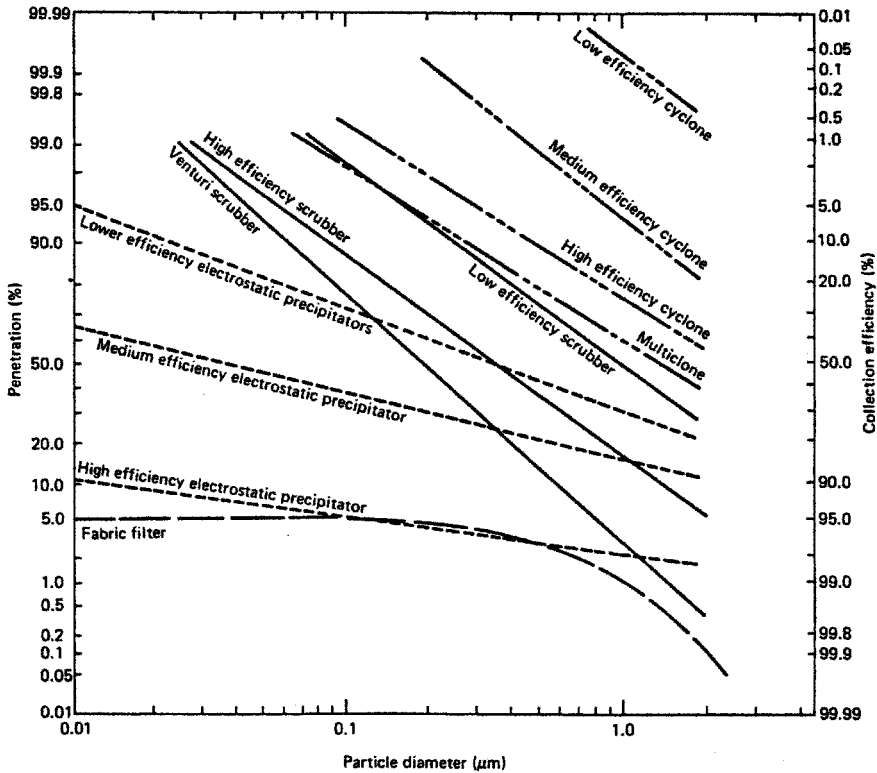


Figure 11.10 Fractional efficiency curves for various air cleaners.

we address the problem of integrating the selected device into the local exhaust ventilation system.

From the point of view of the ventilation system designer, the two most important aspects of the air cleaner are its physical characteristics and the pressure drop it will require at the design airflow. Information about both of these should be available from the device manufacturer. The physical characteristics of the device must be known, of course, so that the final layout of the ventilation system can be specified. It is important that the designer obtain detailed information concerning the device size, weight, and location and size of the inlet and outlet ducts.

Many times the designer will develop a preliminary layout of the exhaust system before the air cleaner is selected; this preliminary design will usually have to be modified after a particular device is specified. Such modifications may be minor, or the air cleaner might be so large (for example) that the entire system layout has to be changed. For reasons such as these it is generally a good idea to select the specific air cleaner *before* attempting a detailed design of the LEV system.

The question of pressure drop presents even more problems to the ventilation system designer. The operating pressure drop of the air cleaner must, of course, be known

in the design stage to determine the required fan static pressure. For many devices it is difficult, if not impossible, to obtain good information on the expected operating pressure drop for a particular operation.

This problem may not be particularly important if the pressure drop across the device is a small fraction of the total static pressure required by the exhaust system. In many cases, however, the pressure drop across the air cleaner is the *predominant* pressure drop for the entire system. The designer may spend many hours obtaining the required static pressure of the exhaust system, only to have this precise number overshadowed by a much larger air cleaner static pressure which cannot be specified closer than a factor of 2.

Many factors contribute to uncertainties about air cleaner static pressure requirements. For some devices, such as fabric filters, the pressure drop is strongly dependent on the particular dust being filtered and the cleaning method employed. For others, such as Venturi scrubbers, the pressure drop is proportional to the collection efficiency; in this case, if the scrubber does not provide the desired collection efficiency, the pressure drop may have to be increased above that selected in the design stage.

The best source of pressure drop data is from an identical air cleaner serving an identical process. The second best source of information is from a pilot-scale device on a pilot plant or sidestream of the exhaust being cleaned. The budget may not allow the collection of such data for small local exhaust systems. In these cases it is best to rely on information supplied by the air cleaner manufacturer.

Equations are available that allow the prediction of pressure drop from basic information about the air cleaner and the process being exhausted; such equations are subject to the uncertainties discussed above. They can be useful in the design stage, however, as an aid to device selection.

The remainder of this section contains brief descriptions of the pressure drop characteristics of each basic type of air cleaner. Included are simple equations for predicting pressure drop, and a discussion of any problems peculiar to that device type. A quick review of this material should convince the reader of the difficulty of using general equations to predict operating pressure drop for a specific device and application; the best sources of pressure drop data almost invariably are those mentioned above.

11.3.1 Gravity Settling Devices

As discussed above, these devices are rarely used because of their large size and low collection efficiency for small particles. In any case, the velocity through the chamber itself is very low, so that any pressure drop is due to the inlet and outlet transitions. The *Ventilation Manual* (2001) states that a typical value for this pressure drop is 1.5 times the duct velocity pressure.

11.3.2 Centrifugal Collectors

Cyclones have been used widely for many years, and thus a large amount of data has been collected on the pressure drop across such devices. The pressure drop is generally independent of dust type or loading, so it is possible to characterize a cyclone

once and use the same data for many applications. Similarly, families of cyclones for different airflows are designed by scaling up dimensions, so pressure drop obtained for one airflow can be used to predict pressure drop at other flows.

Cyclone pressure drops are difficult to predict from theory, so it is best to rely on manufacturer's specifications. Most cyclones are designed to operate at pressure drops in the range 1 to 5 in. H₂O (250–1250 Pa). Pressure drop has been found to vary with the square of the inlet velocity.

11.3.3 Filters

All filters have a pressure drop that varies over time; the nature of this variation depends on the filter design. The pressure drop is lowest when the filter is new. As dust is collected, the pressure drop increases from this baseline value due to the increased resistance caused by the collected dust. This increase in pressure drop cannot continue indefinitely. The system resistance curve becomes steeper, resulting in a new intersection point with the fan curve (Fig. 11.11). The fan and system are now operating at a lower airflow, which may cause dust to start settling out in the ductwork. If this were to continue indefinitely, system airflow would approach zero, so it is necessary for the air cleaner designer to specify a maximum allowable pressure drop. When pressure drop reaches this value, the filter must either be cleaned or discarded.

As the filter collects dust, the system resistance curve gradually becomes steeper, moving from curve A in Fig. 11.11 toward curve B. The clean filter and maximum allowable pressure drops define the limiting points of intersection of the system

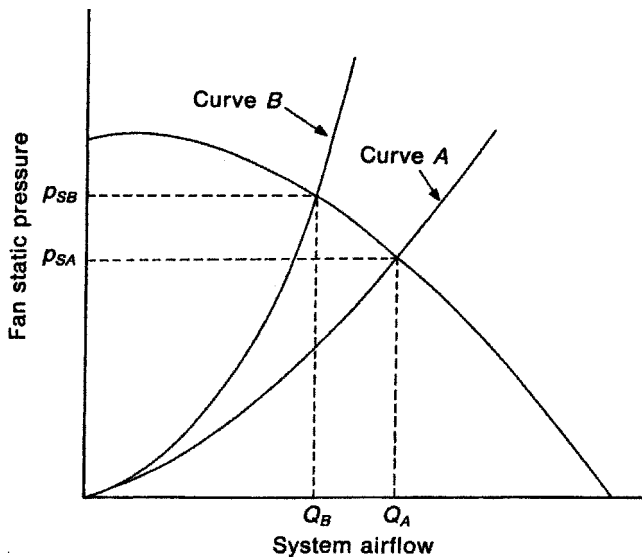


Figure 11.11 Variation of a system resistance curve with change in fabric filter dust loading. Curve A represents low filter loading, while curve B represents a high-loading condition. Note the different intersection points with the fan curve, resulting in different system airflows and pressure drops.

resistance curve and the fan curve. In selecting a pressure drop to assign to the air cleaner, the ventilation system designer should always assume the maximum pressure drop, since this gives the steepest resistance curve. The proper fan can then be selected to give the required airflow (Q_B); when the filter is clean, more air will flow than is necessary (Q_A), thus assuring proper hood operation at all times.

Media Filters. In general, media filters are not cleanable and are changed after a maximum pressure drop, specified by the filter manufacturer, has been attained. The pressure drop across the filter when it is new and at the end of its service life define the limiting values of the system resistance curve.

Media filters vary widely in their design pressure drop, so it is necessary to refer to manufacturers' specifications. Pressure drops across furnace-type filters are generally a few tenths of an inch of water, while large high-velocity filters designed for heavy industrial use can operate at 30 to 40 in. H_2O (7.5–10 KPa).

HEPA Filters. Like media filters, high-efficiency filters cannot be cleaned and are discarded after attaining maximum pressure drop. The pressure drop across such devices when new is generally 0.5–1 in. H_2O (125–250 Pa); since such devices are used only in applications with very low dust loadings, the pressure drop should increase very slowly toward the maximum design value [usually 2 in. H_2O (500 Pa)]. The ventilation designer would do well to choose this maximum value during the design stage, and accept a lower-than-anticipated system pressure drop and higher airflow during early months of operation.

It is important that the pressure drop across all noncleanable filters be monitored continuously during system operation, and that such filters be replaced when maximum allowable pressure drop is attained. If such filters are allowed to operate beyond this point, system resistance will increase to an unacceptable level and airflow will decrease below the amount necessary for efficient hood operation.

Fabric Filters. It is very difficult to predict pressure drop for fabric filters. Several problems are encountered with these devices. The pressure drop is strongly dependent on system variables such as filtration velocity, fabric type, dust type, and cleaning mode. In addition, the pressure drop always *changes* over time, both over the short term during one cleaning cycle and over the long term as the fabric ages and becomes more difficult to clean.

A typical time–pressure drop plot for a fabric filter might look as shown in Fig. 11.12. Given this type of behavior, how is the designer to select one value of pressure drop to insert in the calculation sheet as the pressure drop across the filter? There are several steps that can be taken to simplify matters. First, the initial transient behavior can be ignored, since it is the long-term steady-state pressure drop that is of interest. One value of pressure drop must be selected that characterizes the behavior of the device in region (b) of Fig. 11.12, where the pressure drop cycles between two values during the course of one cleaning cycle. The solution here is to select the *maximum* pressure drop for the design, and ensure that a fan is selected that can handle the range of pressure drops expected.

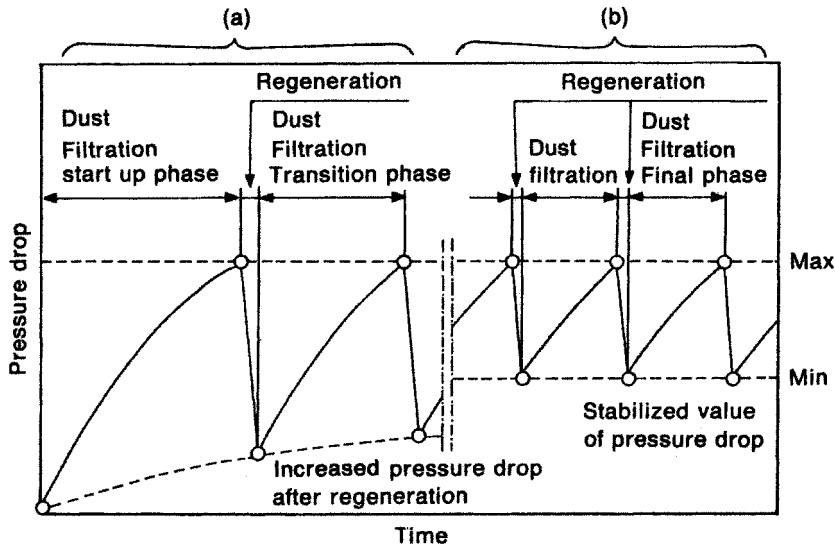


Figure 11.12 Pressure drop versus time for a typical fabric filter. Zone (a) represents the filter's transient behavior during the startup phase, and zone (b) represents normal operation after pressure drop has stabilized.

Some simple equations are commonly used to predict maximum pressure drop in a fabric filter. A basic expression for the pressure drop is

$$\Delta p = \Delta p_f + \Delta p_d \quad (11.1)$$

$$= K_1 V + K_2 V_w \quad (11.2)$$

where Δp = pressure drop (in. H₂O or Pa)

Δp_f = pressure drop across the fabric (in. H₂O or Pa)

Δp_d = pressure drop across the dust (in. H₂O or Pa)

K_1 = clean fabric resistance (in. H₂O/fpm or Pa/m/s)

V = filtration velocity (fpm or m/s)

K_2 = dust deposit specific resistance (in. H₂O/fpm-lb/ft² or Pa-m-s/kg)

w = dust deposit areal density (lb/ft² or kg/m²)

The difficulty in using this equation is determining values for K_1 , K_2 , and w for the particular application. The clean fabric resistance K_1 is a function of the fabric used in the filter and is available from the manufacturer. The dust-deposit-specific resistance K_2 is a complicated function of the dust type, gas viscosity, and dust-fabric interaction and is generally obtainable only from measurements at similar installations or a pilot plant. Similarly, the amount of dust on the fabric per unit area just before cleaning, w , is a complicated function of dust type, fabric type, and cleaning mechanism, and cannot generally be predicted theoretically.

Thus the simple equations given above, while useful in helping to understand what contributes to pressure drop in a fabric filter, are not particularly useful to the ventilation system designer for predicting pressure drop for a particular application. The usual procedure that is followed is to use the manufacturer's data to select a design operating pressure drop, and then adjust the cleaning frequency to attain this pressure drop once the system is operating.

11.3.4 Electrostatic Precipitators

Electrostatic precipitators are among the easiest devices to predict operating pressure drop. From the point of view of the ventilation system designer, electrostatic precipitators are simply large boxes and the pressure drop is low, easy to predict, and will not change significantly during the lifetime of the device. Unfortunately, as was discussed above, these devices are rarely used in local exhaust systems, and thus the designer will rarely have the luxury of designing them into a system. Large single-stage precipitators generally operate at a pressure drop of 0.5–1.0 in. H₂O (125–250 Pa), while that across small two-stage precipitators is even less.

11.3.5 Scrubbers

As described above, there is such a wide variety of wet scrubber designs that it is difficult to classify them systematically. One useful approach is to categorize them by pressure drop (Theodore and Buonicore, 1982). Low-energy scrubbers include all devices with pressure drops less than 5 in. H₂O (1250 Pa); this would include such devices as simple spray towers. Medium-energy scrubbers have pressure drops between 5 and 15 in. H₂O (1250 and 3750 Pa); most packed-bed, impingement plate, and wet centrifugal fan scrubbers fall into this category. High-energy scrubbers, then, have pressure drops greater than 15 in. H₂O (3750 Pa); the most common such device is the Venturi scrubber.

Since these devices operate at a relatively constant pressure drop throughout their lifetimes, and since the desired operating pressure drop is well defined by the device manufacturer, the ventilation system designer's task is relatively straightforward. The major exception to this statement is the Venturi scrubber, which can operate over a wide range of pressure drops, depending on the dust being collected and the collection efficiency desired.

The pressure drop across a Venturi scrubber is primarily a function of the gas velocity in the Venturi throat V_G and the ratio of the liquid flow to airflow, Q_L/Q_G . Pressure drop equations are usually of the form

$$p = KV_G^2 \frac{Q_L}{Q_G} \quad (11.3)$$

where K is a constant for a particular scrubber design. Operating pressure drop is selected to give the desired particle collection efficiency. Typical data illustrating the variation of collection efficiency with particle size and pressure drop are presented in Fig. 11.13.

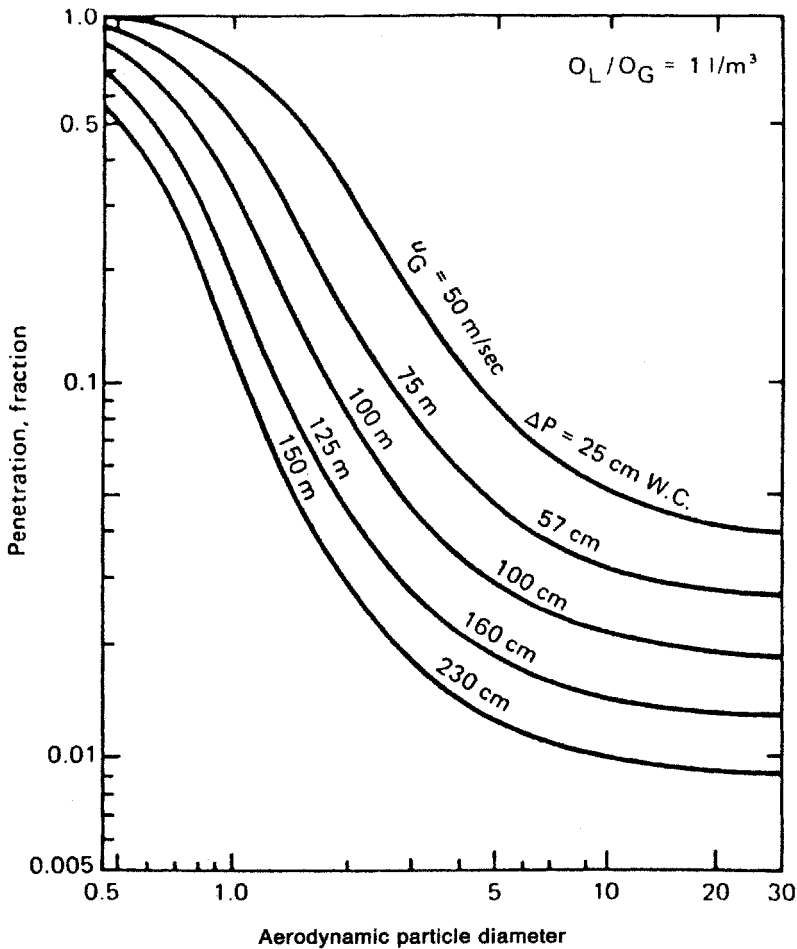


Figure 11.13 Particle penetration versus aerodynamic diameter for a typical Venturi scrubber. Penetration curves are presented for a range of velocities in the Venturi throat (V_G) at a typical liquid-to-gas flow ratio.

11.3.6 Gas and Vapor Removers

The pressure drop characteristics of gas and vapor collection devices are generally well known, and such devices have the distinct advantage that pressure drop generally does not change over the life of the device. Scrubbers for gas adsorption generally fall into the low- or medium-energy categories, typically having pressure drops of a few inches of water but ranging up to 15 in. H_2O (3750 Pa). The pressure drop through an adsorption bed is a function of the bed velocity, bed depth, and size of the granules making up the bed. Typical pressure drop data for granular carbon beds are presented in Fig. 11.14.

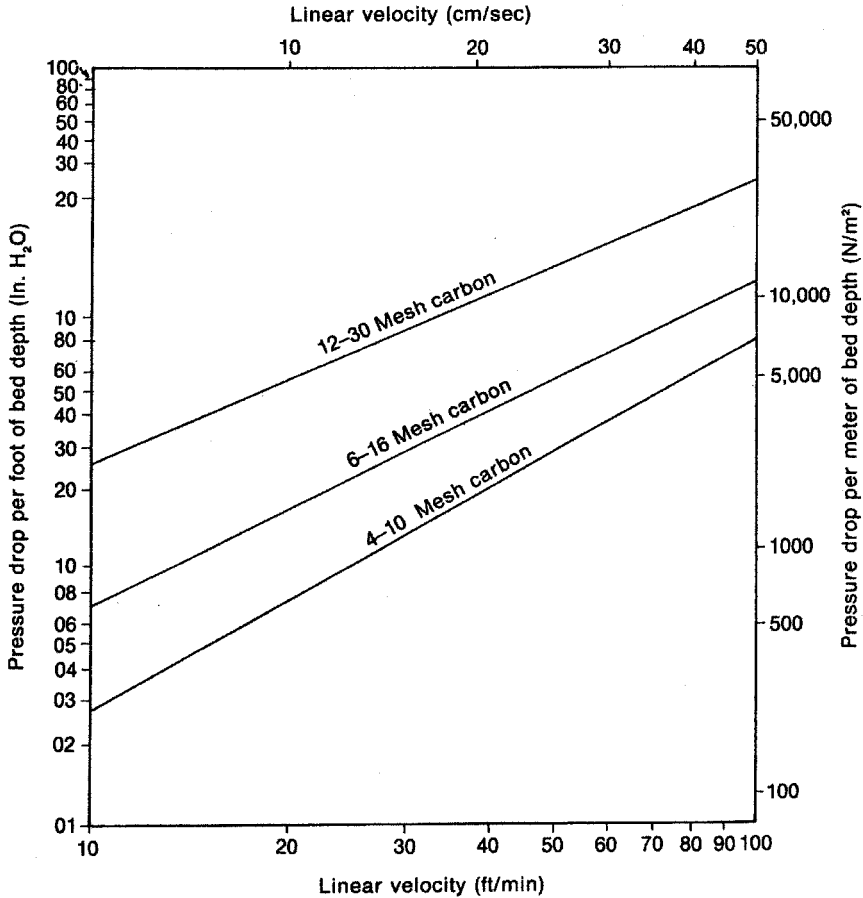


Figure 11.14 Pressure drop versus gas velocity for granular carbon beds with different mesh size granules.

LIST OF SYMBOLS

K	Venturi scrubber constant (Eq. 11.3)
K_1	clean fabric resistance
K_2	dust deposit specific resistance
Q	airflow
Q_G	gas flow in a Venturi
Q_L	liquid flow in a Venturi
V	filtration velocity
V_G	velocity in Venturi throat
w	dust deposit areal density
Δp	pressure drop

Δp_f pressure drop across a clean fabric
 Δp_d pressure drop across a dust deposit

REFERENCES

- American Conference of Governmental Industrial Hygienists (ACGIH), Committee on Industrial Ventilation, *Industrial Ventilation: A Manual of Recommended Practice*, 24th ed., ACGIH, Cincinnati, OH, 2001.
- Cooper, C., and F. Alley, *Air Pollution Control: A Design Approach*, 3rd ed., Waveland Press, Long Grove, IL, 2002.
- Heinsohn, R., and R. Kabel, *Sources and Control of Air Pollution*, Prentice Hall, Upper Saddle River, NJ, 1999.
- Licht, W., *Air Pollution Control Engineering: Basic Calculations for Particulate Collection*, Marcel Dekker, New York, 1980.
- Stern, A., ed., *Air Pollution*, 3rd ed., Vol. 4, *Engineering Control of Air Pollution*, Academic Press, New York, 1977.
- Stern, A., ed., *Air Pollution*, 3rd ed., Vol. 7, *Supplement to Measurements, Monitoring, Surveillance, and Engineering Control*, Academic Press, New York, 1986.
- Strauss, W., *Industrial Gas Cleaning*, 2nd ed., Pergamon Press, New York, 1975.
- Theodore, L., and A. Buonicore, eds., *Air Pollution Control Equipment: Selection, Design, Operation, and Maintenance*, Prentice-Hall, Englewood Cliffs, NJ, 1982.
- U.S. Environmental Protection Agency, *Air Pollution Engineering Manual*, 2nd ed., Publication No. AP-40, J. Danielson, ed., U.S. Government Printing Office, Washington, DC, 1973.
- U.S. Environmental Protection Agency, *Industrial Guide for Air Pollution Control*, Publication No. EPA-625/6-78-004, U.S. Government Printing Office, Washington, DC, 1978.

PROBLEMS

- 11.1** An industrial cyclone is operated at an airflow of 1500 ft³/min and has a pressure drop of 4.4 in. H₂O. If the airflow is increased to 2500 ft³/min, what is the new static pressure across the device?

Answer: 12 in. H₂O

- 11.2** A fabric filter has the following characteristics:

Filtration velocity	2.2 ft/min
Clean fabric resistance	0.27 in. H ₂ O/fpm
Dust deposit specific resistance	1.1 in. H ₂ O/fpm-lb/ft ³
Dust deposit areal density	1.78 lb/ft ²

What is the pressure drop across this filter?

Answer: 4.9 in. H₂O

REPLACEMENT-AIR SYSTEMS

Until the mid-1960s little attention was given to the need for replacement air in the design of industrial ventilation systems. High-quality exhaust systems designed by engineering services would occasionally include a companion design to replace the air exhausted from the workplace, but commonly a local sheet metal contractor would install the local or general exhaust ventilation system with no consideration given to a replacement-air system. Further, existing local exhaust systems routinely were modified and expanded without consideration of replacement air. Many of the difficulties encountered in the performance of exhaust ventilation systems in the past could be assigned directly to the lack of adequate replacement air. These chronic problems began to generate increased interest in the 1960s when a number of state and local agencies started to require that replacement-air systems be installed in conjunction with new exhaust systems.

Limited acceptance of the replacement-air concept by industry prior to 1960 was based on the belief that providing replacement tempered air in the northern latitudes would represent an additional cost. It was not realized that even without a replacement-air system the air was drawn into the building by infiltration and heated before it was exhausted. The well-designed replacement-air system supplies heated air in a much more efficient manner (Fig. 12.1).

The importance of replacement air was beginning to receive acceptance in the 1970s, when mounting fuel costs dampened enthusiasm. This reluctance to introduce replacement-air systems is still being felt today. Even so, the conscientious designer accepts the necessity of providing replacement air and the availability of

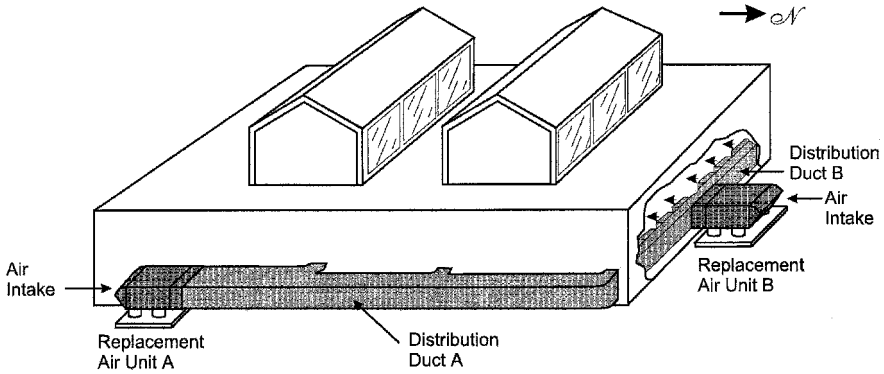


Figure 12.1 Replacement-air systems A and B (RAS-A and RAS-B) consist of basic units and associated distribution ducts. In both cases the units are mounted at ground level outside the building. In RAS-A the distribution duct is positioned along the building perimeter with three duct branches penetrating the sidewall and terminating with air diffusers inside the structure. A single wall penetration from the unit in RAS-B leads to a distribution manifold on an inside wall with a series of diffusers to provide low-velocity air at working height.

a variety of packaged units based on inlet hood, filter, fan, and heating and cooling modules and discharge grilles has made the installation of these systems technically and economically attractive. In addition, the high cost of tempering outside air in northern latitudes has encouraged design innovations to permit recovery of heat from large exhaust streams. The recirculation of exhaust streams after suitable air cleaning is also practiced to a limited extent. This chapter will deal with all three of these issues, with emphasis on the basic issue of introducing replacement air into the plant. Heat recovery and recirculation of air from exhaust streams are covered in detail in other sources.

In this chapter we will use a case study of a large steel foundry in upstate New York plagued by a deficiency in replacement air to demonstrate how a designer first determines the quantity of replacement air needed to balance the exhaust airflow and then considers methods to locate the replacement air unit to deliver the air at a location in the plant where it will work effectively to reduce worker exposure to airborne contaminants without discomfort from severe drafts. The solution to the foundry problem and other heavy industries is to provide a tempered air supply system during the winter season and raw, unconditioned air in the summer.

In some cases where conditions permit, replacement air units in heavy industry may include an evaporative cooler for summertime conditions. In high-technology industries and in research and laboratory facilities where true HVAC systems are specified the equipment choice is based on the discussions in ASHRAE (2000). Calculation of the system losses to permit fan choice for replacement air units is covered in detail in Chapters 8 and 9 of this volume and in other sources (ACGIH, 2001; ASHRAE, 2001).

12.1 TYPES OF REPLACEMENT-AIR UNITS

As noted above, a variety of heating, ventilation, and air conditioning (HVAC) systems described in ASHRAE (2000) can be used as replacement-air units, but the typical major installations use packaged systems that are delivered ready for hookup of services and duct connections. These packaged systems are available: (1) for use with hot water or steam coils, (2) as indirect systems fired by gas or oil with venting of products of combustion to outdoors, and (3) as direct gas-fired units of the type used in the foundry example to be introduced later in this chapter with the products of combustion mixed directly with the air supplied to the workplace as shown in Fig. 12.2.

The conventional hot-water and steam replacement-air units are either available as packaged units or can be assembled from components on site to meet specific airflow requirements and size constraints. The steam units require significant power plant service and are most popular for larger installations; hot-water units are frequently used in smaller systems. The packaged replacement air unit heated by gas or oil with a heat exchange section is commonly used for medium and large systems, where the economy and flexibility of an integral unit are important. This design offers relatively

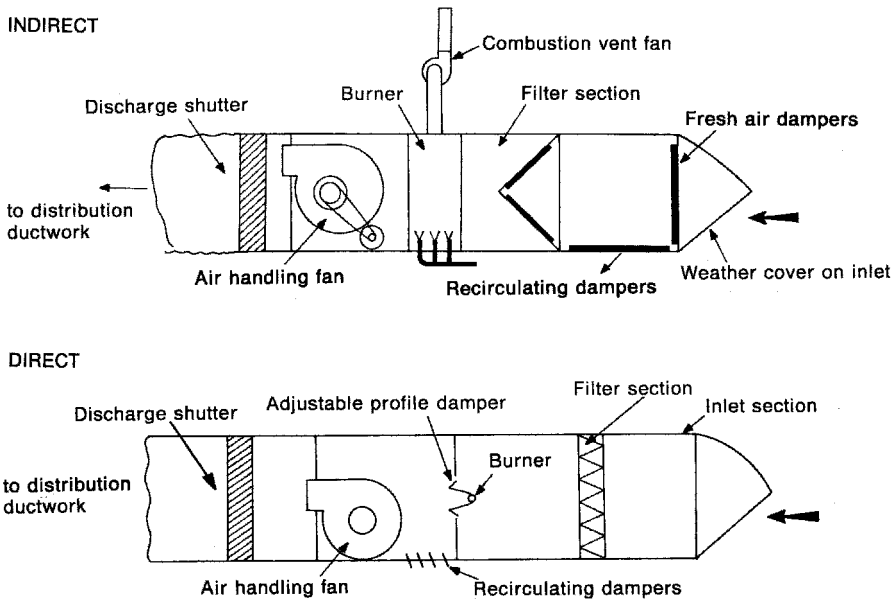


Figure 12.2 Gas-fired replacement-air units (RAUs). The indirect-fired unit is equipped with a burner chamber and heat exchanger, so the replacement airstream and gas combustion process are separate. These units are equipped with recirculating dampers. The products of combustion of the direct-fired gas units are delivered to the workplace. As noted in the text, if air is recirculated from the workplace, it must be introduced downstream of the burner; otherwise, fugitive air contaminants will be thermally degraded in the burner and delivered to the space. The direct-fired replacement air units are equipped with elaborate controls, which permit their safe operation.

high efficiency and, since products of combustion are vented outdoors, is considered safe for all applications.

Where gas is relatively inexpensive, the direct-fired gas units are popular for systems larger than 10,000 cfm ($4.72 \text{ m}^3/\text{s}$). These units are designed with extensive combustion controls to optimize combustion efficiency, thus permitting delivery of the products of combustion to the ventilated space. Recirculation of workplace air through the combustion zone is prohibited since thermal degradation products of certain industrial air contaminants such as chlorinated solvents may present significant health hazards. The direct-fired gas units are usually pre-packaged for ease of delivery and installation at the site. Propeller-type models are commonly available to handle duct resistance up to 0.5 in. H_2O (124.55 Pa); centrifuge-type models are available to handle external resistance as high as 5 in. H_2O (1245.50 Pa).

12.2 NEED FOR REPLACEMENT AIR

Today there is general agreement that exhaust and replacement air should be in balance; that is, when exhaust air is removed from the workplace, replacement air should be introduced. This simple guideline requires interpretation in practice. If a large electroplating and finishing shop operates with a total exhaust of 100,000 cfm ($47.19 \text{ m}^3/\text{s}$), the addition of a small degreaser requiring an additional 2000 cfm ($0.94 \text{ m}^3/\text{s}$) of exhaust should not prompt immediate upgrading of the replacement-air system (RAS). In practice, an RAS is usually not upgraded until the system is out of balance by more than 10%.

Another way to assess the necessity of an RAS is to compare the room volume to the required exhaust rate. Constance (1983) states that replacement air is necessary when the hourly exhaust volume exceeds three times the building volume. No justification is given for this approach. If this guideline were applied to the installation of a new color printer in a room with a total volume of 10,000 ft^3 (283.20 m^3), the required exhaust of 1000 cfm ($0.47 \text{ m}^3/\text{s}$) would warrant a separate RAS or the use of a 1000-cfm ($0.47\text{-m}^3/\text{s}$) supply branch from an existing system.

In an existing facility the need for replacement air is frequently demonstrated by the complaints received from plant personnel. In the large steel foundry in our case study the exhaust ventilation totals 232,800 cfm ($109.60 \text{ m}^3/\text{s}$) with no replacement-air (Fig. 12.3). The complaints received by management are consistent with those noted in buildings with significant deficiency in replacement air. Because of the severe air demand in the building, outside air is drawn through all cracks and openings. Workers in small shops or at isolated workbenches on the perimeter walls complain of strong drafts of cold air in the winter. Such complaints start to be noted with plant negative pressures as low as 0.01 in. H_2O (2.49 Pa). Both pedestrian and material transport doors have significant forces exerted on them under winter conditions due to the negative pressure established by the exhaust fans. It is extremely difficult to open the doors when negative pressures exceed 0.05 in. H_2O (12.45 Pa), and this condition leads to frequent backstrains. Workers stay clear of closing doors to escape the violent slamming.

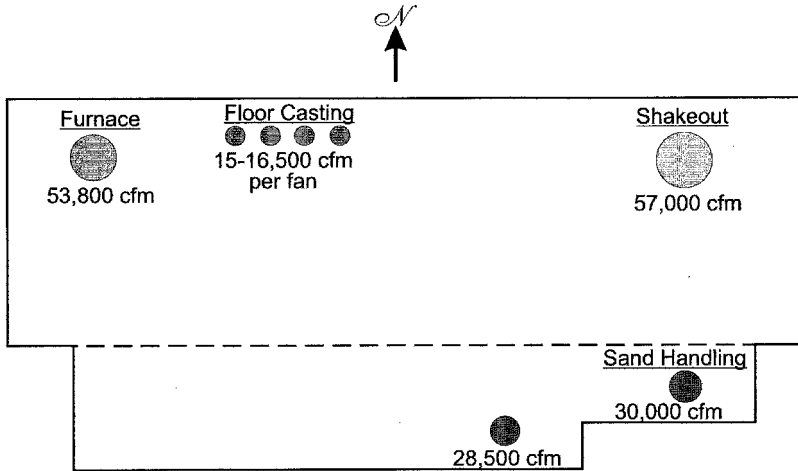


Figure 12.3 Plan view of the foundry showing the foundry building complex with the approximate locations and airflow rates of the exhaust systems in the four major work areas as described in Table 12.2.

Because of the lack of replacement air in the building, even the low static general exhaust fans commonly located in the roof create building negative pressures exceeding 0.05 in. H_2O (12.45 Pa). This condition causes backdrafting of the gravity stacks on unit heaters, ovens, and furnaces resulting in impaired operation of combustion and pollution of the workplace by carbon monoxide.

The performance levels of these the low-static-pressure/high-volume axial flow roof ventilators are, in turn, adversely affected by the operation of the high static fans used in the local exhaust systems. The four roof fans in the foundry pouring area in our case study have a rated flow of 18,000 cfm (8.49 m^3/s) at a static pressure of 0.25 in. H_2O (62.28 Pa). Under the existing air-starved conditions resulting in negative pressures in excess of 0.1 in. H_2O (24.91 Pa), the actual airflow of the roof exhausters drops by 5–10%. Such conditions clearly call for the installation of an adequate RAS.

12.3 QUANTITY OF REPLACEMENT AIR

The first major step in designing a RAS is the selection of the supply airflow. The simplest approach to such a selection is to assume that the supply should equal the exhaust. In practice it is sometimes necessary to generate pressure differentials between major work areas to establish or block airflow from one area to another. Designing a slight imbalance between supply and exhaust can accomplish this. In the foundry example (Fig. 12.3), the air should flow from the general work area toward the furnace area to ensure that the high concentrations of fugitive metal fumes will not contaminate the

rest of the foundry. In this case the replacement air for the electric arc furnace complex should be less than the furnace exhaust, thus creating a slight air demand in the region of the plant where the furnaces are located. In general, it is prudent for the replacement-air flow rate to approximately match the exhaust rates, although supply rates in the range of 90–110% of the exhaust capacity are normally used in practice as design boundaries for replacement-air systems.

Determining the required RAS supply rate for an industrial building can be accomplished in a number of ways. In a small installation an estimate of the magnitude of the supply deficiency can frequently be accomplished by a simple procedure. On a day with little wind, one or two large building access doors can be opened while the building local and general exhaust systems and existing RAS, if any, are operating. If the building is fairly tight and there is an air deficiency, it will be made up by air flowing through the open doors. If the average inward velocity through the doors is then measured, the product of that velocity and the open area of the door represent the deficiency. Even under ideal conditions this procedure will probably give results within only 30% of the values measured by the more accurate methods described below, and it should be used only to obtain a rough measure of the extent of the problem.

A more rigorous approach is that based on a review of the original engineering design plans, which specify the exhaust rates of all installed local and general exhaust ventilation systems. In the case of the steel foundry these data were available in the Engineering Office for all systems except the shakeout as shown in Table 12.1 under “From Prints.” The operating shifts and times for all major exhaust are noted so that suitable RAS distribution can be achieved. No replacement-air systems were installed at the time of the review. We were fortunate that the engineering data were available in this case; however, in a small plant without in-house engineering service, detailed records are seldom available.

If engineering data are not available, an alternative approach is to base the projected exhaust on the consensus standards for industrial ventilation applicable at the time the system is designed. In using engineering design standards to estimate exhaust volume, the designer’s presumption that the original engineer followed the specifications and that a maintenance program was in force to keep the systems operational is probably naive. One manufacturer of replacement-air units agrees that the best approach in determining the airflow requirements is to total the exhaust capacity of all systems. However, the manufacturer states that if these data are not available, the guidelines shown in Table 12.2 can be used. If this approach must be taken, the authors recommend a more rigorous approach based on applying ANSI or ACGIH ventilation standards for various industrial operations.

The fourth and most accurate way to determine how much replacement air is needed is to evaluate the quantity of air currently being exhausted from the plant by direct airflow measurements on each exhaust system using the techniques described in Chapter 3. Since the building may be air-starved, the observed exhaust rate will be less than the design rate if low-pressure exhaust fans are widely used. To minimize this artifact, if weather permits, doors and windows should be opened before taking measurements. Measurements of system submain and main exhausts using the Pitot–static tube

traverse technique provide excellent results, although hood face velocity and hood static pressure measurements are usually adequate for assessment of airflow. A major problem encountered frequently in establishing such an exhaust inventory is the difficulty in measuring the delivery of low static propeller fans used commonly as roof exhausters due to their inaccessibility. Frequently it is necessary to use manufacturers' performance data to estimate delivery of these fans. In the foundry example, actual airflow measurements completed by the authors were used to provide an inventory of exhaust airflow in the "As Measured" column in Table 12.1.

The importance of establishing the required capacity of the replacement units by direct field measurement is noted if one compares the data in Table 12.1 based on direct measurement and those from engineering prints. If one omits the data on the shakeout since engineering prints are not available on that operation, the total measure airflow is 175,000 cfm (82.58 m³/s) and the estimated value from prints is 207,000 cfm (97.7 m³/s). This approach would result in an oversupply of 32,000 cfm (15.10 m³/s) if engineering data alone were used.

12.4 DELIVERY OF REPLACEMENT AIR

The general rules regarding delivery of replacement air to the workplace are that (1) the air should be delivered to the active working zone [less than 8–10 ft (2.44–3.05 m) above the floor], (2) the draft on the worker be minimized by maintaining air velocities below 200 fpm (1.02 m/s), (3) the replacement air should be delivered in a way that minimizes thermal looping as shown in Fig. 12.4, and (4) the replacement air should sweep from the clean to the more contaminated plant area.

In practice it is often difficult to achieve the desired delivery geometry for the replacement air. In a new facility there is a reasonable opportunity to position the distribution duct and the discharge grilles to achieve good delivery patterns by close cooperation between the engineer and the architect. In all cases the ventilation engineer must obtain a firm commitment on the total exhaust rate, the grouping of local exhaust hoods that operate as one system, and the anticipated time of use of each system. Frequently, it is possible to dedicate a RAS to a specific exhaust systems and interlock the replacement air unit with the exhaust fans on that system so they operate as integrated supply exhaust systems. This approach minimizes both the initial cost for the installation and the subsequent operating cost.

In a new system the designer can usually locate the RAS so that an airflow path inside the plant is clearly defined from the RAS delivery grilles to exhaust hoods and is not encumbered by physical obstructions or major draft patterns from other air movers or receiving doors. As noted above, the replacement air should be delivered at the active occupancy level, not the upper reaches of the building. Frequently, it is possible to choose and position adjustable discharge grilles to minimize draft on the worker in the winter but permit cooling air to sweep across the worker in the summer. In many structures the craneway and other obstructions will not permit this placement and the delivery plenum must be positioned at significant heights above

Table 12.1 Replacement-Air Requirements in a Steel Foundry Based on Engineering Specifications and Measured Airflow

(a) In English (U.S. Customary) Units						
Installed Exhaust			Exhaust Airflow		Replacement Air Design	
Process/Operation	Type of Exhaust	Shift	From Prints (cfm)	As Measured (cfm)	System	Distribution
Melting furnace	Hood	1, 2	60,000	53,800	RAS-1	Discharge grille on RAU
Floor casting	Roof fans	1, 2			RAS-2	Three drops
	A		18,000	16,000		
	B		18,000	15,000		
	C		18,000	16,500		
Sand handling	D		18,000	16,000		
	Hoods	1, 2			RAS-3	Three drops
	A		35,000	28,500		
	B		40,000	30,000		
Shakeout	Hood	3	Estimate 50,000	57,000	RAS-4	Discharge grille on RAU
Total exhaust and replacement airflows			257,000	232,800		245,000

Table 12.1 (Continued)

(b) In SI Units						
Installed Exhaust		Exhaust Airflow		Replacement Air Design		
Process/Operation	Type of Exhaust	Shift	From Prints (m ³ /s)	As Measured (m ³ /s)	System	Distribution
Melting furnace	Hood	1, 2	28.3	25.0	RAS-1	Discharge grille on RAU
Floor casting	Roof fans	1, 2				Three drops
	A		8.5	7.6		
	B		8.5	7.1		
	C		8.5	7.8		
Sand handling	D		8.5	7.6		
	Hoods	1, 2			RAS-3	Three drops
	A		16.5	13.4		
	B		18.9	14.2		
Shakeout	Hood	3	Estimate	26.9	RAS-4	Discharge grille on RAU
			23.6			
Total exhaust and replacement airflows			121.3	109.6		115.6

Table 12.2 Manufacturers Recommended Basis for Sizing Replacement Air Units if Engineering Data are not Available

Paint spray booth	125–175 fpm (0.64–0.89 m/s) of face opening
Oven exhaust	One air change per minute of oven volume
Roof exhaust	Duct velocity times average velocity
Dust collector	Duct area times 4000 fpm (20 m/s)
Canopy hood	100–300 cfm/ft ² (0.51–0.14 m ³ /s/m ²)
Combustion air for furnaces	Fuel consumed per hour divided by 6000
Pickling and cleaning tanks	150 cfm (0.08 m ³ /s) per ft ³

the floor, and the throw from high-velocity nozzles is used to achieve delivery to floor level.

Replacement-air units frequently employ ducts of large cross section, and special collaboration with the architect is required to provide the necessary space for the duct runs. Since the architect is usually reluctant to use valuable interior space for this purpose, RAS ducts are frequently located outside the plant with delivery branches penetrating the structure as shown with replacement-air unit A in Fig. 12.1. The installation of 50,000–100,000 cfm (23.60–47.19 m³/s) replacement-air units is difficult because of their size and mounting requirements. If possible, it is good practice to mount the units on footings at ground level or on an exterior structural wall with brackets. This practice usually permits the designer to use a short distribution manifold with resulting low system pressure loss. In this case installation costs are relatively low and the accessibility of the unit encourages routine maintenance. In cold northern climates this duct run should be thermally insulated.

In case where the availability of space on an exterior wall is restricted, roof location of the replacement-air unit may be necessary. Roof installation requires special load-carrying mounting, roof penetrations for electric and fuel services, and, of course, penetration for the air delivery duct. Roof installations frequently require long and expensive duct runs with involved distribution systems. If the mounting locations for

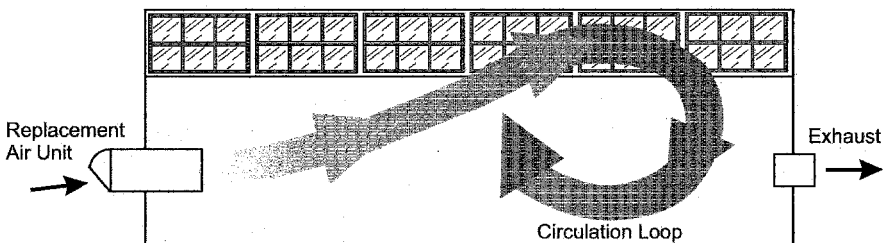


Figure 12.4 Thermal looping occurs when replacement air is heated as it passes over hot processes. Because of the density difference, the replacement air flows to the top of the building, frequently short-circuiting directly to roof exhausters.

the replacement-air units are at the edge of buildings the units can be positioned by crane; large buildings with replacement-air units located in center bays may require transport by helicopter to the mounting pad.

Installation of a replacement-air system for an existing large production facility as typified in the foundry example presents many difficulties not seen in new buildings. As noted earlier, supply volumes for the foundry replacement-air units may be based on engineering data and/or actual measurements of exhaust systems. Although the engineering data may provide reasonably accurate information, direct airflow measurement is the preferred method to establish the existing exhaust volumes and the replacement-air requirements. Obviously, the airflow of any existing replacement-air units should be measured to determine the replacement-air deficiency.

Each type of operation in a foundry results in the generation of an operation—specific contaminant and requires specific exhaust system design features, including duct velocity and air-cleaning type. As in example, the sand-handling operation requires a local exhaust system with a minimum duct velocity of 4500 fpm (22.86 m/s) and an air-cleaning unit designed to remove particles. In all such operations the hoods will be grouped together and served by one exhaust fan. Operations equipped with local exhaust ventilation grouped by function (e.g., sand handling, molding, melting, pouring, shakeout, and finishing) in a high production foundry usually operate continuously, but in the “job shop” foundry in our example each function is carried on for specific periods during the three workshifts (Table 12.1). It is therefore possible to couple the exhaust system with individual replacement-air units and interlock the units and the exhaust fans to conserve energy and ensure adequate air supply during system operation. In this case, the best approach is to have a “one-on-one coupling” of the RAS and the major exhaust systems, that is, if the exhaust fan is turned on the RAS automatically cuts in.

If two major exhaust systems have approximately the same exhaust airflow, do not operate at the same time, and are located in the same part of the plant, it may be possible to use one RAS with a single discharge grille to serve each system as it comes on line. If the exhaust locations are not suitable for one distribution system, then two alternate duct distribution systems can be designed with dampers permitting automatic switching of dampers to the best distribution system for the exhaust system in operation.

Expansion of industrial buildings occurs over decades, resulting in a myriad of roof structures and bay layouts. In such cases it can be very difficult to find a suitable location for the replacement-air unit. The units should be placed close to the optimum air supply location to minimize the length and complexity of the duct run and the mounting location selected to avoid expensive mounting requirements. In addition, the mounting location for the replacement-air unit should be chosen to minimize the likelihood of reentry of air contaminants from exhaust stacks (see Chapter 15). Ideal locations are rarely found, and compromises are usually required. The solutions chosen for the location of the four major replacement-air units (RAUs) in the foundry were made after extended discussions with plant operating and engineering personnel. The capacity of the direct-gas-fired unit to be delivered to the site by the manufacturer is based on the data in Table 12.1.

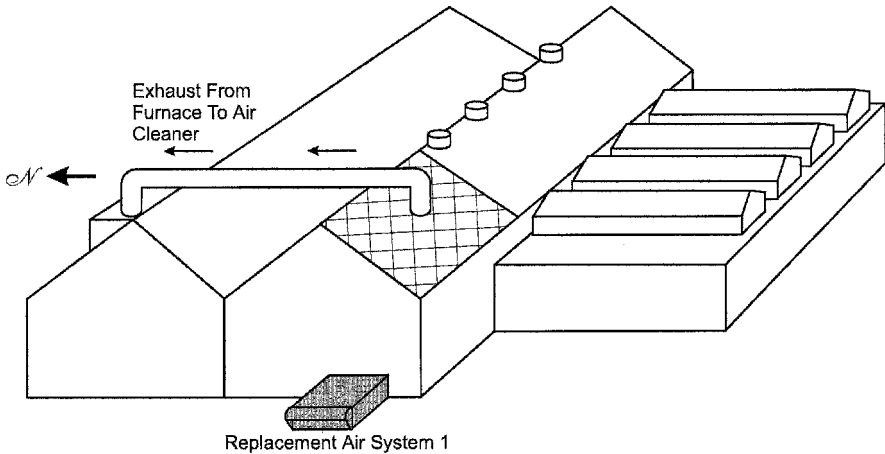


Figure 12.5 Replacement-air system 1 (RAS-1) for the melting furnace area. The exhaust hoods (53,800 cfm, 25.00 m³/s) on the electric furnaces are located under the shaded roof area. The replacement air moves west to east toward the furnace area (viewed from west end of building).

12.4.1 Replacement-Air System 1 (RAS-1), Melting Furnaces

Two large electric arc furnaces provide the melting capacity for this foundry. To control the emissions of iron oxide fume, the furnaces are provided with enclosing hoods (see *Ventilation Manual*, Fig. VS-55-03) and an air cleaner with a total exhaust of 53,800 cfm (25.39 m³/s). Since replacement air is not presently provided, the major infiltration replacement-air flow path is down the main bay from the floor casting area.

In this cast the ventilation designer is fortunate since space is available at ground level at the west end of the building to mount a single 50,000-cfm (23.60-m³/s) RAU interlocked with the furnace exhaust fan (Fig. 12.5). This large unit is mounted on a structural steel base and delivers air directly to the main bay. Since the furnaces are approximately 120 ft (36.58 m) from the delivery point, a plenum and a discharge grille mounted on the wall provide suitable distribution and the airflow path is direct to the exhaust hoods without major obstructions. A minimum residual velocity, less than 200 fpm (1.02 m/s), resulted at the furnace area workplace.

12.4.2 Replacement-Air System 2 (RAS-2), Floor Casting

The steel casting of large floor molds with hot topping of risers in the main bay is a major source of metal fume contamination in this facility. Since an exhausted pouring station cannot be used to control emissions from floor molding, the fugitive fume rises to the main bay roof and is controlled by general exhaust using four 18,000-cfm (8.49-m³/s) roof fans. Because of the negative pressure developed in the building by the high-pressure centrifugal fans exhausting the furnaces, the roof exhausters do not deliver full capacity, but rather 15,000–16,500 cfm (7.10–7.90 m³/s), resulting in poor clearance of the fume during floor casting. The fume blankets the floor

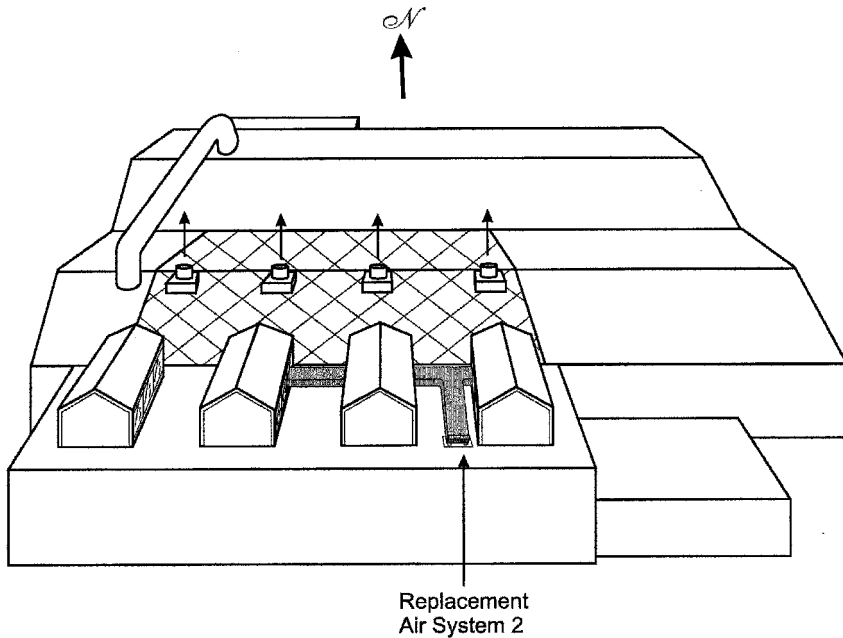


Figure 12.6 Replacement-air system 2 (RAS-2) for the four roof exhausters (63,500 cfm, $30.1 \text{ m}^3/\text{s}$) located over the floor pouring area shown in the shaded roof area (viewed from south end of building).

area and impairs the view of the crane operator and the floor main, making it difficult to conduct operations safely.

A 75,000-cfm ($35.39\text{-m}^3/\text{s}$) RAU is required for this pouring area as noted in Table 12.1. The north side of the building adjacent to the pouring area is blocked by ancillary equipment and is not available for use. The south side of the building is over 200 ft (60.96 m) away from the pouring bay, and the building perimeter space at ground level is limited. However, the building expansion to the south of the main bay is a clerestory design and does offer a solution. A 75,000-cfm ($35.39\text{-m}^3/\text{s}$) roof-mounted replacement-air unit is positioned at the southern edge of the building roof with an outside main duct delivering air to three distribution branches entering the clerestory windows (Fig. 12.6). The three vertical drops are used to deliver the replacement air at craneway height approximately 40 ft (12.19 m) from the main bay. The air demand from the pouring area roof exhausters causes the replacement air to sweep to the bay and clear the metal fumes. The availability of a clerestory roof design frequently proves useful in permitting practical solutions to the location of RAS distribution ducts.

12.4.3 Replacement-Air System 3 (RAS-3), Sand Handling

A multicomponent sand handling system located in the southeastern corner of the building is equipped with two primary exhaust systems, and the total exhaust from the

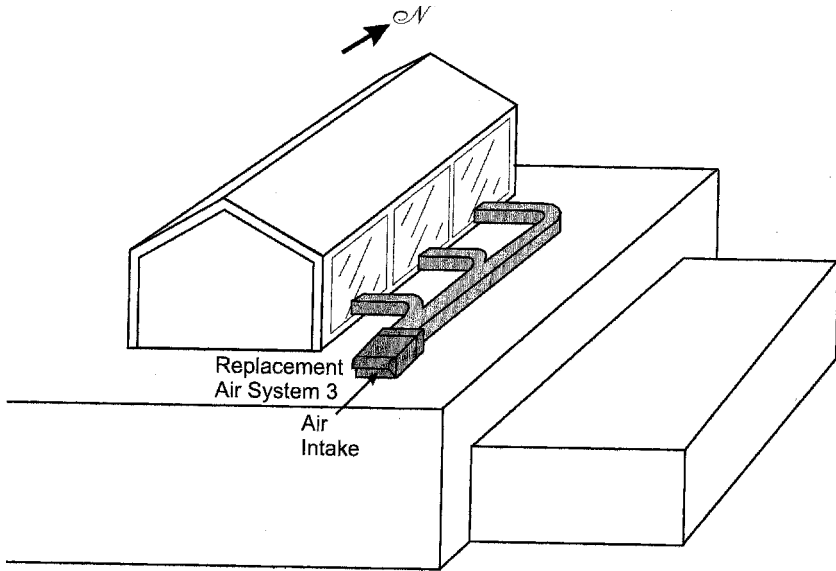


Figure 12.7 Replacement-air system 3 (RAS-3) for the two major local exhaust systems (58,500 cfm, 27.6 m³/s) in the sand handling area located in the shaded area (viewed from the southeast).

two fans is 58,500 cfm (27.37 m³/s). The building perimeter space in this area is heavily utilized for foundry support equipment, and ground-level siting of the RAS is therefore not possible. A roof location for a 60,000-cfm (28.31-m³/s) RAU was again chosen as the best solution (Fig. 12.7). This system is provided with a main duct run along a single clerestory with three duct “drops” discharging through diffusers above the craneway elevation all located approximately 50 ft (15.24 m) from the sand treatment area. Since the sand treatment operations run intermittently on first and second shifts, the replacement-air unit is electrically interlocked with the two exhaust fans in the sand-handling area.

12.4.4 Replacement-Air System 4 (RAS-4), Shakeout

A large shakeout hood located in the main bay with an exhaust of 57,000 cfm (26.90 m³/s) is operated only on the third shift (see *Ventilation Manual*, Fig. VS-20-02 for hood design). The immediate north wall would have been an ideal location for a 60,000-cfm (28.31-m³/s) RAU, in that it would provide cross-bay air sweep, but this space is utilized for a variety of abrasive blasting booths and heat treatment ovens. The nearest ground-level location is on the east wall of this bay approximately 150 ft (45.72 m) from the shakeout (Fig. 12.8). Since there is little other activity underway in the building on the third shift, the possibility of the replacement air short-circuiting to other exhaust sites or thermal looping to the craneway height were minimal and this location was deemed acceptable. The distances from the replacement-air unit to the

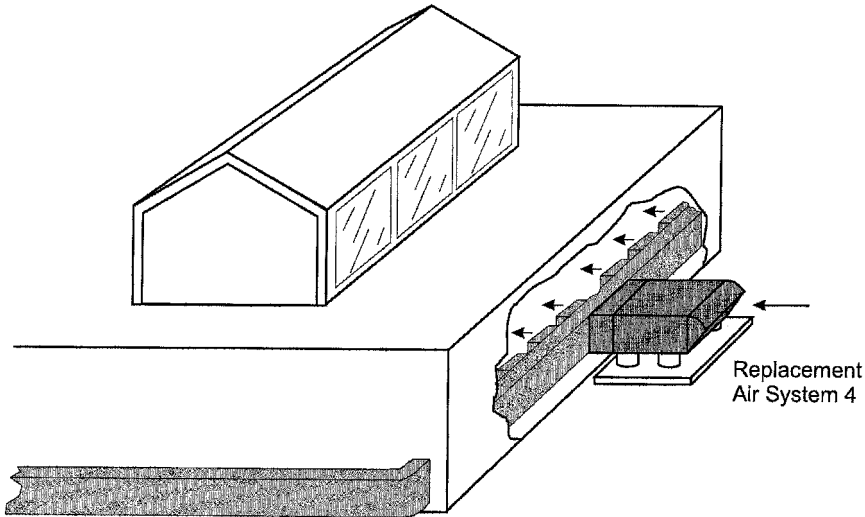


Figure 12.8 Replacement-air system 4 (RAS-4) for the shakeout hood (57,000 cfm, 26.9 m³/s), viewed from the south end of building with replacement air moving from east to west to the shakeout area.

shakeout exhaust hood preclude the need for an extensive distribution duct so a plenum with multiple discharge diffusers mounted directly on the RAU was chosen as noted in Fig. 12.8.

Since there is no pouring or sand treatment on the third shift, RAS-2 and RAS-3 will not be operating. A feasible option in this case is not to install a separate RAS for the shakeout but to use RAS-2, as designed, or RAS-3 with an alternative duct strategically placed to provide replacement air for the shakeout operation.

12.5 REPLACEMENT AIR FOR HEATING

In discussing the application of direct-fired gas replacement-air systems for heavy industry earlier in the chapter, it was stated that these systems are not designed for primary air heating, and thus the delivery air temperature should be approximately room temperature. However, there are occasions when a packaged direct-fired replacement-air unit may provide an inexpensive alternative to a conventional heating system. Such was the case in an unheated granite cutting shed at a New England quarry, where winter workplace temperatures inside the building commonly fell below freezing. Granite was transported from the quarry for manufacture of dimensional and architectural stone.

Approximately 50 people worked at stone-cutting stations scattered over the main bay (100 × 300 ft) (30.48 × 91.44 m), and many of the stations were equipped with local exhaust. Wet drilling and polishing using water as a dust suppressant achieved dust control at other locations. Since the workstations were not fixed, radiant heating

was not appropriate. An expedient solution to alleviate thermal comfort and safety problems was to tighten up the building, insulate the walls and roof with sprayed polyurethane foam, and use two 50,000-cfm ($23.60\text{-m}^3/\text{s}$) direct-fired gas RAUs mounted in a sidewall with direct discharge to the workplace to maintain the air temperatures above 40°F (4°C). This installation satisfied the replacement-air deficiency, improved comfort conditions, and minimized slips and falls and handling accidents caused by ice formation.

12.6 ENERGY CONSERVATION AND REPLACEMENT AIR

When replacement-air systems were first introduced in the United States, plant managers objected to the cost of heating this “new” air. Management did not easily accept the notion that in those plants without designed replacement air, the air that infiltrates the building and is later exhausted is one of the heating loads in a HVAC design. A replacement-air system merely accomplishes this heating in a more efficient manner. This is not to imply that the cost of heating replacement air in northern latitudes is insignificant. The annual cost in the year 2002 to heat the replacement air in the steel foundry in our example located in upstate New York is $\$1/\text{cfm}$ or approximately $\$250,000$.

The techniques available to minimize the energy cost of suitably treated replacement air in various industry settings have been discussed for decades. The energy crisis of the 1970s prompted aggressive action by U.S. industry. The broad approaches to energy conservation in a laboratory setting were discussed in Chapter 7. There are occasions when exhaust airflow is excessive and a reduction in exhaust is possible, permitting a parallel reduction in the replacement-air requirement. When using this approach, the engineer must always demonstrate continued effective contaminant control with the reduced exhaust volumes. Another productive approach is to use the exhaust system and its matching RAS only when the process is operating. Interlocking the exhaust fan with the replacement-air units ensures that heating costs are minimized.

In facilities such as hospitals where one-pass ventilation is practiced, major attention has been given the removal of heat from the air before it is exhausted. A common approach is the so-called head wheel (Fig. 12.9). Warm exhaust air passes through one section of a rotating wheel with a large heat capacity, and the heat is transferred to the

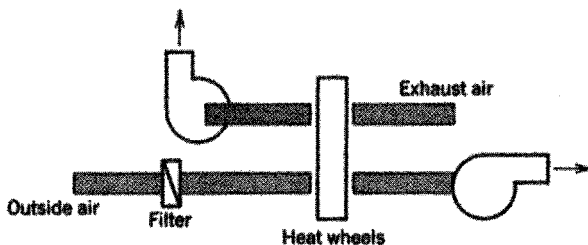


Figure 12.9 Heat wheel system for energy recovery from exhaust air.

wheel. As this wheel sector rotates slowly to the outside supply airstream, the heat is supplied to that stream to increase its air temperature before delivery to the workplace. This technique has limited application in industrial exhaust heat recovery, due to its expense and limited capacity. Furthermore, there is potential for contamination of the wheel packing with air contaminants and their subsequent elution by the outside airstream, resulting in workplace contamination. For these reasons this approach would not be suitable for our foundry example.

The heat pipe is the basis for another thermal recovery unit (Fig. 12.10). The active element in this design is a bundle of heat pipes; each pipe is split along its length by a partition separating the warm exhaust and cold supply airstreams. Heat energy from the warm exhaust stream is transferred to the other end of the individual heat pipe, where it heats the cold incoming air. The manufacturer states that these units recover 60–80% of the difference in sensible heat between the two airstreams.

A third method of recovery of energy from large volumes of air exhausted from industrial ventilation systems (Fig. 12.11) is based on two conventional fin-tubed coils circulating a heat exchanger fluid in a “roundabout loop cycle.” The warm indoor air to be exhausted first passes through one of the heat exchangers, and energy is recovered from the airstream. The heated exchanger fluid then flows to a matching heat exchanger positioned in the cold outdoor stream being introduced into the building where the energy is recovered from the incoming air, resulting in an increase in air temperature.

A major energy conservation approach in industrial exhaust systems has been the removal of the air contaminants from the exhaust stream by suitable air cleaning and the recirculation of the airstream to the workplace. Due to the potential for exposure of employees to toxic air contaminants, this approach has received limited acceptance.

The National Institute of Occupational Safety and Health (NIOSH) has sponsored applied research in this area and held several symposia on the application of the concept (NIOSH, 1978). The legal and regulatory aspects of air recirculation in the workplace have been reviewed by Holcomb and Radia (1986). OSHA does not specifically address air recirculation in its regulations but merely states that exposures in the workplace shall not exceed the OSHA permissible exposure limit (PEL) for selected air contaminants. The most current information available for guidance in the United States is presented in national standards (ANSI, 1998). Certain municipalities specifically prohibit the practice. Canada permits recirculation but requires that the contaminant concentration in the return airstream not exceed one-twentieth of the ACGIH threshold limit value (TLV); the United Kingdom uses this approach but specifies a factor of 0.1 of its exposure standards.

The application of recirculation of exhaust air containing toxic contaminants must be based on detailed knowledge of the form and concentration of the chemical species in the workplace and the performance of the air cleaner for these contaminants. The system must include sensors to indicate when a contaminant concentration has exceeded a critical level, and the sensors must activate a system to discharge the exhaust directly outdoors. If possible, the system should operate in a fail-safe mode.

It is the authors' opinion that the present state of air-cleaning technology is such that air recirculation does have application for particle contamination but has limited

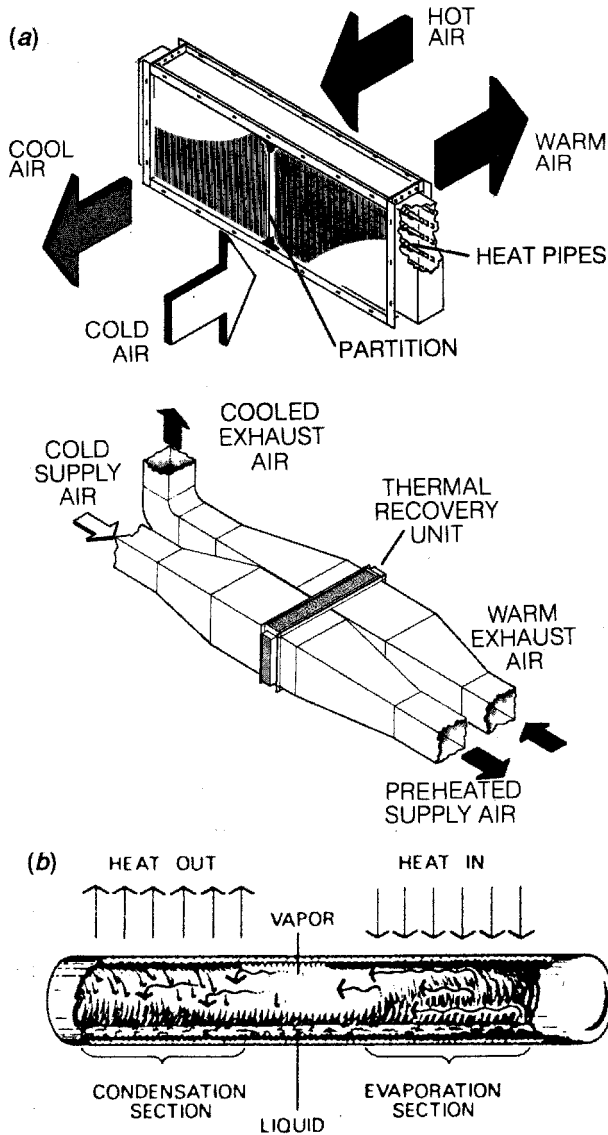


Figure 12.10 The heat pipe coil (a) is positioned across the exhaust and supply duct with a partition separating the pipes into warm (exhaust duct) and cold (supply duct) ends (b). Each heat pipe consists of an inclined tube filled with a refrigerant. As warm air passes over the exhaust duct end of the pipe, the refrigerant vaporizes. The refrigerant vapor passes to the cold incoming airstream, where it condenses releasing the latent heat of condensation, which is transferred to the incoming airstream. The thermal loop continues as the liquid refrigerant flows back to the warm exhaust duct end. A grooved inner wall or other capillary wicking technique facilitates the process of refrigerant transfer between ends. The capacity of the heat pipe can be changed by changing the slope or inclination of the pipe coil and hence the rate of return of the liquid refrigerant to the evaporation (hot exhaust stream) end. (Courtesy of Q Dot Corporation.)

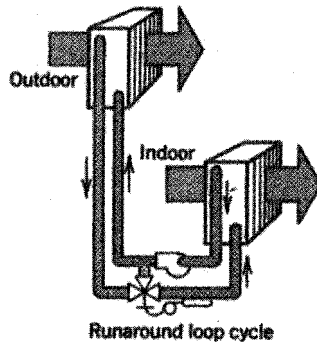


Figure 12.11 Runaround loop cycle for energy recovery from exhaust air.

use for gases and vapors. High-efficiency particle filters used on such applications are “fail-safe,” and the drop in airflow as the filter “loads” can easily be monitored. The downstream particle concentration can usually be measured with sensitive and reliable equipment. However, sorbents used for removal of gases and vapors have a finite life before breakthrough occurs. Monitoring the breakthrough of a gas or vapor contaminant is quite difficult and dependent on the specific contaminant. In any case, recirculation should not be used for human carcinogens or for contaminants with low TLV values.

12.7 SUMMARY

It is important that the designer of industrial ventilation systems recognize the importance of replacement-air systems. In this chapter guidelines are presented to aid in determining whether replacement air is necessary, procedures are outlined for calculating the supply rate of the replacement-air system, and various options are presented for location of the replacement-air unit and distribution ductwork.

REFERENCES

- American Conference of Governmental Industrial Hygienists, Committee on Industrial Ventilation, *Industrial Ventilation Manual*, 24th ed., ACGIH, Lansing, MI, 2001.
- American National Standards Institute; *Recirculation of Air from Industrial Process Exhaust Systems*, ANSI/AIHA Z9.7-1998, April 1998.
- American Society of Heating, Refrigerating and Air Conditioning Engineers, *ASHRAE Handbook—2000 HVAC Systems and Equipment*, ASHRAE, Atlanta, GA, 2000.
- American Society of Heating, Refrigerating and Air Conditioning Engineers, *ASHRAE Handbook—2001 Fundamentals*, ASHRAE, Atlanta, GA, 2001.
- Constance, J. D., *Controlling In-Plant Airborne Contaminants*, Marcel Dekker, New York, 1983, pp. 127–136.

- Holcomb, M. L., and J. T. Radia, "An Engineering Approach to Feasibility Assessment and Design of Recirculating Exhaust Systems," *Proc. 1st Int. Symp. on Ventilation for Contaminant Control*, Oct. 1-3, 1985, Toronto, Canada, H. D. Goodfellow, ed., Elsevier, New York, 1986.
- National Institute for Occupational Safety and Health, *The Recirculation of Industrial Exhaust Air—Symp. Proc.*, Publication No.78-141, Washington, DC, 1978.

QUANTIFICATION OF HOOD PERFORMANCE

It is very important that the performance of exhaust hoods be evaluated once they are installed. Several different tests can be performed, as described below. They are designed to answer one of two important questions:

1. Is the airflow through the hood equal to the design airflow?
2. Is the hood capturing the contaminants given off by the process it is controlling?

The answer to the first question involves making airflow and static pressure measurements. Such measurements (which in the authors' experience are made on only a small fraction of new systems) basically assess the success of the ventilation system design procedure. That is, such tests measure whether the designer has successfully calculated and balanced all the static pressure losses in the system and specified the proper fan; if this is done properly and the construction follows the design specifications (a very big *if*, in some cases), the measured hood airflow will equal the design flow.

Although it is always necessary to measure airflow in newly installed hoods, the second question is fundamentally of greater importance. The success of a hood design rests ultimately in its ability to capture the contaminants given off by the process. Meeting design airflow while capturing only half of the contaminants is not a satisfactory design; it simply means that the proper airflow was not selected during the design process, or the hood was improperly shaped and positioned, or there was some similar defect in the design process.

Traditionally, the success of a ventilation system in capturing contaminants is assessed by measuring the breathing zone concentration of the air contaminants being captured and comparing the results to a standard (e.g., a TLV or a PEL). Alternatively, if the exposed workers move from one location to another, an area sample may be collected in the vicinity of the hood in question. Such measurements, while important, are at best an indirect measure of hood performance. The airborne concentration at any point outside the hood is a function not only of the hood capture efficiency but also of many other factors, such as contaminant generation rate, general room ventilation, operator work practices (for personal samples), and exact sampling location (for area samples). In this chapter we discuss new techniques to measure directly the performance of the hood in capturing contaminants. Measurement of hood capture efficiency should represent the ultimate test of a local exhaust ventilation system.

13.1 HOOD AIRFLOW MEASUREMENTS

The standard procedure used by ventilation engineers and industrial hygienists to evaluate hood performance is simply to measure the total airflow through the hood and compare the measured value to the design value. Once the hood airflow is quantified, its performance can be monitored periodically using the hood static pressure method described in Chapter 3. Techniques for measuring airflow and static pressure are also described in Chapter 3; this discussion will center on the use of such measurements.

The hood airflow measurement method has some great advantages:

1. It is simple and straightforward to perform.
2. It is easy to decide whether the performance is adequate—the flow either meets the design value or it does not.
3. The extent of any required “fix” is equally easy to assess—simply increase (or decrease, perhaps) the airflow to the desired level (by adjusting a blast gate or changing the fan speed, for example).

The chief limitation of this method as a means to quantify hood performance lies in the fact that it measures hood velocities, and knowledge of velocity does not in and of itself ensure adequate hood performance. This is especially true for exterior hoods, which rely on the creation of a capture velocity at the point of contaminant generation sufficient to draw the contaminants into the hood. The difficulties inherent in choosing a capture velocity, and the disruptive effects of cross-drafts, are discussed in Chapter 5.

Such difficulties in choosing the proper capture velocity lead to the very real possibility that an exterior hood may have a measured airflow equal to the design airflow and still not capture the contaminants with high efficiency. Realization of this fact has led researchers to investigate the possibility of measuring hood capture efficiency directly.

13.2 HOOD CAPTURE EFFICIENCY

The authors have been among those looking at the concept of capture efficiency as a means to quantify hood performance. As stated by Ellenbecker et al. (1983):

The advances in ventilation control in the last two decades have been limited to empirical improvements in hood design. . . . Although of demonstrated value, the present design guidelines usually result in the construction of a system whose ability to capture contaminants has only been estimated qualitatively; as a next logical step, we propose a system for the *quantitative* evaluation of exhaust system performance.

Such quantitative evaluation involves the determination of exhaust system capture efficiency, defined as the fraction of contaminants given off by a process actually captured by the exhaust hood(s) used to control that process. This concept of capture efficiency as the best measure of hood performance has received considerable attention from researchers in the 1970s and 1980s (Burgess and Morrow, 1976; Conroy et al., 1988; Conroy and Ellenbecker, 1988; Dalrymple, 1986; Ellenbecker et al., 1983; Fletcher and Johnson, 1986; Flynn and Ellenbecker, 1985, 1986, 1987; Jansson, 1980; Regnier et al., 1986). By the definition above, capture efficiency η is simply

$$\eta = \frac{G'}{G} \quad (13.1)$$

where G = rate of contaminant generation (in, e.g., g/min)

G' = rate at which contaminant is captured by the exhaust system, g/min

In practice, G' may be fairly easy to measure by collecting a sample from the duct located downstream from the exhaust hood(s), but in many cases G is very difficult to measure (or estimate) accurately. Four approaches have been used in an attempt to estimate G : (1) perform a material balance to determine the emission rate; (2) measure airborne contaminant concentrations in the workplace and relate them back to G ; (3) enclose the contaminant source so that all contaminants are captured, and calculate G by measuring the contaminant concentration in the enclosure; and (4) use a tracer to simulate the contaminant emission process.

All four methods have disadvantages. A material balance can rarely be calculated with sufficient accuracy to obtain a realistic estimate of G . The second method is not reliable because of all of the uncertainties involved in translating a generation rate to a resulting airborne exposure. The third method can work well in the laboratory, but is difficult to implement in the field, especially for large contaminant sources. The fourth method is the easiest to use in both the laboratory and the field, but care must be taken to ensure that the tracer accurately simulates the actual emission process.

Both aerosol and gaseous tracers have been used; the most common aerosol is an oil mist, which has the advantage of producing a visible tracer but which is fairly difficult to generate and measure. Gaseous tracers generally are easier to generate and measure than aerosols; the most frequently used is sulfur hexafluoride (SF_6), which can be detected at low concentrations with a properly configured gas chromatograph.

Exhaust hood capture efficiency can also be predicted from theoretical or empirical models. Two theoretical approaches, one using analytical solutions to fluid flow equations and the other using numerical solutions, have been developed. The analytical approach being investigated by the authors and colleagues is described below.

Capture efficiency research is still in its infancy, so that the use of capture efficiency as a system design tool is not widespread. Nonetheless, it represents a powerful new tool for predicting and assessing system performance.

13.2.1 Influence of Cross-Drafts on Hood Performance

As mentioned above, the most important limitation of the hood airflow method of quantifying hood performance is its failure to account for the effects of cross-drafts. In the 1980s work by the authors and colleagues (Conroy and Ellenbecker, 1988; Conroy et al., 1988; Flynn and Ellenbecker, 1985, 1986, 1987; Ellenbecker et al., 1983) resulted in models that can be used to quantify the effect of cross-drafts on hood airflow patterns and capture efficiency. Models have been developed for round, square, rectangular, and slot hoods. The models are based on analytical solutions to Laplace's equation for frictionless, incompressible, and irrotational fluid flow, and they have been validated using wind tunnel tests. Programs have been written for the personal computer that allow a graphical presentation of the models' airflow predictions.

As an example of the use of these models, consider the simple slot hood shown in Fig. 13.1. This hood has a flanged slot 15 in. (0.40 m) long and 1.5 in. (0.13 m) wide (an aspect ratio of 10) and might be used to exhaust a small plating tank. The Flynn, Conroy, and Ellenbecker (FCE) model can be used to visualize the effects of cross-drafts on the performance of this hood. The model was programmed in BASIC; an example of the model output is shown in Fig. 13.2. The figure shows an idealized plan view of this hood, including the flange, the hood opening, and

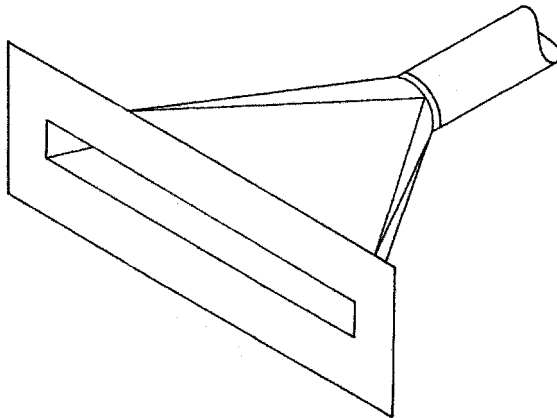


Figure 13.1 Simple flanged slot hood.

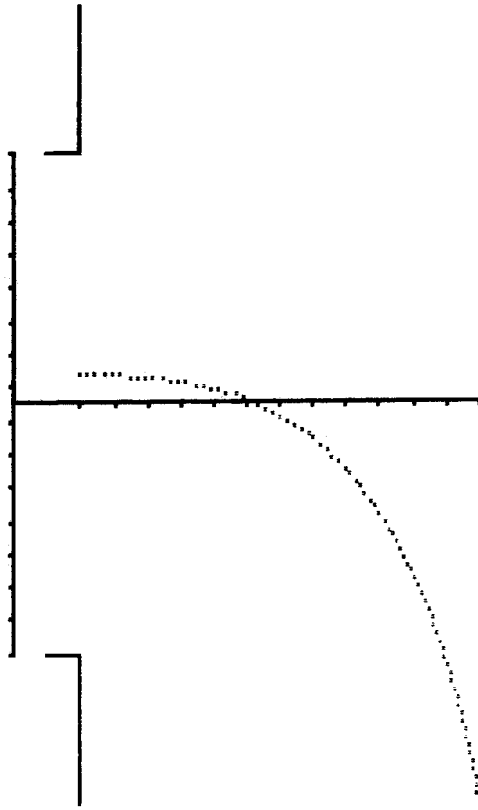


Figure 13.2 Computer model of the hood shown in Fig. 13.1. The slot is seen from above, along with vertical and horizontal distance scales marked 1-in. intervals. $L = 15.0$ in. $w = 1.5$ in., $V_f = 1000$ fpm, $V_d = 25$ fpm. A single streamline is shown for a face velocity of 1000 fpm and a cross-draft velocity of 25 fpm.

reference scales across the hood face and along the hood centerline. Plotted in dotted lines are the airflow streamlines for a particular combination of hood face velocity V_f and cross-draft velocity V_d . In this case the hood face velocity is 1000 fpm (5 m/s) and the cross-draft is relatively low, 25 fpm (0.13 m/s), and blowing directly across the hood face from the bottom of the figure toward the top. A single streamline, starting at a location upstream and 12 in. (0.30 m) in front of the hood, is shown. Such streamlines are useful in visualizing the direction of airflow from any point in front of the hood, and thus are an important feature of the new capture efficiency models. Figure 13.2 and subsequent figures in this chapter show a two-dimensional view of the airflow pattern as it exists on the centerline plane of the hood; any other plane can also be modeled and displayed, so that the entire flow field can be visualized.

Figure 13.3 illustrates the effect of increasing cross-drafts on hood performance; in all cases, the cross-draft is blowing across the hood face (bottom of the figure toward

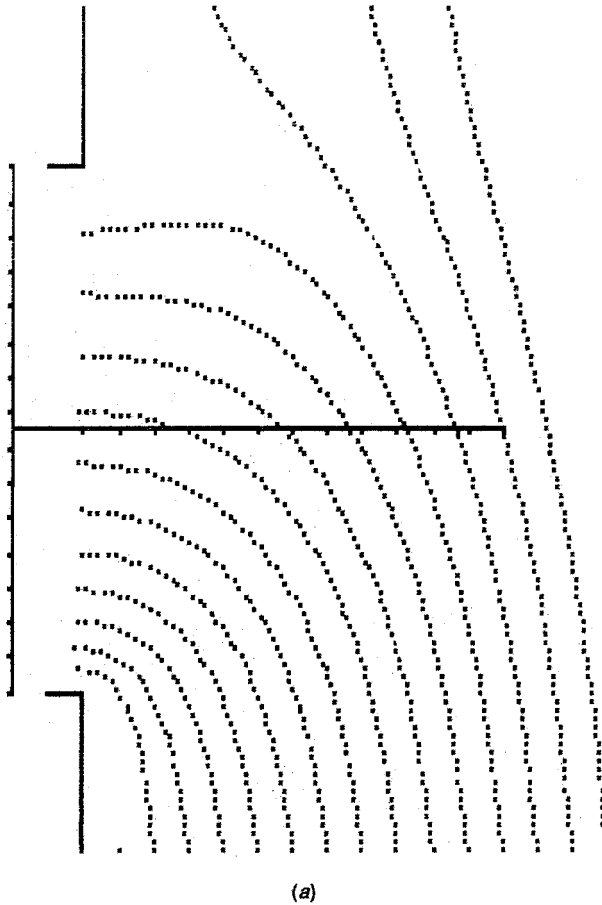


Figure 13.3 The hood shown in Figs. 13.1 and 13.2, illustrating the effect of increasing cross-draft: (a) $V_d = 50$ fpm (0.25 m/s).

the top). As the cross-draft velocity increases, fewer and fewer streamlines enter the hood, so that contaminants would be captured over a smaller and smaller area. When the cross-draft is moderate (e.g., Fig. 13.3a, 50 fpm (0.25 m/s)) the reach of the hood extends about 10 in. (0.25 m) along the hood centerline; when the cross-draft increases to 400 fpm (2.03 m/s) (Fig. 13.3d), the reach is only about 4 in. (0.10 m).

13.2.2 Relationship between Airflow Patterns and Capture Efficiency

Knowledge of the airflow patterns created by an exhaust hood in the presence of a cross-draft can be used to estimate hood capture efficiency. Consider the streamlines shown in Fig. 13.3c; note that one just curves around and enters the hood at the

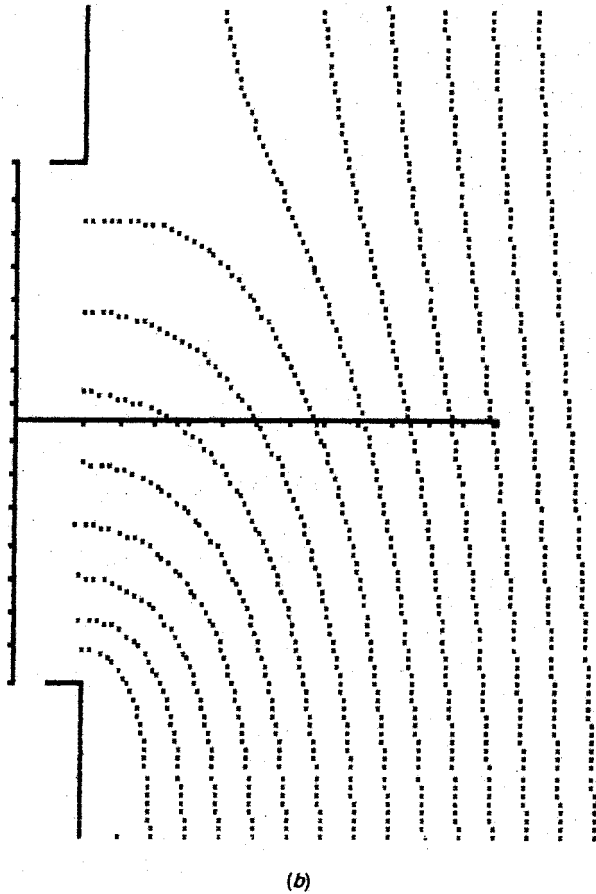


Figure 13.3 (b) $V_d = 100 \text{ fpm}$ (0.5 m/s).

uppermost edge. This streamline is redrawn in Fig. 13.4, where it is labeled the “critical streamline”, since all streamlines closer to the hood enter the hood and all streamlines farther away do not. Air flowing through the crosshatched area of Fig. 13.4 thus enters the hood, so that contaminants given off in this vicinity might be expected to enter the hood and be captured, whereas contaminants given off outside this area would escape the hood.

The predicted performance of the hood at any position in the flow field can now be described. Using the simplistic model of Fig. 13.4, capture efficiency is a step function; inside the crosshatched area it is equal to 1 and outside the crosshatched area it is equal to 0. If capture efficiency is plotted as a function of distance along the hood centerline x the curve of Fig. 13.5a is obtained. The point at which the critical streamline crosses the hood centerline is termed the *critical distance* (x_c); at this point the capture efficiency drops from 1 to 0.

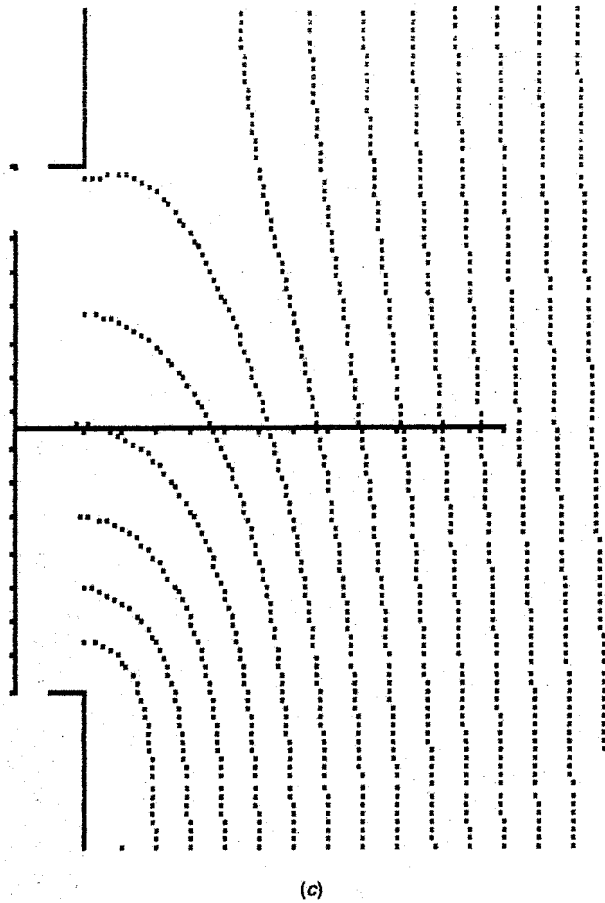


Figure 13.3 (c) $V_d = 200$ fpm (1.01 m/s).

In actual practice turbulence is present in the flow field, which acts to disperse contaminants off their original streamline. This turbulent diffusion should result in a capture efficiency curve that is sigmoidal (Fig. 13.5b). If diffusion is symmetric about the original streamline, the capture efficiency should equal 50% at the critical distance.

Flynn and Ellenbecker (1986) measured the capture efficiency of several flanged circular hoods, and Conroy and Ellenbecker (1988) did the same for flanged slot hoods. They developed models for capture efficiency as a function of hood dimensions (length L and width W or diameter D), hood face velocity (V_f), cross-draft velocity (V_d), position in the flow field, and turbulence intensity (ω). Point sources of gaseous contaminant were used in the experiments so that the behavior of contaminant on individual streamlines could be monitored; the models developed for point sources were then validated for area sources.

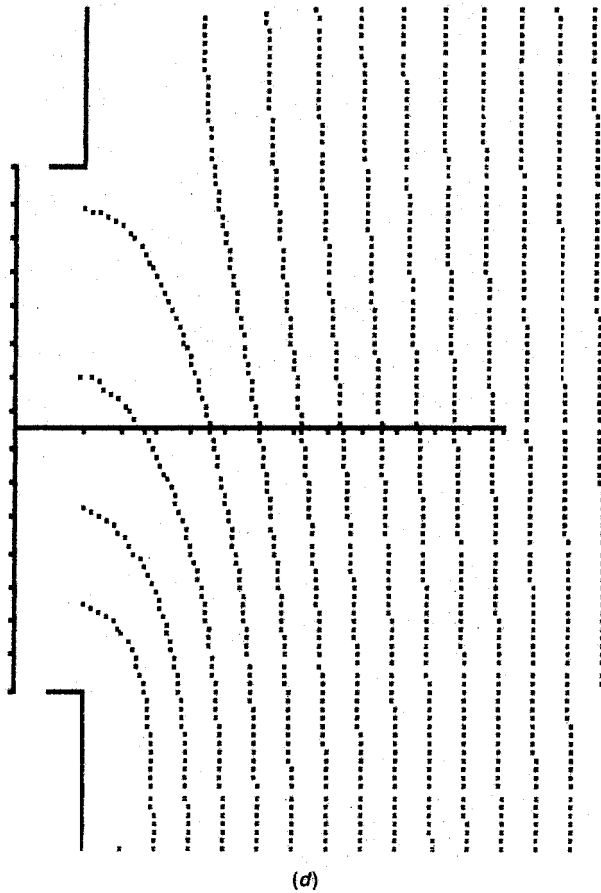


Figure 13.3 (d) $V_d = 400$ fpm (2.03 m/s).

Experimental results confirmed that capture efficiency is best described by a logistic function, which results in sigmoidal capture efficiency curves similar to those in Fig. 13.5b:

$$\eta = \frac{\exp\left(\frac{x - \mu}{\omega}\right)}{1 + \exp\left(\frac{x - \mu}{\omega}\right)} \quad (13.2)$$

where μ is the experimentally measured critical distance, which was found to be very close to the theoretical value x_c . Both μ and ω were found to be functions of the hood dimensions, hood flow, position in the flow field, and cross-draft velocity, as expected.

Typical results using this equation are shown in Fig. 13.6. The four graphs present capture efficiency curves along the centerline in front of a 6-in. (0.15-m) flanged circular hood for different values of V_f/V_d . The first curve (Fig. 13.6a) presents results for

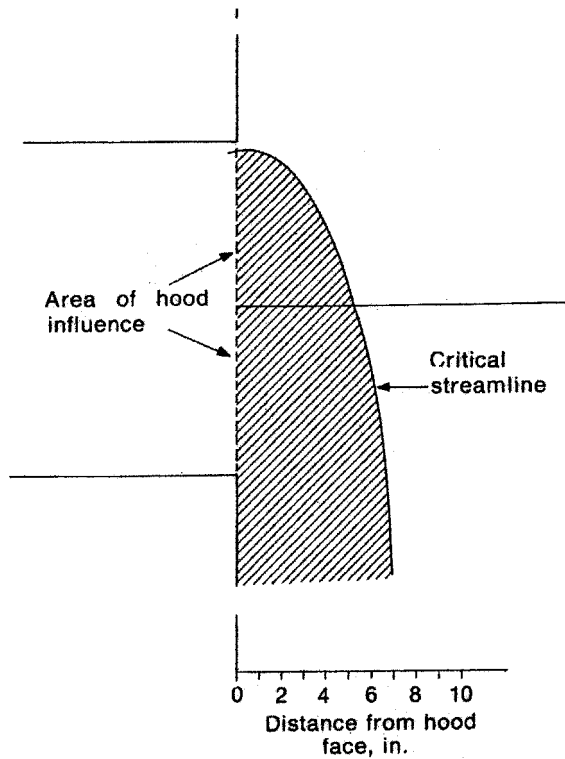


Figure 13.4 The hood of Fig. 13.3 with $V_d = 200$ fpm (1.01 m/s), showing the critical streamline and the area of hood influence.

the lowest ratio tested (0.92). Here the cross-draft quickly predominates and the capture efficiency falls to zero a short distance in front of the hood. The remaining plots illustrate the change in performance as the ratio increases. As the face velocity gets larger relative to the crossdraft velocity, the hood has a greater “reach” and capture efficiency remains high at greater distances from the hood face.

Note also that the slope of the curve changes as the reach increases. This is due to the increased time required for the contaminant to travel into the hood, which in turn results in greater turbulent dispersion around the idealized contaminant streamline. The further the contaminant has to travel, the less the capture efficiency curve looks like the step function of Fig. 13.5a.

Flynn and Ellenbecker (1987) found that for the range of hoods and velocities tested, the critical distance along the hood centerline was given by the following empirical relationship

$$\frac{X}{D} = 0.42 \left(\frac{V_f}{V_d} \right)^{0.6} - 0.08 \quad (13.3)$$

where D is the hood diameter. Critical distances can also be calculated at positions in the flow field not located on the centerline, but no simple empirical relationship

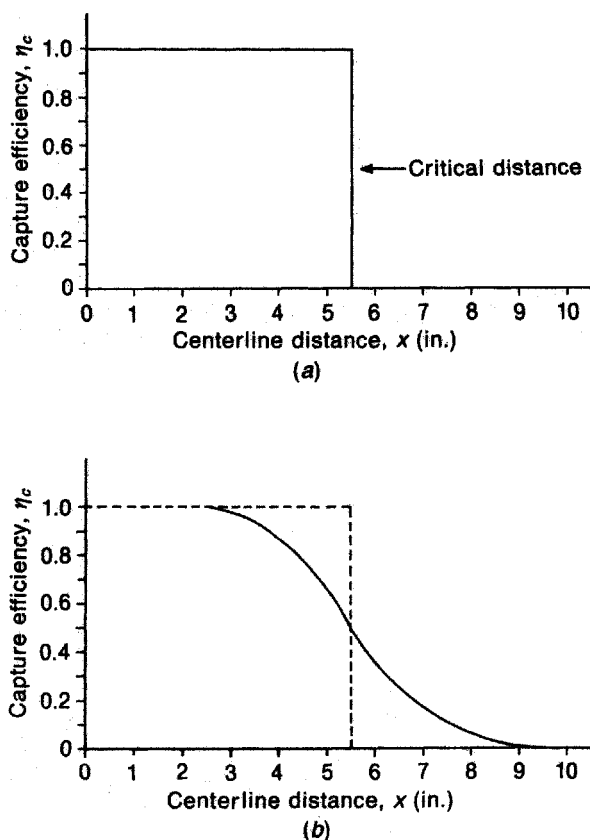


Figure 13.5 Models for hood capture efficiency: (a) with no turbulent dispersion of the contaminant, capture efficiency is a step function, dropping from 100% to 0% at the critical distance; (b) with turbulent dispersion, the capture efficiency curve becomes sigmoidal and drops more gradually, passing 50% at the critical distance.

has been found and the computer model must be used (Conroy and Ellenbecker, 1988).

For a given hood diameter and cross-draft, Eq. 13.3 indicates that the critical distance varies approximately as the square root of the face velocity. This is consistent with the capture velocity findings of DallaValle and others discussed in Chapter 5. The important advance of the capture efficiency method described here over the capture velocity approach now used to describe exterior hood performance is that Eq. 13.2 accounts for the effects of a cross-draft in an explicit, quantifiable manner. That is, if the magnitude and direction of the cross-draft velocity are known, the hood flow required to overcome that velocity can be calculated. This is a considerable improvement over the guidance offered by Table 5.1.

Equation 13.2 can be used to predict capture efficiency for a point source of contaminant located anywhere in front of a flanged exterior hood. For area sources of contaminant release, such as open-surface tanks, the point source capture efficiency

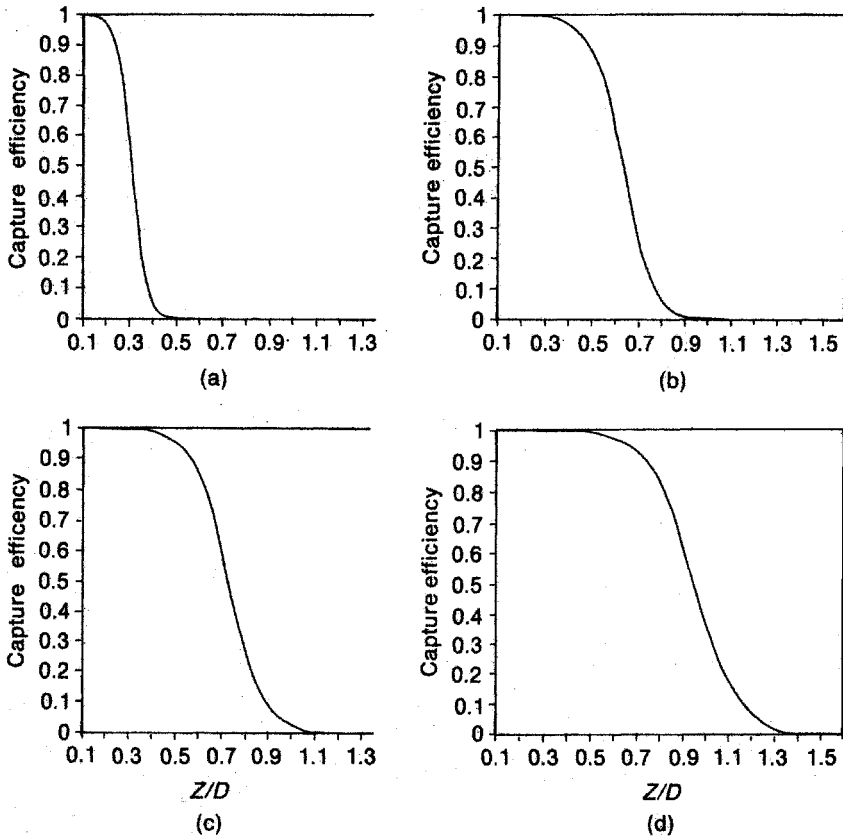


Figure 13.6 Theoretical capture efficiencies for a 6-in. (0.15 m) flanged circular hood at four ratios of face velocity to cross-draft velocity: (a) $V_f/V_d = 0.9$; (b) $V_f/V_d = 2.4$; (c) $V_f/V_d = 3.0$; (d) $V_f/V_d = 4.5$. Note that as the cross-draft ratio increases, the critical distance increases and the shape of the curve becomes flatter.

predictions can be integrated over the area to obtain an overall value of capture efficiency for the source. An example of this procedure is shown in Fig. 13.7. The same 15×1.5 -in. (0.38×0.04 -m) flanged hood as used previously is used here to ventilate a 15-in. (0.38 m)-square open-surface tank, and the conditions are the same as in Fig. 13.3c [$V_f = 1000$ fpm (5.08 m/s), $V_d = 200$ fpm (1.01 m/s)]. The airflow patterns shown in Fig. 13.3 apply with no source present and must be modified to account for the presence of the tank, which prevents airflow from below the centerline plane. The modification can be accomplished by including a symmetric image suction source located below the surface of the tank. The effect is to increase the reach of the hood and move the critical streamline outward from the hood face. The critical streamline shown in Fig. 13.7 reflects this effect. The integrated area source model for this case predicts a capture efficiency of only about 40%, which is not surprising given the high cross-draft velocity and the resulting critical streamline.

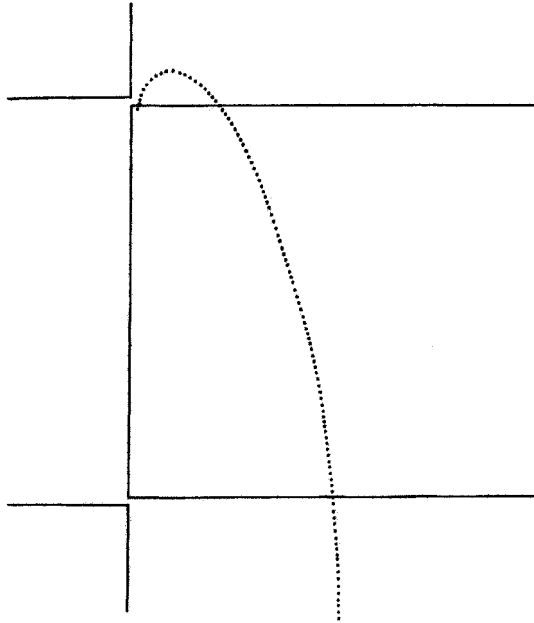


Figure 13.7 Plan view of a 15-in.-square open-surface tank and a 15×1.5 -in. (0.38×0.04 -m) flanged slot hood, showing the critical streamline with $V_f = 1000$ fpm (5.08 m/s) and $V_d = 200$ fpm (1.01 m/s). The area source capture efficiency in this case is 0.41 .

13.2.3 Shortcomings of the Centerline Velocity Approach

The current design procedure for exterior hoods is based on the selection of a proper capture velocity followed by the use of an equation to predict this velocity as a function of hood airflow and distance along the hood centerline. The inadequacies of this procedure in the presence of significant cross-drafts can be illustrated using Fig. 13.3c.

Figure 13.3c indicates that the critical streamline crosses the hood centerline about 5.5 in. (0.14 m) from the hood face. Since the slot width is 1.5 in. (0.04 m), the ratio of critical distance (x) to width (w) in this case is $x/w = 5.5 \text{ in.}/1.5 \text{ in.} = 3.7$. It is instructive to calculate the capture velocity at this distance as predicted by the various models summarized in Table 5.2.

Garrison's empirical model (Eq. 5.60) predicts that

$$\begin{aligned}
 V &= 0.29 V_f \left(\frac{x}{w} \right)^{-1.1} \\
 &= 0.29 \times 1000 \left(\frac{5.5}{1.5} \right)^{-1.1} \\
 &= 69 \text{ fpm } (0.35 \text{ m/s})
 \end{aligned} \tag{5.60}$$

Silverman's equation (Eq. 5.57) predicts that

$$\begin{aligned} V &= 0.36 V_f \left(\frac{x}{w} \right)^{-1} \\ &= 0.36 \times 1000 \left(\frac{5.5}{1.5} \right)^{-1} \\ &= 98 \text{ fpm (0.50 m/s)} \end{aligned} \quad (5.57)$$

while Flynn, Conroy, and Ellenbecker (FCE) (Eq. 5.61) predict that

$$\begin{aligned} V &= \frac{V_f}{2\pi [0.25 + (x/w)^2]^{1/2} [0.25 + (x/l)^2]^{1/2}} \\ &= \frac{1000}{2\pi [0.25 + (5.5/1.5)^2]^{1/2} [0.25 + (5.5/15)^2]^{1/2}} \\ &= 69 \text{ fpm (0.35 m/s)} \end{aligned} \quad (5.61)$$

The validated Garrison and FCE models predict the same capture velocity, while the much older and widely accepted Silverman model predicts a value that is about 40% too high. Garrison's empirical equation (Eq. 5.60) unfortunately was developed only for x/w ratios less than or equal to 4, so that while it can be used in this example, it cannot be used in cases such as Fig. 13.3*b*, where the cross-drafts are lower and the ratio of critical distance to hood width is greater than 4. The FCE theoretical model holds for all values of x/w and has been validated experimentally for x/w values up to 7.5.

The actual velocity at the point where the critical streamline crosses the centerline is the vector sum of the capture velocity created by the hood and the cross-draft velocity. The use of the Silverman equation in this case overpredicts velocity toward the hood, and a design based on the Silverman equation would drastically overestimate the performance of the hood.

The current design procedure for open-surface tank hoods also illustrates the shortcomings of the capture velocity approach. The design procedure described in Chapter 6 involves first determining the hazard potential and the contaminant evolution rate for the process being performed in the tank; these are used, along with the tank aspect ratio and whether the tank is baffled, to determine the necessary airflow. The specified airflow thus accounts for cross-drafts only qualitatively (the tank is either baffled or it is not) and includes a safety factor to account for contaminant toxicity.

The maximum airflow specified is 250 cfm/ft² (1.27 m³/s), with the caveat that while 250 cfm/ft² (1.27 m³/s) "may not produce 150 fpm (0.75 m/s) control velocity at all aspect ratios, the 250 cfm/ft² (1.27 m³/s) is considered adequate for control." It is instructive to evaluate the adequacy of this airflow for the 15-in. (0.40 m)-square source described above, using the area capture efficiency model. With the recommended slot velocity of 2000 fpm (10.2 m/s) and an airflow of 250 cfm/ft² (1.27 m/s),

the required slot width is 1.88 in. (0.05 m). If the cross-draft is 50 fpm (0.25 m/s) the FCE model predicts a capture efficiency of 91%; this value drops to 61% if the cross-draft is increased to 200 fpm (1.01 m/s). A more commonly recommended airflow is 150 cfm/ft²; this airflow gives a predicted efficiency of 84% when the cross-draft is 50 fpm (0.25 m/s) and only 48% when it is 200 fpm (1.01 m/s). For toxic air contaminants, an efficiency of 84% or 91% may be insufficient to produce safe concentrations at worker breathing zones, while 48% or 61% most certainly would be unacceptable.

13.3 USE OF CAPTURE EFFICIENCY IN HOOD DESIGN

At this time the use of capture efficiency models in the design of exhaust hoods is limited to simple hood shapes, such as rectangles and slots. In addition, the experimental validation of the models has occurred in the laboratory under controlled cross-draft conditions. The models must be tested on real systems in the field, and they must be extended to encompass more complex hood shapes. Much more research also needs to be performed on the effects of turbulence on hood performance; all exhaust hoods operate in turbulent fields of varying intensity and scale, and an understanding of such turbulence is key to the quantification of exterior hood performance. This work is now being conducted in several laboratories.

Even at this early stage in its development, the hood capture efficiency concept has proven to be a powerful tool for evaluating hood performance. Although hood capture efficiency has limited practical application at this writing, it is the authors' belief that its incorporation into the design process will result in improved understanding of local exhaust hood performance and the design of better exhaust systems. In Chapter 14 the use of computational fluid dynamics as a tool to better understand the complexity of ventilation and capture efficiency will be introduced.

LIST OF SYMBOLS

D	hood diameter
G	rate of contaminant generation
G'	rate at which contaminant is captured by an exhaust system
V	velocity
V_d	cross-draft velocity
V_f	hood face velocity
w	slot width
x	distance
x_c	theoretical critical distance
η	capture efficiency
μ	experimental critical distance
ω	turbulence intensity

REFERENCES

- Burgess, W., and J. Murrow, "Evaluation of Hoods for Low Volume-High Velocity Exhaust Systems," *Am. Ind. Hyg. Assoc. J.* **37**(9):546-549 (1976).
- Conroy, L., M. Ellenbecker, and M. Flynn, "Prediction and Measurement of Velocity into Flanged Slot Hoods," *Am. Ind. Hyg. Assoc. J.* **49**(5):226-234 (1988).
- Conroy, L., and M. Ellenbecker, "Capture Efficiency of Flanged Slot Hoods under the Influence of a Uniform Crossdraft: Model Development and Validation," *Appl. Ind. Hyg.* **4**(6):135-142 (1989).
- Dalrymple, H. L., "Development and Use of a Local Exhaust Ventilation System to Control Fume from Hand Held Soldering Irons," *Proc. 1st Int. Symp. on Ventilation for Contaminant Control*, Oct. 1-3, 1985, Toronto, Canada, H. G. Goodfellow, ed., Elsevier, New York, 1986.
- Ellenbecker, M., R. Gempel, and W. Burgess, "Capture Efficiency of Local Exhaust Ventilation Systems," *Am. Ind. Hyg. Assoc. J.* **44**(10):752-755 (1983).
- Fletcher, B., and A. Johnson, "The Capture Efficiency of Local Exhaust Ventilation Hoods and the Role of Capture Velocity," *Proc. 1st Int. Symp. on Ventilation for Contaminant Control*, Oct. 1-3, 1985, Toronto, Canada, H. G. Goodfellow, ed., Elsevier, New York, 1986.
- Flynn, M., and M. Ellenbecker, "The Potential Flow Solution for Air Flow into a Flanged Circular Hood," *Am. Ind. Hyg. Assoc. J.* **46**(6):318-322 (1985).
- Flynn, M., and M. Ellenbecker, "Capture Efficiency of Flanged Circular Exhaust Hoods," *Ann. Occup. Hyg.* **30**(4):497-513 (1986).
- Flynn, M., and M. Ellenbecker, "Empirical Validation of Theoretical Velocity Fields into Flanged Circular Hoods," *Am. Ind. Hyg. Assoc. J.* **48**(4):380-389 (1987).
- Jansson, A., "Capture Efficiencies of Local Exhausts for Hand Grinding, Drilling and Welding," *Staub-Reinhalte. Luft* (English ed.) **40**(3):111-113 (1980).
- Regnier, R., R. Braconnier, and G. Aubertin, "Study of Capture Devices Integrated into Portable Machine-Tools," *Proc. 1st Int. Symp. on Ventilation for Contaminant Control*, Oct. 1-3, 1985, Toronto, Canada, H. G. Goodfellow, ed., Elsevier, New York, 1986.

APPLICATION OF COMPUTATIONAL FLUID DYNAMICS TO VENTILATION SYSTEM DESIGN

14.1 INTRODUCTION

Human exposure to airborne contaminants is quantified as a time-weighted average breathing-zone concentration over an interval selected based upon the toxic effects of the agent in question. This concentration is a function of the contaminant generation rate, and the air velocity field that transports it to the breathing zone. For contaminants with significant momentum (an active source), the air velocity field may be strongly coupled with the generation rate, or, if a passive source is involved, independent of it. In either case the time-dependent, three-dimensional, air velocity field is of primary importance in achieving effective exposure control.

Ventilation is an important method used to exert control over the airflow field and achieve acceptable worker exposures. As such, it is an application of the science of fluid mechanics, and involves the use of its basic tools: control volume analysis, dimensional analysis, and differential analysis (White, 1986). As noted in Chapter 13, historically control volume analysis and dimensional analysis have found application in ventilation, including the dilution ventilation equations, and the velocity contour concept for local exhaust inlets, respectively. However, until recently sufficient computational power was not available to make differential analysis feasible for the equations of concern for most real-world ventilation problems. That is changing, and the rapid increase in computing power and the associated improvements in numerical methods have led to explosive growth in this area. The field of computational fluid dynamics (CFD) now offers a powerful complimentary tool for examining ventilation

problems. Currently CFD plays an important role in the design of automobiles, aircraft, and semiconductors, as well as in the prediction of weather.

Computational fluid dynamics is the scientific discipline devoted to the study of numerical (approximate) solutions to the partial differential equations governing fluid motion. For Newtonian fluids such as air and water, these are the conservation equations of mass, linear momentum (Navier–Stokes equations), and energy. An equation of state (the ideal gas law for air) and an empirical relationship for viscosity as a function of temperature may also be required. For turbulent flows additional partial differential equations are introduced to model the Reynolds stresses that arise from random fluctuations in velocity. There are also transport equations for various species and phases (e.g., aerosols). As a complex coupled system, these partial differential equations do not have closed-form analytic solutions, and thus numerical techniques are required to approximate the dependent variables. In addition, these equations require specific boundary and/or initial conditions to be “well posed” for numerical solution. The reader is referred to the Appendix at the end of this chapter and several texts (Anderson et al., 1984; Lapidus and Pinder, 1982) for details.

The use of computational fluid dynamics as a tool for contaminant control ventilation problems requires an understanding of the inputs and outputs associated with the numerical algorithm. In general, a two- or three-dimensional domain is selected to represent the physical world being modeled, such as a box model of a room. The boundary of the domain will contain the known information, such as the physical geometry, inlet velocities, or outlet conditions. The numerical algorithm approximates values for the dependent variables at a fixed number of points within the domain. This discrete approximation is improved in accuracy by refining numerical parameters until an arbitrary accuracy is achieved (convergence). The dependent variables at each point are the air velocities, pressure, density, turbulence parameters, species concentration if present, and possibly temperature. If the problem is time-dependent, these values will change at each point at each timestep of the calculation. From these discrete values integrated estimates (e.g., breathing-zone concentrations) may be reconstructed and/or field values displayed. From the perspective of the occupational hygiene engineer, the capability to simulate exposures, and flow fields prior to pilot-scale testing represents an appealing tool. Alternate ventilation configurations, flows, and work practices, may be examined to optimize the design and efficiency of the controls.

However, the process of using CFD to simulate or model a particular real-world problem is complex and has many sources of uncertainty that may ultimately limit the utility of the results. The problem may be thought of in simple terms as “Have I solved the problem correctly, and have I solved the correct problem?” The first issue relates to how accurately the computational algorithm approximates the solution of the equations, subject to the boundary conditions. All numerical methods are approximate, and the error between the true solution and the numerical approximation can be large. It is only through a careful convergence study and uncertainty analysis that one can address this. The second issue is perhaps more difficult in that one has to make a decision about how well the problem being solved with the computer, represents the reality being simulated. Comparisons between computational results, controlled experiments, and ultimately field data can be helpful here.

Lasher (2001) provides an interesting classification scheme for how well CFD does in predicting experimental and real-world data. In the first category the CFD predictions are within engineering accuracy; in the second group the model is able to predict quantitatively the effects of various changes in geometry, and flow conditions. In category three only qualitative trends are identified and in the final category the model is unable to capture trends of interest. Lasher distinguishes categories 2 and 3 as follows: “[for category 2] a CFD model might under predict drag, but if the geometry is changed the model continues to under predict by the same amount or percentage. In the third category . . . the model shows which of two configurations has the minimum drag, but does not indicate the correct differences.” The ability of CFD to be a useful tool in the analysis of contaminant control ventilation problems clearly requires that the model be in one of the first three categories with respect to breathing-zone concentration, which is the index of system performance. In the remainder of this chapter a brief review of the various methods for solving the relevant equations will be presented, followed by some historical perspectives, current progress, and finally (in Section 14.5) information on some software packages and resources currently available.

14.2 METHODS

Many different methods are used for the numerical solution of the fluid transport equations and partial differential equations in general. Those most commonly used in CFD applications may be divided into grid-based techniques such as finite-difference, finite-element, and finite-volume methods; and grid-free approaches such as vortex methods. A reasonably comprehensive review of grid-based methods may be found in Lapidus and Pinder (1982), while the text by Anderson et al. (1984), focuses on finite difference methods for the Navier–Stokes equations. Patankar (1980) published a very readable text with details of the SIMPLE(R) (*semi*implicit *pressure-linked equations*) algorithms, which now play a central role in most commercially available grid-based codes for the Navier–Stokes equations. A good review of vortex methods can be found in Puckett (1993). A brief overview of each of these approaches is given below, followed by some of the issues related to obtaining solutions.

In all cases when approximating a solution to a differential equation with a numerical method, the issue of convergence is central to the analysis and interpretation of the results. A convergent numerical method is one that is both stable and consistent, in a practical sense this means that as the numerical parameters (e.g., mesh size, time step, number of vortex elements) are refined, the difference between the numerical approximation and the true solution becomes arbitrarily small. Without a careful examination of the solution under such refinement, conclusions drawn from simulations are suspect, and may in fact be so far from the true solution as to be useless. This important aspect of numerical simulation has often been omitted in studies using CFD for ventilation (and other) work since the calculations require a significant amount of computer memory and time.

This issue of convergence cannot be overstated and is of major concern in determining the utility of the CFD prediction. If the mesh size and/or timestep is not small enough, or there is not enough resolution with respect to other numerical parameters, the solution may be so inaccurate that no reasonable conclusions can be drawn (a category 4 model by Lasher's scheme). As finer and finer meshes and timesteps are used, the model may converge to within some arbitrary accuracy of the true solution, and if the "correct problem has been input to the program," a highly accurate and useful model may result (category 1, perhaps). The problem often becomes one of obtaining enough computer memory and speed to solve the problem in a reasonable time. Thus there is a tradeoff between resources and the accuracy possible for any given numerical simulation.

There are at least two major sources of numerical error in CFD simulations of ventilation problems relating to contaminant control. These problems are invariably high Reynolds number flows that involve a nonlinear convective acceleration term in the momentum equations. This means that one must initially guess a velocity field and then recalculate the solution over and over until arbitrarily small differences exist from one iteration to the next. This is the so-called nonlinear error in the Navier–Stokes equations. The other major source of uncertainty is truncation error that arises from approximating the partial derivatives by a truncated Taylor series that has vanishing higher-order terms as the mesh size and/or timestep is reduced. Both of these sources of uncertainty require evaluation, to characterize the quality of the numerical approximation.

14.2.1 Grid-Based Methods

The essence of all grid (or mesh)-based numerical methods is to transform a continuous problem (infinite degrees of freedom) into a discrete problem, where the solution is sought at a finite number of points or nodes in the domain. The grid defines these nodes and the discretization method makes an assumption about how the unknowns (e.g., velocity components) vary between the nodes (linear, quadratic, etc.). The result is a linear algebra problem with N equations and N unknowns, where N is the product of the number of nodes in the system and the number of unknowns per node. Thus, if one is seeking the solution of a three-dimensional turbulent flow problem at 1000 nodes and there are 6 unknowns per node (three velocity components, pressure, and two turbulence parameters), the total number of entries in the coefficient matrix is 36,000,000! Fortunately many of the entries are zero, and effective methods exist for storage, which reduces the memory required. However, the accuracy of the numerical method improves as the number of nodes increases (mesh size decreases), and eventually the coefficient matrix exceeds the core memory available and the program must swap to disk, which is a very slow process in relative terms. Hence the major problem in grid-based approaches is obtaining sufficient computer time and memory to solve the large linear algebra problems required for accurate solutions.

The first grid-based methods were finite-difference techniques that used Taylor series expansions to generate difference equations for the derivatives. These methods

formed the basis for most of the initial work done in computational fluid dynamics. Subsequently the *method of weighted residuals* provided an alternative. This approach starts by equating an integral of the product of a weighting function and the residual (difference between the true solution and the approximation) to zero. The different weighting functions define the particular method.

Method of Weighted Residuals (MWR). Let $L(u)$ represent a differential operator, and f , a scalar valued real function then for the equation $L(u) = f$ the residual ε is defined by

$$L(\hat{u}) - f = \varepsilon \quad (14.1)$$

where \hat{u} is an approximation of u . The MWR multiplies this residual by an orthogonal weighting function w ; thus

$$\int w [L(\hat{u}) - f] d\Omega = 0 \quad (14.2)$$

where Ω is the domain of integration. This form allows a host of numerical approximations, including collocation, subdomain (finite-volume), and Galerkin methods. The weighting and interpolation functions are of compact local support and zero elsewhere, thus generating an $N \times N$ sparse system of simultaneous equations for the discrete problem. In the Galerkin approach the functions used to approximate u are the same as the weighting functions. Finite-element approximations for the Galerkin method follow directly from this approach. Petrov–Galerkin methods employ different functions for the weights and approximations. In the finite-volume method the weighting function is one over the cell volume.

14.2.2 Grid-Free Methods

All the CFD ventilation studies to date employing commercially available software packages use a fixed grid with either finite-element or finite-volume discretizations. A significant amount of time and effort go into creating the mesh for these problems, and one limitation is the ability to generate adequate, efficient meshes. In addition, all of these codes employ either a RANS (Reynold’s averaged Navier–Stokes) approach with scalar eddy viscosity turbulence models, such as k -epsilon; or a large eddy simulation (LES) approach with a subgrid turbulence model. Both approaches require assumptions and empirically determined fit factors to complete the model.

A different approach is possible, one that employs no assumptions about turbulence but solves the Navier–Stokes equations directly. This *direct numerical simulation* (DNS) approach can be implemented without a mesh via the *discrete-vortex method* (DVM) developed by Chorin (1973). This method has several appealing advantages and some drawbacks. Here a time-dependent calculation is used to solve the vorticity transport form of the incompressible Navier–Stokes equations, and discretize the vorticity into little “blobs.” The method works well for certain types of high-Reynolds-number flows with boundary-layer separation, and has been applied to

ventilation and worker exposure problems (Flynn and Miller, 1991; Flynn et al., 1995). Although the large linear algebra problem inherent in mesh-based methods is not encountered here, there is an equally challenging “*N*-body” problem resulting from the interaction of each vortex blob with all others.

The advantage of solving the time-dependent Navier–Stokes equations at high Reynolds numbers without a mesh using the DVM is its “self-adaptivity” or the ability to resolve sharp flow gradients by clustering computational elements in regions that require them. For a mesh-based method to do this, the grid must be adaptive and reform periodically to capture relevant features of the flow. At present a commercial vortex code is unavailable, and significant resource questions remain; however it appears to be a promising tool with application to exposure simulations.

14.3 APPLICATIONS

As noted above, there are various possible applications for CFD in the ventilation field, including qualitative flow visualization, ranking alternative designs based on relative exposures, prediction of contaminant reentry into buildings, and finally quantitative prediction of exposure for a given scenario. In addition, flows of interest range in complexity from relatively simple flow into unobstructed local exhaust hoods, to complex, turbulent, time-dependent flows with heat and mass transfer, such as worker exposure studies. The computational resources needed to solve these various problems cover a wide range.

Most CFD calculations applicable to contaminant control ventilation focus on solutions to the incompressible Navier–Stokes equations. These are the only types of simulations addressed here. The term *incompressible* in this context means that the pressure and density are uncoupled, and from a practical perspective, air speeds are less than about 30% of the speed of sound. This does not necessarily mean that density is constant, although this is often true. Within the incompressible formulation, buoyancy-driven flows, such as those in indoor environments, are addressed using the Boussinesq approximation, which allows for density variations to impact the momentum equations.

14.3.1 Historical Perspectives

The earliest attempts to construct mathematical models of fluid flow involved the assumption that viscous (frictional) forces in the fluid were negligible. The governing equations reduce to Laplace’s equation, and the velocity field is recovered as the gradient of the potential function; hence the term *potential flow*. The potential flow assumptions are reasonable for unobstructed flows into exhaust hoods at high Reynolds numbers, and analytic solutions exist for flanged circular (Drkal, 1970) and rectangular (Tyaglo and Shepelev, 1970) hoods. In addition, several simple approximations based on potential flow theory have also been developed for flanged hoods (Flynn and Ellenbecker, 1987; Conroy et al., 1988). Unflanged hoods do not have analytic solutions, and several investigators (Flynn and Miller, 1989; Kulmala,

1995) have explored various numerical techniques to solve for flow fields into these hoods. Potential flow solutions have also been used to estimate hood capture efficiency in the presence of cross-drafts (Flynn and Ellenbecker, 1986).

As the availability of computing power increased and numerical algorithms for fluid flow improved, simulations of the full Navier–Stokes equations became possible and more realistic and complex simulations were undertaken. Several studies were devoted to examining the flow into unobstructed local exhaust hoods (Kulmala, 1993, 1995), and in general the predicted velocity fields were in good agreement with the potential flow solutions and experimental data. Although modeling flows into unobstructed exhaust hoods represents an important step in applying numerical tools to ventilation for contaminant control, the real challenge is to use this technology to reduce exposure. Initial CFD simulations that attempted this appear to have begun in the 1970s with the work of R. J. Heinsohn et al., at The Pennsylvania State University. In his text, Heinsohn (1991) illustrates various applications of CFD to rim exhausters for open-surface tanks, and also for grinding operations. At about the same time in Denmark work by P. V. Nielsen (Nielsen et al., 1978) at the Technical University of Denmark focused on the HVAC and indoor air arena. Although CFD was well established in other areas, these investigators made some of the most significant initial contributions in the ventilation arena.

14.3.2 Current Progress

There are many current examples of CFD applications in the contaminant control ventilation field, and only a few can be included here. An effort has been made to select studies that have undertaken at least some evaluation of the numerical uncertainties. The focus here is on applications primarily concerned with controlling exposure or evaluating exhaust hood performance using CFD. The reader is referred to Awbi's text *Ventilation of Buildings* and the *Industrial Ventilation Design Guidebook* for CFD applications focusing on indoor air and HVAC applications. (Awbi, 1991; Goodfellow and Tahti, 2001).

Kulmala (1994) conducted steady, three-dimensional, CFD simulations of the air velocity and tracer gas concentration fields into a ventilation unit for powder handling and made experimental measurements in the laboratory to examine the results. The computer simulations were run using FLUENT version 3.02 with a standard k -epsilon turbulence model, and did not include a representation of a worker. Because of the symmetry of the problem, only half of the ventilation unit was simulated, and approximately 25,000 cells were employed. The nonlinear error tolerance achieved was 0.001, but a mesh convergence study was not conducted. The level of agreement between the predicted and measured velocities and concentrations depended strongly on achieving a good match between experimental and numerical boundary conditions, specifically uniform flow at the inlet of the ventilation unit. While reasonable qualitative agreement was observed in some cases significant differences were also present.

In a related study (Kulmala et al., 1996) a numerical simulation of relative breathing-zone concentrations was undertaken for a stationary mannequin in a uniform flow. Emphasis was on the near-wake region, and both three-dimensional velocity

fields and “relative concentrations” were reported. The same version of FLUENT and turbulence model were used as in the previous study. Two different mesh densities were reported: one with approximately 13,000 cells the other with about 24,000 cells; again only half of the domain was simulated because of the symmetry. Sufficient convergence was assumed with a nonlinear error tolerance of 0.001, the mesh refinement errors were not reported, but the investigators noted no significant differences between results on the two different meshes. The relative concentrations were calculated with tracer particles and normalized by the highest concentration observed. The results suggested good qualitative agreement.

Flynn and Sills (2000) examined the use of CFD to assess exposure quantitatively for compressed air, spray painting applications, and developed a process for examining the uncertainties that may arise in using such simulations. The worker is modeled simply as a circular cylinder of finite height. Integrating work practices into the CFD simulations is also considered. Figure 14.1 shows the situation selected for simulation.

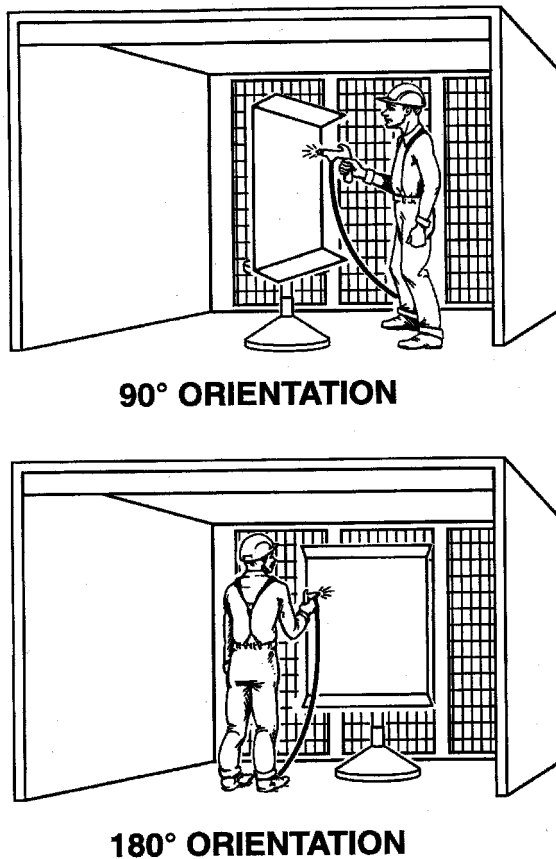


Figure 14.1 Worker performing compressed air spray painting in cross-flow booth in either orientation A (90°) side-to-flow or orientation B (180°) back-to-flow.

Three-dimensional, steady-state predictions of paint transfer efficiency, tracer gas concentration (designed to mimic solvent exposure), air velocity, and particle-size-specific breathing-zone concentrations were made using FIDAP version 8.01 (Fluent Inc., Lebanon, NH), a finite-element package. A standard *k*-epsilon turbulence model was used, and particle tracking using a generalized drag equation and in-house concentration code were employed. The nonlinear error tolerance of 0.001 was used, and three different mesh densities were employed with up to 170,000 cells.

The effect of worker position on exposure was evaluated using the simulations indicating the superiority of the back-to-flow orientation over the side-to-flow position. Figures 14.2–14.7 illustrate the results of the simulations graphically as contours of equal concentration for the various orientations. These figures were generated using visualization software from Advanced Visual Systems (AVS, Waltham, MA) based on the computed outputs from the CFD package. The ability to visualize the data is particularly important in interpreting the results and also as an educational tool in worker training. The study relied on the use of dimensional analysis as well as numerical simulations to relate a dimensionless breathing-zone concentration to a momentum flux ratio.

This preliminary work was followed by a second study (Flynn and Sills, 2001) that conducted a “higher-resolution” simulation of aerosol exposures that matched wind tunnel experimental data reasonably well. The potential for extension of the use of such steady simulations to actual field exposures was also explored, with a favorable comparison with field data. Five different meshes were employed with up to approximately 600,000 nodes. The effect of timestep and number of trajectories on particle breathing-zone concentrations were also examined. Figures 14.8 and 14.9 indicate the aerosol trajectories for two different-size particles in the 90° orientation.

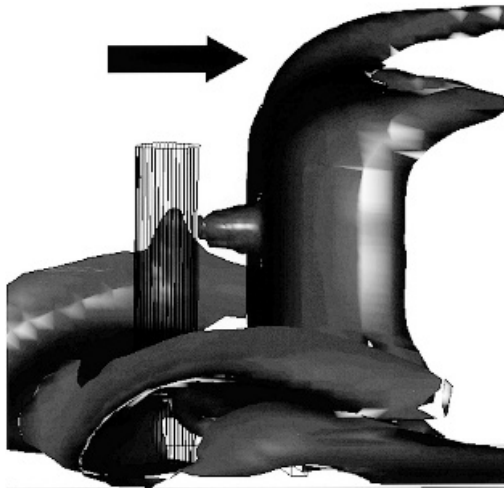


Figure 14.2 The 0.05 mole fraction isoconcentration contour for simulated solvent vapors in orientation B (180°).

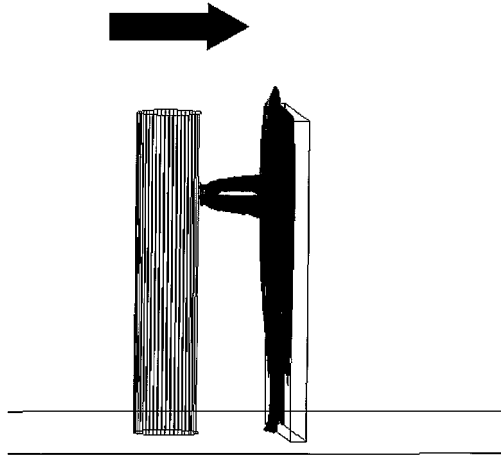


Figure 14.3 The 0.125 mole fraction isoconcentration contour for simulated solvent vapors in orientation B (180°).

A study by Brohus (1997) addressed issues related to the thermal plume from the body and its significance relevant to some of the inertial forces in the fluid. In the previous work cited above, the body was assumed in thermal equilibrium with the air, and there was no need to solve an energy equation. In the Brohus study a constant convective heat flux on the body was input as a boundary condition for the energy equation. The study made comparisons between numerical predictions of tracer gas concentration, velocity, and temperature distributions and detailed laboratory experiments of a breathing thermal mannequin in a booth ventilated by

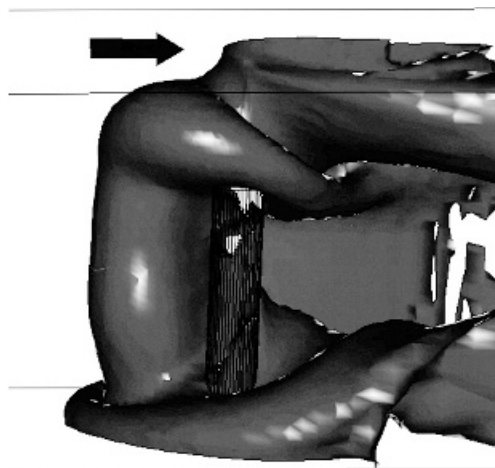


Figure 14.4 The 0.05 mole fraction isoconcentration contour for simulated solvent vapors in orientation A (90°), side view.

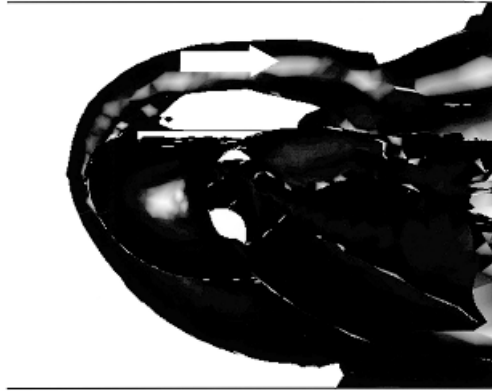


Figure 14.5 The 0.05 mole fraction isoconcentration contour for simulated solvent vapors in orientation A (90°), top view.

two circular extracts on the back wall. The computational and experimental work suggested that at low air velocities the thermal plume effect is important, but that as the velocity increases, the significance of the buoyancy diminishes. The study also considered different rectangular surrogate shapes for the human body. Unfortunately, grid refinement studies apparently were not conducted, and the nonlinear error tolerance achieved was not stated, making evaluation of the simulations difficult.

Subsequently Hyun and Kleinstreuer (2001) examined the geometry that Brohus looked at above and conducted 3-d steady and time-dependent simulations with

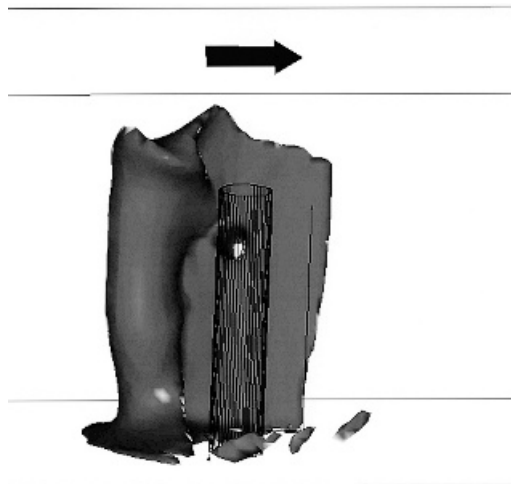


Figure 14.6 The 0.125 mole fraction isoconcentration contour for simulated solvent vapors in orientation A (90°), side view.

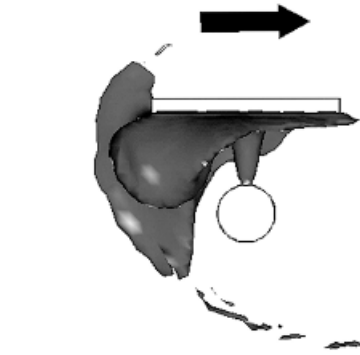


Figure 14.7 The 0.125 mole fraction isoconcentration contour for simulated solvent vapors in orientation A (90°), top view.

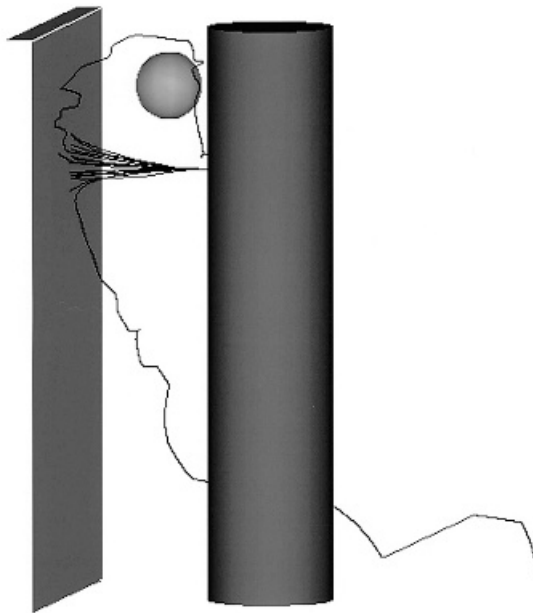


Figure 14.8 Particle trajectories for the $52.5\text{ }\mu\text{m}$ size in orientation A (90°)—small sphere indicates virtual breathing zone.

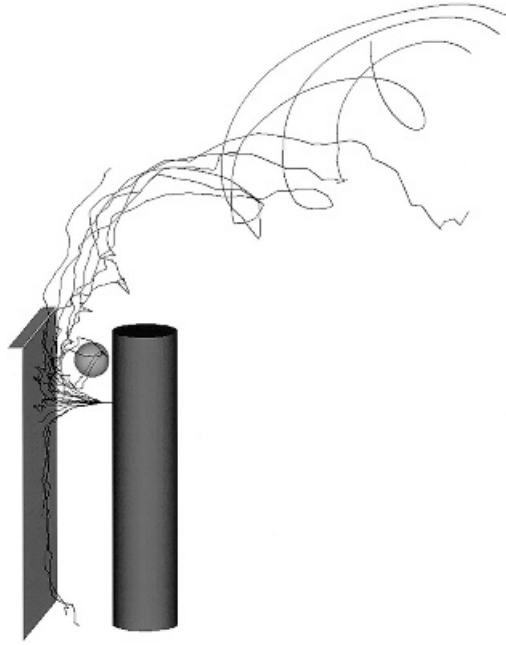


Figure 14.9 Particle trajectories for the $27.5\ \mu\text{m}$ size in orientation A (90°)—small sphere indicates virtual breathing zone.

an RNG (renormalized group) turbulence model. They used the CFX 5.3 (AEA the Technology) finite-volume computer program with up to 350,000 cells in the domain. The authors looked at four different mesh sizes and concluded that an intermediate size was best. One would expect the finer mesh to be the more accurate solution, and no explanation was provided for the selection of the coarser approximation. The non-linear errors were reduced to 0.0001. The timestep size was not given, and a convergence study with respect to its refinement was apparently not conducted. The inlet velocity to the booth was 0.15 m/s. The comparison between thermal and nonthermal effects (i.e., a heated or unheated virtual mannequin) on what they termed “personal dose” appeared to be minor.

14.4 ISSUES ON THE USE OF COMPUTATIONAL FLUID DYNAMICS

Computational fluid dynamics (CFD) will continue to be applied to problems related to human exposure control and ventilation design. Time-dependent, three-dimensional flow in complex geometry, with moving boundaries is clearly the desired end-point. However, computational speed and memory are the key resources governing the feasibility of such calculations and the quality of the results. At present there are

several important issues affecting the use of CFD as a tool in occupational hygiene engineering applications. One of the most important is selecting the necessary and sufficient representation of reality to input into the computer. This deals with issues such as how complex a geometry to employ, what equations to solve, and what boundary conditions should be used. All must be considered in light of the anticipated use of the model output. There will always be constraints on the resources available, and some judicious approximations will be required. Careful communication between occupational hygiene and CFD engineers is important in achieving meaningful results.

Another area that requires research is the process of verification and validation of CFD codes. These terms are being used in the mechanical (ASME, 1993) and aerospace (AIAA, 1997) engineering fields to document and quantify the numerical uncertainties (verification) and the uncertainties between simulated and measured results (validation). For the nonlinear Navier–Stokes equations at high Reynolds numbers, these are difficult issues that require enormous computational resources.

14.5 COMMERCIAL CODES: PUBLIC-DOMAIN INFORMATION

Several CFD codes are commercially available. The finite-element package FIDAP, and the finite volume-code FLUENT, are both sold by Fluent Inc., Lebanon, NH. The CFX code, also a finite-volume package, is available from AEA Technology, UK. Links to these and other CFD resources can be found at the following Website: <http://www.cfd-online.com>.

REFERENCES

- American Institute of Aeronautics and Astronautics (AIAA), *Guide to Uncertainty in Computational Fluid Dynamics Simulations*, AIAA G-077, draft of a recommended practices document, 1997.
- American Society of Mechanical Engineers (ASME), "Editorial Policy Statement on the Control of Numerical Accuracy," *ASME J. Fluids Eng.* **115**(3) (1993).
- Anderson, D. A., J. C. Tannehill, and R. H. Pletcher, *Computational Fluid Mechanics and Heat Transfer*, Hemisphere Publishing, New York, 1984.
- Awbi, H. B., *Ventilation of Buildings*, E&FN Spon, London, 1991.
- Brohus, H., *Personal Exposure to Contaminant Sources in Ventilated Rooms*, Ph.D. thesis, Aalborg Univ. Denmark, 1997.
- Chorin, A. J., "Numerical Study of Slightly Viscous Flow," *J. Fluid. Mech.* **57**:785–796 (1973).
- Conroy, L. M., M. J. Ellenbecker, and M. R. Flynn, "Prediction and Measurement of Velocity into Flanged Slot Hoods," *Am. Ind. Hyg. Assoc. J.* **49**:226–234 (1988).
- Drkal, F., "Stromungsverhältnisse bei runden Saugöffnungen mit Flansch," *Z. Heinz Luft Klim. Haus.* **21**:24–25 (1970).
- Flynn, M. R., and M. J. Ellenbecker, "Capture Efficiency of Flanged Circular Local Exhaust Hoods," *Ann. Occup. Hyg.* **30**:497–513 (1986).

- Flynn, M. R., and M. J. Ellenbecker, "Empirical Validation of Theoretical Velocity Fields into Flanges Circular Hoods," *Am. Ind. Hyg. Assoc. J.* **48**:380–389 (1987).
- Flynn, M. R., and C. T. Miller, "The Boundary Integral Equation Method (BIEM) for Modeling Local Exhaust Hood Flow Fields," *Am. Ind. Hyg. Assoc. J.* **50**:281–288 (1989).
- Flynn, M. R., and C. T. Miller, "Discrete Vortex Methods for the Simulation of Boundary Layer Separation Effects on Worker Exposure," *Ann. Occup. Hyg.* **35**:35–50 (1991).
- Flynn, M. R., M. M. Chen, T. Kim, and P. Muthedath, "Computational Simulation of Worker Exposure Using a Particle Trajectory Method," *Ann. Occup. Hyg.* **39**:277–289 (1995).
- Flynn, M. R., and E. Sills, "On the Use of Computational Fluid Dynamics in the Prediction and Control of Exposure to Airborne Contaminants—an Illustration Using Spray Painting," *Ann. Occup. Hyg.* **44**:191–202 (2000).
- Flynn, M. R., and E. Sills, "Numerical Simulation of Human Exposure to Aerosols Generated During Compressed Air Spray Painting in Cross-Flow Ventilated Booths," *ASME J. Fluids Eng.* **123**:64–70 (2001).
- Goodfellow, H. D., and E. Tahti, eds, *Industrial Ventilation Design Guidebook*, Academic Press, San Diego, CA, 2001.
- Heinsohn, R. J., *Industrial Ventilation: Engineering Principles*, Wiley, New York, 1991.
- Heinonen, K., I. Kulmala, and A. Saamanen, "Local Ventilation for Powder Handling—Combination of Local Supply and Exhaust Air," *Am. Ind. Hyg. Assoc. J.* **57**:356–364 (1996).
- Hyun, S., and C. Kleinstreuer, "Numerical Simulation of Mixed Convection Heat and Mass Transfer in a Human Inhalation Test Chamber," *Int. J. Heat Mass Transfer* **44**:2247–2260 (2001).
- Kulmala, I., "Numerical Calculation of Air Flow Fields Generated by Exhaust Openings," *Ann. Occup. Hyg.* **37**:451–467 (1993).
- Kulmala, I., "Numerical Calculation of a Local Ventilation Unit," *Ann. Occup. Hyg.* **38**:337–349 (1994).
- Kulmala, I., "Numerical Simulation of Unflanged Rectangular Exhaust Openings," *Am. Ind. Hyg. Assoc. J.* **56**:1099–1106 (1995).
- Kulmala, I., A. Saamanen, and S. Enbom, "The Effect of Contaminant Source Location on Worker Exposure in the Near-Wake Region," *Ann. Occup. Hyg.* **40**:511–523 (1996).
- Lapidus, L., and G. F. Pinder, *Numerical Solution of Partial Differential Equations in Science and Engineering*, Wiley, New York, 1982.
- Lasher, W. C., "Computation of Two-Dimensional Blocked Flow Normal to a Flat Plate," *J. Wind Eng. Ind. Aerospace* **89**:493–513 (2001).
- Nielsen, P. V., A. Restivo, and J. H. Whitelaw, "The velocity Characteristics of Ventilated Rooms," *ASME J. Fluids Eng.* **100**:291–298 (1978).
- Patankar, S. V., *Numerical Heat Transfer and Fluid Flow*, Hemisphere Publishing, New York, 1980.
- Puckett, E. G., "Vortex Methods: An Introduction and Survey of Selected Research Topics," in *Incompressible Computational Fluid Dynamics*, M. D. Gunzburger and R. A. Nicolaides, eds., Cambridge Univ. Press, Cambridge, UK, 1993.
- Tyaglo, I. G., and I. A. Shepelev, "Dvzhenie Vozdushnoo Potoha Vytyazhnomu Otverstiyu," *Vodosnab. sanit. Tekh.* **5**:24–25 (1970).
- White, F. W., *Fluid Mechanics*, 2nd ed., McGraw-Hill, New York, 1986.

APPENDIX

The equations generally selected to model airflow in ventilation studies are either the time-dependent or steady, incompressible, Reynolds averaged Navier–Stokes (RANS) equations. A turbulence model is required and the one most often used is the standard k -epsilon model. This requires two additional partial differential equations. If heat and/or multiple chemical species are present, advective–dispersive equations may be solved subsequent to the velocity field (uncoupled approach), or if they introduce significant effects on the momentum equation, they may be coupled with them. If aerosol particles are present in the flow, they may be tracked in the flow field according to drag equations. The equations given below are for time-dependent, isothermal airflow. A transport equation is given for a passive scalar (e.g., solvent vapors), and aerosol transport equations are shown for nonevaporating particles. These equations were employed in the FIDAP program to solve for the flow fields shown in the figures in this chapter:

$$u_{j,j} = 0 \quad (14A.1)$$

$$\rho \left[\frac{\partial u_i}{\partial t} + u_j u_{i,j} \right] = -p_{,i} + \left[\mu(u_{i,j} + u_{j,i}) - \rho \overline{u'_i u'_j} \right]_{,j} \quad (14A.2)$$

$$\rho \left(\frac{\partial C}{\partial t} + u_j C_{,j} \right) = \left(\rho \alpha C_{,j} - \rho \overline{u'_j C'} \right)_{,j} \quad (14A.3)$$

where u , p , and C are the velocity, pressure, and concentration respectively; μ is the coefficient of laminar viscosity; and α is the diffusivity of the passive scalar. The Einstein convention for repeated indices and comma notation for derivatives are used, and the superscript primes denote fluctuating quantities according to the usual Reynolds decomposition. To close these equations, we invoke Boussinesq constitutive relationships for the Reynolds stresses:

$$-\rho \overline{u'_i u'_j} = 2\mu_t S_{ij} - \frac{2}{3} \rho k \delta_{ij} \quad (14A.4)$$

where

$$k = \frac{1}{2} \overline{u'_i u'_i} \quad \text{and} \quad S_{ij} = \frac{(u_{i,j} + u_{j,i})}{2} \quad (14A.5)$$

$$\text{and for species} \quad -\rho \overline{u'_j C'} = \alpha_t T_{,i} \quad (14A.5)$$

$$\mu_t = \rho c_\mu \frac{k^2}{\varepsilon} \quad \text{and} \quad \alpha_t = \frac{\mu_t}{\rho S_t} \quad \text{and} \quad \varepsilon = \frac{\mu}{\rho} \overline{u'_{i,j} u'_{i,j}} \quad (14A.6)$$

The turbulence kinetic energy k and dissipation ε are obtained from the semiempirical k -epsilon model given below:

$$\rho \left[\frac{\partial k}{\partial t} + u_j k_{,j} \right] = \left[\mu + \frac{\mu_t}{\sigma_k} k_{,j} \right]_{,j} + G + \rho \varepsilon \quad (14A.7)$$

$$\rho \left[\frac{\partial \varepsilon}{\partial t} + u_j \varepsilon_{,j} \right] = \left[\mu + \frac{\mu_t}{\sigma_\varepsilon} \varepsilon_{,j} \right]_{,j} + c_1 \frac{\varepsilon}{k} G - c_2 \rho \frac{\varepsilon^2}{k} \quad (14A.8)$$

Here

$$G = 2\mu_t (s_{ij}) u_{i,j} \quad (14A.9)$$

The constants are $c_\mu = 0.09$; $\sigma_k = 1.00$; $\sigma_\varepsilon = 1.30$; $c_1 = 1.44$; $c_2 = 1.92$. Then $S_t = 0.9$.

Aerosol Trajectories. In the case where particles do not transfer significant momentum to the fluid, but are subject to drag as they move through it, they may be tracked according to a generalized drag equation:

$$\frac{d\mathbf{v}}{dt} = \frac{\mathbf{u} - \mathbf{v}}{\tau} + \frac{\rho_p - \rho_a}{\rho_p} \mathbf{g} \quad (14A.10)$$

where

$$\tau = \frac{4\rho_p D_p^2}{3\mu C_D \text{Re}_p} \quad (14A.11)$$

and

$$C_D = \frac{24}{\text{Re}_p} \left(1 + 0.15 \text{Re}_p^{0.687} \right) \quad (14A.12)$$

$$\text{Re}_p = \frac{D_p |\mathbf{u} - \mathbf{v}| \rho_a}{\mu} \quad (14A.13)$$

where \mathbf{u} = air velocity vector

\mathbf{v} = particle velocity vector

Re_p = particle Reynolds number

C_D = particle drag coefficient

D_p = diameter of aerosol particle

τ = particle relaxation time

ρ_a, ρ_p = density of the air and particle, respectively

REENTRY

Reentry in the context here is the inadvertent return of a vented contaminant back into a nearby air intake or other building opening. This condition is illustrated in Fig. 15.1, which shows a portion of the exhaust from a stack being drawn back into the building through intakes located on the roof or side of a building. Figure 15.2 shows an actual exhaust-to-intake configuration that resulted in a reentry problem.

The most common reentry problems arise from offending air contaminants with low olfactory thresholds, such as food odors from a restaurant kitchen or mercaptans from a laboratory hood. Less common, but of great importance, are cases where detrimental health effects may occur as a result of the quantity or nature of the reentered contaminants. Infrequently, reentered contaminants are reported to cause equipment damage, such as accelerated corrosion to a ventilation system.

There are many documented cases of reentry, and the undocumented cases in industrial, laboratory, and medical facilities certainly exceed that number manyfold. Indeed, it is the rare production or research facility that has not experienced this problem. In one case (Held, 1962) it is reported that a building was evacuated several times because of the reentry of phosgene and chlorine releases. This reference also reports an illness where the cadmium-laden exhaust from a machine shop electroplating unit was drawn directly back into the room.

At another facility (Barrett, 1963), the exhaust from a sodium dichromate tank was drawn into the plant through the building windows. The resulting indoor chromic acid concentrations were sufficient to cause respiratory irritation and perforated nasal septa. In another case at the same site, the exhaust from a trichloroethylene degreaser was

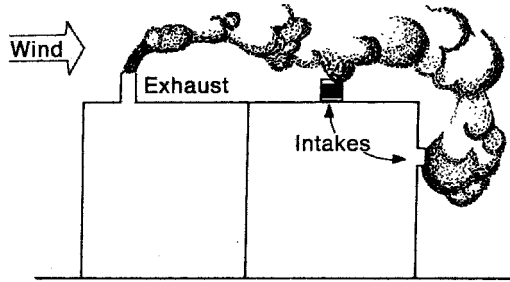


Figure 15.1 Schematic of reentry. Some portion of stack exhaust reenters though roof and side intakes.

drawn through a direct-fired air heating system. The hydrochloric acid that resulted from pyrolysis of the vapor caused rapid corrosion of the heat exchanger. In Fig. 15.3, the author described a case where the diesel exhaust from an emergency generator was drawn into the air inlets on the side of the building. Truck exhaust from the loading dock area (Fig. 15.4) was also in close enough proximity to cause occasional odor complaints.



Figure 15.2 Actual reentry situation. Design flaws include insufficient stack height, proximity of stack to HVAC intakes and the presence of a rain cap.



Figure 15.3 Reentry problems caused by near-ground-level exhaust and HVAC intakes at side of building.

An understanding of contaminant reentry requires knowledge of several related subjects. Initially, it is important to consider the relationship of reentry to the airflow around buildings. Within this context, exhaust system design to prevent reentry requires good engineering practices in determining stack height, location, and other exhaust and intake characteristics. This may be difficult since stack and intake designs vary greatly and often depend on considerations other than potential reentry problems. Architectural aesthetics may impede design from the reentry prevention perspective.

Tracer techniques can be used to determine the potential hazard of existing exhaust intake configurations and to investigate incidents. Wind tunnel and water channel tests have also been used to characterize systems and to offer models and data for improved design. Computational methods can be used to predict contaminant dilution for a proposed or existing system.

Each of these subjects will be discussed in this chapter. Although there is still a good deal of art in the science of stack and intake design, many of the problems that occur today can be prevented by applying available knowledge.

15.1 AIRFLOW AROUND BUILDINGS

Airflow around even simple and isolated rectangular buildings is complex (Fig. 15.5) (ASHRAE, 1997; Wilson, 1979). As building height H above the ground increases, the mean wind speed U_H increases. Also, as shown in Fig. 15.5, a stagnation zone



Figure 15.4 Reentry problems caused by proximity of loading dock to HVAC intakes at side of building.

exists on the upwind wall. As the flow separates at the sharp edges, recirculating flow zones are formed that cover the downwind surfaces of the building. If the building has sufficient length L in the direction of the wind, the flow will reattach to the building.

The flow patterns along the upwind wall are determined in part by the characteristics of the approaching wind. Higher wind speed at roof level causes a relatively higher stagnation pressure on the upper part of the wall and downwash on the lower portion of the upwind surface. The airflow on the more elevated upwind surface continues up and over the roof. When the building height H is ≥ 3 times the width W , the airflow in an intermediate height can pass around the building.

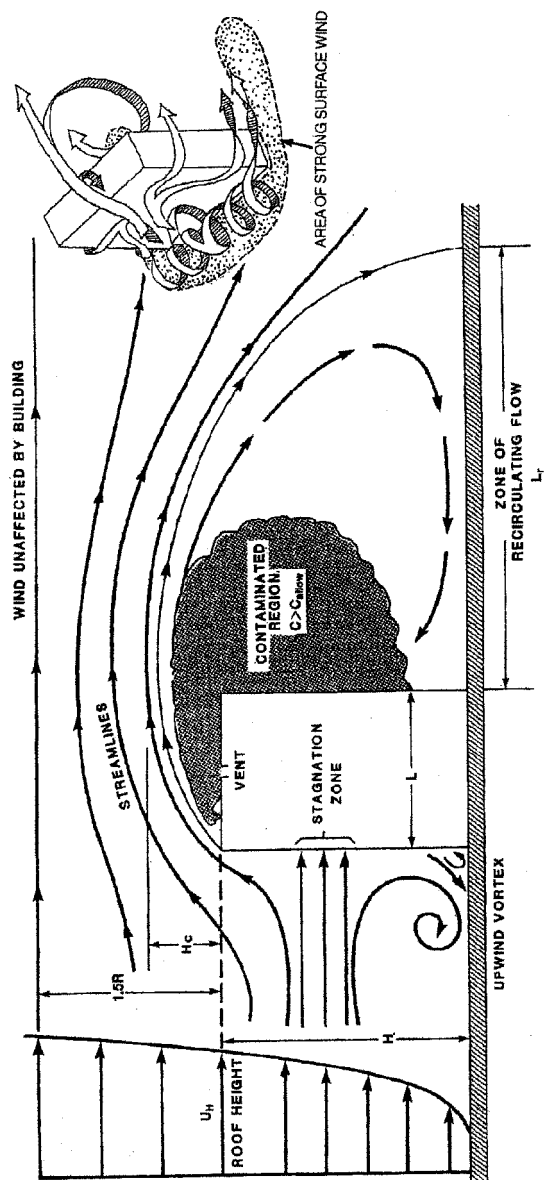


Figure 15.5 Airflow around simple and isolated rectangular building. [Reprinted with permission of ASHRAE (1997).]

It is useful to find a scaling length R according to Wilson (1979) as

$$R = B_S^{0.67} B_L^{0.33} \quad (15.1)$$

where B_S = smaller of upwind building face dimensions H and W

B_L = larger of upwind building face dimensions H and W

When B_L is larger than $8B_S$, use $B_L = 8B_S$.

The distance above the roof level where a building influences the airflow is approximately $1.5R$ (Fig. 15.5). Also shown in this figure is L_r , a zone of recirculation with approximate scaling of $L_r = 1.0R$.

The area above the roof where turbulent recirculation occurs is called the "cavity". The height of the cavity H_C (Fig. 15.5) is important in designing stacks. Release into the cavity can lead to entrainment of contaminants into the turbulent zone above the roof and in the downwind recirculating zone. The maximum cavity height is found when the wind is normal to the upwind building face. At other approach angles, more complex flow patterns develop that tend to reduce the cavity height.

Using the building scaling length from Eq. 15.3, Wilson (1976) found that for a flat-roofed building (see Fig. 15.4)

$$H_C = 0.22R \quad (15.2)$$

$$L_C = 0.9R \quad (15.3)$$

Above the cavity is a zone where the streamlines are affected by the building but do not enter the downwind recirculation zone. Contaminants released into this zone are less likely to cause reentry problems but may cause downwind pollution in neighboring streets, buildings, and parking areas. Above this zone, the streamlines are unaffected by the building. When a building is located in rough terrain, is near other buildings, or has a nonideal shape, as is often the case, the flow patterns will be very complex. Figure 15.6 shows the effect of such a flow pattern on stack exhaust. Theoretical determination of stack height and location in these cases becomes more difficult; empirical measurement or visualization with scale models may be necessary.

15.2 MEASUREMENT OF REENTRY

In evaluating a potential case of reentry, it may be clear that a serious problem exists without resorting to measurements. An example is the manufacturing building schematically depicted in Fig. 15.7, where the dense nesting of exhausts and intakes on the roof inevitably led to reentry problems. In cases such as this it is possible to forgo reentry measurements and work immediately on design changes.

In most cases the extent of a reentry problem is not so clear-cut and the extent of reentry can be measured directly with a tracer. A known amount of the tracer is released into an exhaust point, such as a laboratory hood or a local exhaust vent on a mix vessel, while measurements of the tracer concentration are concurrently made at the building's replacement-air inlet or at various interior locations.

The ideal tracer (Turk et al., 1968) will be

- Detectable at very low concentrations to facilitate measurement across several orders of magnitude
- Nontoxic
- Odorless
- Stable (i.e., it will not thermally or chemically degrade during use)
- Rarely found in the atmosphere, so background ambient levels will not interfere with the test

Several materials have been used successfully in tracer experiments. Sulfur hexafluoride (SF_6) and other halogenated compounds have best met the criteria above (Dietz and Cote, 1973). These compounds can be detected with great sensitivity by electron capture gas chromatography; the detection limit for SF_6 can be as low as 1 part in 10^{13} . Samples can be collected over time (e.g., in an air sampling bag) and taken to a laboratory for analysis, or a variety of commercial portable gas chromatographs can be used for direct field measurements. Lamb and Cronn (1986) used an array of portable automated syringe samplers at up to 40 locations to yield isopleths on and around a laboratory building. Passive sampling devices have been used with a family of perfluorinated cyclic hydrocarbon tracers to obtain long-term average measurements (Dietz and Cote, 1982). Analysis by gas chromatography allows a six-order-of-magnitude capability with this sampling method.

Other materials, including fluorescent dyes, smoke plumes, oil fogs, and antimony oxide, have been used as tracers although the "public relations" issues with releasing tracer materials have increased over time. Munn and Cole (1967), for example, used a fluorescent uranine dye particle to measure the dilution of a building exhaust. A time-weighted average concentration was obtained by filter collection of the tracer over a 20-min period.

It may be feasible to use the offending material itself as a tracer. If the release rate of a contaminant can be quantified and the downwind concentrations can be measured, this contaminant can be used in the same manner as the more common tracers. In a field study by one of the authors, methylene chloride, being released in a laboratory hood, was used as the tracer to measure reentry potential via charcoal tube vapor collection at the roof intake and inside several areas of the building.

There are several important factors to consider in reentry measurements. Wind speed and direction are critical and should be measured on the roof with portable equipment at the time of the tracer release or, at least, qualitatively estimated. Stack temperature and volume should be at normal operating values, and if they vary significantly with time, they should be measured at the time of the reentry measurement. If a short-term measurement is made inside a building, it is important to know the percentage of outside air in the replacement-air system. This value may vary between 10 and 100% depending on the type of HVAC system installed in the building, and on outside temperature and humidity. This measurement is especially important in variable-air-volume HVAC systems.

In some cases a yes-or-no answer is adequate in defining whether reentry is occurring for a given stack intake configuration. For this, the tracer can be released without quantification, although it must be in sufficient quantity to ensure adequate detection limits. In the more usual situation, a tracer is released at a known rate into an exhaust stream with known airflow to create a known exhaust concentration C_e

$$C_e = \frac{Q_t}{Q_e} \quad (15.4)$$

where Q_t is the released tracer flow and Q_e is the exhaust airflow.

A building dilution factor D_b can be defined as the ratio of the outside replacement airflow Q_i and the exhaust airflow containing the trace gas Q_e :

$$D_b = \frac{Q_i}{Q_e} \quad (15.5)$$

Further, an observed dilution factor D_o is defined as the ratio of the exhaust tracer concentration C_e to the indoor concentration C_i resulting from reentry:

$$D_o = \frac{C_e}{C_i} \quad (15.6)$$

The fraction reentry F_R is equal to the ratio of the amount of tracer reentering the building to the amount being exhausted:

$$F_R = \frac{Q_i C_i}{Q_e C_e} \quad (15.7)$$

Substituting Eqs. 15.3 and 15.4 into Eq. 15.5 yields

$$F_R = \frac{D_b}{D_o} \quad (15.8)$$



Figure 15.6 Effect of complex wind pattern on stack exhaust. Three photos taken within minutes of each other show widely varying flow patterns.



Figure 15.6 (Continued)

The indoor concentration C_i can be measured at the replacement-air inlet or at various locations inside the building. Using the highest measured tracer concentration as the value for C_i gives the minimum value for D_o and allows for a conservative approach to reentry evaluation.

In a series of dilution measurements, variables such as wind speed and direction are expected to produce variations in reentry, and for this reason field measurements of dilution may vary over several orders of magnitude. Drivas et al. (1972), for example, in two SF_6 tracer tests of a system with exhaust and intake in very close

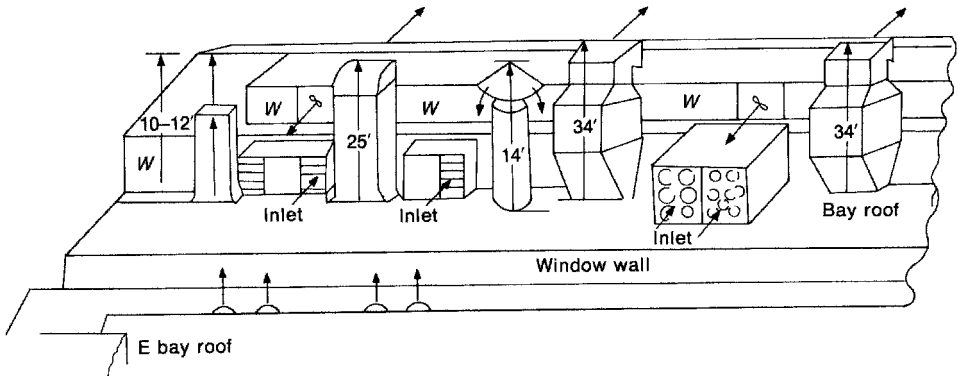


Figure 15.7 Sketch of dense nesting of exhausts and intakes on roof of manufacturing building indicates need for immediate design changes.

proximity, found a variation in D_o from 400 to 10,000, depending in large part on wind direction.

In one field study conducted by the authors, reentry was measured in a chemical research laboratory building in response to several odor complaints. Sulfur hexafluoride (SF_6) was released in a laboratory hood at a known rate, and samples were collected elsewhere inside the building by personal air sampling pumps and air sample bags. Analysis of the collected air on site with a portable electron capture gas chromatograph showed varying SF_6 concentrations with varying meteorological conditions.

As an example of one run of this field study, SF_6 was released at a rate of $0.04 \text{ ft}^3/\text{min}$ ($1.9 \times 10^{-5} \text{ m}^3/\text{s}$) into an exhaust flow of $12,100 \text{ ft}^3/\text{min}$ ($5.7 \text{ m}^3/\text{s}$) from a building with replacement-air flow of $55,200 \text{ ft}^3/\text{min}$ ($26.1 \text{ m}^3/\text{s}$). The computed exhaust concentration was

$$C_e = \frac{Q_i}{Q_e} = \frac{0.04 \text{ ft}^3/\text{min} (1.9 \times 10^{-5} \text{ m}^3/\text{s})}{12,100 \text{ ft}^3/\text{min} (5.7 \text{ m}^3/\text{s})} = 3.3 \times 10^3 \text{ ppb}$$

The building dilution factor was

$$D_b = \frac{Q_i}{Q_e} = \frac{55,200 \text{ ft}^3/\text{min} (26.1 \text{ m}^3/\text{s})}{12,100 \text{ ft}^3/\text{min} (5.7 \text{ m}^3/\text{s})} = 4.6$$

The maximum concentration measured inside the building was 2.4 ppb, so the minimum observed dilution was

$$D_o = \frac{C_e}{C_i} = \frac{3.3 \times 10^3 \text{ ppb}}{2.4 \text{ ppb}} = 1.4 \times 10^3$$

The reentry, expressed as a fraction of the released material brought back into the building, was

$$F_R = \frac{D_b}{D_o} = \frac{4.6}{1.4 \times 10^3} = 0.003$$

The worst case in a series of these measurements showed 5% reentry. With the reentry potential thus defined, a more detailed modeling study was initiated to evaluate the necessary stack height and configuration to prevent reentry (see Section 15.4).

For a given situation with reentry potential, the measured dilution factor can be used to set safe conditions of use. For example, assume that a laboratory hood exhausts phosgene during a synthesis reaction. The value of D_o (based on the maximum SF_6 value found at the inlet under a variety of meteorological conditions) is found to be 250. If the hood exhaust airflow is $500 \text{ ft}^3/\text{min}$ ($0.24 \text{ m}^3/\text{s}$), the maximum generation rate of phosgene in the hood should be about 355 ml/min to ensure values at the intake less than the TLV of 0.1 ppm. This is an illustration of the application of this method. Of course, depending on the toxicity of the material and local regulatory needs, more or less stringent restraints may be imposed.

Reentry measurements require equipment, are time-consuming, and depend on variables, such as wind direction, beyond control of the investigator. Their great advantage is that they do offer a direct measure of a given complex system.

15.3 CALCULATION OF EXHAUST DILUTION

Given a known contaminant concentration in exhaust airflow as well as the exhaust-to-intake configuration, an empirically derived equation can be used to predict the contaminant concentration at an intake. The calculation gives the expected (initial) dilution D_o . The conservative approach, using the smallest dilution D_{\min} , provides the most useful result. The concentration at the replacement-air intake is then calculated using Eq. 15.6. Several empirical methods are summarized below. For the complete methods, the reader is referred to the original work.

The intake concentration C_i can be calculated directly by the method of Halitsky (1982). In this model the concentration C at any point near a building exhaust will be proportional to the contaminant volume release Q_c and inversely proportional to the wind speed U and a reference building face area A :

$$C = \frac{K_c Q_c}{AU} \quad (15.9)$$

where K_c is a dimensionless concentration coefficient at the coordinate location. A limited number of wind tunnel experiments (Halitsky, 1963; Wilson, 1976) provide values of K_c so that Eq. 15.9 can be solved for the concentration.

If a suitable experimental model for K_c is lacking, the following approach (ASHRAE, 1997) can be used to estimate D_{\min} . Key variables are the exhaust to intake stretched-string distance S and the effective stack height h_s (Fig. 15.8). The stretched-string distance is the equivalent of the shortest length of string connecting the point on a stack where $h_s = 0$ (defined as either the height of obstacles such as a roof penthouse close to the stack in question or the boundary of any roof recirculation region through which the stack passes) to the nearest point on an air intake. ASHRAE (1997) reviews three cases of the use of S to calculate the minimum dilution:

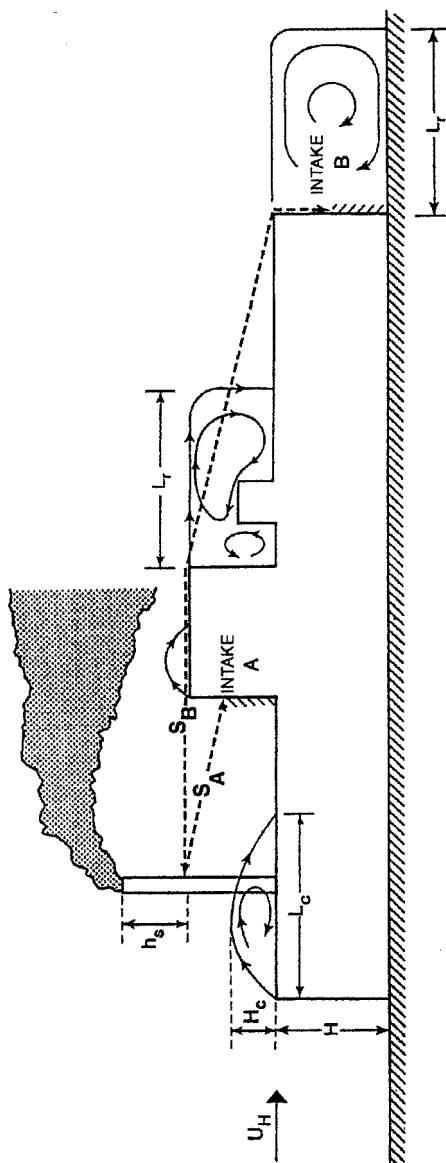


Figure 15.8 Flow recirculation regions and exhaust to intake stretched string distances. [Reprinted with permission of ASHRAE (1997).]

Case 1: block building with surface vents or short stacks with significant jet rise

$$D_{\min} = \left[\alpha + \frac{0.11(1+0.2\alpha)S}{A_e^{0.5}} \right]^2 \quad (15.10)$$

where α is a numerical constant related to building shape, emission velocity ratio, building orientation to wind, and stack height (Halitsky, 1963) and A_e is the stack exit face area.

Case 2: multiwinged building with surface vent or short stack exhaust with emission velocity ratio $V_e/U_H \approx 2$

$$D_{\min} = M \left[3.16 + \frac{0.1S}{A_e^{0.5}} \right]^2 \quad (15.11)$$

where M = intake location factor, $M=1.5$ when the intake is on same roof as the source, $M=2.0$ when source and intake are on different wings separated by airspace, and $M=4.0$ when intake is substantially lower than the source.

Case 3: building with zero exhaust height on flat roof

$$D_{\min, 0} = \left[D_0^{0.5} + D_s^{0.5} \right]^2 \quad (15.12)$$

where $D_0 = 1 + 13.0\beta (V_e/U_H)$ and $D_s = B_1(U_H/V_e)(S^2/A_e)$, where D_0 is the apparent initial dilution at roof level caused by internal turbulence in the exhaust jet, D_s is the distance dilution caused by combined action of building and atmospheric turbulence, β is capping factor ($\beta = 1.0$ for vertical uncapped exhaust, $\beta = 0$ for capped, louvered, or downwind-facing exhausts), and B_1 is the distance dilution parameter.

Wind speed is a variable in several of the equations above. Two competing effects cause a critical windspeed U_c that will result in the minimum dilution. The first effect is that the plume rise due to momentum or buoyancy will decrease with increasing wind speed, with a resulting increase in rooftop concentrations. In contrast, turbulent diffusion increases in the plume as ambient air is entrained with a resulting decrease in rooftop concentrations. Halitsky (1982) concluded that a wind speed of 13.6 mph (21.9 km/h) is the critical value for minimum dilution of a typical laboratory hood. In discussing the maximum intake concentration for flush vents on a flat-roofed building, Wilson (1982) related the critical windspeed to the ratio of a plume rise factor to the downwind distance to the intake. He found that in the range 0.5–3.0 U_c , the roof-level concentration varied by a factor of 2.

Wilson (1984) considered the total dilution between the exhaust and intake (or other receptor point at roof level) as the product of three components: internal system dilution, wind dilution, and dilution due to stack height. If the critical windspeed is used, this approach predicts the minimum dilution. The internal system dilution is a result of in-stack dilution and is obtained by combining exhausts. The

wind dilution results from the entrainment of ambient air between the exhaust and the receptor point, assuming a vent flush with roof level and no plume rise. Finally, dilution is included as a result of stack height and plume rise from vertical exhaust velocity. Modification of the equation for plume rise in the presence of a rain cap or a downward-facing gooseneck is also discussed.

The calculations discussed above are very useful for a quick determination of the approximate dilution for an existing or planned system. Use of the equations for the worst-case scenario (i.e., the lowest dilution) is especially valuable. Since real-world situations have many complex conditions that cannot be fully accounted for by the theoretical and empirical bases of these equations, these techniques should be used with caution.

15.4 SCALE MODEL MEASUREMENT

Scale models can be used to quantify data on flow around buildings, to validate mathematical models for reentry, and to predict reentry for a given design configuration. The great advantage of scale models is that they can include such empirical factors as rough terrain, surrounding buildings, complex building shape, and other variables not fully accounted for by theoretical analysis. Scale models can also be used to test pre-construction designs to evaluate, for example, the effect of a change in stack height on roof concentration contours when the wind is from the least favorable direction. Models are costly in terms of both time and money and thus usually require strong justification before use.

The complex airflow around an existing or planned structure can be investigated with a geometrically scaled physical model where the flow field is simulated by air or water. Such models have been used extensively in civil engineering since being used by the French engineer, Alexandre-Gustave Eiffel.

General modeling criteria (Snyder, 1972; ASHRAE, 1997) are used to ensure that a group of parameters are chosen such that the model and the building are analogous. One criterion is that there must be similarity of the natural wind. This requires modeling the flow characteristics of the atmospheric boundary layer where the flow is affected by the degree of surface roughness. The vertical thermal distribution is usually uniform in wind and water tunnels so that neutral stability conditions are modeled. Thermal stratification can be modeled in a specially designed facility. There must also be geometric similarity between the building and the surrounding topography and kinematic and dynamic similarity of the exhaust effluents.

For modeling in the near field of a point source such as a stack, it is necessary to duplicate closely the local geometry in the area of the source (Plate, 1982). The interior of the model stack might require roughening, for example, to duplicate the exhaust flow properties. The buoyancy and momentum of the exhaust gas must also be scaled. Buoyancy has been modeled by using differing proportions of air-helium mixtures. The exit and intake velocities must be equal in the model and prototype to ensure dynamic similarity.

The near field of a stack is determined not only by its configuration and exhaust rate but also by the turbulence of the atmospheric flow field. To best reproduce this turbulence, it is more important to model the buildings and topographic features in the stack vicinity than to have an exactly scaled profile of the approach wind.

Several tracer techniques have been used in wind tunnel studies (Plate, 1982). Early experiments depended on smoke patterns for mapping contours. Smoke can also be used for quantitative measurements with the use of a photometer. Another early method used ammonia as a tracer with sample analysis by titration. A variety of other tracers and detection systems have been used. These include radioactive tracers such as Krypton-85 with Geiger-Mueller counter detection, helium with a mass spectrometer leak detector or with a thermal conductivity meter, and hydrocarbons with a flame ionization detector.

Open-surface water channel systems have also been used to model the flow field around a stack. Colored dye can be used to visualize flow patterns around buildings of various shapes and sizes in the water channel. Electrical conductivity probes have been used to measure tracer concentrations in a water channel. Thymolphthalein, blue in basic solution, has also been used with different pH values to visualize the isoconcentration lines around an exhaust stack model. Wilson et al. (1998) summarizes ASHRAE Research Project 897, which used water channel simulation to evaluate 1700 different configurations of adjacent-building height, width, spacing, stack location, stack diameter, height, and exit velocity. A fluorescent dye tracer was used with illumination by thin-laser light sheets. Digital video images measured the dilution levels at roof-level air intake locations.

Petersen et al. (1993) used scale modeling to determine stack height with the effect of a nearby hill and later (Petersen et al., 1999) used scale models to study the influence of architectural screens on rooftop concentrations. In both studies, hydrocarbon tracers such as methane, ethane, and propane in mixtures of nitrogen and/or helium to scale density were used with detection via flame ionization or gas chromatography with dual-flame ionization detectors to measure different hydrocarbon tracers released from separate sources.

A model was built of a research building (see Section 15.2) in an urban area (Durgin and Eberhardt, 1981). With a scale of 1:300, the 90-in. (229-cm)-diameter model scaled to a 2250-ft (686-m)-diameter section of the urban area (Fig. 15.9). Smoke was used to visualize flow from the stacks and to define reentry qualitatively by proximity of the smoke to roof inlets. All visual data were recorded for

1. The existing roof design at eight wind directions and four wind speeds
2. Stacks of different incremental heights at the worst-case wind direction and speed
3. The “solution” stack at eight wind directions and four speeds to verify the choice

This experimental sequence led to a compromise recommendation for stack height and design that would minimize reentry at most wind speeds and directions.

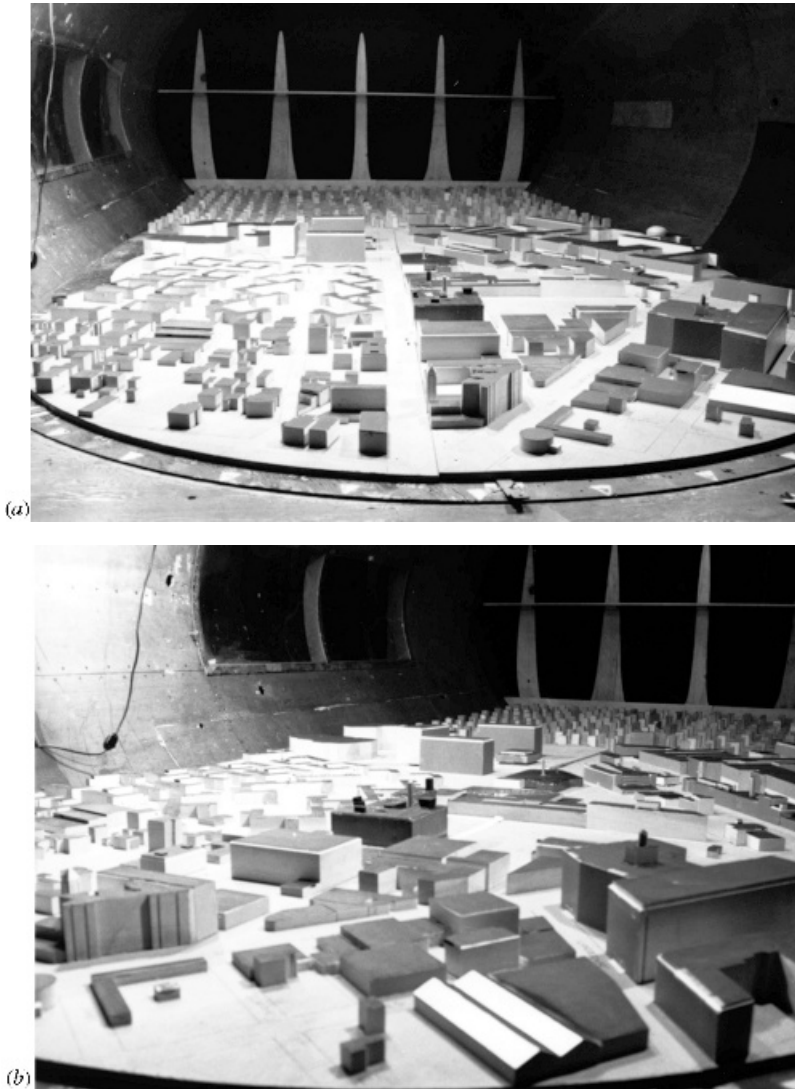


Figure 15.9 (a) Wind tunnel scale model looking upstream. Note the small blocks in the background that reproduce atmospheric turbulence. (b) Close-up of test building.

15.5 DESIGN TO PREVENT REENTRY

The removal of contaminants from an exhaust stream before they leave the stack, as described in Chapter 11, is the surest way to prevent reentry problems. In many facilities contaminant removal is not feasible; in such cases an understanding of airflow around buildings and how reentry is affected by each exhaust stack parameter makes it possible to design or modify a building to minimize reentry problems. Past

experience, translated into good engineering practices and coupled with effective use of empirical and theoretical calculations, permits effective design.

15.5.1 Stack Height Determination

Initially, stack height criteria were based on the assumption that cavity height equaled 1.3–2.0 times the building height (Clarke, 1963). A rule of thumb for power plants with tall stacks called for a stack height of at least 2.5 times the height of the largest nearby building (Thomas et al., 1963), although this probably had little theoretical basis. For power plants and other facilities with very large discharge requirements, air pollution dispersion and not reentry is often the deciding criterion in choosing very tall stacks. The *Industrial Ventilation Manual* (ACGIH, 2001) uses $H_c = 0.22R$. This is based on the work by Wilson (1976), who used water channel laboratory tests to define the turbulence zones above the roofs of a variety of building shapes. These tests also included model buildings with discontinuities such as penthouses, or sudden drops, and rules are suggested for incorporating these into the scaling factor R .

ASHRAE (1999b) uses a geometric stack height design resulting in a recommended effective stack height above rooftop obstacles h_s

$$h_s = h_{sc} - h_r + h_d \quad (15.13)$$

where h_{sc} = required height of capped exhaust stack to avoid excessive intake contamination

h_r = plume rise of uncapped vertical exhaust jet

h_d = downwash correction to be subtracted from stack height

An alternative to a stack height design predicated on cavity height is to design for the needed dilution. Wilson (1984) discusses this approach and points out that design using the cavity height calculation format will give the same conservative treatment to minor nuisance odors that it does to highly toxic contaminants. He presents a design based on “available dilution” that has components of internal system dilution, wind dilution, and dilution from stack height (as discussed in Section 15.3). With this approach a given desired dilution can first be chosen and used to solve for the required stack height.

Ratliff and Sandru (1999) combine dilution prediction equations (ASHRAE, 1997) with the dilution criteria of Halitsky (1988). These authors believe this strategy to lead to less conservative results with application to relatively simple building geometries with no larger adjacent buildings. They calculate the required stack height versus distance of source to air intake for varying exhaust rates, with variable assumptions included from upcoming ASHRAE publications. Their calculations predict a side intake to be beneficial and allow for shorter stack designs.

These stack height design estimates are most applicable in relatively simple situations. They give the designer guidance in choosing parameters and give insight in cases of existing reentry problems.

15.5.2 Good Engineering Practices for Stack Design

There are numerous references in the literature for stack and intake design to help prevent reentry problems. Stack downwash is created by the negative-pressure zone on the downwind side of a stack. When the stack exit velocity is low relative to the wind velocity, downwash can occur, increasing contaminant concentrations up to six stack diameters into the stack eddy zone. The effective stack height is decreased by this mechanism. To prevent downwash, stack velocity should be at least 1.5 times the wind velocity (Clarke, 1965). For most areas in the United States, the maximum wind velocity is less than or equal to 20 mph (1770 fpm or 9.0 m/s) 98% of the time. Using this value for the wind velocity, the stack velocity should be $1770 \times 1.5 = 2660$ fpm (13.5 m/s). The terminal velocity for a raindrop is about 2000 fpm (10.2 m/s) (Laws and Parsons, 1943). Thus the design stack velocity of 2500–3000 fpm (12.7–15.2 m/s) will prevent downwash and keep rain out of the stack.

It is sometimes desirable to add a tapered cone to a stack to increase the exit velocity. The added pressure drop, however, must be considered in the system design and fan specification. Halitsky (1982) states that plume rise h is related to exit velocity V_e and exhaust air flow Q_e by

$$h \propto V_e^{1/3} Q_e^{1/3} \quad (15.14)$$

For a reduction in stack diameter by a factor of 2 with constant airflow, the velocity will increase by a factor of 4 and the plume rise by a factor of $4^{1/3} = 1.6$. The increased velocity obtained from a tapered tip may also be important in preventing downwash.

The *Industrial Ventilation Manual* (ACGIH, 2001) recommends a stack velocity of 3000 fpm (15.2 m/s) to

- Prevent downwash in typical wind conditions
- Increase effective stack height
- Allow use of a smaller centrifugal exhaust fan to provide more stable operation point on applicable fan curve
- Allow for dust in exhaust (or if air-cleaning device fails)

An exception to general stack velocity recommendations may apply for discharge of corrosive condensate droplets (ASHRAE, 1997). An in-stack velocity of 984 ft/min. (5 m/s) with a condensate drain is recommended to help limit droplet emission.

ASHRAE (1997) presents recommended and poor stack designs for proper vertical discharge and rain protection (Fig. 15.10). Rain caps, once very commonly used, are a poor practice in stack design since they are not very effective in keeping out the rain (Clarke, 1963) unless they are very close to the discharge point. Caps blunt the momentum benefit of a straight exhaust and deflect the exhaust horizontally and downward. An uncapped stack will project exhaust at significant velocities at greater than 12 stack diameters upward.

Minimum stack heights are discussed in several publications. NFPA Standard 45 (1996) recommends that exhaust stacks be at least 10 ft (3 m) above the highest point

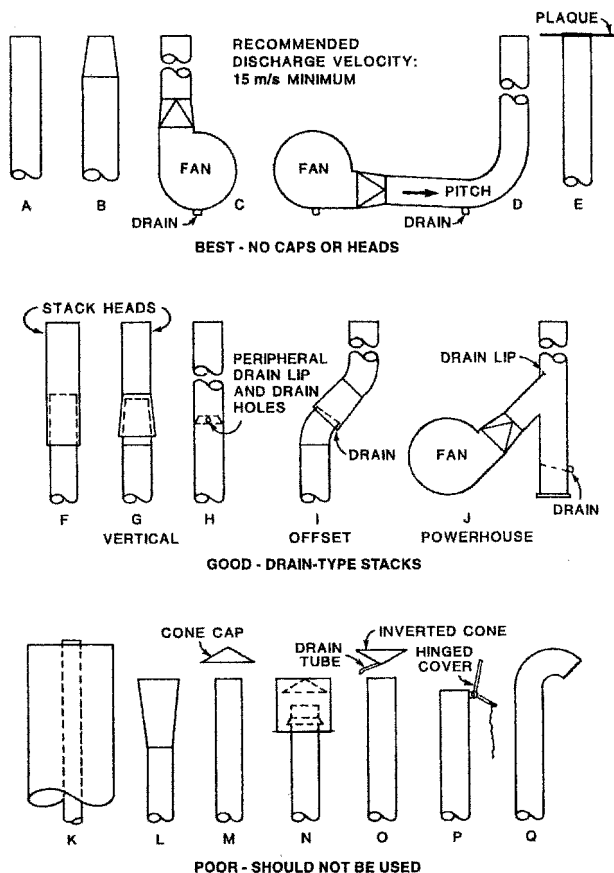


Figure 15.10 Recommended and poor stack designs. [Reprinted with permission of ASHRAE (1997).]

on the roof. This criterion is established to protect personnel on the roof. The BSR AIHA Z9.5 *Laboratory Ventilation Standard* (2000, draft) also recommends discharge to be 10 ft (3 m) above adjacent roof lines and air intakes.

The relative locations of exhaust and intakes are, of course, a primary concern in preventing reentry. The roof is normally the best location for exhausts. On the side of the building, vents may exhaust into the downward flow on the upwind face. Building contamination may arise from a side exhaust as described in Barrett (1963), with direct flow back into the building through windows or intakes (Fig. 15.11). On buildings with several roof levels, locations of the stack on the highest level is usually most effective in promoting the greatest dilution.

Considerable design time should be spent on the spatial relation of the exhausts and intakes in the design of a new facility. Methods range from placing the intake at the base of a "well-designed" exhaust stack (Clarke, 1965) to the more usual method of maximizing the distance between the two. The effects of varying distance can be



Figure 15.11 Side exhaust from side of building may lead to reentry condition.

compared using the computations methods discussed in Section 15.3. Where all exhausts of concern are emitted from a single relatively tall stack or cluster of stacks, locating an intake in this immediate vicinity may work well (ASHRAE, 1997). Prevailing wind direction should not be relied on exclusively in planning intake location. Reentry can be a serious problem even if the potential exists only during infrequent wind directions.

Wilson et al. (1998) examined a multitude of configurations of adjacent-building heights, widths, spacing, stack location, stack diameter, height, and exit velocity. Some resulting general guidelines are

- Avoid locating stacks near edge of a roof where plume can be deflected into roof edge recirculation cavity.
- With emitting building upwind, a stepdown roof of a lower adjacent building will always have higher dilution than would occur on a flat roof at the emitting building height.
- When the lower adjacent building is upwind of the emitting building, it will block the flow approaching the emitting building and will increase the dilution on the emitting building roof.
- Designers can produce jet dilution from higher exhaust velocity when the plume will be trapped in the recirculation cavity from a high upwind adjacent building.

Intake locations should account for all potential contamination sources to the fullest extent feasible. Intakes should not be located within the same architectural screen

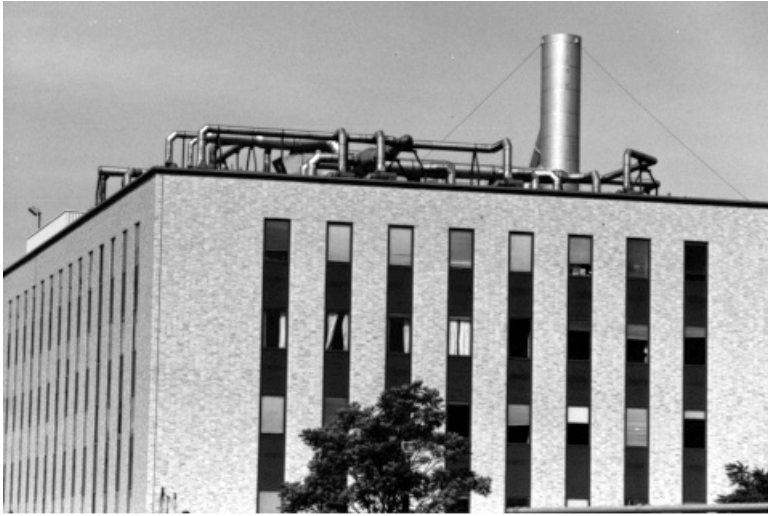


Figure 15.12 Separate exhaust systems from many laboratory hoods combined into one large release stack.

enclosure as the exhaust stacks. Additionally, intakes near loading dock or other ground-level contamination sources, should be avoided.

In some cases, it has proved wise to choose a large central exhaust system rather than many smaller ones (Rydzewski, 1999). A central exhaust system has both advantages and disadvantages, as discussed in Chapters 6 and 9. With regard to reentry, having one larger stack rather than several smaller ones gives a higher release point. Also, Eq. 15.14 demonstrates that a larger exhaust volume, even with a constant velocity, results in an increase in plume rise. Another important advantage of a central system is the added dilution of unforeseen or occasional high contaminant production from a single exhaust point in the total system. This may be a consideration, for example, in the semiconductor industry, where gas cabinets with relatively small exhaust volumes may be called on to handle a highly toxic chemical leakage. An example of a building exhaust system modified to release all exhaust points through one larger stack is shown in Fig. 15.12 (Bearg, 1987). As discussed in Chapter 9, however, the use of several separate fans allows individual exhaust hoods to be shut down when not needed, with a savings in energy costs. There may also be concern about exhaust flexibility and the possible loss in production time at all work sites if the one central fan is down for servicing or repair.

As noted in Chapter 6, many new laboratory buildings are being designed with exhaust stacks that entrain ambient air to provide both dilution and added plume height to the stack exhaust ("strobic air"). This type of stack, seen in Fig. 15.13, can entrain up to 175% by volume of outside air.

Much has been learned from past mistakes in exhaust design that can be used, in conjunction with the most recent theoretical and model studies, to design and modify exhaust systems to prevent reentry problems. As knowledge and concern about



Figure 15.13 Stacks that entrain ambient air into the exhaust.

chemical exposures have increased, attention to careful roof and stack design is becoming recognized as an important part of the overall design effort of a facility.

LIST OF SYMBOLS

A	area of building face
A_e	area of exhaust opening
C	concentration
C_e	concentration in exhaust
C_i	concentration measured downstream from exhaust, at intake or indoors
D_b	building dilution factor
D_0	apparent initial dilution
D_{\min}	minimum observed dilution factor
D_o	observed dilution factor
D_s	distance dilution
F_R	fraction reentry
H	building height
H_C	cavity height
h	plume rise
h_d	downwash correction
h_r	plume rise
h_s	effective stack height
h_{sc}	capped stack height
K_c	dimensionless concentration coefficient
L	building length

L_c	cavity length
L_r	zone of recirculation
Q_c	contaminant flow
Q_e	exhaust airflow
Q_i	replacement airflow
Q_t	tracer flow
R	scaling length
S	shortest distance from exhaust to intake
U	wind speed
U_c	critical wind speed
U_H	wind speed at building height
V_e	exhaust velocity
W	building width

REFERENCES

- American Conference of Governmental Industrial Hygienists (ACGIH), Committee on Industrial Ventilation, *Industrial Ventilation Manual*, 24th ed., ACGIH, Lansing, MI, 2001.
- American National Standards Institute (ANSI), American National Standards for Laboratory Ventilation, American National Standards Institute (ANSI) Z9.5-2003, AIHA, Fairfax VA, 2003.
- American Society of Heating, Refrigerating and Air Conditioning Engineers (ASHRAE), "AirFlow Around Buildings," *ASHRAE, Handbook—1997; Fundamentals*, ASHRAE, Atlanta, GA, 1997, Chapter 15.
- American Society of Heating, Refrigerating and Air Conditioning Engineers (ASHRAE), "Laboratories," *ASHRAE Handbook—HVAC Applications*, ASHRAE, Atlanta, GA, 1999a, Chapter 13.
- American Society of Heating, Refrigerating and Air Conditioning Engineers (ASHRAE), "Building Air Intake and Exhaust Design," *ASHRAE Handbook—HVAC Applications*, ASHRAE, Atlanta, GA, 1999b, Chapter 43.
- Barrett, I. C., letter in "Open for Discussion," *Heat. Piping Air Cond.* **35**:78 (Aug. 1963).
- Bearg, D., Life Energy Associates, Concord, MA, personal communication, 1987.
- Clarke, J. H., "The Design of Exhaust Systems and Discharge Stacks," *Heat. Piping Air Cond.* **35**:118–132 (May 1963).
- Clarke, J. H., "The Design and Location of Building Inlets and Outlets to Minimize Wind Effect and Building Reentry of Exhaust Fumes," *Am. Ind. Hyg. Assoc. J.* **26**:242–247 (1965).
- Dietz, R. N., and E. A. Cote, "Tracing Atmospheric Pollutants by Gas Chromatographic Determination of Sulfur Hexafluoride," *Env. Sci. Technol.* **7**:338–342 (1973).
- Dietz, R. N., and E. A. Cote, "Air Infiltration Measurements in a Home Using a Convenient Perfluorocarbon Tracer Technique," *Env. Int.* **8**:419–433 (1982).
- Drivas, P. I., P. G. Simmonds, and F. H. Shair, "Experimental Characterization of Ventilation Systems in Buildings," *Env. Sci. Technol.* **6**:609–614 (1972).
- Durgin, F. H., and D. S. Eberhardt, *Wright Brothers Wind Tunnel*, MIT Report No. WBWT-TR-1 141, 1981.

- Halitsky, J., "Diffusion of Vented Gas around Buildings," *J. Air Pollut. Control Assoc.* **12**:74–80 (1962).
- Halitsky, J., "Gas Diffusion Near Buildings," *ASHRAE Trans.* **69**:464–485 (1963).
- Halitsky, J., "Estimation of Stack Height Required to Limit Contamination of Building Air Intakes," *Am. Ind. Hyg. Assoc. J.* **26**:106–115 (1965).
- Halitsky, J., "Atmospheric Dilution of Fume Hood Exhaust Gases," *Am. Ind. Hyg. Assoc. J.* **43**:185–189 (1982).
- Halitsky, J., "Dispersion of laboratory exhaust gas by large jets," 81st Annual Meeting of the Air Pollution Control Association, Dallas, Texas, Paper 88-75.1 (1988).
- Hama, G. M., letter in "Open for Discussion," *Heat. Piping Air Cond.* **35**:80 (Aug. 1963).
- Held, B. J., "Planning Ventilation for Nuclear Reactor Facilities," *Am. Ind. Hyg. Assoc. J.* **23**:83–87 (1962).
- Lamb, B. K., and D. R. Cronn, "Fume Hood Exhaust Re-entry into a Chemistry Building," *Am. Ind. Hyg. Assoc. J.* **47**:115–123 (1986).
- Laws, J. O., and D. H. Parsons, "Relations of Rain Drop Size to Intensity," *Trans. Am. Geophys. Union* (Part II):452 (1943).
- Meroney, R. N., "Turbulent Diffusion near Buildings," in *Engineering Meteorology*, E. J. Plate, ed., Elsevier, Amsterdam, 1987.
- Munn, R. E., and A. F. W. Cole, "Turbulence and Diffusion in the Wake of a Building," *Atmos. Env.* **1**:33–43 (1967).
- National Fire Protection Association (NFPA), *Standard on Fire Protection for Laboratories Using Chemicals*, NFPA 45, 1996.
- Petersen, R. L., D. K. Parce, J. L. West, and R. L. Londergan, "Effect of a Nearby Hill on Good Engineering Practice Stack Height," paper presented at AWMA Conf., Denver, CO, 1993.
- Petersen, R. L., J. J. Carter, and M. A. Ratcliff, "Influence of Architectural Screens on Rooftop Concentrations Due to Effluent from Short Stacks," *ASHRAE Trans.* **105**(Part 1) (1999).
- Plate, E. J., "Wind Tunnel Modelling of Wind Effects in Engineering," in *Engineering Meteorology*, E. J. Plate, ed., Elsevier, Amsterdam, 1982.
- Ratcliff, M. A., and E. Sandru, "Dilution Calculations for Determining Laboratory Exhaust Stack Heights," *ASHRAE Trans.* **105** (1999).
- Rydzewski, A. J., "Design Considerations of a Large Central Laboratory Exhaust," *ASHRAE Trans.* **105** (1999).
- Snyder, W. H., "Similarity Criteria for the Application of Fluid Models to the Study of Air Pollution Meteorology," *Boundary-Layer Meteorol.* **3**:113–134 (1972).
- Thomas, F. W., S. B. Carpenter, and F. E. Gartrell, "Stacks How High?" *J. Air Pollut. Control Assoc.* **13**:198–204 (1963).
- Turk, A., S. M. Edmonds, H. L. Mark, and G. F. Collins, "Sulfur Hexafluoride as a Gas-Air Tracer," *Env. Sci. Technol.* **2**:44–48 (1968).
- Wilson, D. J., "Contamination of Air Intakes from Roof Exhaust Vents," *ASHRAE Trans.* **82**(1):1024–1038 (1976).
- Wilson, D. J., "Flow Patterns over Flat-Roofed Buildings and Application to Exhaust Stack Design," *ASHRAE Trans.* **85**(2):284–295 (1979).
- Wilson, D. J., "Critical Wind Speeds for Maximum Exhaust Gas Reentry from Flush Vents at Roof Level Intakes," *ASHRAE Trans.* **88**(1):503–513 (1982).

Wilson, D. J., "A Design Procedure for Estimating Air Intake Contamination from Nearby Exhaust Vents," *ASHRAE Trans.* **90**:136–152 (1984).

Wilson, D. J., I. Fabris, and M. Y. Ackerman, "Measuring Adjacent Building Effects on Laboratory Exhaust Stack Design," *ASHRAE Trans.* **104**(2) (1998).

PROBLEMS

15.1 For a rectangular building with height of 35 ft (10.7 m) and width of 75 ft (22.9 m), what is

- (a) Scaling length, R
- (b) Distance above roof where building influences the airflow
- (c) Zone of recirculation, L_r
- (d) Cavity height, H_C
- (e) Cavity length, L_C

Answers:

- (a) 45 ft (13.7 m)
- (b) 67 ft (20.2 m)
- (c) 45 ft (13.7 m)
- (d) 9.9 ft (3.0 m)
- (e) 41 ft (12.5 m)

15.2 In a tracer experiment, the following variables are given:

$$\text{Tracer release rate} = 0.1 \text{ ft}^3/\text{min} \quad (4.72 \times 10^{-5} \text{ m}^3/\text{s})$$

$$\text{Exhaust rate} = 10,000 \text{ ft}^3/\text{min} \quad (4.72 \text{ m}^3/\text{s})$$

$$\text{Outside replacement-air flow} = 40,000 \text{ ft}^3/\text{min} \quad (18.88 \text{ m}^3/\text{s})$$

$$\text{Measured indoor concentration} = 5 \text{ ppb}$$

- (a) What is the observed dilution factor for this run?
- (b) What is the fraction reentry for this run?

Answers:

- (a) Observed dilution factor, $D_o = 2000$
- (b) Fraction reentry, $F_R = 0.002$

15.3 In ASHRAE (1997), for a building with surface vents or short stacks with significant jet rise (case 1, use of the stretched string distance), what is the effect on D_{\min} of doubling the stretched string distance from 25 m to 50 m, given

$$\alpha = 4.0$$

$$A_e = 5.38 \text{ ft}^2 \quad (0.5 \text{ m}^2)$$

Answer:

$D_{\min} = 566$ at 25 m and $D_{\min} = 1901$ at 50 m. The effect on D_{\min} is to increase it by a ratio of $1901/566 = 3.36$ for the doubling in stretched string distance.

- 15.4** According to Halitsky (1982) on plume rise, what is the change in plume rise if
- (a) Exit velocity increases from 500 fpm (2.54 m/s) to 3000 fpm (15.24 m/s)?
 - (b) Exhaust airflow decreases from 3000 cfm (15.24 m/s) to 1000 cfm (5.08 m/s)?

Answers:

- (a) Plume rise increases by factor of 1.8.
- (b) Plume rise decreases by factor of 0.69.

INDEX

- Absolute pressure, airflow principles, 16
- Absorbers, air-cleaning devices, 322–324
- Administrative controls, worker rotation, 3
- Adsorbers, gas and vapor removers, 324–325
- Air-cleaning devices, 311–337
 - gas and vapor removers, 322–325
 - absorbers, 322–324
 - adsorbers, 324–325
 - chemical reaction devices, 325
 - importance of, 311–312
 - particle removers, 312–322
 - centrifugal collectors, 313–319
 - electrostatic precipitators, 319–320
 - gravity settling, 312–313
 - scrubbers, 320–322
 - problems, 337
 - selection of, 325–326, 327–328
 - ventilation system integration, 326, 329–336
 - centrifugal collector particle removers, 330–331
 - electrostatic precipitator particle removers, 334
 - filters, 331–334
 - gas and vapor removers, 335–336
 - gravity settling devices, 330
 - scrubber particle removers, 334–335
- Air contaminants:
 - control methods, classifications of, 2
 - ventilation control, 3–5
- Air ejectors, 287–288
- Airflow, 12–42
 - around buildings, reentry, 393–396, 404–406
 - assumptions in, 13
 - continuity relation, 14–15
 - density, 13–14
 - electroplating operations, 155–159
 - elevation, 20–22
 - granular materials, 167
 - head, 18–20
 - historical perspective, 12–13
 - losses, 26–30
 - frictional, 26–28
 - shock losses, 28–30
 - losses in fittings, 30–37
 - branch entries (junctions), 36–37
 - contractions, 32–35
 - elbows, 35–36
 - expansions, 30–32
 - physics, 12
 - pressure, 16–18
 - measurements, 16–17
 - types, 17–18
 - pressure relationships, 22–26
 - problems, 39–42
 - spray painting, 163–165
- Airflow limitation, chemical laboratory ventilation, energy conservation, 225–227
- Airflow measurements, 43–89
 - bridled vane anemometer, 71–72
 - deflecting vane anemometer (Velometer), 68–71
 - heated-element anemometer, 72–75
 - hood performance quantification, 359

- Airflow measurements (*Continued*)
 hood static pressure method, 77–79
 instrument calibration, 79–80
 orifice meter, 76
 overview, 43–45
 Pitot-static tube, 45–61
 applications and errors, 60–61
 pressure measurements, 47–50
 traverse, 57–59
 velocity profile in duct, 50–56
 problems, 87–89
 resources, 87
 rotating vane anemometer, 61–67
 Venturi meter, 76–77
 visible tracers, 80–85
 application, 84–85
 design, 81–84
 vortex shedding anemometer, 75–76
 Airflow patterns, hood performance quantification, 363–370
 Air movers. *See* Fans
 Air replacement. *See* Replacement-air systems
 American Conference of Governmental Industrial Hygienists (ACGIH), 3, 4, 6
 Anemometer:
 bridled vane, airflow measurement techniques, 71–72
 deflecting vane (Velometer), airflow measurement techniques, 68–71
 heated-element, airflow measurement techniques, 72–75
 rotating vane, airflow measurement techniques, 61–67
 vortex shedding, airflow measurement techniques, 75–76
 Atmospheric pressure, airflow principles, 16
 Auxiliary air supply hoods, chemical laboratory ventilation, 212–213
 Axial flow fans, 283–285
- Backward-curved-blade fans, 286
 Banbury mixer hood, single-hood systems design, 234–241, 248–249, 252
 Blast gate balance method, multiple-hood systems design, 265
 Blowers, defined, 282. *See also* Fans
 Blowing air, exhausting air compared, hood airflow determination, 125–126
 Booth-type hoods:
 described, 110, 112
 design of, 117–119
 Branch entries (junctions), losses, airflow principles, 36–37
- Brazing operations, hood design, 169–177
 Bridled vane anemometer, airflow measurement techniques, 71–72
- Calibration, of instruments, airflow measurement techniques, 79–80
 Capture velocity determination:
 experimental, 127–131
 exterior hood design, 120–124
 slot hoods, 131–135
 Centerline velocity approach:
 exterior hoods, 144–148
 limitations of, hood performance quantification, 370–372
 Centrifugal collector particle removers, air-cleaning devices, 313–319, 330–331
 Centrifugal fans, 285–287
 Chemical laboratory ventilation, 204–231
 design types, 205–213
 auxiliary air supply hoods, 212–213
 horizontal sliding sash hoods, 209–212
 vertical sliding sash hoods, 205–209, 210
 energy conservation, 224–228
 airflow limitation, 225–227
 diversity, 227
 ductless hoods, 227–228
 heat recovery, 227
 operating time reduction, 224–225
 exhaust system, 217–220
 configuration, 217–218
 construction, 218–220
 face velocity for, 214–216
 general ventilation, 229
 historical perspective, 204
 hood performance factors, 220–224
 laboratory layout, 220–222
 work practices, 222–224
 performance, 228–229
 special-purpose hoods, 216–217
 terminology, 204
 Chemical processing operations, hood design, 177–187
 Chemical reaction devices, gas and vapor removers, 325
 Compressor, defined, 282. *See also* Fans
 Computational fluid dynamics, 374–390
 accuracy of, 376
 applications, 379–386
 current progress, 380–386
 historical, 379–380
 commercial codes available, 387
 defined, 375

- equations, 389–390
- error sources in, 377
- field of, 374–376
- issues in, 386–387
- methods, 376–379
 - generally, 376–377
 - grid-based, 377–378
 - grid-free, 378–379
- Computer-aided manufacturing/design (CAM/CAD), 6
- Conservation of matter, airflow principles, 14–15
- Contaminant matching, air-cleaning devices, 325–326
- Continuity relation, airflow principles, 14–15
- Contractions, losses, airflow principles, 32–35
- Cross-drafts, hood performance quantification, capture efficiency, 361–363
- Deflecting vane anemometer (Velometer), airflow measurement techniques, 68–71
- Degreasing tank, slot hoods, single-hood systems design, 241–247
- Density, airflow principles, 13–14
- Dilution (general) ventilation. *See* General exhaust (dilution) ventilation (GEV)
- Direct numerical simulation (DNS), grid-free computational fluid dynamics, 378–379
- Discrete-vortex method (DVM), grid-free computational fluid dynamics, 378–379
- Diversity, chemical laboratory ventilation, energy conservation, 227
- Doorways, chemical laboratory ventilation, 220–221
- Ductless hoods, chemical laboratory ventilation, energy conservation, 227–228
- Dust, granular materials, hood design, 165–169
- Elbow losses:
 - airflow principles, 35–36
 - Banbury mixer hood, single-hood systems design, 239, 241
- Electroplating, 152–159
 - airflow, 155–159
 - hood design, 152–155
 - multiple-hood systems design, static pressure balance method, 262–265, 272–278
- Electrostatic precipitator particle removers:
 - air-cleaning devices, 319–320
 - ventilation system integration, air-cleaning devices, 334
- Elevation, airflow principles, 20–22
- Enclosing hoods:
 - described, 109–110, 111–113
 - design of, 116–120
- Energy conservation, 224–228
 - airflow limitation, 225–227
 - ductless hoods, 227–228
 - heat recovery, 227
 - operating time reduction, 224–225
 - replacement-air systems, 353–356
- Equations, general exhaust (dilution) ventilation (GEV), 93–99
- Equivalent foot method, frictional losses, airflow principles, 27
- Exhaust hood, defined, 108. *See also* Hood design (general applications); Hood design (specific applications)
- Exhausting air:
 - blowing air compared, hood airflow determination, 125–126
 - theoretical considerations, hood airflow determination, 126–127
- Exhaust system, chemical laboratory ventilation, 217–220
- Exhaust system resistance curve, local exhaust ventilation (LEV), fans, 302–303
- Expansions, losses, airflow principles, 30–32
- Exterior hoods:
 - centerline velocity models, 144–148
 - described, 110, 113–115
 - design of, 120–135
 - capture velocity determination, 120–124
 - hood airflow determination, 125–135
 - shape and location, 135
- Fabric filters:
 - centrifugal collector particle removers, 316–319
 - ventilation system integration, 332–334
- Face velocity, chemical laboratory ventilation, 214–216
- Fan laws, 295–297
- Fans, 282–310
 - performance curve tables, 288–298
 - fan curves/fan tables relationship, 297–298

Fans (*Continued*)

- fan laws, 295–297
- mechanical efficiency curve, 293, 295
- power curve, 291–293, 294
- static pressure curve, 289–290
- problems, 309–310
- selection procedure, 305–308
- types of, 283–288
 - air ejectors, 287–288
 - axial flow, 283–285
 - centrifugal, 285–287
- use of, 298–305
 - general exhaust (dilution) ventilation (GEV), 298–300
 - local exhaust ventilation (LEV), 300–305

Filters:

- centrifugal collector particle removers, 315–319
- ventilation system integration, 331–334

Fittings. *See* Losses, in fittings

Flammable gases, general exhaust (dilution) ventilation, 91

Floor casting, replacement-air systems, 349–350

Fluid dynamics. *See* Computational fluid dynamics

Forward-curved-blade fans, 286

Foundry cleaning room system, multiple-hood systems design, 260–262, 267–271, 280–281

Frictional losses:

- airflow principles, 26–28
- Banbury mixer hood, single-hood systems design, 238–239, 240

Fume hood. *See* Chemical laboratory ventilation

Gage pressure, airflow principles, 16

Gas and vapor removers, 322–325

- absorbers, 322–324
- adsorbers, 324–325
- chemical reaction devices, 325
- ventilation system integration, 335–336

General exhaust (dilution) ventilation (GEV), 90–107

- air contaminants, 4, 5
- air replacement, 103–104
- concepts in, 91
- elements in, 90–91
- equations for, 93–99
- fans in, 298–300
- generation rate variations, 99–100
- inlet/outlet locations, 101–102, 103

limitations of, 91–92

local exhaust ventilation compared, 90, 105–106

mixing, 100–101

problems, 107

worker location, 102–103

Glove boxes, hood design, 110, 111

Granular materials, hood design, 165–169

Gravity settling particle removers:

- air-cleaning devices, 312–313
- ventilation system integration, 330

Grid-based computational fluid dynamics, 377–378

Grid-free computational fluid dynamics, 378–379

Grinding operations, receiving-type hood design, 138–141

Head, airflow principles, 18–20

Head units, airflow principles, 17

Heated-element anemometer, airflow measurement techniques, 72–75

Heated processes, receiving-type hood design, 135–138

Heating, replacement-air systems, 352–353

Heat recovery, chemical laboratory ventilation, energy conservation, 227

HEPA filters:

- centrifugal collector particle removers, 315–316
- ventilation system integration, 332

Hood airflow determination, exterior hood design, 125–135

Hood design (general applications), 108–150

- classification, 109–116
 - enclosures, 109–110, 111–113
 - exterior hoods, 110, 113–115
 - receiving hoods, 115
- elements in, 108
- enclosing hoods, 116–120
- exterior hoods, 120–135
 - capture velocity determination, 120–124
 - centerline velocity models, 144–148
 - hood airflow determination, 125–135
 - shape and location, 135
- performance evaluation, 141–142
- problems, 148–150
- receiving hoods, 135–141
 - grinding operations, 138–141
 - heated processes, 135–138
- Hood design (specific applications), 151–203

- chemical processing operations, 177–187
- electroplating, 152–159
 - airflow, 155–159
 - hood design, 152–155
- granular materials, 165–169
- low-volume/high-velocity systems (portable tools), 192–201
- overview, 151
- semiconductor manufacturing, 187–192
 - entry loss, 190
 - optimum exhaust rate, 191–192
- spray painting, 159–165
 - airflow, 163–165
 - hood design, 159–163
- welding, soldering, and brazing, 169–177
- Hood entries, losses, airflow principles, 32–34
- Hood performance quantification, 358–373.
 - See also* Performance curve tables (fans); Performance evaluation
 - airflow measurements, 359
 - capture efficiency, 360–372
 - airflow patterns, 363–370
 - centerline velocity approach limitations, 370–372
 - cross-drafts, 361–363
 - design implications, 372
 - importance of, 358–359
- Hood static pressure:
 - airflow measurement techniques, 77–79
 - Banbury mixer hood, single-hood systems design, 237–238
- Horizontal sliding sash hoods, chemical laboratory ventilation, 209–212
- Industrial hygiene, literature review, 1
- Inlet/outlet locations, general exhaust (dilution) ventilation (GEV), 101–102, 103
- In-line centrifugal fan, 287
- In-line contractions, losses, airflow principles, 34–35
- Instrument calibration, airflow measurement techniques, 79–80
- Iron-ore mines, 7–8, 10
- Junctions (branch entries), losses, airflow principles, 36–37
- Kinetic energy, airflow principles, pressure types, 17–18
- Laboratory hood. *See* Chemical laboratory ventilation
- Lake Superior iron-ore mines, 7–8, 10
- Laminar flow, airflow principles, pressure relationships, 24–26
- Law of the conservation of matter, airflow principles, 14–15
- Literature review, ventilation control, 1
- Local exhaust ventilation (LEV). *See also* Multiple-hood systems; Single-hood systems design
 - air contaminants, 4–5
 - fans in, 300–305
 - general exhaust (dilution) ventilation compared, 90, 105–106
 - single-hood systems, 232
- Log-linear method, Pitot-static tube traverse, 57–59
- Losses:
 - airflow principles, 26–30
 - frictional, 26–28
 - shock losses, 28–30
 - elbow, Banbury mixer hood, single-hood systems design, 239, 241
 - in fittings, 30–37
 - branch entries (junctions), 36–37
 - contractions, 32–35
 - elbows, 35–36
 - expansions, 30–32
 - frictional, Banbury mixer hood, single-hood systems design, 238–239, 240
 - single-hood systems design, slot hood system (for degreasing tank), 243–245
- Lower flammable limit (LFL), general exhaust (dilution) ventilation, 91
- Low-volume/high-velocity systems (portable tools), 192–201
- Maintenance, visible tracers, airflow measurement techniques, 85
- Measurement techniques. *See* Airflow measurements
- Mechanical efficiency curve, fan performance curves, 293, 295
- Media filters:
 - centrifugal collector particle removers, 315
 - ventilation system integration, 332
- Melting furnaces, replacement-air systems, 349
- Method of weighted residuals (computational fluid dynamics), 377–378

- Mixing, general exhaust (dilution) ventilation (GEV), 100–101
- Modified ellipsoidal Pitot-static tube, velocity pressure measurement, 46
- Multiple-hood systems design, 254–281.
 - See also* Local exhaust ventilation (LEV); Single-hood systems design
 - applications of, 254–255
 - approach to, 256–260
 - blast gate balance method, 265
 - computational methods, 265–266
 - static pressure balance method, 260–265
 - electroplating shop, 262–265, 272–278
 - foundry cleaning room system, 260–262, 267–271, 280–281
- Natural ventilation, general exhaust (dilution) ventilation, 103–104
- Operating time reduction, chemical laboratory ventilation, energy conservation, 224–225
- Orifice meter, airflow measurement techniques, 76
- Paper chromatography, special-purpose hoods, chemical laboratory, 216–217
- Particle removers, 312–322
 - centrifugal collectors, 313–319
 - electrostatic precipitators, 319–320
 - gravity settling, 312–313, 330
 - scrubbers, 320–322
- Pedestrian traffic, chemical laboratory ventilation, 221
- Performance curve tables (fans), 288–298
 - mechanical efficiency curve, 293, 295
 - power curve, 291–293, 294
 - static pressure curve, 289–290
- Performance evaluation. *See also* Hood performance quantification
 - chemical laboratory ventilation, 228–229
 - hood design, 141–142
- Personal protection devices, 3
- Pitot-static tube, 45–61
 - applications and errors, 60–61
 - pressure measurements, 47–50
 - traverse, 57–59
 - velocity profile in duct, 50–56
- Portable tools, low-volume/high-velocity systems, 192–201
- Potential energy, airflow principles, pressure types, 17–18
- Potential flow, computational fluid dynamics, 379–380
- Power curve, fan performance curves, 291–293, 294
- Pressure (airflow principles), 16–18. *See also* Static pressure; Velocity pressure measurements, 16–17
 - types, 17–18
- Pressure plot, single-hood systems design, 247
- Pressure units, airflow principles, 16–17
- Propeller fans, 283–284
- Push-pull hoods, air contaminants, 5
- Radial blade fans, 286
- Receiving-type hoods:
 - described, 115
 - design of, 135–141
 - grinding operations, 138–141
 - heated processes, 135–138
- Rectangular duct, Pitot-static tube traverse, 58–59
- Reentry, 391–416
 - airflow around buildings, 393–396, 404–406
 - defined, 391
 - documented cases, 391–392
 - exhaust dilution calculation, 401–404
 - measurement of, 396–401
 - prevention, 406–412
 - stack design, 408–412
 - stack height determination, 407
 - problems, 415–416
 - related subjects, 393
 - scale models, 404–406
- Replacement-air systems, 338–357
 - delivery, 344, 347–352
 - floor casting, 349–350
 - melting furnaces, 349
 - sand handling, 350–351
 - shakeout, 351–352
 - energy conservation, 353–356
 - general exhaust (dilution) ventilation, 90–91, 103–104
 - heating, 352–353
 - historical perspective, 338
 - importance of, 338–339
 - needs assessment, 341–342
 - quantity assessment, 342–344, 345–346
 - types of, 340–341
- Restrained airflow, airflow principles, 13

- Reynolds number, airflow principles, pressure relationships, 24–26
- Roof fan, 286
- Rotating vane anemometer, airflow measurement techniques, 61–67
- Round duct, Pitot-static tube traverse, 57–58
- Sand handling, replacement-air systems, 350–351
- Scale models, reentry, 404–406
- Scrubber particle removers:
 - air-cleaning devices, 320–322
 - ventilation system integration, 334–335
- Semiconductor manufacturing, 187–192
 - entry loss, 190
 - optimum exhaust rate, 191–192
- Shakeout, replacement-air systems, 351–352
- Shipyards, 9
- Shock losses, airflow principles, 28–30
- Silicosis, 7–8
- Single-hood systems design, 232–253. *See also* Local exhaust ventilation (LEV); Multiple-hood systems design
 - Banbury mixer hood, 234–241, 248–249, 252
 - chemical laboratory ventilation, 217–218
 - local exhaust ventilation (LEV), 232
 - overview, 232–233
 - pressure plot for, 247
 - problems, 252–253
 - slot hood system (for degreasing tank), 241–247
 - steps in, 233–234
 - velocity pressure calculation sheet, 245–247, 250–251
 - velocity pressure plot, 247
- Slot hoods:
 - capture velocity determination, 131–135
 - single-hood systems design, for degreasing tank, 241–247
- Soldering operations, hood design, 169–177
- Special-purpose hoods, chemical laboratory ventilation, 216–217
- Specimen digestion, special-purpose hoods, chemical laboratory, 216
- Spray painting, 159–165
 - airflow, 163–165
 - hood design, 159–163
- Stack design, reentry prevention, 408–412
- Stack height, reentry prevention, 407
- Static pressure, airflow principles, 18. *See also* Pressure (airflow principles)
- Static pressure balance method (multiple-hood systems design), 260–265
 - electroplating shop, 262–265, 272–278
 - foundry cleaning room system, 260–262, 267–271, 280–281
- Static pressure curve, fan performance curves, 289–290
- Streamline flow, airflow principles, pressure relationships, 24–26
- Tangential method, Pitot-static tube traverse, 57–59
- Total pressure, airflow principles, 18
- Tracers:
 - airflow measurement techniques, 80–85
 - application, 84–85
 - design, 81–84
 - reentry measurement, 396–401
- Training, of employees, airflow measurement techniques, 84
- Tubeaxial fans, 284
- Tuberculosis, 7–8
- Tunnel-type hoods:
 - described, 110, 113
 - design of, 117
- Turbulent flow, airflow principles, pressure relationships, 24–26
- Unrestrained airflow, airflow principles, 13
- Upblast roof fan, 286
- Vaneaxial fans, 284–285
- Variable-air-volume (VAV) hood, chemical laboratory ventilation, energy conservation, 226
- Velocity pressure. *See also* Pressure (airflow principles)
 - airflow principles, 18
 - calculation sheet, single-hood systems design, slot hood system, 245–247, 250–251
 - frictional losses, airflow principles, 27–28
 - measurement, Pitot-static tube, 45–61
 - pressure relationships, 22–26
 - single-hood systems design, Banbury mixer, 248–249, 252
- Velocity profile, in duct, Pitot-static tube, 50–56
- Velometer (deflecting vane anemometer), airflow measurement techniques, 68–71

- Ventilation control:
 - air contaminants, 3–5
 - applications, 5–7
 - case studies, 7–9
 - literature review, 1
 - options in, 2–3
- Venturi meter, airflow measurement techniques, 76–77
- Venturi scrubber particle removers, air-cleaning devices, 320–322
- Vermont granite workers, case study, 7–9
- Vertical sliding sash hoods, chemical laboratory ventilation, 205–209, 210
- Video-concentration tape, 5–6
- Viscous flow, airflow principles, pressure relationships, 24–26
- Visual tracers. *See* Tracers
- Vortex shedding anemometer, airflow measurement techniques, 75–76
- Weighted residuals method (computational fluid dynamics), 377–378
- Welding:
 - hood design, 169–177
 - shipyards, 9
- Windows, chemical laboratory ventilation, 221
- Worker location:
 - administrative controls, 3
 - general exhaust (dilution) ventilation (GEV), 102–103
- Worker training, airflow measurement techniques, 84